

SOCIETY OF FLIGHT TEST ENGINEERS

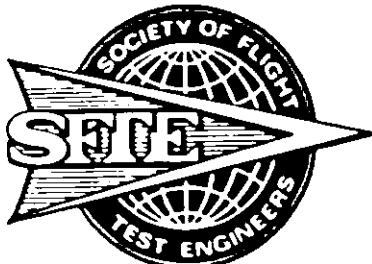
**ELEVENTH ANNUAL SYMPOSIUM
PROCEEDINGS**

FLIGHT TESTING IN THE EIGHTIES

AMERICAN MOTOR HOTEL

**Atlanta, Georgia
August 27 - 29, 1980**

sponsored by



SOUTHEASTERN CHAPTER

PUBLICATION POLICY

Technical papers contained herein may not be reproduced in any form without written permission from the Society of Flight Test Engineers or the respective authors. The Society reserves the exclusive right of publication in its periodicals of all papers at the annual SFTE symposium. Abstracts of these papers may be published without permission provided credits are given to the author, the symposium, and the Society of Flight Test Engineers.

For further information concerning publications policy write to:

Society of Flight Test Engineers
Post Office Box 4047
Lancaster, California 93534

Library of Congress Catalog Number: 75-26226

Copyright 1980 by the Society of Flight Test Engineers

FOREWORD

The theme of the 11th Annual Symposium is intended to recognize the dynamic changes that are taking place in the many engineering and scientific disciplines of aerospace engineering. These include but are not limited to Computer Sciences, physics, electronics, meteorology and avionics, as well as all engineering fields.

These new and on going technologies are presented in the following papers. I thank the authors and their organizations for their willingness to share that technology with the Society.

C. W. James
Symposium Chairman



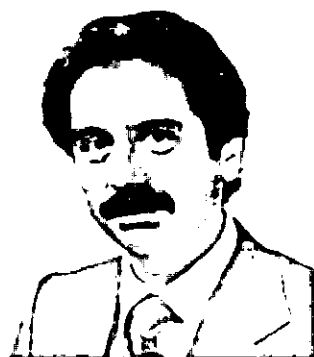
C. W. "Jim" James
Lockheed-Georgia Co.
Southeastern Chapter Director
Symposium Chairman

H. E. "Hugh" Smith, Jr.
Lockheed-Georgia Co.
Technical Papers &
Session III Chairman



N. D. "Norm" Frank
Lockheed-Georgia Co.
Southeastern Chapter Treasurer
Financial & Registration Chairman

A. "Rosey" Rosende, Jr.
Lockheed-Georgia Co.
Southeastern Chapter
Vice-President
Banquet & Session II
Chairman



E. A. "Ed" Reed
Lockheed-Georgia Co.
Southeastern Chapter Secretary
Vendor Chairman

L. P. "Lefty" Shoaf
Lockheed-Georgia Co.
Southeastern Chapter
President
Reproduction & Mailout
Chairman

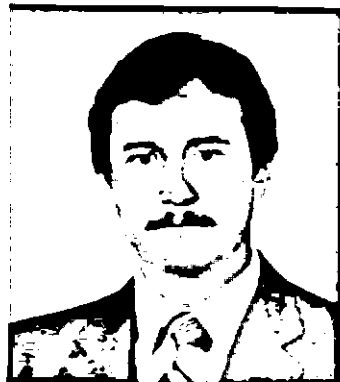




S. N. "Sam" Glass
Lockheed-Georgia Co.
Reception Chairman



R. G. "Glenn" Allen
Lockheed-Georgia Co.
Visual & Audio Aids
Chairman



R. "Rich" Jennings
Lockheed-Georgia Co.
Session I Chairman



H. "Harvey" Gambrell
Lockheed-Georgia Co.
Session IV Chairman



W. C. "Bill" Bahr
Lockheed-Georgia Co.
Publicity Chairman



Rose V. James
Special Activities
Co-Chairperson



Eleanor Smith
Special Activities
Co-Chairperson



"KELLY" JOHNSON AWARD

DONALD D. ARCHER

Mr. Archer attended the Coast Guard Academy and the University of Washington where he graduated with a B.S. Degree in aeronautical engineering. Following graduation, he served a tour of duty in the Air Force as a 1st Lt assigned to the Air Force Flight Test Center, Edwards AFB, California. At Edwards, he worked as a performance engineer on the T-37, B-57, B-66, C-133 and F-89J test programs. On most of these programs, he also served as his own instrumentation engineer, planner, data transcriber and program manager. As a result, he became thoroughly familiar with almost all aspects of flight testing.

Upon completion of his tour of duty with the Air Force, he joined the Flight Test Department of The Boeing Company in November 1957. This was in the early days of the development and FAA certification of the 707 airplane. Since that time, he has had an active part with increasing responsibilities in the development and or certification of the 707-100, 720, 707-320, 727, 737, 747, 747SP, C8A, QSRA, YC-14, AWACS and Command Post airplanes and their derivatives. He has also been involved in numerous proposal programs such as the Supersonic Transport, etc. With the advent of digital electronics he has had increased responsibilities in seeing that these programs with digital autothrottle, auto pilots and flight management systems are a success.

In addition to his in-house activities, he has established himself throughout the flight test community as a professional in the testing field with the ability to apply good engineering techniques and practical solutions to problems at hand.

He has been instrumental in the development of FAA rules for the certification of jet airplanes with emphasis on "Rational Landing Rule," SR 422B and amendments to FAR 25. He has been active in the various regulatory groups and currently serves on the project for the AIA Transport Airworthiness Requirements Committee. He has also represented The Boeing Company for many years on the AIA Flight Test Operations committee.

He is currently Assistant Director of Flight Test Engineering for The Boeing Commercial Airplane Company and is responsible for expanding the Flight Test Organization to certify two new model airplanes in an overlapping time period.

He is a member of the originating group of the SFTE and was instrumental in making the Sixth Symposium at Rosairo Resort in the San Juan Islands a success.



WILLIS M. HAWKINS

BANQUET SPEAKER

Willis M. Hawkins retired for a second time on May 13, 1980. Hawkins, who elected to take early retirement in 1974 after a career spanning 37 years with Lockheed, returned to serve as president of the Lockheed-California Company in 1976, the position he held until his Senior vice president-aircraft assignment in April 1979. He has been a member of the board of directors since 1972.

Hired in 1937 as a junior detail engineering draftsman in Lockheed's engineering department in Burbank, California, Hawkins advanced through a number of key engineering positions, becoming engineering department manager in 1944 and chief preliminary design engineer in 1949.

From 1953 to 1957 he was director of engineering at Lockheed Missiles & Space Division, and in 1959 was appointed assistant general manager of that division. He was elected a vice president of Lockheed Corporation in 1960.

In 1961 Hawkins received the U.S. Navy Distinguished Public Service Medal for his contributions to the Polaris missile program.

Before assuming duties as the corporation's vice president-science and engineering in 1962, he served for more than a year as vice president and general manager of the Lockheed Missiles & Space Company's Space Systems Division.

Hawkins served as Assistant Secretary of the Army for Research and Development for nearly three years beginning in 1963. He received the Distinguished Civilian Service Awards in 1965 and 1966 for his contributions to the Army's research and development programs and his direction of the U.S.-German main battle tank development. He returned to Lockheed in July 1966 to resume his duties as vice president-science and engineering. Hawkins was advanced to senior vice president-science and engineering of Lockheed Corporation in 1969, a position he held until 1974.

Hawkins was born on December 1, 1913, in Kansas City. He graduated from the University of Michigan in 1937 with a bachelor of science degree in aeronautical engineering. He received an honorary doctor of engineering degree from the University of Michigan in 1965, and an honorary doctor of science degree from Illinois College in 1966.

He is a member of many professional societies, including Tau Beta Pi (honorary engineering society) and the National Academy of Engineering, and is a Fellow of both the American Institute of Aeronautics and the Royal Aeronautical Society.

Hawkins and his wife, Anita, reside in Encino, California.

SESSION III: HUGH SMITH - CHAIRMAN (CONTINUED)

PAGE

ANALYSIS OF FLIGHT TEST MEASUREMENTS IN
GROUND EFFECT

Dr. E. K. Parks, University of Arizona
R. C. Wingrove, NASA-Ames Research Center
Moffett Field, CA 17-1

SUITABILITY OF THE ALL FIBERGLAS XVIIA AIRCRAFT
FOR FUEL EFFICIENT GENERAL AVIATION FLIGHT RESEARCH

Dr. George Bennett
Aerospace Engineering
Mississippi State University, MS 18-1

A COMPREHENSIVE FLIGHT TEST FLYOVER NOISE PROGRAM

James W. Vogel
Lockheed-California Company
Palmdale, CA 19-1

SESSION IV: HARVEY GAMRELL - CHAIRMAN

SIZE REDUCTION - FLIGHT TEST INSTRUMENTATION

J. W. Gierer
McDonnell Aircraft Company
St. Louis, MO 20-1

DATA SYSTEMS ORGANIZATION - A CHANGE FOR THE BETTER

Robert D. Samuelson
McDonnell Aircraft Company
St. Louis, MO 21-1

SIMULATOR DATA TEST INSTRUMENTATION:

FLIGHT TEST CHALLENGE OF THE EIGHTIES
William L. Curtice III
ASD Wright-Patterson AFB, OH 22-1

BOEING FLIGHT TEST AND THE COMPUTER, 1980

Jerry Zanatta
Boeing Commercial Airplane Company
Seattle, WA 23-1

INSTRUMENTATION REMOTE "MINI" GROUND STATIONS

Jack Nixon
Boeing Commercial Airplane Company
Seattle, WA 24-1

COLOR GRAPHICS BASED REAL-TIME TELEMETRY PROCESSING SYSTEM

Thomas M. Randall
Lockheed-Georgia Company
Marietta, GA 25-1

SESSION II: ARMAND ROSENDE - CHAIRMAN (CONTINUED) PAGE

GENERAL AVIATION FUEL CONSERVATION IN THE 1980's G. R. Bromley Beech Aircraft Corp., Wichita, Kansas	9-1
FLIGHT TEST RESULTS OF ACTIVE CONTROLS CERTIFICATION FOR THE LOCKHEED DASH 500 John W. Pieper Lockheed-California Company Palmdale, CA (Paper not available)	10-1
FLIGHT TESTING THE AIR LAUNCHED CRUISE MISSILE Richard R. Hildebrand AFFTC, Edwards AFB, CA	11-1
DETERMINING PERFORMANCE PARAMETERS OF GENERAL AVIATION AIRCRAFT Gifford Bull/Phil Bridges Aerospace Engineering Mississippi State University, MS	12-1

SESSION III: HUGH SMITH - CHAIRMAN

TORNADO - AVIONIC DEVELOPMENT TESTING E. K. Obermeier Messerschmitt-Bolkow-Blohm GmbH Flugplatz, West Germany	13-1
DESIGN DEVELOPMENT AND FLIGHT TESTING OF A JET-POWERED SAILPLANE Bernard S. Smith Caproni Vizzola Costruzioni Aeronautiche Spa, Italy	14-1
SMALL SCALE FREE FLIGHT RESEARCH AT LOCKHEED-GEORGIA M. W. M. Jenkins Lockheed-Georgia Company Marietta, GA	15-1
PERFORMANCE FLIGHT TEST EVALUATION OF THE BALL-BARTOE JW-1 JETWING STOL RESEARCH AIRCRAFT Ralph D. Kimberlin University of Tennessee Space Institute Tullahoma, TN	16-1

TABLE OF CONTENTS

	<u>PAGE</u>
SESSION I: RICHARD JENNINGS - CHAIRMAN	
INITIAL F-18 CARRIER SUITABILITY TESTING James W. Hakanson McDonnell-Douglas Corp. Patuxent River, MD	1-1
ICING PROGRAM MANAGEMENT TECHNIQUES Frederick S. Doten, Major U.S. Army Aviation Engineering Flight Activity, Edwards AFB, CA	2-1
F-16 INFLIGHT AND GROUND ICING TEST Charles M. Core, Major ASD, Wright-Patterson AFB, OH	3-1
HELICOPTER - ICING SPRAY SYSTEM Daumants Belte U.S. Army Aviation Engineering Flight Activity, Edwards AFB, CA	4-1
MODERN TECHNIQUES OF CONDUCTING A FLIGHT LOADS SURVEY BASED ON EXPERIENCE GAINED ON THE BLACK HAWK HELICOPTER William P. Groth Sikorsky Aircraft, Stratford, CT	5-1
JP-8 FUEL CONVERSION EVALUATION Robert A. Stambovsky AFFTC, Edwards AFB, CA	6-1
SESSION II: ARMAND ROSENDE - CHAIRMAN	
INSTRUMENTING A TEST AIRPLANE IN BRAZIL Arturo Garza Cantu Boeing Commercial Airplane Co. Seattle, WA	7-1
DEVELOPMENT OF A SIMPLE, SELF-CONTAINED FLIGHT TEST DATA ACQUISITION SYSTEM Ronald R. L. Renz Flight Research Lab University of Kansas Space Tech Center Lawrence, Kansas	8-1

INITIAL F-18 CARRIER SUITABILITY TESTING

James W. Hakanson*
McDonnell Douglas Corporation, NATC
Patuxent River, Maryland

ABSTRACT

The F-18 Hornet made the first shipboard arrested landing on the USS AMERICA October 30, 1979. After four days of exercising the aircraft in every aspect of carrier operations and logging 32 arrested landings and 32 catapults without missing a flight period, the Hornet completed what was considered the most successful "Sea Trials" in recent history.

"Sea Trials" was preceded by six months of vigorous, productive flight testing. The aircraft was evaluated for flying qualities, structural integrity, steam ingestion, jet blast deflector compatibility, electromagnetic compatibility, systems performance, and deck handling.

Problems were defined early which allowed maximum recovery time. The aircraft was deemed ready for shipboard operations by McDonnell Aircraft Company, a division of the McDonnell Douglas Corporation, and accepted by the U. S. Navy October 3, 1979 for four weeks of shore-based familiarization and evaluation flying by the two USN pilots selected to participate in "Sea Trials". On the 30th of October, LCDR Richards flew towards the USS AMERICA with confidence that he and the Hornet were ready.

This paper discusses the Carrier Suitability Flight Test Program from beginning through "Sea Trials" including test conditions, techniques, instrumentation and data systems.

INTRODUCTION

The F-18 is built by McDonnell Douglas for the U. S. Navy and Marine Corps. It is designed to replace the F-4 and A-7 with performance superior to both in their respective roles. Major emphasis was placed on designing the F-18 for excellent carrier suitability which includes catapult, approach, arrestment and deck handling. The F-18 is designed to catapult with heavy payloads and arrest with little or no wind-over-deck. The F-18 first flight was November 18, 1978; a major goal was to get the carrier suitability test aircraft on an aircraft carrier by October 1979, within a year of the F-18 first flight.

*James W. Hakanson is a McDonnell Douglas F-18 Senior Flight Test Engineer at the Naval Air Test Center, McDonnell Douglas Corporation, Patuxent River, Maryland.

AIRCRAFT DESCRIPTION

The F-18 is a single place, twin tail, twin engine high performance fighter/attack aircraft for the U. S. Navy and Marine Corps. Its size falls between the A-7 and F-4. Three F-18s take the same space as one F-4 and two A-7s approximately the ratio of aircraft it will replace aboard ship.

The avionics system is designed for a one man operation. Centered around a new multi-mode radar and two central digital computers, the avionics equipment is tied together with a multiplex system providing flexibility for altering or adding new equipment.

The armament is carried on nine store stations; two wing tips, two pylons on each wing, a pylon on the centerline of the fuselage and the two "corners" of the fuselage. These stations offer the flexibility of a full complement of air-to-air and conventional air-to-ground weapons, as well as guided bombs. The aircraft also has a 20mm gun and nuclear capability.

Approximately 11,000 lbs of fuel is carried in the fuselage and wings. Each of the inboard wing stations and the fuselage centerline station can carry a 315 gallon external fuel tank for extended range.

Two 16,000 lbs thrust class F404 low by-pass engines provide power for the F-18. An auxiliary power unit supplies self starting and the capability to run all of the systems on the ground for full checkout with no external power.

The airframe is a balance of conventional materials and graphite/epoxy. The wing skins, flaps, ailerons, stabilators, vertical tails and many access doors are made of graphite material which comprises over 13% of the structure.

Approximately every ninth F-18 is a two-place, mission trainer. All equipment and displays are duplicated in the back seat except for the head-up display. The differences between the F and TF are the back seat equipment, a larger canopy, and the removal of less than 500 lbs of fuselage fuel.

The third F-18 was designated as the carrier suitability test aircraft. It was instrumented with strain gages, accelerometers, cameras, gear positions, sink rate radar and basic engine and flight control parameters.

PREPARATION

Prior to the flight test program, laboratory tests were performed to verify component and system integrity. The total structure was loaded to simulate catapult and arrested landings using the static and fatigue test articles. Figure 1 shows the static test article during the catapult tow loads testing.

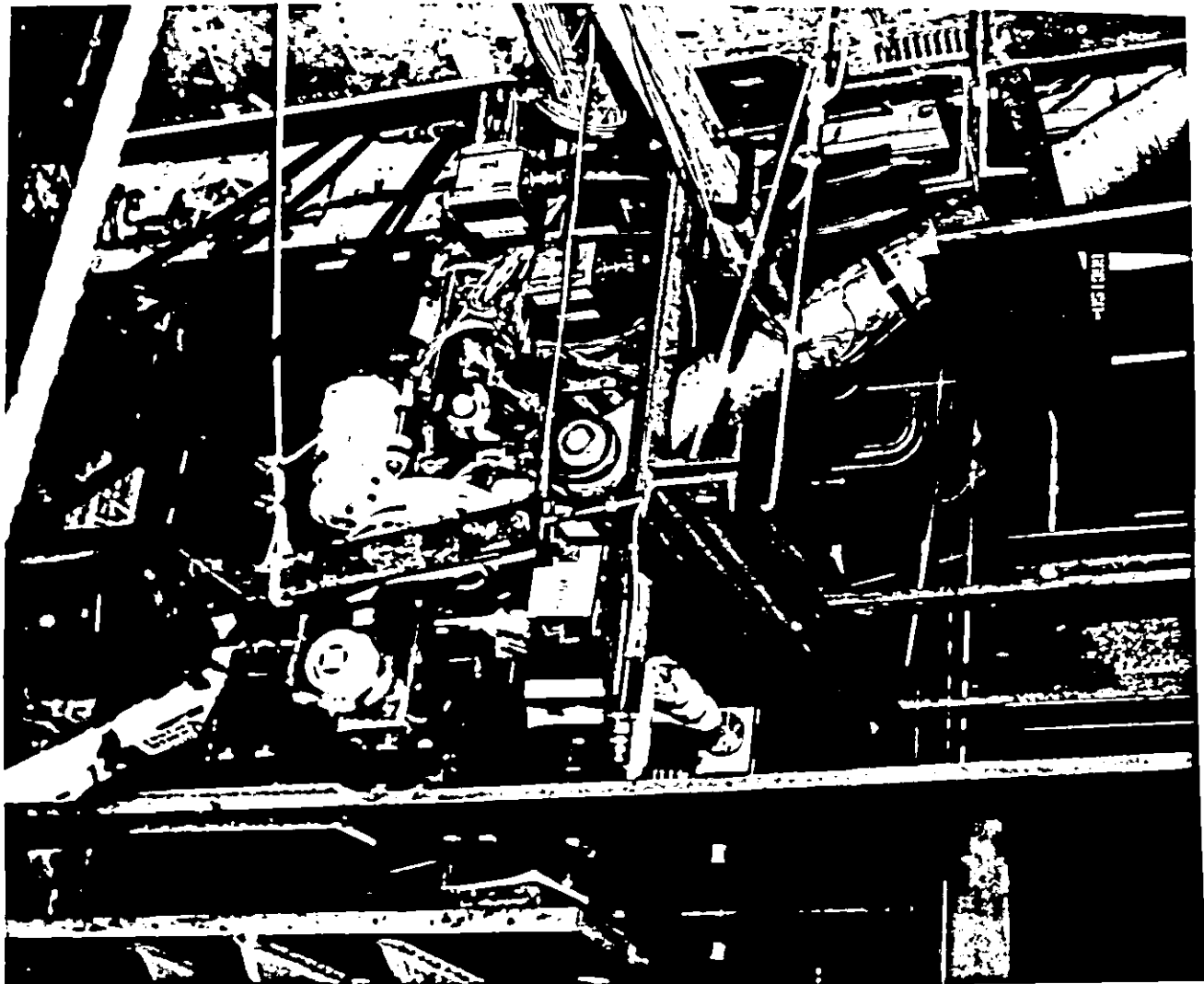


FIGURE 1
STATIC TEST ARTICLE DURING CATAPULT TOW LOAD TESTING

High sink landings were simulated by the drop test article. Figure 2 shows the drop test article in position for a drop with a pre-determined sink speed, wing lift and approach speed. The wheels are spun backwards to represent wheel spin-up forces at the target approach speed. The drop test article also proved to be valuable in selection of strain gage locations for the flight article.

The virtual image take-off and landing (VITAL) simulator was used to evaluate and develop flying qualities and displays. The simulator had the capability of simulating ground effects, the bubble, crosswinds, throttle sensitivity, launch bar release and gear dynamics. Figure 3 presents the simulator field-of-view on approach.

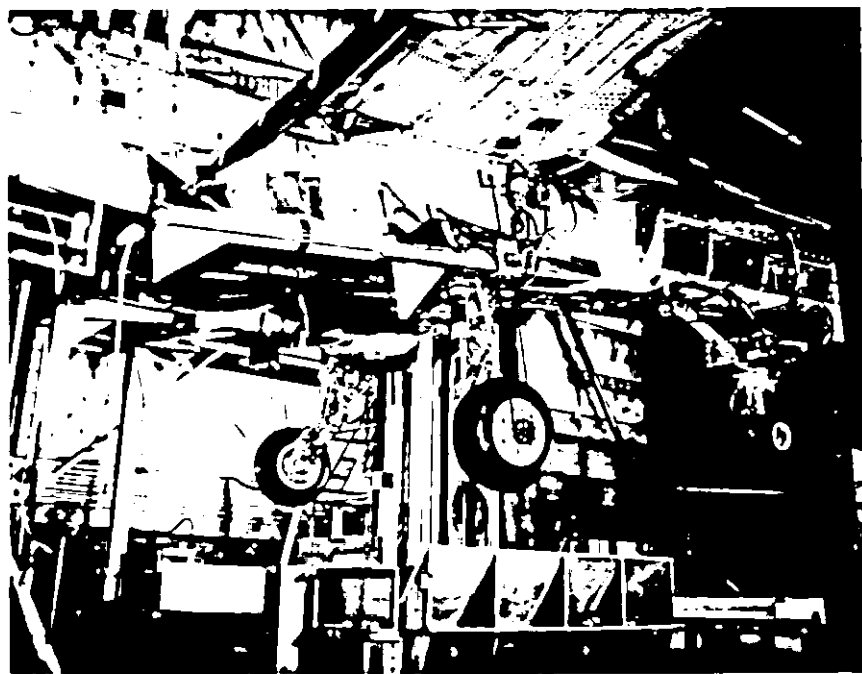


FIGURE 2
DROP TEST ARTICLE IN POSITION FOR DROP

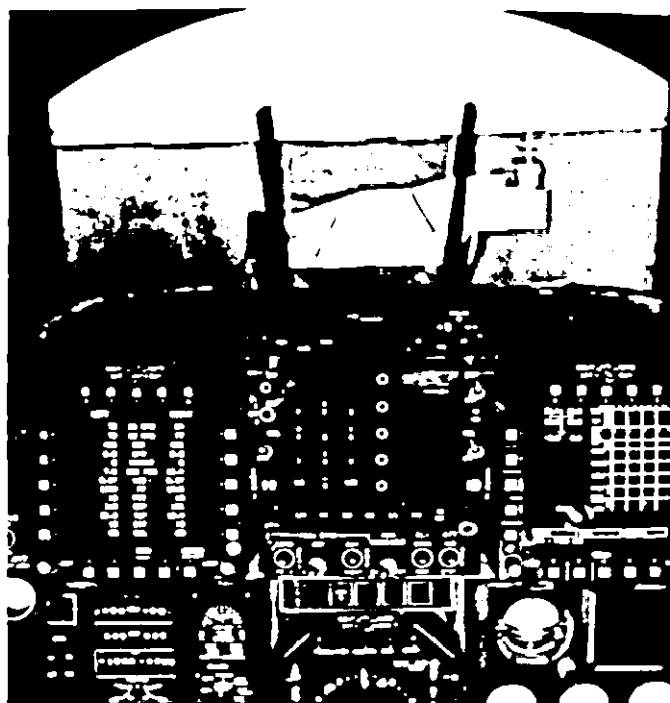


FIGURE 3
VITAL CARRIER APPROACH DISPLAY

ARRESTMENTS

A series of touch and go landings and taxi-in engagements were performed in preparation for the actual arrests. These tests allowed the pilot to become familiar with the aircraft on the glideslope and "in the wire" as well as gaining confidence in the instrumentation and data systems. The selection of the first arrested landing was a challenge. Selecting a low glideslope angle increases the chance of a free-flight engagement while a high glideslope angle results in high gear loads. High airspeed results in high hook loads and low airspeed results in less pilot control of the engagement conditions. Therefore, it was decided to start with a point in the middle of the envelope - a 3 1/2° glideslope with the pilot flying "on speed". The first arrested landing attempt resulted in a hook skip bolter and the second was an uneventful arrestment.

The arrestment envelope was then expanded in the following areas:

- o Off-Center (to 20 ft)
- o High Sink Speed (to 19.5 fps)
- o Pitch Attitude (0 to 8°)
- o Rolled Attitude (to 10°)
- o Rolled/Yawed (to 6° roll with 6° yaw)
- o Deck Obstructions
- o Full and Half Flaps

The ability to control the aircraft attitude and speed at touch down are of paramount importance for a carrier suitability structural test program. The F-18 mission computer capability and flexibility afforded us the opportunity to use a tool we called "Dial-An-Alpha". The test engineer would take into consideration wind, gross weight and glide-slope angle to select the proper angle-of-attack for the pilot to fly to get the desired touchdown variables (pitch angle and engagement speed). The pilot would dial in the required angle-of-attack and fly the velocity vector on the center of the HUD indexer. Figure 4 presents the HUD display and resultant geometry. This was an improvement over previous test programs which utilized the LSO to report airspeed verbally (based on the SPN 44 tracking radar).

Prior to "Sea Trials" 141 arrestsments were accomplished. The following pertinent problems were apparent early in the arrestment test program:

PROBLEM	SOLUTION
1. Approach speed higher than required (~ 5 kts);	Acceptable for "Sea Trials" with wind-over-deck; Production fix in work;
2. Poor bolter performance;	Installed unsnagged stabilators and reprogrammed the flight control computers;
3. Excessive throttle friction;	Installed boosted throttle system; Reduced friction to 2-3 lbs per throttle;

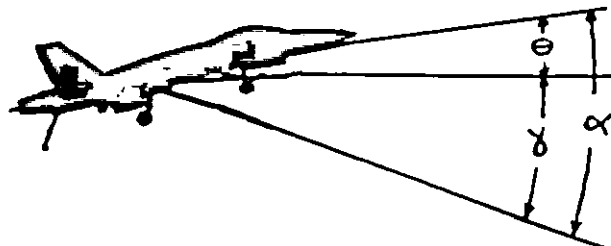
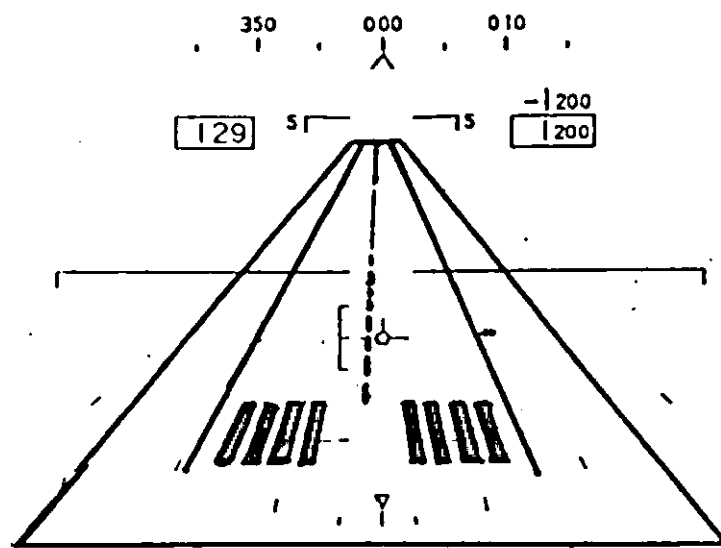
PROBLEM

4. Throttle too sensitive at approach speeds;
5. Tail hook extension time too slow;

SOLUTION

Acceptable for "Sea Trials";
Final throttle gradient design in work;

Modified vertical damper to decrease extend time to two seconds.



θ Pitch Angle
 γ Glideslope Angle
 α Angle-of-Attack

FIGURE 4
DIAL-AN-ALPHA PRESENTATION AND RESULTANT GEOMETRY

The aircraft was very stable and easy to fly on approach and was well damped during engagement. Difficult-to-attain attitudes were performed routinely. The bolter rate was low even though the test facility uses one pendant whereas a carrier has four.

CATAPULTS

Selecting the first catapult test condition also posed a problem. Because of the NATC catapult layout (see Figure 5), the aircraft would have to negotiate a 9° left turn 2150 feet after the catapult stroke if not airborne. This precluded a build-up sequence from low speed to fly-away speeds. One taxi-away catapult was performed at idle to 70 kts followed by normal braking. The next catapult was decided to be a fly-away.

The areas of concern were:

- o Engine blowout
- o Degradation of flight controls
- o Structural integrity
- o Over rotation
- o Stick handling at end of stroke

The above were all taken into consideration and the first fly-away conditions were:

- o 5000 lbs fuel
- o 130 kts end airspeed
- o Mil power
- o Stabilator trim (-4°) pilot holding (-15°)

Although the F-18 was designed for "hands off" catapults, the first catapult was performed with the pilot holding the stick to give -15° of stabilator. The -15° of stabilator was selected based on a series of take off's to evaluate rotation characteristics with various stabilator positions and centers of gravity.

The aircraft flew away from the catapult with comfortable characteristics. The remaining catapults were performed to expand the catapult envelope in the following areas:

- o Increased tow forces
- o Increased longitudinal acceleration
- o MLG off-center spotting (22 inches)
- o Stabilator trim optimization
- o Steam ingestion

The aircraft had good catapult characteristics; however, at forward centers of gravity there was insufficient stabilator trim. This problem was attributed to the flight control system dumping 5° to 7° of stabilator at nose wheel lift off because of the rapid nose-up pitch rate resulting from the stored energy in the nose gear strut. Sixty catapults

were performed during the build-up phase and the following problems were defined:

PROBLEM	SOLUTION
1) FCES ram door opened during catapult stroke;	Open (temporarily solved by riveting door closed);
2) Repeatable release spring cartridge assembly is understrength;	Interim configuration available for "Sea Trials"; Final fix in work;
3) Launch bar extension too rapid; Personnel hazard and damaging to deck ramp;	Installed orifice to slow extension time to approximately four seconds;
4) Not enough nose up trim for hands off catapults (forward CG and heavy weights); Also, stabilator dumped trim at end of catapult stroke;	Imposed center of gravity and endspeed restrictions during "Sea Trials"; Production fix is in work (increased longitudinal trim and pitch rate feedback wash out);
5) Repeatable release hold back bar dynamics after release;	Modified by vendor/minimal dynamics after release;
6) Force to manually raise launch bar increases with number of cycles on power unit until unacceptable;	Increased mechanism tolerances.

Steam ingestion was evaluated by degrading the C-7 catapult to simulate the worst steam leakage possible in the fleet catapults. Out of 27 catapults, two resulted in afterburner blowouts. The A/B automatically relit each time and was therefore deemed acceptable. Figure 6 shows the F-18 at the end of the degraded catapult.

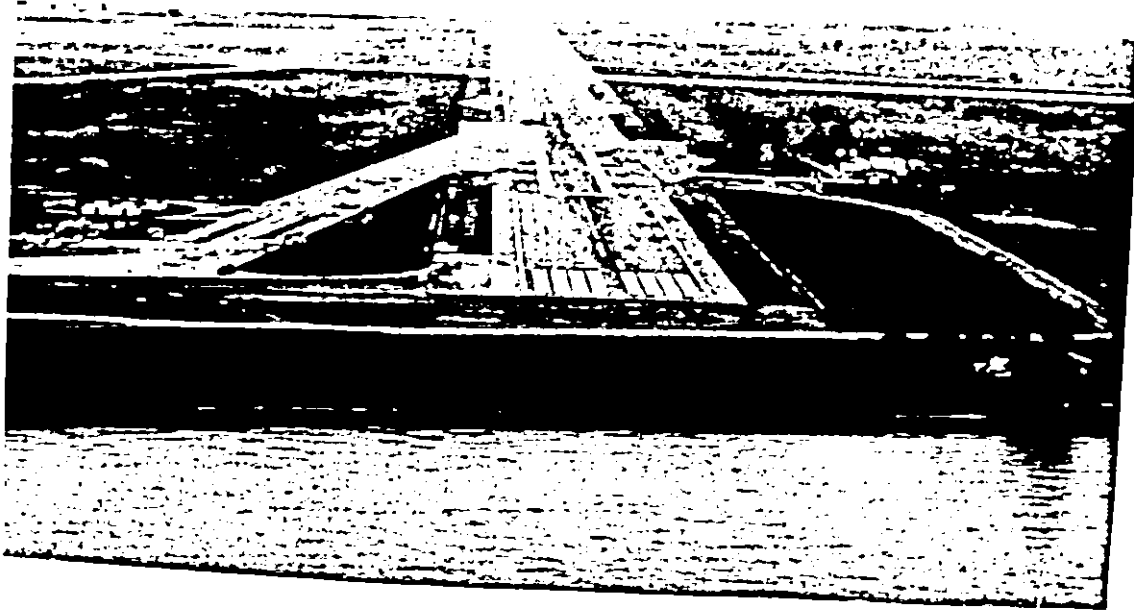


FIGURE 5

NATC C-7 CATAPULT AND MK-7 MOD 3 ARRESTING GEAR FACILITY

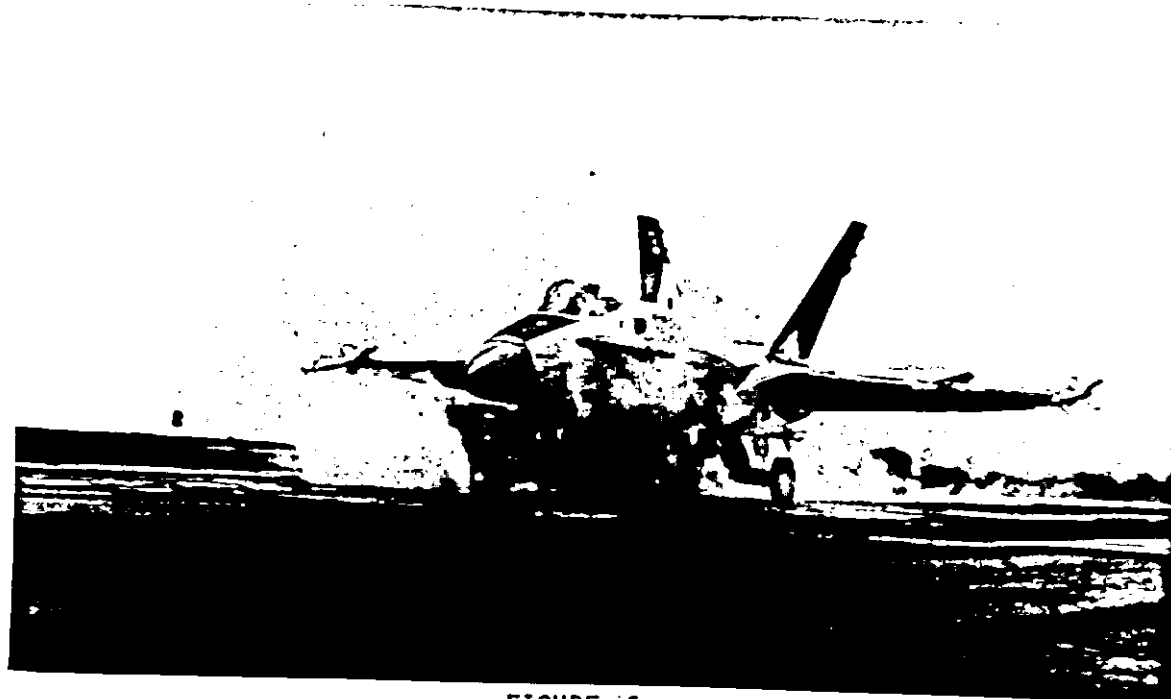


FIGURE 6

STEAM INGESTION CATAPULT

ELECTRO-MAGNETIC COMPATIBILITY (EMC)

Two periods of EMC testing were required; the first period was used to define problems and the second to verify problems had been solved and/or establish operating restrictions. The tests were performed at NATC EMC Facility. Figure 7 shows the aircraft avionics compartments being radiated by A band radiation. The tests were performed with a pilot in the cockpit and all systems operational.

DECK HANDLING/OPERATION

The aircraft was evaluated for carrier environment during the following tests:

- o Tip Back
- o Spotting Dolly Compatibility
- o Wet Brake Tests
- o Aft Towing
- o Engine Starts with Tail Winds
- o Low and High Pressure Huffer Engine Starts
- o Ship Inertia Navigation Alignments
- o Hoisting (see Figure 8)
- o Chain Tie Down

INSTRUMENTATION

The onboard data system consisted of a time division multiplex/frequency division multiplex system (TDMS/FDMS), a 14-track magnetic tape recorder and a telemetry transmitting system. The TDMS data were recorded in serial digital form, pulse code modulation (PCM). The FDMS data were recorded in analog form using frequency modulated constant bandwidth (CBW) subcarrier channels. The telemetry system transmitted all PCM, some CBW measurands and pilot's voice. Also, the following noteworthy items were installed:

- o Two TM transmitters capable of transmitting 24 FM measurands;
- o Instrumented landing gear - strain gaged to allow matrix solution for vertical, side and drag loads;
- o Ryan sink rate radar;
- o Documentation cameras capable of high speed movie coverage of main landing gear, nose landing gear or tail hook operations;
- o High usage of MUX parameters.

Portions of the instrumentation requirements were satisfied using the following NATC supplied systems:

- o SPN 44 tracking radar (approach and engagement speed);
- o Laser tracker (approach and engagement speed);
- o Mechanical trips and chronographic sensors (catapult endspeed);
- o Cinerama and Cameraflex cameras (sink speed and touch down attitude);
- o Portable ground station for use onboard carrier.

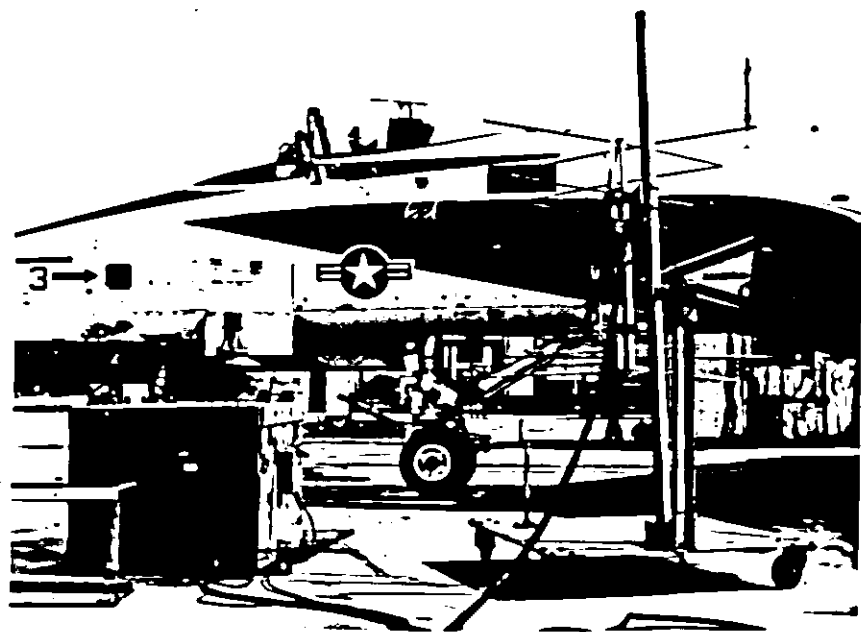


FIGURE 7
F-18 AT NATC EMC TEST FACILITY

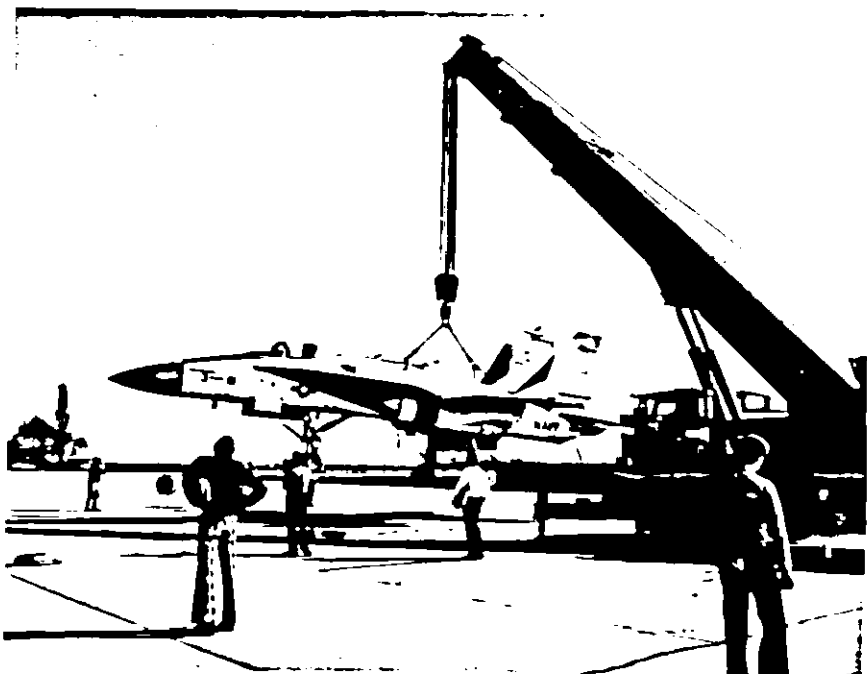


FIGURE 8
F-18 DURING HOISTING TESTS

DATA SYSTEM

There were two types of data used, real time quick look data and final data. The real time system used was the NATC real time telemetry processing system. Final data was processed in St. Louis. The pre-processed data was transmitted to St. Louis via the Bell system and processed and transmitted to Northrop and NATC.

"SEA TRIALS"

Prior to the shipboard tests, the two U. S. Navy pilots were trained in the MCAIR simulator and each had 25 hours of F-18 flight time. The flight profiles included flying qualities, engine handling, bingo schedules, ground controlled approaches, inflight refueling, simulated single engine approaches, catapults and arrested landings. This testing was accomplished using the same aircraft that would go aboard the ship.

The F-18 arrived at the USS AMERICA 30 October 1979, the day for which we had been planning and waiting. Figure 9 shows the Hornet arriving at the ship. The months of preparation and effort would finally be put to the test. There was a feeling of anxiety until LCDR Dick Richards made the first touch and go and demonstrating that the bubble was not a problem. After a series of touch and go's and wave-offs were completed, the pilot extended the hook and made an uneventful arrestment, engaging the number 3 wire.

Thirty-two catapults and 32 arrested landings were performed during six deck periods from 30 October to 3 November, 1979. The aircraft was very stable on the glideslope and flew through the bubble with little pilot compensation. Approximately 75% of the arrestments caught the target, number 3 wire.

There were no unintentional bolters. The aircraft also demonstrated excellent pendant shedding characteristics. The catapult launches went well also; the hook-ups to the shuttle were easy and all launches were "hands off".

The five days of "Sea Trials" resulted in the following accomplishments:

- o Engine starts using APU, engine crossbleed, low and high pressure huffer;
- o Engine starts in tail winds up to 22 knots;
- o Mil and max power catapults;
- o C-13 and C-13-1 catapults;
- o Bow and waist catapults;
- o Intentional bolters (to determine hook point wear);
- o Controlled carrier approaches;
- o Ship's inertial navigation alignments (cable and RF);
- o Taxi tests with centerline external fuel tank for clearance tests;
- o Electro-magnetic interference check at various positions on the deck;

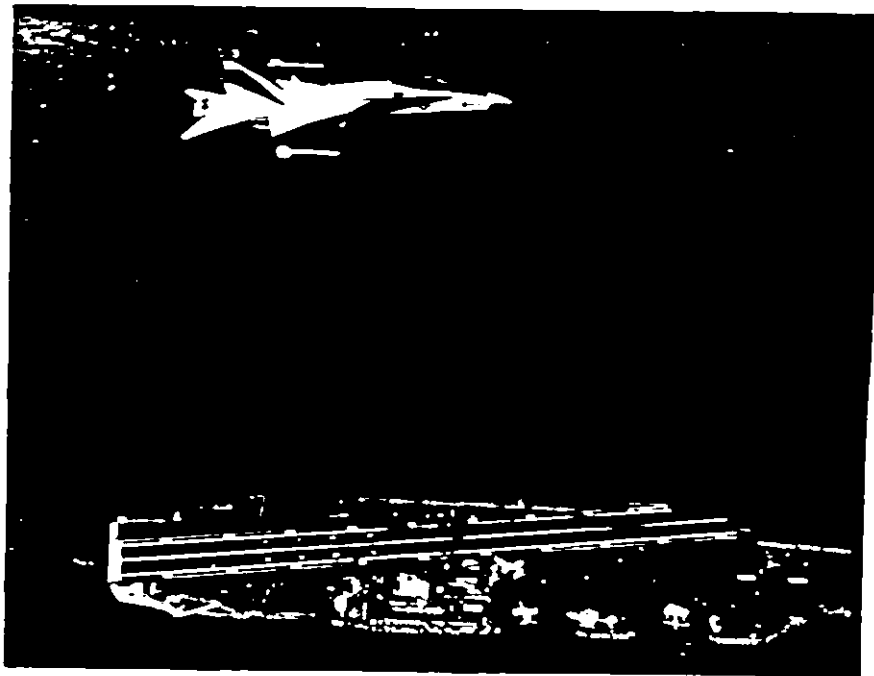


FIGURE 9
THE HORNET ON ARRIVAL AT THE USS AMERICA

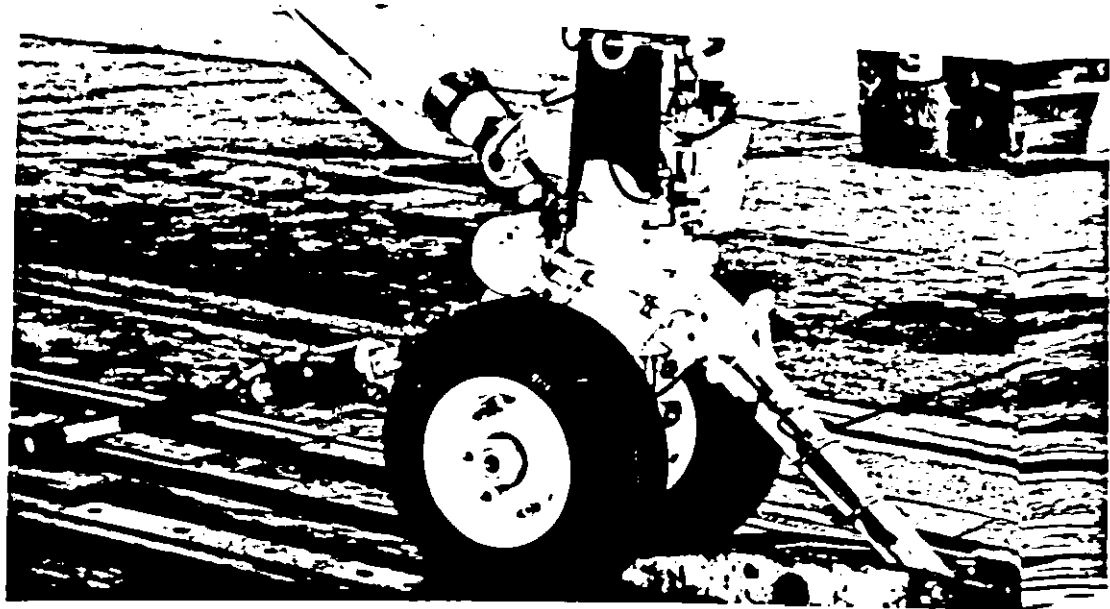


FIGURE 10
F-18 NOSE GEAR LAUNCH MECHANISM

- o Chain tie downs at various positions on flight and hangar decks;
- o Catapult endspeeds from 137 to 174 KCAS
- o Simulation of various maintenance items on the flight deck;
- o Various centers of gravity during catapult launches;
- o Two tests including the spotting and flight deck dollies;
- o Use of maximum power holdback fitting;
- o Demonstration of an engine change;
- o Emergency brake accumulator tests;
- o APU foot print tests with MLG wheels at scupper;
- o Simulated single engine approaches.

During the above mentioned tests the following problems were apparent:

- o Excessive sink off the bow - this problem was apparent during the shore-based testing; however, the fix for this required increased longitudinal trim and a pitch rate feedback washout fix which wasn't ready in time.
- o Repeatable release holdback spring cartridge was understrength during arrestsments. Figure 10 presents the nose gear launch mechanism. Subsequent laboratory tests determined that the lower nose wheel spin-up speeds caused a resultant excess load which caused us to fail several spring cartridges, one of which was responsible for engine foreign object damage.
- o Throttle Sensitivity - Again, this was expected, but the fix was not available in time. This problem was compensated for by the pilot training period prior to shipboard operations.
- o Stiff Catapult Stroke - With nose tow aircraft, the catapult stroke results in a higher G rate than experienced with the bridle type catapult hardware. However, the F-18 appeared to be more severe than other nose tow type aircraft. The result of this problem was the pilot's inability to read the HUD parameters. Pilot concern was lessened because of the "hands off" capability which allows plenty of recovery time.

CONCLUSIONS

The initial F-18 carrier suitability testing was completed with a successful "Sea Trials". The test program included all aspects of carrier interface testing. Problems were defined early which allowed maximum recovery time. The two U.S. Navy pilots were thoroughly trained and familiar with the F-18 Hornet in order to make a comprehensive evaluation of the aircraft. The problems revealed during "Sea Trials" are being reviewed by MCAIR and will be solved and solutions demonstrated so that at the end of the contractor carrier suitability program, the aircraft will be ready for the fleet.

ICING PROGRAM MANAGEMENT TECHNIQUES

Major Frederick S. Doten
TEST PILOT

U.S. Army Aviation Engineering Flight Activity
Edwards Air Force Base, California

ABSTRACT

The Army has instituted a centralized management system as a means of conducting several icing tests at one test location. This system, in conjunction with the use of innovative management techniques have minimized the logistical and support requirements and reduced the overall cost of the flight testing. The use of leased apartments and automobiles, locally hired personnel and established military facilities with similar resources have been major factors in this reduction. Techniques used by the military are applicable to the flight test endeavors of non-military organizations.

INTRODUCTION

The United States Army for the past several winters has been conducting icing tests in order to determine the capability of their helicopter fleet to operate in an icing environment. Since the initial winter where only a small effort was made, the icing program has grown to its present size and complexity. During the 1979-80 season, the icing and cold weather effort involved four helicopters, 65-plus individuals and close to one-half million dollars. As this effort has grown, the management and logistical requirements have escalated to the point where preparation for the icing season commences in June or July. In addition to this pre-planning, the Army has adopted several techniques that have reduced the overall cost and personnel required. These techniques will be discussed individually and then will be followed by a descriptive outline of how a typical program is conducted.

MANAGEMENT TECHNIQUES

Centralized Management Team

Previously, the icing test for a specific helicopter was an entity in itself and each had its own icing team. These teams included the test pilots and engineers; instrumentation, maintenance and photographic support; safety/chase crews.

Frederick S. Doten (Retired-US Army), Test Pilot and Consultant for Flight Research, Inc., Mojave, California.

and the Helicopter Icing Spray System (HISS) crew (the HISS is the subject of a later paper). Each team was under the direction of the Project Officer who was responsible for all phases of his test. In addition to planning and conducting the test, he was responsible for moving equipment to the test site, securing test site facilities and quarters and local transportation. Each team was independent even though co-located with another team. Generally, both teams were identical in composition and only varying in size due the complexity of the individual test.

The centralized management team was introduced to decrease the Project Officer's workload, the number of support personnel and the total cost of the overall icing effort. This team, under the direction of a Program Director, was responsible for all test site coordination, movement of equipment, test support and test site logistics. Because of the management team, each test team was reduced to the test pilots and engineers, one being the Project Officer. A typical wiring diagram is shown in figure 1. Although shown under the supervision of the Program Director, each icing test team is independent and is only under the Program Director for logistical support.

The centralized management team consists essentially of six individuals; the Program Director, the Logistics Technician, the Maintenance Supervisor, the Instrumentation Supervisor, the Photographic Supervisor and the Flight Support Supervisor. Of these individuals only the first two have major roles during the establishment of the test site. The other individuals, along with the Project Officers, only provide technical advise and support requirements. These same individuals also control the various technicians supporting the tests.

The Program Director is the overall coordinator of the icing program. Based on the requirements dictated by individual team members, the Program Director will coordinate for office and work facilities, quarters, local transportation, logistical and personnel support and any other requested requirement. After coordination is completed, the Program Director will publish the applicable movement orders and time schedules to insure an orderly and efficient movement of all personnel and equipment to the test site. He will then coordinate all suport elements to insure the maximum utilization of equipment and personnel once the test site is established and the test teams are operational. The major advantage of the Program Director is that he alleviates the Project Officers of their logistical and support coordination requirements and allows them to direct 100% of their effort toward the completion of the test mission.

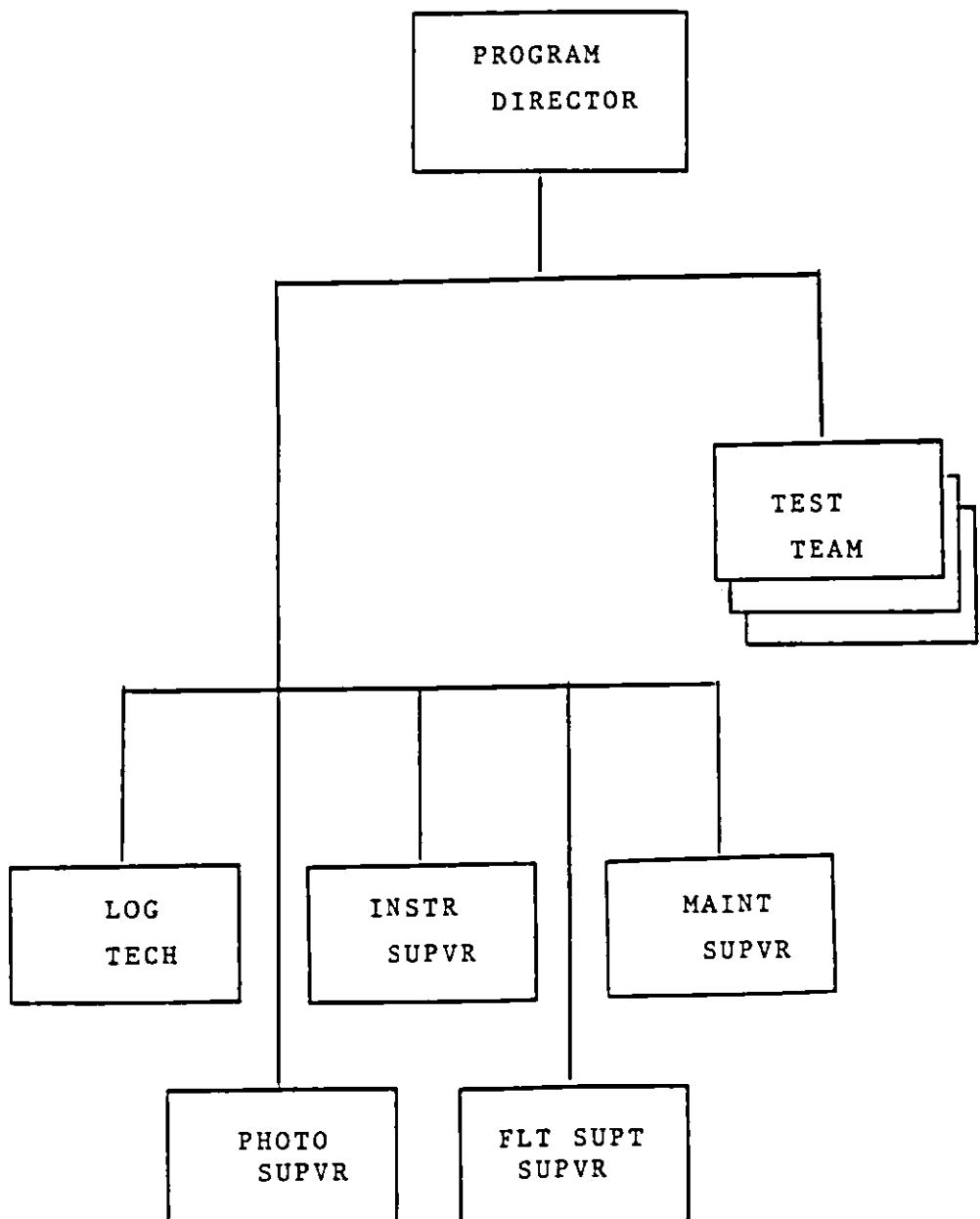


Figure 1--MANAGEMENT TEAM

The Logistics Technician is the Program Director's right hand man in the establishment of the test site. This individual is responsible for the acceptance of all facilities and equipment, the establishment of local maintenance and support accounts, the procurement and reception of all supplies and, at the completion of the icing program, the termination of all contracts and the shipment of test equipment and supplies. He consolidates the efforts of several individual Project Officers into one position.

The Instrumentation and Maintenance Supervisors have identical functions. Their primary function is to coordinate the efforts of all maintenance and instrumentation at the test site. They insure that each test team receives their requested share of the support and during periods when special assistance is required, provide the additional personnel and/or equipment needed. They also function as advisors for the Program Director and Project Officers. Their major asset is the consolidation of the efforts of several Project Officers into a single position.

The Photographic Supervisor is responsible for all photographic requirements during the icing program. Prior to the icing program he will advise both the Program Director and Project Officers of the photographic requirements. He is also responsible for the procurement of all equipment and supplies. During the icing program he supervises all photographers and allocates resources to support all programs. He is also responsible for the processing of all film, the repair of all equipment and the documentation of the icing program. His efforts reduce the total number of photographers and cameras required.

The Flight Support Supervisor is responsible for all aircraft support during the icing program. He will coordinate the efforts of the HISS and all chase aircraft and insure air crews are available and briefed. He will act as an advisor to the Program Director and the Project Officers. During the icing program he will eliminate the requirement of each Project Officer supervising the support crews and equipment.

Leased Apartments

The use of furnished apartments during the icing program for the test personnel was considered a tremendous cost savings in addition to being a great morale booster. Two-bedroom apartments were leased and operated similar to a motel by the Program Director. The number leased was based on the arrival and departure schedule of the various test teams and the total personnel support requirement. The apartments were leased unfurnished with supplemental contracts for furniture (w/tv), kitchen utensils, linen exchange (towels and bedding), maid service and garages.

Minimum lease on the apartments was two months. Use of supplemental contracts for the additional services reduced the overall costs as each apartment, even though rented, was not provided with these services until occupied. It was determined with double occupancy that the break-even point was 20 days for a two-month lease. During the test period an 85% occupancy rate was achieved with 100% occupancy quite common. The 85% occupancy was considered an advantage as it allowed the accommodation of visiting dignitaries. Figure 2 portrays graphically expected savings from ten apartments for four months.

Leased Automobiles

Local transportation on all test programs, especially those of long duration; is without an exception one of the major factors in determining a successful program. During the icing program over 20 automobiles were provided the test teams to meet their commitments. These cars were leased from GSA motor pools at minimal cost when compared to the local rental agencies. Leased vehicles, either commercial or government, are more advantageous than rental cars. These

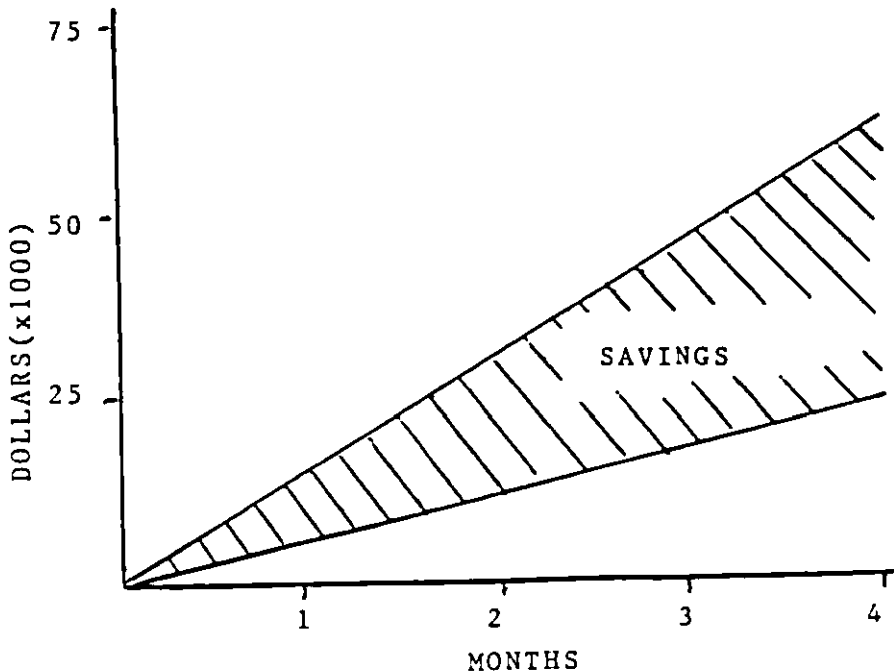


Figure 2--SAVINGS, 10 APARTMENTS VS MOTELS

cars when combined with organizational credit cards for fuel and minor maintenance require minimal administrative support and no personnel support. Comparative cost for rentals, government and commercial lease are shown in figure 3.

Government Support Facilities

During the icing programs the Army satellite itself on the local National Guard and Reserve units. This fact had numerous side benefits for the Army as well as National Guards and Reserves. For the Army there was hangar and office facilities and at no or minimal cost, access to the Army supply channels, a source of aircraft special tools and repair parts, and most importantly, organizations familiar to Army procedures. As both were aviation units, emergency and crash rescue procedures were already established. In conjunction with the above, support aircraft and equipment was available for lease allowing the icing program to reduce its shipping requirement and consequently total cost.

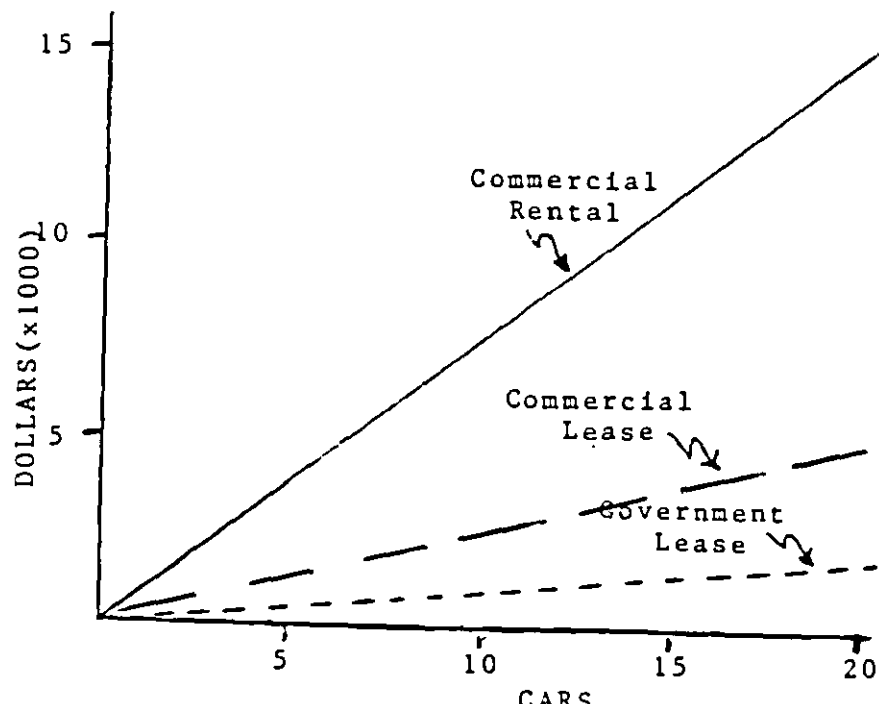


Figure 3--CAR RENTAL COST PER MONTH

For the local unit, the housing of active Army units in their facilities provided additional monies to be made available either through aircraft leasing fees or rental agreements. Additionally, the majority of the locally hired personnel were members of the local units who were unemployed. Hiring these individuals through the local commanders assured a positive relationship, enhanced inter-organizational cooperation and promoted inter-service harmony.

Locally Hired Personnel

Locally hired personnel to augment test teams provide a very viable solution for reducing test expenses, personnel requirements and logistical support. These reductions are countered with only a minimal administrative increase if local employment agencies, especially government agencies, are used.

During the icing program helicopter pilots, aircraft mechanics, fuel handlers and secretaries were hired. Additional talents considered but not hired included firemen, medics, photographers and avionic technicians. Based on a 40-hour week and using only the funds available from the \$50.00 daily per diem rate an average salary of \$8.75 an hour is possible. This figure adequately paid the average salary of those hired. Use of locally hired personnel reduced transportation costs, housing requirements and travel expenses. There was an additional side benefit of leaving key personnel at Edwards AFB to support other tests. Also, the use of locally hired personnel supports the local economy and enhances community acceptance of outsiders.

Fuel Procurement

The past procedure during tests away from Edwards AFB was to purchase fuel from the local airport supplier. This procedure was based on the relatively low cost of fuel, short test duration and limited fuel requirements. On long duration tests where large quantities of present day cost fuel are used, use of government fuel is economical.

During the icing program the test teams were provided government fuel dispensed from a government tanker driven by a locally hired operator. This type service provided rapid turn around of test and support aircraft with cheap fuel at negligible cost in both money and personnel. Use of a locally hired driver, rather than a military driver was more advantageous as it was cheaper, required less logistical support and provided a driver with cold weather driving experience. Savings amounting to 15% of the fuel cost were realized during the icing test.

Medical Facilities

Due to the large number of personnel involved in the icing program, coordination for medical support was made. By making prior arrangement, all team members were guaranteed immediate medical attention. All out-of-state insurance policies were accepted and processed without delay or question. Army personnel were seen at no expense to the individual as direct billing to the government had been prearranged. All doctors were cognizant of the aviation medical requirements; therefore, issued no medication detrimental to flying. No monetary benefit was achieved from this coordination; however, the effect on morale was extensive.

THE ICING PROGRAM

The start of the icing program commences with the assignment of the icing tests to the Project Officers and the designation of the Program Director. This generally takes place in early summer to allow sufficient planning time. Once individuals are identified, planning commences and the initial survey of the test site is made. The initial survey is always conducted to identify possible support facilities and problem areas.

After the initial survey has been completed and the Project Officers have a preliminary test plan, coordination meetings are conducted to identify the following:

1. Test Dates.
2. Test Facility Requirements.
3. Personnel Requirements.
4. Instrumentation Support Requirements.
5. Maintenance Support Requirements.
6. Photographic Requirements.

Armed with the above information, the Project Officer is now prepared to commence planning. His next several weeks are the most important as during this period the plan of operation is developed. It is during this time period that he finalizes his personnel, test facility, vehicle and apartment requirements. These requirements must be identified early in order to allow sufficient time to negotiate contracts.

It is also imperative that the Project Officers concur with the Program Director's findings as the results of their tests are predicated on the support received. Generally, once the requirements have been identified, another survey is conducted after preliminary negotiations for support have been made and is conducted by the Program Director who is accompanied by the Project Officers. Areas coordinated with each project officer include but are not limited to:

1. Hangar and Office Facilities.
2. Logistical Support.
3. Weather Support.
4. Air Traffic Control Support.
5. Fuel.
6. Apartments.
7. Vehicles.
8. Test Areas.

From this survey comes the final Test plans, movement orders and concept of support.

The Logistics Technician is the first individual at the test site and he should be on station at least three weeks prior to the first increment of support personnel. During this time, he will accept the arrival of support equipment, sign for and inspect apartments, supervise setting up of office equipment and coordinate for the installation of communication and other rental equipment. He will also arrange for the arrival of the remainder of the management team who should be on station 4 to 5 days prior to the arrival of the main support group.

Once the first test team is on-station testing commences. Support to the test team is allocated by the Program Director as it is requested. As additional test teams arrive on station the support force is augmented with additional personnel from Edwards AFB. Apartments are allocated according to a prearranged time schedule. When more than two test teams are working, allocation of support resources becomes critical. Priorities are established daily for the following day's testing. Deviations from schedules are coordinated through the Program Director and are varied only on his approval. This constant monitoring assures maximum utilization of all resources. Support aircraft which under the old procedure flew only sparingly in support of one test aircraft now are capable of flying 5-7 hours daily in support of two or more test crews. This procedure optimizes the use of equipment, personnel, facilities and weather. As each test team completes its test it returns to Edwards AFB and takes excess support personnel with it. Its mission is now to complete the final report. The problems of securing the test site are not their concern allowing more time for the primary purpose of flight testing.

At the completion of all testing the test site is closed by the Program Director and the Logistics Technician. They are supported by the support personnel during the packing and shipping; however, the responsibility of terminating all contracts and closing all facilities is theirs. Closing of the test site is accomplished with minimal personnel and delay.

The use of a centralized management team and the other cost saving techniques have an application to non-military flight testing. Flight testing areas where it would be applicable include:

1. Weapons Testing.
2. Hot Weather Testing.
3. Cold Weather Testing.
4. System Testing (icing, electronics, etc.).

Also the co-location of several companies and sharing resources is economical and conceivable. Whether one company or an outside resource provides the management team a benefit for all is there.

CONCLUSION

The combination of several icing test teams at one location with a centralized site support management team has proven very cost effective without degradation to the support provided and the overall test results. Using the techniques established during the icing programs can reduce personnel requirements and lodging and facility needs, and concurrently increase the productivity of all test and support personnel. The centralized management team concept is applicable to the non-military aviation industry.

F-16 Ground and Inflight Icing Testing

By

Major Charles M. Core Jr.

ASD/YPDT

Wright-Patterson AFB Ohio 45433

ABSTRACT

The F-16 aircraft is susceptible to ice accretion and subsequent ice shedding which causes engine first stage fan damage. This engine damage has not indicated a flight safety problem, however, the maintenance and materiel impacts are significant to the USAF. The first stage fan blade damage can requires engine removal, borescope inspection, fan blade replacement, and reinstallation of the engine. The majority of the icing damage incidents have required blending of curled tips or dented fan blades. The blending is accomplished with "Swiss" files and emery cloth for a smooth finish. After blending the damaged blades are marked with a blue dye. The blend limits are described in detail in the engine maintenance technical orders. These limits are not as liberal as previous USAF aircraft engines (J-57/79).

This F-16 ice foreign object damage (FOD) problem was identified during the F-16 climatic laboratory test (May 1978) and the initial inflight icing test (Dec 1978). Initial TAC operational experience (Jan-May 1979) at Hill AFB UT highlighted the operational significance of the problem. At the same time (Feb-May 1979), the first combined operational and adverse weather test was being accomplished in the harsh European winter weather with three F-16s. The above European Test and Evaluation (ET&E) was conducted in Norway, Denmark, Germany, and the United Kingdom and the ice ingestion problem was again identified in Norway and Denmark.

Due to this critical problem, more innovative icing tests had to be planned, managed, and accomplished on an accelerated basis to identify production engine and airframe fixes. Realistic operational ground icing tests were devised and accomplished to identify the principle contributors to the ice ingestion engine FOD problem. The major fixes were designed by the contractor using heat transfer models and test data provided from ground icing testing in the climatic laboratory at Eglin AFB FL. The test data was used to modify the heat transfer model for both ground and flight icing conditions.

The following personnel contributed to F-16 icing test significantly:
Mr. Lorin D. Klein, Mr. Timothy P. Nasal, and Mr. William V. Tracy of
6510TW/TEES Edwards AFB CA. Mr. Richard D. Toliver of 3246 TW/TERW
Eglin AFB FL.

INTRODUCTION

In order to understand the complexity of the F-16 ice ingestion FOD problem, this paper is organized as follows: general and systems description of the F-16, airframe and engine icing specifications, operational experience, chronological history of testing, future icing tests, and summary. A general review of the aircraft and the pertinent systems is necessary prior to discussing the specific icing tests.

F-16 - GENERAL AND SYSTEM DESCRIPTIONS

The F-16 is a single-engine, multi-role, tactical fighter with air-to-air and air-to-ground combat capabilities. The F-16 aircraft is powered by the F100-PW-200 turbofan engine, which is in the 25,000 pound thrust class. An airframe mounted accessory drive gearbox powers aircraft accessories. A jet fuel starter provides self-starting of the engine. The fuselage is characterized by a large bubble canopy, forebody strakes, and an under fuselage engine air inlet. The wing and tail surfaces are thin and feature moderate aft sweep. The wing has leading edge flaps which are deflected automatically to enhance performance over a wide speed range. Flaperons are mounted on the trailing edge of the wing and combine the functions of flaps and ailerons. The horizontal stabilizers have a small amount of negative dihedral and provide pitch and roll control through symmetrical/differential deflection. The vertical tail, augmented by twin ventral fins, provides directional stability. All flight control surfaces are actuated hydraulically by two independent hydraulic systems that are directed by signals through a fly-by-wire flight control system.

The aircraft is equipped with a split speedbrake at the aft end of the fuselage and an arresting hook under the fuselage aft section. The hydraulic brakes are actuated by toe action on the rudder pedals as modified by an anti-skid system. The tricycle landing gear has a steerable nosewheel which is controlled by the rudder pedals. The cockpit is enclosed by an electrically operated clamshell canopy. Internal fuel is contained in the fuselage and wing. Additional fuel can be carried in external tanks. The fuel system incorporates both in-flight and a single point ground refueling capabilities. The radar with search and tracking capability, a radar electro-optical display and a head-up display. A stores management system presents a control panel and visual display to the pilot for inventory, control, and release of all stores. Basic armament includes a left wing root-mounted multibarrel 20mm gun and an air-to-air missile on each wingtip. Additional stores of various types can be carried on seven pylons mounted under the wings and on the fuselage centerline. The overall dimensions of the aircraft are: Span - 32 feet, 10 inches; Length - 49 feet, 6 inches; Height - 16 feet, 5 inches; Tread - 7 feet 9 inches, and Wheelbase - 13 feet, 2 inches.

The gross weight of the aircraft including pilot, full internal fuel, oil, two tip missiles and a full load of 20mm ammo is 23,500 pounds. Maximum gross weight is 35,400 pounds.

The dimensions and specific locations of airframe components is essential to help identify possible contributors to the ice ingestion problem. The initial production configuration of the aircraft and the anti-ice system has changed to solve the ice ingestion problem. Changes will be described in the testing section of this paper. The original aircraft configuration is as follows: 1) The engine inlet lower lip is 39 inches and the upper lip is 56 inches above the ground for the maximum gross weight; 2) The length of the engine air inlet duct is approximately 17 feet from the engine face; 3) The exposed length of the airframe inlet strut is 22 inches, and 4) It is 11.5 inches and 33 inches from the edge of the lower lip and upper lip respectively. This inlet strut is a tension member to prevent permanent deformation in shape of the oval inlet structure during engine compressor stalls. Refer to Atch 1 and 2 for pictorial display. The ice detector, as shown in Atch 3, is located 34 inches in front of the engine face and 8 inches left from center. The engine design is based on the modular concept in which functionally and physically associated parts are removable as units for improved maintainability. The three-stage fan (low pressure compressor) is driven by a shrouded, two-stage low pressure turbine. The 10-stage high pressure compressor is driven by a two-stage, air-cooled high pressure turbine. Variable stator vanes are used in the fan and high-pressure compressor for improved performance and stall margin. The annular combustion is designed for smokeless operation. Continuous ignition in the combustor is provided by dual ignitor circuits. The afterburner is a mixed flow design incorporating seven variable area spray rings grouped into five segments for continuous thrust modulation. Afterburner ignition is momentary and is provided for a single electric-spark ignitor. Power is extracted from the high-pressure rotor for driving all engine and aircraft-mounted accessories.

The engine gearbox, mounted on the bottom of the engine, is driven by a shaft from the high-pressure rotor. The gearbox drives the main fuel pump, the oil pump assembly, the engine alternator, and the power takeoff shaft, which delivers power to the airframe-mounted gearbox. Fuel is supplied by the main fuel pump and an air-turbine driven augmentor fuel pump. Bleed air is extracted from 7th and 13th stages of the compressor. The environmental control system uses bleed air from both 7th and 13th stage ports. The 13th stage air is also supplied to the nacelle ventilation ejectors and the emergency power unit. During engine starting, bleed air from the 7th stage compressor is vented into the fan duct to facilitate starting. Compressor 7th-stage air bleed is used for anti-icing the engine only. The initial production anti-ice system routes heated air from the engine compressor 7th stage to and through the fixed inlet guide vanes and the nose cone

to prevent ice formation. Attachment 4 is a photograph of the engine, the 7th stage anti-icing valve, and the four anti-ice manifold lines. Atch 5 is a drawing of the 7th stage bleed air flow through the anti-icing valve, the manifold line, the fixed inlet guide vane, and the compressor inlet nose cone. The frontal view of the engine face is presented as Atch 6. A cross-sectional view of the fixed and variable inlet guide vanes is presented as Atch 7. The variable inlet guide vanes are more commonly called flaps and are scheduled by the engine electronic control as a function of corrected fan speed (see Atch 8).

The anti-ice system is controlled by a two-position anti-ice switch located on the forward end of the right console. The switch is normally operated in the automatic (AUTO) position, causing the engine anti-icing valve to open when the ice detector in the inlet duct accumulates ice. If ice accumulates on the ice detector, electrical power to the anti-ice valve is lost and the valve is opened by a mechanical spring to allow bleed air through.

The ice detector is a vibrating rod or probe type and as ice forms on the rod the natural frequency of the rod is reduced. This reduced frequency is compared to a reference frequency and when the frequency difference exceeds a predetermined level two timing circuits are energized. One circuit timer controls the duration (cycle time - 4.5 seconds) of the ice detector probe heaters. The other circuit timer controls the time duration (cycle time - 60 seconds) for the 28VDC anti-ice signal that maintains the anti-ice valve open. This timer is designed to reset automatically if another icing signal occurs before the 60 seconds has elapsed.

This completes the systems descriptions of the anti-icing capability for the F-16 aircraft. In this program, military specifications were used to define design criteria and requirements for the F-16 anti-icing capability. Two key military specifications were used as a design criteria for the F-16 airframe and engine anti-icing requirements.

ANTI-ICING SPECIFICATION REQUIREMENTS

MIL-E-38453A Environmental Control, Environmental Protection, and Engine Bleed Air Systems, Aircraft, General Specification For, 2 Dec 1971 was used principally as design criteria for the aircraft environmental control system. However, there are selected portions of this specification related to anti-icing of aircraft. The key airframe components mentioned are transparent areas (canopy), radomes, antennas, ram air inlets, and flight surfaces. The aircraft shall be designed to operate under meteorological conditions defined by Atchs 9 and 10 respectively. This specification statement was not used for the F-16 design criteria due to the lack of requirement for anti-icing of airframe surfaces and canopy.

MIL-E-5007C Engines, Aircraft, Turbojet, and Turbofan, General Specification For, 30 Dec 1965 was used primarily as the engine design criteria for the engine anti-icing system. From a flight safety standpoint, the specification was very adequate and the contractor met the ice ingestion test requirements. The meteorological conditions specified by Attachment 11 conditions are not in agreement with the MIL-E-38453A specification or the worst case icing conditions of MIL-STD-210B, Climatic Extremes for Military Equipment, 15 Dec. 1973. Both Military Specifications (MIL-E-38453A & MIL-E-5007C) should be made consistent and specify the appropriate meteorological conditions. The aircraft should then pass a ground and inflight icing qualification test with no engine damage. MIL-STD-210B conditions represent highest recorded and the 0.5 percent risk level concentration.

Three paragraphs of MIL-E-5007C are worthy of quote and the key points are underlined. 3.2.5.7 Anti-Icing. The Engine shall operate satisfactorily under the meteorological conditions included in Tables VII and VIII with not more than 5% loss in net thrust available and 5% increase in specific fuel consumption at all operating conditions above 50% maximum continuous rated power lever position shall be such that 95% of any thrust desired above 50% maximum continuous rated power lever position can be obtained within the normal acceleration time. The effect on engine performance and engine characteristics when continuously operating the anti-icing system with and without the environment of icing is provided by the electronic automatic machine performance presentation defined in 3.2.1.1.1.8.3. 3.2.5.8 Ingestion Capability. The engine design shall be such that the ingestion of foreign objects such as large particles, birds, sand, ice and hail will not cause uncontrollable fires, engine disintegration, catastrophic failure, flameouts, lengthy power recovery time, or severe sustained power losses, although some damage of engine parts may occur. 3.2.5.8.3 Ice Ingestion. The engine shall be designed to ingest ice with a specific gravity of .8 - .85 as follows with no more than 10% power loss. a) One inch hailstones at the maximum continuous power setting, b) ice slabs of 24 square inches area by one inch thick at intermediate power setting. c) random aircraft inlet ice formations up to 1-1/2 x 2 x 15 inches at intermediate power. This specification was changed to MIL-E-5007D on 15 Oct. 1973 and paragraph 4.6.4.2 specifies ground icing test run procedures, conditions, engine performance requirement, and no engine damage requirement due to this FOD problem, a review of operational experience is necessary.

OPERATIONAL EXPERIENCE

Two operational aircraft in the USAF use the F100 engine today. The F-15 was the first aircraft to use the F100 engine and then the F-16. Operational units of both aircraft have devised interim procedures to reduce the impact of the ice ingestion FOD incidents. The majority of incidents for the F-15 operational units were at Bitburg AB Germany. The majority of the F-16 incidents were at Hill AFB UT. The CY 1979

number of incidents for the F-15 and F-16 are presented in Atch 12. The interim procedures for the F-16 will be discussed only for the 388 TFW at Hill AFB UT.

Hill AFB weather personnel notify the command post of ice FOD alert when weather conditions are temperatures below 45°F and visible moisture present. The command post then notifies flying and maintenance squadrons of the ice FOD alert. The maintenance personnel position an ice dolly underneath the engine inlet to prevent the inlet vortex from forming. The first F-16 starts the engine and idles for four minutes. If no ice forms on the airframe inlet strut or the lower inlet lip, the remaining aircraft start engines and continue the mission. While flying, the Hill AFB pilots have been reducing exposure time to icing conditions by modifying departure and penetration procedures. The number of sorties cancelled due to icing conditions could not be determined, however, the percent of sorties cancelled by weather per calendar month in 1979 is shown in Atch 12.

ICING TEST HISTORY

Pratt & Whitney Aircraft, at West Palm Beach, FL performed the original anti-ice system tests in 1972-73. Two tests performed were as follows: 1) F-100-PW-100 Engineering Test and Evaluation Report and Analytical Evaluation for Anti-Icing, P&WA Report No. FR-6199 dated 12 Dec 1973 and 2) F-100-PW-100 Engineering Test and Evaluation Report for Ice Ingestion Capability, P&WA Report No. FR-5369 dtd 1 Nov 1972.

The above first test key conclusions were that: 1) The anti-icing system will achieve 95 percent of engine thrust and 105% of thrust specific fuel consumption when the anti-icing system is on for all power settings at intermediate or below; 2) The fixed inlet guide vane will satisfactorily anti-ice at all power settings above 50 percent maximum continuous rated power level position (approximately 80 percent N2); and 3) Continuous operation of the anti-icing system will not be detrimental to the engine. This test did not, however, impose icing conditions on the inlet or engine face. The majority of the conclusions were accomplished from an analysis and the instrumented fan inlet case. In retrospect, the lack of anti-icing for the variable inlet vanes, the inadequate heating of the fixed inlet vanes at idle power settings, and the fact that actual icing conditions were not tested has resulted in the USAF identification of the ice ingestion FOD problem at a much later date than desired. Atch 13 is a graphical representation of the 7th stage anti-ice flows and respective temperatures of the fixed inlet vanes.

The P&WA ice ingestion capability test was the first indication of the ice ingestion FOD problem to the USAF. The test results are annotated as Atch 14. This test does adequately assess the flight safety aspects of ice ingestion, however, additional testing was still needed to simulate operational icing conditions.

The first realistic icing test for the F-16 was conducted during the F-16 Climatic Laboratory Test, May 1978. The worst case icing condition

used was 0.5 gm/m³ liquid water content (LWC) which is representative of light-to-moderate icing conditions in the real world. The Atch 15 test run at MIL engine power resulted in damage to four first stage fan blades. The test run time and icing conditions of this test did not adequately simulate the real world in severity; but some key deficiencies of the F-16 icing problem were correctly identified such as: 1) Anti-ice system did not effectively prevent ice accumulations on the engine front frame and nose cone at all power settings; 2) Anti-ice system did not have ON switch; 3) Anti-ice detector did not operate satisfactorily, and 4) Anti-ice system did not have an indicator light similar to other USAF aircraft. The next test scheduled was the inflight icing test.

The F-16 inflight icing test was completed in Dec 1978 at Edwards AFB CA. Artificial icing clouds were provided by a modified NKC-135 icing spray tanker aircraft. The airborne tests were accomplished in a build-up manner for each type of ice and icing severity (ice depth). Ice depth indicators were installed on the left wing, left horizontal tail, vertical tail, left outside of the engine inlet duct, and at the engine inlet strut. The F-16 was flown in the landing and cruise configuration while in the icing cloud. For all ice accretion and shedding test runs, the F-16 aircraft would exit the icing cloud and a T-38 photo/chase aircraft was used to visually evaluate the F-16 icing characteristics. Additionally, photographs and 16mm motion pictures were taken to document the icing results. After each flight, the airframe, engine front face and first stage fan blades were inspected for damage and documentary photographs were taken. The icing test conditions are worthy of specific comment, since, these conditions do not adequately simulate real world inflight icing conditions.

The Air Force Design Handbook and the Weather Forecaster's Guide on Aircraft Icing were used to define the artificial icing cloud liquid water content for specified icing severity levels. For this test, light icing was defined as 0.23 gm/m³, moderate icing as 0.90 gm/m³ and heavy icing as 1.20 gm/m³. Rime ice was visually observed at true outside ambient temperature near -20°C and glime ice at -10°C. Rime ice is a milky, opaque, bubbly looking ice form which appears to be crusty and very brittle. The coefficient of adhesion of ice is not nearly as high as clear ice because of the cold brittle bond between the ice and surface. Glime ice is a mixture of clear and rime ice and can be defined as a rough, bubbly, wet-looking ice. Glime ice may well be the toughest ice because it has both the molecular tenacity of clear ice and the semi-hardness of rime ice.

The artificial icing cloud mean droplet diameters ranged from 2 to 140 microns for all test conditions. Droplet diameters in the natural environment range from 10 to 50 microns with a mean of 20 microns. Theoretically, this difference in droplet diameters means that artificial ice accretion rates were therefore slightly higher than those expected in the natural environment for blunt objects, such as the canopy windscreens with insignificant differences for sharper airfoil shapes. From an F-16 program standpoint, this

inability of the Air Force Flight Test Center to provide a real world icing cloud has caused test credibility problems with both the contractors (General Dynamics and Pratt & Whitney Aircraft). Additionally, the inability to visually monitor engine face icing during the test caused test controversy between the two contractors. When ice ingestion engine damage occurred during the test, it was not concluded what caused the damage.

The test results indicated the ice accretion sequence was as follows: top of the inlet lip (or top inside of the inlet duct), inlet strut, sides of the inlet lip, and bottom of the inlet lip. The inlet strut iced along total length for the cruise configuration and the bottom first for the landing configuration. In most instances, the inlet strut ice shed prior to the F-16 exiting the cloud and was ingested into the engine inlet. Five test flights were completed during the test with no engine damage. Icing conditions completed were light, moderate, and heavy rime ice and light glime ice. On the sixth test flight (moderate glime icing conditions) at least 5/8 inch (thickness) of ice from the inlet strut was ingested prior to exiting the spray icing cloud. After exiting the spray cloud, the test pilot felt a bump that may have been ice ingestion but the engine operated normally. After the flight, an inspection found 19 first stage fan blades were damaged and four of the blades were beyond blendable limits. Engine damage from this test was similar to Atch 6 and testing was terminated due to this damage. Tear down inspection revealed damage to the first seven stages and the tenth and eleventh stages. Besides this engine damage three more deficiencies were identified in the test: 1) During exposure to moderate icing, the pilot reported that visibility was restricted to the extent that an approach could not be safely accomplished; 2) Selecting MAX defog prior or after the icing exposure had no apparent effect on ice accretion rates and would not remove ice from the canopy windscreens; and 3) Accreted ice on the inlet strut was structurally unstable and would normally shed during exposure for any type of ice. Some key F-16 program decisions were made after the termination of the incomplete inflight icing test. These decisions were as follows: 1) The airframe inlet strut would be electrically heated to prevent ice accumulations; 2) The three-position anti-ice switch would be retrofit into production aircraft; 3) The canopy windscreen visibility problems were discarded due to the icing cloud droplet size problem; and 4) The Air Force Flight Test Center was required to improve the artificial icing cloud prior to resuming F-16 inflight icing test.

After the inflight icing test in Dec 1978, the first operational base (Hill AFB UT) was activated in Jan 1979. Also, a key F-16 European operational and adverse weather test was conducted in four European countries (Norway, Denmark, Germany, and United Kingdom) from Feb to May 1979. This initial operation of the F-16 at Hill AFL UT resulted in icing ingestion damage incidents when ambient temperatures were freezing (20 to 45°F) and water or slush was on the ground. The European F-16 test team identified the vortex problem also, however, no engine ice FODs occurred during the test. Simply stated, the F-16 engine creates an inlet vortex at all power settings during

normal ground operations. This visible engine generated vortex (white tornado) picked up and carried small water droplets into the engine inlet. These droplets subsequently froze and ice accreted on the following primary areas: 1) airframe inlet strut, 2) lower inlet lip, 3) engine nose cone, and 4) variable and fixed engine inlet guide vanes. A small scale ground icing test was performed on the Hill AFB UT taxiway number 6 from 28 Mar to 11 Apr 1979.

Twenty-two ground test runs were conducted during this test. This was the first USAF ground environment (vortex) induced icing test conducted in the history of ASD aircraft development programs. The key variables in the visual strength of the white tornado were: 1) depth of pooled water, 2) engine power setting, 3) pavement condition (a rough concrete surface produced lower surface energy and thus increased water content in the vortex), 4) wind direction and speed (worst case was visually observed as quartering tailwind at 10 to 15 kts), and 5) dimensions of the pooled water.

The test results led to the following conclusions: 1) visible vortices (non self-sustaining) were possible and the F-16 could accrete and shed enough ice to FOD engine for normal engine ground run times (15 to 30 minutes); 2) The ice accreted on the previously mentioned primary areas of the F-16; 3) The key variables for the vortex formation were as mentioned previously; and 4) A visual vortex was not created while taxiing at 5 to 20 knots over a damp and flooded taxiway. Recommendations and deficiencies from the test were as follows: 1) The ice on the airframe inlet strut appeared to have the highest potential for engine damage and 2) The engine anti-ice detector is not properly located to sense ground icing conditions. These deficiencies were previously identified, but the operational significance of them was not discovered until this test.

It became apparent to me that I had to plan an operational realistic ground icing test to identify the principle contributors of this F-16 ice ingestion problem and eliminate the controversy between the two contractors. The planning, organizing, modifying of aircraft, and scheduling for this test began in Jun 1979 after the F-16 European test. This test was conducted in two phases, Phase I from 4-11 Sep 1979 and Phase II from 19 Oct to 5 Nov 1979.

Phase I test objectives were as follows: 1) evaluate effectiveness of icephobic materials in preventing ice accretions and subsequent shedding of ice, 2) evaluate effectiveness of lattice grate over pooled water in preventing ice accretions, and 3) identify the principle sources of engine FOD due to ice ingestion. The engine was operated in each icing condition for 30 minutes or until one-half inch of ice accumulated on the airframe inlet strut. The 30 minute time limit was chosen because it was operationally representative of engine run time on the ground prior to takeoff. During these test runs, the engine was shut down mainly for significant ice sheds or above ice limits. The engine was damaged during four (4) test runs due to ice shedding; however, it was impossible to determine the FOD source due to

the lack of real time video instrumentation. The three icephobic materials (Dow Chemical E-3382-100A/B, General Electric G-697, and Star Brite Auto Wax) tested did not, in any icing condition, allow continuous shedding of accumulated ice from the airframe inlet strut or the fixed and variable inlet guide vanes. The ice accumulations were essentially identical and the icephobic materials would not preclude engine FOD or a probable FOD condition. The engine ground operation test over a grate covered puddle prevented ice accumulations for 30 minutes of continuous engine operation at various power settings. The dimensions of the interim recommendation grate were: Length - 4 feet; Width - 4 feet; Minimum Height - 1 1/4 inch; Minimum Weight - 36 pounds, Plain Bearing Bars - 1 1/4 inch x 1/8 inch minimum on 1 3/16 inch centers maximum, and cross bars - 3/4 inch x 1/8 inch minimum on 4 inch max. centers.

This interim recommendation for TAC operational units to locally procure the lattice grate was provided in early Oct 1979. TAC units subsequently decided to locally manufacture an ice dolly (4 ft. x 6 ft. x 3/4 in plywood sheet with casters and 4 ft. x 6 ft. x .093 in. steel plate with casters) for F-16 ground operations in icing conditions. This brief test provided an interim workaround for the F-16 ice ingestion problem; however, Phase II of the test was instrumental in determining the principle contributors to this problem.

Phase II test objectives were as follows: 1) identify the principle sources of engine FOD due to ice ingestion, 2) evaluate the electrically heated airframe inlet strut, 3) evaluate the anti-ice system performance using 13th stage compressor bleed air, 4) evaluate reduced idle thrust engine operation in ground icing conditions, 5) determine the effect of a freezing point depressant (urea) on ice accretion characteristics, and 6) evaluate maintenance FOD screen during engine operation in icing conditions. The real time instrumentation added for this test was as follows: 1) engine inlet mounted video tape camera; 2) external video camera for the airframe inlet strut; and 3) selected key aircraft and laboratory parameters to include pressures, dew points, temperatures, and valve positions. The engine inlet real time video camera was used to monitor ice accumulation rates on the engine face. This was the first time a video camera had been installed in the F-16 engine inlet and it provided a high resolution mirror image of the upper half of the engine face which was the most critical. The Phase I test limitations were used for the majority of the Phase II test runs except for operational scenario test runs. Thirty-eight engine test runs at four power settings were completed in icing conditions defined in MIL-E-38453A and NACA-TN-1855. The icing conditions were the puddle or pooled water at 30°F and supercooled fogs of 0.5, 0.8, and 1.0 g/m³ at 20°F. Two of these test runs were operational scenarios of 15 and 30 minutes. The first test run was in a 0.5 g/m³ supercooled fog at idle power (63.5% N2) for 15 minutes then military power (90% N2) for 1 minute simulating takeoff power setting. Three first stage fan blades were damaged beyond blendable limits and the 30 minutes run was cancelled for safety reasons. This damage was caused by the fixed and variable inlet guide vane ice shedding. The

photograph of Atch 16 highlights the reason for cancelling run. The 30 minute test run was later accomplished in the puddle icing conditions since the ice accumulations were less severe. All first stage fan blades (38) were damaged (9 major, 10 intermediate, and 19 minor), during an operational scenario run over puddle, by ice shedding from principally the variable inlet guide vanes which are not heated. These and other test runs conclusively proved that the engine face was one of the principle contributors to the F-16 ice ingestion FOD problem. Previous icing test results and these test results identified again the airframe inlet strut as a principle contributor to the FOD problem. Atch 17 is a typical ice accumulation on strut which sheds and causes damage. Potential FOD sources (ice accumulations greater than 1/2 inch) were also identified as follows: the lower engine inlet lip for puddle icing condition only and a two-foot by three-foot area on the upper duct wall around the airframe inlet strut for puddle icing condition only. Atchs 18 and 19 are photos of typical formations of ice accumulations on inlet lip and duct wall. The ice accumulations on the fixed and variable inlet guide vanes presented the most potential for serious engine FOD. The inlet lip and duct wall ice accumulations were considered low potential for FOD and would be technically unsolvable at this time. The second test objective was the electrically heated airframe inlet strut. An external electrical power supply (115 VAC, 400 Hz) controlled manually by a variable transformer, provided the strut heating. The leading edge contour of the strut was altered to reduce ice catch efficiency. The test results indicated that the change in strut contour did not significantly reduce ice accretion rate, type of accumulation, shedding characteristics, or engine FOD potential. The strut remained clear of ice in a supercooled fog (LWC of 0.5 g/m³) at engine power settings of RIT, IDLE, 70% N2, and MIL. The LWC of the supercooled fog was increased to 1.0 gm/m³ and an engine power setting of MIL. During this test run, the heater voltage supply was increased to 125 VAC and the strut remained clear of ice. The third objective was the anti-ice system effectiveness using 13th stage compressor bleed air. Test results indicated that the modification design did not satisfy the intended objective of improved engine anti-icing. The bleed air temperatures agreed with the predicted values; however, bleed airflows appeared restricted. The fourth test objective was the RIT power setting evaluation. Test results indicated no operational significant difference in ice accumulations for this two percent lower power setting. The fifth test objective was urea in the puddle water. Although a slight ice characteristic change was observed, no appreciable change in ice accretion rates, and no significant reduction in FOD potential resulted from use of urea up to a 2.0 percent concentration by weight in water. The maintenance FOD screen, sixth objective, did not significantly decrease the strength of the engine inlet vortex. Engine face and inlet wall ice accumulations were reversed in location with use of the FOD screen and the potential FOD source (ice) was still there.

After the completion of the above test, an engine icing action team was formed (Dec 1979) with representatives from the F-100 engine SPO, F-16

SPO, F-15 SPO, Pratt & Whitney Aircraft, General Dynamics Corp., and McDonnell Douglas Corp. The primary task of this team of engineers and testers was to solve the F-100 engine icing problem. I was and still am a key member of this team. Pratt & Whitney Aircraft was tasked through the Component Improvement Program to actively pursue engine design changes to solve the engine face ice accumulation FOD problem. The design goal was to have an ice free engine at 0°F and 0.28 g/m³ LWC. The P&WA initial recommendations were as follows: relaxation of blend limits for fan blades, insulation of the 7th stage bleed air lines, strut/flap film heating (7th stage bleed air), axial flaps, strut/flap film heating (13th stage bleed air), reduced leading edge wall thickness of the struts (cutbacks), electrical anti-ice heating, and internally heated flaps. A parametric study of the various design options was conducted (Mar 1980) using previous icing test data, an analytical model, and the design goal of ice free. From this study various engine configurations were chosen for the next two phases of ground icing tests.

Phase I of the Improved Anti-Ice System Test was conducted at Eglin AFB FL from 14 Apr to 2 May 1980. The test objectives were as follows:
a) evaluate production equivalent airframe inlet strut, b) evaluate alternate anti-ice sensor location in inlet, c) evaluate 7th and 13th stage bleed line insulation, d) evaluate axial flaps at idle power only, e) evaluate 13th stage bleed air at four bleed air mass flows, f) evaluate reduced leading edge wall thickness of the struts (cutbacks), and g) bleed air heated hollow flaps. Test termination criteria was defined by a 1/2 inch thick ice accumulation on the engine face or 15 minutes in the icing condition. This time limit was chosen due to previous test results and stabilization of ice accumulations at that timeframe. The test instrumentation was improved by adding approximately 50 parameters for the anti-ice bleed air lines, the engine inlet case, and engine face (struts and flaps). Also, the same real-time cameras were used for the engine face and the airframe inlet strut. The icing test conditions were as follows: 0°F, LWC of 0.3 g/m³; 20°F, LWC of 0.5 g/m³; 28°F, LWC of 0.6 g/m³; and puddle simulation. Three engine power settings were used IDLE, 70% N₂, and MIL. Tests were conducted using four 13th stage engine core mass flows: 2.1, 1.7, 1.3, and 0.9 percent; and the production 7th stage bleed air flow was also used. Preliminary test results were prepared by the AFFTC in Jun 1980 and are discussed in the same order as objectives.

The leading edge of the production electrically heated inlet strut remained free of ice for all conditions tested. A small amount of glaze ice, formed by freezing runback from the forward portion of the strut, was accumulated during IDLE power runs at 0°F and 20°F and the MIL power runs at 30°F. Refer to Atch 2 for a typical ice accumulation. Both the alternate anti-ice sensor location (just forward of rise in the lower inlet) and the production sensor location did not provide a satisfactory detection signal for the puddle conditions or during some supercooled fog conditions. The recommendation to move the anti-ice sensor probe is still valid. The next in-flight icing test will determine if it works

properly. The existing sensor design would be moved to the test identified ideal location, however, there are significant airframe accessibility problems with this location. Test results of the bleed line insulation (7th and 13th stages bleed air) were very negative and no discernible difference in ice accumulations was noticed for insulated versus uninsulated. Leading edge mass temperatures of the IGV strut increased by 2°F using insulation with 7th stage bleed air and by 1.8°F for the 13th stage max bleed air flow. The IGV flaps were scheduled axial for an engine power setting of IDLE only and tested in the various icing conditions. The axial flaps accumulated (more than 1/2 inch thickness) ice from approximately the midspan point outboard to the outside diameter on the high pressure side and from the midspan point inboard to the inside diameter on the low pressure side. Refer to Atch 20 for a pictorial view of ice accumulations. A non flight worthy modification was used to change the anti-ice system for 13th stage bleed air. Four engine core mass flows were tested at 0°F and 0.3 g/m³ LWC with the following results:

1) 2.1 percent core mass flow - Continuous shedding of the production struts was observed while the cutback struts remained free of ice. The IGV flap ice accumulations exceeded 1/2 inch in thickness. Atch 21 is a good photo of ice at the worst case icing condition, 2) 1.7 percent core mass flow - Continuous shedding of the production struts was observed and some struts accumulated ice in excess of 1/2 inch. Cutback struts accumulated ice 1.2 inch long by 0.1 inch in thickness starting at the inside diameter, 3) 1.3 percent core mass flow - No shedding of production struts was observed and ice accumulations exceeded 1/2 inch in thickness. Cutback struts accumulated ice along the entire leading edge and shed from the outside diameter to the midspan point. The test cutback struts remained free of ice for all flows and the production struts shed portions of ice accumulations at the 0.9 percent mass flow. The test results at 28°F yielded no strut ice accumulations. It was obvious that leading edge strut temperatures were higher (54°F for max flow and 20°F for min flow) when using 13th stage bleed air. The cutbacks (2) remained free of ice at 20°F and 28°F. At 0°F, the cutback struts remained free of ice at 2.1 percent core mass flow and the other flows had accumulations as mentioned earlier. The last test objective was the hollow flaps (2). Tests conducted at 0°F and 20°F resulted in a clear area extending from the leading edge outside diameter, diagonally across the face of the flap, to the trailing edge inside diameter. This clear area corresponded to the direction of the internal bleed air flow through the hollow flap. Immediately behind the clear area a freezing runback ice (very hard) accumulated over 1/2 inch thick. The hollow flaps remained free of ice at 28°F and 0.6 g/m³ LWC fog condition and the puddle condition. The most effective combination of modifications on this test was the 13th stage bleed air (max flow), cutback struts, and hollow flaps. Atch 22 is a hollow flap with baffles for future testing, which will improve the internal bleed air flow.

FUTURE ICING TESTS

Phase II of the Improved Anti-Ice System Test is scheduled from 14 Jul to 15 Aug 1980 at Eglin AFB FL. Refer to Atchs 22 and 23 for a description of engine modifications to be tested. Two new engine design concepts

will be tested. The first is film heating of the flap and the other is internal baffles inside the hollow flap which guides the flow of bleed air in the flap. This test will be very similar to the Phase I test with one main exception. The liquid water content of the icing conditions will be increased incrementally up to 1.0 g/m³ at 0°F and 2.0 g/m³ at 20°F. The test goal is to satisfy the MIL-E-5007D icing condition limits.

Another ground icing test is scheduled in Jan 1981 to test the production version of the anti-ice system fixes. My experience and best guess for the production version is to use 13th stage bleed air (2.1 percent of engine core mass flow) with the cutback struts and the double baffle hollow flaps (leading edge first pass). The development of a new flight worthy 13th stage anti-ice valve is an extremely long process (18-24 months).

The next inflight icing test is tentatively scheduled for Oct 1981 after Pratt & Whitney Aircraft completes the required ground and safety of flight testing of the new 13th stage anti-ice valve. If the above production substantiation test proves successful, the inflight icing conditions envelope could be expanded to meet the MIL-E-5007D specification envelope.

SUMMARY

The all-weather capability of USAF aircraft should be drastically improved with effective anti-icing systems that prevent damage to the engine. The lessons learned for icing testing of this system were formally passed to USAF organizations in May 1980 by myself. These lessons learned effectively summarize the F-16 icing tests in the following areas: test scheduling, anti-ice specifications, test instrumentation, and test results.

The ground and inflight icing test was too late in the F-16 development program to affect early design of aircraft airframe or engine anti-icing systems. The retrofit costs, if anti-icing system is deficient, are always more expensive. Two military specifications (MIL-E-5007D and MIL-E-38453A) should be expanded to include requirements for ground and inflight icing tests, ground vortex icing test, and the same meteorological (icing) conditions. The military standard (MIL-STD-210B) should be expanded to include 1.0 percent and 10 percent risk levels for icing conditions. The tables (pages 34 & 35) should be converted to median droplet diameters for consistencies with the above specifications. This data would provide a substantial improvement over existing (highest recorded concentrations of icing) design criteria for ground and flight operations in icing conditions. Test instrumentation is absolutely essential for ground and inflight icing tests. Real time camera coverage (ground and inflight) of the engine face and inlet lip region will help define ice accretion rates, thickness of ice that causes engine damage, specific locations of ice, and ice shedding characteristics. Pressure and airflow measurements of the bleed air will help determine anti-icing

system effectiveness. Temperature measurements of the engine strut leading edge surfaces were above 45°F for the idle power setting test runs thus prevented FOD potential ice accumulation. The appropriate design goals for engine leading edge surfaces should be at least running wet surfaces at idle power settings. The F-16 ground icing test results identified the principle contributors to the ice ingestion FOD problem and the probable fixes that will reduce the problem. Further ground and inflight icing tests are required to substantiate the production modifications to the engine and aircraft.

REFERENCES

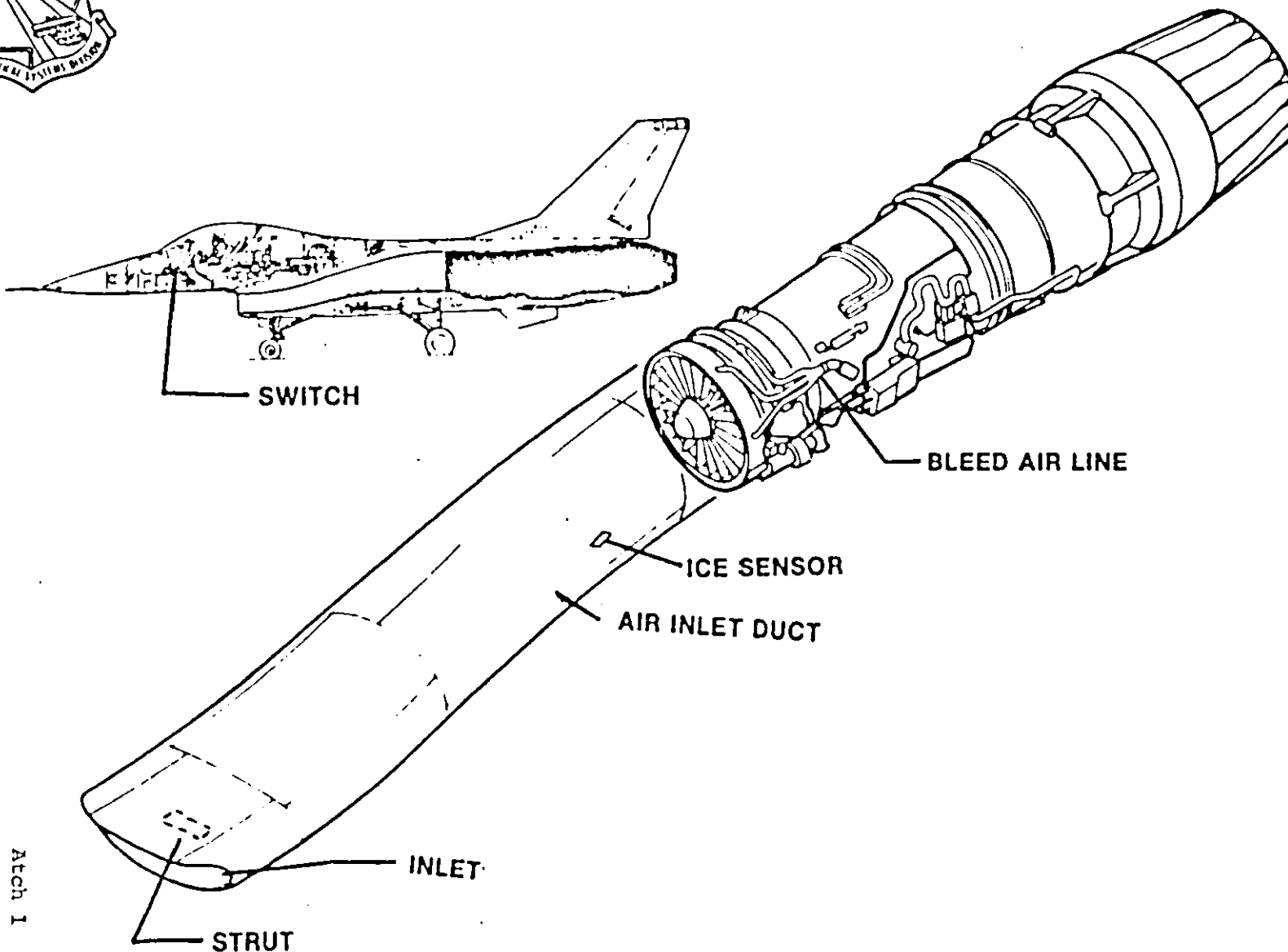
1. F-100-PW-100 Engineering Test and Evaluation Report for Ice Ingestion Capability, FR-5369, Pratt & Whitney Aircraft, West Palm Beach FL, 1 Nov 1972.
2. F-100-PW-100 Engineering Test and Evaluation Report and Analytical Evaluation for Anti-Icing, FR-6199, Pratt & Whitney Aircraft, West Palm Beach FL, 12 Dec 1973.
3. F-16 Climatic Laboratory Test, TER AW-1, 21 Jun 1979, Timothy P. Nasal, Steven D. Peterson.
4. F-16 Pre-European Deployment Artificial Inflight Icing Test, TER I/R-2, Air Force Flight Test Center, Edwards AFB CA, 6 Jul 1979, William V. Tracy, Jr.
5. F-16 Ground Environment Induced Icing, TER I/R-3, Air Force Flight Test Center, at Hill AFB UT, 26 Oct 1979, William V. Tracy, Jr.
6. F-16 Icophobic Materials Test and Evaluation, TER I/R-4, Air Force Flight Test Center, at Eglin AFB FL, 15 Oct 1979, Lorin D. Klein.
7. F-16 Climatic Laboratory Ground Icing Evaluation, TER I/R-6 Air Force Flight Test Center, at Eglin AFB FL, 21 Mar 1980, Timothy F. Nasal, and Lorin D. Klein.
8. F-16 Climatic Laboratory Improved Engine Anti-Ice System Tests Phase I, Preliminary Letter Report, Air Force Flight Test Center, at Eglin AFB FL, 12 Jun 1980, Lorin D. Klein and Timothy P. Nasal.
9. MIL-E-38453A Environmental Control, Environmental Protection, and Engine Bleed Air Systems, Aircraft, General Specification for, 2 Dec 1971.
10. NACA-TN-1855 Recommended Values of Meteorological Factors to be Considered in the Design of Aircraft Ice -Prevention Equipment, Mar 1949, Alum R. Jones and William Lewis.
11. MIL-E-5007 C and D, Engines, Aircraft, Turbojet and Turbofan, General Specification For, 30 Dec 1965 and 15 Oct 1973 respectively.
12. T.O. 1F-16A-1, Flight Manual F-16A/B USAF/EPAF Series Aircraft, 13 Apr 1979.
13. F-16 Adverse Weather and European Test and Evaluation Report, TER AW-5, Feb 1980, Timothy P. Nasal.

APPENDIX

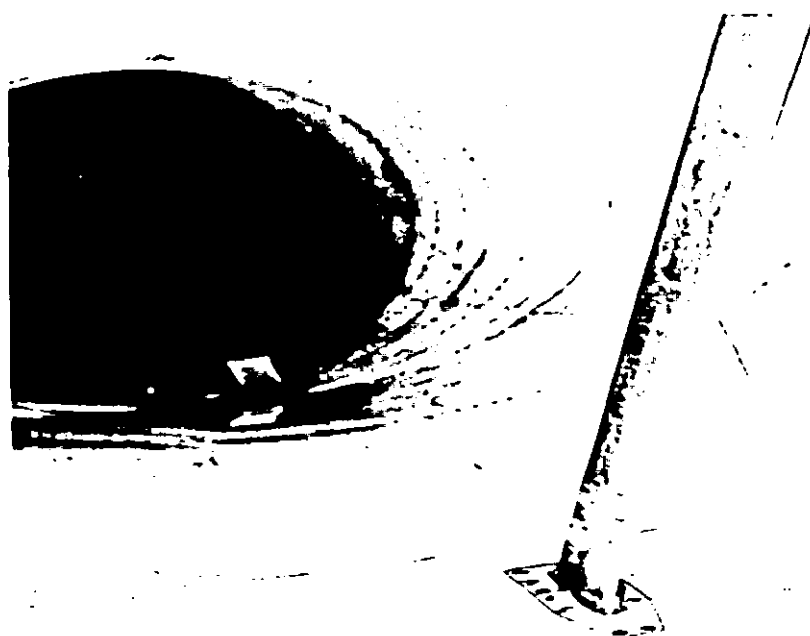
- Atch 1 - F-16 anti-ice system components
- Atch 2 - F-16 electrically heated inlet strut
- Atch 3 - Photograph of anti-ice detectors (production and alternate) with engine removed and upper inlet camera
- Atch 4 - Photograph of anti-ice system bleed air lines and engine
- Atch 5 - Drawing of bleed air routing through engine inlet case
- Atch 6 - Frontal view of the engine face after operational scenario test run. Damaged first stage fan blades are visible.
- Atch 7 - Cross sectional drawing of production and cutback strut and the flap positions
- Atch 8 - Flap scheduling versus engine power setting
- Atch 9 - Continuous maximum MIL-E-38453A meteorological conditions
- Atch 10 - Intermittent maximum MIL-E-38453A meteorological conditions
- Atch 11 - MIL-E-5007 C/D Anti-icing conditions
- Atch 12 - F-15/F-16 operational experience (ice FODs)
- Atch 13 - Anti-ice flows and strut temperatures
- Atch 14 - Ice ingestion test results
- Atch 15 - Photograph after three minute MIL power test run
- Atch 16 - Engine face ice accumulation after 30 minute test run in supercooled fog ($21.5^{\circ}\text{F}/0.5 \text{ g/m}^3$)
- Atch 17 - Three minute ice accumulation on the inlet strut
- Atch 18 - Inlet lip ice accumulation
- Atch 19 - Upper duct wall ice accumulation
- Atch 20 - Axial flap ice accumulations
- Atch 21 - Engine face ice accumulation after 15 minute test run in supercooled fog ($0^{\circ}\text{F}/0.3 \text{ g/m}^3$). Bleed air flow through #6 strut was restricted due to instrumentation wires
- Atch 22 - Baffled hollow flap drawing
- Atch 23 - Fan inlet case configuration for Jul-Aug 1980 icing test



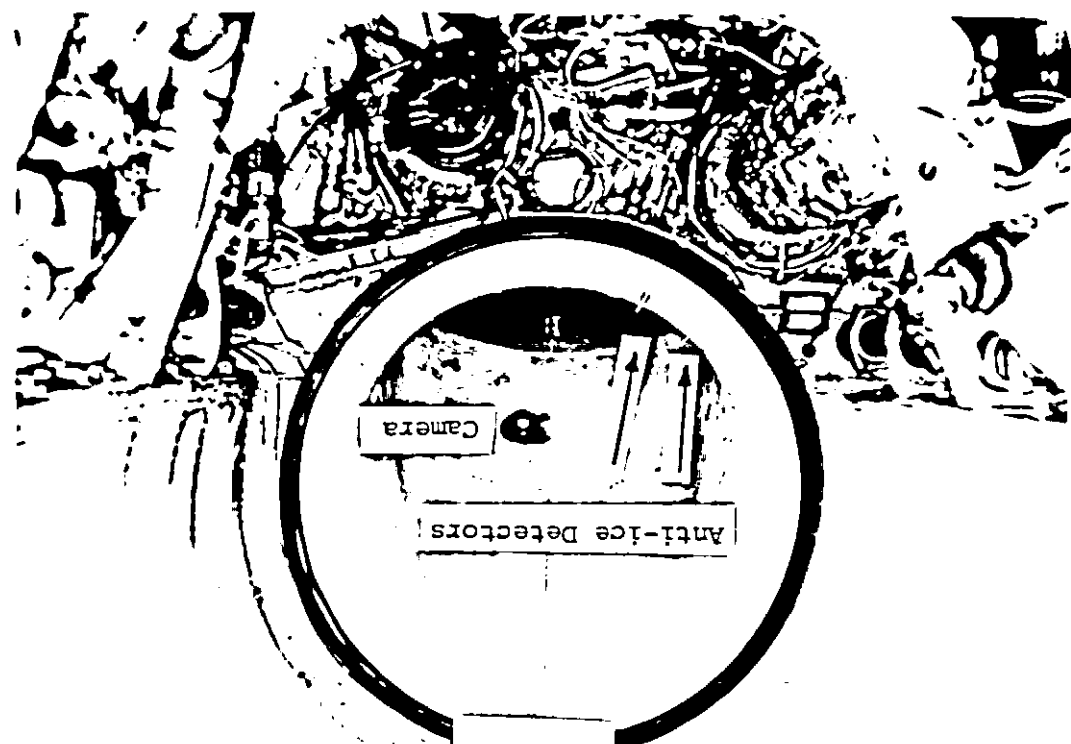
F-16 ANTI-ICE



3 - 19

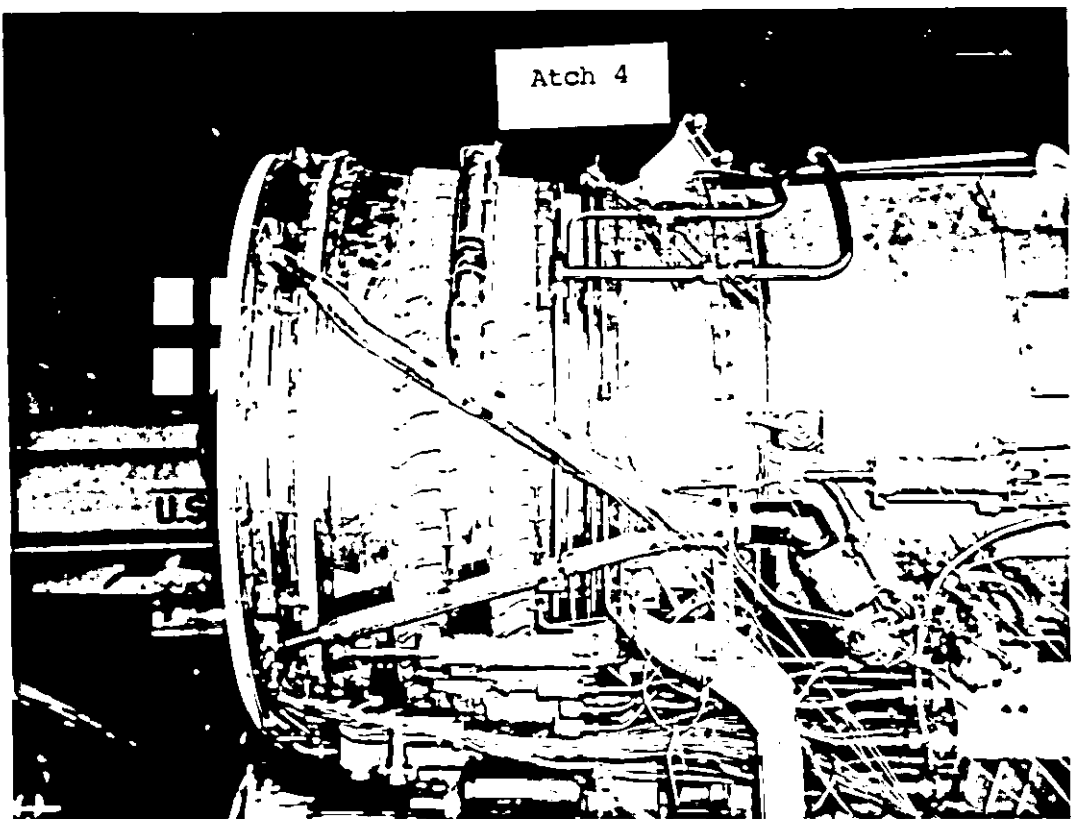


Atch 2

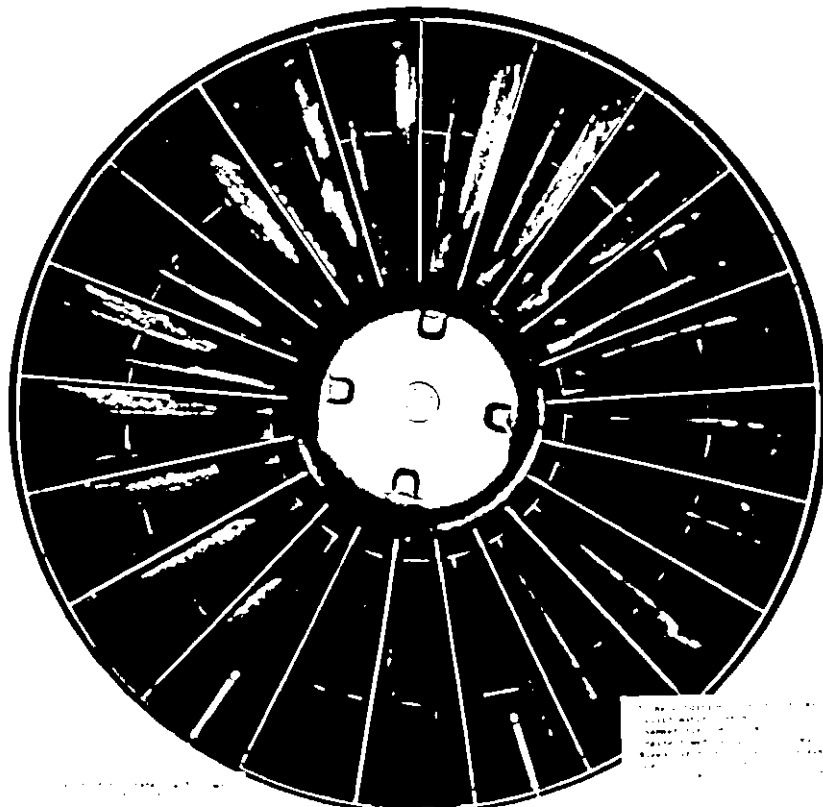


Atch 3

Atch 4

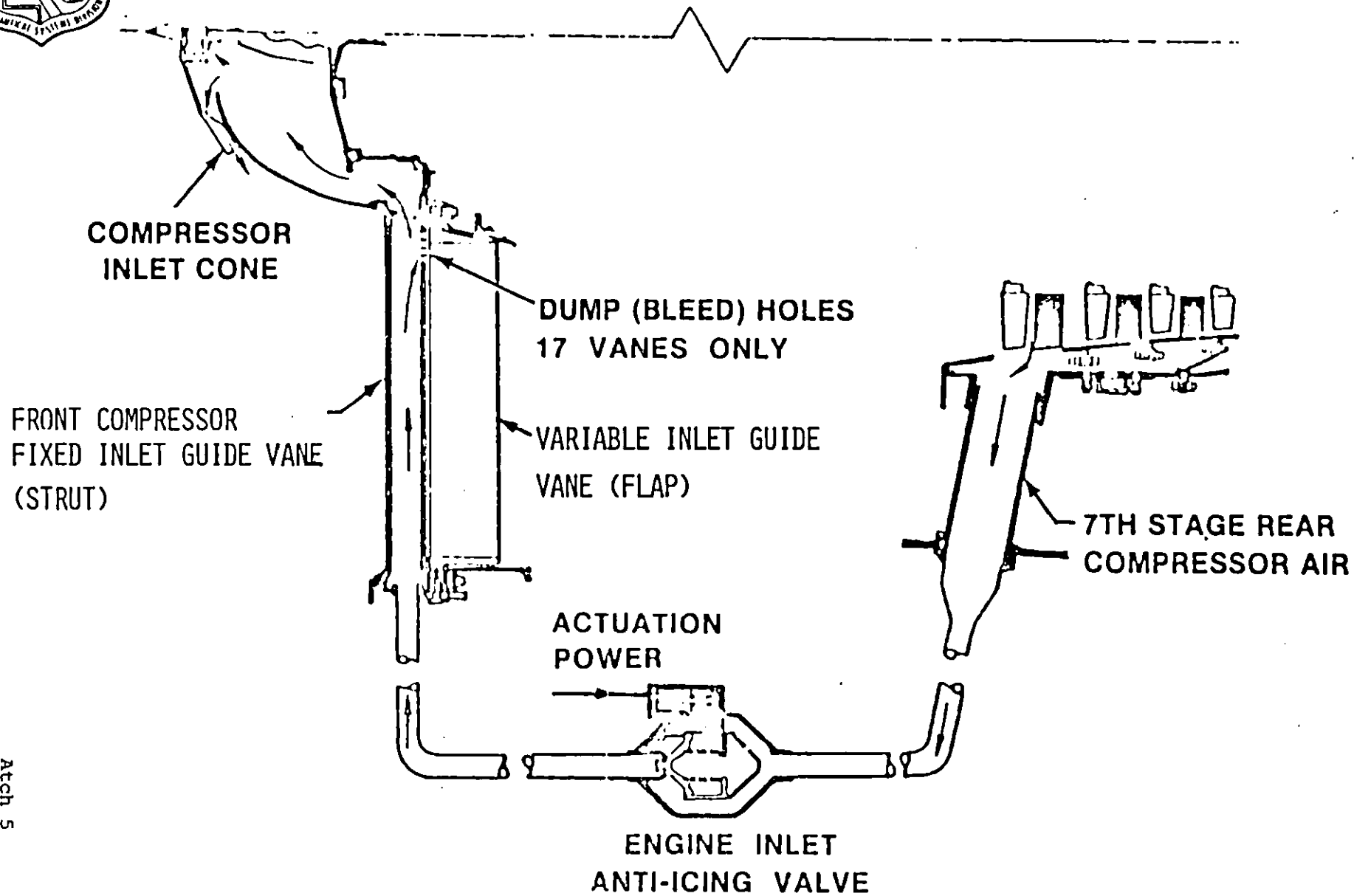


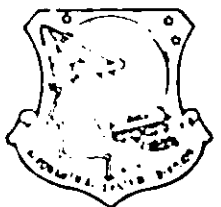
Atch 6



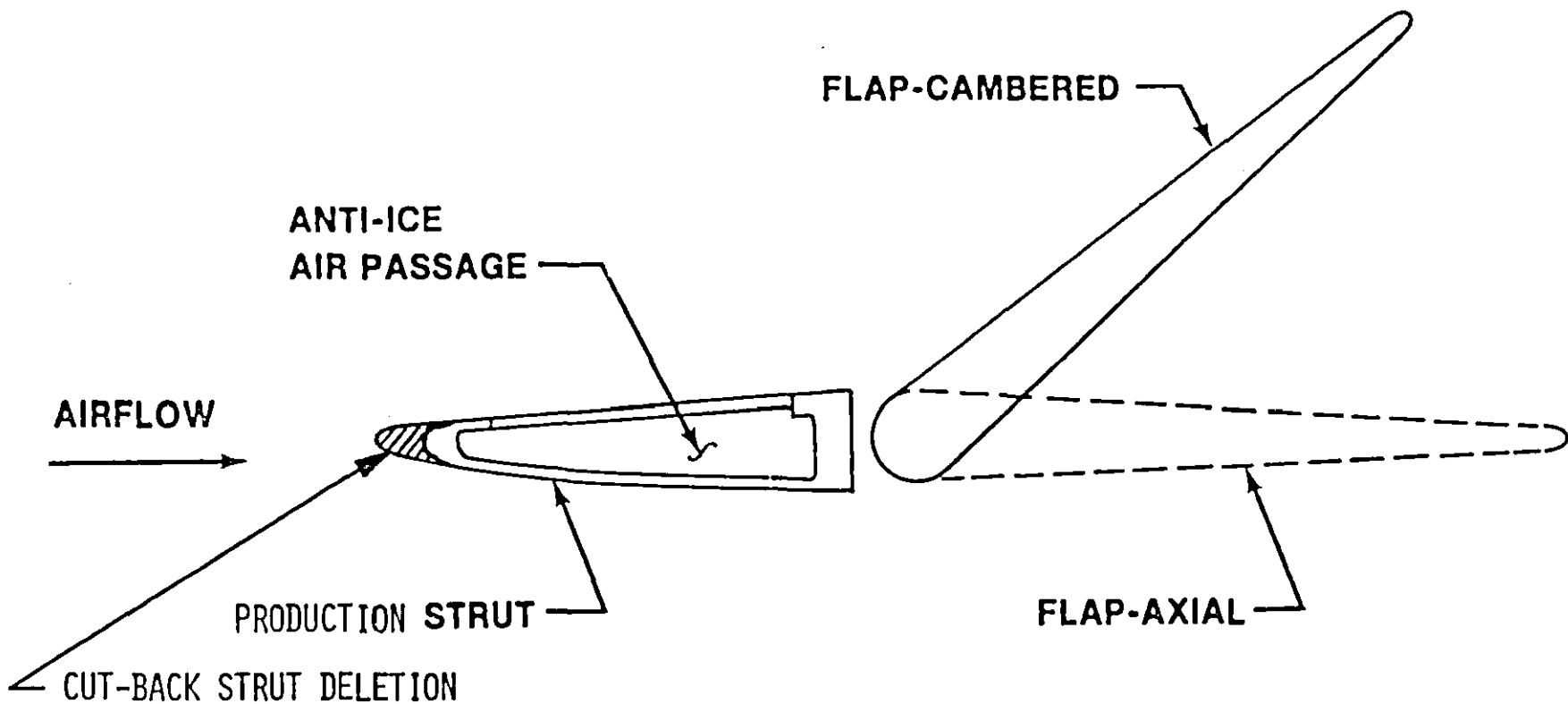


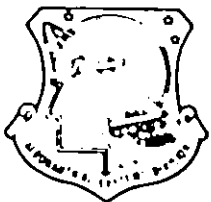
F100 ANTI-ICE SYSTEM





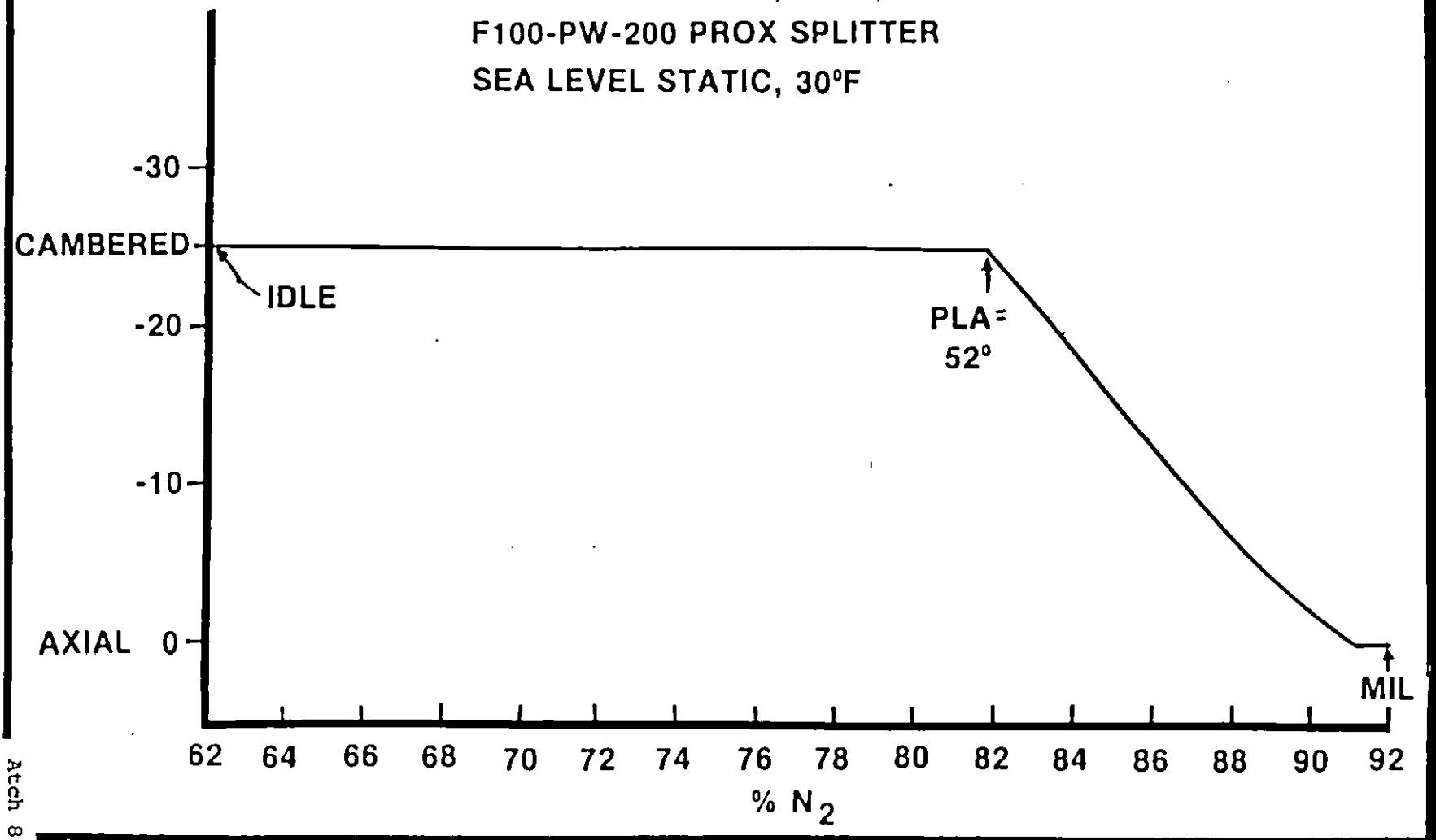
INLET GUIDE VANE CROSS-SECTION



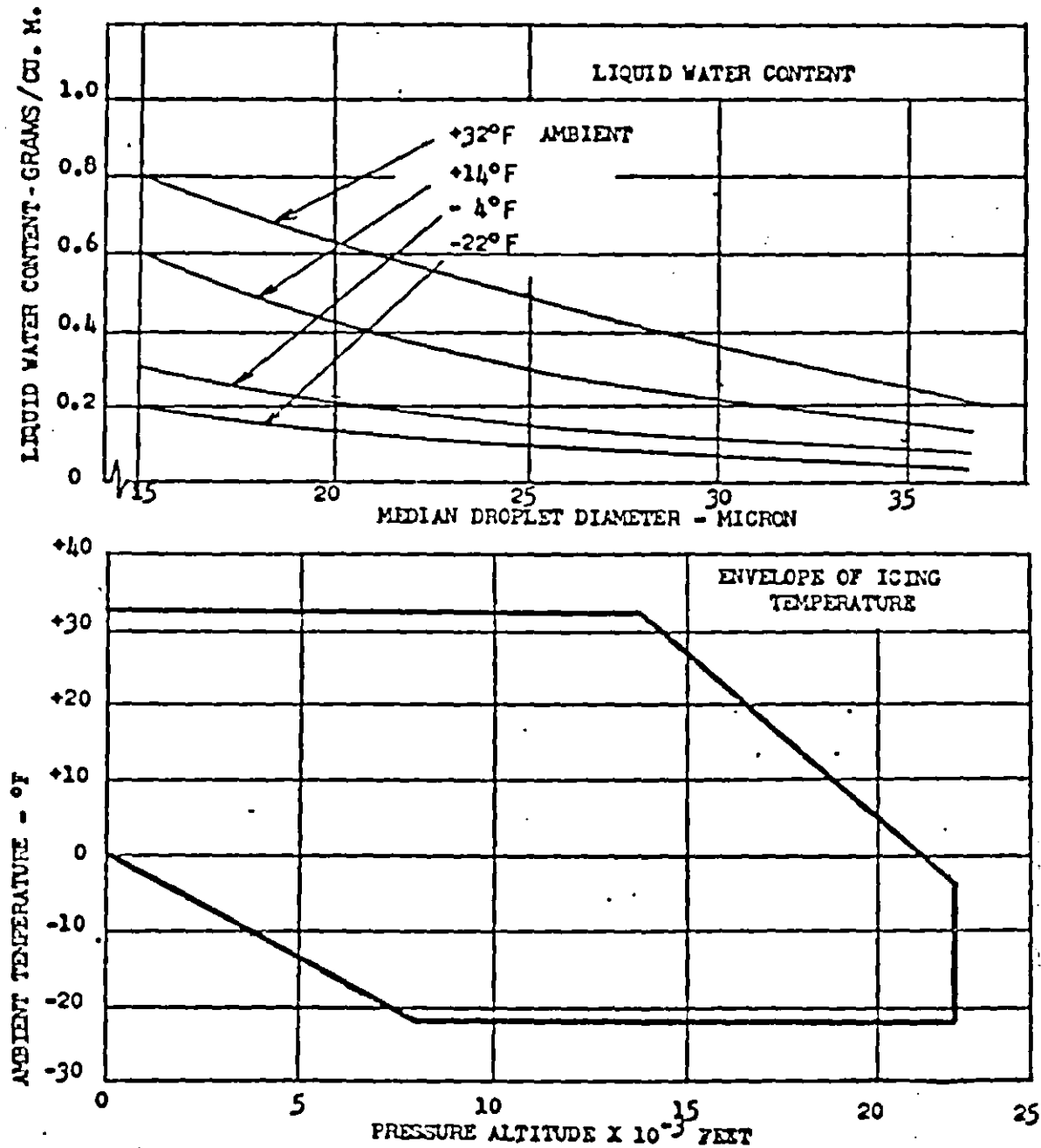


FLAP VS N_2

F16 INSTALLATION, ANTI-ICE ON
F100-PW-200 PROX SPLITTER
SEA LEVEL STATIC, 30°F



- (1) ALTITUDE; SEA LEVEL TO 22,000 FEET
- (2) MAXIMUM VERTICAL EXTENT; 6,500 FEET
- (3) HORIZONTAL EXTENT; 20 STATUTE MILES



Continuous Maximum Icing Conditions

Atch 9

(1) ALTITUDE; 4,000 TO 22,000 FEET
 (2) HORIZONTAL EXTENT; 3 STATUTE MILES

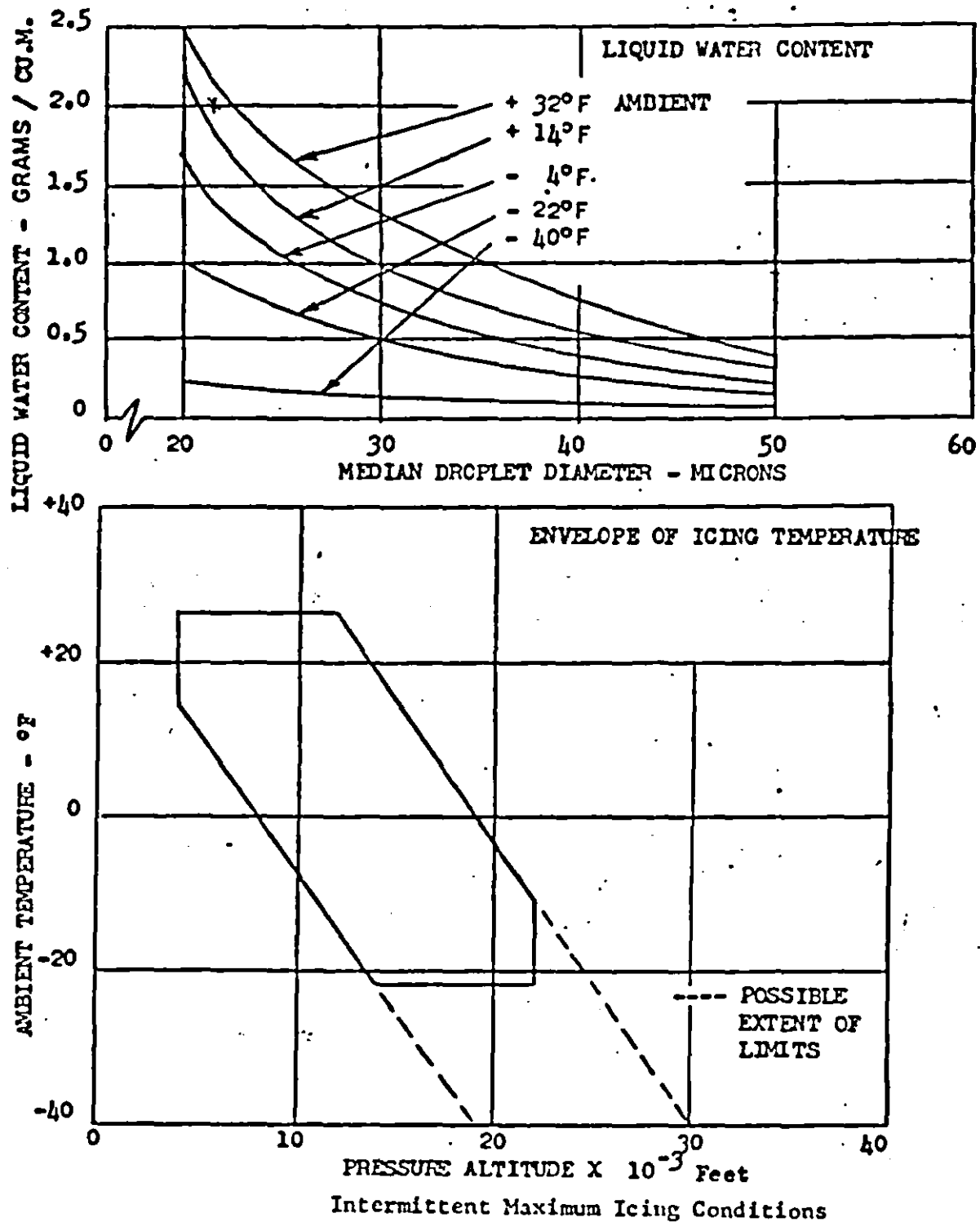


Table VII. Sea Level Anti-Icing Conditions (Ref. 3.2.5.7)

Attribute	Condition I	Condition II
Liquid Water Content	1 gram per cubic meter	2 grams per cubic meter
Atmospheric Air Temperature	-4°F (-20°C)	+23°F (-5.0°C)
Flight Velocity	Static	Static
Altitude	Sea Level	Sea Level
Mean Effective Drop Diameter	15 microns	25 microns

Table VIII. Altitude Anti-Icing Conditions (Ref. 3.2.5.7)

Attribute	Condition I	Condition II
Liquid Water Content	0.5 gram per cubic meter	0.5 gram per cubic meter
Inlet Air Temperature	-4°F (-20°C)	-4°F (-20°C)
Flight Velocity (Mach No.)	0.32	0.71
Altitude	20,000 ft	20,000 ft
Mean Effective Drop Diameter	15 microns	15 microns

Atch 11

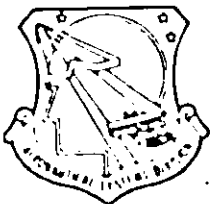
F-15/F-16 OPERATIONAL EXPERIENCE (CY1979)

<u>F-15 BASE</u>	<u>ENGINES DAMAGED</u>	<u>OPERATION</u>	<u>ENGINE REMOVAL</u>	<u>BLADES BLENDABLE</u>	<u>BLADES REPLACED</u>
BITBURG	40	TAXI OR FLT	NONE	NONE	6 OR LESS PER ENGINE
CAMP NEW AMSTERDAM	1	TAXI OR FLT	1	1	6
EGLIN	0	N/A	N/A	N/A	N/A
HOLLOMAN	3	TAXI OR FLT	NONE	NONE	AS REQ'D
LANGLEY	0	N/A	N/A	N/A	N/A
LUKE	1	TAXI OR FLT	NONE	NONE	AS REQ'D
NELLIS	2	MAINTENANCE	NONE	NONE	AS REQ'D
	<u>47</u>		<u>1</u>	<u>1</u>	

<u>F-16 HILL AFB</u>	<u>ICE FOD EVENTS</u>	<u>ENGINE REMOVAL</u>	<u>BLADES DAMAGED</u>	<u>BLADES BLENDABLE</u>	<u>BLADES REPLACED</u>
GROUND	12	4	73	64	9
FLIGHT	<u>2</u>	<u>1</u> 5	<u>3</u> 76	<u>3</u> 67	<u>0</u> 9

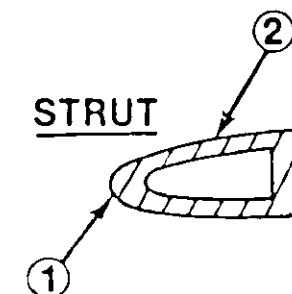
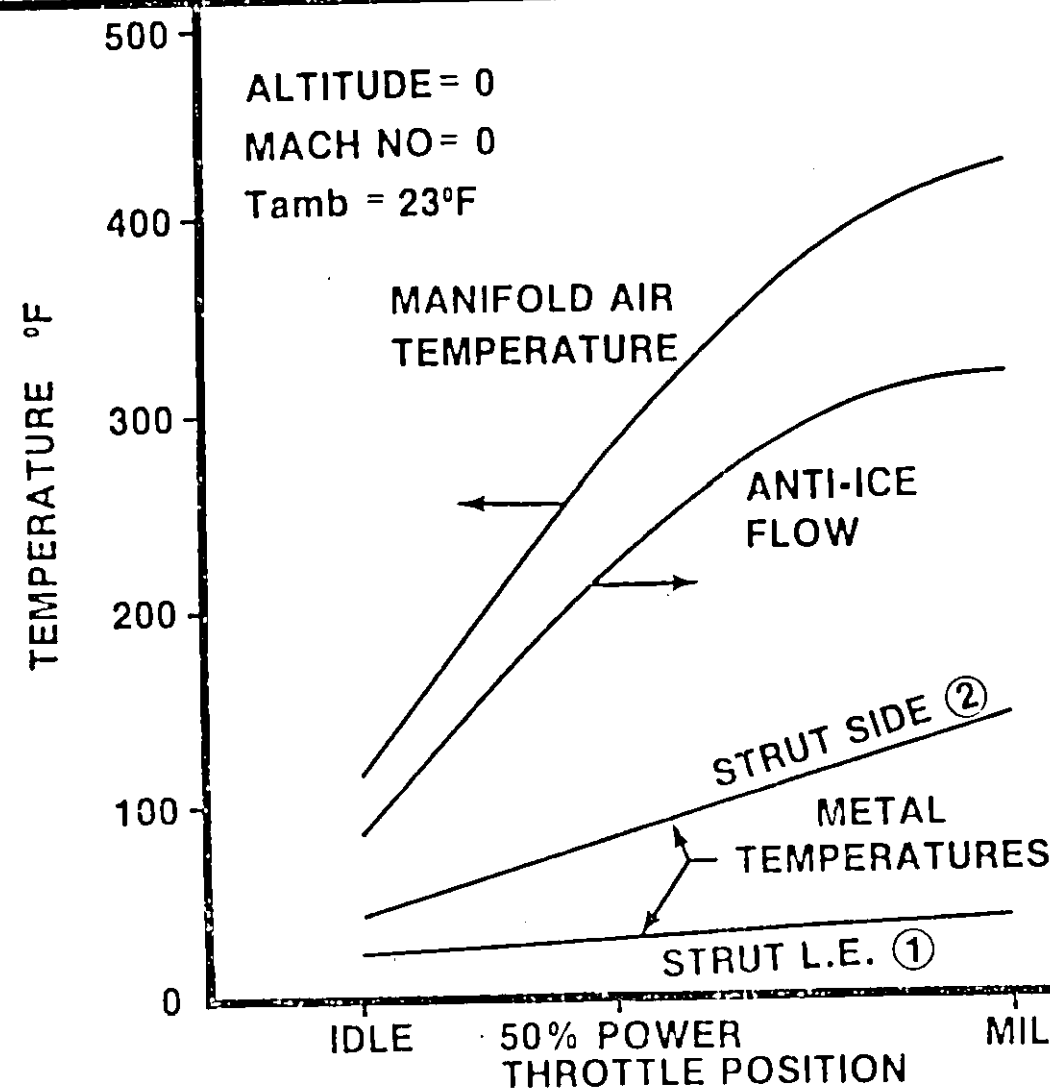
PERCENT WEATHER CANCELS BY CALENDAR MONTH (CY 1979)

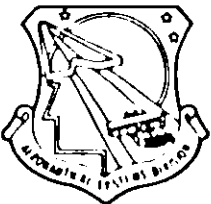
	<u>JAN</u>	<u>FEB</u>	<u>MAR</u>	<u>APR</u>	<u>MAY</u>	<u>JUN</u>	<u>JUL</u>	<u>AUG</u>	<u>SEP</u>	<u>OCT</u>	<u>NOV</u>	<u>DEC</u>
HILL AFB	25%	24%	13%	4%	6%	0	0	0.4%	0.6%	2.3%	8.6%	2.0%



F100 ENGINE

ANTI-ICE FLOWS AND TEMPERATURES





DESIGN VERIFICATION – ICE INGESTION

INGESTED

OPERATING CONDITIONS

RESULTS

2 - 1" DIAMETER BALLS

MILITARY

2 CURLED 1st BLADES
NO THRUST LOSS

1 - 1 1/2 X 2 X 15" ROD

MILITARY

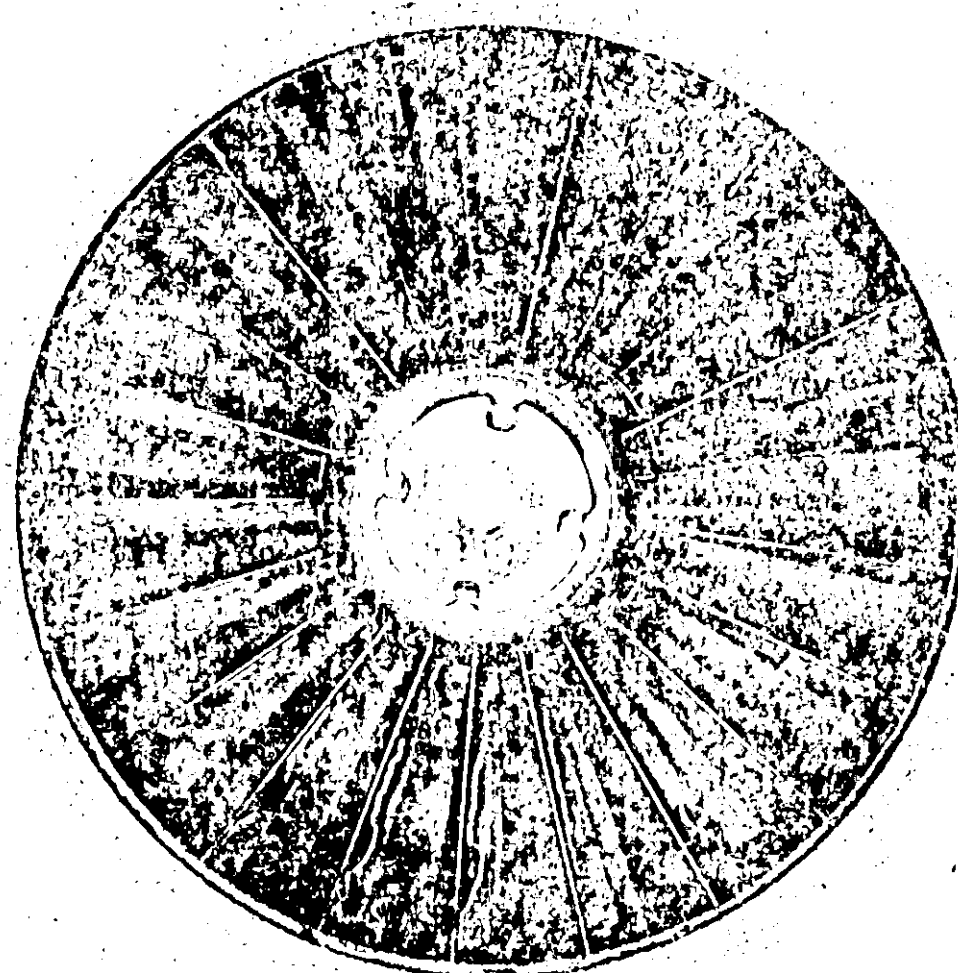
16 BENT 1st BLADE TIPS
THRUST LOSS 5%

1 - 1" X 4" X 6" SLAB

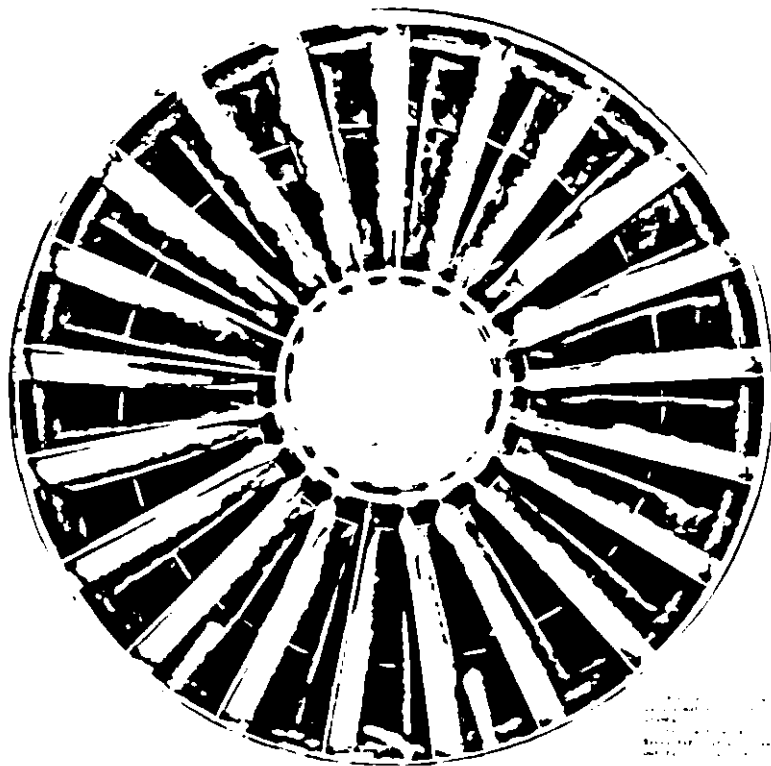
MILITARY

28 BENT 1st STAGE BLADES
1 TORN BLADE TIP
THRUST LOSS <10%

Typical Engine Inlet Guide Vane and Nose Cone Ice Accumulations Test No. 26 Mil Power
Liquid Water Content $0.3 \text{ g}/\text{m}^3$ Anti-Ice AUTO



Atch 16



Atch 17



3 - 31

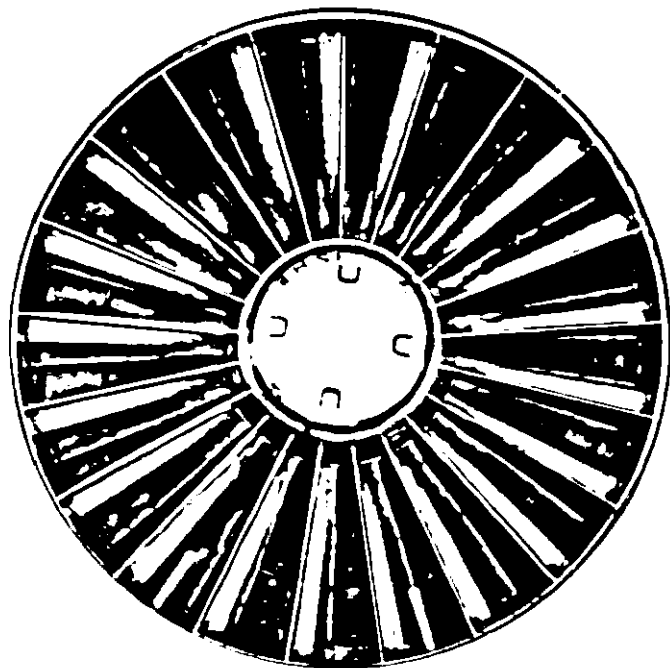


Atch 18

Atch 19



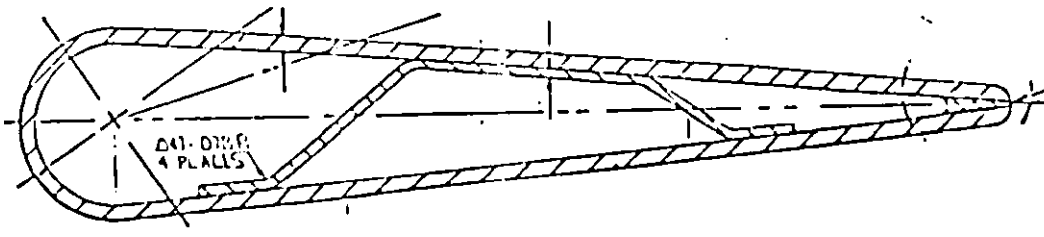
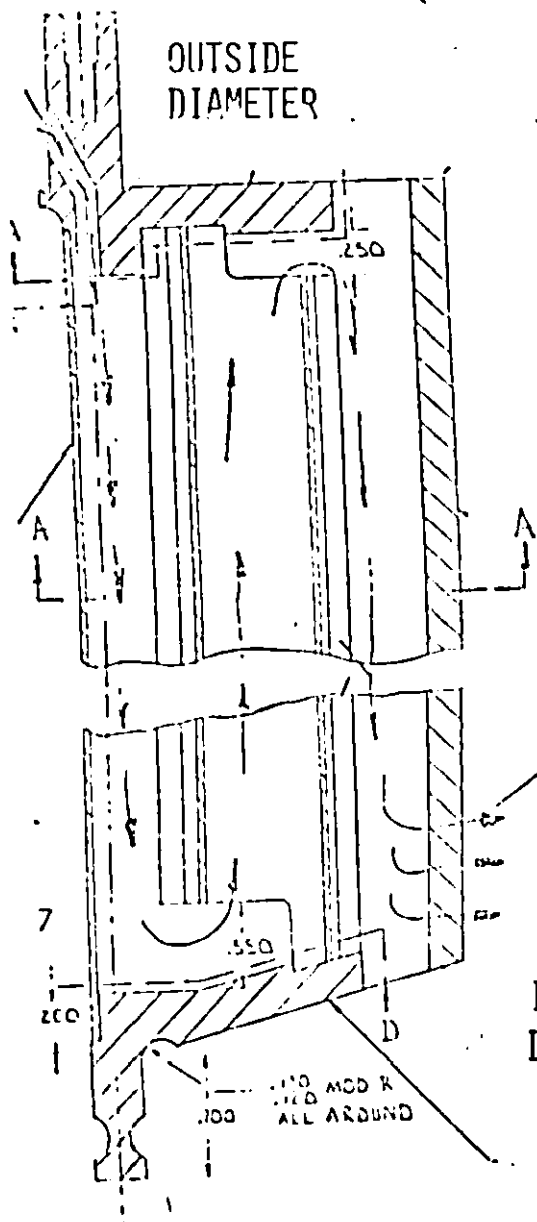
Atch 21



Atch 20

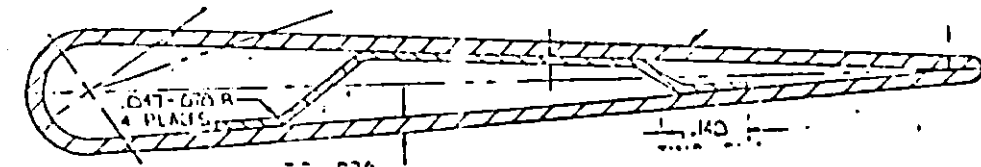


F100 ENGINE HOLLOW FLAP

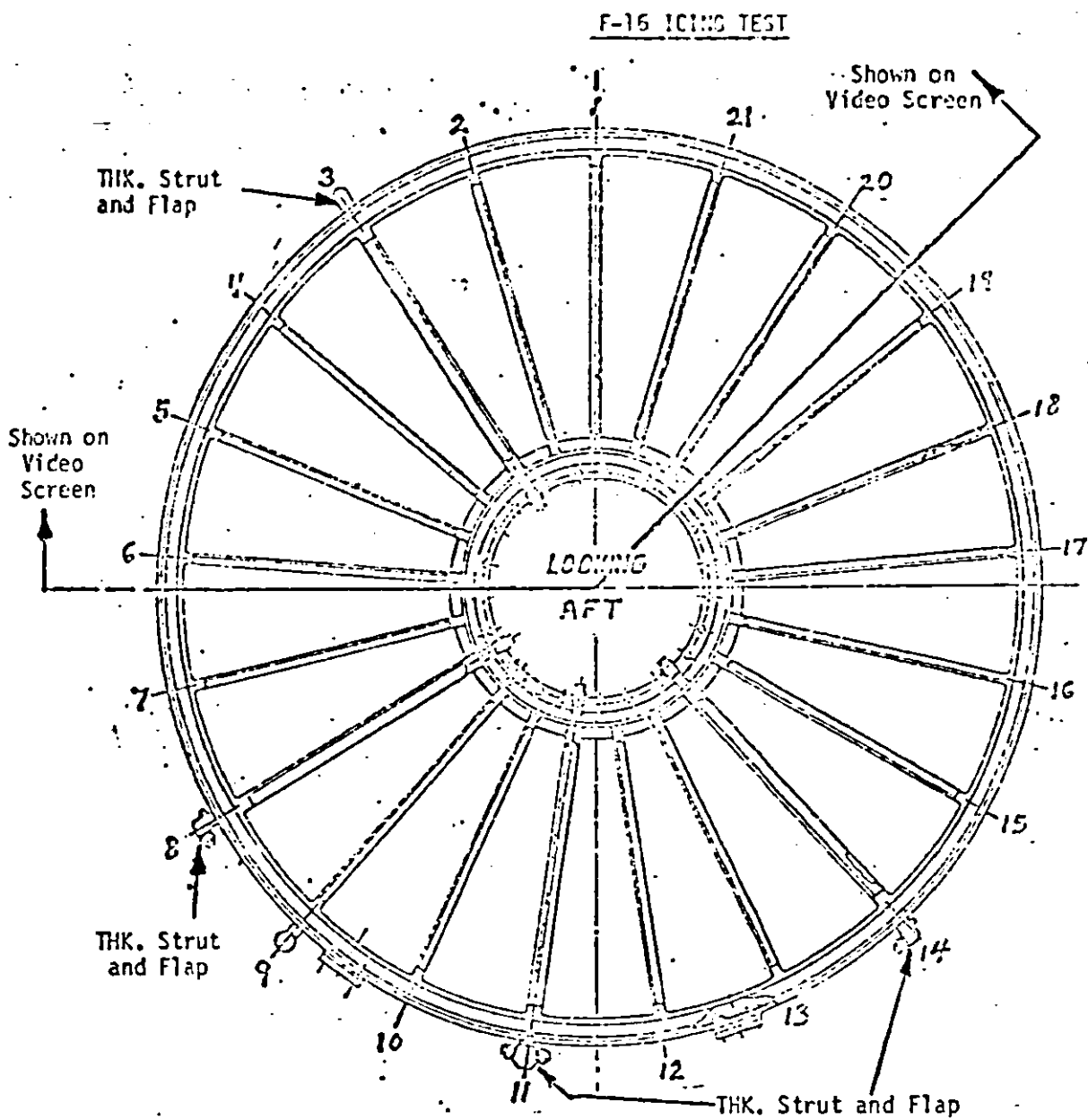


SECTION A-A
THICK FLAP

TOTAL (9) HOLES
.168" DIA.



SECTION A-A
THIN FLAP



F100(3) FAIRING CASE CONFIGURATION

<u>POSITION</u>	<u>STRUT MODIFICATION</u>	<u>FLAP MODIFICATION</u>
20	Cut-Back L.E. Strut	Film Heating (30, 1/8 in. dia.hole)
21	B/I	B/I
1	Cut-Back L.E. Strut	Double Baffle (L.E., 1st Pass)
2	Cut-Back L.E. Strut	Double Baffle (T.E., 1st Pass)
3	Cut-Back L.E. Strut (THK.)	Hollow Flap (YF100)
4	Cut-Back L.E. Strut	Film Heating (EG, 1/16 in. dia.hole)
5	B/I	Hollow Flap (YF100)
6	Cut-Back L.E. Strut	Hollow Flap (YF100)
7 through 19	Cut-Back L.E. Strut	Hollow Flaps (YF100)*

*Several of these flaps will be B/I to balance flow used for film heating.

HELICOPTER ICING SPRAY SYSTEM

Daumants Belte
US Army Aviation Engineering Flight Activity
Edwards Air Force Base, California

Abstract

The US Army has used a CH-47C as an airborne spray tanker since 1973 for helicopter qualification testing in icing conditions. The initial icing cloud it produced was found to consist of much larger diameter drops than natural clouds, and problems existed in uniformity and control of its liquid water content. A program was undertaken in 1979 to modify the system to generate a spray plume more closely resembling a natural cloud. This effort included ground and icing wind tunnel evaluation of spray atomizers, a flight survey of turbulence behind the spray aircraft, and in-flight evaluation of atomizer spray characteristics. Modifications were incorporated, and the new system was used for icing tests in 1980. Evaluation of the new spray cloud characteristics shows a vastly improved drop size distribution and a more homogeneous liquid water content, closely resembling that of a natural cloud.

Introduction

The US Army has long recognized a need to equip its helicopter fleet with an adverse weather operational capability, to include flight into natural icing conditions. Development of new aircraft and ice protection systems creates a requirement to qualify them for operation in the icing environment. Conducting tests in a simulated instead of natural icing environment offers several advantages such as the ability to control icing condition variables and continuous availability. Safety of a flight test program is enhanced by the ability to easily enter and exit the icing environment, and to accomplish a controlled buildup in icing severity.

In early 1971, the Aviation Research and Development Command (AVRADCOM) conducted a study to define a specific program for flight qualification of Army helicopters in icing conditions. At this time, only three facilities were available to conduct controlled artificial icing tests of an entire helicopter, none of which the study considered entirely adequate. The Climatic Laboratory at Eglin Air Force Base permits tied-down operations only; a 9 x 60 ft spray rack is used to simulate a natural icing cloud. The Canadian National Research Council Icing Spray Facility in Ottawa permits hovering in and out of ground effect in winds from 5 to 30 KTS and uses a 15 x 75 ft ground based assembly to generate an icing cloud. A C-130 fixed wing aircraft operated by the Air Force as a spray tanker can conduct in-flight helicopter icing tests at airspeeds above 100 KTS. It uses a palletized water tank and 4-ft diameter spray ring assembly to create a useable cloud at a standoff distance of 500 to 600 ft. A KC-135 is also available for testing above 135 KTS.

The study noted the inherent limitations of each of these facilities, and recommended development of a new airborne spray system capable of producing a controlled in-flight icing environment compatible with Army helicopter sizes and speeds. This led to the development in 1972 and 1973 of an Army Helicopter Icing Spray System (HISS).

Helicopter Icing Spray System

The HISS was developed under contract by the All American Engineering Company (AAE) and consists of an internally mounted 1800-gallon water tank in a CH-47C helicopter, and an external spray boom assembly suspended beneath the aircraft from a cross-tube through the cargo compartment. A schematic is shown in figure 1. Hydraulic actuators rotate the cross-tube to raise and lower the boom assembly. Both the external boom assembly and water supply can be jettisoned in an emergency. Because of gross weight and center of gravity limitations, the aft fuel cells of the helicopter are left empty and only 1500 gallons of water are carried. A calibrated outside air temperature probe and a dew

point hygrometer provide accurate temperature and humidity measurement. An aft-facing radar altimeter is mounted at the rear of the HISS to allow positioning the test aircraft at a known standoff distance. Commonly used standoff distances range from 150 to 250 ft. The spray cloud is generated by pumping water at known flow rates from the tank to the nozzles mounted on the boom assembly, using aircraft engine compressor bleed air to atomize the water. For icing tests, a chemical with coloration properties similar to sea marker dye is added to the water and imparts a yellow color to the ice. This improves in-flight photo documentation and provides a means to distinguish between natural and HISS-generated ice. While the design airspeed range for icing tests is from 60 to 150 KTS, use of a 90 knots true airspeed (KTAS) has predominated in the past, as a practical compromise between HISS capability and test aircraft performance.

The HISS has existed in two configurations since it was first assembled in 1973. The original version had a single spray bar suspended 15 ft beneath the aircraft, with a tip-to-tip boom width of 75 ft. This version of the HISS conducted seven artificial icing test programs between September 1973 and March 1975. Several shortcomings of this early configuration became apparent.

1. Shallow cloud depth from the single spray bar precluded icing the fuselage and main rotor simultaneously.
2. Presence of light to moderate turbulence within the cloud interfered with assessment of icing induced changes in flight characteristics.
3. Downwash behind the CH-47C placed the test aircraft in a flow field equivalent to a 500 to 1000 ft/min rate of climb with a corresponding power required increase over level flight.
4. The arrangement and spacing of nozzles on the spray boom prevented proper overlap and mixing of the spray cloud, producing non-uniformity in liquid water content.

Modification to the spray boom in 1975 replaced the single bar with a 60 ft wide dual trapeze assembly. The assembly was lowered 4 ft below the original to reduce turbulence and downwash at the test aircraft. A second center section was added 5 ft beneath the first to increase cloud depth. The outriggers were swept back and angled downward to counteract the roll up tendency at the edges of the spray cloud. Nozzle locations were rearranged to increase cloud uniformity. This configuration completed six icing programs between October 1976 and April 1979.

These changes alleviated but did not entirely eliminate the original shortcomings. An additional problem that appeared was formation of ice near various nozzles on the spray boom during operation. These ice accumulations, or "popsicles" would block nozzles and affect cloud consistency by disturbing airflow around the boom. Periodic shedding of this ice presented a potential hazard to the test aircraft.

Natural Icing Environment

Existing literature addresses many aspects of aircraft icing in a natural environment, from identification of atmospheric conditions conducive to ice formation and description of the range over which they vary, to correlation of these variables with expected icing severity and the types of ice formations produced. Three atmospheric parameters are generally associated with aircraft icing: temperature, liquid water content (LWC), and drop size distribution. The type of icing considered here occurs from flight through clouds or precipitation composed of supercooled water drops.

The mechanism of ice accretion on an aircraft surface presents a complex picture of heat transfer, momentum exchange, diffusion, and phase change at the boundary layer. Different types of ice formation are characteristic for different combinations of temperature, LWC, and drop size.

Rime ice: requires temperatures colder than -12°C, characterized by low LWC and small drop size. It forms when drops freeze immediately on impact, and has a milky white, smooth appearance with a streamlined shape.

Glaze or clear ice: occurs at temperatures between -8°C and 0°C, characterized by high LWC and larger drop size. It forms when impinging drops flow along the surface in liquid form before freezing, and is transparent. Glaze ice deposits are aerodynamically much less favorable than rime ice, since they frequently assume a mushroom shape with double horn protrusions from the stagnation point.

Glime ice: a mixture of the above two types, common at intermediate combinations of temperatures, LWC, and drop size.

Measurements of natural clouds made by various investigators show a strong correlation of drop size distribution with cloud type. Figure 2 shows characteristic drop diameter spectra for stratus, cumulus, and stratocumulus clouds (ref 1). Stratus clouds display a narrow distribution between 7 and 9 μm , and a maximum diameter of less than 50 μm . Particle density decreases exponentially with increasing diameter. Cumulus clouds show an even distribution across the 5 to 20 μm range, with maximum diameters around 80 to 100 μm . Stratocumulus clouds are characterized by the exponential distribution found in stratus and the size range found in cumulus.

Values of LWC show less correlation with cloud type, and can change radically within an individual cloud. This occurs partly because the density of a cloud varies greatly and partly because the water content of a drop depends on the third power of the drop radius. A slight shift in the drop spectrum to larger particle sizes can cause a pronounced increase in the associated LWC. Values of LWC commonly vary from .1 to .9 gm/m³, but severe intermittent conditions can include values as high as 2 and 3 gm/m³.

Pre-Improvement Simulated Icing Environment

LWC and drop distribution are of primary interest in relation to spray tanker development, as they specify the desired cloud composition. Comparison between properties of natural clouds and the HISS generated spray plume indicates how successful a simulation has been attained. Prior to this year's activity, four efforts were made to measure and quantify the HISS spray cloud characteristics in flight, with varying degrees of success. In general, these measurement programs attempted to relate LWC, drop size distribution, and number densities to water flow rate, airspeed, distance behind the spray booms, and vertical and horizontal dimensions of the spray cloud.

Measurements in the early configuration were made using a hot-wire anemometer array mounted on a UH-1M (ref 2), and with a gelatin coated glass slide droplet collector on a Piper Aztec (ref 3). Following the dual-boom modification, the spray plume was surveyed with a Piper Aztec carrying a cloud particle spectrometer (ref 4). As part of the 1979 icing program, a UH-1H used an axially scattering probe and two cloud particle spectrometers to gather data both in the HISS spray cloud and in natural icing conditions (ref 5).

These programs found large variation in LWC, and drop distributions characterized by much larger diameters than those of natural clouds. Cloud characteristics showed little measurable dependence on flow rate, distance behind the spray boom, vertical position in the cloud, or airspeed. This was a disappointing lack of quantitative change in the plume structure with changes in control variables.

A convenient parameter used to characterize drop distributions where LWC is important are the median and mean volume diameters. Median volumetric diameter (MVD) evenly divides the mass, or volume, of the spray into halves such that half of the total mass of water is contained in drops larger and half in drops smaller than this diameter. Mean volumetric diameter is the droplet size whose volume, if multiplied by the number of drops, will equal the total volume of water in the sample. Mean and median drop diameters of

natural clouds are usually very close to each other. In general, natural clouds can be characterized as having a drop distribution MVD in the 10 to 30 μm range, with a 20 μm MVD as a rough average condition. Representative volumetric diameters in the HISS spray plume were a 50 μm mean and a 140 μm median. The occurrence of large drops caused difficulty with sampling statistics and introduced scatter, as presence of a single large drop in a given sample radically increases its LWC. The median diameter is important as an indicator of the LWC contained in the large drops. While 90% of the drops were smaller than 50 μm diameter, they only contained 10% of the liquid water, and drops with diameters greater than 100 μm contained about 70% of the liquid water. Drop concentrations in natural clouds commonly range from 20 to 100 particles per cubic centimeter; densities measured in the spray plume varied from .5 to 4 drops per cubic cm.

In 1979, three particle sizing probes furnished by Meteorology Research, Inc. (MRI) were carried on a UH-1H in Minnesota to make measurements of simulated and natural icing clouds. The same probes were used again in this year's tests and in the icing wind tunnel. All of the probes count and size droplets into 15 size classes, each probe having a separate size interval range. The axially scattering probe measures over a 3 to 45 μm range, and operates on a light scattering principle. Both of the other probes were of the optical array type, which measure drop size by the number of elements shadowed. Physically similar but equipped with different optics, the cloud particle spectrometer sizes particles in the 35 to 300 μm range, and the precipitation particle spectrometer in the 140 to 2100 μm range. Drop concentration estimates of the various size intervals measured are used to calculate particle concentration, LWC, drop size distribution, and mean and median diameters. The axially scattering probe was mounted on the left side of the aircraft and either of the other two on the right side.

As anticipated from the earlier HISS cloud measurements, considerable scatter was encountered, and the presence of very large drops interfered with sampling statistics. Drop MVDs near the top of the cloud ranged from 50 to 100 μm , and at the bottom from 200 to 300 μm , shown in figure 3. Liquid water content was extremely nonuniform, and little correlation existed with the programmed flow rates, as shown in figure 4. A comparison of the HISS spray plume with a natural cloud measured by the same aircraft and sensors is shown in figure 5. The drop concentration of the simulated cloud is too low, slope of the distribution fall-off with drop size is very shallow, and most of the LWC is contained in drops entirely too large. Difficulty of obtaining repeatable and consistent LWC measurements suggested the presence of a significant number of large drops that do not always get measured.

Improvement Program

Collection efficiency, or the amount of water impinging onto a surface, is affected by size of the aircraft component involved and the drop diameter. Smaller drops follow airflow streamlines more closely than large ones. The HISS drop distribution was of sufficiently large size to impinge on most of the airfoil and aircraft structure, resulting in concentrated ice accumulations spread over a greater surface area than in natural icing. One viewpoint considers that while the HISS spray plume was not a valid simulation of a natural cloud, it nevertheless represented a more severe icing environment than the natural one. In this capacity, it served as a useful tool to verify the ability of ice protection system to cope with extreme conditions, but its failure to duplicate the types of ice formation and effect on aircraft resulting from the smaller drops of natural clouds reduced its validity as a simulation. For example, in 1979 tests of the CH-47C Fiberglass Rotor Blade aircraft, ice accretion in the vicinity of the aft rotor droop stops would prevent them from engaging during shutdown (ref 6). This problem occurred only after flights in natural ice, and not in the icing environment produced by the HISS. In this instance, the HISS was not credible as a valid simulation, and a need for improvement was apparent.

The obvious deficiencies of the drop size distribution indicated the spray atomizers were a logical starting point for improvement. The spray boom is fitted with a total of 172

receptacles on the boom surface, and is assembled of concentric metal tubing as shown in figure 6. The inner pipe of 1-1/2" diameter acts as the water supply and leads to 30 manifolds spaced approximately 3 ft apart along the boom exterior. The 4" diameter outer pipe contains bleed air from the aircraft engines. The nozzle receptacles are spaced at 1 ft intervals along the top and bottom of the boom and are staggered to provide alternating upward and downward ejection ports every 6 inches. The original AAE nozzles were held in the receptacles by snap rings, and used air pressure to atomize water into drops. Bleed air from the boom entered at the base of the nozzle and water was supplied to the side from the manifolds through external plastic pipes. Although 172 nozzle receptacles existed, only 51 nozzles were installed and used. To define a baseline during the 1979 icing tests, operating pressures of air and water at the boom were measured over the full range of water flow rates, shown in figure 7.

From this point, two approaches were used to identify and incorporate improvements to the HISS before the 1980 season. A contract was let with Boeing Vertol through AVRADCOM and the FAA to conduct a wind tunnel investigation in the NASA-Lewis Icing Research Tunnel (IRT). Concurrently, an in-house AEFA effort would also investigate ways to achieve an improvement to the simulated spray cloud with the contracted services of Mr. Earle Binckley of SON Enterprises. This effort included ground and airborne testing of alternate nozzles, engine bleed airflow measurement, and a qualitative in-flight wake survey behind the HISS.

Single-Nozzle Ground Tests

The objective of the ground nozzle investigation was to qualitatively assess existing AAE nozzle performance and to compare and screen alternate nozzles for suitability as replacements. Flow rate directly affects cloud LWC, since mass conservation provides a linear relation between flow rate, airspeed, LWC, and cloud crosssectional area. The LWC requirement determines the desired flow rate range for a single nozzle.

A simple test set-up was constructed as in figure 8 with a control panel to regulate air and water pressure normally available in the hangar. Flexible metal hoses connected the panel to the individual nozzle, and a test matrix of air and water pressures was developed. Repeatable water flow rate data for each nozzle were obtained by collecting and weighing water spray over a timed interval.

A 20-ft long collection pool on the ground in front of the nozzle was divided into 5-ft bins to hold water and reveal drop impacts. An effective indication of relative drop sizes could be obtained by observing the spray and its drop trajectories. Distance from the nozzle that drops contacted the surface of the pool and the size of impact quickly revealed large drops and their relative frequency.

Tests with AAE nozzles confirmed the presence of unacceptably large drops, and no combination of reasonable air or water pressures would produce small drops. An internal resonance, detectable by a loud whistling noise, could be induced for certain air and water pressure settings while increasing pressure. The same resonance could not be duplicated at the same conditions while decreasing pressure. This peculiar resonance lowered water flow rate and improved atomization when compared to identical conditions without resonance. Another characteristic was a steady dripping of water from the nozzle orifice while spraying. This tendency would explain the origin of ice accumulation on the booms during icing flights. The spray characteristics of the AAE nozzle in these tests was unsatisfactory from all aspects.

In selecting and testing alternate nozzles, some general characteristics and considerations became apparent. The variety of available nozzles is diverse, having been designed for a multitude of applications and operating fluids. Adding energy to a flow of water achieves small drop size by creating additional surface area. Single fluid atomizers are capable of producing a very fine spray mist, but flow per nozzle is low and high pressures are required. In dual fluid atomizers, the lowest air pressure resulting in effective

atomization was around 20 psig. Increasing the air pressure improves atomization and reduces water flow rate at a constant water pressure. Pressures of air and water are not independent in this type of nozzle; changes in each affecting the other. With nozzles producing a fine spray at a given air pressure, atomization would deteriorate as increasing water pressure started to approach air pressure. A clear breakdown in nozzle performance occurred near this point and large drops would suddenly appear. Flow rate is not necessarily linear with number of nozzles when they operate from a common air and water supply; doubling number of nozzles may not double total flow rate at a given air and water pressure.

Approximately 17 different nozzle configurations were evaluated. When compared to the AAE nozzles, the dual fluid types that produced improved atomization within a reasonable pressure range all operated at much lower water flow rates. Two nozzles were identified that showed potential for a large improvement in the HISS spray cloud, functioned within available pressure limits, and could be readily adapted to the existing booms. Figure 9 shows their performance as determined by the single nozzle ground tests. However, these tests could only provide a qualitative assessment of microphysical spray characteristics. To quantitatively define the cloud composition a wind tunnel program was also conducted.

Wind Tunnel Test

The wind tunnel test conducted by Boeing Vertol at the NASA-Lewis IRT during October was aimed at identifying necessary system modifications to achieve a spray cloud with a minimum LWC variation and a droplet distribution with an MVD from 15 to 40 μm . A schematic of the test set-up is shown in figure 10. A full scale 9-ft long section of the HISS spray boom was fabricated and installed in the 6 x 9 ft test section of the IRT. The boom was equipped with water and air supplies, and instrumented for pressure, temperature, and flow rate. Installed 21.5 ft downstream was an instrumentation platform assembly to measure spray cloud characteristics using the previously mentioned MRI particle measuring spectrometers.

Operating the wind tunnel over a range of airspeeds and temperatures produced conditions closely resembling an actual icing flight, with the exception of a reduced standoff distance. Boom air and water pressures and flow rates could be varied within and beyond HISS limits, allowing measurement of their effect on the spray plume. Plume characteristics were measured for a variety of nozzles, including the baseline AAE, Spray Systems 1/4J series, Sonic Development Corporation (Sonicore), and the nozzle used by the Air Force's KC-135 spray tanker. Single and multiple nozzle arrangements were tried with various orientations to the airstream. While complete results are given in reference 7, some of the interesting findings are listed below.

1. The baseline AAE nozzle showed good agreement with previous in-flight data, in that droplet MVD ranged from 200 to 300 μm . Increasing air pressure did not result in acceptable performance. Ice formation near the nozzle orifice occurred several times during low temperature runs.

2. For the type of circular cross section spray boom used, nozzle ejection perpendicular to the airstream produced the best spray patterns. Downwind ejection produced a turbulent, uneven spray, causing splashback onto the boom.

3. Presence of large drops from a given nozzle could be identified by the visual appearance of the perpendicular spray plume. Inertial separation between large and small drop trajectories produced a well defined "roostertail" effect, the airstream carried away small drops much more rapidly than large ones. In the worst case of the baseline AAE nozzle test, large drops would hit the tunnel ceiling.

4. Water drops did not become supercooled in the 0.13 seconds while traveling the 21.5 ft distance from the nozzles to the probe platform, as they would have at the greater standoff distance behind the HISS. The type of ice formations seen on the MRI probes and

instrumentation platform showed runback of liquid water and subsequent freezing, resulting in rapid ice build up. Because of this short distance from nozzle to impact, ice shape characteristics and area coverage were not indicative of in-flight performance and traditional identification of ice types could not be relied on.

5. Temperature gradient, even across this short 9 ft boom section, was significant when operating at cold temperatures. At -26°C, warm supply air entering one end of the boom at 60°C would cool to 4°C at the other end. A procedure developed to alleviate freezing of water in the external lines and nozzles used hot bleed air to purge the water lines until just prior to start of water flow.

6. A measurable difference in LWC and drop distribution existed between runs at room temperature and cold conditions for the same nozzle settings. A higher LWC and increased number of both large and small drops were measured at cold conditions. Considerably fewer drops with diameters below 40 μm were seen at room temperature. The difference became more pronounced with increasing flow rate. The reason for this difference is not clearly understood.

7. Nozzles of the type used by the Air Force icing spray tanker produced unacceptably large drops within HISS operating condition limits.

8. Both the Spray Systems 1/4J No. 29 and Sonicore nozzles generated a spray cloud with acceptable drop MVD. The Sonicore nozzle was favored since it did not experience freeze-up problems as did the 1/4J No. 29, adaption to the spray boom was simpler, and the drop distribution was narrower around the MVD. This nozzle had the best potential to duplicate a natural cloud within existing HISS operating constraints.

Effect of Humidity and Evaporation

One characteristic of a natural icing cloud that cannot be controlled or duplicated in a spray simulation is its 100% relative humidity. Even if the nozzles generate a spray cloud with identical LWC and drop distributions, evaporation will act on the ejected plume to change its composition with time. Over the range of airspeeds and standoff distances used in these icing tests, the pertinent time varies from 1.2 to 1.6 seconds. The amount of water that can evaporate into dry air, or its saturation capacity, varies from about 5 gm/m³ at 0°C to 1 gm/m³ at -20°C, with relative humidity defining the percentage actually present. Since the spray cloud is generally programmed for a LWC below 1 gm/m³, its rate of evaporation prior to reaching the test aircraft may be significant.

Cloud drop evaporation is governed by the drop diameter, water vapor diffusion coefficient, and vapor densities of the drop surface and surrounding air. With various simplifying assumptions and approximations, change in drop size can be calculated as a function of ambient temperature and relative humidity (ref 3). At the 1.4 second time frame of interest, evaporation can have a strong effect on drops of 20 μm diameter and less, as shown by the calculated time histories in figure 11. Since the 20 μm MVD desired for natural cloud simulation implies that half the water content exists in drops smaller than this, their extinction can significantly change the spray LWC and distribution prior to reaching the test aircraft. Even at 70% relative humidity, a 20 μm drop will lose 60% of its LWC at 0°C and 20% at -20°C. The implication is that simulation of a natural cloud with known LWC and drop distribution at the test aircraft involves precise knowledge and control of spray nozzle drop distribution with flow rate to compensate for evaporation.

Humidity measured during icing tests can vary over a wide range of values. The 1979 programs using the HISS in Minnesota encountered relative humidity conditions from 20 to 95%. Visible differences in the spray cloud occurred as a function of test day humidity. On high humidity days, vapor condensation within the low pressure vortex cores was commonly seen trailing from the blade tips as a result of cooling by thermal expansion. In this environment, the visible spray cloud was much denser and created an opaque fog. Distribution of small drops present, whether created by the nozzles or condensation effects, was clearly

different from that at a low-humidity condition. Initial water temperature influences the extent of evaporation as well as the extent of supercooling before reaching the test aircraft. Evaporation is certainly a major factor when tests examining spray cloud composition are made in ambient temperatures well above freezing. The humidity difference between a natural cloud and the test environment affects the thermal and physical process of ice formation on aircraft surfaces, and once formed, the extent of ice retention through sublimation.

Rotor Wake Survey

The downwash wake created by the HISS rotors was known to influence the spray cloud geometry. Two flights were made to define the usable test air volume and the extent of turbulence behind the HISS spray bars. Nine electrically actuated smoke grenades were clamped to the boom assembly and ignited in level flight at 80 and 100 KTAS (fig 12). It was felt that the smoke, having negligible ejection velocity and particle size, would follow the flow field more closely than a water plume and would minimize inertial effects. Two photo chase aircraft were positioned in formation to obtain lateral and overhead views of the HISS and a 500 ft long area behind it. This was adequate to include the test air volume and the area where the rotor tip vortices penetrated the cloud. A 300 ft height was maintained over a ground track to allow ground observation.

Analysis of the film coverage showed:

1. Distance behind the spray bars at which the rotor tip vortex disturbance intersected the central portion of the cloud was approximately 250 ft at 80 KTAS and 400 ft at 100 KTAS. The flow field behind the two center sections was relatively undisturbed forward of this point.
2. Smoke trails from the outrigger tips were entrained in the vortex roll at less than half this distance, causing them to diverge outward from the central trails.
3. A wave phenomenon of fixed frequency similar to a Von Karman street could be seen trailing closely behind the cylindrical spray pipes.

These findings indicate a maximum usable stand-off distance of approximately 250 feet behind the spray bars to operate in an icing cloud at 90 KTAS. This is where vertical aircraft movement above the upper edge of the visible cloud intersects turbulence from the HISS rotor wake, as shown in figure 13. Spray from the outriggers becomes entrained in the vortex roll-up well before this, and lateral movement of the test aircraft penetrates this turbulence, as in figures 14 and 15. This lateral flow separation from the outriggers creates an uneven gap in LWC, and tends to sort droplets by size at the edges. When the outriggers are used, these discontinuities make cloud cross sectional area estimation difficult. The small scale wave effects immediately behind the booms also creates turbulence causing inertial drop sorting.

Available Supply Air Pressure

Since available air pressure has a major influence on nozzle performance, measurements of actual engine bleed air output were taken to better define the existing configuration. Bleed air pressure from the engines is a function of power setting and ambient pressure and temperature. Probes to measure total and static air pressure and total temperature were inserted in the engine bleed air lines that supply the boom system. With the aircraft in hover, power setting was varied from 30 to 70% torque, both with the boom system isolated and while spraying water from the AAE nozzle configuration. Without airflow to the boom, pressure in the bleed air lines near the engines varied from 35 to 49 psig; when flowing, measured pressure range was from 21 to 32 psig. Mass flow of air per engine varied from .45 to .62 lbs/sec. Previous in-flight measurements taken at the boom had shown a maximum of 24 psig, evidencing pressure loss between the source and the nozzles. Ideal gas law pressure

change caused by the large bleed air temperature difference between the engines and the boom nozzles, particularly at icing test conditions, accounts for some of this loss.

In-flight Nozzle Comparison

Prior to actual modification of the entire spray assembly, a partial array of both Sonicore and Spray Systems nozzles were mounted on the boom outriggers to check in-flight operation at Edwards AFB. The new nozzles were placed in adjacent mounting locations on the outrigger tips, giving a 6-inch spacing between nozzles with alternating upward and downward ejection, as in figure 16. One outrigger was used for each new nozzle type, while the AAE nozzles remained installed in the two center sections. Since the three nozzle types were separated from each other on the booms by several feet, this configuration allowed side by side comparison of their spray behavior in flight, as in figure 17.

The visible spray plumes agreed with anticipated characteristics. The closer spacing of the new nozzles produced a more homogeneous spray having a denser consistency than the AAE nozzles. The characteristic "roostertail" shapes of the AAE nozzles plumes were not present in the other two, indicating an absence of large drops capable of laterally penetrating the airstream. The cloud depth produced by the new nozzles was consequently less. A denser cloud was generated by the Sonicore nozzles than the Spray Systems, consistent with their higher flow rating for the same pressures. In-flight nozzle operation was satisfactory, and the qualitative comparison with the AAE spray cloud was encouraging.

New Spray System Characteristics

Icing tests conducted by AEFA in Minnesota this year extended from January through March, and included evaluation of the YCH-47D, UH-60A, and ice phobic coatings on a UH-1H in both natural and HISS simulated environments. The UH-1H, equipped with the MRI particle spectrometers, assessed spray cloud characteristics of the newly modified HISS.

Two HISS configurations were evaluated, both involving replacement of the AAE nozzles with the Sonicore type. Schedule constraints precluded in-flight assessment of the Spray Systems nozzles. For the first three flights, 160 Sonicore nozzles were installed, filling all available center section locations and the inboard three quarters of each outrigger. The remainder of the HISS flights were completed with 97 nozzles installed in the center sections only. For these, the outriggers were physically isolated from the air and water supplies by metal plates bolted between the boom flanges at the outrigger junctions.

Operational Characteristics

Measured boom air and water pressures for both configurations are shown in figure 18. Boom air pressure with 160 nozzles was around 10 psig, about half of that measured with 97 nozzled configuration. Previous tests had shown that minimum pressure required for proper nozzle atomization was around 20 psig, rendering the first configuration unsuitable. The difference in pressure between the two configurations is attributed to the change in total boom air orifice area resulting from increased number of nozzles. Comparison of the operating air and water pressures in the final 97 nozzle configuration shows that water pressure equals and exceeds air pressure beyond a 30 gpm water flow rate, setting an upper flow rate limit of about 25 gpm to retain satisfactory spray atomization.

Several other characteristics of the new system were observed in operation. Flow blockage from freezing of nozzles was a problem initially, but could be alleviated by a procedural change similar to that developed in the wind tunnel. Valving bleed and purge air continually through the air and water lines from takeoff until actual start of water flow proved effective to temperatures as low as -20°C, if all residual water had first been eliminated from the boom. However, because of hardware design, thoroughly draining all

residual water prior to flight was not always possible in practice, and occasional problems persisted.

Temperature measurements at various air and water boom locations were observed to change with position on the boom, ambient temperature, flow rate, and time. In general, boom temperatures were higher after the outriggers had been blocked off, and ranged from 15 to 30°C above ambient. Icing operations at -20°C resulted in near freezing temperatures at certain boom locations. In these cases, potential for freezing and flow blockage existed if any discontinuous event resulted in further cooling.

One of the chief questions concerning use of the new configuration was whether the formation of "popsicles" on the boom would continue to be a problem. Most ice accretion on the spray boom this year occurred as a result of leakage from loose fittings between the nozzles and water manifolds, and from spray impingement onto the uplock latches on the top bar that holds the boom in place when stowed. These were remedied by removal of two nozzles and retightening fittings. Some ice accretion developed around the nozzles when flow blockage was experienced, but this was not a regular occurrence in normal operation. For practical purposes, formation of ice on the boom has been eliminated as a significant concern.

Partial blockage of some nozzles occurred on one flight when residual debris from the water tank entered the boom system. A 70 gpm capacity in-line water filter with 100 µm elements was added and successfully eliminated this problem. One interesting development occurred during initial use of the filter. Flowing engine bleed air through the water lines prior to start of spray resulted in freezing and ice formation inside some nozzles. However, these nozzles were blocked by normal white ice, not the dyed yellow ice characteristic of the HISS. Hot air flow through the moist filter elements while purging had vaporized some of their contained water, which then recondensed and froze at the nozzles. Rerouting the purge air line to bypass the filter eliminated this phenomenon.

Evidence of uneven flow rates between the upper and lower booms was apparent when operating at low water flow. Downward flow routing from common sources and a difference in static head pressure due to 5 ft vertical separation resulted in a visibly thicker spray emanating from the lower boom. At extremely low flows, spray from the upper boom would be intermittent.

Installation of the Sonicore nozzles increased weight of the 1634 lb boom assembly by approximately 91 lbs with 160 nozzles, or 55 lbs with 97 nozzles. Interaction between the suspended boom assembly and aircraft dynamics in flight has always existed. The added weight and drag characteristics of the new nozzles noticeably aggravated boom dynamics problems, and increased aircraft sensitivity to turbulence.

Cloud Size

Size of the visible spray cloud produced by the final configuration was approximately 8 ft deep and 36 ft wide. This compares to an estimated 10 to 12 ft depth with the dual boom configuration in previous years, and a 5 ft depth with the original single boom. Reduction in cloud thickness by use of the Sonicore nozzles resulted from shorter drop travel distance as a consequence of smaller drop size and 2/3 less flow per nozzle.

Depth of the spray cloud is still not adequate for comprehensive testing of all ice protection systems, even if immersion is divided in phases between rotor and fuselage. Test aircraft ice detection systems must be exposed to the same environment as the aircraft components they are designed to protect, and this is not always possible with the present cloud depth. In testing the YCH-47D this year, forward and aft rotor heads could not be exposed to the plume simultaneously. With the forward rotor immersed, its corresponding ice detector would be on the lower fringes of the plume, while most of the aft rotor and lower fuselage remained outside the cloud. Complete exposure of both rotors and their ice detectors as well as the fuselage would require a spray plume roughly three times as deep.

Width of the cloud, estimated at 36 feet, was less than any test aircraft rotor diameter. However, full span ice accretion was demonstrated on all aircraft rotor systems, including the 60-ft diameter of the YCH-47D. Since each part of the blade passes through the plume at least once every revolution, the main question centers on definition of the applicable spanwise LWC. The inboard portions are always within the plume, while the outer portions experience less exposure. Combined with the test aircraft lateral motions in the cloud and the effect of its induced velocity downwash components in forward flight, distribution of LWC for any given blade remains problematic. Use of the HISS outriggers extends cloud width and permits more lateral leeway for the test aircraft but its entrainment and roll-up in the HISS wake does not simplify calculation of LWC.

Cloud Composition

Procedures used to obtain in-flight measurements of the microphysical cloud properties resembled those of previous efforts, where flow rate, standoff distance, and vertical and horizontal positions in the cloud were varied. Analysis of these measurements showed a vast improvement over previous years in drop size distribution and LWC consistency (ref 8).

Variation of drop MVD with vertical position in the cloud is shown in figure 19. Measured MVD varied from 17 to 30 μm at the top of the cloud and 20 to 65 μm at the bottom. Overall comparison with the 10 to 30 μm MVD range possible in natural cloud is favorable and represents a large improvement over the previous HISS configuration (fig 3). Representative drop distributions are compared in figure 20. Numerical drop concentration is greatly increased over last year, and compares favorably with that of a natural cloud. The slope of concentration fall off with increasing diameter indicates the extent of size variation in the distribution: the greater the slope the fewer large drops and less variation from the mean. A natural cloud has a tailing slope of about 8 decades per decade (1 in 10^{-8}). The present spray cloud has a slope of about 5, and last year's cloud had a slope of 3. Mass distributions are compared in figure 21. The present cloud still contains some water in drops larger than 100 μm and less mass than a natural cloud in the 10 to 20 μm range.

Measurement of spray cloud LWC was considerably more successful than in the past, in that correlation with flow rate could be obtained, and a reasonable distribution existed as a function of position within the cloud. Figure 22 shows vertical distribution within the visible cloud for three flow rates. Increased concentration in the lower part of the cloud is consistent with the larger drop MVD measured near the bottom, as well as with the visual difference in spray output between the upper and lower booms. In the previous cloud (fig 4), preponderance of very large drops and wider gaps between individual plumes created a nonhomogeneous spray in which repeatable LWC measurements were not possible. Ability to obtain consistent LWC measurements within the present cloud is attributed to the improved drop size distribution and more uniform cloud consistency resulting from closer nozzle spacing.

Conclusions

Test results from the 1979-1980 icing program indicated that microphysical properties of the new spray plume approach those of a natural cloud, and show vast improvement over previous configurations. Ice accretions on test aircraft resembled those encountered in natural icing more closely than those prior to modification. Dimensions of the spray cloud present difficulty in simulating complete immersion of test aircraft. Experience gained through this program provided valuable insight on the subject of icing simulation, and indicated several areas for future investigation. Pursuit of a continued modification program can further improve the quality of the drop size spectrum, enlarge icing cloud dimensions, and expand the operating test envelope.

References

1. Fowler, Mary Grace; Facci, Edward W. Jr.; Blau, Henry H. Jr.; "Cloud Microstructure Studies, The Bering Sea Expedition - Flight 8", Environmental Research & Technology, Inc.

Project P-554, Aug 1973

2. Russo, A.; "Test and Demonstration Report, Helicopter In-Flight Icing Test Facility", All American Engineering Co., TR-333, Nov, 1973
3. Easterbrook, Calvin C.; "Measurement of the Microphysical Properties of a Water Cloud Generated by an Airborne Spray System", CALSPAN Report No. CH-5391-M-1, Dec 1973
4. Fowler, Mary Grace; Kebabian, Paul; Blinn, John C; "Characteristics of a Spray Plume", Environmental Research & Technology, Inc., Report No. P-1840, Apr 1976
5. Wilson, LTC Grady W.; Woratschek, Ralph; "Microphysical Properties of Artificial and Natural Clouds and their Effects on UH-1H Helicopter Icing", US Army Aviation Engineering Flight Activity, Report No. 78-12-2, August 1979
6. Niemann, John R.; Bowers, CPT Frame J III; Spring, MAJ Sherwood C.; "Artificial Icing Test Ch-47C Helicopter with Fiberglass Rotor Blades," US Army Aviation Engineering Flight Activity, Report No. 78-18, July 1979
7. Lynch, C. P.; "Helicopter Icing Spray System (HISS) Improvement Program - Final Report", Boeing Vertol Report No. D210-11570-1, Jan 1980
8. Humbert, M.E.; Jahnson, L.J.; Dzamba, L.D.; "Droplet Size and Liquid Water Characteristics of the USAAEFA (CH-47) Helicopter Spray System and Natural Clouds as sampled by a JUH-1H Helicopter", Meteorology Research Inc. Report 80 dFR-1748, April 1980

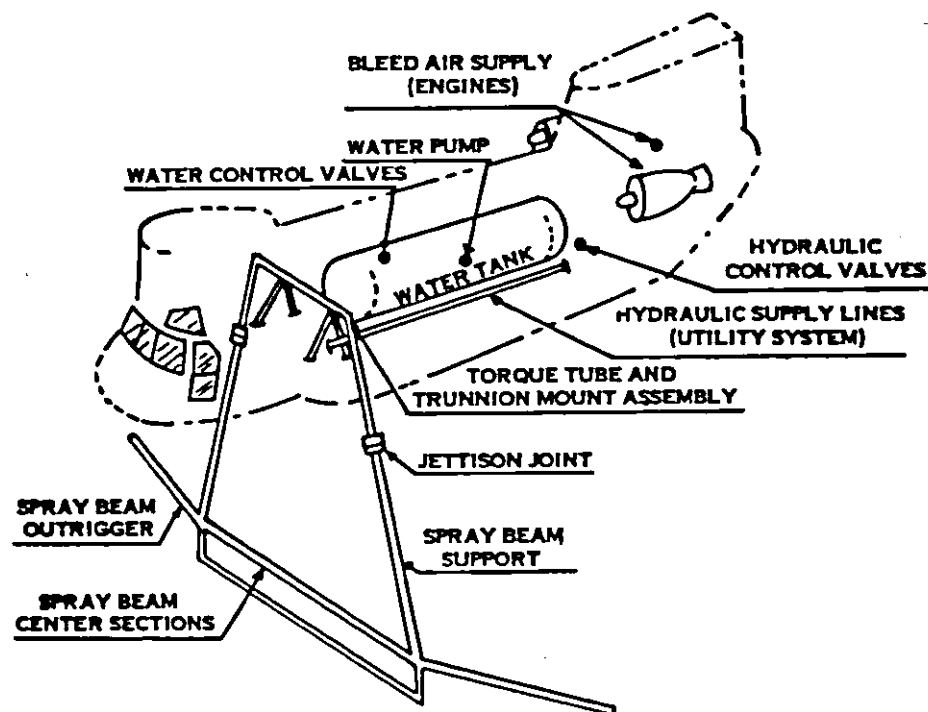


Fig. 1 HISS Schematic

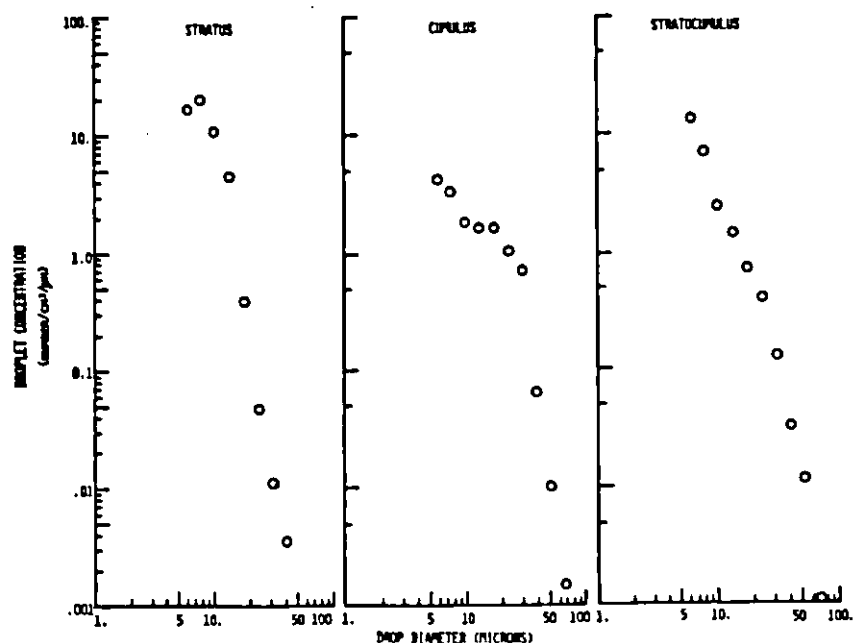
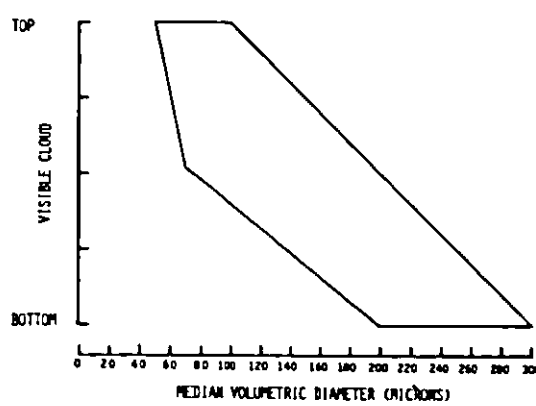
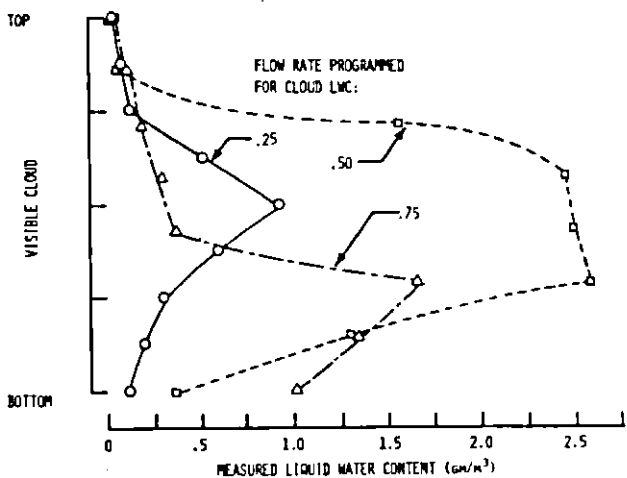


Fig. 2 Representative Drop Size Spectra for Stratus Cumulus, and Stratocumulus Clouds



**Fig. 3 Vertical Variation of Cloud
Droplet MVD**



**Fig. 4 Vertical Variation of Visible Cloud
Liquid Water Content**

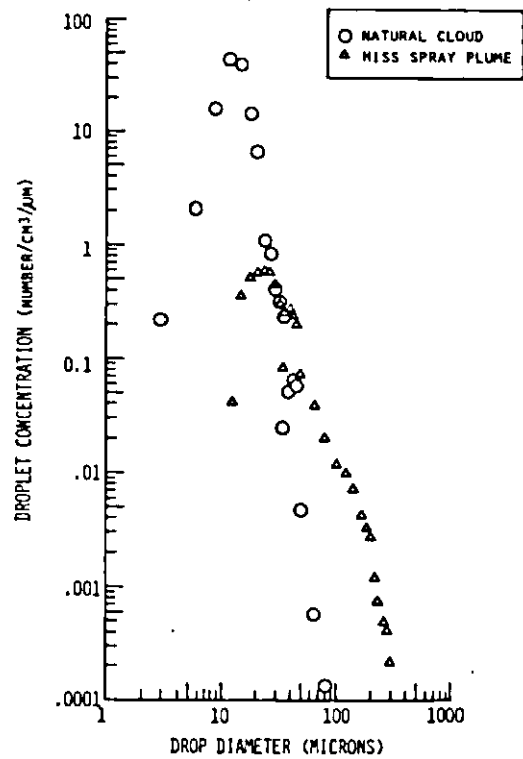


**Fig. 5 Comparison of Drop Size Spectra
Measured in a Natural Cloud and
the HISS Spray Plume**

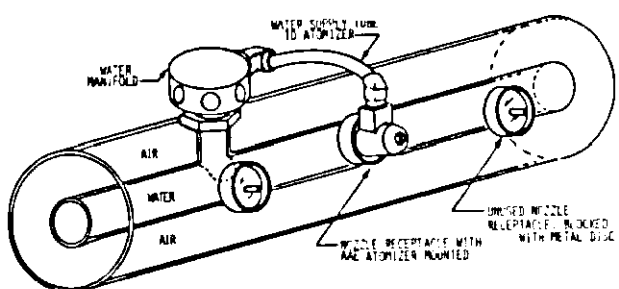


Fig. 6 Schematic of Spray Boom Section

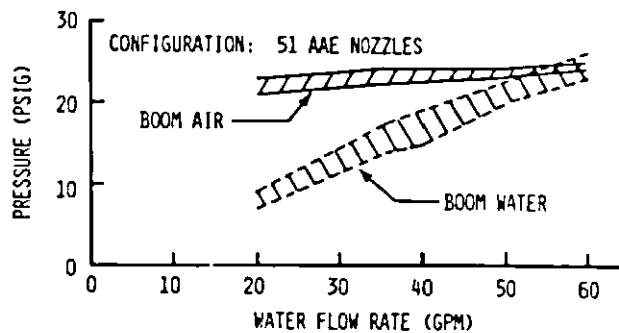


Fig. 7 Spray Boom Air and Water Pressure

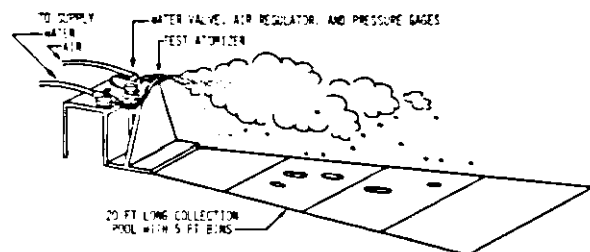


Fig. 8 Schematic of Single-Nozzle Ground Test Set-Up

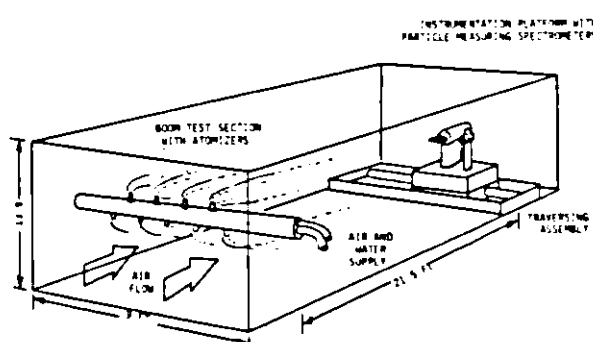


Fig. 10 Schematic of Test Set-Up in the NASA-Lewis Icing Research Tunnel

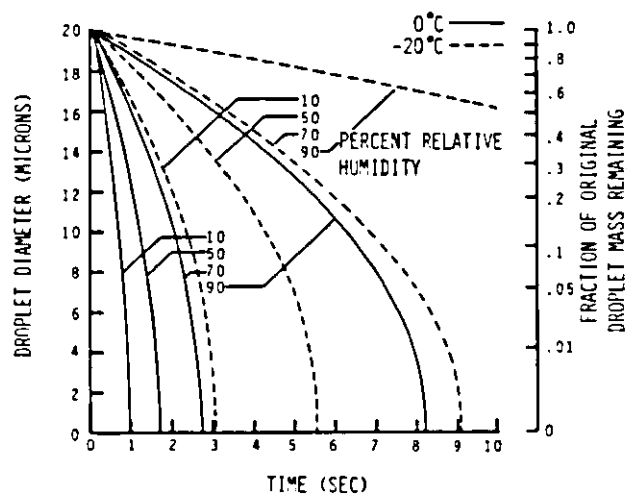


Fig. 11 Evaporative Size Change of a 20-Micron Diameter Drop with Time

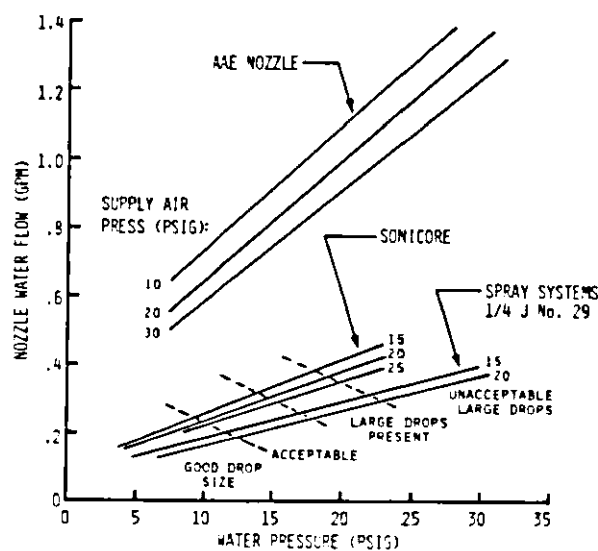


Fig. 9 Comparison of Atomizer Performance from Single-Nozzle Ground Tests



Fig. 12 Smoke Trails During Rotor Wake Survey

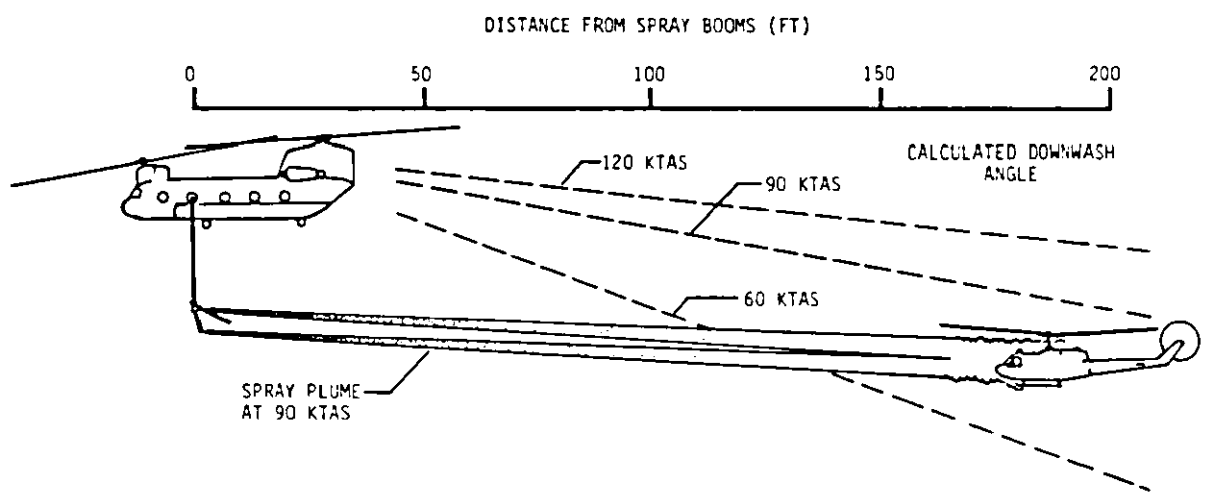


Fig. 13 Approximation of Main Rotor Downwash and Spray Plume Interaction

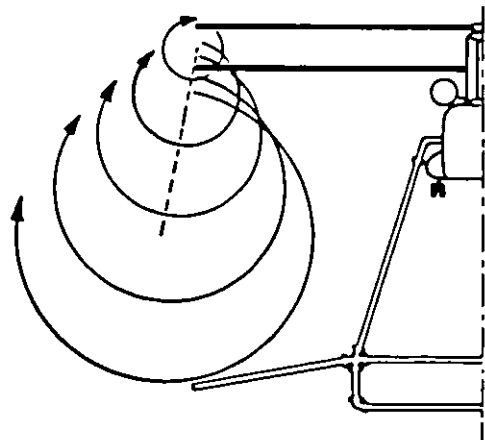


Fig. 14 Approximation of Rotor Vortex Effect on Outrigger Spray



Fig. 15 Rear View of Smoke Entrainment in Vortex Roll-Up



Fig. 16 Ten Sonicor Nozzles Installed on Left Outrigger

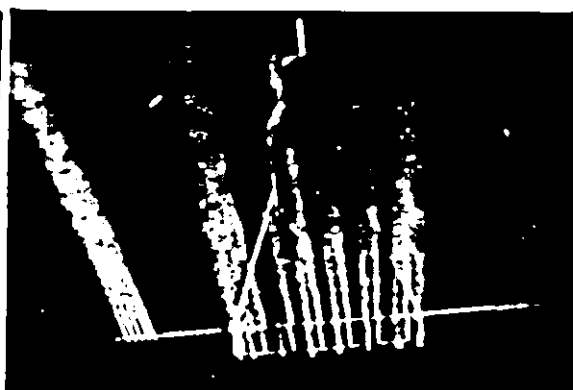


Fig. 17 Visual Spray Comparison (Left to Right) Sonicore AAE, and Spray Systems Atomizers

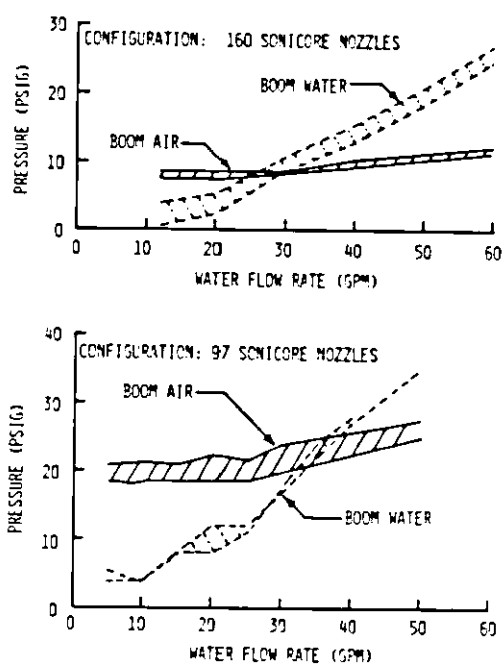


Fig. 18 Spray Boom Air and Water Pressure

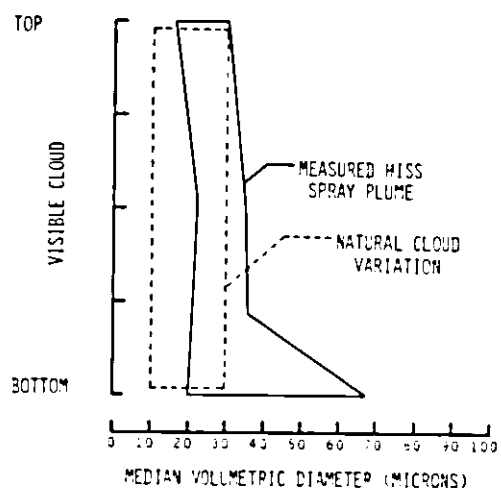


Fig. 19 Vertical Variation of Cloud Droplet MVD

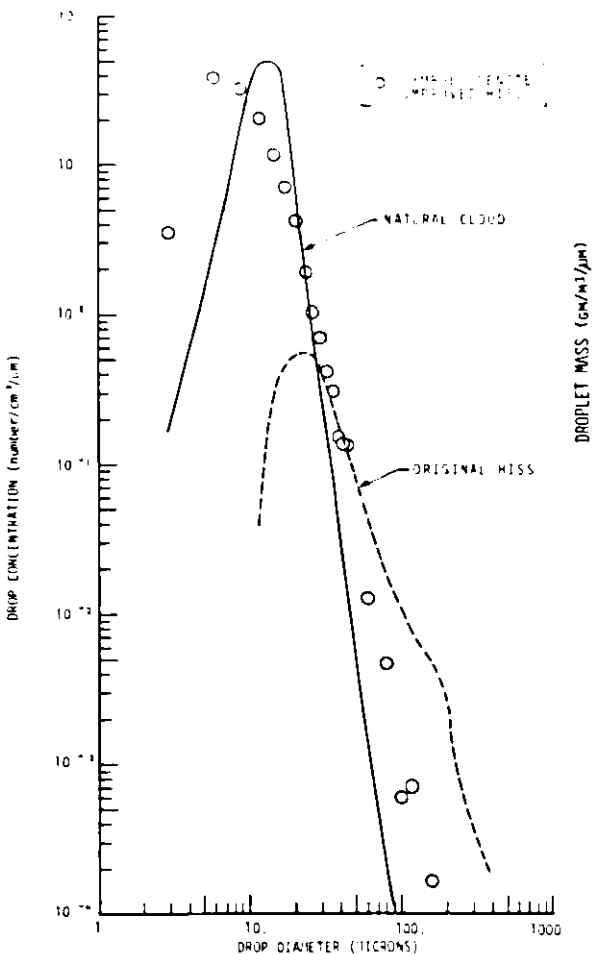


Fig. 20 Representative Drop Size Spectra Measured in HISS Spray Plume after Improvement

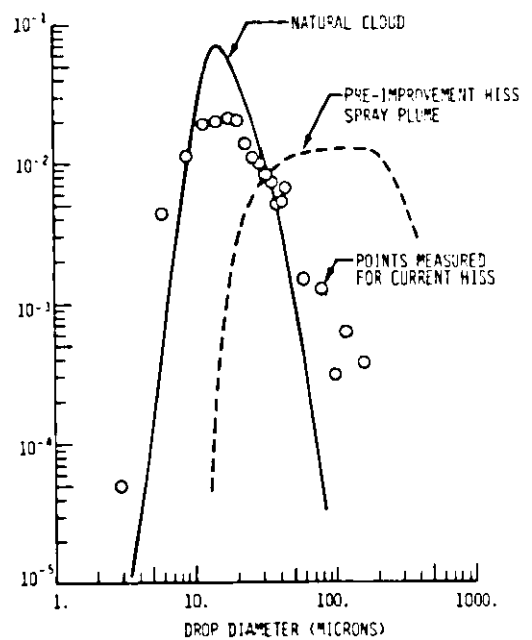


Fig. 21 Droplet Mass Distributions of a Natural Cloud and HISS Spray Plume, Before and After Modification

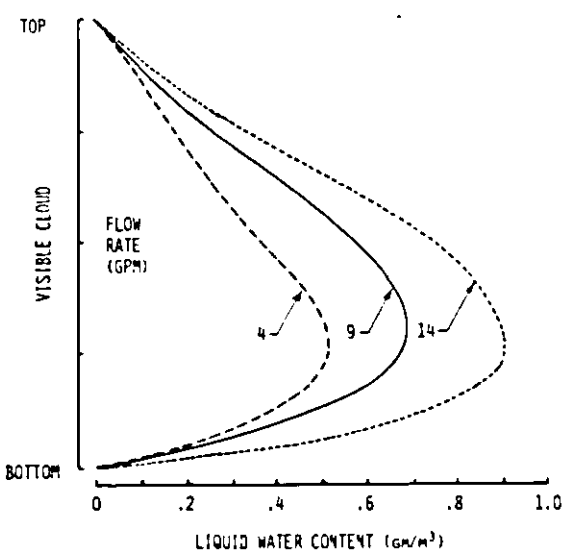


Fig. 22 Vertical Variation of Visible Cloud Liquid Water Content

MODERN TECHNIQUES OF CONDUCTING A FLIGHT LOADS SURVEY
BASED ON EXPERIENCE GAINED ON THE BLACK HAWK HELICOPTER

W. P. Groth
G. M. Chuga
V. S. Nelson

SIKORSKY AIRCRAFT DIVISION
UNITED TECHNOLOGIES CORPORATION
Stratford, Connecticut

ABSTRACT

The ever increasing demand on the helicopter manufacturer for development and qualification of new aircraft with improved performance, reliability and mission capabilities within stringent budgetary constraints has surfaced a need to re-evaluate and improve the methods, techniques and procedures (methodology) utilized during qualification testing. Previous flight test experience at Sikorsky Aircraft clearly indicates that the critical path to early production procurement is the successful completion of the aircraft structural qualification program with the Flight Loads Survey being the key element during aircraft alight qualification.

This paper addresses the techniques developed and utilized during the recent BLACK HAWK (UH-60A) qualification program and shows how the Flight Loads Survey provides the basis for flight envelope definition, mission utilization, fatigue analysis and also provides interactive data to support and/or update predicted loads criteria. The importance of development and implementation of new flight test methodology to flight loads survey criteria is shown to be a primary consideration for timely and successful completion of major aircraft test programs.

NOTATION

UTTAS	Utility Tactical Transport Aircraft System
NPE	Navy Preliminary Evaluation
APE	Army Preliminary Evaluation
STA	Static Test Article
GTV	Ground Test Vehicle
YAPS	Yaw and Pitch Sensor

INTRODUCTION

Past experience associated with the development of both fixed wing and rotary wing aircraft has shown that the uncertainties of design provide the basis for test requirements. As a result government specifications have been developed for use by the helicopter manufacturer to demonstrate the airworthiness of his design. References 1 and 2 are examples of comprehensive specifications developed by the Army and Navy for the planning and execution of qualification test programs on military helicopters.

Reproduction right granted by the American Helicopter Society.

In the case of the helicopter, qualification of a new model usually requires ground substantiation of components and subsystems using wind tunnel, bench and static tests followed by an extensive flight test evaluation. As specified in References 1 and 2, airworthiness cannot be demonstrated in accordance with government specifications until numerous flight surveys and demonstrations are satisfactorily completed on the entire helicopter system. Test experience at Sikorsky Aircraft based on more than 30 years of qualification testing of both commercial and military aircraft, Figures 2 through 5, indicate that the critical path to early and continued production deliveries of a successful model is the aircraft structural qualification. Flight test experience also shows that the Flight Loads Survey is the key element during the aircraft flight qualification phase since it is the pacing item for initiation of other surveys and demonstrations and must also provide data/verification to support design and ground test criteria.

Since the calendar time and flight test hours required to demonstrate airworthiness of a new design is extensive, new management techniques have been applied in attempting to reduce the schedule and associated costs of the test program. However, since the Flight Loads Survey is the key element during the structural flight qualification with numerous interactions with other areas, it is obvious that proper management alone is not sufficient. The management effort must be supported with improved and updated test methods, techniques and procedures if the helicopter manufacturer is to remain competitive.

The recent BLACK HAWK (Figure 1) development and qualification test program conducted by Sikorsky Aircraft is an excellent example of how new test methodology can be implemented during the Flight Loads Survey resulting in the timely and successful completion of a major aircraft test program. Subsequent paragraphs will address the techniques developed and utilized during the BLACK HAWK program and are considered a step forward in the development of new Flight Loads Survey Methodology.

BACKGROUND

Planning Airworthiness Qualification

Airworthiness is "a demonstrated capability of an aircraft or aircraft subsystem or component to function satisfactorily when used within prescribed limits".³ Accordingly, airworthiness of the helicopter is demonstrated in accordance with established government specifications to show compliance with contractual design requirements and performance guarantees. Although the qualification process is dependent on performing the specific tests described in the specification, the planning, testing techniques and execution is left up to the contractor with subsequent review and approval by the procuring government agency. The contractor's qualification test planning is therefore considered a principal element in the overall coordinated effort for development and delivery of a new helicopter system. It is this area of contractor responsibility to which the manufacturer's test engineer must continually apply his ingenuity and know how if the manufacturer is to remain competitive and successful.

To provide better management of the individual disciplines involved, the planning is generally segregated into four phases as illustrated in Table A consisting of:

- (1) design analysis
- (2) ground qualification tests
- (3) aircraft flight tests
- (4) government service and evaluation tests

Although specific substantiation requirements are defined for each phase the airworthiness qualification is a continuous process with interactive data provided to support previous test results and define where modifications and requalification may be necessary.

Analytical Structural Substantiation

A well planned helicopter development program must rapidly provide minimum risk development to meet safety, performance and producibility goals within program budget and schedule constraints prior to formal qualification testing. This qualification begins with the analytical load predictions, static and dynamic structural analysis which form the basis for the initial structural substantiation from an analytical standpoint. Due to the assumptions made and the uncertainties involved in the analytical process, verification is required on the physical hardware.

Ground Qualification Tests

Ground qualification tests for major aircraft development programs usually consist of model and/or full scale wind tunnel tests conducted early in the development phase followed by bench, whirl and subsystem qualification tests. Static tests are also conducted to limit, ultimate or failure loads using full scale components and actual airframe structure to verify design analysis. Eventually ground tests are conducted on an actual aircraft or a specially designed ground test vehicle. Some of the ground qualification tests normally performed at Sikorsky Aircraft are illustrated in Figures 6 through 11.

Basic objectives of the ground testing are to:

1. minimize risk during flight testing.
2. provide early development of the aircraft and aircraft subsystems to reduce costly modifications later in the test program.
3. demonstrate to the procuring agency that the components and subsystems have met contract guarantees in compliance with the specified mission requirements.

Aircraft Flight Tests

Flight tests of the aircraft system provide the final data necessary to confirm compliance with contractual design performance requirements and verify that the aircraft is safe for operation within its assigned mission. The aircraft flight test program consists of a series of surveys and demonstrations which comprise the airworthiness qualification tests. A summary of these is provided in Table A. However, the specific tests required for each particular test program can vary with specific aircraft configuration and mission requirements.

Demonstrations are primarily go/no go type tests conducted at specific test conditions to show compliance with contract or detail specification requirements. Some demonstration tests (such as structural demonstrations) go well beyond the flight limits used during normal operation of the helicopter. Surveys on the other hand gather information/data concerning components, hardware, equipment or subsystems over a wide range of test conditions. The test data is obtained at flight conditions both within as well as outside the flight envelope eventually recommended for normal service operation.

A comprehensive Flight Loads Survey measures the influence of all variables such as gross weight, altitude, airspeed, rotor speed and center of gravity on the structural data. This must also include effects due to changes in mission or configuration requirements such as the carrying of external loads, Figure 4, or the installation of auxiliary equipment such as external fuel tanks or armament. Additionally, the Flight Loads Survey provides the basis for defining operating limits to be complied with during service operations.

Table A illustrates how the Flight Loads Survey, due to its various interactions with other elements of the airworthiness qualification, is the key element during the structural qualification and supplies the basic data to support other disciplines. Specifically, the Flight Loads Survey:

- establishes the flight envelope. Conduct of the test defines limitations and restrictions which determine flight envelope boundaries. Interim flight envelopes provide capability to initiate parallel discipline subsystem flight qualification testing on other aircraft and permit early assessment of flight characteristics by government pilots. The final flight envelope is established based on composite survey data (including flight loads) with the appropriate limitations and restrictions included in the pilot's Flight Handbook.
- provides the basic load and stress data used for fatigue substantiation to establish component replacement times. Primary emphasis is placed on obtaining extensive data for dynamic components, control systems and other specific areas where failure of components or subsystems could be catastrophic.
- provides iterative data to support and/or update predicted loads criteria. Correlation of the flight measurements with design analysis verifies or negates design assumptions used for prediction of flight loads applied in structural analyses of dynamic components, airframe, empennage or other aircraft subsystems. When discrepancies are evident, inspection requirements may be established to permit continuation of flight testing pending redesign and requalification of the affected areas.
- provides verification of critical load distributions and load application methods during structural ground tests. If flight test results indicate critical loads or techniques used during static, whirl or bench testing are not appropriate, modifications to ground qualification testing must be made to provide compliance with actual flight experience.
- provides a historical library of test data to support future development activity. As new mission requirements develop and changes to the original design are introduced the baseline flight data is available for additional fatigue and/or design analysis or load trend predictions.

Government Service Tests/Evaluations

With the exception of preliminary evaluations performed periodically during the contractor's test program, government service tests normally follow completion of the contractor's testing and are performed on production type aircraft to evaluate operational suitability. These usually continue beyond initiation of production deliveries and are considered beyond the scope of this paper. The preliminary evaluations (NPE, APE) are normally performed by government engineering test pilots during the development program but are restricted to verification of performance, handling qualities and system operational characteristics. Since neither the early government evaluations nor the subsequent service tests provide structural substantiation the basic structural qualification must be provided by the contractor's Flight Loads Survey.

Shortcomings of Previous Load Surveys

The planning of an effective Flight Loads Survey in the past has been hampered by the methods and tools available to the test engineer. Restrictions imposed by the airborne data acquisition system, Figures 12 and 13, along with time and cost constraints resulted in fewer data samples based on a limited number of measurements. Conservatism was introduced during the data reduction, analysis and application procedures due to the interpretations and individual experience of the analyst. As a result it was difficult to reduce cost and weight penalties associated with the conservatism without compromising safety.

With the development and implementation of more sophisticated magnetic tape airborne recorders, computerized automatic data processing and on-line telemetry capabilities for real-time data analysis and verification the tools became available to stimulate the development of new flight test methodology. Although the initial emphasis was placed on the development of new hardware and procedures for data collection and processing, it became obvious that other areas of the Flight Loads Survey test criteria needed re-examination and improvement. Some of the more significant areas included:

- improved instrumentation features on the aircraft to provide more flexibility and reliability as well as provisions for redundant measurements.
- new approach to development flight testing to provide a greater population sample of data, including data from more than one aircraft, to reduce uncertainties.
- verification of loads and stresses on the final production article.
- incorporation of methods to account for statistical load variations due to weather conditions, pilot techniques, measurement accuracy and test procedures/tolerances.
- new flight test technology to expedite safe envelope expansion and substantiation of configuration changes based on pre-determined static and fatigue test limits.

As requirements materialized for qualification of a new utility tactical transport helicopter for the U.S. Army, Sikorsky Aircraft quickly realized that new flight test methodology must be applied in all possible areas to provide a competitive aircraft for government evaluation. With the implementation of the new methodology supported by a new test philosophy Sikorsky was able to meet the challenge of providing a superior production aircraft safely, on schedule and with record efficiency.

BLACK HAWK TEST EXPERIENCE

The U.S. Army's UTTAS (BLACK HAWK) specification required development and qualification of a new aircraft system with improved performance, reliability and mission capability within more severe budgetary and schedule constraints than previously sought by any procuring agency. The successful completion of this task provided an excellent opportunity at Sikorsky to demonstrate the importance of development and utilization of new flight test methodology during the Flight Loads Survey. The technology and philosophy used during the BLACK HAWK testing are highlighted in the following sections.

New Test Methodology

Requirements to accomplish simultaneous development and flight qualification of the aircraft with unprecedented efficiency dictated the development of new planning, organization and flight test technology to provide:

- redundant multi-discipline test aircraft each capable of rapid interchangeable test roles and possessing the capability of providing structural Flight Loads Survey data.
- new test tools to permit rapid expansion of the flight envelope as well as development testing with primary emphasis on new methods of data acquisition, processing and analysis to permit on-line decision making and rapid aircraft turnaround between flights.
- a dedicated test organization capable of conducting multi-discipline testing during development as well as qualification.

To implement this concept Sikorsky provided three test aircraft with redundant/back-up test instrumentation as shown in Figure 14. Each aircraft was configured with a full set of instrumentation including telemetry capability for 20 channels of real time data, Figure 15. The airborne instrumentation package also incorporated features to provide the necessary flexibility for quick turnaround of measurements as based on test objectives, Figures 16a, 16b and 16c.

- Quick disconnects were provided on all instrumented components including the sliprings and terminal board to minimize the down time required when replacing components.
- A programmable patch board provided the means to quickly select the required parameters for each test.
- Interchangeability of instrumentation components such as encoders, voltage control oscillators and tape recorders from aircraft to aircraft.
- Redundant strain gage bridges were provided for all critical parameters.
- Aircraft center of gravity control was provided to compensate for migration with fuel burnoff to allow for longer flights within the c.g. tolerance applicable to the loading of the aircraft, Figure 16d.

Improved flight test techniques were also developed to expedite safe flight envelope expansion and evaluation of configuration modifications. These include new decisioning procedures for the test engineer. Structural endurance and Do Not Exceed (DNE) limits were established prior to test conduct and enabled the flight director to make a quick and sound assessment of structural adequacy during flight. When the pre-determined endurance values were exceeded, damage tracking was initiated to assure adequate residual component life. DNE limits were set at a level which would maintain safety for a short period of exposure while still permitting investigations to the extremes of the flight envelope. Test directors were provided with standardized procedures to follow in the event DNE limits were encountered.

Computer software was developed to allow for inflight evaluation of test data in addition to the post flight analysis. A stability monitoring program was developed and used for inflight determinations of system frequency and content. This permitted safe probing of aeroelastic stability and rotor/airframe modifications by the telemetry test team while incrementally expanding the flight envelope.

Sikorsky's RAPID (Real-time Acquisition and Processing of Inflight Data) system also provided significant advantages during the load surveys as well as other tests. Tabulated and plotted data were available within hours after each flight. New computer programs were developed for semi-automatic data editing, harmonic analysis and damage tracking to assist in test engineering decisions. As a result, not only were the time and cost of final edited data reduced, but standardization of the data was also achieved.

To provide multiple-discipline testing dedicated test teams were assigned to each aircraft. A designated test director was responsible for test conduct on each aircraft with support from flight test specialists provided from other disciplines. During critical development testing specialists from the Design Organization were also assigned to the test team to provide additional support.

Test flights were designed to obtain simultaneous data in several disciplines (structures, vibrations, handling qualities and performance) while combining basic envelope expansion with the assessment of development aircraft configuration changes. Alternate flights were planned for each day to take optimum advantage of existing weather conditions or potential configuration/instrumentation delays.

New Test Philosophy

Specification requirements for the BLACK HAWK dictated a two phase development and qualification program as illustrated in Table B. The initial phase, designated the Basic Engineering Development (BED) Phase, required early delivery of a production prototype aircraft for government competitive testing with subsequent production contract award based on the results of the competitive evaluation. During the follow-on Maturity Phase the selected contractor developed and qualified his aircraft to full U.S. Army requirements. This philosophy of a competitive fly-off evaluation prior to production commitment was new to the helicopter industry and required each contractor to use all the available resources at his disposal. Some of the methodology introduced by Sikorsky to secure a production contract was discussed previously. The new philosophy, however also demonstrates that acquisition of valid flight loads data that accurately represents the final product is not easily obtained. Sikorsky's experience, especially during the BLACK HAWK program, indicates that three basic steps must be considered during good Flight Loads Survey planning. These include:

- a. A preliminary evaluation phase to develop and define the final aircraft configuration. Problem areas are investigated and measurement requirements are finalized. Measurements obtained during these tests are preliminary but provide early assessment of a satisfactory configuration. In some cases where only subsystems or aircraft derivatives are being qualified, the preliminary evaluation may consist of a minimum "Shakedown" program. In the case of the BLACK HAWK qualification, the preliminary evaluation (BED) phase was extensive with numerous secondary surveys and demonstrations conducted to qualify the aircraft for competitive evaluation. In all cases, however, the primary goals of the initial evaluations are to develop and verify the aircraft configuration as early as possible, thereby minimizing risk during subsequent qualification of the production article.
- b. A comprehensive Flight Loads Survey conducted in accordance with government specification requirements. This testing is conducted with a final instrumentation package which includes all critical measurements and with all modifications retrofitted to the aircraft. During the BLACK HAWK qualification, this phase was represented by the Maturity testing and substantiated production changes to the main and tail rotor dynamic systems as well as the stabilator as based on results of the BED phase testing. The data recorded during this phase forms the basic data bank for flight envelopes, fatigue analysis and future reference and must therefore accurately define the load environment of the aircraft.
- c. A data verification phase during which the primary loads and stresses used for substantiation are verified on the final production article. Due to changes in manufacturing techniques, tolerance build-up, aircraft performance as well as statistical loads variations the loads obtained during the Flight Loads Survey may differ from the loads experienced during actual service usage. Since government service tests seldom provide for structural type measurements, this area is most often ignored. During the BLACK HAWK program, the production aircraft showed an increased level flight airspeed capability as compared to the prototype aircraft. As a result, the influence of the additional speed capability on the critical components had to be investigated and the results included in the fatigue analysis.

Although all three steps may not be a pre-requisite for all Flight Loads Surveys, they should be considered in the planning effort since the procedure can be successfully utilized to reduce cost and weight with minimum risk during aircraft development.

Results

The new test philosophies and methods implemented during the BLACK HAWK development and qualification program provided a data base unprecedented in the number of data units for the structural qualification of any helicopter in the history of Sikorsky Aircraft. The population sample from the three production prototypes and one production aircraft represented a wide cross section of data to account for variability between aircraft differences, piloting techniques and weather conditions as well as for specific operating conditions such as variables in gross weight, center of gravity, rotor speed, altitude and load factor. This allowed a more accurate definition of the load environment throughout the extremes of the envelope limits from which data was extracted and applied to fatigue strength and mission spectrum data to provide the component replacement times required to meet the Army specification.

The standardization of the measurement methods such as locations, recording equipment, and data processing provided the means for an early evaluation of the structural adequacy of the aircraft systems. As new fatigue origins were identified in the laboratory, the flight loads were available to assess the impact on the retirement times.

The processing of flight data standardized through the use of the computer not only provided data to the engineers within hours after the completion of a flight for evaluation purposes, but formed a library from which data was available for correlation and comparative purposes. The data processing was standardized with respect to its grouping as either steady state, where the basic aircraft controls remained fixed throughout the data record or transient where the controls were moved as required to perform the intended maneuver. For the steady state condition as presented in Figure 17, a statistical analysis was performed on the data samples within the data burst, to calculate the 95th percentile oscillatory load level along with the arithmetic mean of the steady load. Figure 18 shows the output of data processed for the transient conditions. It provides a summary of the maximum recorded oscillatory loads with the associated steady levels grouped according to specific maneuvers for the entire survey.

The implementation of the new methods and philosophies demonstrated a step forward in the state of the art of flight testing, all of which revolves about the flight loads data providing the key for future development and continued success of the production aircraft to perform the intended mission.

CONCLUSIONS AND RECOMMENDATIONS

1. With the introduction of more demanding mission and test requirements by government agencies the manufacturer must continually update present state-of-the-art test methodology.
2. Since the Flight Loads Survey data has such a pronounced influence on numerous other areas during the airworthiness qualification process every effort should be made to conduct a comprehensive survey on the final configuration being qualified to avoid significant structural modifications during the testing. The critical structural loads should also be verified on a final production article to account for differences due to manufacturing techniques, tooling and production tolerances.
3. It has been demonstrated during the BLACK HAWK qualification testing that new equipment and methods can be used effectively to provide standardization in the areas of data acquisition and processing. Similar standardization of procedures should be implemented in the areas of data analysis and application methods.

REFERENCES

1. AMC Pamphlet No. 706-203, Engineering Design Handbook, Helicopter Engineering, Part Three Qualification Assurance, by U.S. Army Material Command - April 1972.
2. Military Specification MIL-D-23222A (AS), Military Specification Demonstration Requirements for Helicopters, by Department of the Navy, Naval Air System Command - March 1971.
3. AMCR 70-33, Aeronautical Design Standards for U.S. Army Aircraft Systems.
4. Stutz, R.G., Kreutz, F., and Fenaughty, R.R., Sikorsky YUH-60A UTTAS Helicopter Flight Test Program, Presented at the 8th Annual Symposium of the Society of Flight Test Engineers, - August 1977.
5. Mard, K.C., YUH-60A Test Operations Presented at the 32nd Annual National V/STOL Forum of the American Helicopter Society, Washington, D.C., - May 1976.
6. Mard, K.C., The Challenge for New Test Methods, Presented at American Society for Testing and Materials Symposium on Testing for Prediction of Material Performance in Structures and Components, Anaheim, California, - April 1971.
7. Wolfe, R.A. and Arden, R.W., U.S. Army Helicopter Fatigue Requirements and Substantiation Procedures, Paper from Report No. 674, Helicopter Fatigue.

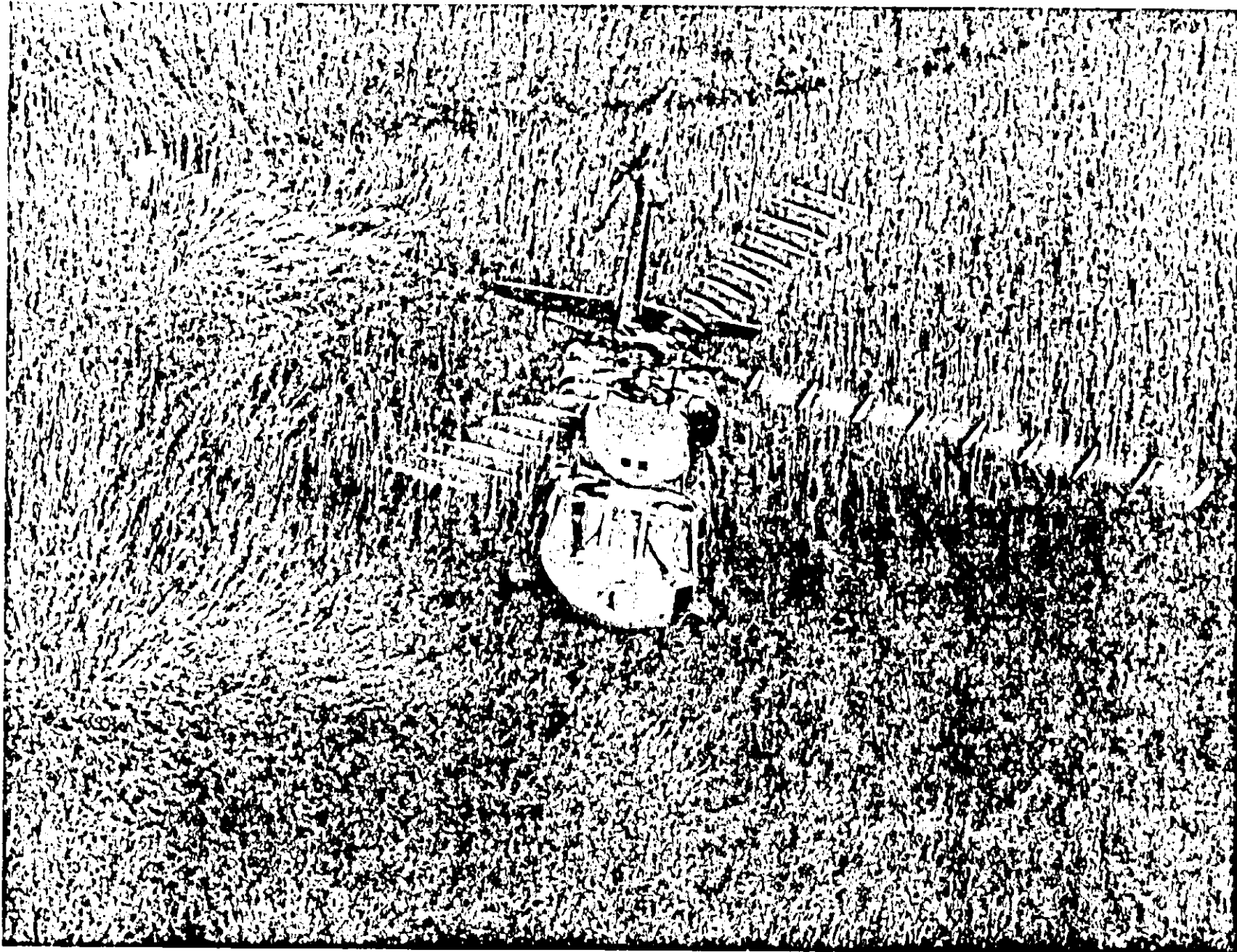


FIGURE 1 SIKORSKY (UH-60A) BLACK HAWK HELICOPTER



FIGURE 2 - Sikorsky S-58 (Military)



FIGURE 3 - Sikorsky S-61 (Commercial)

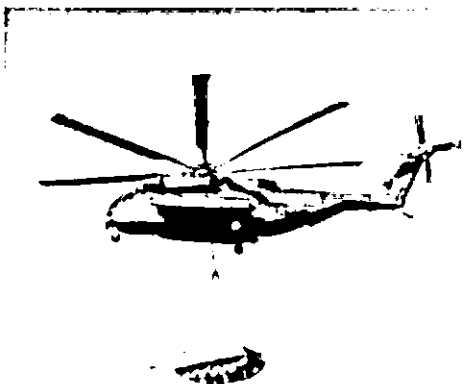


FIGURE 4 - Sikorsky CH-53E (Military)

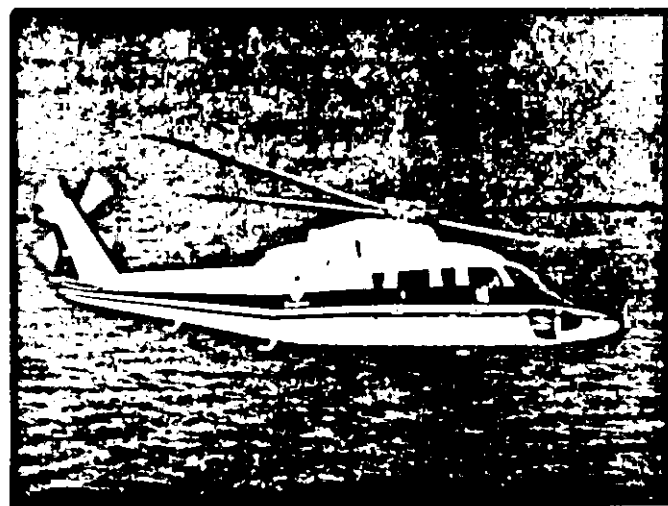


FIGURE 5 - Sikorsky S-76 (Commercial)

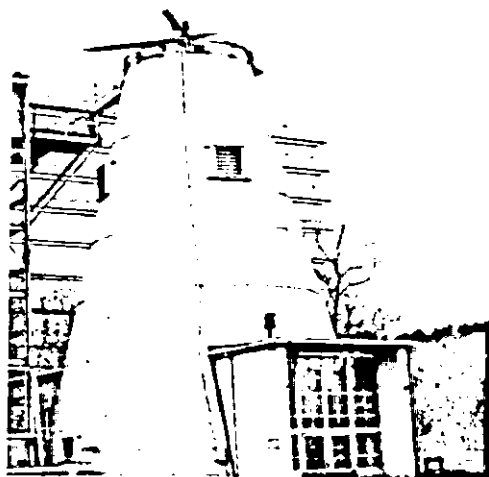


FIGURE 6. Main Rotor Whirl Test

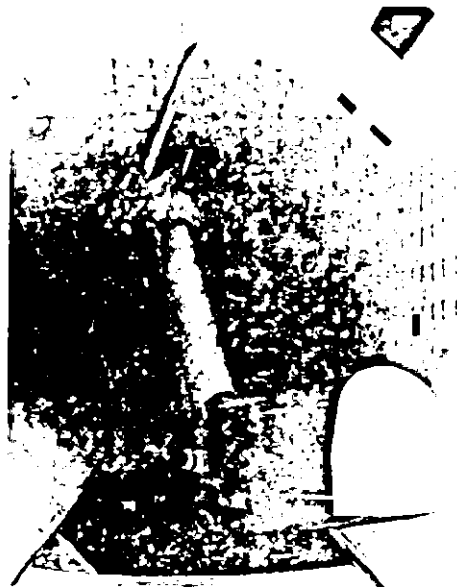


FIGURE 7. Tail Rotor Wind Tunnel Test

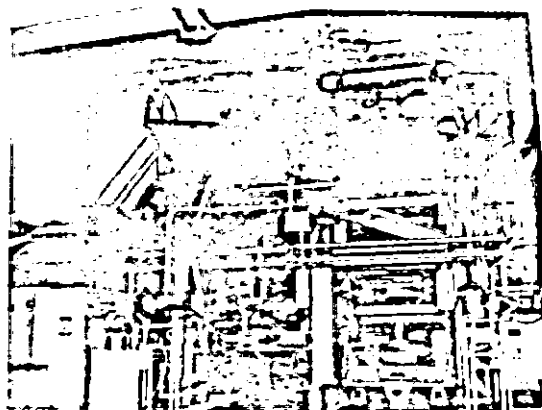


FIGURE 8. Main Transmission Test



FIGURE 9. Static Test

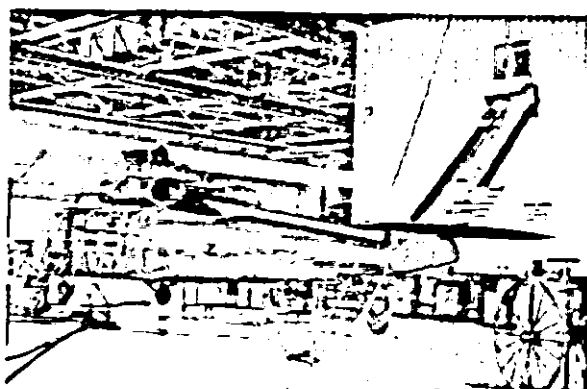


FIGURE 10. Aircraft Shake Test



FIGURE 11. Ground Test Vehicle

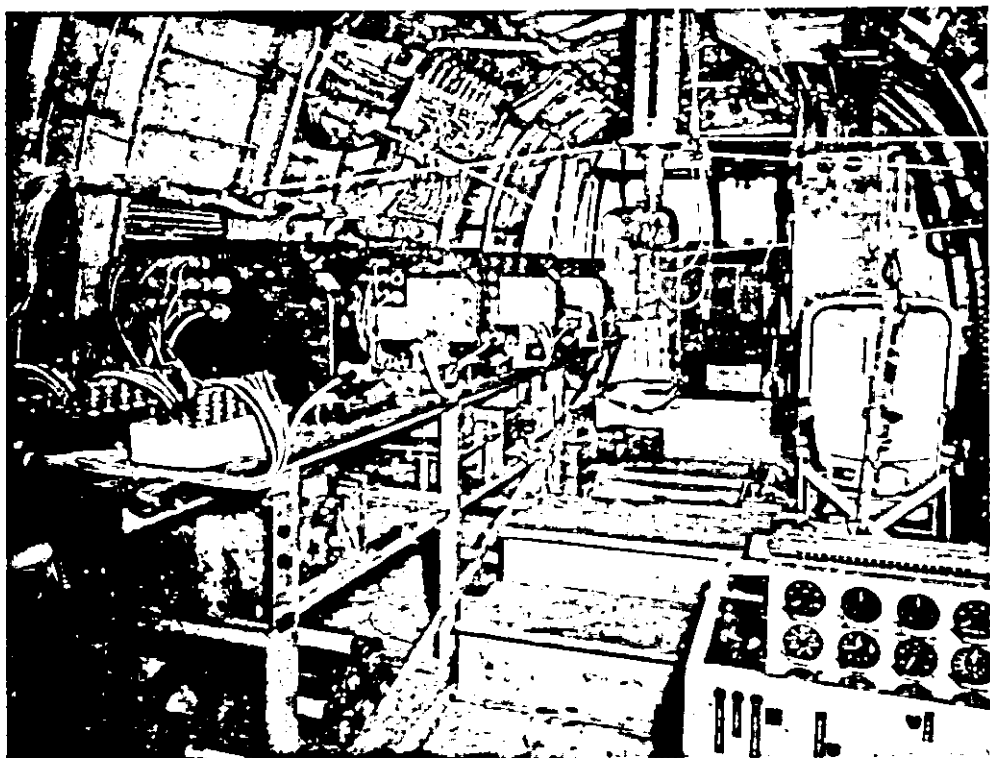


FIGURE 12 - Oscillograph Installation on Test Aircraft

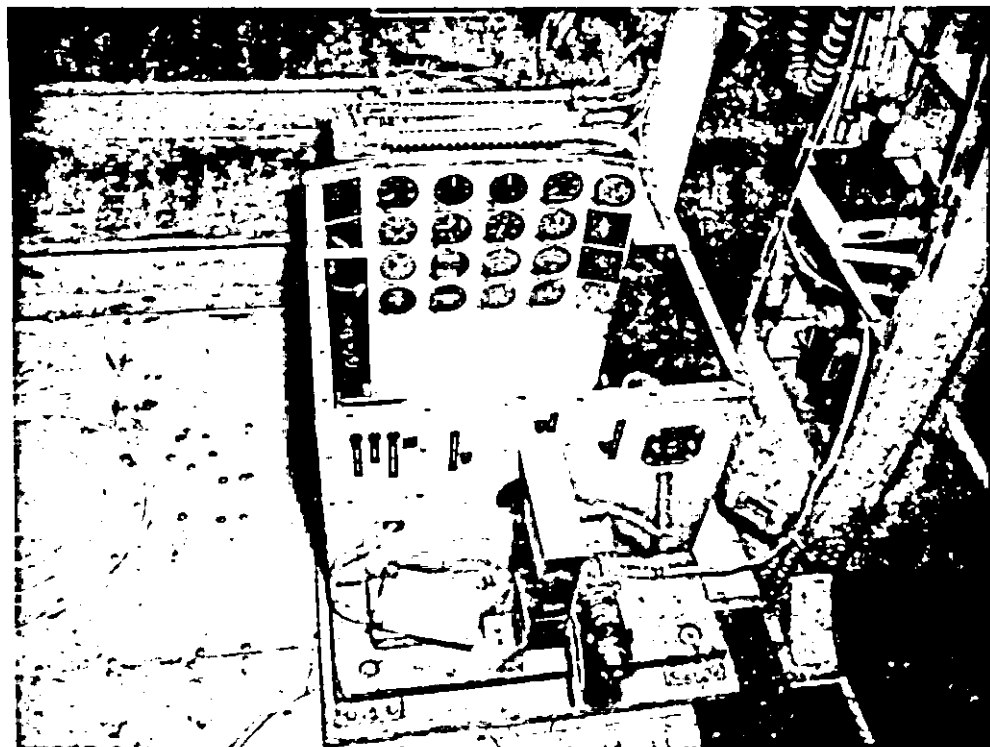
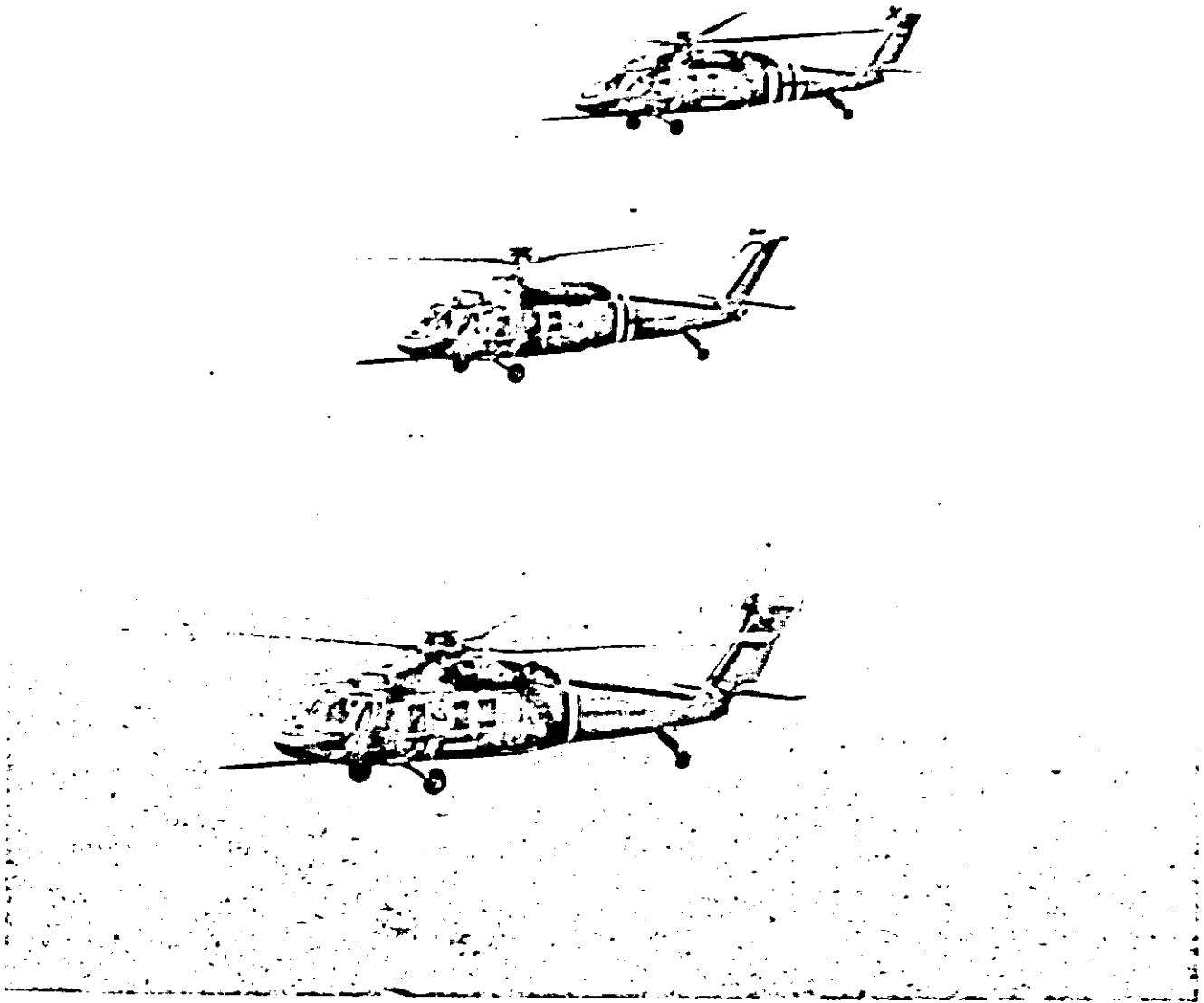


FIGURE 13 - Photopanel Installation on Test Aircraft



	<u>A/C I</u>	<u>A/C II</u>	<u>A/C III</u>
Primary Test Instrumentation	Structures/ Vibration	Handling Qualities	Powerplant/ Mission Equip.
Back-Up Test Instrumentation	Powerplant and Handling Qualities	Struct/Vibration Mission Equipment	Struct/Vibration and Handling Qualities

FIGURE 14 - Multi-Discipline Test Aircraft

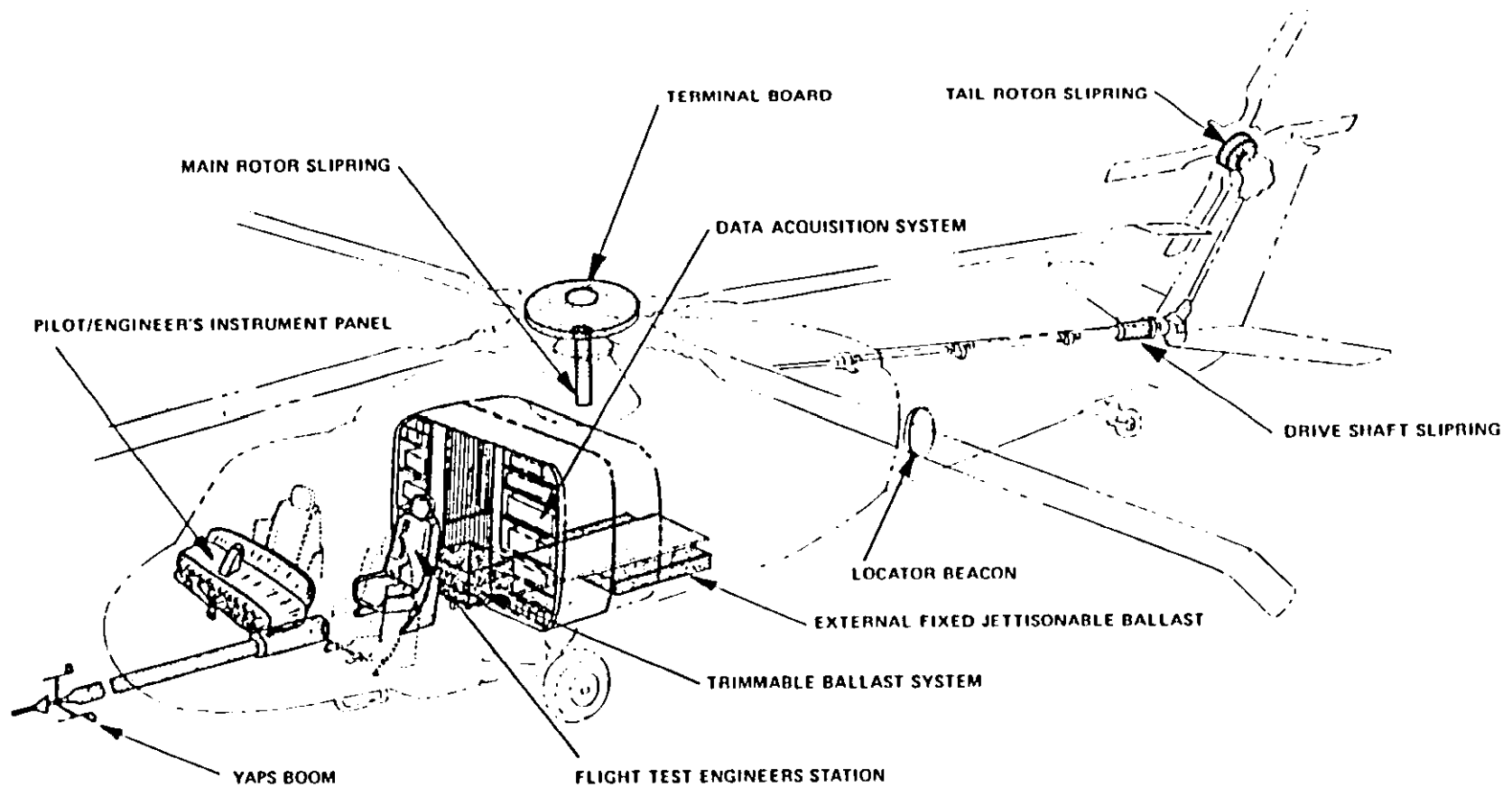
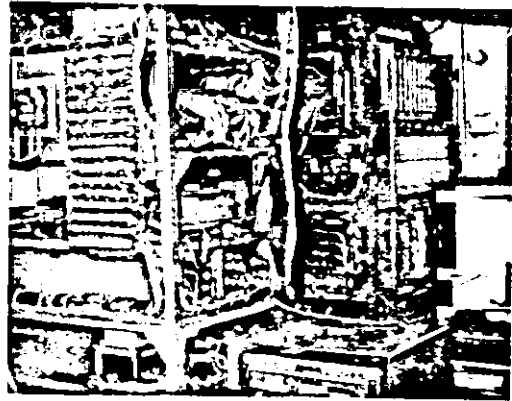


FIGURE 15 UH-60A INSTRUMENTATION SCHEMATIC



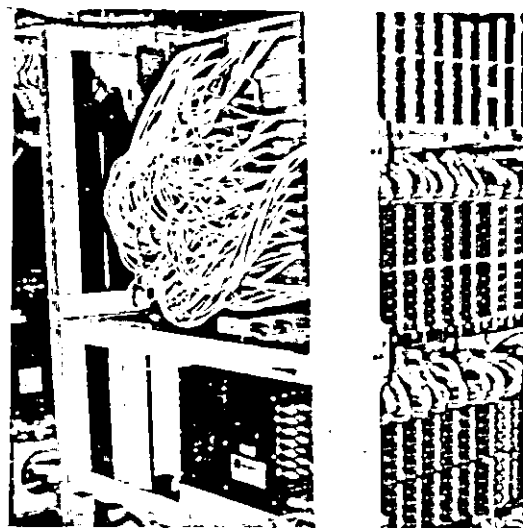
Instrumentation Installation

(a)



Instrumentation Installation

(b)



Programmable Patchboard

(c)



Trimmable Ballast Cart

(d)

FIGURE 16 - UH-60A INSTRUMENTATION INSTALLATIONS

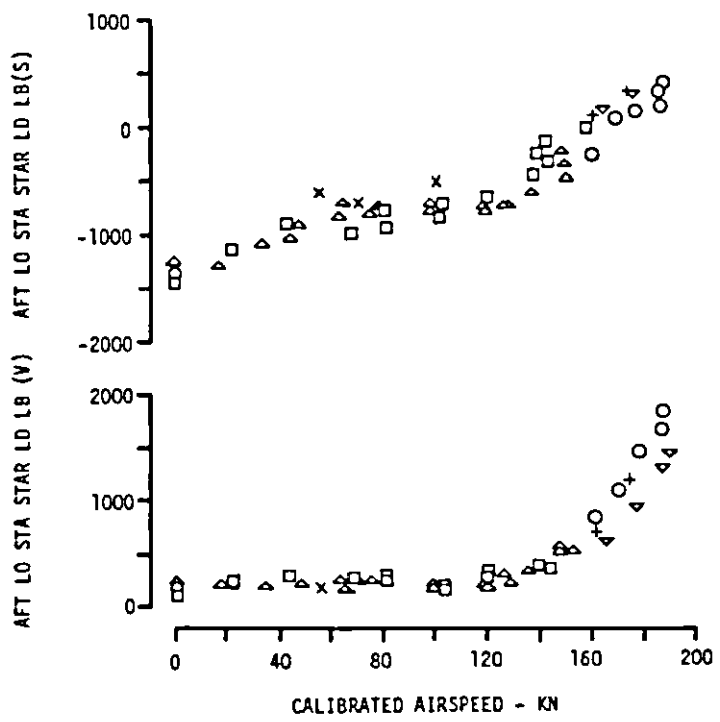


FIGURE 17 - Data Samples vs. Airspeed

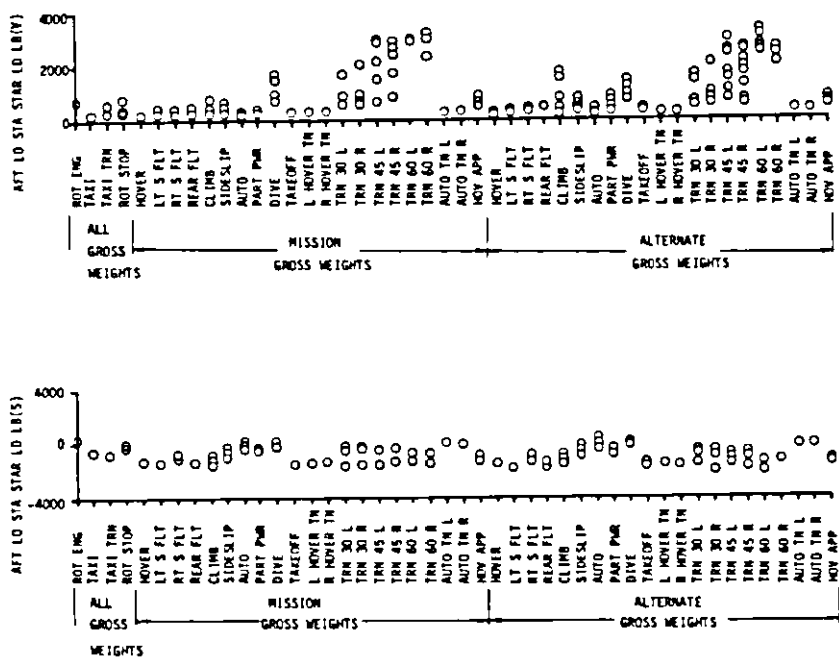


FIGURE 18 - Maneuver Loads vs. Mission Spectrum

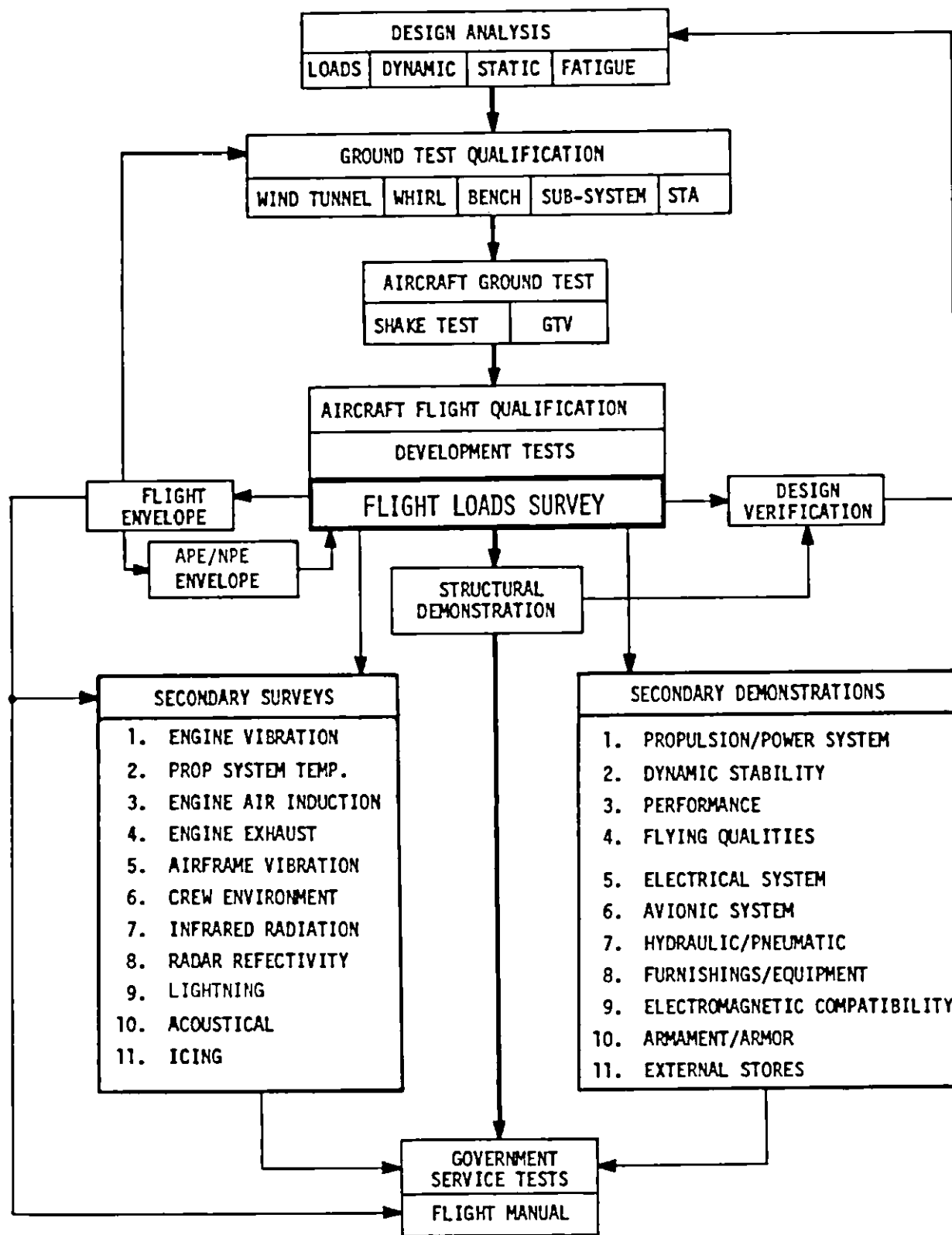


TABLE A

Interactions of Flight Loads Survey with Other Test Requirements

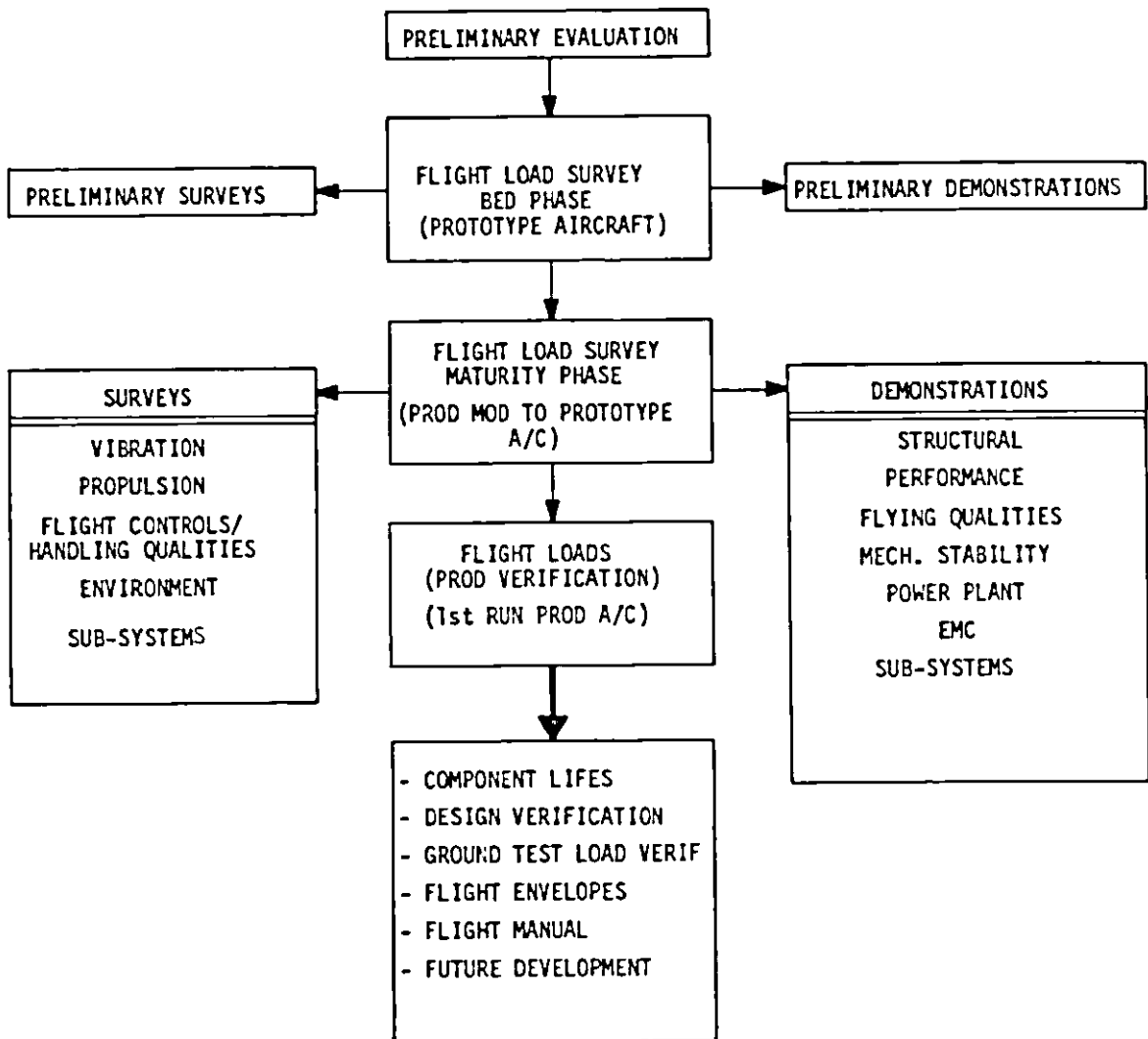


TABLE B
BLACK HAWK Airworthiness Flight Qualification

JP-8 FUEL CONVERSION EVALUATION

Robert A. Stambovsky
United States Air Force Flight Test Center
6510th Test Wing/TEES
Edwards Air Force Base, CA 93523

ABSTRACT

An evaluation was performed as part of an overall fuel conversion effort established by Headquarters United States Air Force (USAF) for land based jet aircraft to use JP-8 (NATO F-34 fuel). All USAF aircraft systems subject to operation in the North Atlantic Treaty Organization (NATO) theatre are effected. The San Antonio Air Logistics Center (SA-ALC), as system manager for the OV-10A, F-5 and the A-37B, requested that the Air Force Flight Test Center (AFFTC), Edwards Air Force Base, conduct a program to evaluate JP-8 fuel for normal use in the OV-10A, F-5 and A-37B aircraft. The objectives of this fuel conversion evaluation were to determine the suitability of JP-8 fuel for use in the aircraft and to identify any problems of operational significance which may exist.

Ground and flight tests were structured to collect data to support technical data changes authorizing JP-8 fuel and to determine the appropriate fuel category as a function of fuel control density settings and engine trim. Because it could not be assumed that the aircraft will be operating on one or the other fuel exclusively, testing was done with JP-4 and JP-8 in both "on" and "off" trim conditions; "off" trim meaning operating with a given fuel when the fuel control setting was adjusted for another fuel. The baseline case was JP-4 "on" trim. Specific tests which were accomplished included airstarts, throttle transients, low temperature tests, thrust stand tests, weight and balance, and smoke evaluation.

The JP-8 airstart tests were conducted at Edwards AFB, CA. Airstart attempts were made at altitudes from 5,000 feet to 20,000 feet pressure altitude. The low temperature ground tests were conducted at the McKinley Climatic Laboratory, Eglin Air Force Base, Florida. Test temperatures ranged from ambient (70 to 80 degrees F) to -50 degrees F in increments, including 0 degrees F, -25 degrees F, -40 degrees F, and -50 degrees F. Aircraft flight test instru-

Robert A. Stambovsky, Project Flight Test Engineer, 6510th Test Wing, Systems Branch, Flight Test Engineering Directorate

mentation was not available for the flight test evaluations. All aircraft data presented in this paper were manually recorded from production cockpit indicators.

Recommendations for limitations including airstart envelope, preheating procedures, fuel control gravity settings, were forwarded to be incorporated in the appropriate technical orders as a result of the engine performance during this evaluation using JP-8 fuel.

INTRODUCTION

This fuel conversion fuel program was established by Headquarters, U.S. Air Force, to determine the suitability of JP-8 Jet Fuel for normal use in NATO theatre USAF aircraft. Specific tests covered in this paper include low temperature ground starts, airstarts, weight and balance, throttle transient, and thrust stand performed using a production OV-10A and A-37B aircraft. Low temperature ground start testing was conducted using a production F-5E aircraft, and airstart tests were conducted on C-5A aircraft.

DISCUSSION

JP-8 vs JP-4 Fuel:

JP-8 (NATO code No. F-34) is a kerosene type fuel similar to jet A-1, properties of which are specified in MIL-T-83133. JP-4 (NATO code No. F-40) is a wide cut, gasoline type fuel. Properties of JP-4 are specified in MIL-T-5624K. A characteristics comparison is found in the following table.

JP-8 fuel has an increased average specific gravity as opposed to JP-4 (6.7 lb/gal vs. 6.5 lb/gal) as well as a higher flash point (100 + degrees F vs. \pm 10 degrees F).

The fact that JP-8 fuel exhibits a higher flash point and lower vapor pressure than JP-4 tends to lend itself to safer handling and less evaporation; however, JP-8 also exhibits a more limited airstart envelope capability, as well as adding an average of 0.20 pounds per gallon of fuel to the aircraft weight.

AIRCRAFT DESCRIPTIONS

The OV-10A test aircraft was a production twin engine observation/attack turboprop powered by two Garrett Air Research T76-G (L/H-10A, R/H-12A) center-rotating turboprop engines which produce 715 shaft horsepower each at sea level. The test aircraft was tested without armament or external fuel. The internal fuel system consists of four in-wing outboard fuel tanks which flow into a central wing

JP-4 AND JP-8 FUEL CHARACTERISTICS

<u>Characteristic</u>	<u>Fuel</u>	
	<u>JP-4</u>	<u>JP-8</u>
Flashpoint, deg C (deg F)	--	38 (100)
Density, kg/m ³ , min (degrees API, max) at 15 degrees C	751 (57.0)	775 (51.0)
Density kg/m ³ , max (degrees API, min) at 15 degrees C	802 (45.0)	840 (37.0)
Vapor pressure, 37.8 degrees C, psi, min	2.0	--
Vapor pressure, 37.8 degrees C, psi, max	3.0	--
Freezing point, degrees C (degrees F) max	-58 (-72)	-50 (-58)
Viscosity at -20 degrees C, max centistokes	--	8.0
Net heat of combustion, Btu/lb, min	18,400	18,400

feed tank incorporating motive flow type boost pumps. For starting, a fuel enrichment module feeds extra starting fuel directly into the engine combustor. This flow is automatically cutoff when exhaust gas temperature (EGT) reaches 450 ± 50 degrees C, or upon attaining 50 percent gas generator speed (rpm). This aircraft accommodates a two-man crew in tandem, and has a maximum gross take-off weight of 14,000 pounds, including 248 U.S. gallons of fuel.

The A-37B aircraft was a production twin engine attack/counter-insurgency (COIN) aircraft, powered by two General Electric J-85-17A single spool, axial flow engines each producing 2,850 pounds of military thrust at sea level. The test aircraft underwent airtstart testing with four pylon fuel tanks and two wingtip tanks attached. The internal fuel system consists of eight wing fuel cells, four leading edge fuel cells, tip tanks, and a fuselage feed tank incorporating a feed boost pump. This aircraft holds 468 U.S. gallons of fuel (453 usable), and has a gross take-off weight of 12,500 pounds. This aircraft accommodates a two-man crew (side-by-side) and has air refueling capability.

The F-5E aircraft was a production twin engine, single seat fighter, powered by two afterburning (A/B) General Electric J-85-21A single spool turbojets, each producing 3,500 pounds of thrust at military power and 5,000 pounds of thrust at maximum power (MAX A/B) at sea level. The test aircraft underwent low temperature testing while configured with two 150 gallon pylon tanks, and a 275 gallon centerline tank. The internal fuel system consisting of fore and aft fuselage tanks. The forward fuel cell holds 392 U.S. gallons, and the aft fuel cell holds 306 U.S. gallons. The forward cell feeds the left engine, while the aft tank feeds the right engine, however, there was a cross-feed capability. Fuel transfer from external tanks was accomplished by using engine compressor bleed air pressure to pump fuel back into the fuselage tanks.

LOW TEMPERATURE TESTS

Test Objective:

The objective of these tests was to determine suitability of JP-8 for cold weather ground starting and operation in A-37, OV-10A, and F-5E aircraft. The evaluation was to be accomplished with the engines in the on and off trim conditions. Test results would be analyzed for cold weather operation information which would be added or amended in the aircraft flight manuals.

Test Method:

The low temperature testing was conducted at the McKinley Climatic Laboratory, Eglin AFB, FL. During a six week test period, the test aircraft were subjected to temperatures ranging from ambient (70-80 degrees) to -50 degrees F. The aircraft were positioned on jack stands in the climatic chamber, after which they were secured to the laboratory floor by using grounding cables. The tie down procedure was to prevent any turning of the aircraft due to assymetrical loading during engine runs.

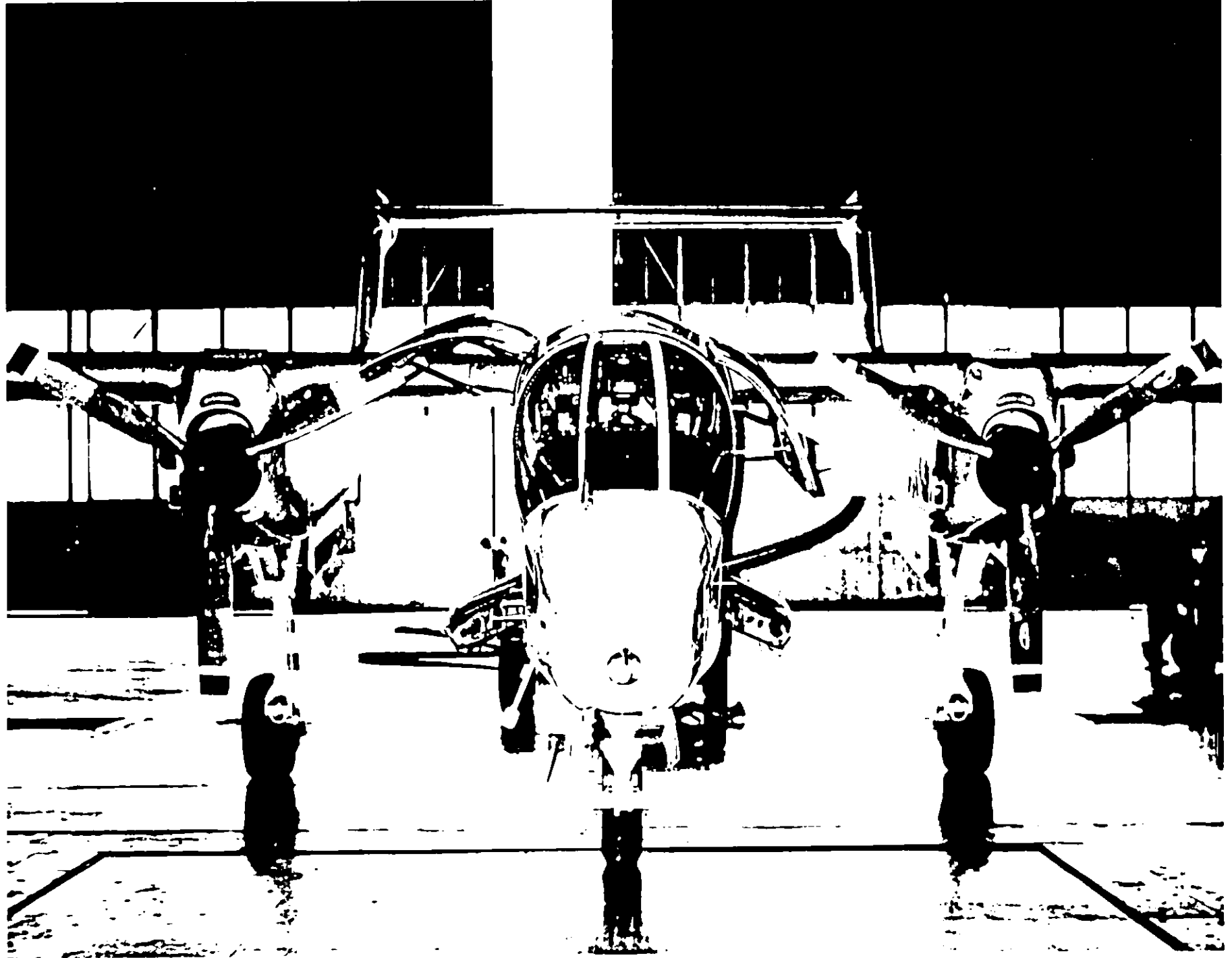
The test engines were started and run at various temperature intervals between 0 degrees F, and -50 degrees F. All starts were performed according to flight manual procedures. Instrumentation consisted mainly of thermocouples placed in the aircraft fuel tanks to observe aircraft fuel temperature, thermocouples placed at the nose and wingtips of the aircraft to monitor ambient temperature. Engine parameters were hand recorded from the cockpit indicators. Cold soak periods between the start attempts averaged 24 hours. Fuel samples were taken prior to engine run as well as after refueling.

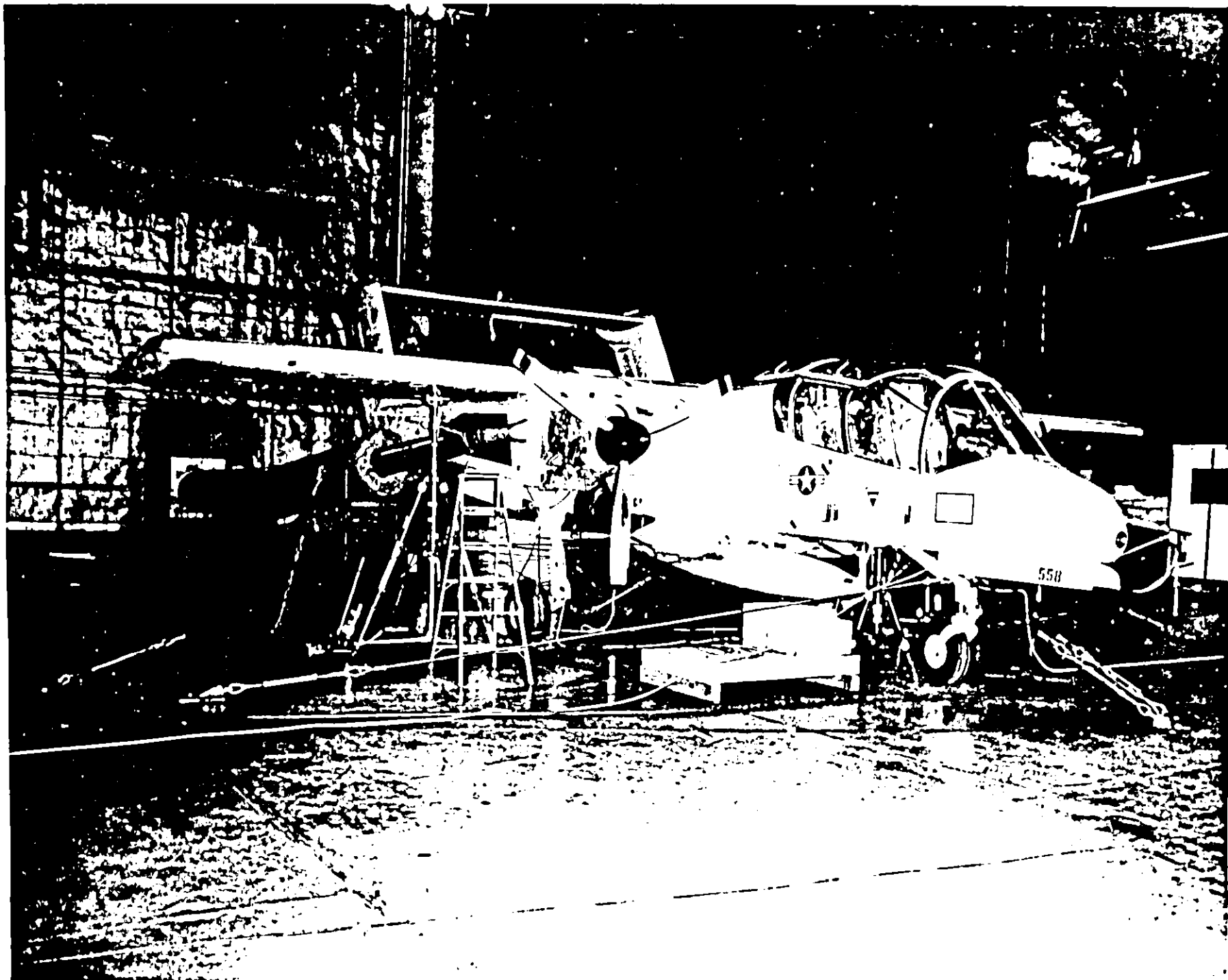
The required preheating was accomplished by using an H-1 gas/electric heater, which output varied between 130 degrees to 145 degrees F, in proportion to the laboratory temperature. Heat was applied to the engine area 30 minutes prior to the start attempts.

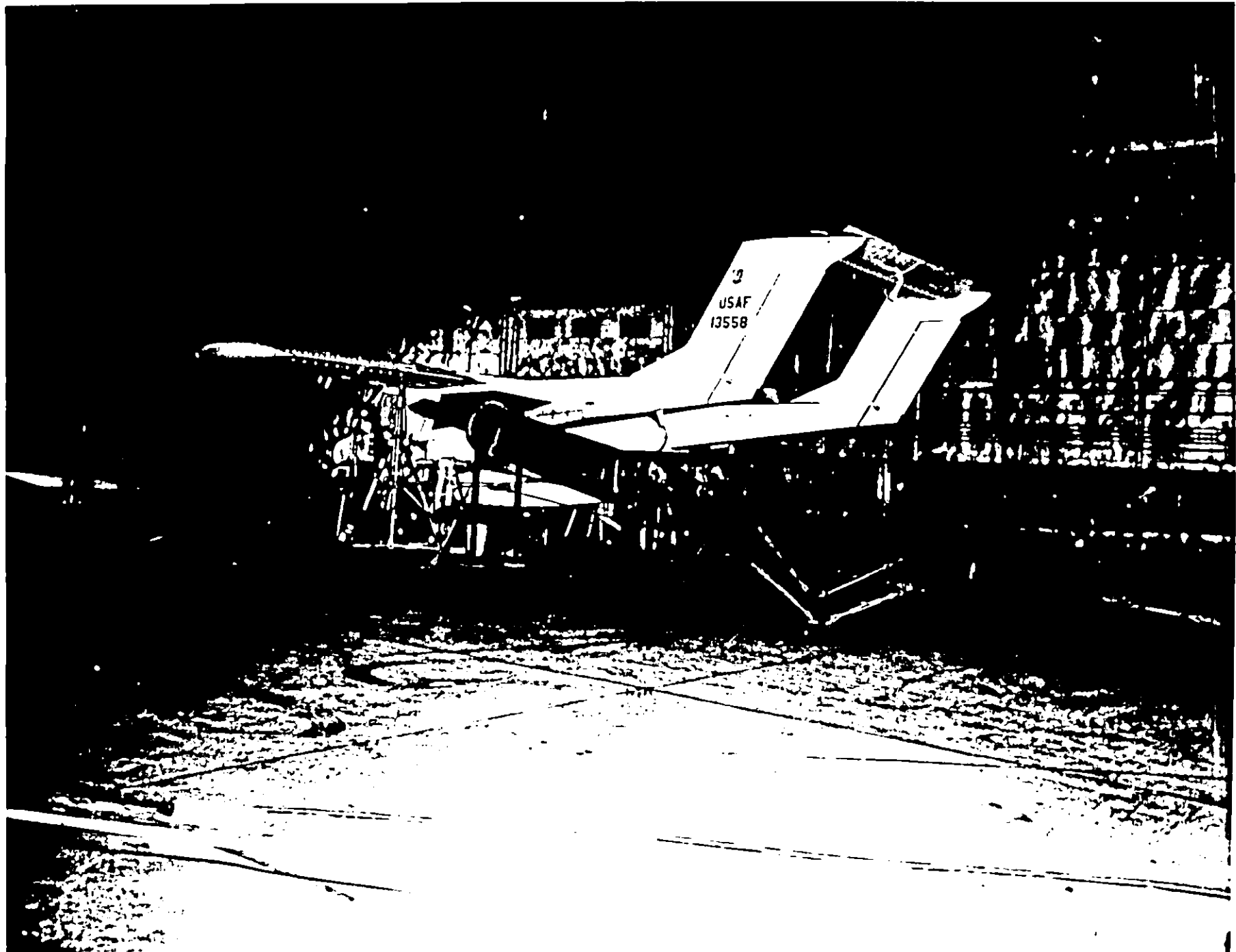
Engine starts and run cycles were conducted both on and off trim for the same test condition, using JP-4 fuel/JP-4 trim as baseline data at the various outside air temperatures. Engine run cycle was from stabilized idle to stabilized military power.

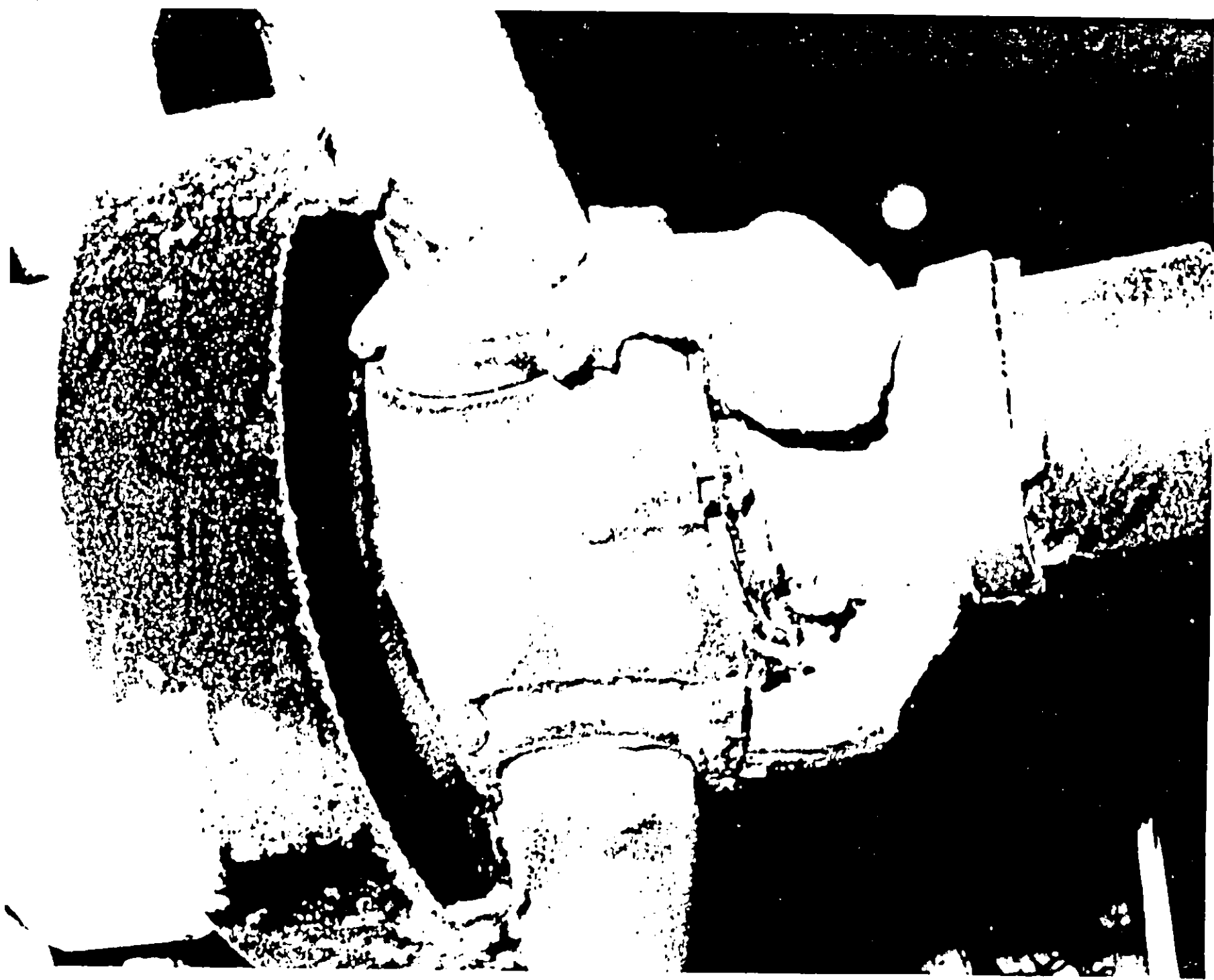
Test Results:

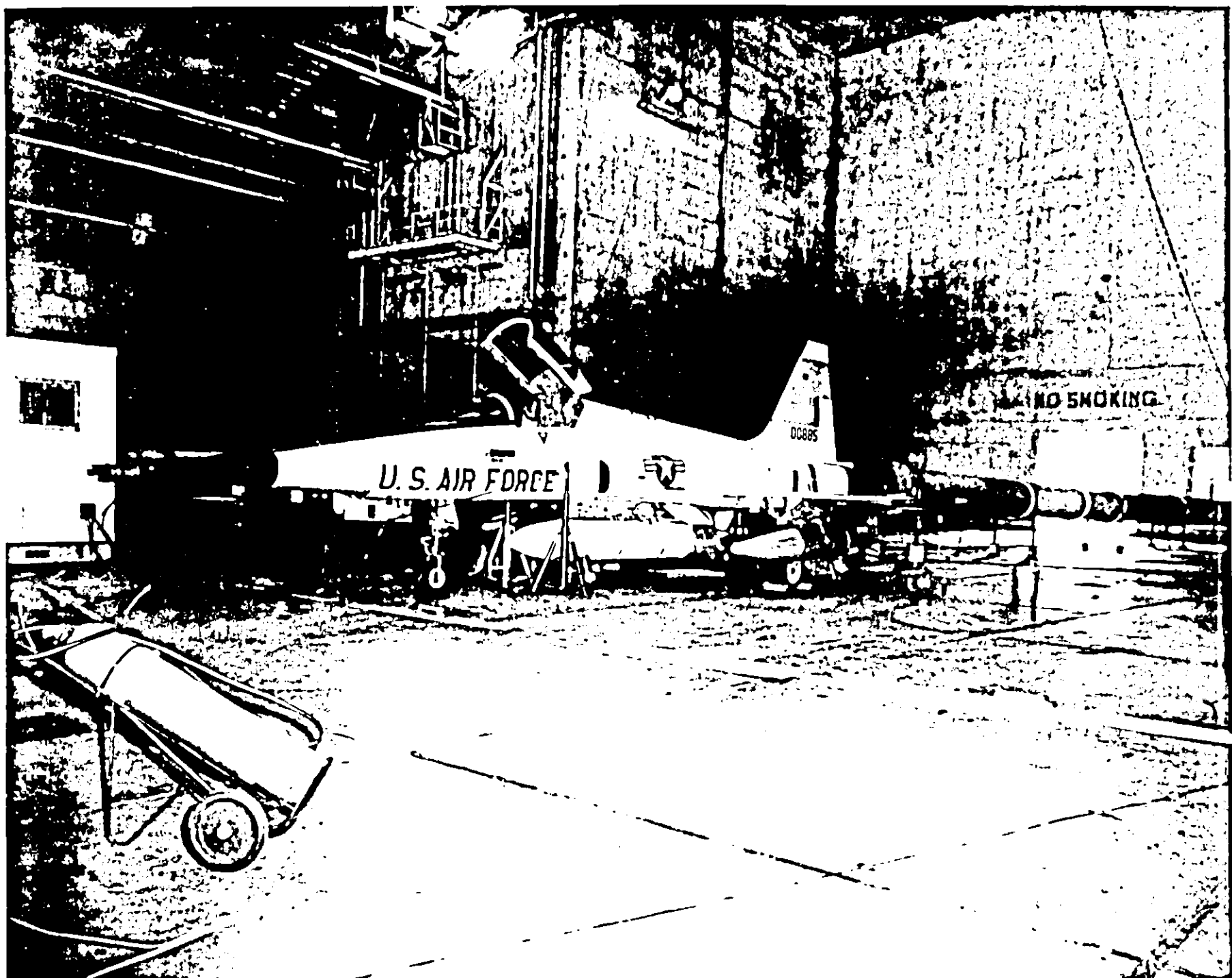
Both OV-10A aircraft engines were started at 0 degrees F without prior heating. During the starts and runups, all engine parameters remained within operating limits while using both fuels at both trim conditions. When engine starts were attempted below -25 degrees F, a 90 percent rpm upper limit for engine runs to preclude possible over-torquing the engines.

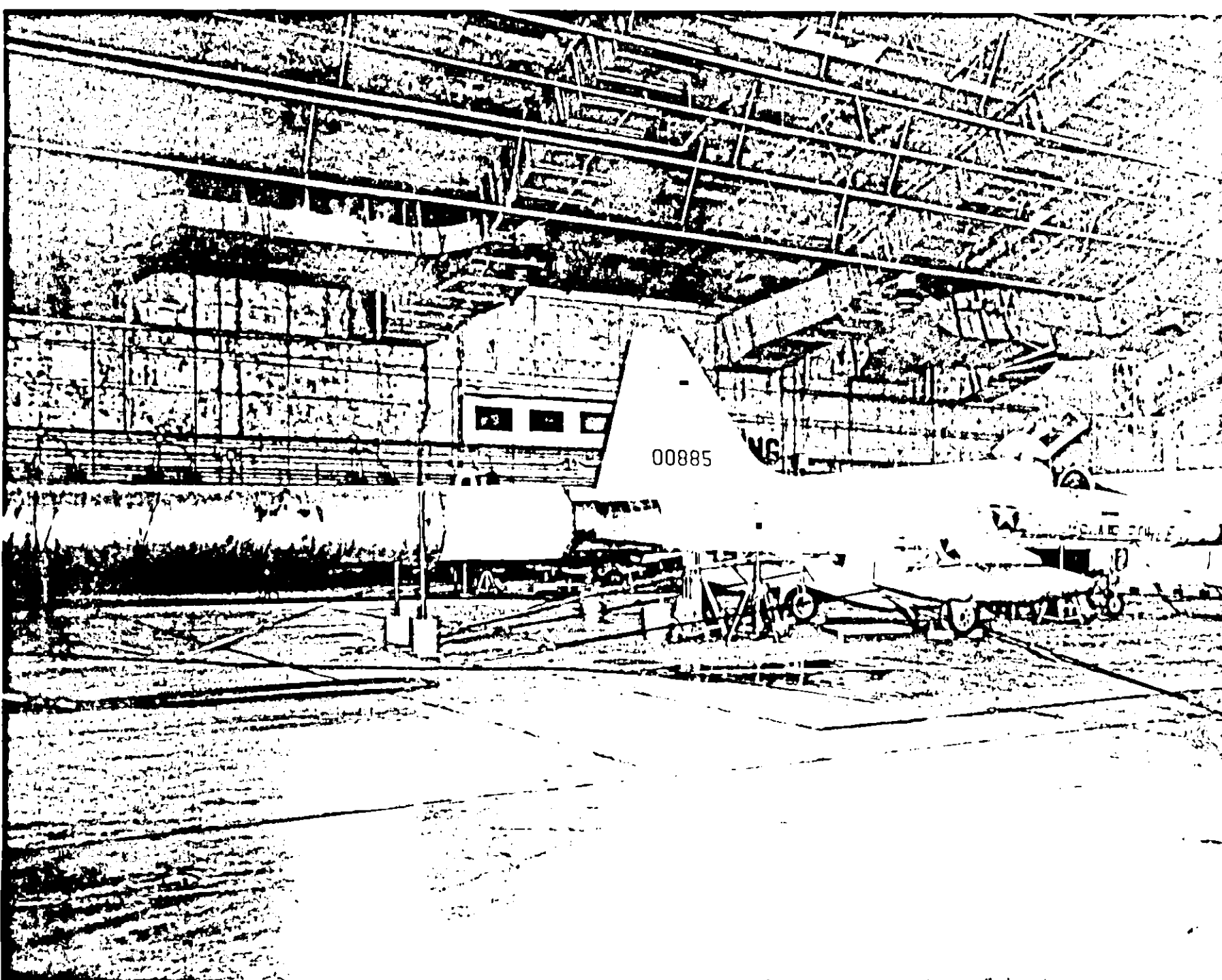


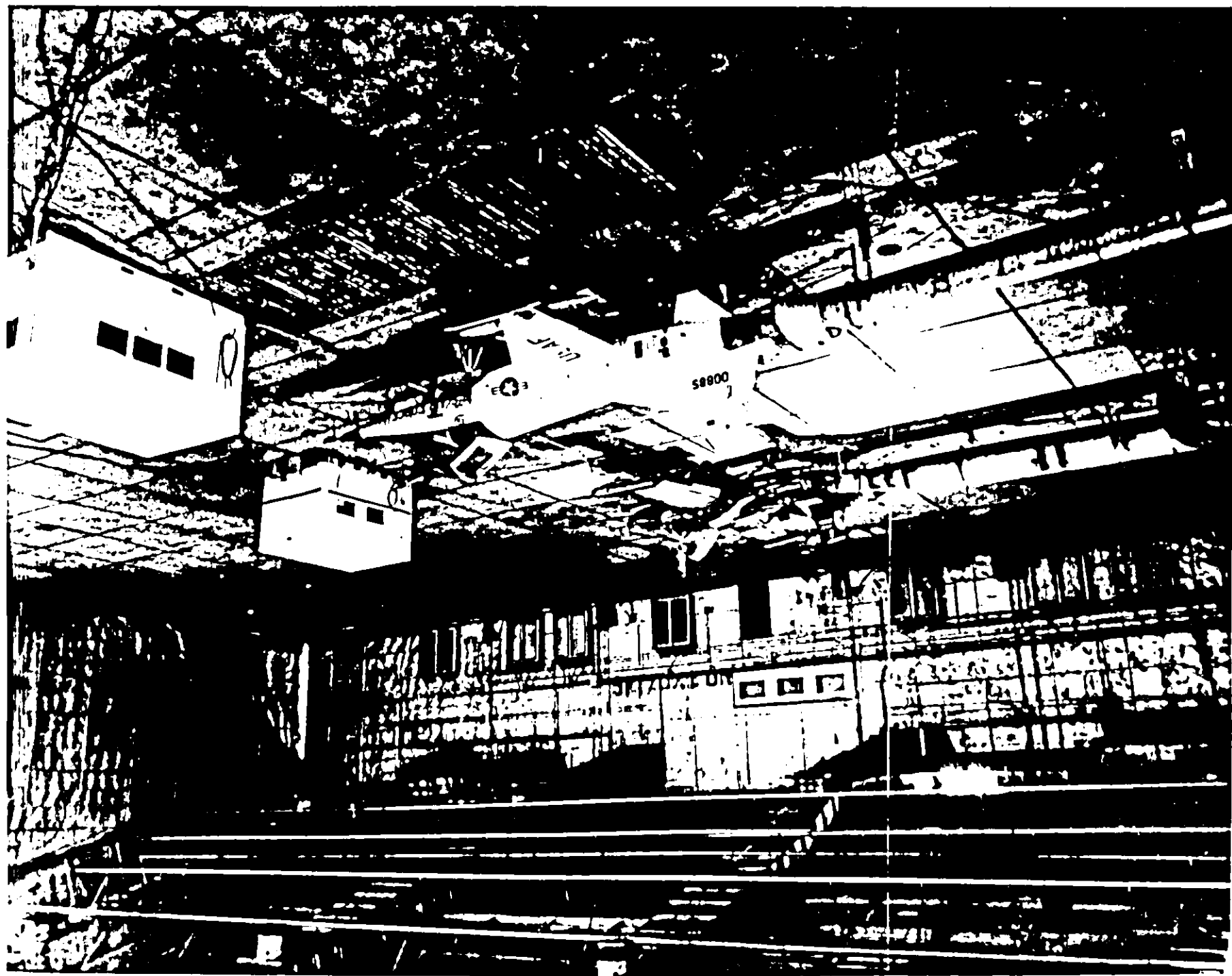


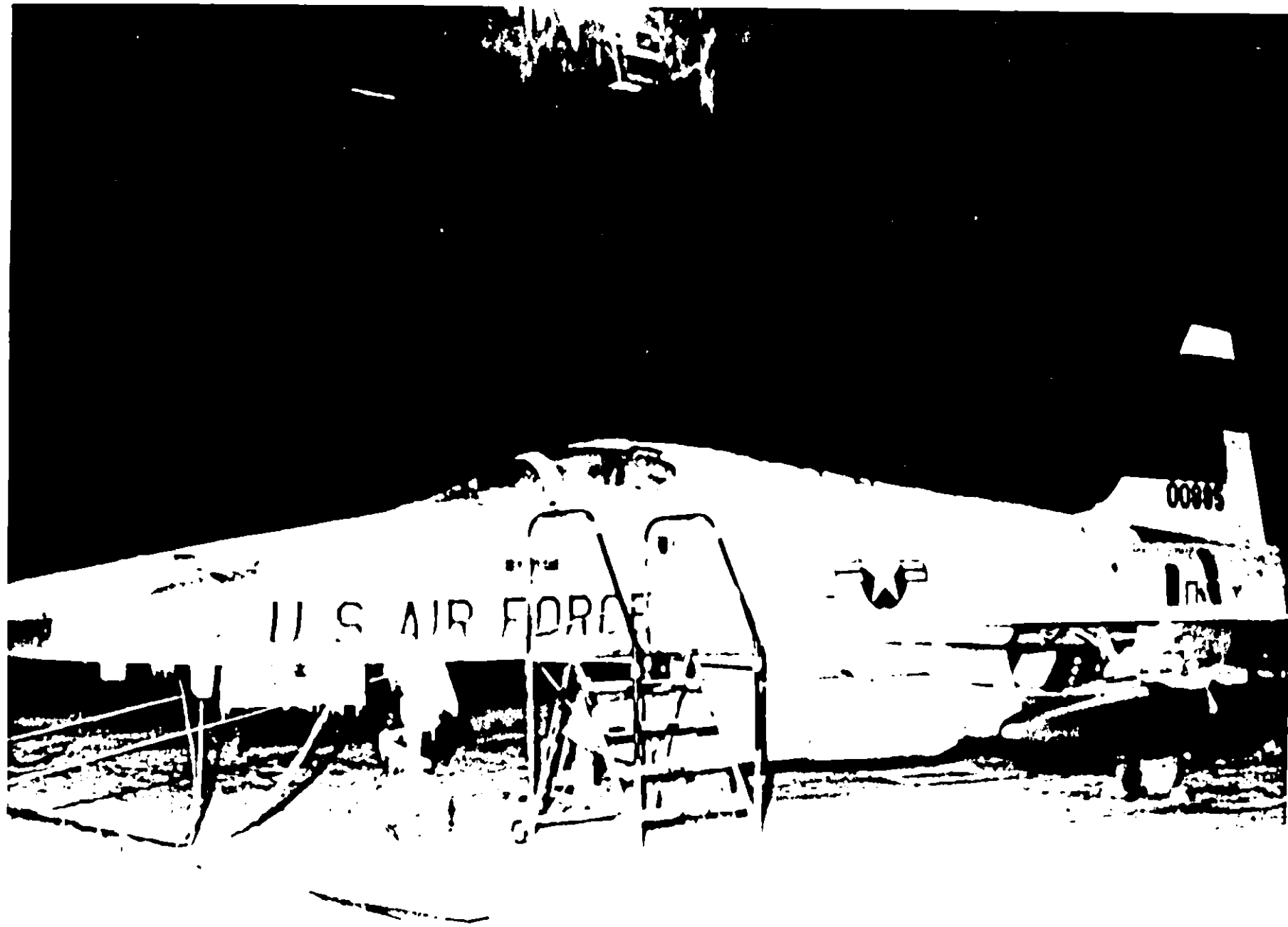












Both engines of the F-5E aircraft could be started at all temperature ranges while using JP-4 with either trim. In most cases, engine start times were in excess of the flight manual limit, however, no engine run problems evolved from excessive start times. JP-8 with either trim exhibited no significant change in thrust.

Both engines in the A-37B aircraft required preheating below -25 degrees F, regardless of fuel type or trim for a period at least twenty minutes prior to the start attempt. No significant difference was noted during cold weather starts while using JP-4 on and off trim, or JP-8 fuel on trim. JP-8 off trim exhibited slightly higher peak EGT during the start sequence however, engine parameters remained within limits.

AIRSTART TESTS

Test Objective:

The objective of these tests was to evaluate the A-37B, C-5A, and OV-10A airstart envelope using JP-4 and JP-8 fuels, on and off trim. Nominal test points within the current JP-4 airstart envelope were selected to obtain a viable cross-section of the aircraft operational altitudes and airspeeds.

Test Instrumentation:

Data for the airstart tests consisted of flight and engine parameters manually recorded from production aircraft instruments. Time to ignition and idle were measured with a stopwatch.

Test Method and Conditions:

The OV-10A airstart envelope used for this evaluation was derived from the Engine Operating and Start Limits (pressure altitude vs. Mach number) envelope presented in the T76 engine model specification SC-5715-3. The airstart test points for both the OV-10A and A-37B aircraft were 20,000 feet pressure altitude (PA) 100 knots indicated air-speed (KIAS), 130 KIAS, 155 KIAS; 15,000 feet PA 100, 130, and 155 KIAS; 10,000 feet PA 100, 130, and 155 KIAS; and 5,000 feet PA 100, 130 and 155 KIAS.

The test engine was airostarted from the feathered condition using the Flight Manual procedures and starting limits. As a safety precaution, the initial airostart for each fuel/trim combination was at a nominal point of 10,000 feet PA and 130 KIAS. Times to ignition and idle were measured from Airstart Switch ON, and engine ignition was determined by an increase in EGT. An airostart was considered successful if the engine attained idle speed and if engine parameters remained within aircraft flight manual limits. The Starting Fuel Module was installed and operational for these tests.

A-37B airostart data were obtained during airostarts with the engine inlet screens both down and up. At selected points, the engine was cold soaked for a minimum of five minutes prior to the airostart attempt. Aim airspeed and altitude were established with the test engine at idle power. The test engine was shut down, and the airostart was attempted when windmill rpm had stabilized or at the end of the cold soak period. The Flight Manual normal airostart procedure and emergency airostart procedure for double engine failure during flight were used, except that the engine starter was not activated for the emergency procedure. Airostarts using the emergency procedure are referred to as windmill airostarts in this report. Times to light off and idle were measured from throttle to idle, and engine light off was determined by an increase in EGT. An airostart was considered successful if the engine parameters remained within limits and if the time to idle was 40 seconds or less.

C-5A airostart attempts were performed with engines number 2 and number 4. Aim airspeed and altitude were established with the test engine held at idle power for five minutes for engine temperature stabilization prior to shutdown. An unassisted airostart was attempted when windmill revolutions per minute (rpm) had stabilized. If the unassisted airostart was unsuccessful, an assisted airostart was attempted. The initial airostart attempt at a given altitude and airspeed was assisted if the previous higher airspeed point at the same test altitude required an assisted airostart with that engine. Flight Manual airostart procedures were used. For one JP-4 and JP-8 airostart, a one hour cold soak preceded the airostart attempt. Times to idle and ignition were measured from fuel and start ignition switch to AIR START for unassisted starts or to RUN for assisted starts. Engine light off was determined by an increase in Turbine Inlet Temperature (TIT). An airostart was considered seccessful if:

1. The engine parameters remained within limits.
2. The time to ignition was 30 seconds or less.
3. The time to idle was two minutes or less.

APU airstarts were also attempted at various airspeeds and altitudes. Airstart attempts were performed with both the LH and RH APUs. An APU airstart was considered successful if limits were not exceeded and the CN SPEED light illuminated within the aim times. Time to ON SPEED was measured from APU control switch to START/RUN.

Test Results:

For the seven successful airstarts, peak EGT's averaged 713 degrees C. The initial precautionary airstart at 10,000 feet PA, 130 KIAS, was successfully accomplished with a peak EGT of 780 degrees C. Two other 10,000 feet PA airstarts were successfully accomplished at airspeeds of 100 to 155 KIAS. Five other airstart attempts were unsuccessful due to overtemperature tendencies. Of seven airstart attempts at 15,000 feet PA, only two were successful, both of which were performed above 155 KIAS. Peak EGT's for these starts reached 730 and 750 degrees C. A third attempt above 155 KIAS was unsuccessful due to overtemperature tendency (795 degrees C peak EGT). All JP-8/JP-4 airstart attempts at 5,000 feet PA and below 155 KIAS were aborted as EGT reached 800 degrees C during the start.

Airstart performance with JP-4 fuel, on and off trim, was satisfactory. Airstart performance with JP-8 fuel on trim was satisfactory. Peak EGT's during these airstarts were approximately 100 degrees C higher than the baseline case. Based on airstart performance with JP-8 fuel, the T76 engine fuel control density setting should be adjusted to 0.82.

Experience with other aircraft indicates that airstart performance is significantly improved when a starter assist procedure is used. The OV-10A Flight Manual does not contain a starter assist procedure for airstarts.

A total of 118 normal and 22 windmill airstarts were attempted during the A-37B airstart tests. For all airstart attempts, the stabilized engine windmill speed was above the six percent minimum specified in the Flight Manual.

A total of 36 assisted and 47 unassisted airstarts were attempted with the C-5A aircraft. Evaluation of airtstart test results indicate slightly degraded airtstart performance for JP-8 when compared to JP-4 at 35,000 feet pressure altitude. At 30,000 feet and below airtstart performance on either fuel was comparable. Comparison with Category II Evaluation of the C-5A Propulsion System indicated similar results were achieved for JP-4.

An airtstart attempt after a one hour engine cold soak was performed with both JP-4 and JP-8 fuel. A successful unassisted airtstart was achieved on JP-4 fuel. The cold soaked JP-8 engine was successfully started without assist.

No specific airtstart envelope is delineated in the Flight Manual. The Flight Manual states that normal airtstarts will be made with starter assist. The Flight Manual also states that unassisted airtstarts can "probably" be made if N₂ rpm is greater than 10 percent below 10,000 feet or minimum of 210 KIAS is maintained above 10,000 feet. According to the Flight Manual, airtstarts can be accomplished up to 30,000 feet and can be attempted at higher altitudes. Results of this test with both JP-4 and JP-8 fuels generally confirm the preceding statements. Unassisted JP-8 airtstarts were attained consistently at 25,000 feet when above 210 KIAS.

Smoke was observed during three JP-8 airtstarts. No smoke was observed during airtstarts with JP-4.

APU airtstarts were accomplished at both 15,000 feet and 25,000 feet with both JP-4 and JP-8 fuels. One JP-8 APU airtstart had a peak EGT of 810 degrees C (limit is 815 degrees C).

Overall engine airtstart performance with JP-8 was adequate. No change to the existing Flight Manual procedures or notes is required for airtstarts for JP-8 fuel.

THROTTLE TRANSIENT TESTS

Test Objective:

The objective of these tests was to evaluate compressor stall/engine flameout susceptibility during throttle transients when using JP-4 and JP-8, both on and off trim.

Test Instrumentation:

Data for the throttle transient tests consisted of flight and engine parameters manually recorded from production aircraft instruments.

Test Method and Conditions:

The OV-10A throttle transient test sequence consisted of rapid (one second or less) accelerations from flight idle to military (accels), rapid decelerations from military to flight idle (decels), and interrupted decelerations

with return to military (bodies). The test engine was allowed to stabilize before initiation of power lever movement. Throttle transients were performed in straight and level 1-g flight, and during steady heading sideslips with full left and right rudder deflection, Dutch roll (yaw damper off), and windup turn (3-g) maneuvers. The aircraft was tested in the cruise (CR) and power approach configurations. Test points were: 5,000 feet PA, 100 KIAS; 10,000 feet PA, 155 and 180 KIAS; and 15,000 feet PA, 155 and 180 KIAS. As a safety precaution, the test engine was airstarted at 10,000 feet PA, 130 KIAS, at the beginning of each throttle transient test flight.

A-37B aircraft transients consisted of rapid (one second or less) accelerations from idle to military (accels), rapid decelerations from military to idle (decels), and interrupted decelerations with return to military (bodies). The test engine was allowed to stabilize before initiation of throttle movement. Throttle transients were performed in straight and level (S&L) 1-g flight, and during steady heading sideslips (SHS) with full left (L) and right (R) rudder deflection, Dutch roll (DR), and windup turn (WUT) maneuvers. The aircraft was tested in the cruise (CR) and power approach configurations. The left engine was the primary test engine.

The throttle transient series for the C-5A aircraft consisted of:

1. An accel from idle to military power (in one second or less).
2. A decel from military power to idle (in one second or less).
3. A bodie which consisted of an accel (in one second or less) to military power with the throttle held at military for at least one second followed by a decel to idle in one second or less.

The aircraft's number 2 and 4 engines were used for these tests. At each flight condition the target EPR for military power was determined from Flight Manual data. The pilot marked the throttle quadrant position that developed the target EPR prior to throttle series at the test flight condition. Throttle transients were performed in straight and level 1-g unaccelerated flight and during steady heading sideslips. Sideslips were performed in a direction such that the yawing moment due to the throttle transient would tend to restore the aircraft to straight flight. For example, an accel and a bodie on number 2 engine was performed in a left sideslip. Tests were performed in both cruise and power approach configurations. All tests were performed on both test engines. Selected points were performed with engine anti-ice on.

Test Results:

Both JP-4 and JP-8, on and off trim, in straight and level flight, exhibited no adverse characteristics during accels, decels, or bodies at any of the test conditions with the OV-10A aircraft. Throttle transients during steady heading sideslips, with full rudder deflection, exhibited no engine stall tendencies with either JP-4 or JP-8, on and off trim. Windup turns were conducted at only one altitude (10,000 feet PA, 180 and 155 KIAS) due to time restraints and power available limitations. Accels, decels, and bodies using both fuels, on and off trim, exhibited no adverse characteristics. Dutch roll testing was conducted at 10,000 feet PA, 155 and 180 KIAS, with the yaw damper off. Accels, decels, and bodies performed at these test points had no adverse effect on engine operation with either fuel, on and off trim.

Peak EGT's obtained during throttle transient tests should be considered inaccurate due to the extreme lag exhibited by the EGT indicator. This lag was most apparent during body transients when the EGT continued to decrease, even after the power lever was returned to military.

A-37B data reflected that of the 275 throttle transients on the left engine, four resulted in stall and engine flameout, and one resulted in a self-recovering stall.

The four stall/flameout conditions occurred during SHSL maneuvers at 25,000 feet PA and 160 KIAS with the speed brake extended. Two of these stall/flameout cases were during operation with JP-8 fuel/JP-8 trim, and one each was during operation with JP-4/JP-8 and JP-8/JP-4. Since these stall/flameout events occurred while operating with differing fuel/trim combinations but during identical maneuvers and test conditions, engine inlet airflow distortion was the suspected cause. With a positive sideslip angle, the left engine inlet is in a region of disturbed airflow from the forward fuselage. This airflow is further disturbed by extension of the speed brake. To verify this suspicion, throttle transients were performed on the right engine during SHSR (negative sideslip) maneuvers with the speed brake extended. The results were similar with two occurrences of stall/flameout in three attempts. The Flight Manual discussion of engine compressor stalls indicated that the engines are highly susceptible to stall and flameout during throttle transients in high g maneuvers with the speed brake extended. The Flight Manual discussion of engine stall/flameout susceptibility should also include uncoordinated flight maneuvers with the speed brake extended as a major contributing factor to engine stall and flameout.

The self-recovering engine stall occurred during a body transient in 1-g, S&L flight at 25,000 feet PA and 250 KIAS. The fuel/trim combination for this test was JP-8/JP-4.

With the JP-4/JP-4 condition as baseline, acceleration times were lower and peak fuel flows were higher for the JP-8/JP-4 configuration. For the JP-4/JP-8 condition, peak fuel flows were lower with no significant difference in acceleration times.

The test results demonstrated that there was no increase in compressor stall/engine flameout susceptibility when operating with JP-8 fuel, on trim. Off trim operation with JP-8 fuel may result in increased compressor stall susceptibility due to decreased acceleration times and higher peak fuel flows. Although not clearly demonstrated by these tests, operation with JP-4/JP-8 could result in speed hangup during acceleration or slow acceleration. The J85-GE-17A engine fuel control density setting should be adjusted to the value specified in T.O. 1A-37B-2-5 for the fuel being used.

No engine stalls or flameouts with either JP-4 or JP-8 fuel were experienced during any of the 245 throttle transients performed on the C-5A aircraft. Eight of the 113 throttle transients with JP-4 resulted in a slow accel (greater than 20 seconds). Of those eight slow accels, six occurred during anti-ice ON points. Five of the 132 JP-8 throttle transients resulted in a slow accel. All five of the JP-8 slow accels were during anti-ice on points. Slow accels with anti-ice selected was a phenomenon experienced during Category II tests. Engine performance during throttle transients with JP-8 was not degraded over JP-4 performance for any condition tested. The TF39-GE-1A engine requires no change in pilot throttle technique when using JP-8 fuel.

WEIGHT AND BALANCE TESTS

Test Objective:

The objective of these tests was to evaluate weight and balance changes between JP-4 and JP-8 fuels.

Test Instrumentation:

These tests were performed in the AFFTC Weight and Balance Facility. This facility is equipped with four Fairbanks-Morse flush mounted mechanical platform scales each with a capacity of 300,000 pounds, a volumetric fuel flow meter, and fuel specific density/temperature measuring equipment.

Test Methods and Conditions:

The OV-10A aircraft was fueled with JP-4 prior to being positioned on the weighing scales. The aircraft was weighed and the center of gravity was computed. The aircraft was defueled and weighed in increments. When the aircraft was defueled, the final weight and balance was performed.

Due to time restraints, the only JP-8 weight and balance performed was that of full fuel load. The aircraft was fueled with JP-8 and weighed. Full fuel balance was then performed.

Both JP-4 and JP-8 weight and balance was computed by using the information in T.O. 1-1B-40, DD 365B, aircraft #66-13558, and the specific density of the fuels determined at the weight and balance laboratory.

The A-37B weight and balance calibration was performed in accordance with T.O. 1A-37B-56. Initially the aircraft was defueled into a fuel truck. Additional fuel was drained from the wing and fuselage tanks through the defueling valve, and each tip tank was drained through the drain valve located on the bottom of the tank. The fuel remaining aboard after defueling in this manner was trapped fuel. The aircraft weight and center of gravity (cg) with trapped fuel was determined. The aircraft was then fully fueled using the over-the-wing procedure described in the Flight Manual, and the weight, cg, and indicated fuel quantities were recorded. The aircraft was incrementally defueled from the fuel feedlines located on the engine firewalls. Normal in-flight fuel sequencing (tiptanks, then internal fuel) was used. At each increment the aircraft was leveled and weighed, the cg was determined, and the indicated fuel quantities were recorded. The fuel remaining onboard after defueling in this manner was unusable fuel. Over-the-wing refueling was then performed in two increments with data recorded at each increment.

Fuel system operating characteristics were evaluated concurrently with the weight and balance calibration. Fuselage tank fuel quantity levels were recorded when the proportioner pumps started and shutoff and when the low fuel indicator illuminated and the fuel gravity feed system actuated.

Fuel samples were taken, and the fuel temperature and density were recorded for the defueling and refueling operations.

Test Results:

Due to time restraints, the OV-10A aircraft JP-8 zero fuel weight and balance was derived by computation only. When compared to zero fuel weight with JP-4, the only difference in weight was a two pound weight increase due to denser JP-8 in figuring trapped fuel (six U.S. gallons). JP-4 to JP-8 center of gravity differed by 0.7 percent mean aerodynamic chord (MAC).

JP-8 full fuel weight exhibited a weight increase of 96 pounds. The full fuel center of gravity data showed that the MAC change was less than one percent.

The A-37B aircraft test shows a cg range from 30.2 to 32.2 percent MAC for JP-4 and 30.4 to 32.7 percent MAC for JP-8, for a maximum difference of 0.5 percent MAC. In both cases the maximum aft cg occurs when the tiptank fuel is depleted.

As a further check on the test data, a mathematical analysis of weight and balance was performed. This analysis was based on weights data for A-37B S/N 70-01310 with moments determined from T.O. 1A-37B-5. All fuel volumes (including unusable fuel volume) were assumed to be constant, and standard fuel densities of 6.5 pounds per gallon for JP-4 and 6.8 pounds per gallon for JP-8 were used.

Both the test data and the mathematical analysis show the change in cg with JP-8 fuel to be minimal. Changes in fuel weights can be mathematically computed using standard fuel densities. Fuel weight information presented in A-37B technical data should be revised to include fuel weights for JP-8 fuel at a standard density of 6.8 pounds per gallon.

The indicator errors at the full level were slightly higher for JP-8 than for JP-4. At the low fuel level, the errors were -10 pounds (1.5 gallons) for JP-8 and -15 pounds (2.2 gallons) for JP-4. The errors in both cases were acceptably small.

The FUEL LOW LEVEL warning light activated when fuel in the fuselage tank reached an indicated level of 280-290 pounds for JP-4 and 290-300 pounds for JP-8. Both indications were within the 295 ± 20 pound limit specified in the Flight Manual and T.O.s 1A-37B-5 and 1A-37B-2-5. Fuselage tank indicated quantities at proportioner pump start and shutoff were within limits for JP-4 fuel but were 10 to 30 pounds above limits for JP-8 fuel. These differences are not significant operationally. However, to insure accurate interpretation of the technical data presented

in the Flight Manual and T.O. 1A-37B-2.5, discussions of fuel system operating characteristics should note that data are based on JP-4 fuel properties.

Fueling and defueling operations were qualitatively evaluated during this test. The over-the-wing procedure was used for fueling. Fuel draining was accomplished through the fuselage tank defueling valve located on the bottom centerline of the aircraft. The use of JP-8 fuel in these operations did not present any additional difficulties and did not require any procedural changes.

THRUST STAND TESTS

Test Objectives:

The objective of these tests was to measure installed static thrust using JP-4 and JP-8 fuels, on and off trim.

Test Instrumentation:

This test was performed using the AFFTC Aircraft Horizontal Thrust Stand Facility, located at Pad 18. This facility is equipped with four Hunter-Bristol thrust platforms, each having a measurement capability of 125,000 pounds. Parameters included wind speed and direction, outside air temperature, barometric pressure, test day engine thrust output, and standard day engine thrust output. Aircraft engine parameters were hand recorded from cockpit indicators.

Test Method and Conditions:

OV-10A installed static thrust was measured at military with the condition levers in the normal flight position, and military with the condition levers in the takeoff position. Generator switches were on for all test conditions.

A-37B installed static thrust was measured at approximately 20 percent engine rpm increments from idle to military and back to idle for both single engine and dual engine operation. The left engine was tested on and off trim while the right engine was tested on trim only. All conditions were tested with engine inlet screens down. Selected conditions were also tested with inlet screens up. Bleed air switches were ON, inlet anti-ice was OFF, and generator switches were ON for all test conditions. The engines were allowed to stabilize at each power setting for three minutes before recording data. Fuel samples were taken for the JP-4 and JP-8 thrust calibration tests.

Test Results:

OV-10A thrust information represent uncorrected data for relative comparison only.

The torque output was obtained from the aircraft cockpit indicators. Using JP-4 fuel on and off trim, both engines attained or exceeded the target torque. Using JP-8 fuel on and off trim, only the L/H engine attained or exceeded target torque; however, the R/H engine exhibited increased thrust with reduced torque.

Although JP-8 off trim produced the best thrust output this condition is not recommended due to poor airstart capability.

With the A-37B aircraft, for the JP-4/JP-8 condition, corrected gross thrust was lower in all cases. EGT was lower in all cases. Fuel flow was lower in all cases. In the JP-8/JP-4 case, thrust was lower in all cases, ECT was lower, and fuel flow was higher in four of the six comparison points. For the JP-8/JP-8 condition, thrust was lower in all cases, EGT was lower in eight of twelve cases, and fuel flow was higher in ten of twelve cases. The difference were minimal at power settings above 80 percent rpm, but became more significant at lower power levels.

Data indicates a trend towards slightly increased fuel consumption for operation with fuel or trim setting other than JP-4/JP-4. Changes in thrust and EGT at higher power settings were minimal and should not have any operational impact for the A-37B.

NOTE: The effect of the higher viscosity of JP-8 on the volumetric fuel flow meters in the A-37B was not determined. Also, the fuel flow meters were not test calibrated.

CONCLUSIONS

The OV-10A engine starting characteristics with JP-4 and JP-8 fuels, on and off trim, were satisfactory.

A-37B engine starting characteristics were within Flight Manual limits for all cold weather starts with JP-4 and JP-8 fuels, on and off trim. Differences in cold weather fuel system operating characteristics were not operationally significant. The overall low temperature test results demonstrated that JP-8 is a suitable alternate fuel for use in the A-37B.

The F-5E engines were shown to start and operate down to -47 degrees F ambient temperature using JP-8. Based on the ground tests conducted, either a JP-4 or JP-8 main fuel control specific gravity (MFC sp gr) setting may be used.

OV-10A airstart performance with JP-4 fuel, on and off trim, was satisfactory. OV-10A airstart performance with JP-8 on trim was satisfactory at lower operational altitudes; however, peak exhaust gas temperatures (EGTs) during these airstarts were approximately 100 degrees C higher than the baseline case.

A-37B engine airstart test results indicated that airstart performance was degraded when using JP-8 fuel or when the engine was operating off trim. The most significant degradation occurred when using JP-4 fuel with a JP-8 fuel control density setting.

The OV-10A throttle transient test results demonstrated that there was no increase in compressor stall/engine flameout susceptibility when operating with JP-8 fuel, on and off trim. Peak EGTs obtained during throttle transient tests were inaccurate due to the extreme lag exhibited by the EGT indicator.

A-37B throttle transient test results demonstrated that there was no increase in compressor stall/engine flameout susceptibility when operating with JP-8 fuel, on trim.

C-5A engine performance during throttle transients with JP-8 was not degraded over JP-4 performance for any condition tested. The TF39-GE-1A engine requires no change in pilot throttle technique when using JP-8 fuel.

The results of the OV-10A weight and balance testing indicate that the difference in JP-4 and JP-8 fuel density resulted in a center of gravity shift of less than one percent mean aerodynamic chord (MAC). Takeoff weight was increased by 96 pounds with JP-8 fuel. The aircraft remains well within weight and balance limits with JP-8 fuel.

The A-37B weight and balance calibration and mathematical analysis showed that changes in cg with JP-8 were minimal. Changes in fuel weights due to differing fuel densities can be mathematically computed using standard fuel densities.

Calibration of the total fuel quantity indicating system showed that indicator errors for JP-8 fuel were slightly higher than for JP-4. However, the errors in both cases were acceptably small.

The results of the OV-10A thrust stand test indicate that the left and right engines attained or exceeded target torque values using JP-4 fuel, on and off trim. The left engine only attained or exceeded target torque values using JP-8 fuel, on and off trim. The left engine exhibited approximately eleven percent more thrust output than did the right engine, using JP-4 and JP-8, on and off trim.

A-37B installed static thrust calibrations of the J35-GE-17A engine using JP-4 and JP-8 fuels, on and off trim, indicated that differences in thrust and EGT at higher power settings were minimal and should not have any operational impact on the A-37B. The data did indicate a trend towards slightly increased fuel consumption for operation with fuel or trim setting other than JP-4/JP-4.

The test objectives of the ground and flight test program were successfully accomplished. JP-8 fuel was found to be suitable as an alternate fuel for the test aircraft, provided that the engine fuel control specific gravity was adjusted to the appropriate setting.

REFERENCES

Organizational Maintenance - Power Plant C-5A, T.O. 1C-5A-2-4, 26 August 1971, Change 33, 27 April 1979.
UNCLASSIFIED

Military Specification, Turbine Fuel, Aviation, Grades JP-4 and JP-5. MIL-T-5624K, 1 April 1976, amended 12 November 1976.
UNCLASSIFIED

Military Specification, Turbine Fuel, Aviation, Kerosene Type, Grade JP-8. MIL-T-33133, 5 May 1976.
UNCLASSIFIED

Flight Manual - C-5A, T.O. 1C-5A-1, 12 September 1975, Change 9, 29 June 1979.
UNCLASSIFIED

Category II Evaluation of the C-5A Propulsion Subsystem, FTC-TR-71-45, December 1971.
UNCLASSIFIED

Organizational Maintenance - Power Plant and Fuel System - A-37B, T.O. 1A-37B-2-5, 1 March 1975, Change 8, 1 August 1979.
UNCLASSIFIED

General Electric Company, Model Specification E1134, Engine Aircraft, Turbojet, J85-GE-17A, 12 October 1966.
UNCLASSIFIED

Organizational Maintenance - Basic Weight Check List, T.O. 1A-37B-5, 1 December 1975, Change 2, 1 October 1977.
UNCLASSIFIED

Flight Manual - A-37B, T.O. 1A-37B-1, 1 March 1976, Supplement 72, 17 July 1979.
UNCLASSIFIED

Flight Manual, USAF Series F-5E Aircraft T.O. 1F-5E-1, 1 August 1978, Change 2, 1 April 1979.
UNCLASSIFIED

Intermediate Maintenance Manual, General Electric J85-GE-21/21A Turbojet Engine, T.O. 2J-85-96-1, May 1977, changed August 1977.
UNCLASSIFIED

Stanford, Ronald E., Sandstrom, Clair K., Category II
Evaluations of F-5A Aircraft, ASD-TR-65-13, September 1965.
UNCLASSIFIED

Functional Check Flight Procedures, USAF Series F-5E and
F-5F Aircraft, T.O. 1F-5E-5CF-1, 1 June 1979.
UNCLASSIFIED

Flight Manual OV-10A, T.O. 1L-10A-1, 1 June 1978.
UNCLASSIFIED

Air Research Manufacturing Company, Model Specification
SC-5715-B, Engine, Aircraft, Turboprop, T76-G-10A and
T76-G-12A, 3 November 1970.
UNCLASSIFIED

BIBLIOGRAPHY

Anderson, James R., Limited Evaluation of the A-37B Aircraft Using JP-8 Fuel, AFFTC-TR-79-29, Air Force Flight Test Center, Edwards AFB, California, January 1980.

Boucher, Lance M., Second Lieutenant USAF, and Ford, James A., F-15 Reevaluation in the Climatic Laboratory, AFFTC-TR-77-37, Air Force Flight Test Center, Edwards AFB, California, December 1977.

Day, Thomas B., First Lieutenant USAF, and Rhynard, Wayne E., Major USAF, Limited Evaluation of the F-106A Using JP-8 Fuel, AFFTC-TR-79-31, Air Force Flight Test Center, Edwards AFB, California, To Be Published.

Eschweiler, Ronald R., Captain USAF, and Novakowski, Leonard E., Major Canadian Forces, Flight Evaluation of JP-8 Fuel, FTC-TR-73-4, Air Force Flight Test Center, Edwards AFB, California, March 1973.

Fischer, Richard R., Captain USAF, F-111E/F-111F/M32A-60A Cold Temperature Starting Evaluation with JP-8 Fuel in the McKinley Climatic Laboratory and F-111F/JP-3 Airstart/Afterburner Light Evaluation, SM-ALC-TR-78-179, Sacramento Air Logistics Center, McClellan AFB, California, November 1978.

Hall, Ken J., et al, F-111/CT-39/M32A-60 Cold Weather Starting Evaluation with JP-8 Fuel, SM-ALC-TR-78-116, Sacramento Air Logistics Center, McClellan AFB, California, April 1978.

Myers, Lawrence P., First Lieutenant USAF, and Thompson Addison S., Lieutenant Colonel USAF, B-57E and HC-13H/JP-8 Fuel Evaluation, Technical Letter Report, Air Force Flight Test Center, Edwards AFB, California, July 1978.

Stambovsky, Robert A., OV-10A/JP-8 Fuel Conversion Tests, AFFTC-TR-79-28, Air Force Flight Test Center, Edwards AFB, California, To Be Published.

Webb, Allan T., F-5E/JP-8 Fuel Climatic Evaluation, AFFTC-TR-79-23, Air Force Flight Test Center, Edwards AFB, California, November 1979.

A-10/JP-8 Fuel Compatibility Test, Fairchild Republic Division, July 1978.

Poch, Richard C., Captain USAF, C-5A/JP-8 Fuel Limited
Flight Tests, AFFTC, TR-79-32, Air Force Flight Test Cen-
ter, Edwards AFB, California, To Be Published.

LIST OF ABBREVIATIONS

<u>Item</u>	<u>Definition</u>	<u>Units</u>
AFB	Air Force Base	--
AFFTC	Air Force Flight Test Center	--
APU	auxiliary power unit (used interchangeably with GPU)	--
C	centigrade	--
cg	center of gravity	pct MAC
DR	Dutch roll	--
EGT	exhaust gas temperature	deg C
F	Fahrenheit	--
ft	feet	--
g	acceleration due to gravity	32.2 ft per sec ²
gal	gallons	--
GPU	ground power unit (used interchangeably with APU)	--
KIAS	knots indicated airspeed	--
MAC	mean aerodynamic chord	in.
NATO	North Atlantic Treaty Organization	--
PA	pressure altitude	--
psi	pounds per square inch	--
rpm	revolutions per minute	--
SA-ALC	San Antonio Air Logistics Center	--
SHSL	steady heading sideslip with left rudder (positive sideslip)	--
SHSR	steady heading sideslip with right rudder (negative sideslip)	--
S&L	straight and level	--

<u>Item</u>	<u>Definition</u>	<u>Units</u>
S/N	serial number	--
sp. gr.	specific gravity	--
T.O.	Technical Order	--
TSFC	thrust specific fuel consumption	lb per hr/lb
USAF	United States Air Force	--
USAFE	United States Air Force Europe	--
WUT	windup turn	--

INSTRUMENTING A TEST AIRPLANE IN BRAZIL

Arturo Garza Cantu
The Boeing Commercial Airplane Company
Seattle, Washington

In Brazil in 1980
There's a group of men that say,
"Aviation is where our hearts are
And aviation is where they'll stay."
Ask any one of them
Who was first in powered flight,
And they will tell you not the brothers
On that cold December day.
"It was Santos Dumont," they exclaim,
With a twinkle in their eye,
And with their hearts all filled with pride
They make sure you don't forget.
For you see he was Brazilian
And in 1898
He took off and traveled Europe
In his powered hot air balloon.
His contributions were enormous
That is plain as night and day,
And without him
Who knows where we'd be today.
These men are his successors
And though lacking tools and wealth,
They have the same ambition
And the drive to make it play.

- 0 -

I was sitting in a tavern
In Sao Paulo one fine day
When a man came sat beside me
With a stench that made me say:
"Begging your pardon sir
I don't mean to be unkind,
But you smell like rotten horsemeat
Thats been hanging in the sun.
And if you don't mind, my good man,
I shall take my drink and move
To the corner by the window
On the far side of the room."
"Hold it there young fellow,"
He said as I stood up,
And he motioned to me gently
Lest I think him out of line.
"You can move if you've a mind to
And there's nothing I can do,

But first listen to my story
So you'll know I'm not unclean."
He said, "I am working for an airline
And it is my job, you see,
To scrub and clean the bathrooms
Of the planes as they come in.
And no matter how carefully
I perform my work, you see,
When I remove the toilet bags
Some of it always gets on me.
I know this is a problem
And at the end of work each day
I go home and bathe and change my clothes
And use deodorants and creams.
But apparently its insufficient
Though I soak and rub and clean,
To properly refresh myself
And remove the stink from me.
If you have any suggestions
I would follow them indeed,
For my wife would be most thankful
And my friends would speak to me."
I thought it over for a moment
And I knew what I would do,
If I found I had this problem
With my job, my wife and you.
"The answer is simple, friend," I told him,
"Here's what you must do,
You must get a different job,
One that doesn't stick with you."
He frowned.
He squinted at me with his eyes.
And with his voice raised in anger said,
"What, and get out of aviation!!"

- 0 -

I gulped my drink and left there
With my nose still feeling pain.
But he left me with a thought that's still deep within my mind,
That that kind of dedication is extremely hard to find.

- 0 -

And dedicated they are these Brazilians. They are putting a tremendous amount of effort and capital into making their aviation industry one of the largest in the world. They are putting an equal amount of energy into making it one of the best in the world. In one of the flight test hangars at the Centro Tecnico Aeroespacial (Aerospace Technical Center, better known as CTA) they have a sign which proclaims in three feet high letters that "IN AVIATION, ONLY PERFECTION IS ACCEPTABLE." And they mean it. They are doing the best they can to make their industry competitive world wide.

October 22, 1968, was the first flight date of an all metal, twin turboprop airplane, the prototype of the Bandeirante. This was the first airplane totally designed, developed and built in Brazil by Brazilians. The name Bandeirante refers to the first pioneers who left the easy life on the coast of Brazil and braved the rugged interior to form settlements and begin to develop the enormous natural resources of that country. Like its namesakes, the Bandeirante airplane was a pioneer conceived and backed by the government and developed by the personnel at CTA. After a successful year of testing the prototype, a private company was formed to put the airplane into production. The company was named Embraer. Today, in a little over ten years since its formation, Embraer has turned into the sixth largest manufacturer of airplanes in the western world in terms of airplanes produced yearly, over 400 per year. The Bandeirante is now certified to British, French and U.S. FAR Part 23 standards and it is flying in 16 different countries. In 1979 over 50 airplanes were exported to countries in Europe, Africa and Latin America as well as to the United States and Australia.

The EMB-110 Bandeirante is powered by two PT6A turboprop engines. There are several versions of the airplane. The one shown in this slide is the 18 passenger commercial version, the EMB-110P2, which is in service with many commuter airlines around the world. Another version is the C-95 military troop transport which because of its wide door can also be used as a cargo airplane or to deliver paratroopers. Yet another version is the R-95 photographic airplane which is used for all types of aerial photography including mapping missions in the vast interior of the Amazon jungles. This shoreline patrol version, the P-95, with its powerful radar is said to be able to detect a small fishing boat 60 miles away in rough waters. On its right wing it carries a 50 million candlepower search light and it is fully equipped for over water search and rescue missions.

But the Bandeirante is not the only airplane made by Embraer. Through a licensing agreement with the Piper Aircraft Corporation, they manufacture almost the entire line of Piper airplanes. In addition they designed and built their own agricultural airplane, the EMB-201A, called the Ipanema. They have already built and delivered more than 400 of these agricultural airplanes. The Ipanema is used not only for crop dusting but also for planting certain crops such as rice and for seeding lakes and rivers with new species of fish and with some species that are in danger of extinction.

In the military area again, they also manufacture the EMB-326GB Xavante which is a military jet trainer of Italian design. Over 150 of these jet trainers have been delivered to the Brazilian Air Force.

One of the newest entries in the constantly expanding line of Brazilian designed and built airplanes is the EMB-121 Xingu. This is a 6 passenger executive type airplane of which approximately 30 have been built. The Xingu is a major step forward for the still young Brazilian aviation industry since it is their first pressurized airplane. This airplane is a kind of stepping stone in reaching their most ambitious goal to date, the EMB-120 Brasilia. The Brasilia which is scheduled to fly in the next two years will be a 30 passenger, pressurized, twin turboprop commuter.

All of these achievements become even more impressive when you remember that just about eleven years ago the Brazilian aviation industry was practically nonexistent.

I was fortunate enough to spend 17 months working at CTA. Since Embraer was formed, CTA has taken over the role of certification agency. A few years ago the United States signed a treaty with Brazil in which Brazil agreed to use the American FAR's as their certification standards. My particular assignment was to teach methods and procedures used in performance and flying qualities testing to comply with the FAR's Part 25. In addition to lectures and conferences I thought it would be of value to do some actual testing. Little did I know that this was to lead to one of the most fun and challenging experiences I have ever had. We were provided with a Bandeirante C-95 airplane with which to do the testing. The training tests were to be combined with additional testing which had been requested by the Air Force to better define the performance of the older versions of the Bandeirante. But in order to do the testing, first we had to instrument the airplane. It was decided that a high speed PCM system which had previously been purchased by CTA but which had never been installed on an airplane would be used for our test program. I immediately yelled for help and was able to enlist an old friend and one time instrumentation engineer into the project. Between us and with the help of a very enthusiastic although completely inexperienced Brazilian crew we set out to make wiring diagrams, signal conditioning cards, transducer installations, wiring installations and instrumentation calibrations. I would like to point out that I myself had no experience at this type of work. In our first attempt after installing about half the wiring we found ourselves with what looked like a spaghetti factory inside the airplane and that wouldn't have passed the wiring code for a chicken coop in southern Mexico. In our second attempt we set up a patchboard type arrangement which was much more successful although we did end up with an intermittent problem with the engine torque instrumentation which somehow caused erroneous aileron position data. We solved that problem after we discovered we had 110 volts a.c. driving our attitude gyros instead of the required 28 volts d.c.

In any case, after four months and a very rigorous safety check we made first flight and celebrated with a big "churrasco" which is a Brazilian barbeque with plenty of "Pinga," the national sugar cane firewater. After I returned to the states, I understand that the instrumentation system continued to work successfully.

During my stay in Brazil I found the people to be extremely friendly and hospitable. Their country along the coast and in the mountains is beautiful and their food is delicious. If you ever get a chance to visit there, I highly recommend it, especially around carnival time in February. They are very proud of the progress they have made in their aviation industry in the last few years, and well they should be.

DEVELOPMENT OF A SIMPLE, SELF-CONTAINED
FLIGHT TEST DATA ACQUISITION SYSTEM

Ronald R. L. Renz*, Robert Clarke**, and Jan Roskam†

ABSTRACT:

This paper describes work done under NASA Dryden Grant during the period January 21, 1979, through March 31, 1980. This ongoing program encompasses the development of a simple, self-contained flight test data acquisition system. Phase I, which has been completed to date, consisted of two parts. These were 1) an extensive literature survey of flight testing methods, and 2) development of a proof of concept system.

The literature survey was completed in July 1979. This was used as a primary data base for system selection.

This paper describes the system concepts selected, as well as results of the flight test program conducted to show these concepts as valid.

This instrumentation package embodies transducers to allow both stability and performance analysis of general aviation class airplanes, although it can easily encompass most other types of aircraft. Due to the nature of the data reduction method utilized, a minimum number of (high accuracy) transducers are required. Data from these transducers are recorded using an on-board microprocessor and digital cassette recorder. This has proven a simple, reliable method to obtain accurate flight data. As a minimum modification requirement to the test aircraft was the primary design factor for the entire system, it was decided to use a rechargeable battery pack for airborne power. This has allowed total isolation from the aircraft systems, which simplifies installation, enhances safety, and eliminates many electrical noise problems in the transducer signals. The transducers are all contained on one module, except for the following: total pressure probe, static pressure probe, and control position transducers. A minimum of installation is also required for these devices, as they are literally sticky-taped to the airframe.

The system constructed for Phase I has proved, under flight test, that these concepts were valid for longitudinal stability analysis. Throughout this flight test program (conducted using a Cessna 172 airplane) no major problems were encountered, and the package proved extremely reliable.

Ongoing development is now being conducted to complete the system to allow also lateral stability, and performance analysis.

* Project Manager

** Research Assistant

† Director Flight Research Lab; Professor Aerospace Engineering

NOMENCLATURE

A_x	Longitudinal acceleration	$C_{m_T} = \frac{\partial C_m}{\partial (\frac{U}{U_1})}$	Variation of thrust pitching moment coefficient with speed
A_y	Lateral acceleration	$C_{m_{E,c}} = \frac{\partial C_m}{\partial \delta_{E,c}}$	Variation of pitching moment coefficient with elevator or canard angle
A_z	Vertical acceleration	$C_{T_x} = \frac{T_x}{qS}$	Thrust force coefficient in X direction
[A]	Stability matrix	$C_{T_x} = \frac{\partial C_T}{\partial (\frac{U}{U_1})}$	Variation of thrust force coefficient with speed
[B]	Control matrix	$C_{x_a} = \frac{\partial C_x}{\partial \alpha}$	Variation of longitudinal force coefficient with angle of attack
B.S.	Body station	$C_{x_u} = \frac{\partial C_x}{\partial (\frac{U}{U_1})}$	Variation of longitudinal force coefficient with speed
{c}	Vector of unknowns for MMLE	$C_{x_{\delta_{E,c}}} = \frac{\partial C_x}{\partial \delta_{E,c}}$	Variation of longitudinal force coefficient with elevator or canard angle
\bar{c}	Mean aerodynamic chord	$C_{z_o} = \frac{\partial C_z}{\partial \alpha}$	Nondimensional longitudinal force equation bias
C.G.	Center of gravity	$C_{z_u} = \frac{\partial C_z}{\partial (\frac{U}{U_1})}$	Variation of vertical force coefficient with angle of attack
$C_D = \frac{D}{qS}$	Drag force coefficient	$C_{z_{\delta_{E,c}}} = \frac{\partial C_z}{\partial \delta_{E,c}}$	Variation of vertical force coefficient with elevator or canard angle
$C_{D_\alpha} = \frac{\partial C_D}{\partial \alpha}$	Variation of drag coefficient with angle of attack	$C_D = \frac{D}{qS}$	Drag force
$C_{D_u} = \frac{\partial C_D}{\partial (\frac{U}{U_1})}$	Variation of drag coefficient with speed	$D - E = \delta_g$	Elevator angle
$C_{D_{\delta_E}} = \frac{\partial C_D}{\partial \delta_E}$	Variation of drag coefficient with elevator angle	$[D]$	MMLE weighting matrix
$C_L = \frac{L}{qS}$	Lift force coefficient	\mathbf{g}	Force of gravity
$C_{L_\alpha} = \frac{\partial C_L}{\partial \alpha}$	Variation of lift coefficient with angle of attack	$[G]$	MMLE observation matrix
$C_{L_{\dot{\alpha}}} = \frac{\partial C_L}{\partial (\frac{\dot{\alpha}}{2U_1})}$	Variation of lift coefficient with rate of change of angle of attack	$G.W.$	Gross weight
$C_{L_q} = \frac{\partial C_L}{\partial (\frac{qC}{2U_1})}$	Variation of lift coefficient with pitch rate	$[H]$	MMLE observation matrix
$C_{L_u} = \frac{\partial C_L}{\partial (\frac{U}{U_1})}$	Variation of lift coefficient with speed	$[I]$	Identity matrix
$C_{L_{\delta_E}} = \frac{\partial C_L}{\partial \delta_E}$	Variation of lift coefficient with elevator angle	I_{yy}	Moment of inertia about the Y axis
$C_m = \frac{M}{qSc}$	Pitching moment coefficient	J	MMLE cost function
$C_{m_\alpha} = \frac{\partial C_m}{\partial \alpha}$	Variation of pitching moment coefficient with angle of attack	L	Lift force
$C_{m_{\dot{\alpha}}} = \frac{\partial C_m}{\partial (\frac{\dot{\alpha}}{2U_1})}$	Variation of pitching moment coefficient with rate of change of angle of attack	L	Iteration number
$C_{m_q} = \frac{\partial C_m}{\partial (\frac{qC}{2U_1})}$	Variation of pitching moment coefficient with pitch rate	m	Perturbed pitching moment
$C_{m_u} = \frac{\partial C_m}{\partial (\frac{U}{U_1})}$	Variation of pitching moment coefficient with speed	M	Mass
C_{m_T}	Pitching moment coefficient due to thrust	M_0	Total pitching moment
			Dimensional variation of pitching moment with angle of attack

NOMENCLATURE (continued)

M_a	Dimensional variation of pitching moment with rate of change of angle of attack	x_o	Longitudinal force equation bias
M_q	Dimensional variation of pitching moment with pitch rate	$\{y(t)\}$	Computed observation vector
M_u	Dimensional variation of pitching moment with speed	$y_i = \{y(i)\}$	Computed observation vector at time i
M_{T_a}	Dimensional variation of pitching moment due to thrust with angle of attack	$\{z(t)\}$	Measured observation vector
M_{T_u}	Dimensional variation of pitching moment due to thrust with speed	$z_i = \{z(i)\}$	Measured observation vector at time i
$M_{\delta_{E,C}}$	Dimensional variation of pitching moment due to elevator or canard angle	z_o	Dimensional variation of Z-force with angle of attack
M_o	Pitching moment equation bias	z_u	Dimensional variation of Z-force with rate of change of angle of attack
M_g	Dimensional variation of pitching moment with pitch angle	$z_{\delta_{E,C}}$	Dimensional variation of Z-force with pitch rate
p	Roll rate	z_v	Dimensional variation of Z-force with speed
p_d	Dynamic pressure		Vertical force equation bias
p_s	Static pressure		
q	Pitch rate	α	Angle of attack
\dot{q}	Dynamic pressure	θ	Euler pitch angle
r	Yaw rate	ϕ	Euler roll angle
s	Wing area	δ_e	Bias in Euler pitch rate equation
t, T	Time point	δ_A	Elevator angle
T	Temperature	δ_R	Aileron angle
T_x	Thrust force in X direction	δ_c	Rudder angle
u	Perturbed speed	w_n	Canard angle
U	Total speed	$\{n(t)\}$	Undamped natural frequency
$\{u(t)\}$	Control vector	∇_c	Noise vector
$\{v\}$	MLE variable bias vector	∇_c^2	Gradient with respect to c
\dot{v}	Perturbed velocity in Z direction		Second gradient with respect to c
w	Weight		
$\{x(t)\}$	State vector	<u>Subscript</u>	
X_a	Dimensional variation of X-force with angle of attack	I	Initial
X_u	Dimensional variation of X-force with speed	D	Dutch roll
X_{T_u}	Dimensional variation of X-force due to thrust with speed	P	Phugoid
$X_{\delta_{E,C}}$	Dimensional variation of X-force with elevator or canard angle	SP	Short period
		<u>Superscript</u>	
		$*$	Transpose
		\cdot	State vector derivatives

A dot over a quantity denotes the time derivative

INTRODUCTION

This paper describes work done under the first phase of a continuing program to develop a simple, self-contained flight test data acquisition system. Phase I, which has been completed to date, comprised two aspects: 1) a literature survey of flight testing methods (Ref. 1), and 2) the development of a proof-of-concept system (described in detail in Ref. 2). This paper discusses the concepts used for design of the system, describes the actual instrumentation system constructed, and discusses the data reduction methods used for initial tests.

PURPOSE OF PROJECT

Flight testing has always required a high degree of complex instrumentation to get accurate results. This, in the past, and still evident today, has taken a great deal of time and money to equip each individual flight test article. Traditional systems are placed on aircraft on an individual basis, utilizing what is available at that time, coupled with the specific requirements of a particular test program. This has never really led to ideal or totally thought-out systems and normally results in high costs or in too much time being required for instrumenting the airplane.

With the accurate instrumentation available today, and with the recent advances in microcomputer technology, it was seen that an accurate, multi-purpose data acquisition system could be developed. The system described here has been developed to do just that.

The basis for design of this system is as laid out here.

EASE OF INSTALLATION - This has been a major design consideration. If possible, NO permanent modification should be done to the airplane. The system must be universally easy to install and should require a minimum of installation time and no special procedures. This factor includes calibration of the system installed on the airplane.

SELF-CONTAINED - The system should be totally self contained. This should include all data sources, data recording methods, power requirements and data reduction techniques.

SIMPLE - The system must be simple in concept and easy to use. The need for complex instrumentation, difficult calibration, and specialized operator knowledge must be kept to a minimum.

FLIGHT TESTING - The system should not require any specialized piloting techniques to obtain accurate results.

CLASS OF AIRCRAFT - The system to be developed is primarily applicable to the general aviation type airplane. This criterion does not restrict the methods and theories, but it does define the requirements for the transducer ranges and accuracies.

RESULTS - The system is aimed at stability and performance parameter identification, but it must permit adaptation to other test requirements.

COSTS - The system constructed under Phase I has shown all of the above requirements to be feasible at relatively low cost.

The system described here has been developed only to prove the concept and was not intended to be the "full-house" * system. For this phase the testing was restricted to longitudinal stability analysis only.

INSTRUMENTATION SYSTEM

The system constructed satisfies all the design requirements stated above. The package can be broken up into the data gathering system, transducers, power supply, and pilot control console. A block diagram of the system is shown in Fig. 1. Following is a description of these components.

DATA GATHERING SYSTEM

The trade-offs considered in this area are those of analog vs digital storage, and airborne recording vs telemetry.

In the past, most on-board systems made use of analog recording, due primarily to the high cost and complexity of digital systems. In recent years, however, vast inroads have been made in the digital field. This has resulted in small, inexpensive, and reliable digital devices, most available as solid-state integrated circuits. The recent advances in digital electronics technology have reduced both the complexity and costs. Coupling this with the lower likelihood of error in digital systems, it was decided to use a totally digital system for this package.

In the past, telemetry has been a much-used means of transmitting data to be recorded on the ground. This is primarily due to the large size and complexity of the older recording media. Many improvements have also been made in this regard, with the advent of small, reliable cartridge and cassette recording systems. This improvement is also attributed to the recent advances in digital technology. Telemetry still has a place in aircraft flight testing, primarily in high-risk operations (such as flutter tests, spin testing, etc.). Its major disadvantages are the requirement of a ground station, and its associated high cost and complexity. For this system on-board recording, making use of a digital cassette recorder, has been chosen.

The airborne part of the system is shown in Figs. 2 and 3, and the ground part of the system is shown in Figs. 4 and 5.

* A "full-house" system would be a ready-for-application package allowing both longitudinal and lateral stability analysis.

The heart of the unit is a Rockwell AIM 65 microcomputer with 4000 bytes of memory. This is coupled through a Rockwell expansion interface to the rest of the system. The other two major components of the air-borne package's recording system are the Datel MDAS-16 multiplexer and analog-to-digital converter, and the TEAC MT2-02 digital cassette tape transport.

The AIM-65 is an eight-bit interactive microcomputer using an R6502 microprocessor. It is capable of being programmed by the user. The AIM-65 is used for control of the data acquisition in flight and for control of read-back of these data from the TEAC tape drive and transferring the data to the data reduction computer.

The AIM-65 is coupled, by use of the MDAS-16, to the transducer package. The MDAS-16 is a 16-channel multiplexer coupled with a 12-bit analog-to-digital converter. This unit has the capability of addressing channels as desired (either random or sequentially), using a microprocessor controller. Voltage input ranges can be selected as desired (-5 volt to +5 volt was chosen for this system). The unit has a 50 KHz through-put rate with 20 μ sec access time per channel.

The other major component of the data acquisition system is the TEAC tape transport. This unit is a low-cost magnetic tape unit designed specifically for digital applications. It makes use of standard audio type cassette tapes for data storage. All interfacing required is included in the tape package. Input requirements are TTL*-compatible; and the tape unit requires only control signals, provided by the AIM-65 microcomputer, and parallel data input. All detailed control functions required by the tape unit are handled on board by the unit for both recording and playback. Only simple control signals are required to initiate the various functions.

The data acquisition system is also used for data playback and transfer to the data reduction computer. An interface system compatible with standard computer RS232 ports is used. It was decided to use the same recorder and computer system for in-flight recording and playback of data. This avoids possible problems due to mismatch of tape drives and also reduces overall system costs. Once all the data are on the data reduction computer, the Rockwell system is no longer required in the data reduction process.

TRANSDUCERS

The transducers used, the ranges required, and the accuracies selected for the system are listed in Table 1. References 3-9 were the primary input aid in selection of these requirements. Discussion with personnel at NASA, Dryden Flight Research Center, was the secondary input for transducer selection. The transducers selected allow optimal use of the data reduction technique considered.

During a specific maneuver, T, Pg and Pd need only be measured at the start and finish to define the initial and final conditions. The

*TTL = Transistor-Transistor-Logic: Electrical standard.

other 11 channels require measurement throughout the maneuver to determine the dynamic characteristics and analyze stability and performance properties of the airplane.

To select the acquisition rate, the following factors must be considered:

- Minimum rate must be higher than the undamped natural frequency of the airplane to be tested.
- Minimum rate must be high enough to avoid time skewing of the data points.
- Minimum rate must be as low as possible to allow economy in the recording media and data reduction process.

In data analysis, to obtain reasonable representations of the frequency response, an acquisition rate of at least five times the undamped natural frequency should be used (Ref. 10). In the class of aircraft considered for this instrumentation system, the natural frequencies are of the following order:

$$\omega_{n_{SP}}, 0.5 - 1.0 \text{ Hz}; \omega_{n_p}, 0.01 - 0.03 \text{ Hz}; \omega_{n_D}, 0.25 - 0.60 \text{ Hz}.$$

Therefore, the maximum frequency ($\omega_{n_{SP}}$) requires an acquisition rate of $1.0 \times 5 = 5/\text{sec}$. This is the minimum data requirement.

From Reference 9 and discussion with the authors it was determined that an acquisition rate of 100/sec is required to avoid time skewing problems. From the practical applications of the maximum likelihood estimation methods, this rate (100/sec) also results in an excess of data that unnecessarily increases the computation time and costs.

Using a computer-controlled acquisition system allows scanning of the transducers as rapidly as possible (20 $\mu\text{ sec}/\text{channel}$, 220 $\mu\text{ sec}$ total)*, and then waiting until the next data point is required (0.1 sec later)*. These data are temporarily stored in memory and then output to the TEAC tape. This technique allows a high scanning rate to avoid time skewing between channels (equivalent to 4545/sec)* and a low overall acquisition rate (10/sec)* to provide economy and the minimum data requirement.

The transducers were mounted on one pallet. This is shown in Fig. 6. It was possible to include all transducers on the pallet with the exception of the pitot tube, static cone, and elevator position transducer.

The pallet was mounted as close to the center of gravity of the airplane as possible. In this flight test program the pallet has been clamped to the seat tracks of the Cessna 172, directly aft of the forward seats.

Following are descriptions of the individual transducers used for Phase I of this program.

* Values for the University of Kansas Flight Research Lab (KU-FRL) system

Accelerometers

Both accelerometers used are of the force feedback type. They are made by Schaevitz Engineering (LSB series). The response characteristics of these accelerometers were such that they picked up the aircraft vibration caused by the engine. To reduce this noise, a double-pole active filter with a cutoff frequency of 10 Hz was designed.

Attitude Gyro

Both roll attitude and pitch attitude were obtained from a Humphrey VG-24 vertical gyroscope. This unit has sufficient damping in its operation to filter out the high frequency vibrations caused by the engine. Thus no additional filtering is required, and the signal is recorded directly.

Pitch Rate Gyro

The pitch rate gyro used is a Humphrey RG51 gyroscope. This unit is a displacement type unit. It should be noted that this instrument does not meet the accuracy requirements specified in Table 1. It was found that to obtain the required accuracy of $0.1^\circ/\text{sec}$, force feedback gyros are required. The KU-FRL had the Humphrey gyros available at no cost, and they were used for the present phase for that reason. The Humphrey gyro has sufficient accuracy for stability analysis; however, for the performance analysis to be carried out in Phase II of this program, this gyro will be replaced by the more accurate force feedback type.

Elevator Position Transducer

A linear displacement transducer manufactured by Space-Age Control, Inc., was used to measure elevator position. Due to the small size of this unit, it was decided to place it externally on the airframe. The transducer is installed as shown in Fig. 7.

A novel technique for attaching the control position transducer (as well as the total pressure tube) has been used. Double-sided foam tape attaches the external devices onto the airframe. The mounting technique is depicted in Fig. 8. The mounting method was first tested in the KU-FRL subsonic wind tunnel for wind speeds up to 119 mph. The tests in the tunnel were run for periods of up to 4 hours, with no degradation in rigidity of the mount (see Ref. 11). The method has proven to give excellent results in the flight test program. The tape used is 3M number 4265 neoprene foam, the properties of which are included in the table in Fig. 8.

It was anticipated that the mounting location for the elevator position transducer would result in a non-linear calibration curve. However, the calibration curve appeared to have a linear character (linear regression correlation coefficient of 0.9997) for the mounting location used.

Static and Dynamic Pressure Transducer

A B&D Instruments Company 2504 series transducer was used for the static and dynamic pressure measurement. This device includes its own signal conditioning and converts the pressures to electrical signals utilizing semiconductor pressure transducers. This type of transducer is largely affected by the ambient temperature. The B&D unit allows for this by heating the case and maintaining this at a constant temperature.

The pitot tube was designed and constructed according to Reference 12. The pitot tube is attached to the underside of the wing (see Figs. 9) using the foam tape method shown in Fig. 8. The pitot tube allows a high angularity of the flow and still provides true readings. The distance from the wing is such that the tube is out of the boundary layer and thus provides a true total pressure reading as long as the pitot tube axis is close to the direction of airflow ($\pm 15^\circ$). The tube is mounted along the wing, halfway between the propeller arc and the wing tip. This location minimizes flow effects due to the propeller slip stream and the wing tip vortices.

For the accurate measurement of static pressure, a trailing static cone was selected (see Ref. 13). Initial flights showed difficulty in deployment of the static cone after takeoff. As an accurate determination of static pressure was not necessary for this proof-of-concept phase, it was decided to delay further design of the static cone deployment method until the second phase. The performance testing slated for the second phase will require accurate determination of the static pressure.

The transducers selected have shown that the basic decision regarding specific transducers, ranges and accuracies were correct. They have all proved reliable, with no failures encountered; and none required any specialized signal conditioning or difficult calibration procedures.

POWER SUPPLY MODULE

The options considered for supplying power for this instrumentation system are 1) to tap off the aircraft electrical system, or 2) to carry a separate battery package on the flight.

Considering option one, using the aircraft power system, offered several advantages. These were reduction in size of the instrumentation system, and no limited usage time due to battery rundown. It was realized, however, that there are several voltage standards on the current general aviation fleet. This would therefore require either a complex voltage control system or several systems to account for the various voltages available in the airplanes to be considered. Coupled with this is the high cost of voltage conversion systems. Also, modification would be required to the airplane's electrical system to install this instrumentation package.

It was decided to explore the second option. A suitable rechargeable battery was found, manufactured by Eagle-Picher. These lead acid batteries are sealed, rechargeable, and maintenance free. These batteries can also be used in any position. The batteries allow a minimum of 3 hours running time between recharge of the batteries (for the "full-house" system to be used in Phase II). In Phase I the longest flight to date has required four hours of system operation, which was accomplished without problems.

The biggest disadvantage when batteries are used is that of weight. The battery module, complete, weighs 60.5 lbs. This is the heaviest component in the entire system. (The computer module weighs 34.5 lbs.; the transducer pallet, 17 lbs. See Fig. 2.) Total weight of the entire instrumentation system including all cables is 115.1 lbs. This system weight is not a problem for the majority of general aviation airplanes.

PILOT CONTROL CONSOLE AND TRANSDUCER READOUT

The pilot controls the entire system using a box which can be placed on the seat beside him. The controls contained on this box are as follows:

Three System Control Switches

The first is the tape initialize switch. This is a momentary contact switch which is used only after insertion of a fresh data tape. This prepares the beginning file mark on the data cassette and readies it to accept data.

Second, the STBY/RUN toggle switch is used to control when data is being recorded. In the STBY position the system is non-active. In the RUN position, data is recorded.

The third control switch is the REWIND switch. This is used at the end of a cassette or flight. Activation of this switch places an end-of file mark on the tape and rewinds the tape back to the start position.

One Transducer Readout Control

A high impedance voltmeter is provided to the pilot so that he can observe a particular transducer as he requires. A rotary switch (on the pilot control console) controls the signal which is observed.

This feature is also used to verify that all transducers are operating correctly prior to a test flight.

INSTALLATION

The package described above is easily placed in the airplane without any permanent modifications (see Ref. 11). It is shown installed in the KU-FRL Cessna 172 in Figs. 10-12.

DATA REDUCTION METHOD

This chapter describes the data analysis procedures used in this phase for longitudinal stability analysis. The overall method is best depicted via the flow chart shown in Fig. 13.

For this phase the system described above was used for airborne data acquisition. The KU-FRL's Hewlett Packard (HP9825) microcomputer was used for all further data processing. This system is a 24000-byte microcomputer complete with hard copy printer and digital plotter. Segmenting the various data reduction programs into the blocks as shown in Fig. 13 allowed effective data analysis. It should be noted, however, that the data reduction method used is operating on the verge of the capability of this computer. The HP9825 operates in BASIC language using an interpretive line-by-line procedure. Thus the numerous calculations required take a great deal of time. For example, typical time required for the analysis of one maneuver using the MMLE method is in the order of five hours of execution time. Phase II of this program will make use of a compiler on another microcomputer, which will decrease execution time of the programs a factor of 10-20 compared to the HP9825 system.

MODIFIED MAXIMUM LIKELIHOOD ESTIMATOR

The flight data were processed through the Modified Maximum Likelihood Estimator (MMLE) developed by NASA (see Refs. 6, 9, 14). This technique has been used by NASA for over 12 years. A simplified program (NASA Dryden "BONES" version of MMLE) has been placed on the HP9825 computer. Described here is the theory used in this technique, and some of the assumptions made for the KU-FRL version.

Parameter Estimation

The MMLE estimator determines the coefficient of a given set of linear equations describing the motion of the aircraft. It does this by comparing the difference between actual in-flight measured responses of various states, and the predicted responses of these states using an estimate of the coefficients. The actual measured control input is used as the input for the estimating procedure. The estimated coefficients are updated each iteration, using the error as determined above. The flow chart of Fig. 14 shows the MMLE concept. The details of the mathematics are presented in Appendix A.

Microcomputer and MMLE

There are several aspects that must be realized when using the MMLE technique on the current microcomputers. Most of these systems still have limited capacity, and thus the overall MMLE estimator must be broken up into various program stages. This is caused primarily by memory availability and execution time required (especially for an interpreter type machine such as the HP9825; see Fig. 15).

The HP9825 system at the University of Kansas has a physical limit of operating on a maneuver with 325 data points (32.5 seconds with the acquisition rate used in this system). This is due to the length of data tape available.

The execution time required is in the order of 1 hour per iteration. To reduce the possibility of data loss, due to power outages, etc., the entire computer memory is saved on the data tape after each iteration. This then limits the possible loss of run time at a maximum of 1 iteration.

FLIGHT TEST MANEUVER

Traditional flight testing methods have utilized primarily steady-state flight paths for data collection. This was due mostly to the data acquisition systems available. Unfortunately, this required a highly trained and competent test pilot to obtain realistic and valuable results.

With the current transducer and acquisition system technology available, flight testing need no longer rely on steady-state maneuvers to allow accurate state measurement. This development has resulted in the newer flight testing methods utilizing dynamic maneuvers.

The literature indicates that the nature of the maneuver is not critical to determine the aircraft characteristics. What is important when using the techniques such as MMLE is to ensure that the proper aircraft modes have been excited. For example, a longitudinal maneuver should excite both the short-period and phugoid modes of the airplane. This realization (i.e., non-critical flight path) leads to the possibility of using lesser qualified pilots and still obtaining accurate results. All testing done on this program has been done by a pilot who had no previous flight test experience.

The control input used for this phase was an elevator pulse, or series of elevator pulses, approximating a sinusoidal input. It was found that this maneuver sufficiently excited the Cessna 172 used and provided reducible data. The results of the flight tests are presented in the next section.

RESULTS OF FLIGHT TEST PROGRAM

Presented here are the results of a typical maneuver (see Fig. 16). The fit of the estimated states and actual states is good. The A_x estimate is the only one that differs significantly from the measured quantities. Also provided are predicted time histories of several states that are not measured (\dot{q} , U , α). These are a result of the mathematical model used for the MMLE method.

The result obtained with the KU-FRL system is compared with flight test results done at NASA Langley on a Cessna 172 (Ref. 16) and with analytical methods of Reference 15. This correlation is shown in Table 2. It is seen that there is good correlation between some deriv-

atives but not between others. Further work will be required in Phase II to determine the source of this discrepancy.

CONCLUSIONS

The proof-of-concept system designed and evaluated under this program has met the objectives outlined in Chapter II. The system is easy to install, is virtually self contained, is simple in operation, requires no complex flight maneuvers, is applicable to general aviation airplanes, is capable of longitudinal stability analysis, and is low in cost. This system has shown that the technology used is capable of the tasks to be performed.

Areas have been discovered where further work is required. A comprehensive list is included in Appendix B.

REFERENCES

1. Renz, R. R. L.; Clarke, R.; Roskam, J.; "A Literature Survey of Performance and Stability Flight Testing"; University of Kansas Flight Research Lab; KU-FRL-407-1; 1979.
2. Renz, R. L.; Clarke, R.; et al.; "Phase I: Development of a Simple Self-Contained Flight Test Data Acquisition System"; University of Kansas Flight Research Lab; KU-FRL-407-3; 1980
3. Gerlach, O. H.; "Determination of Performance, Stability and Control Characteristics from Measurements in Non-Steady Maneuvers"; Stability and Control, AGARD Conf. Proc. No. 17, p. 497-523; 1966.
4. Smetana, F. O.; Fox, S. R.; "Flight Test Evaluation of Predicted Light Aircraft Drag, Performance, and Stability"; NASA CR-158076; 1979.
5. Sorensen, J. A.; Tyler, J. S.; Powell, D. J.; "Evaluation of Flight Instrumentation for the Identification of Stability and Control Derivatives"; AIAA Paper 72-963; September 1972.
6. Iliff, K. W.; Maine, R. E.; "NASA BONES"; NASA Dryden; unpublished computer program.
7. Klein, V.; Gregory, R.; "A Proposal for Self-Contained Instrumentation System for Flight Research on Stability Control"; Report CIT-FI-72-013; March 1972; Cranfield Institute of Technology.
8. Eckholdt, D. C.; Wells, W. R.; "A Survey of AFFDL Parameter Estimation Efforts and Future Plans; Parameter Estimation Techniques and Applications in Aircraft Flight Testing"; NASA TN D-7647; 1973.
9. Iliff, K. W.; Maine, R. E.; "Practical Aspects of Using a Maximum Likelihood Estimation Method to Extract Stability and Control Derivatives from Flight Data"; NASA TN D-8209; 1976.
10. Mace, W. D.; Pool, A.; (editors); "Flight Test Instrumentation Series"; AGARD No. 160, Vols. 1-8; 1973 to 1977.
11. Renz, R. R. L.; "Flight Test Instrumentation Certification Report"; University of Kansas; KU-FRL-407-2; 1980.
12. Wuest, W.; "Measurements of Flow Speed and Flow Direction by Aerodynamic Probes and Vanes"; AGARD Conf. Proc. 32; 1967.
13. Ikhtiar, Paul A.; Marth, V. G.; "Trailing Cone Static Pressure Measurement Device"; p. 93-94; Journal of Aircraft, Vol. 1, No. 2; March 1969.
14. Main, R. E.; Iliff, K. W.; "A Fortran Program for Determining Stability and Control Derivatives from Flight Data"; NASA TN D-7831; 1975.
15. Roskam, J.; "Airplane Flight Dynamics and Automatic Flight Controls"; Roskam Aviation and Engineering Corporation; Ottawa, Kansas; 1979.
16. Suit, W. T.; Cannaday, R. L.; "Comparison of Stability and Control Parameters for a Light, Single Engine, High-Winged Aircraft Using Different Flight Test and Parameter Estimation Techniques"; NASA Tech Memorandum 80163; 1979.

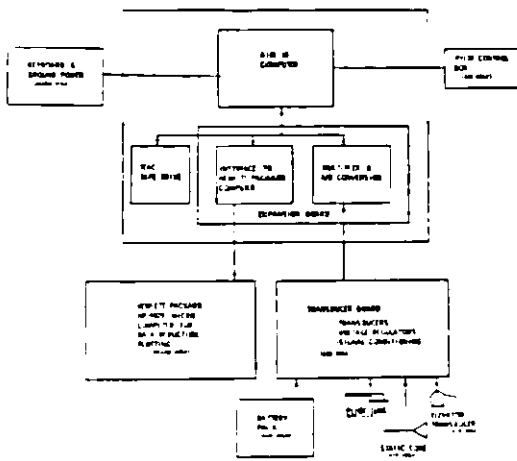


Figure 1 Block diagram of the overall system

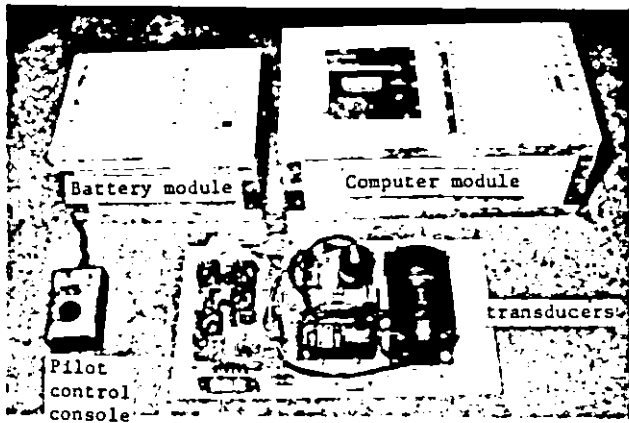


Figure 2 Major components of the airborne system

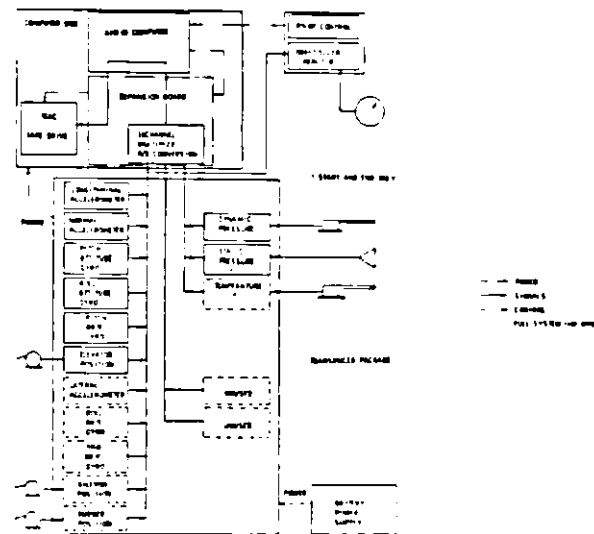


Figure 3 Block diagram of the airborne system



Figure 4 AIM-65 ground system

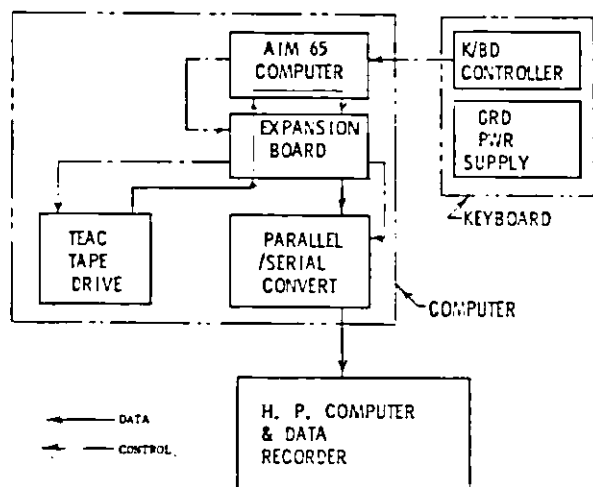


Figure 5 Block diagram of the data transfer system

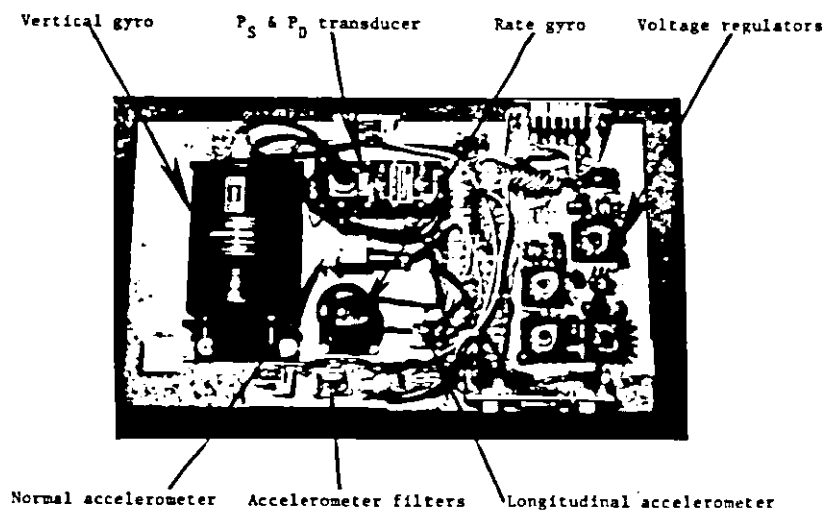


Figure 6 Transducer board

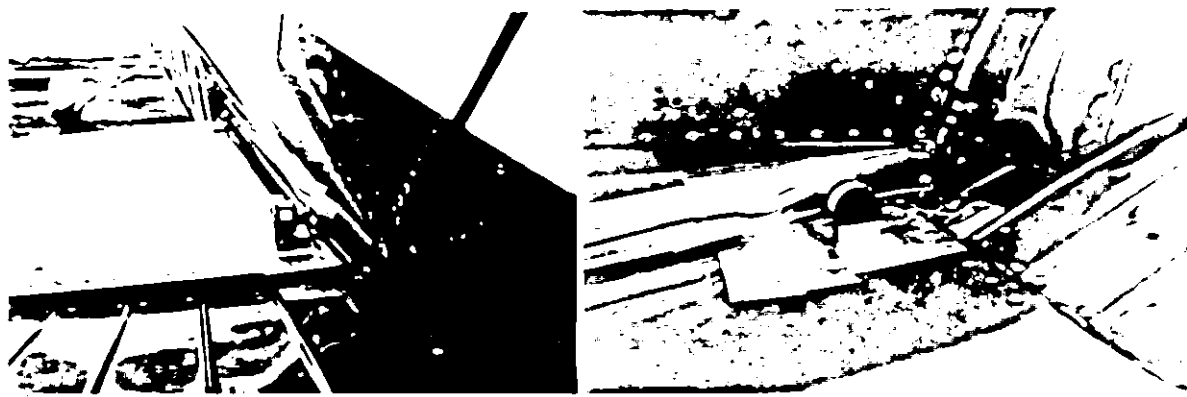


Figure 7 Elevator control position transducer mounted on airplane

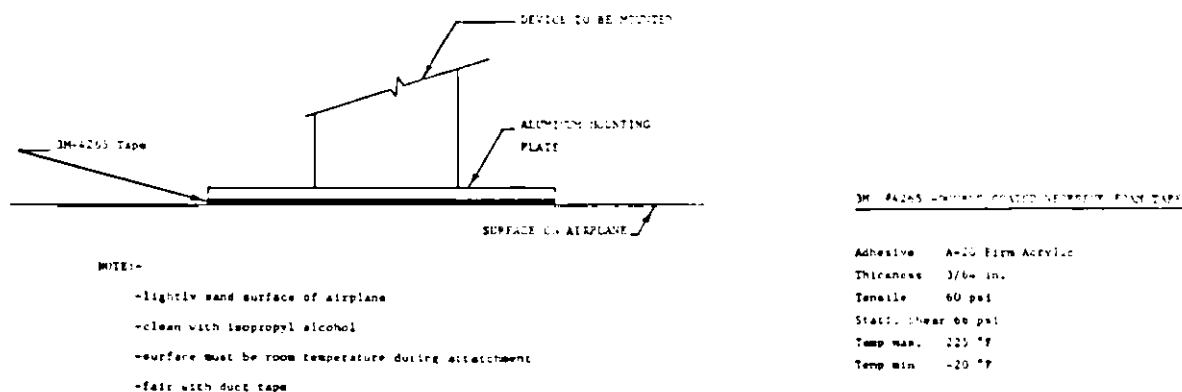


Figure 8 Mounting technique for external devices



Figure 9 Pitot tube mounted on airplane

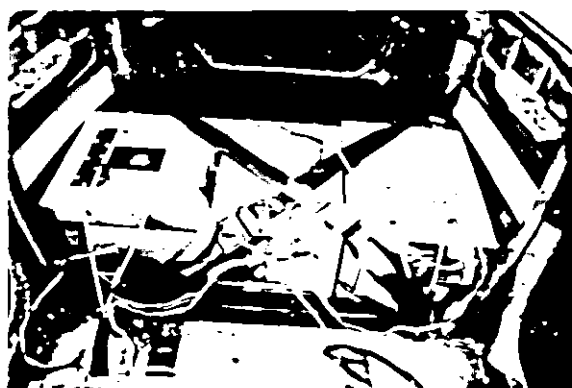


Figure 10 Computer controller and battery module
installed in airplane

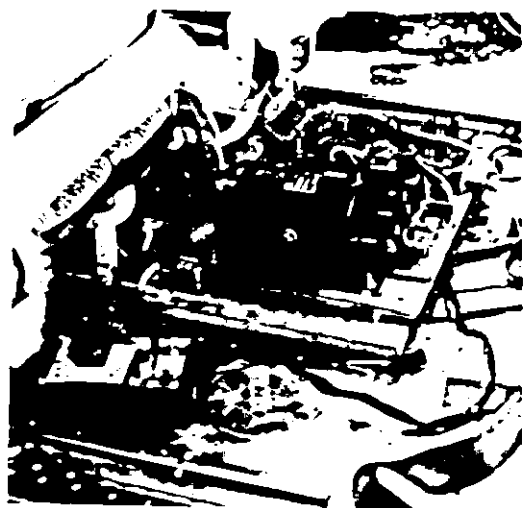


Figure 11 Transducer module installed in airplane

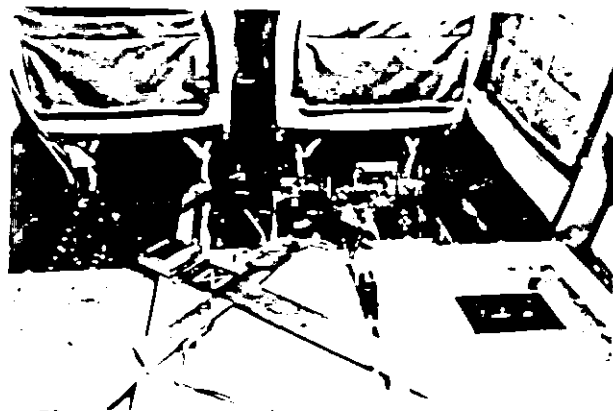


Figure 12 Cockpit instrumentation installation

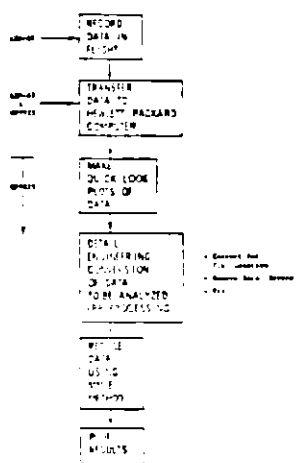


Figure 13 Data processing flow chart

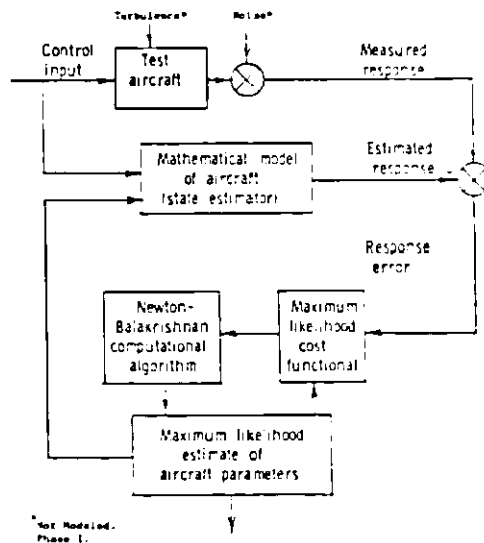


Figure 14 Maximum likelihood estimation concept
(from Reference 9)

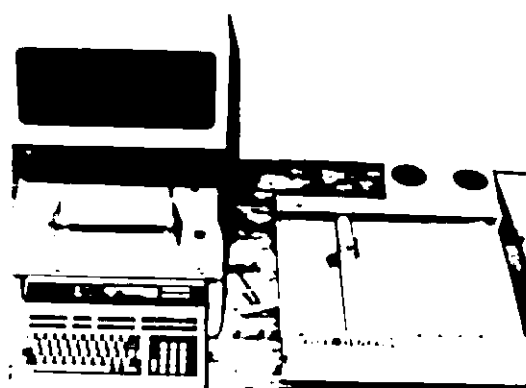


Figure 15 H.P. 9825 microcomputer

REDUCED TIME HISTORIES

FLIGHT 4 RUN # 15

120 mph (IAS)

3800 ft (pressure altitude)

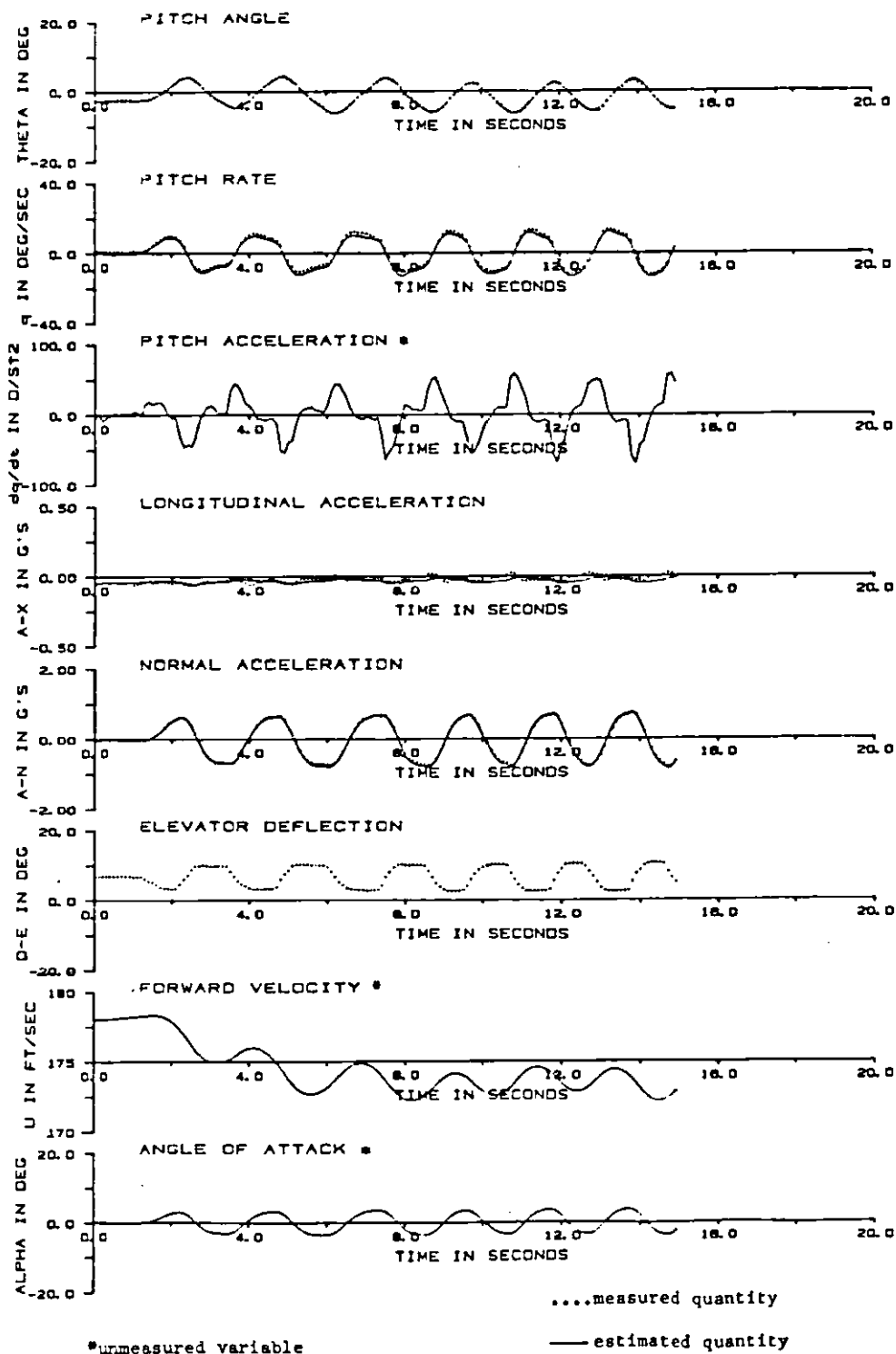


Figure 16 Reduced time history, flight 4

Table 1 Transducer accuracy and ranges used Phase I

SYMBOL	SENSOR	ACCURACY	RANGE
A_x	longitudinal acceleration	.002 g	-1 g to +1 g
A_y	lateral acceleration	.002 g	± 0.5 g
A_z	normal acceleration	.002 g	-1.5 g to 4 g
ϕ	pitch angle	0.5 °	± 30 °
θ	roll angle	0.5 °	± 30 °
p	pitch rate	0.1 °/sec.	± 50 °/sec
q	roll rate	0.1 °/sec.	± 50 °/sec
r	yaw rate	0.1 °/sec.	± 50 °/sec
δ_E	elevator position	0.4 °	
δ_A	aileron position	0.4 °	
δ_R	rudder position	0.4 °	
T	temperature	+ 2 °F	-20 to +120 °F
P _S	static pressure	+ 10 feet	0 to 25K feet
P _D	total pressure	+ 2 knots	40 to 150 knots
			40 to 400 knots

* Indicates transducers used for longitudinal stability analysis in Phase I.

+ Indicates transducers used to define initial and final conditions.

Table 2 Comparison of results

STICK FIXED, AIRSPEED 178.0 ft/sec (120 mph)

Estimation Method	KU-FRL MMLE	LAWLEY-Maximum Likelihood (Reference 16)	Roskam (Analytical) (Reference 15)
C.G. (3.5. in.)	40.4	42.3	40.3
C.W. (lb.)	2160	1848	2160
Parameter			
\dot{C}_{nq}	-23.48	-19.36 (-18%)	-17.380 (-26%)
$C_{n\alpha}$	0.160		0.013 (-92%)
$C_{n\beta}$	-0.593	-0.678 (14%)	-0.890 (50%)
$C_{n\delta_E}$	-1.246	-1.16 (-5%)	-1.263 (11%)
$C_{m\alpha}$	-0.177		
C_{x_u}	-0.049		-0.049 (0%)
C_{x_a}	-0.081	0.54 (-76%)	0.199 (-346%)
$C_{x\delta_E}$	-0.096		-0.060 (-38%)
$C_{x\phi}$	0.093		
C_{s_u}	-0.323		-0.0018 (-95%)
C_{s_a}	-4.44	-5.22 (+18%)	-4.375 (+3%)
$C_{s\delta_E}$	-0.533	-0.402 (-23%)	-0.575 (-20%)
$C_{\dot{x}_a}$	0.703	-0.36 (-15%)	

(*) As compared with the KU-FRL MMLE results.

*

* C_{nq} has a large $C_{n\alpha}$ component which cannot be predicted.

- Expansion to include all transducers listed in Table I. This requires addition of A_y , P_x , G_x , and T sensors. This then allows longitudinal and lateral stripline movement analysis.

- Development of a stable and reliable deployment method for the stripline system.

- Deployment of a step and fallable deployment method for the transducer.

- The means to allow lateral stripline assembly analysis should be added to the MUL routine. This is easily accomplished using the current HPG825 file.

- Addition of a more capable microcomputer than the HPG825 is suggested to reduce the time needed for data reduction. Substitution of an interface card can be made by use of a computer with a capability, rather than a general purpose board to allow performance analysis (I.e., time HPG825 program).

- Purchasing study is suggested to allow performance analysis (I.e., time HPG825 program).

- Design (part) of the new stripline.

- Tests are recommended to other general vibration applications to demonstrate the system's adaptability. Recommended are tests on a high-performance, single-stage testarticle.

- All transducers should be calibrated as a system. Using the self-test feature into the possible "uniqueness" problem. This should be a definitive test of the calibration package for transducer calibration as suggested.

- The tests suggested above would also aid in providing confidence in the design of the C.G. of the stripline if located area of research, to validate the MUL (or similar) concepts.

- A means for determining where the C.G. of the stripline is located as a means to reduce calibration errors.

APPENDIX B: RECORDENDATIONS FOR PHASE II

www.vedic.org.in | www.srimadbhagavat.org | www.vediclibrary.com | www.vedicastrology.com

GENERAL AVIATION FUEL CONSERVATION IN THE 1980'S

George R. Bromley
Beech Aircraft Corporation
Wichita, Kansas

ABSTRACT

Until recently, general aviation pilots showed little interest in long-range cruise control; they purchased airplanes more for speed than fuel economy. Accordingly, general aviation manufacturers, for several decades, limited the amount of handbook guidance for saving fuel and installed larger and larger engines to increase speed.

Now, however, manufacturers take the lead role in helping pilots save fuel. Their first efforts have been to issue rules-of-good-practice and money-savings tips that encouraged pilots to think about economy. Secondly, they have been revising the formats for performance data to highlight the tradeoffs between fuel economy and speed. Meanwhile drag clean-up programs improved the flight efficiencies of several models. Now flight planning innovations (some exploiting the latest computer technology) help pilots more easily determine the optimum altitudes and power settings for various winds and trip lengths. Additional flight testing will more clearly identify optimum climb and descent schedules. And, for airplanes of the future, new design criteria will place more emphasis on fuel economy than on top speed or STOL-like performance.

Flight test engineers are at the center of this activity. No other group knows better how to measure, process, and present performance and how to identify wasteful practice. This paper urges general aviation flight test engineers to maintain a leadership role in aviation fuel conservation.

INTRODUCTION

The cliche that there is nothing new under the sun, typifies the approach in this paper. Trouble comes when things, once known, are forgotten. Changing interests and perceptions cause issues to vanish, only to reappear in other eras under different guises. So it is with aviation fuel conservation. Fuel conservation in aviation was once thought of as competition for range and endurance records. Later it was the means of escape from enemy-held territory. Now it is business survival. The only thing that is "new" is our perception: how we see the problem and the techniques and innovations we envision to solve the problem.

George R. Bromley, Flight Test Engineer - Fuel Conservation Programs, Engineering Flight Test

HISTORY

Pilots straggling home with battle-damaged airplanes in World War II, didn't always have the fuel to make it. Stories describe desperate efforts to stretch fuel.

These pilots didn't worry about fuel cost and the supply at the pump, yet their struggles to get more MPG dealt with the same operating principles faced by today's pilots because of fuel cost and availability.

In those life-or-death situations, WW II pilots invented their own ways to extend fuel. Some worked and some didn't. Training did little to prepare pilots and, indeed, little was known anywhere about how the engines tolerated high power and extra lean mixtures. And airspeeds for maximum range in high-drag configurations, with some engines caged, were usually unknown.

Following WW II, fuel cost and availability were still not problems but unrefueled range remained crucial. To reach new targets in the cold war era, B-29's, B-50's and B-36's needed intercontinental range. This need to fly farther with a given amount of fuel required better engine technology, better sizing of the engine to the airframe, and better cruise control technique.

The B-36 design and operation brought together the best of these efforts for reciprocating engines. Extensive performance tests established optimum airspeeds for long range on any combination of engines, weight, and drag configuration. B-36 performance charts illustrate, perhaps, the most comprehensive set of cruise control data to this date. The R-4360 engines got their high brake specific fuel consumption using manual leaning, manual spark advance, a complex turbo-boost system, and cooling provisions that allowed continuous operation at high brake mean effective pressures (BMEP's).

When B-52's replaced the B-36's, it wasn't long before virtually the entire military fleet was turbine powered. Turbine power greatly simplified cruise control. Aircraft performance engineers (of which there were two on each B-36) soon took other jobs. Turbine powered airplanes, in general, simply flew as high as practical (giving some consideration for winds) to get the best miles per gallon. Where long range remained important, air refueling eliminated the requirement for maximum miles per gallon in favor of higher cruise speeds.

General aviation, meanwhile, had plenty of avgas at attractive prices and general aviation manufacturers advertised speed to attract customers. Designers, for the most part, simply called for bigger engines whenever they wanted more speed.

As in the auto industry, fuel efficiency with its attendant poky performance, would not generate sales. Range and duration were lackluster subjects. Record setting flights for range and duration in civil aircraft had gone out of fashion with the passing of the 1930's.

And so, with the passing of a generation of pilots following WW II and the early cold war years, pilots and manufacturers, alike, lost the knack (and incentive) for extending fuel.

Today, however, due to the energy shortage, the incentive for getting maximum range has returned; this time on a broad front. Although the wherewithal to conserve fuel has been misplaced by years of neglect, it is now being rediscovered.

THE PROBLEM

The problem, nevertheless, is that a pilot's means of conserving fuel are still limited; where fuel considerations apply to the total flight, not the cruise portion alone.

The general aviation industry is acting, however, and some remedies are already evident.

The General Aviation Manufacturers Association (GAMA) is rewriting its Pilots Operating Handbook (POH) Specifications to increase emphasis on fuel conservation in the performance section of the handbook. Light general aviation airplanes, even as they exist today, have good fuel efficiency when compared to other forms of transportation, and the additional efficiency available by flying them at optimum altitudes and airspeeds can be achieved without hardware changes. Refinement of the performance data suffices as a relatively quick, low-cost method of capitalizing on the latent economy which these airplanes already possess.

With respect to modifying airplanes, in recent years most manufacturers conducted drag clean-up projects. Through the 1950's and '60's, many lightplane designers had opted for slab sides, protruding rivets, minimal filleting, and big cowl flaps and exhaust stacks on oversize engines to get the appearance of good performance with lowered production cost. During the '70's, however, this effort largely spent itself while fuel prices started to climb. Drag clean-up projects on existing models became fashionable in the industry with the Mooney 201 taking most of the press.

For the future, totally new designs will not only be cleaner aerodynamically, they will also feature engine-to-airframe matching criteria that place higher priority on fuel conservation.

The immediate problem, however, is developing the best format to comply with the GAMA POH specification and help pilots determine optimum power settings and altitudes for their particular operations. Although such information may appear mostly in the performance sections of POH's, separate manuals and hand-held calculators (preprogramed with performance algorithms) are attractive adjuncts.

In search of the best format to comply with the new GAMA POH specification, a fundamental understanding of cruise control principles is essential.

CRUISE CONTROL FUNDAMENTALS

In general terms, cruise control is simply flying in the most efficient way to accomplish a given performance objective. Objectives can be minimum fuel consumption, maximum duration, minimum flight time, low noise, controlled arrival time, or whatever; obviously one objective usually precludes another. The following discussion emphasizes the objective of conserving fuel.

The basics of range performance, (which implies fuel conservation), inevitably include the concept of specific range, preferably in terms of ground nautical miles per pound (or gallon) of fuel.

Specific range can be plotted in several formats. The plot in Fig. 1 is typical. Airspeed is on the abscissa and specific range is on the ordinate. A family of curves results when various weights or other drag configurations are represented. Lines of constant power or thrust run diagonally across the curves. The plot presents the entire performance spectrum in a single view. Each performance

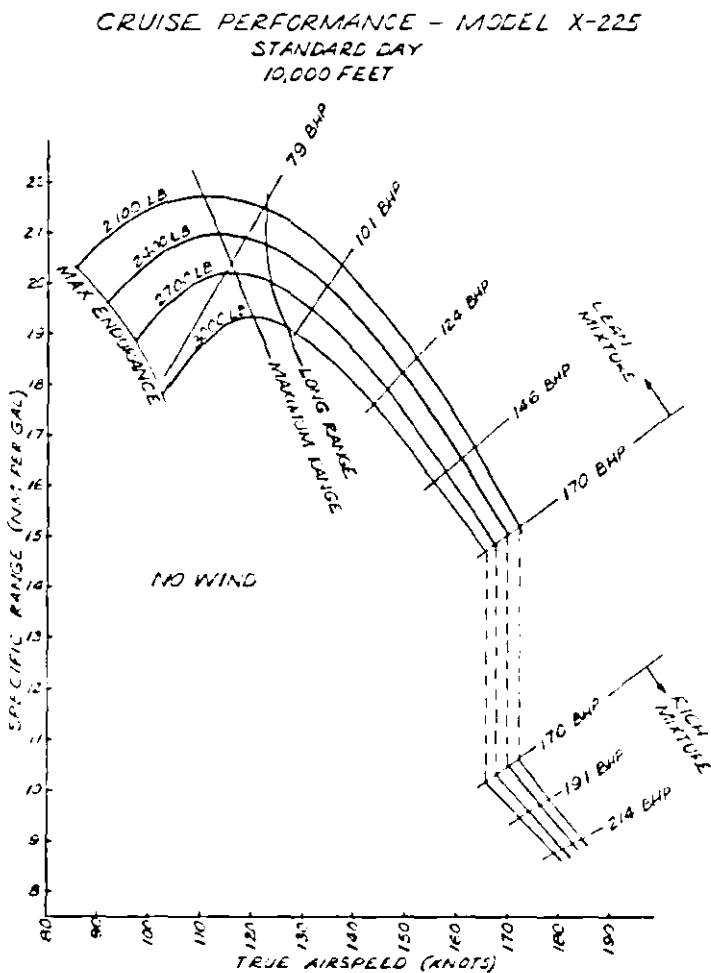


Fig. 1

point appears in the context of all other points.

Although performance commonly appears this way in military and other professional manuals, the POH's for light general aviation airplanes have not, until recently, used such presentations. Only recently, for example, has Mooney chosen to include specific-range curves in its M-20K POH. Fig. 2a shows the specific-range chart for the M-20K at 10,000 feet. Performance is given for two weights under no-wind conditions. The chart only applies to cruising, of course, and it is well to remember that climbing and descending also exist in the optimization equation for every flight.

Not depicted on the Mooney chart is what is known as a long-range airspeed line. Such a line defines the airspeed and power for optimizing the specific range in cruise. The line is traditionally defined as the locus of points across a family of weight curves where the specific range is 99 percent of maximum range (Fig. 1). Flying at this condition is preferable to flying at the maximum-range airspeed because, for a negligible decrease in range, the airspeed is significantly faster. This extra airspeed usually makes an airplane easier to fly and airspeed fluctuations in turbulence are less apt to cause the airspeed to slip to the back side of the power curve.

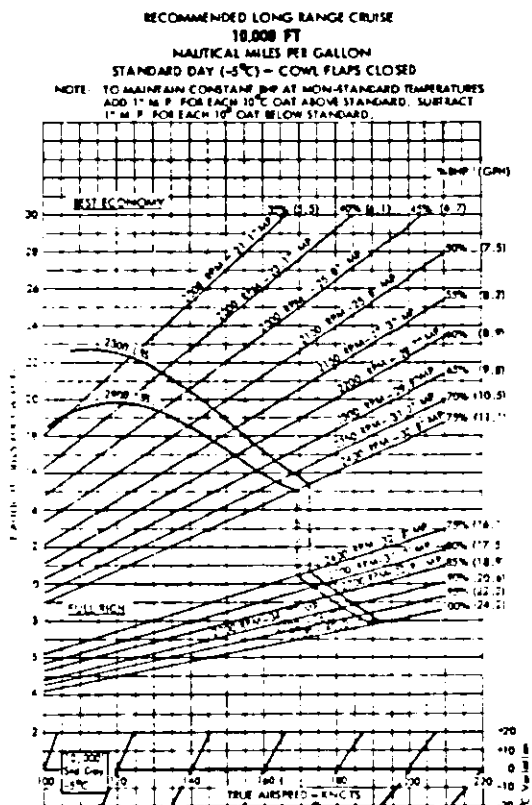


Fig. 2a

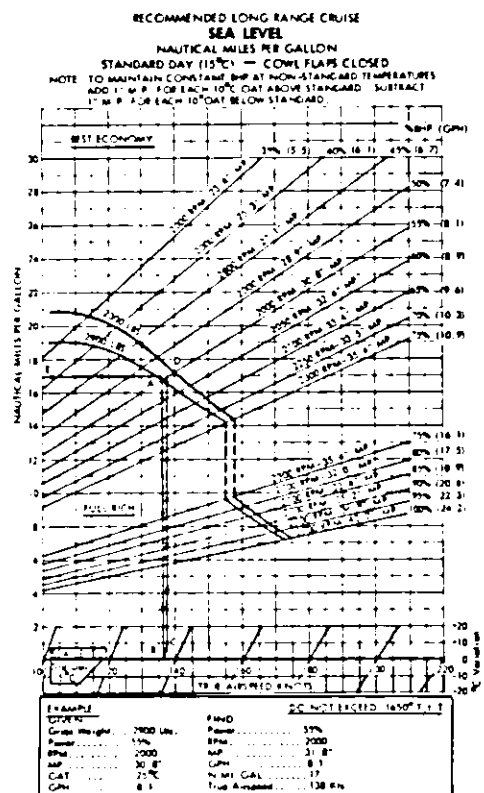


Fig. 2b

Fig. 3a through Fig. 3e shows other forms of the specific-range chart. All forms involve the same principles. Depending on the manufacturer's application and associated data, some handbooks use one form and some another.

In any case, flight planning with specific-range charts makes it possible to see, graphically, the tradeoffs between fuel consumption, speed, power, weight, and altitude. Because of varying mission requirements, it is not always desirable to operate in either the long-range or maximum-speed condition. Conveniently, the chart shows fuel consumption (in terms of specific range) for flights at any speed within the operational envelope; in other words, for any combination of airspeed and power.

If the specific-range data appears in tables rather than graphically, the tradeoffs are less apparent.

Unfortunately, specific-range charts as discussed so far, and as traditionally used, are not sufficient, in themselves, for planning an optimum flight. As implied, the effects of wind and temperature at various altitudes and the fuel used for climbing and descending are important factors.

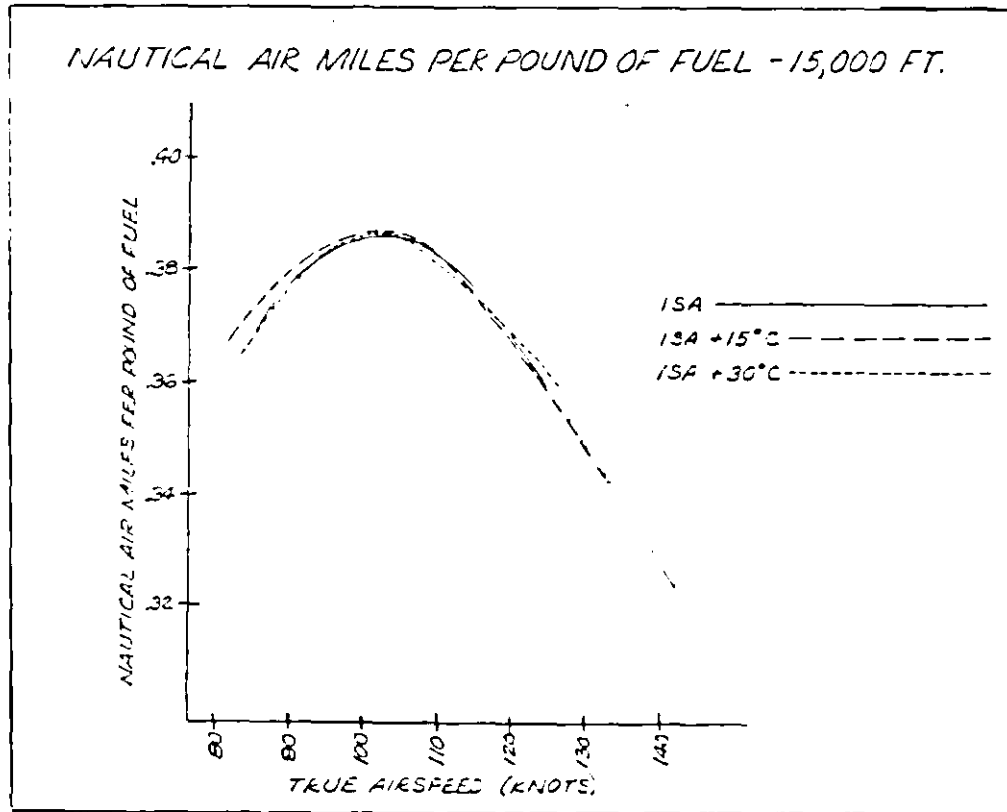


Fig. 3a

NAUTICAL AIR MILES PER POUND OF FUEL - 15,000 FT.

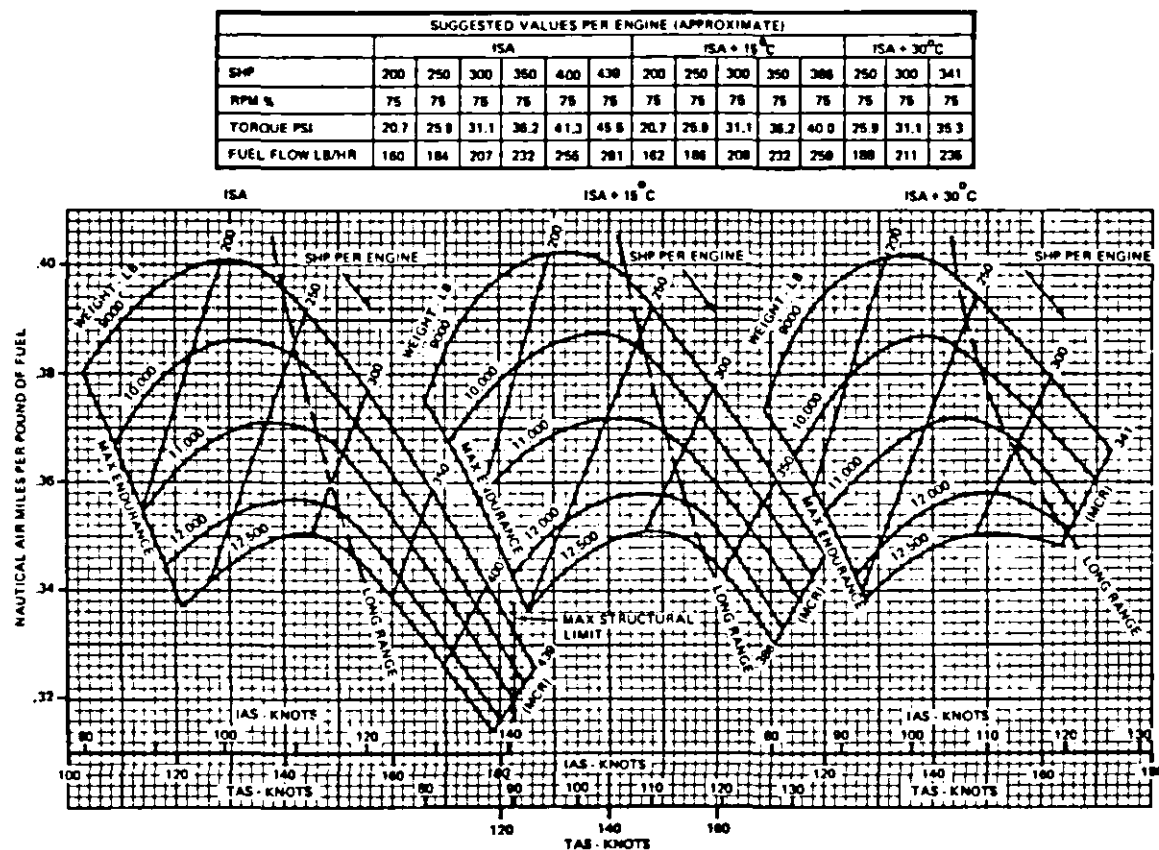


Fig. 3b

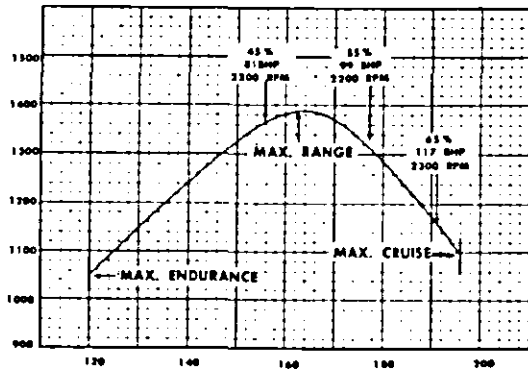
RANGE AT ALTITUDE

10,000 FEET

LEAN MIXTURE
4000 POUNDS
NO RESERVE
112 GALLONS

10000 FT.

RANGE — MILES



TRUE AIRSPEED — MPH

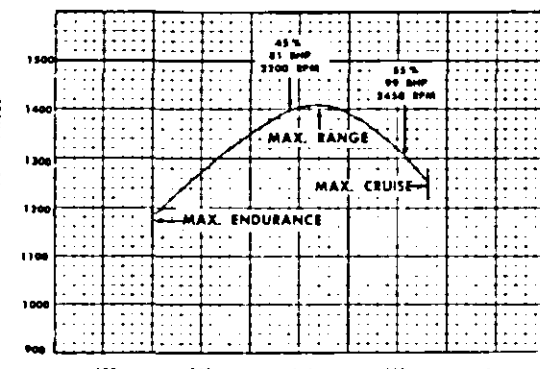
RANGE AT ALTITUDE

15,000 FEET

LEAN MIXTURE
4000 POUNDS
NO RESERVE
112 GALLONS

15000 FT.

RANGE — MILES



TRUE AIRSPEED — MPH

Fig. 3c

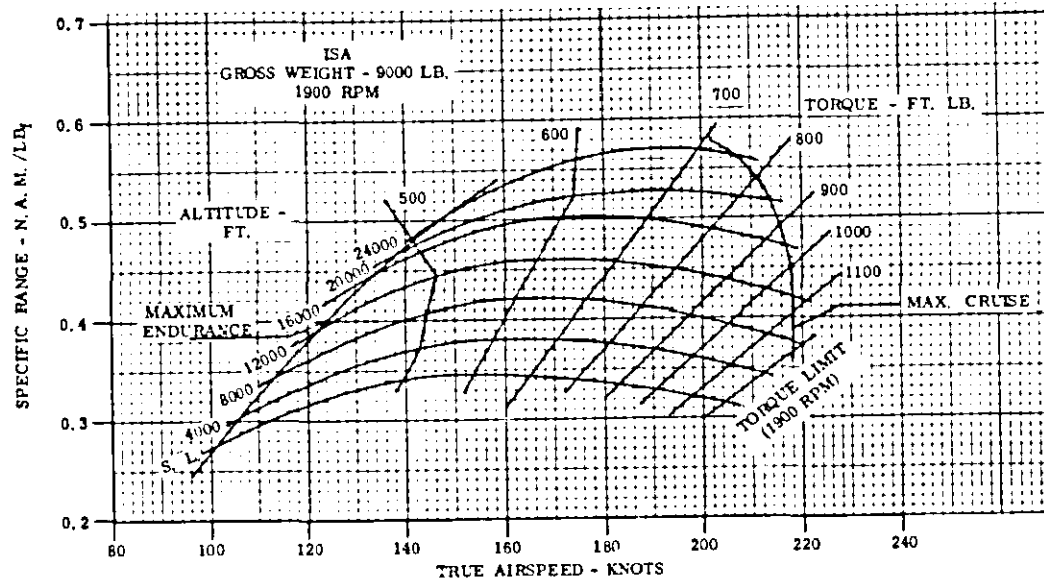


Fig. 3d

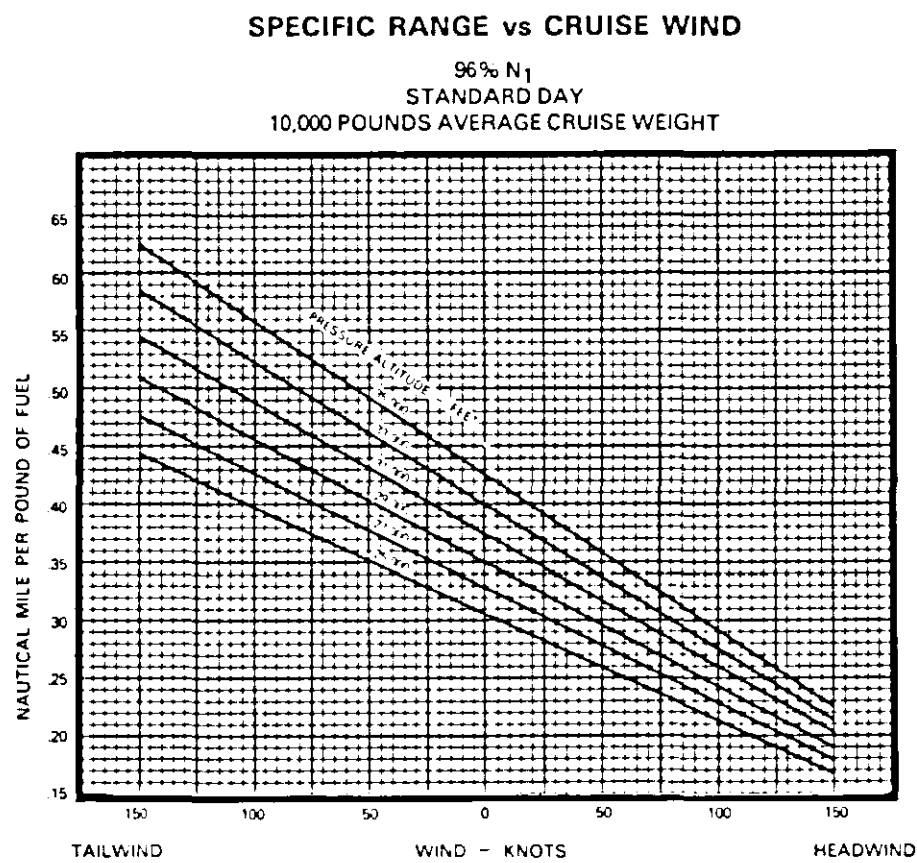


Fig. 3e

Partial compensation for this is possible by constructing specific-range curves for various wind components. Assuming that a no-wind specific-range curve is plotted for a single weight (Fig. 4a), so the chart is not filled with a family of curves, other curves can be laid down for various wind conditions simply by using groundspeed instead of airspeed in the calculations. Note in Fig. 4b that the shape of each wind-related curve is unique, thus it is not possible to use one curve and merely shift the ordinate scale according to the wind strength.

Drawing a line through the peak of each wind-related curve (Fig. 4c), defines the maximum-range airspeeds based on wind. Again, this is valid for only one weight and one altitude.

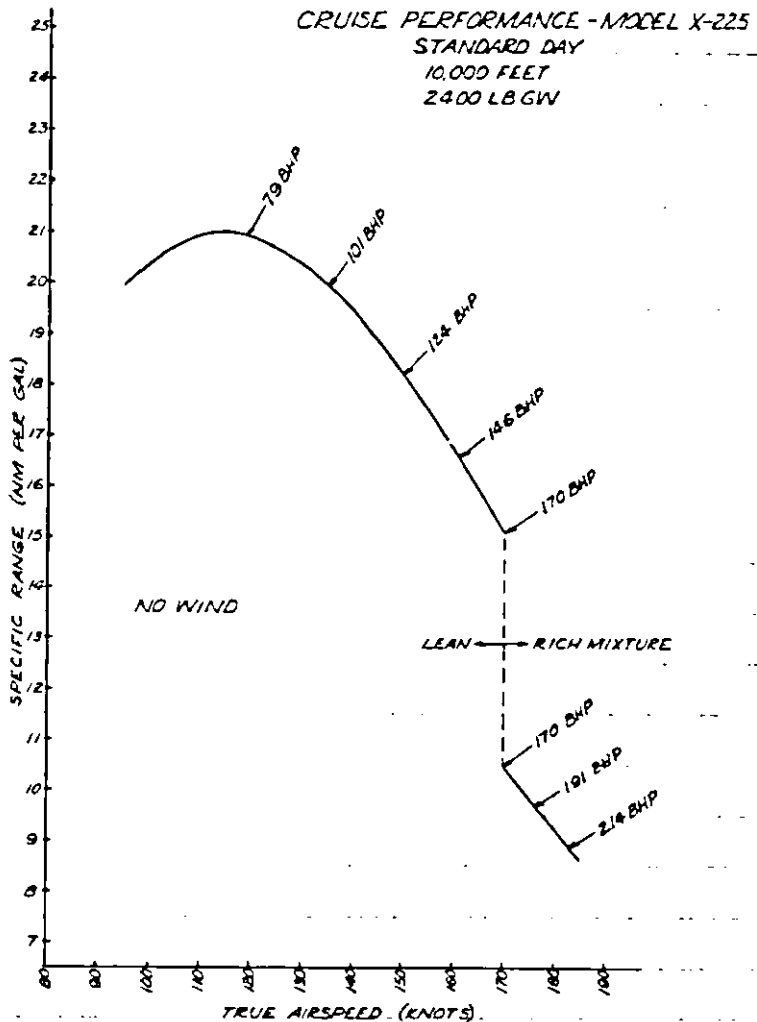


Fig. 4a

Since operation is usually preferable at long-range rather than maximum-range airspeeds, Fig. 4d shows the long-range line based on flying at 99 percent of maximum range. Note that the long-range airspeed for the no-wind curve coincides with the maximum-range airspeed for a 28-knot headwind. This illustrates why, when flying long-range cruise control, airspeed is not increased for flying with headwinds unless the headwind exceeds a rather high value. In this case, maximum-range airspeed is used instead of long-range airspeed. Some range benefit comes from slower airspeeds with tailwinds but the benefit is offset if handling qualities deteriorate.

With wind accounted for in specific-range charts, the long-range airspeed lines would still show only the optimum speeds to fly for economy; they would not show the best

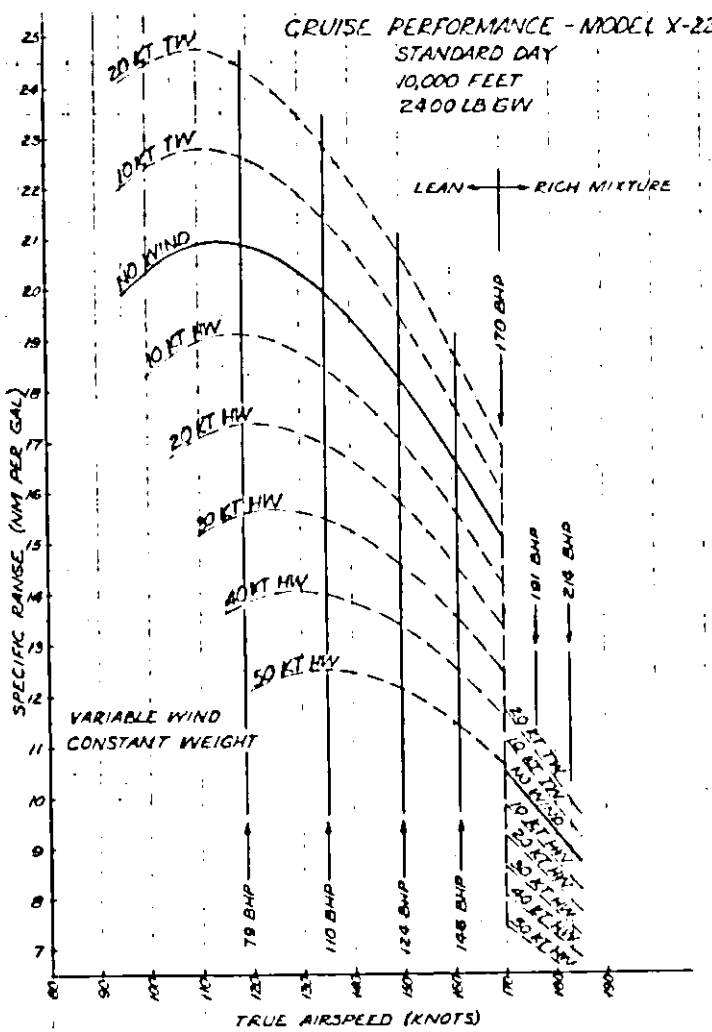


Fig. 4b

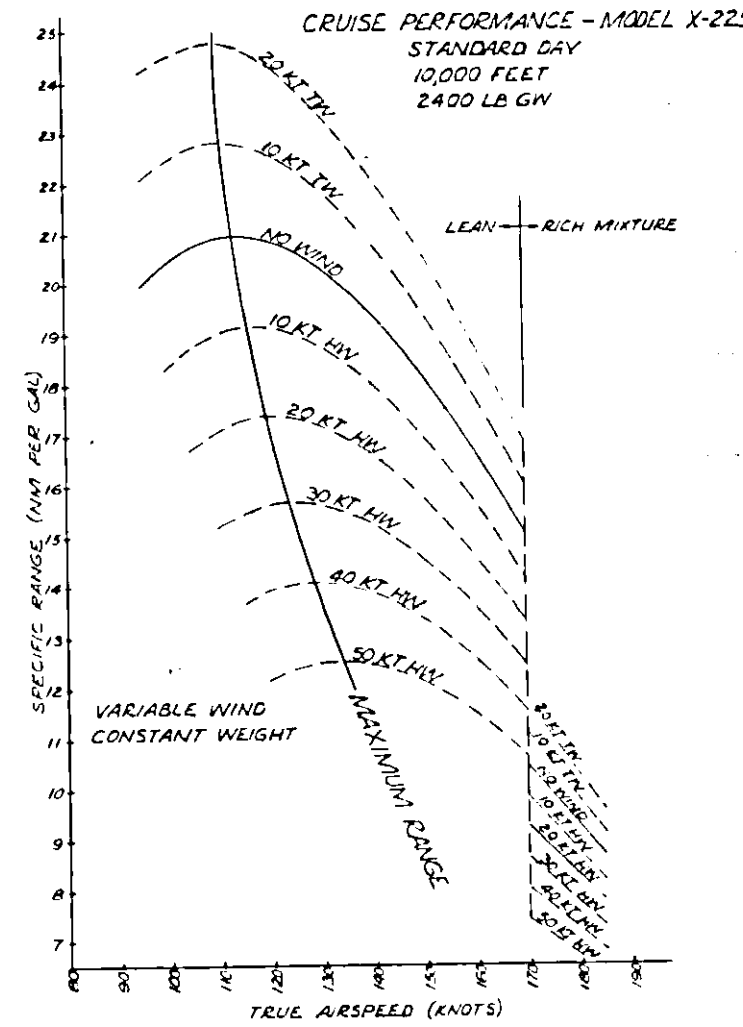


Fig. 4c

altitude. In general, the lesser fuel flow rate in descent does not entirely compensate for the greater fuel flow rate in climb. To optimize the overall flight, the specific range in cruise must be good enough to justify the net excess fuel expenditure of the climb over the descent. This, in turn, is a function of cruise distance.

Another aspect of cruise control is engine operation at RPM, manifold pressure, and mixture combinations that give the best brake specific fuel consumption. This subject, alone, would constitute another paper.

Suffice to say here, tradeoffs must be made with the greater heat rejection attendant to high BMEP (and consequent cooling drag), and reduced engine life. Certification for operation at high BMEP's involves warranty safeguards, acceptable vibration characteristics, the integrity of instrumentation to accurately set and monitor power, etc.

CRUISE CONTROL AND THE PRIVATE PILOT

Though the foregoing may seem elementary to engineers who work with it routinely, cruise control intimidates private pilots. This is probably because training does not include it and POH's usually avoid it.

Many pilots are thus unmindful of the potential savings their airplanes offer. And, for those who suspect savings, the wherewithal to maximize them is only now becoming available.

A curious Mooney 231 pilot, for example, can use his

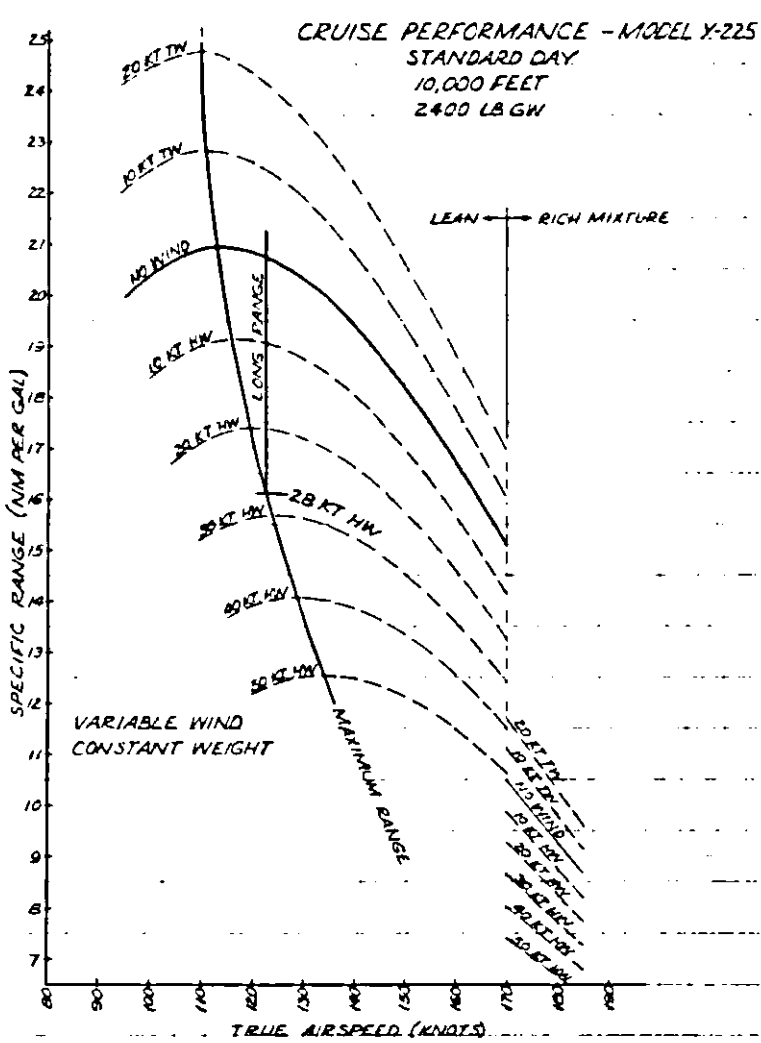


Fig. 4d

Though the foregoing may seem elementary to engineers who work with it routinely, cruise control intimidates private pilots. This is probably because training does not include it and POH's usually avoid it.

Many pilots are thus unmindful of the potential savings their airplanes offer. And, for those who suspect savings, the wherewithal to maximize them is only now becoming available.

specific-range charts to learn that, based on \$2.00 per gallon fuel, cutting 18 minutes off of a 163-mile cruise segment (4000 ft., no-wind), costs him \$6.13. But he cannot, in a simple way, assess the combined effect of climb, choice of altitude with winds aloft, and descent on the overall cost and time for his flight, yet these factors can radically change his analysis.

In the past, performance data available to general aviation pilots, private and professional alike, has not often made a thorough cruise control analysis possible. For most general aviation pilots, cruise control consisted of little more than rules-of-thumb: one power setting for climb, another for cruise (usually based on the noise and vibration levels in a leaned condition), and descent power set by reducing throttle according to the rate of descent while keeping the airspeed from becoming excessive. Until the fuel crunch, there was little inducement to do otherwise.

Through the years, general aviation manufacturers accommodated pilot complacency about cruise control by not complicating performance data. Tables were used wherever possible to avoid the graphs which might cause pilots to avoid the POH performance sections altogether. And without the multi-dollar benefit from slowing to long-range airspeeds, cruise control was simply left out of pilot training.

The "jump-in-and-go" concept prevailed for most of general aviation, perhaps not so much because pilots didn't care, but because they didn't have the wherewithal and knowledge to do otherwise.

NEW WAYS TO PROVIDE PILOTS WITH THE INFORMATION THEY NEED TO SAVE FUEL

Today the challenge to make performance data more comprehensive while simultaneously simplifying its use, goes to flight test engineers. And increasing emphasis on fuel conservation by the government, as well as simple economics, makes the effort essential.

The flight planning method devised for any model, is best when it accounts for the performance characteristics and normal use of the model. The detail and complexity of the method, however, as well as the time needed to employ it, must be warranted by the economic benefit to the pilot.

Within these guidelines, Beech engineers are studying different ways to present and apply flight planning information. Changes will be phased in with the present system as follows:

First, currently published performance is retained intact while various devices help apply it. Chief among

these devices, to date, is a read-only memory module for the HP41-C hand-held calculator. The module is preprogramed for the performance of the Beech Super King Air 200 and provides all the data in the 1700 RPM, recommended power, cruise range plus run-up, taxi, takeoff, climb and descent performance. The programing accounts for winds and temperatures aloft plus takeoff weight. It uses the calculators alpha-numeric display to ask for inputs and then display altitude, torque, fuel used and duration for minimum fuel, as well as minimum time, flight plans.

Another device for the King Air 200, still retaining the POH performance section intact, is a performance catalog. This catalog, like other catalogs, allows a pilot to look up the cost and availability of an item when he enters with his requirements. If he needs the cost in time and gallons to go x miles in y atmosphere, he looks it up under distance, altitude temperature, and wind component. The catalog is, in effect, a compilation of "all possible flight plans," worked-out and listed in convenient increments of distance, wind, and temperature conditions for all altitudes. The volume is no larger than a medium-size telephone book.

Depending on customer acceptance, Beech will offer or refine either or both of these flight planning devices as well as apply them to other models. Both have the feature of not disturbing currently published data and, as such, can be offered independent of POH's, much in the fashion that small, circular calculators are offered to help determine power settings.

In a continuing search for ways to improve the performance section of POH's and to comply with the GAMA requirement for emphasis on fuel conservation, Beech is reviewing many performance formats including modified versions of the specific-range charts, improved climb and descent schedules, and new flight planning algorithms. In time, this may entail additional flight testing to establish, for example, the most economical ways to climb and descend.

Flight test engineers throughout general aviation have developed a variety of charts and tables for presenting performance. Some, such as the specific-range chart, have not been widely used but are being reconsidered for use to save fuel. Other charts are recent developments which, in some cases, have never been published. With increasing demand for more sophisticated flight planning data, the best of these charts are sure to appear within this decade.

An example of innovation on specific-range charts, appears in the Mooney M-20K POH. Specific-range charts are normally

for the standard atmosphere and, accordingly, the Mooney charts specify standard-day conditions. Nevertheless, on their sea-level chart (Fig. 2b), Mooney illustrates a way to adjust for nonstandard atmospheric temperatures. A manifold pressure adjustment, prescribed above the chart, compensates power while a corresponding true airspeed adjustment at the bottom of the chart, revises the specific range.

Mooney, on the other hand, did not include a calibrated (or indicated) airspeed scale in conjunction with the true airspeed scale. Such a dual scale is common on specific-range charts, generally, and is helpful inasmuch as airspeed indicators usually do not show true airspeed.

Another of the more interesting charts (which might compete with the specific-range chart), comes from Cessna and appears in Fig. 5a. Like the specific-range chart, it shows each performance point as it relates to the entire performance spectrum. The pilot notes immediately where his operation lies relative to the performance boundaries and senses, at least to some degree, which parameters are most critical in obtaining the desired performance. Some airplanes are more sensitive to weight burn-off, for example, while others are especially sensitive to altitude.

The chart is an enhanced version of the ordinary speed-power polar. In Fig. 5b, a single polar represents a given airplane configuration at one weight and one altitude with the speed and power scales drawn to show their origin. A line from the origin, drawn tangent to the curve, touches the curve at the speed-power combination that corresponds to maximum range. If the line is drawn from the right of the origin by the amount of a headwind, or from the left of the origin by the amount of a tailwind, the point of tangency corresponds to the maximum-range speed and power for the respective wind.

Cessna engineers plotted a family of these curves for various flight weights, expanded the power and airspeed scales to accommodate all altitudes, and showed the maximum-range lines for various wind components as the locus of points across the various weight curves (Fig. 5a). The chart, in addition to defining maximum-range operation, shows maximum endurance as the lowest point on each curve. The power for any other airspeed is included along the remainder of the appropriate curve. Like the proverbial "picture that's worth a thousand words," one of these charts is equivalent to pages of tables.

Several other charts that have not had widespread use in the past are interesting. Fig. 6 shows time and fuel consumed over an entire flight of a given distance. The chart accounts for takeoff, climb, cruise, and an allowance for descent. A matrix of altitude and power shows the relative effects of all combinations of power and altitude on fuel economy. Unlike the previous chart (as well as the specific-range

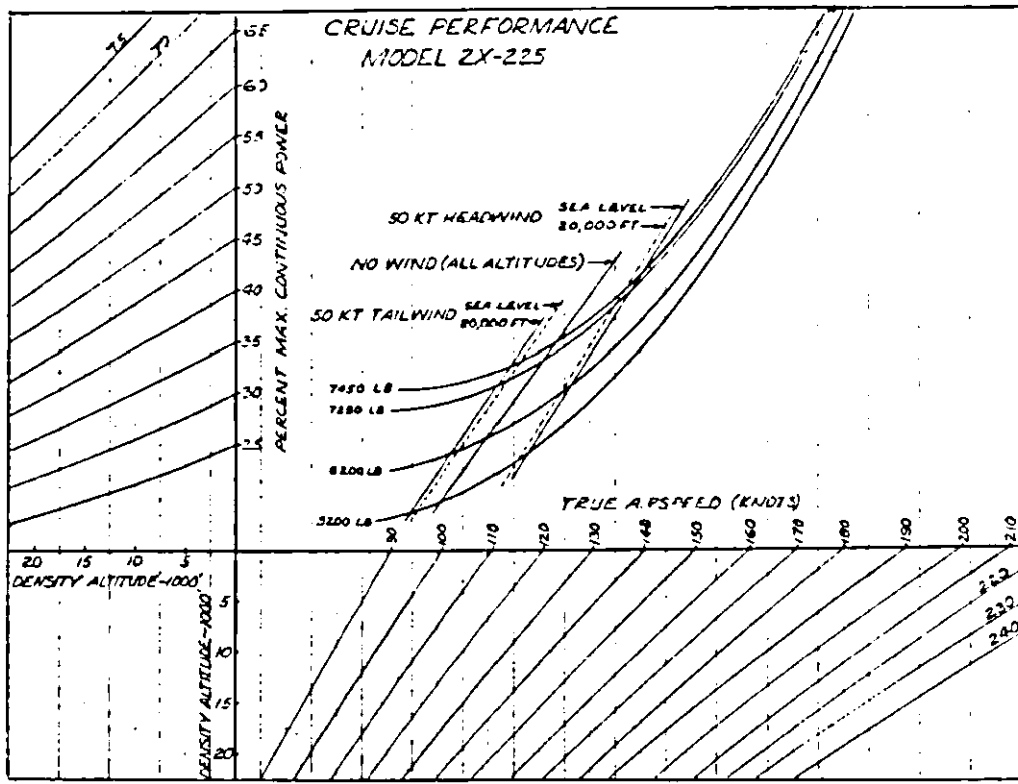


Fig. 5a

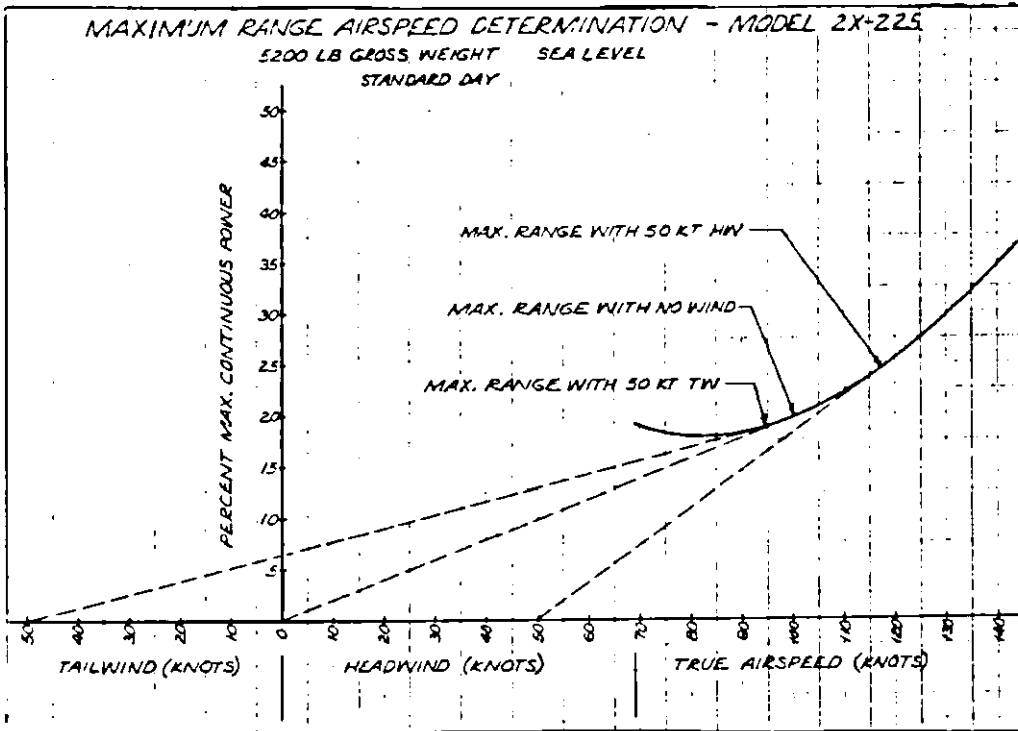


Fig. 5b

chart), the total flight is accounted for so a true optimization results. A series of such charts in practical increments of distance might constitute a book, however the pilot would use only one chart per flight.

Although Fig. 6 represents a no-wind case, charts can be made equally well for increments of headwind and tailwind or, alternatively, "no-wind" charts can be used and, where wind exists, the chart distance can be redefined as air miles instead of ground miles. This necessitates an initial guess at air distance (which is a function of time aloft) so an approximate flight time can be found and, in turn, a more accurate air distance can be

established, until satisfactory accuracy exists. This juggling should be possible without pencil and paper while flipping between two charts.

The chart in Fig. 7 is a simpler but less sophisticated version of the Fig. 6 chart. It is more in keeping with past practice, perhaps, but it does not reveal the flight duration.

Fig. 8a through Fig. 8e shows still other charts, all of which are common formats but none of which, alone, enable a pilot to establish the power and altitude for minimum fuel consumption on a given trip. When combined with other data, however, the charts have value, either for interim application or where cruise control operations are less significant, such as primary trainers and agricultural airplanes.

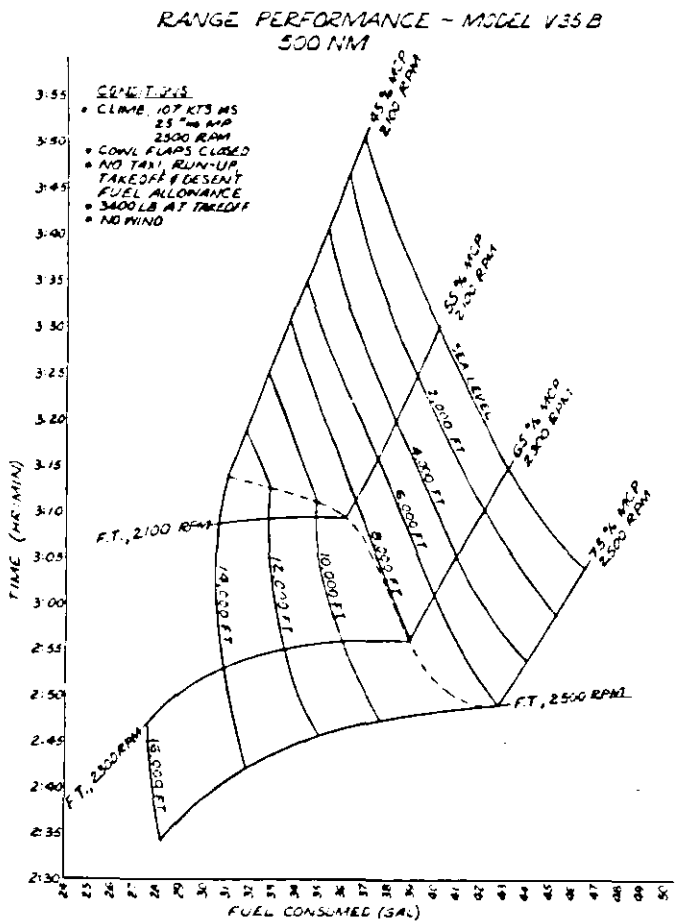


Fig. 6

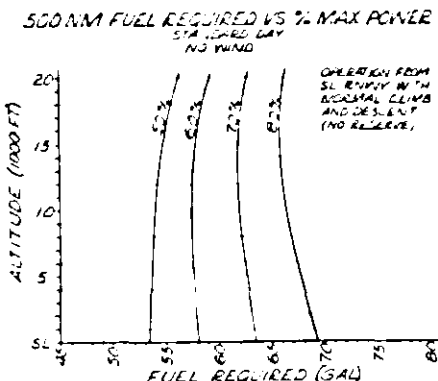


Fig. 7

To augment such charts, manufacturers issue guidelines such as

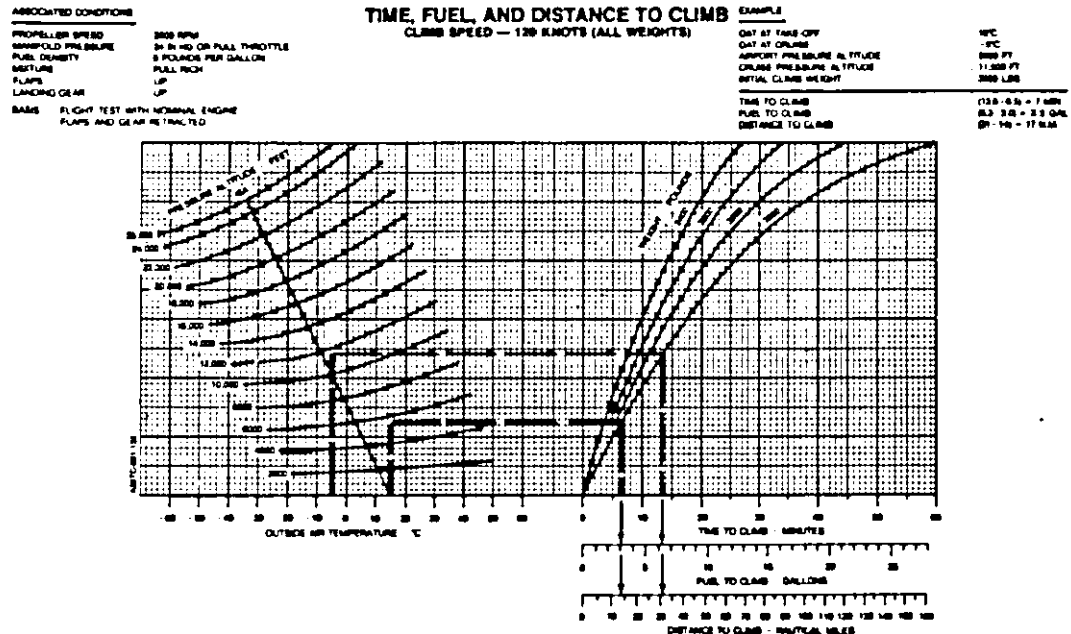
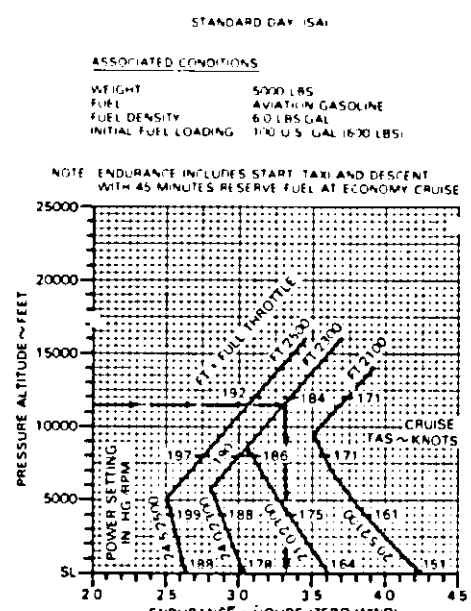


Fig. 8a

ENDURANCE PROFILE - 100 GALLONS

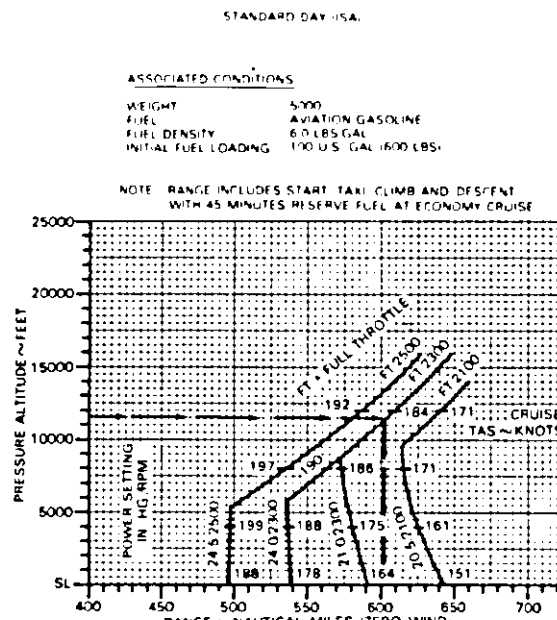


EXAMPLE

PRESSURE ALTITUDE 11500 FT
POWER SETTING 2300 RPM
ENDURANCE 3.3 HRS

ENDURANCE 3.3 HRS - 18 MIN.

RANGE PROFILE - 100 GALLONS



EXAMPLE

PRESSURE ALTITUDE 11500 FT
POWER SETTING 2300 RPM
RANGE 6.4 NM

Fig. 8b

Fig. 8c

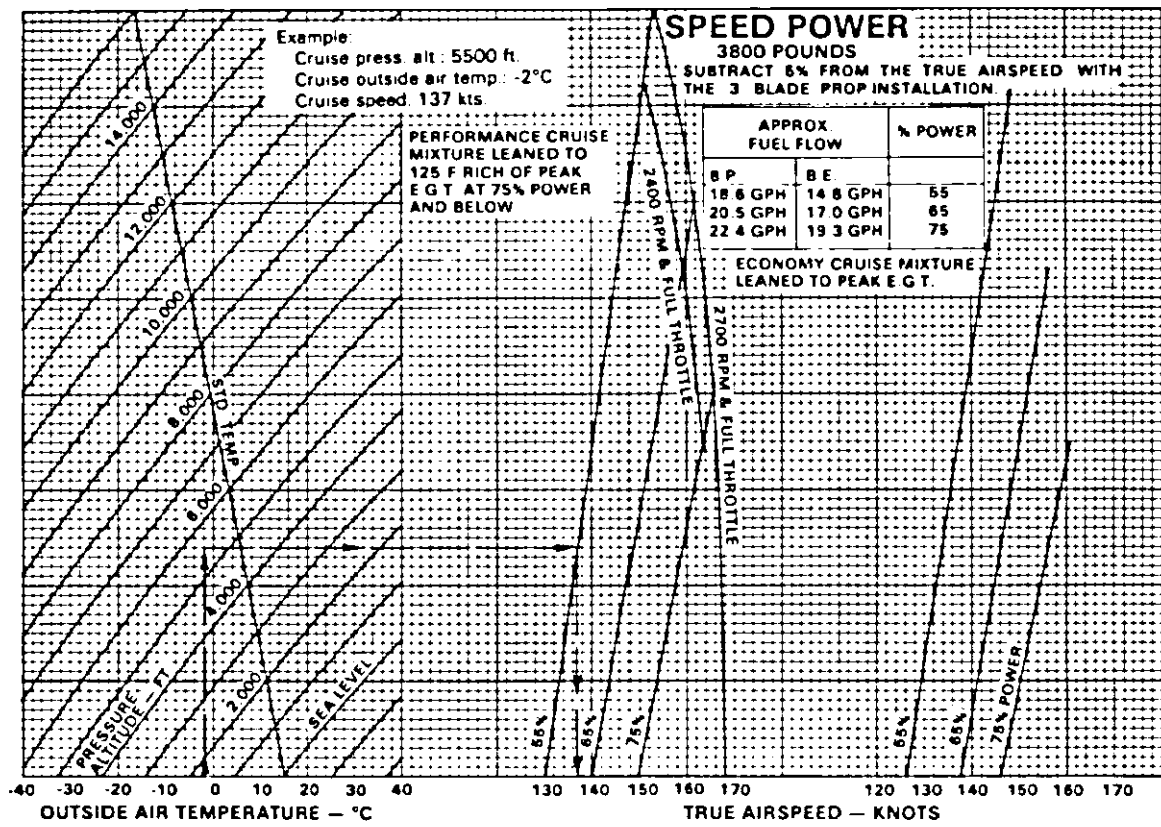


Fig. 8d

DESCENT

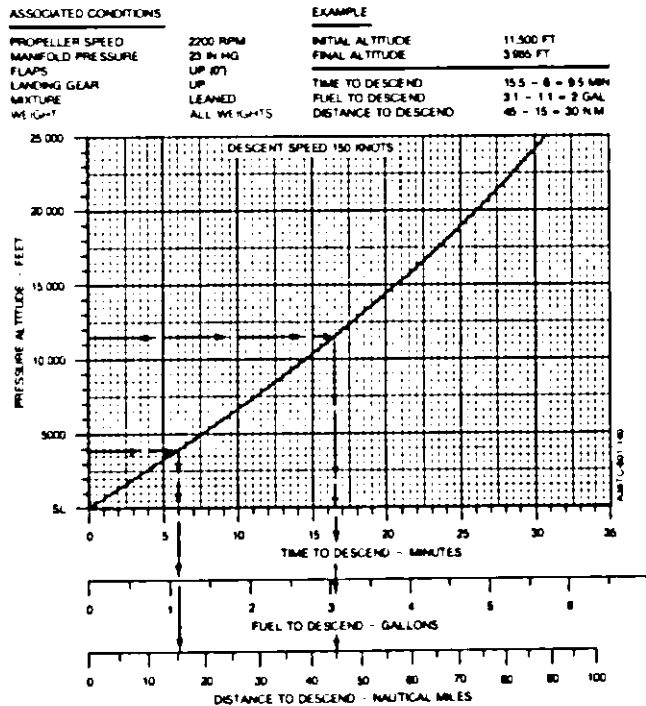


Fig. 8e

RULES OF THUMB

1. Cruise at or below 55% power.
2. Optimum altitude vs. stage length.
- NOTE:** 8000 ft. for less than 250 miles. Increase altitude 8000 feet for each additional 100 miles. Optimum altitude can be varied \pm 3000 feet with little effect.
3. Select the altitude which will give the best wind advantage.
- NOTE:** Winds are primary in selecting altitude, especially for distances between 300 and 500 miles.
4. To take advantage of higher altitudes the increase in TAS with altitude at a constant power setting must be greater than any wind disadvantage at the higher altitude.
5. Extra weight is extra drag.
6. Extra distance is wasted fuel.
7. Good maintenance saves fuel.
8. Throttle back and conserve fuel.

Fig. 9a

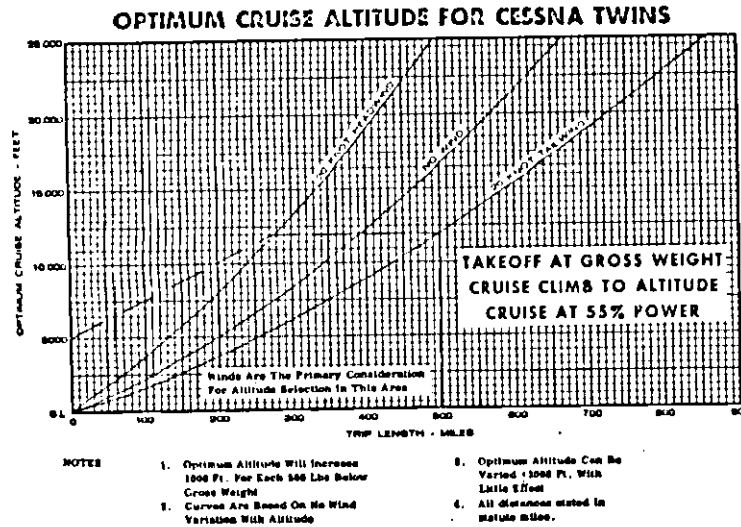


Fig. 9b

CESSNA AIRCRAFT COMPANY, WICHITA, KANSAS

IF YOU'RE GOING TO GET MAXIMUM USE OF YOUR AIRPLANE AND HELP OUR NATION SAVE ENERGY, YOU WILL HAVE TO CONSERVE FUEL—MAKE THE AVAILABLE FUEL GO FURTHER. HERE ARE TWELVE IDEAS TO HELP:

1. **KEEP GROUND OPERATIONS TO A MINIMUM.** Plan arrival and departure times to avoid peak hours of operation at the airport. Substantial fuel can be saved by reducing the time that the airplane is operated on the ground. A cool to the lower before starting the engine, reduced power and a short run-up before takeoff will all result in fuel savings.
2. **CLIMB EFFICIENTLY.** Use the speeds recommended in your Pilot's Operating Handbook. Lean your engine during climb—your Pilot's Operating Handbook tells you how. Higher powers are normally used during climb and fuel is consumed at a high rate. During this time—proper leaning can result in substantial fuel savings.
3. **ALTITUDE SELECTION.** For a given power setting true air speed increases with altitude, resulting in more miles per gallon of fuel. Long range trips can be made with less fuel when flying high. Cessna airplanes can gain from 5% to 10% additional gasoline mileage by operating at higher altitudes. For short trips (up to approximately 250 miles) these advantages are offset by fuel used to reach a high altitude. Don't fly at an altitude where the speed gain is offset by unfavorable winds.
4. **RIDE THE WINDS.** Ask for winds aloft information and take advantage of altitudes where favorable winds are available. This can save substantial fuel. For example, a 20 mph tailwind adds 10% to a 200 mph airplane resulting in a 10% savings in fuel. If you throttle back to travel at the same speeds, you'll still save 10%.
5. **THROTTLE BACK AND LEAN THE MIXTURE.** The use of lower power settings and efficient leaning methods are the most important things which can be done to reduce fuel consumption. Generally, the total fuel consumption on any given trip will be reduced by approximately 12% to 15% by selecting 55% power instead of 75%. Although the percent of savings varies slightly from model to model, the rule applies to single or multiengine Cessnas. The additional time added for each 100 miles of cruise flight will average only four to six minutes. Always lean carefully to at least the Recommended Lean mixture setting as described in your Pilot's Operating Handbook. Further reductions in fuel consumption can be achieved by the use of best economy mixture settings as described in your Pilot's Operating Handbook. This can effect a further 5% to 8% improvement in economy with only a slight additional increase in trip time.
6. **FLY A STRAIGHT LINE.** Planning so that your flight will be direct to the airport closest to your destination is a very simple matter when flying VFR and very practical when operating IFR by requesting direct routing and enroute vectors. Modern navigation equipment can be effectively utilized to fly direct and shorten the miles between points. After takeoff, turn on course as soon as practical. On arrival at your destination, request a straight in approach whenever it is to your advantage.
7. **KNOW YOUR AIRPLANE.** Your Pilot's Operating Handbook contains many pages of operating and maintenance information about the most efficient and reliable use of your airplane. Particular attention is called to the cruise performance charts, which establish power settings for maximum range and endurance of your airplane. Knowing this information can give you substantial fuel savings.
8. **MAINTAIN YOUR AIRPLANE.** Good mechanical condition of your airplane is very important for efficient operation and, therefore, the best use of fuel. Even cleanliness is important. A clean exterior, especially on the wing leading edges, results in better fuel economy. Place your airplane in the hands of your Dealer for proper care.
9. **PLAN AHEAD.** Time spent on the ground in flight planning will avoid needless delays on the ground, unnecessary fuel stops and other conditions that can be wasteful of time and fuel.
10. **FILL EMPTY SEATS.** Whether it's a company flight operations or an individual business trip, a little effort in coordinating and scheduling can provide many miles of travel with no additional use of fuel by using empty seats.
11. **PREFLIGHT.** When practical, carry only the required fuel to safely complete the trip. When practical, plan flights to arrive and depart high density areas during periods of low traffic.
12. **FLIGHT PROCEDURES.** If an optional EGT system is used, operate at peak EGT at or below 55% power; an additional fuel savings of 8% can be realized over and above normal lean operation. Avoid using drag devices such as gear or flaps, reduce power instead. If holding is necessary, reduce to maximum endurance power setting and lean the mixture accordingly. Delay extending the gear and flaps until the final approach if, when IFR or as late as safety practical when VFR.

YOUR CESSNA AIRPLANE IS ONE OF THE MOST ENERGY-EFFICIENT FORMS OF TRANSPORTATION AVAILABLE — MUCH BETTER THAN SOME CARS.

USE YOUR AIRPLANE — IT'S A RESPONSIBLE USE OF FUEL.

PLEASE DISPLAY IN FLIGHT AND SALES OFFICE

Fig. 9c

in Fig. 9a through 9c. The guidelines help. Their adequacy depends on pilots' requirements. As pilots become more sophisticated in their flying, the guidelines may cease to be enough.

A pilot's enthusiasm for flying at optimum altitude and air-speed (ie., cruise control) will be in direct proportion to how easily he can determine those altitudes and speeds.

In this connection, the pilot of a lightplane might appreciate a chart like Fig. 10a (or an alternate form shown in Fig. 10b). It gives the optimum altitude for saving fuel over any trip length in terms of air miles. The pilot can enter with ground distance, read flight time for the most economical power and speed, and then multiply the wind component times the flight time to determine the extra air-miles due to wind. Adding the extra miles to the ground distance gives him a reasonably accurate total air-miles with which to re-enter the chart and read his final fuel, duration, power settings, airspeed, and altitude. For the lower altitudes at which non-turbocharged lightplanes fly, wind strengths are rarely high enough to destroy the applicability of this analysis. The chart, incidentally, accounts for run-up, taxi, takeoff, and reserve fuel.

At the risk of more clutter on such a chart, the horizontal lines of fuel consumption and duration can be extended to nearly the full width of the chart so off-optimum performance can be read; then the pilot can establish his own tradeoff between economy and speed with the knowledge of how many dollars it is costing him.

If such a chart is turned on end to the right, it can easily be thought of as a table with increments of distance down the left side and increments of altitude across the top. This is, in fact, the form of Beech's performance catalog referred to earlier.

HOW FLIGHT TEST ENGINEERS CAN HELP

In general aviation, particularly in lightplanes, pilots are not equipped, either by training or inclination, to do burdensome flight planning or make meticulous inflight calculations. Nor should they be expected to.

With imaginative application of current technology, flight test engineers are in the best position to devise simple, quick ways of helping pilots get more economical performance, even without altering airplanes. They need not wait for top management to order highly specific programs. Management alone, in fact, may not be mindful of all the possibilities that specialists can foresee.

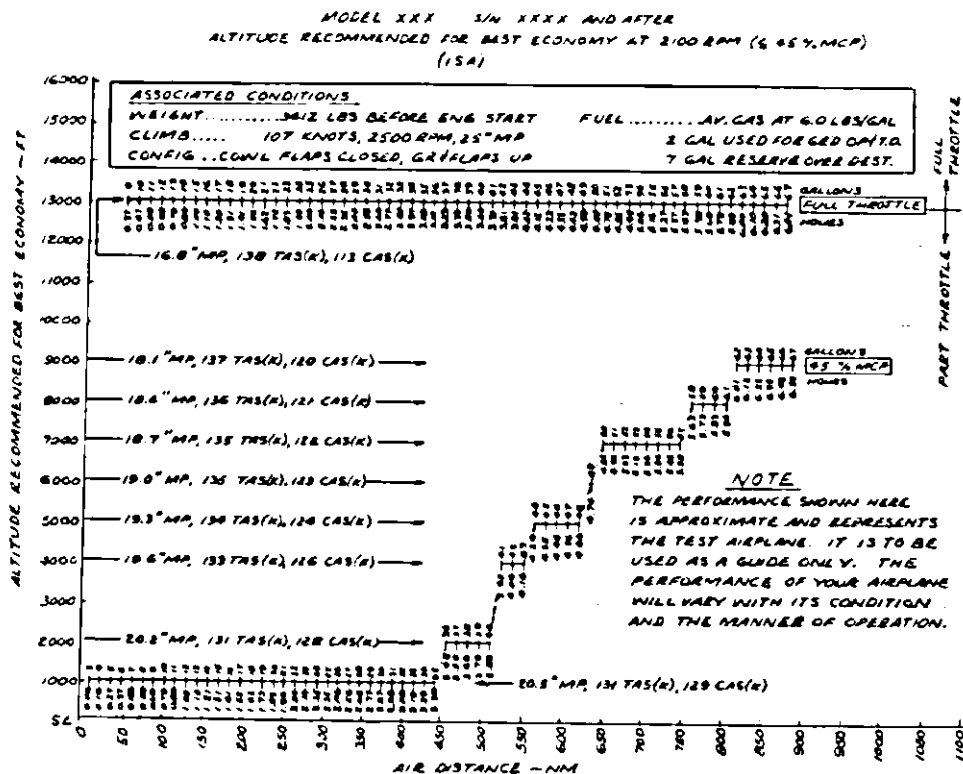


Fig. 10a

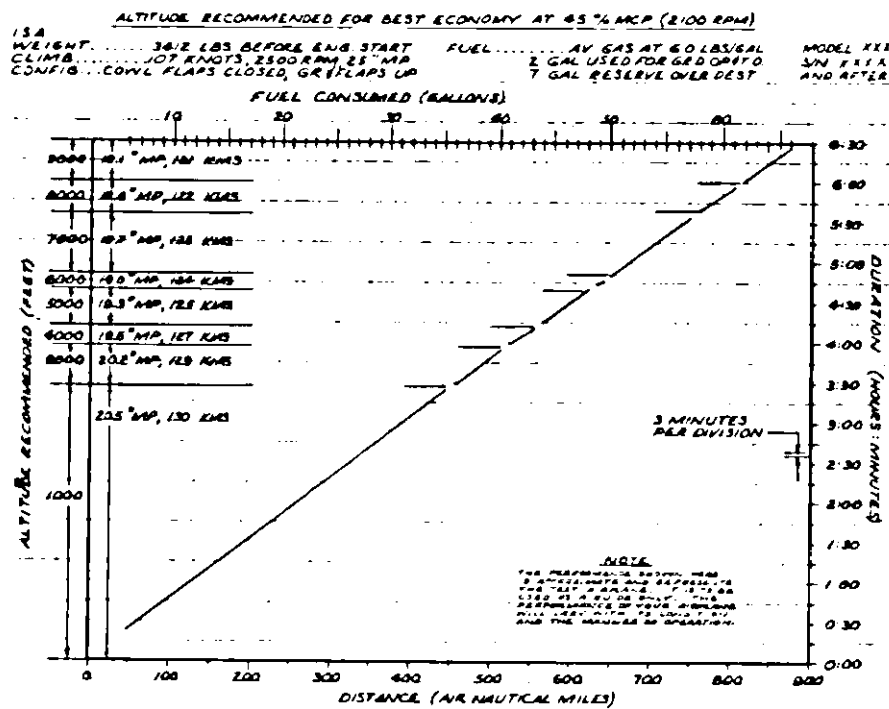


Fig. 10b

The intent of this paper is merely to broach the subject, to suggest some ideas, and to encourage those in the best positions to help, the general aviation flight test engineers.

Most of the ideas need more development, not only to improve them but also to suggest still other ideas that will supersede them.

Furthermore, all the ideas don't relate to cruise control; aerodynamic refinements, better propulsion efficiency, and structural weight reductions also save fuel. Flight test engineers have daily contact with these disciplines.

Last, but very important, for those flight test engineers that don't mind dealing with the unwashed, there is a need for teachers, authors, and lecturers to explain cruise control theory and practice.

CONCLUSION

Any new flight planning method or device must be simple and quick if it is to gain much use. Not only that, the dollars saved by it must be immediate and apparent.

Flight test engineers know what has been done in the past and why. They know not only how test data is reduced and expanded, but also how best to display and interpret it.

As implied in the opening paragraphs, cruise control techniques established years back have simply laid in the bottom drawer; there was little market value left in them.

Until recently.

Now international politics, the domestic economy, patriotic incentive, and computer technology have come into phase. The old knowledge can be applied in new and imaginative ways.

Flight test engineers can put it all together with the assurance that the pilots will buy it, the companies (and government) will support it, and engineers will get the credit.

Note:

The charts in this paper are presented for illustration, only, and are not intended to represent the actual performance of any airplane.

FLIGHT TESTING
THE AIR LAUNCHED CRUISE MISSILE

Richard R. Hildebrand
Air Force Flight Test Center
Edwards Air Force Base, California

ABSTRACT

The Air Launched Cruise Missile (ALCM) program was the top priority flight test effort in DOD during 1979-80. The unique characteristics of the weapon system posed new and exciting challenges to the team charged with designing and conducting this flight test effort. The recently concluded competitive phase, which resulted in the selection of the Boeing AGM-86B as winner, is described. The plans for continued development and operational testing of the B-52/ALCM are briefly summarized.

Richard R. Hildebrand, Deputy Director of the Air Launched Cruise Missile Combined Test Force, 6510th Test Wing Directorate of Test Forces

INTRODUCTION

It's been three years since the Carter administration's decision not to authorize production of the B-1 bomber, but to instead accelerate development of the Air Launched Cruise Missile (ALCM). During that period two vehicles were developed and built, one by General Dynamics Convair and the other by the Boeing Aerospace Company. An extensive cruise missile test capability was established, essentially from scratch, to conduct an intense flight test competition. This paper chronicles the successful completion of the competition, selection of a winner, production authorization and continuing test activities.

SYSTEM DESCRIPTION

The role of the ALCM in the United States' strategic plans for the near future is to extend the offensive striking footprint of the B-52 bomber. As will become evident in a moment, the capabilities of the ALCM are designed to that end and, in conjunction with offensive and defensive avionics improvements, are key to preserving the manned bomber leg of the Strategic Triad through the next decade. The "system" to be fielded consists of the cruise missile married to the B-52G equipped with an Offensive Avionics System (OAS) which is currently under development by the Boeing Military Airplane Company and which enters flight test in September of this year. A three-pronged approach was selected for total system development, namely to independently develop the ALCM air vehicle and the Offensive Avionics System to a common interface and then integrate the two. This development is well underway.

Air Vehicle

As I mentioned in the introduction, two ALCM systems were developed to the same set of requirements. The approximate sizes of both the General Dynamics' AGM-109 and the Boeing AGM-86B were twenty feet in length, two feet in fuselage cross-section, wing span of approximately ten feet, and weight around 3,000 pounds fully fueled. Details of the different configurations of the two missiles are readily apparent in figures 1 through 4. Several major components were common to both ALCMs and were provided to the competing contractors by the Government. These were the engine, the inertial navigation element and radar altimeter, and the ALCM-modified B-52s and external pylons. The W-80 warhead, under simultaneous development by the Department of Energy, was common to both missiles.

The expansion of the B-52's offensive footprint is readily apparent when you consider the range of these relatively tiny vehicles - over 1350 nautical miles (2500 kilometers). Each B-52 will have the capability to carry twelve ALCMs externally on pylons and up to eight ALCMs internally on a rotary launcher. The rotary launcher can also be used to carry AGM-69A SRAMs (Short Range Attack Missiles) or any combination of ALCMs and SRAMs. The requirement to be interoperable with SRAMs and the SRAM Carrier Aircraft Equipment of the B-52 was a big driver in the design of the ALCM and its software.

Features which enhance the ALCM's ability to penetrate enemy defenses are extremely low observables (i.e., size, radar cross-section, noise and infrared signatures, etc.) and high subsonic speeds, about 500 miles per hour. These features combined with the ability to terrain follow, that is to hug the ground closely, make them very, very difficult to acquire, track, and destroy.

The heart of the missile's capability is the navigation subsystem, the primary components of which are the inertial platform, the radar altimeter, the air data system, and the computer. Some time prior to missile launch, mission information is fed into the memory of the missile computer. This information contains specific mission routes with certain points identified as fix points. The mission information includes a computer representation of the altitude profiles ("maps") of the terrain in the vicinity of each fix point. After the B-52 communicates present geographical position to the missile, it is launched. Immediately upon ejection from the B-52, the engine inlet opens. The missile computer then directs the control surfaces to unfold, the engine to start and the wings to extend. The missile inertially navigates its way to the first fix point where, through use of radar altimeter measurements, it takes an altitude profile of the terrain along its flight path (figure 5). The computer then compares this profile with the stored "map" and determines its precise location at fix time. In comparing its actual location against where the platform thought it would be at fix time, the computer arrives at the "position error." The computer then apportions this error among a number of so-called Kalman filter "states." This Kalman filter process then biases the inertial platform alignment and the missile proceeds to the next fix point. Through successive fixes the system alignment gets better and better so that it is capable of achieving extremely high accuracy by the time it arrives

at the target. When the vehicle computes that it is at the target, it sends a firing signal to the warhead.

Offensive Avionics System

The second half of the total system, as I mentioned previously, is the B-52 with the OAS improvements. The current B-52G utilizes an old analog bombing and navigation system which has become a maintenance nightmare. In order to increase availability, decrease maintenance costs, and realize improved performance, this equipment is being replaced with a digital Offensive Avionics System. The main features of the OAS are a MIL STD 1553 data bus, dual inertial navigation system, new common strategic doppler, new radar altimeter, and modified bombing/navigation radar. The integration of ALCM and OAS is expected to preserve the effectiveness of the aged B-52 through the 1980's.

THE ALCM COMPETITION

The decision to accelerate development of the ALCM and the desire to reap the benefits of competition led the Office of the Secretary of Defense to order that the ALCM program be a "competitive full scale development." This is in contrast with other prototype competitions such as the Lightweight Fighter (YF-16 versus YF-17) and Advanced Medium STOL Transport (YC-14 versus YC-15) programs where there was no commitment to production and thus many cost-saving shortcuts were possible. Examples of these were soft tooling, makeshift support equipment, little documentation, no validated and verified technical data, etc. For full scale development, considerable resources and effort are expended "up front" so that later year savings in the maintainability and supportability of the weapon system result in the lowest possible life cycle cost. What this meant to the flight test program was that no stone could be left unturned in assessing the relative acquisition risks and evaluating the operational utility and effectiveness of the competing designs. To this end the test program has been structured as a combined DT&E/OT&E (development test and evaluation/operational test and evaluation). By this I mean that there is a single test team, the Combined Test Force (CTF), composed of people from all of the organizations participating in the flight test program; specifically, the Air Force Flight Test Center (AFFTC), the Air Force Test and Evaluation Center (AFTEC), the Strategic Air Command (SAC), Air Force Logistics Command (AFLC), the Air Training Command (ATC), and the Department of Energy (DOE). To these government participants are than added the competing contractors and their associates whom I'll describe shortly. The objectives of all participating organizations have been combined into a single test plan and program.

The ALCM competitive flyoff and source selection were conducted under the overall management of the Joint Cruise Missiles Project Office (JCMPO) which was formed by the Secretary of Defense to manage all cruise missile development. The JCMPO charter includes assuring the maximum practical commonality between ALCM, the Navy Tomahawk Sea Launched Cruise Missile (SLCM), the Air Force Ground Launched Cruise Missile (GLCM), and the joint service Medium Range Air to Surface Missile (MRASM).

The missile system contractors directly involved as competitors were General Dynamics Convair with the AGM-109 and Boeing Aerospace Company with the AGM-86B. McDonnell-Douglas Astronautics Company-East was teamed with General Dynamics on the AGM-109 as the navigation-guidance contractor.

Williams Research Company provided the common engine for both ALCM designs. The only engine differences were those such as accessory locations necessary for interface with the two airframes.

The final participants, playing a very crucial role in the development and especially in the ultimate fielding of the B-52/ALCM system was the Boeing Military Airplane Company (termed the Cruise Missile Integration contractor) under the management of the Strategic Systems Program Office (SSPO) at Wright-Patterson Air Force Base, Ohio.

One of the more unusual aspects of cruise missile testing is the tremendous dedication of resources, particularly aircraft, required to assure the safe conduct of a test mission and the acquisition of test data. The best way to describe the function of all the participating aircraft is to describe a typical ALCM launch and free flight mission.

The ALCM is prepared for flight in the Integrated Maintenance Facility, transported to the flightline, and uploaded onto the B-52 pylon or rotary launcher. The B-52 then takes off. Following system alignment and after extensive onboard and telemetry evaluation of missile and flight safety system health, the ALCM is launched on its preprogrammed mission profile to the target at the Utah Test and Training Range and subsequent midair recovery. The support fleet consists of:

- The B-52 launch aircraft. Three were "owned" by the Combined Test Force.
- Three chase/safety F-4Es which rotate to and from KC-135 aerial refueling tankers. These aircraft have the

capability to take remote command control of the missile or terminate flight if required. A total of eight F-4Es were dedicated to ALCM support.

- Approximately three KC-135 aerial refueling tankers. These were SAC airplanes provided through a "Tanker Task Force" set up at Travis Air Force Base, California, for ALCM support.

- An Advanced Range Instrumentation Aircraft (ARIA), to receive telemetry from the ALCM and retransmit it to the mission control center at Edwards AFB. These NKC-135s were modified for the Apollo program and follow the ALCM at high altitude. Two were further modified for ALCM support.

- T-38 chase aircraft with aerial photographers to record launch and the deployment of the recovery parachute system at mission's end. Aircraft from the general support fleet at the Air Force Flight Test Center were used.

- H-53 Mid-Air Recovery helicopters to catch the missile at mission's end and return it for evaluation and possible reuse. A total of three H-53s were available for ALCM support.

- A UH-1 helicopter for aerial photography of the Mid-Air Recovery and subsequent docking. UH-1 helicopters were also used to transport security and recovery teams to the sites of unplanned terminations.

The magnitude of the airborne effort can perhaps best be appreciated by looking at the totals. 689 sorties totalling 3990 flight hours were flown by all participating aircraft. Up to 26 different aircraft were involved in a single mission.

In order to evaluate the ALCM under the most operationally realistic conditions possible, a network of routes were established in conjunction with the FAA, extending from the Pacific Ocean to the Great Salt Lake desert in Utah. Figure 6 depicts such a route and the seven Government Test Ranges which were utilized. One of the most difficult challenges which we faced was the tremendous coordination effort required to tie all this together to successfully support a mission.

The competitive flyoff itself consisted of ten launches of each type missile, supporting captive carriage flights, and a program to determine/demonstrate physical compatibility with the B-52G. The activity is summarized in figure 7.

As you know from the resulting publicity, not all of the launch and free flights were 100 percent successful. Eight missiles, four of each type, terminated prematurely. However, with the data available we were able to determine the likely cause of each premature termination and fixes were developed to prevent recurrence. There were no repeat anomalies with either competing system.

Now, you might ask, what did we accomplish with all this? Basically, and most important, we feel we got a better system at lower cost than would have been the case without competition. We got a good look at both systems - figure 8 lists many of the areas of test which were addressed. As you can see, this is a very comprehensive listing. The incentive for the individual contractors to "do better" was very real. For example, because of the competition, Boeing developed and demonstrated an innovative cast fuel tank in lieu of the previous welded tank. This innovation alone is expected to save \$700 million in production costs, well in excess of the cost of carrying a second contractor through the competition. Substantial benefits accrued to the Sea and Ground Launched cruise missile versions of the AGM-109 as a result of design improvements and lessons learned from the ALCM competition.

Very significantly, the competition was sufficiently thorough to give the decision makers confidence in making a full production decision. The Defense Systems Acquisition Review Council (DSARC) on 17 April 1980 approved the full ALCM production. This long term guidance provides the program manager with a tremendous opportunity to utilize cost effective strategies and actions because he knows what to expect in future years.

A few words about program management are now in order. As mentioned previously, the ALCM competition, as well as all US cruise missile development was managed by the Joint Cruise Missiles Project Office. Following the selection of the AGM-86B as the winner and the subsequent production decision, the transition of program management authority from JCMPO to the Air Force was directed as planned. This transition has been made and the ALCM program is now managed by the Strategic Systems Program Office at Wright-Patterson Air Force Base, Ohio.

FUTURE PLANS

As I mentioned in the early portion of this paper, the total system development concept is to independently develop the ALCM and B-52 OAS and then integrate the two. Much effort still remains. Figure 9 lists the developmental objectives of future testing and figure 10 depicts where we

are from the flight test perspective. The ALCM competition is complete and we have begun what is termed Phase II, the continued DT&E/OT&E of the selected AGM-86B ALCM. In the summer of 1981, the first launches of ALCM and SRAM are planned from an OAS-equipped B-52G. These launches follow a period of testing of the OAS itself which is planned to begin in September of this year. The ALCM/OAS integration effort is termed Phase III and is expected to continue until the end of 1981, at which time the developmental testing should be complete. Phase IV is the term used to describe the Operational Test and Evaluation which continues until the First Operational Capability in December 1982. At that time a full wing of ALCM and OAS equipped B-52Gs will be in place and operationally ready to perform their role in the strategic posture of the United States.

CONCLUSION

The Air Launched Cruise Missile posed a new challenge to the flight test community. This challenge has been successfully met with the establishment of a flight test system and organization which is unparalleled. An intense competition was conducted, a winner selected, and full production authorized in the span of one year. Efforts are well underway with the continued ground and flight testing required to lead to a full operational capability in December of 1982.

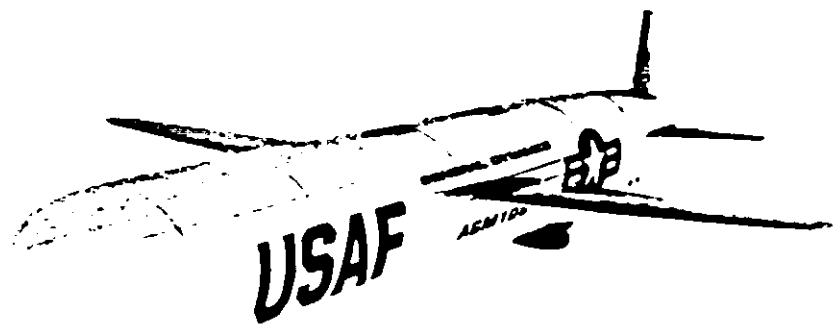
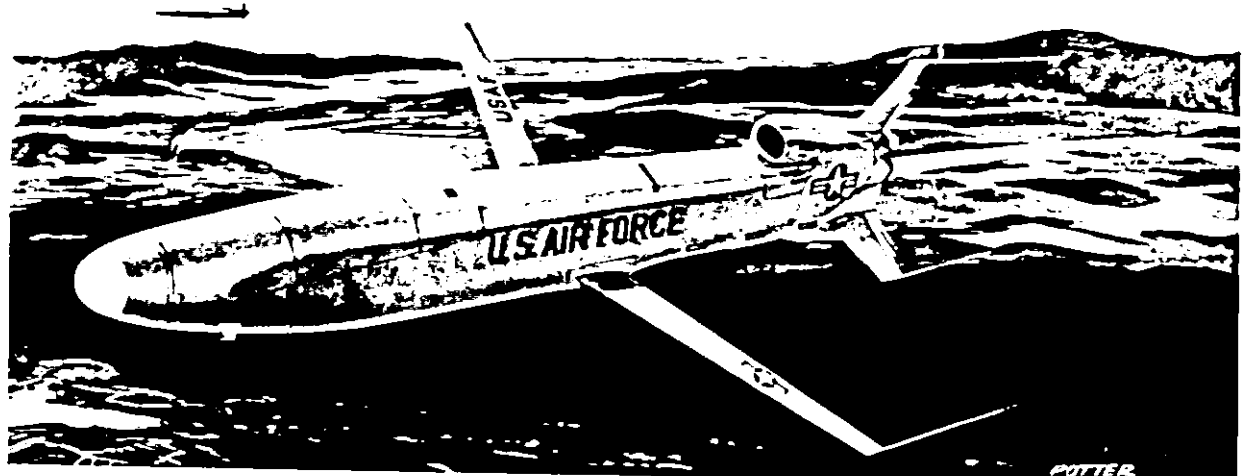


FIGURE 3
AGM-86

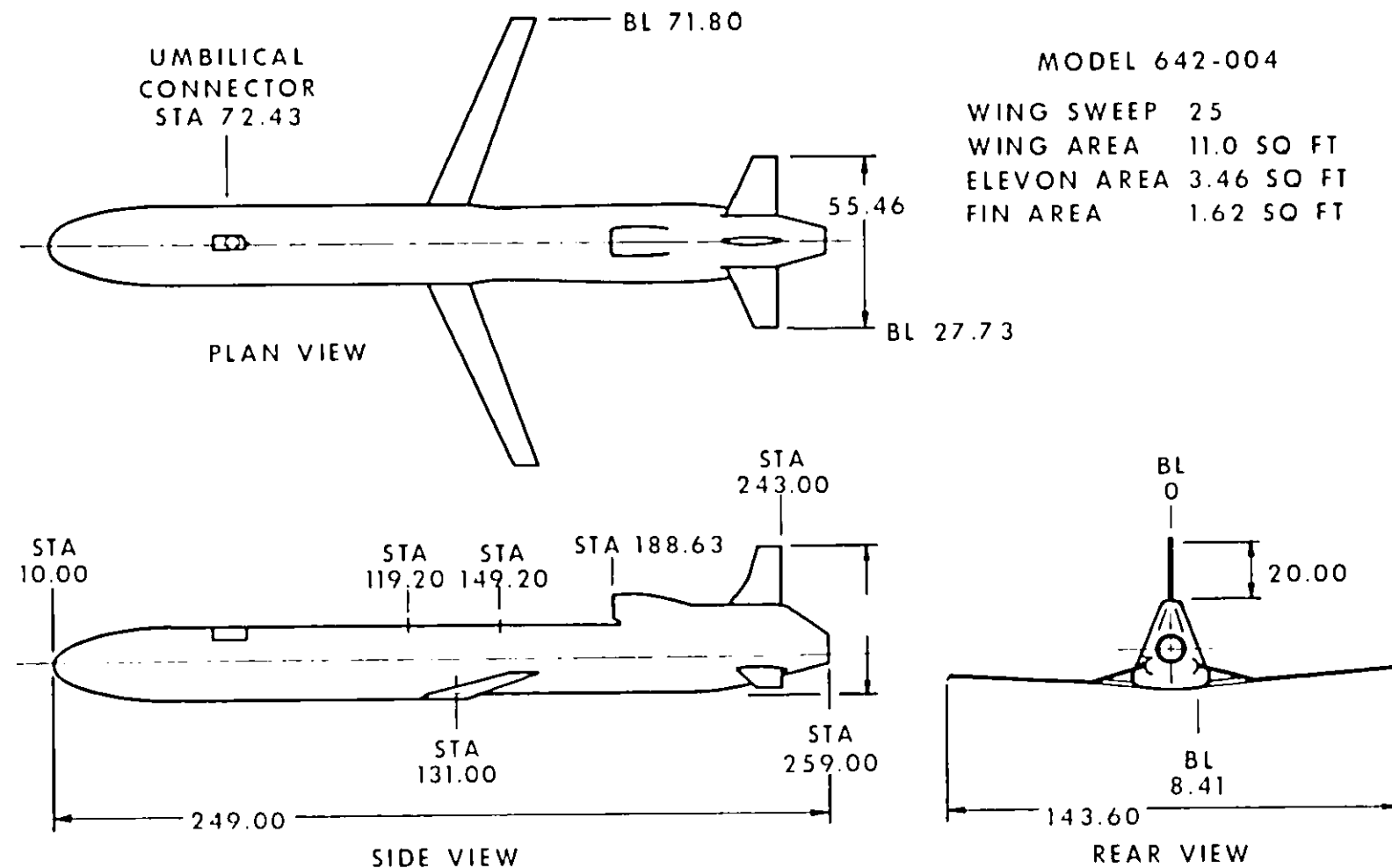
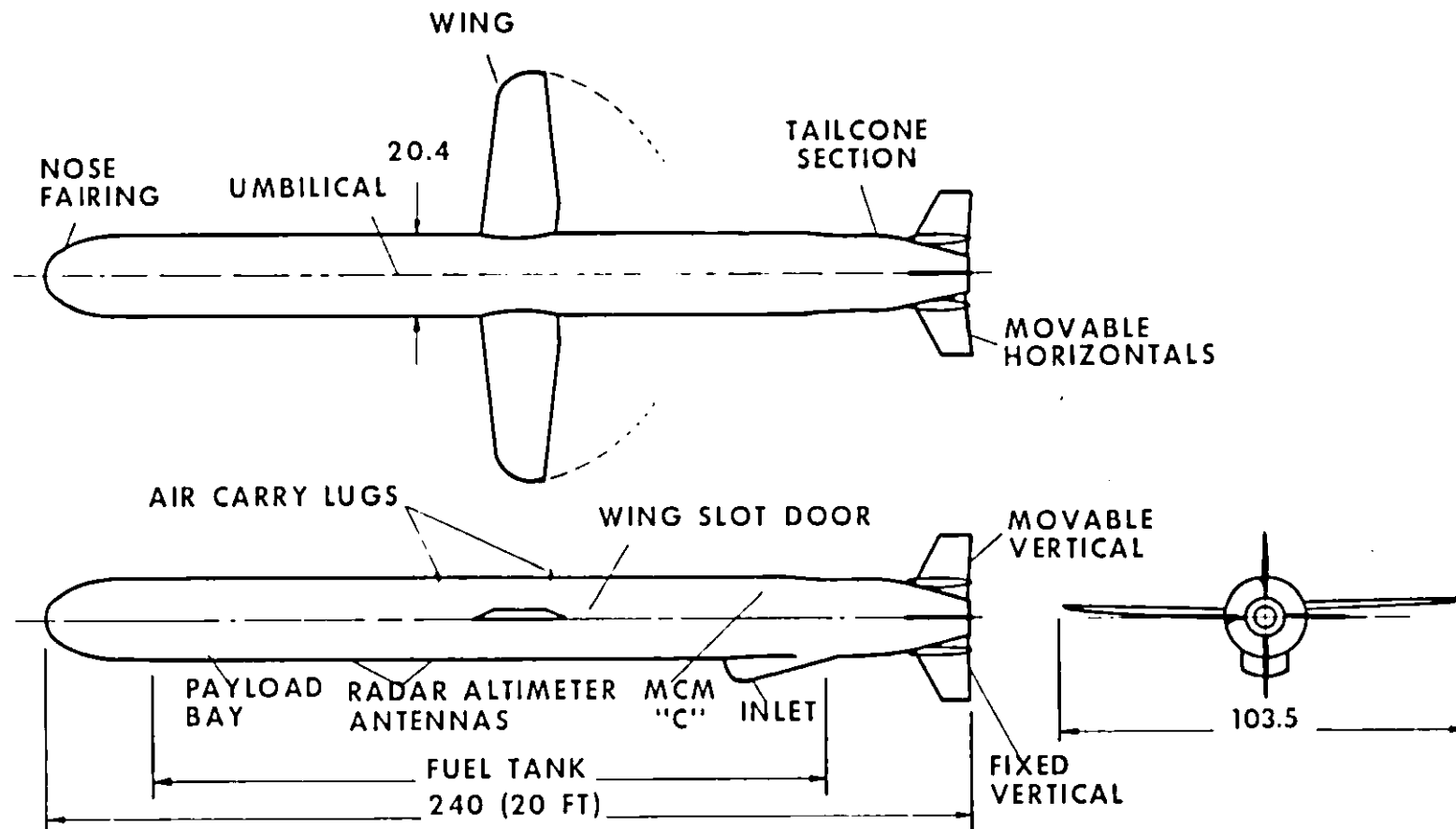


FIGURE 4

AGM-109



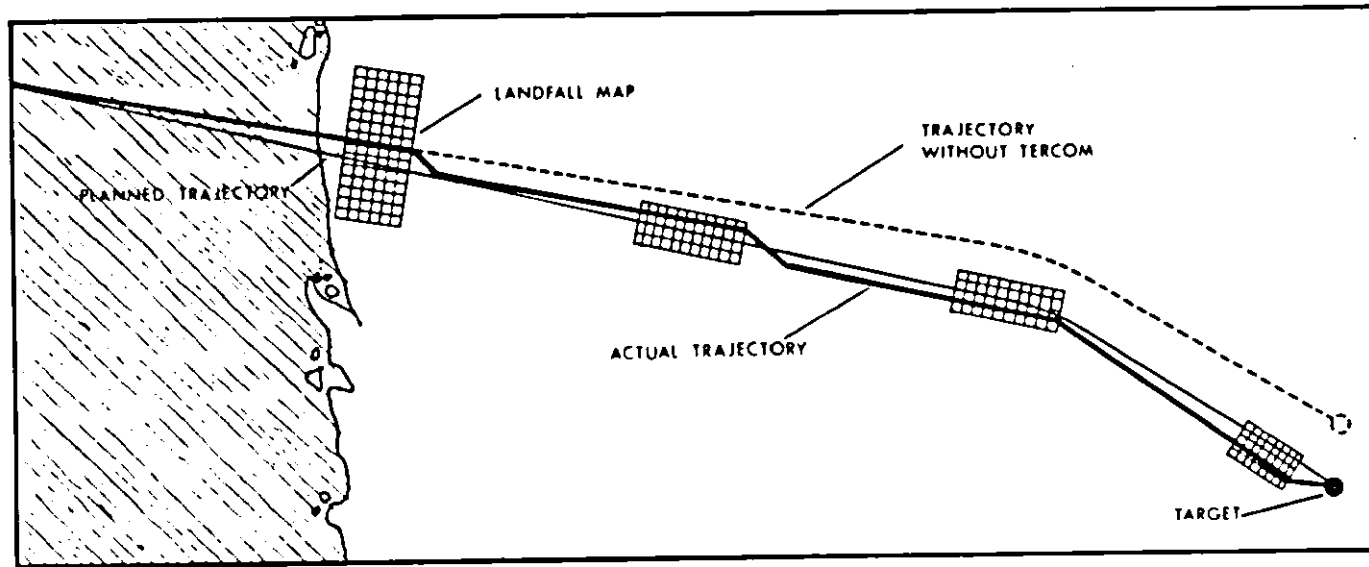
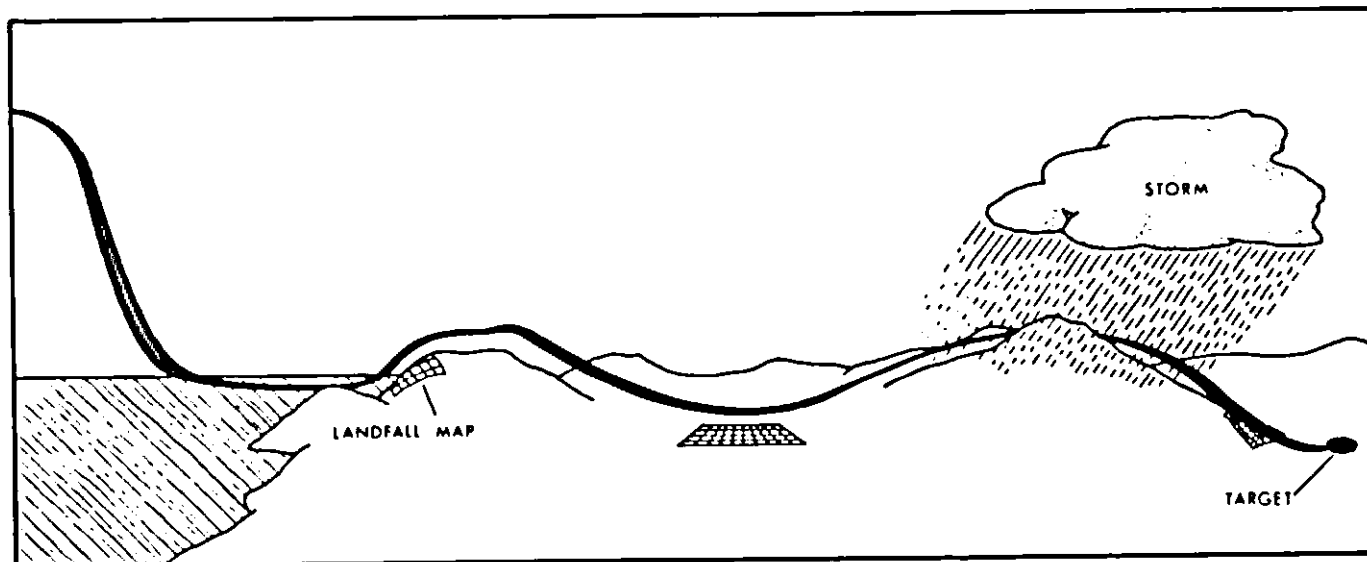


Figure 5 -- ALCM Navigation Concept

FIGURE 6

INLAND ROUTE & TEST RANGES

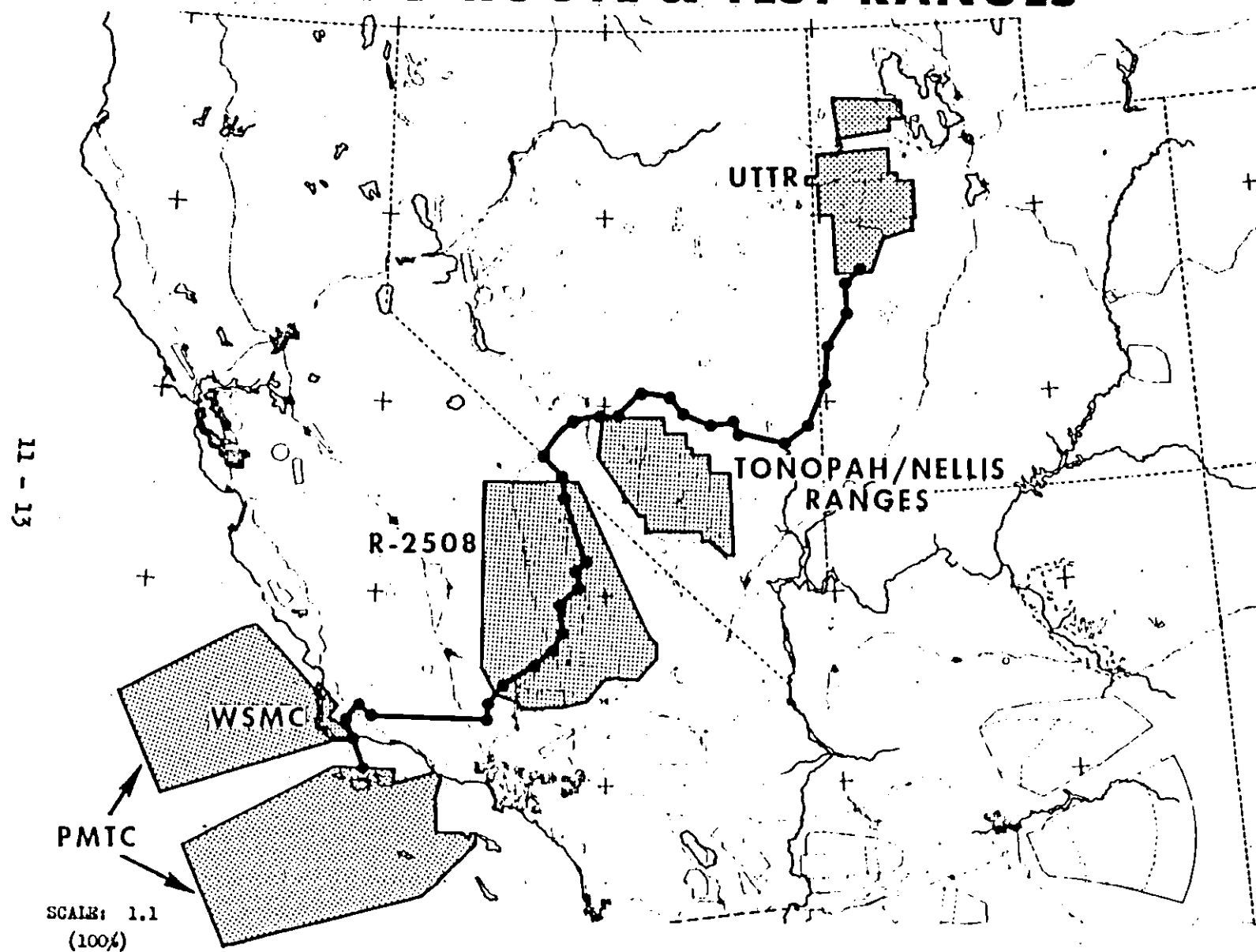


FIGURE 7

ALCM COMPETITION SUMMARY

	AGM-86B	AGM-109	TOTAL
FREE FLIGHTS	10	10	20
TOTAL FLIGHT TIME	31.7 HOURS	22.6 HOURS	54.3 HOURS
TOTAL DISTANCE FLOWN	12,915 NM	9582 NM	22,497 NM
CAPTIVE CARRIES	12	11	23
ALCM JETTISON TESTS	9	8	17
SRAM JETTISON TESTS	1	1	2
TOTAL B-52 SORTIES/HOURS	44/279	30/208	129/725.5*

* INCLUDES PERFORMANCE, FLYING QUALITIES, FLUTTER, AIR ABORTS, ETC.

TEST OBJECTIVES ACCOMPLISHED

- ALCM/B-52 COMPATIBILITY
- B-52 FLIGHT CHARACTERISTICS WITH EXTERNAL ALCMS
- INFLIGHT ALIGNMENT
- TERRAIN CORRELATION UPDATES
- INTERNAL AND EXTERNAL JETTISON
- INTERNAL AND EXTERNAL LAUNCH
- ALCM FLUTTER
- ALCM STABILITY AND CONTROL
- TERRAIN FOLLOWING
- ACCURACY
- AERO PERFORMANCE/RANGE
- ENGINE/AIRFRAME COMPATIBILITY
- RADAR CROSS SECTION
- INFRARED SIGNATURE
- NUCLEAR SURVIVABILITY (EMP)
- COMPATIBILITY WITH W-80
- ALCM/SRAM PHYSICAL COMPATIBILITY
- RELIABILITY
- MIDAIR RECOVERY
- MISSION PLANNING
- SUPPORT EQUIPMENT

FIGURE 8

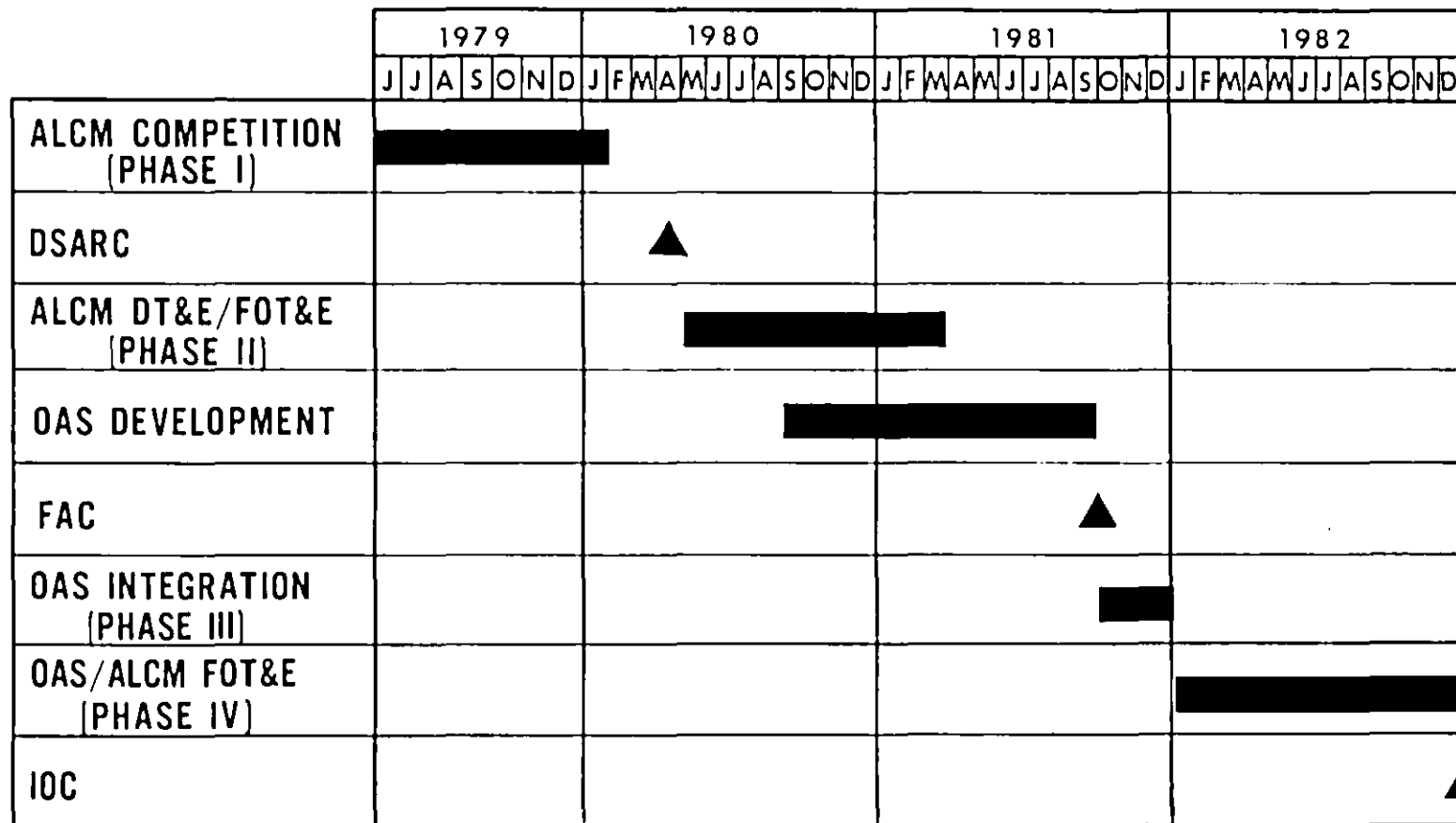
FIGURE 9

REMAINING DEVELOPMENTAL OBJECTIVES

- EXPAND MISSILE DATA BASE (PERFORMANCE) FOR SIOP PLANNING: NAVIGATION GUIDANCE, AND MISSION PLANNING
- INTEGRATE WITH B-52 OFFENSIVE AVIONICS SYSTEM
- COMPLETE VALIDATION AND VERIFICATION OF TECHNICAL DATA
- DEVELOP REMAINING AUTOMATIC TEST EQUIPMENT
- QUALITY SUPPORT EQUIPMENT
- CONDUCT PYLON JETTISON TESTING
- INTEGRATE NEW MISSILE RADAR ALTIMETER(S)
- RADAR CROSS SECTION (RCS): PRODUCIBILITY CHANGES AND TEST CONFIGURATIONS
- LAUNCH ENVELOPE EXPANSION
- ICING TEST
- ELECTROMAGNETIC VULNERABILITY (EMV)
- HIGH LATITUDE NAVIGATION
- AIR VEHICLE COMPONENT QUALIFICATION
- PAINT SELECTION AND QUALIFICATION

FIGURE 10

B-52 OAS/ALCM FLIGHT TEST SCHEDULE



Determining Performance Parameters of
General Aviation Aircraft

Gifford Bull and Philip D. Bridges
Department of Aerospace Engineering
Mississippi State University
Mississippi State, Mississippi 39762

ABSTRACT:

A method for determining propeller efficiency and drag from flight tests, using relatively simple instrumentation, is under development at Mississippi State University. Flight test data from several simple maneuvers are combined to produce sufficient information to determine the desired parameters. Information obtained from the transient response of airspeed to a step change in power or drag in level flight is utilized. Theory is developed and results of preliminary computer studies and preliminary flight test are presented.

NOTE

This paper is a report of research now in progress at Mississippi State University on the measurement of performance of airplanes. At this time, preliminary results are available.

Work performed at Mississippi State University under NASA Research Grant NAG-I-3, NASA Langley Research Center, Dr. Bruce J. Holmes, Technical Officer.

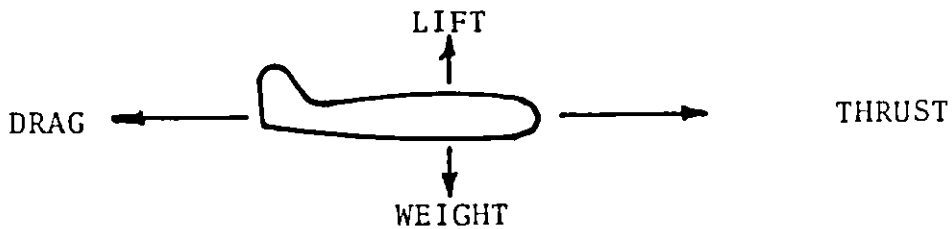
Gifford Bull, Associate Professor and Chief Test Pilot
Philip D. Bridges, Research Associate and Test Pilot
Raspet Flight Research Laboratory, Mississippi State
University

INTRODUCTION

The Problem

Operational performance information needed by the pilot, such as cruising speed or range, can be determined directly from flight tests but the factors which influence the performance are not so readily accounted for. The engineer needs to know these factors, such as drag and propeller efficiency, to decide where efforts to improve the performance will be most productive. He also needs to be able to measure the results of those efforts. However, the airspeed in steady flight which results from a given power is affected not only by the drag but also by characteristics of the power plant such as propeller efficiency. The usual flight test methods do not provide enough information to separate the factors. The engineer cannot tell, for example, whether disappointing performance is caused by too much drag or an inefficient propeller.

To clarify the problem, consider the forces which must be in balance on an airplane in steady level flight.



$$\text{Drag} = \text{Thrust}$$

or

$$\text{parasite drag + induced drag} = \frac{\text{Thrust horsepower}}{\text{speed}}$$

or

$$\text{parasite drag + induced drag} = \frac{(\text{Propulsive Efficiency})}{\text{speed}} \frac{(\text{engine horsepower})}{\text{speed}}$$

or

$$(1) \quad \left(C_{D_0} + \frac{C_L^2}{\pi A Re} \frac{1}{2} \right) p V^2 S = \frac{n p \text{ BHP}}{V}$$

In level flight, Lift equals Weight, or:

$$(2) \quad L = W = mg$$

$$(3) \quad L = C_L \frac{\rho S V^2}{2}$$

Expanding equation (1) and replacing C_L with terms that are more directly measurable:

$$\left(C_{D_0} \right) \frac{\rho S}{2} V^2 + \frac{2m^2 g^2}{\rho S \pi AR} \left(\frac{1}{e} \right) \frac{1}{V^2} = \left(\eta_p \right) \frac{BHP}{V}$$

or

$$(4) \quad \left(C_{D_0} \right) \frac{\rho S}{2} V^3 + \frac{2m^2 g^2}{\rho S \pi AR} \left(\frac{1}{e} \right) \frac{1}{V} = \left(\eta_p \right) BHP$$

The unknown quantities are enclosed in parentheses and the quantities to be measured in flight are in bold characters. Thrust is affected by the unknown propulsive efficiency and drag is affected by both parasite drag and airplane efficiency factor. Speed for a given power can be measured, but that speed is affected by the propulsive efficiency and the components of drag. Thus, if the airplane goes slower than expected, is it because the parasite drag is high or because the propulsive efficiency is low? We have used the term propulsive efficiency to indicate the efficiency of the propeller as installed on the airplane as opposed to the efficiency of the isolated propeller. A common practice is to assume a propulsive efficiency and then use speed-power data from flight tests to determine drag. This is useful but it still leaves doubts as to whether the assumed propulsive efficiency was correct.

Design parameters of interest, such as drag, propeller efficiency and airplane efficiency, are related to speed and thrust or power by the equations describing the motion of the airplane. If the motion is measured sufficiently accurately under circumstances that provide at least as many equations as the number of unknowns, then presumably the unknowns can be determined. Even with sophisticated statistical smoothing of the data, the character of the equations is such that measurements must be made to a very high degree of accuracy. Instrumentation of this accuracy and the necessary analytical techniques are available, and are used successfully in the flight testing of military and large transport airplanes. An example of a comprehensive investigation into application of these modern methods to determination of performance and stability characteristics of smaller general aviation airplanes is given in Reference 1 & 2. However, the instrumentation and analytical methods required by these techniques have been beyond the reach of much of the general aviation industry. A need exists, therefore, for flight test methods which are relatively simple and use affordable instrumentation and analytical procedures. The Raspet Flight Research Laboratory at Mississippi State University is engaged in a theoretical and experimental investigations of methods for measuring performance of airplanes,

methods which use relatively simple instrumentation and data extraction techniques which are well established from other fields. The test airplane is a T 34 B, Figure 1. The work is sponsored by NASA Langley Research Laboratory.



Fig. 1 T-34B Test Airplane

Requirements on the instrumentation are minimized by selection of maneuvers which limit the number of variables in a given test. Data is taken in simple one degree of freedom maneuvers as well as in steady flight. Examples are measurements of power, speed and rate of climb at constant speed; measurements of power and time history of speed and speed in a steady turn; or measurement of power, speed and power change when a given drag increment is deployed. Use of the transient response in speed, as used here in performance tests, is believed to be novel. This method makes use of the information contained in the transient response of an airplane to a change in power or drag, in addition to the information obtained from steady-state performance of the airplane.

If the power is suddenly increased in an airplane flying steadily at constant altitude and the altitude is held constant, the airspeed will increase to a new steady-state value. When the power is first increased, the thrust will be greater than the drag and the airplane will start to accelerate. As the speed increases, the drag increases and although the thrust may vary with speed, depending on the engine characteristics, the excess thrust will decrease and the acceleration of the airplane will become smaller. The time history of the speed will be in the form of a decreasing exponential, as represented by the response of a first order system to a step input. The time constant describing the motion will be affected by the momentum of the airplane and the drag; large momentum and small drag will give a long time constant.

The transient response in airspeed in level flight has been investigated before, Reference 3, but the emphasis has been on stability and other considerations rather than on development of a method to measure performance. Acceleration in level flight has also been used widely as a means of measuring excess thrust or power for climb performance and these methods are summarized in texts, Reference 4. The transient response in speed is one element of aircraft response exploited in methods known as equations of motion of parameter identification methods. To our knowledge, the transient response in speed or altitude has not previously been separated out and used in a relatively simple manner to determine drag and propeller efficiency.

The method is developed in some detail in Appendix A. The results show that the time history of the speed change following a step change in power has the form:

$$(5) \quad \Delta V(t) = A (1 - e^{-at})$$

Both coefficients, A and a, contain terms for propulsive efficiency and drag. Determination of these quantities requires measurement of initial and final speed and power and the time constant associated with change in speed in level flight. A preliminary error analysis, using numbers typical of the T-34B airplane, showed that a 5% change in C_{D_0} changed $T_{1/2}$ from 33.2 to 29.5 seconds, which should be readily measured.

Assumptions were made to permit a closed solution to the equations to clarify the relationship between the variables. Included were the assumptions of constant n_p , C_{D_0} and e over the speed range to be covered in the individual tests. Thus, the change in power should be relatively small, to produce a reasonably small speed change. Assumptions of constant propeller efficiency and parabolic drag polar are not essential to the fundamental method; variations in propeller efficiency and airplane efficiency with speed could be accounted for and handled in a numerical solution of the equations. Constant altitude is assumed. Variations in altitude which last a short time compared to the time to reach a new speed can be accounted for, since they represent a simple exchange of potential and kinetic energy. In other words, speed data taken while an altitude error existed for a short time can be corrected to the speed which would have been measured at constant altitude.

Keeping the altitude constant reduces the performance problem to a single degree-of-freedom and simplifies the problem of making the necessary measurements. Notice that measurements of pitch angle, longitudinal and vertical

acceleration, etc. which are required in some parameter identification flight tests, are not required here. Keeping the altitude constant reduces requirements on the instrumentation but it imposes a requirement for accurate flying by the pilot. Questions have been raised as to how accurately a pilot can maintain constant altitude. Given a sufficiently good reference, a pilot can readily maintain altitude in smooth air to within a few inches, as shown by close formation flying or flying very close to the ground or the top of an agricultural crop. At altitude the pilot does not normally have such good reference. For these tests, the altitude information provided by the test instrumentation was used to drive meters in the cockpit (Figure 2) indicating rate of climb and incremental altitude to a maximum of ± 20 feet from a reference altitude. With this information the pilot can maintain altitude to within a foot or so.

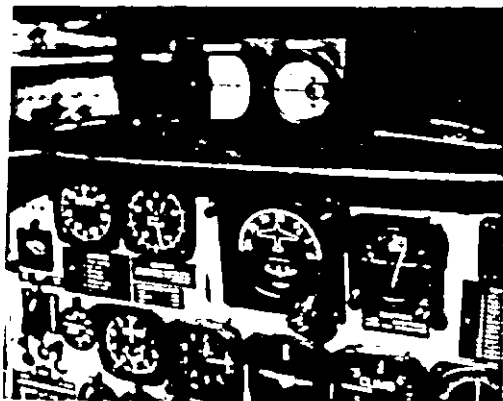


Fig. 2. Incremental Altitude Indicators



Fig. 3. Recording Instrumentation

Two examples of preliminary flight test data are shown. Figure 4 shows a measurement of the time history of airspeed change following a step change in power, using only cockpit instrumentation. A time constant calculated from this data produced a theoretical curve well matched to the flight data, showing that the exponential response predicted by the equations developed in Appendix represents the behavior of the airplane. It can also be seen that the instrumentation requirements are not extreme. Figure 5 shows data taken in another preliminary test using the instrumented T-34 with an earlier version of present instrumentation. Performance parameters extracted from this test are included in Figure 5.

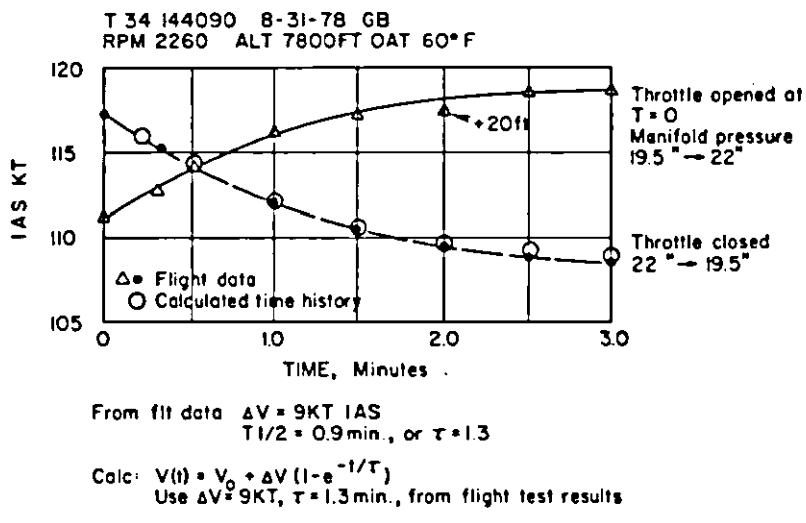


Fig. 4. Measured Response in Speed T.
Step Change in Power

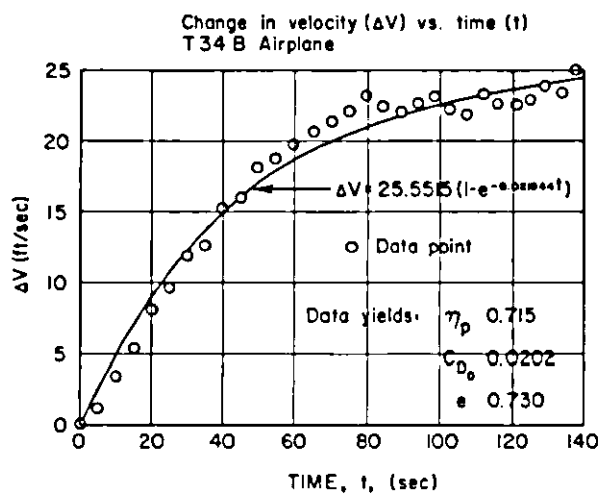


Fig. 5. Measured Response to
Step Power Change

EVALUATION BY COMPUTER SIMULATION

The next step was to evaluate this flight test technique using a digital off-line simulation. There were three areas in which the simulation could be useful. These were to verify the basic technique, to examine the limitations of the solution, and to evaluate the impact of input errors on the computed values of C_{D_0} , N_p and e .

The simulation used was the NASA Langley General Aviation Aircraft Simulation Program coded on the Mississippi State University Univac 1100/80 computer. This program is a six degree-of-freedom simulation that represents a Cessna 172 aircraft. The program was modified so that the aircraft had a parabolic drag polar and a constant value of propeller efficiency; zero-left drag coefficient, and wing efficiency. A constant speed propeller was also added, since the T 34B flight test aircraft had a constant-speed propeller. No attempt was made at this time to change the simulation to that of a T34-B, since this would require a large number of aerodynamic and mass property inputs, most of which are unknown.

The first use of the simulation was to prove the concept. If this ideal airplane in straight and level flight is given a step input in power and constrained to hold its altitude, will the response be exponential in nature and can flight test data be extracted from this response? To determine this, the simulation was initialized in straight and level flight at 5,000 feet with a velocity of 160 feet/second. At a specified time the throttle was increased $2\frac{1}{4}\%$ (of full throttle). The simulation autopilot constrained the maximum altitude change to one foot or less. The change in velocity is shown in Figure 6. The plotted points are from the simulation, and the fitted line is a least squares type of curve fit formulated by Marquardt, Reference 5. It can be seen that the exponential form

$$\Delta V = A(1 - e^{-at})$$

provides an excellent curve fit.

The coefficients of this fit were then used to find the computed values of C_{D_0} , N_p , and e . These values, shown compared with the actual values in the first line of Table 1, show very close agreement. It is obvious that this method can yield data in an ideal case.

The second problem was to examine the limitations of this technique. The limitations included the size of the throttle change and the effect of not holding constant altitude.

The first to be examined was the size of the throttle change. Simulations were run with 5% and 10% throttle changes and the exponential curve fitted to the change in velocity. The computed values of these cases are shown in Table 1. As can be seen, the larger the throttle change, the less accurate are the calculated values. This was to be expected, since a Taylor series expansion was used to solve the differential equation of motion. This approximation becomes less accurate as one uses larger throttle changes.

For the altitude changes, the simulation autopilot was modified to produce a roller coaster motion with height deviations of 10-15 feet from the desired altitude when the throttle was increased. It was felt that this was the maximum deviation that would be seen in a flight test. The results of these runs are also shown in Table 1. Comparing the dispersed cases with those having no altitude changes, it is clear that the computed wing efficiency is the parameter most affected by the altitude dispersions, the propeller efficiency is less affected, and the computed drag coefficient is relatively insensitive to the altitude changes.

The third goal of the simulation was to examine errors in the input data to the program evaluating C_{D_0} , N , and e . In this instance it was assumed that the velocity and time were measured perfectly during the test flight. An exponential curve was fitted to the data to obtain the A and B coefficients. However, a wrong value of initial power, change in power, air density, or aircraft weight was used in the calculation of the unknown parameters. The errors used were representative of what could reasonable be encountered on a flight test. By examining the results of this, it would be possible to identify the accuracy requirements for measurement of these variables. The results of these errors are shown in Table 2. According to these results, the most critical measurement is the change in power. As before, the parameter most affected was the computed wing efficiency, with the computed drag coefficient affected least. To minimize these errors, it will be necessary to carefully calibrate the torque meter and to make multiple runs to average out random noise.

Further studies of the technique are now in progress. The effect of a non-parabolic drag polar, variable propulsive efficiency, and random noise, on the computed parameters will be investigated, along with other flight test techniques that will be integrated with this procedure.

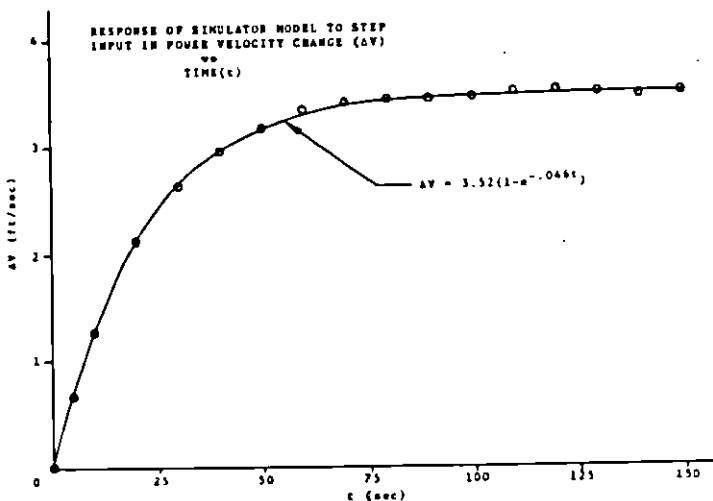


Fig. 6. Response of Simulator Model to Step Input in Power

TABLE 1

Simulation Model: $C_{D_0} = .038$, $N_p = 0.8$, $e = 0.67$

No Altitude Deviation

TEST CONDITION	C_{D_0}	N_p	e
2½% Throttle Increase	.0381	.7987	.6719
5 % Throttle Increase	.0393	.8265	.6422
10% Throttle Increase	.0414	.8714	.6058

±10-15 Ft. Altitude Deviation

2½% Throttle Increase	.0394	.7906	.7550
5 % Throttle Increase	.0396	.7803	.8412
10% Throttle Increase	.0410	.8529	.6344

TABLE 2

Simulation Model $C_{D_0} = .038$, $N_p = 0.8$, $e = 0.67$

2½% Throttle Increase, No Altitude Deviation

INPUT ERROR	C_{D_0}	N_p	e
Power Change 5% High	.0375	.7601	.7818
Power Change 5% Low	.0388	.8414	.5814
Initial Power 1% High	.0383	.7986	.6531
Initial Power 1% Low	.0380	.7983	.6929
Air Density 2% High	.0373	.7985	.6573
Air Density 2% Low	.0388	.7985	.6841
Aircraft Mass 1% High	.0385	.8063	.6789
Aircraft Mass 1% Low	.0378	.7907	.6658

INSTRUMENTATION

The T34B test airplane, Figure 1, is the same airplane used in earlier NASA-sponsored performance investigations at Mississippi State University, Reference 6.

Data is recorded on a Hewlett-Packard Data Logger. Digital voltmeter readings are printed directly on a paper tape, with four digit accuracy. The instrument is self-scaling so all the digits can be significant, yielding recording accuracy to one part in 10,000. A MSU timing circuit is arranged to adjust timing of data collection and printing to fit requirements of different tests. This device also incorporates a digital clock to record time on the tape.

Engine horsepower is calculated from measurements of torque and rpm. Torque is measured with a Lebow torquemeter and is displayed in the cockpit as well as recorded on the logger. Engine rpm is measured by counting pulses from a magnetic pickup on one magneto. RPM is displayed in the cockpit as pulse period or frequency, and is recorded on the logger. Indicated airspeed and altitude are measured by Rosemont transducers with the voltage outputs recorded on the logger. Airspeed can be read to within ± 0.1 knot, and altitude to within 20 feet at 10,000 feet. The instrument can show changes in altitude of a few inches at 5,000 feet.

The excellent altitude resolution of the Rosemont altitude transducer is used to provide an incremental altitude indication to help the pilot maintain constant altitude. This instrument, Figure 2, shows full scale at about 20 feet from a reference altitude. The pilot can maintain altitude within ± 1 foot for longer than the several minutes required to complete a data run. Rate of change of altitude is provided by the same transducer. This information is also displayed to the pilot, Figure 2, and is of considerable assistance in maintaining level flight.

Fuel flow and fuel consumed are measured by a Silver Fueltron. This data is used to calculate weight as fuel is used.

Static and total pressures are provided by a swivelling head mounted on 5-foot boom at the wing tip.

The general arrangement of the recording instrumentation in the rear cockpit is shown in Figure 3.

IMPLICATIONS FOR OTHER FLIGHT TESTS

OF THE TRANSIENT IN AIRSPEED

Information contained in the transient response of airspeed to a step change in power or drag is used here to help measure propulsive efficiency and drag. An understanding of this response is helpful in other applications. For example, how long does it take to reach steady state airspeed in flight testing and in operational flying? Manipulation of the equations developed in the Appendix leads to

$$\text{time constant} = \frac{\text{momentum}}{3 \text{ profile drag} - \text{induced drag}} \frac{\text{Constant-Speed}}{\text{Propeller}}$$
$$\text{time constant} = \frac{\text{momentum}}{2(\text{Profile drag} - \text{induced drag})} \frac{\text{Turbojet}}$$

These expressions, which are not satisfactory for flight at speeds near minimum power required, lead to time constants ranging from 15 sec for a light, slow, high drag airplane to several minutes for a heavy fast low drag airplane. Information of this type can be of real assistance to the test pilot and test engineer in planning data flights. The information also bears up on the problem of pilot technique in adjusting and controlling airspeed.

EXTENSION OF PERFORMANCE MEASUREMENT WORK

This paper reports progress to date on development of improved methods of measuring performance. Work continues on other topics, including bringing results from different maneuvers to bear on the measurement of performance parameters, and consideration of engines in which power varies with speed, as a fixed pitch propeller, or thrust varies with speed, as a fan jet. The requirement to measure engine power can be eliminated by expressing power in terms of drag and steady speed. This results in a system which will produce information on parasite and induced drag but not propeller efficiency. Changes in drag (produced perhaps by jettisoning a drogue) can be used instead of changes in engine horsepower, with implications for instrumentation and for assumptions of constant propulsive efficiency.

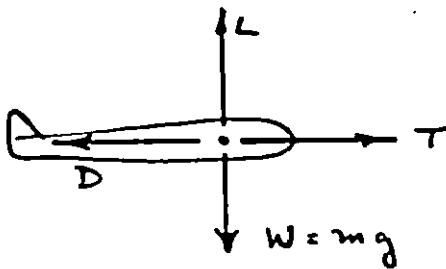
REFERENCES

1. Smetana, F. O. and Fox, S. R. Recent Results Obtained with a New Method for Measuring Aircraft Power and Drag in Flight. SAE Technical Paper 790616, April 1979.
2. Smetana, F. O. and Fox, S. R. Flight Test Evaluation of Predicted Light Aircraft Drag Performance and Stability. NASA CR 15092, May 1979.
3. Neumark, S. Problem of Longitudinal Stability below Minimum Drag Speed, and Theory of Stability Under Constraint. British ARC R & M 2983, July 1953.
4. Small, S. M. and Prueher, J. W. Fixed Wing Performance Theory and Flight Test Techniques. US Naval Test Pilot School FTM 104, July 1977.
5. Kuester, J. L. and Mize, Joe H. Optimization Techniques with Fortran McGraw-Hill Book Company, New York, 1973.
6. Bridges, P. D., Cross, E. J., and Boatwright, D. W. Flight Test Evaluation of a Method to Determine the Level Flight Performance of a Propeller-Driven Aircraft. SAE 770470, April 1977.

APPENDIX - Theory of Transient Response in Airspeed

The transient response method will be developed here for the case of measurement of the time history of airspeed in response to a change in power as the altitude is held constant.

Consider an airplane in steady level flight. The engine power is changed by a relatively small amount and the resulting time history of the change in airspeed is measured. The engine brake horsepower and airspeed are also measured.



Summing horizontal forces, we have:

$$\Sigma F_{HORIZ} = ma = mV = T - D \quad (1)$$

Assuming a parabolic drag polar.

$$D = (C_{D_0} + \frac{C_L^2}{\pi A Re}) \frac{1}{2} \rho V^2 S = C_{D_0} \frac{\rho V^2 S}{2} + \frac{2m g^2}{\rho S \pi A Re V^2} \quad (2)$$

$$T = \frac{\eta_p BHP}{V} \quad (3)$$

Substitution of these expressions into equation 1 leads to the differential equation which describes the motion

$$\dot{V} = \frac{\eta_p BHP}{m V} - \frac{C_{D_0} \rho S V^2}{2 m} - \frac{2m g^2}{\rho S \pi A Re V^2} \quad (4)$$

Expansion of the terms of equation 4 in a Taylor series and solution of the equation using LaPlace transforms yields an expression for speed as a function of time following a step change in power

$$\Delta V(t) = \frac{\frac{\eta_p}{m} \frac{\Delta BHP}{V_o}}{\left[\frac{\eta_p}{m} \frac{BHP}{V_o^2} + \frac{C_D}{m} \frac{\rho S V_o}{V_o} - \frac{4mg}{\rho S \pi A Re V_o^3} \right] t}$$

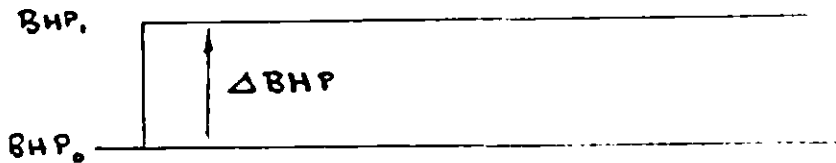
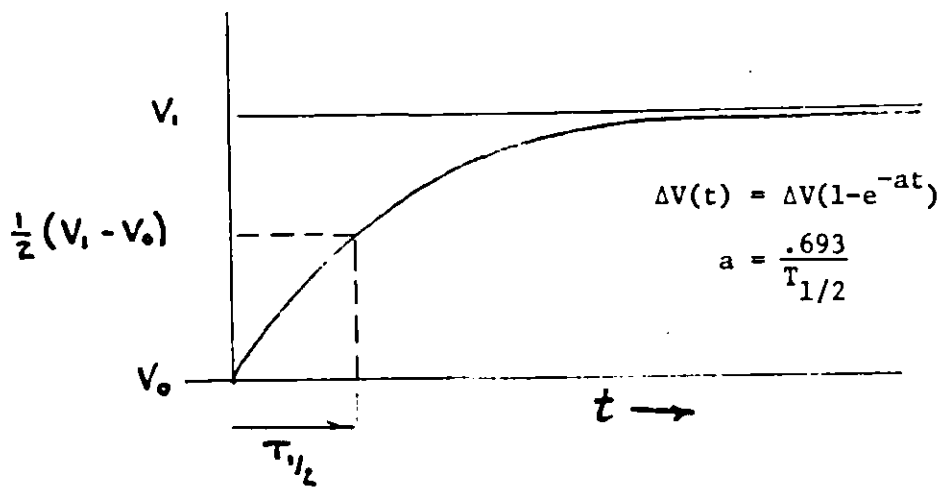
(5)

This expression has the form of a first-order system

(6)

$$\Delta V(t) = A(1-e^{-at})$$

which implies that the exponent in equation 5 can be evaluated by measuring the time constant of the response to a step change in engine power. If, in addition, measurements are made of the initial power and speed, and the change in power and speed, enough information is available to solve for the three unknowns, propeller efficiency, parasite drag coefficient, and aerodynamic efficiency. To illustrate, let the speed and power in the initial steady-state condition to be V_o and BHP_o , the change in power be ΔBHP , the final speed and power V_1 and BHP_1 , and the time to reach half of the change in speed by $T_{1/2}$.



At V_o , $T_o - D_o = 0$

$$\frac{\eta_p BHP_o}{V_o} - \frac{C_{D_o} \rho S V_o^2}{2m} - \frac{2m g^2}{\rho S \pi A R e V_o^2} = 0$$

At V_1 , $T_1 - D_1 = 0$

$$\frac{\eta_p BHP_1}{V_1} - \frac{C_{D_o} \rho S V_1^2}{2m} - \frac{2m g^2}{\rho S \pi A R e V_1^2} = 0$$

At $T_{1/2}$

$$\frac{\eta_p BHP_o}{m V_o^2} + \frac{C_{D_o} \rho S V_o}{m} - \frac{4mg^2}{\rho S \pi A R e V_o^3} = \frac{.693}{T_{1/2}}$$

These are simultaneous equations and can be solved for η_p , C_{D_o} , and $T_{1/2}$

- e. Notice that the measured quantities are initial and final speeds, the time history of the speed change, and the initial and final powers, all of which are amenable to flight test measurements.

TORNADO-AVIONIC DEVELOPMENT TESTING

Erwin K. Obermeier
Messerschmitt-Bölkow-Blohm GmbH
Manching, Germany

ABSTRACT

The TORNADO was designed as a multi-role aircraft capable of carrying large payloads in all weather conditions in either day or night operations, over long ranges at high speeds, whilst hugging the terrain below the enemy radar by use of its high precision navigation and attack equipment.

The TORNADO avionic system is orientated around a digital computer into which main and secondary sensor information is fed. Navigation information is presented to the navigator on the combined radar projected map and television display and to the pilot on the repeater projected map display. Flight director and weapon-aiming symbology is presented to the pilot on the head-up display.

The automatic terrain following subsystem was designed to ensure a safe flightpath over the terrain under low-level high-speed conditions, at whatever clearance-height and ride-mode the pilot has selected.

Subsequent analysis is carried out by utilising onboard recorded data and by using ground based measuring equipment data. So far, the avionic trials have been extremely successful and only comparatively, minor problems have been encountered. These flight tests have confirmed the systems performance predictions.

Erwin K. Obermeier, Flight Test Engineer with Messerschmitt-Bölkow-Blohm GmbH, works extensively with avionic flight test development program.

Acknowledgement

The author would like to acknowledge the effort of H.G. Dexel and H.J. Suratny for the suggestions and review of the paper.

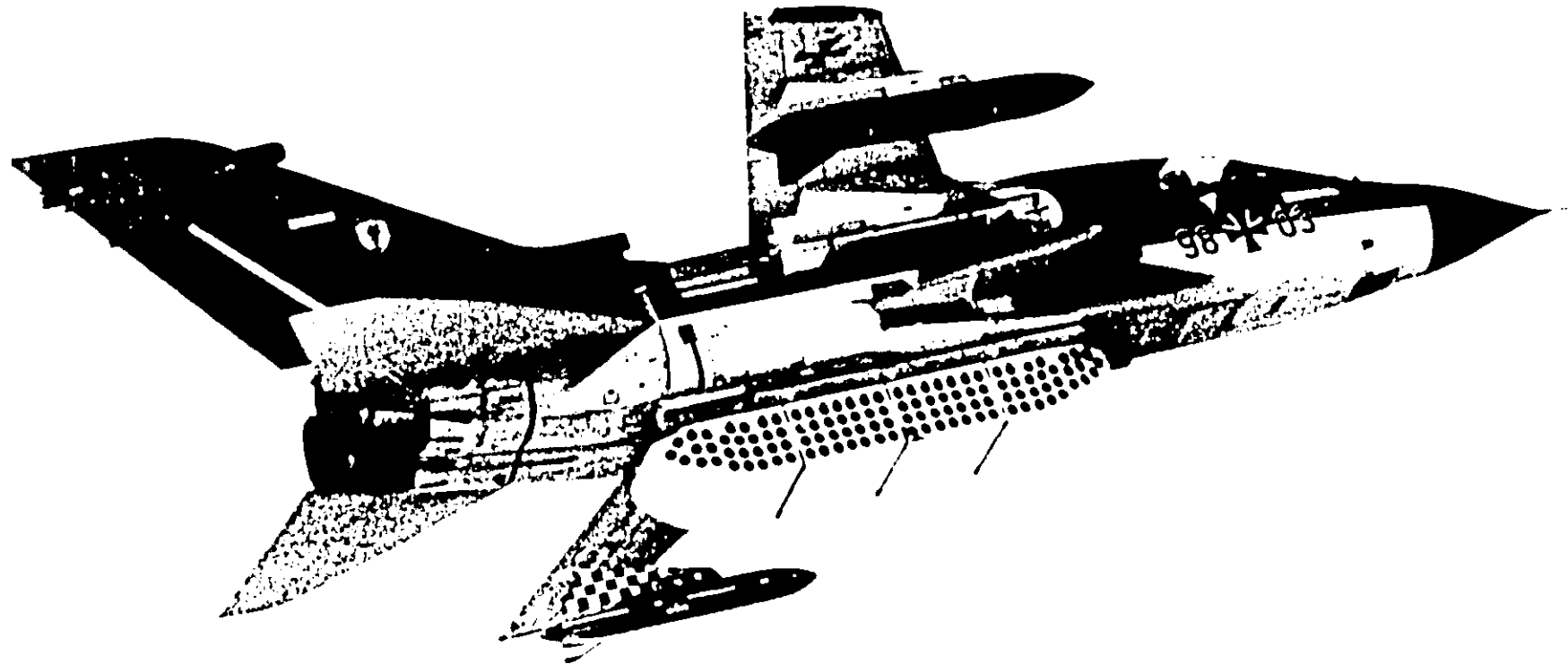
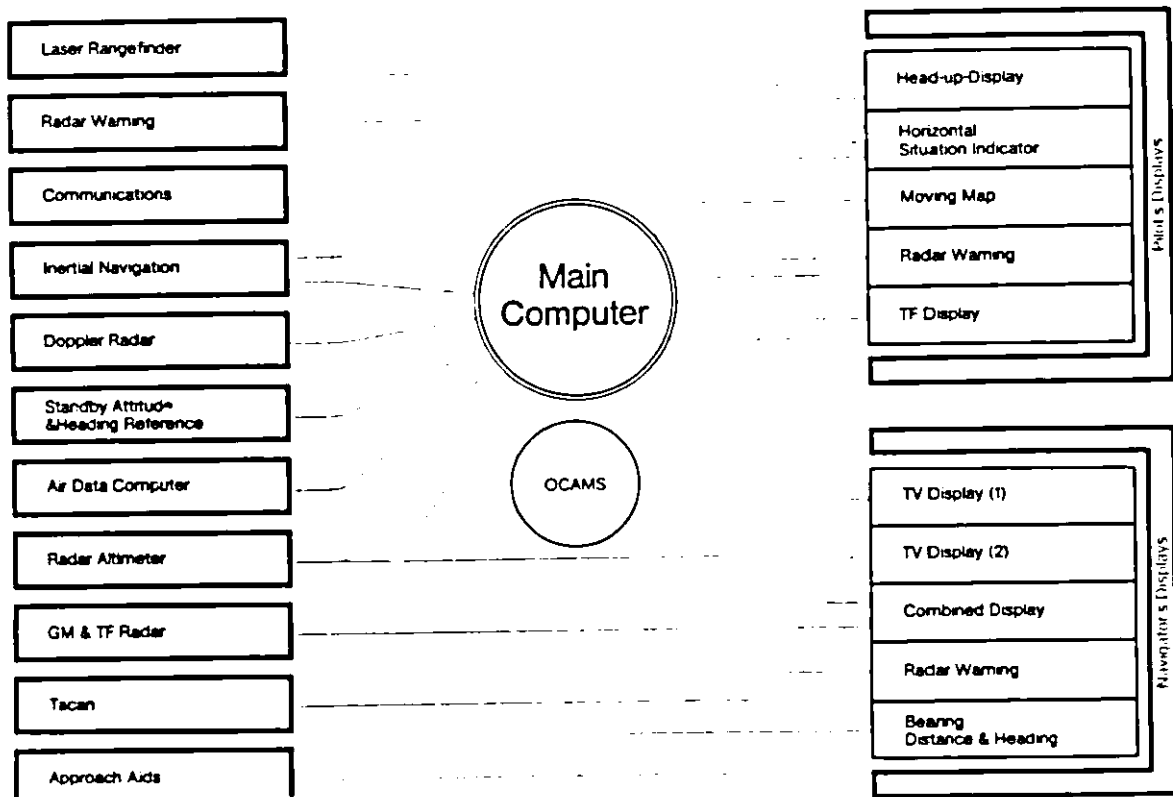


Figure 1, TORNADO - typical mission configuration

INTRODUCTION

To be sure that the TORNADO (produced in partnership with Air Italia (AIT) British Aerospace (BAe) and Messerschmitt-Bölkow-Blohm (MBB)) can fulfil its specific tasks, - such as interdiction/strike, counter-air and close air support mission - and in order to provide repeatable effectiveness, it was essential to furnish the aircraft with the most advanced equipment. Generally, that equipment necessary to achieve the navigation and weapon delivery accuracy required is defined by the term avionics.

The TORNADO avionic system is orientated around the digital Main Computer (MC) into which main and secondary sensor information is fed (Figure 2).



OCAMS = On board Checkout and Monitoring System

Figure 2 TORNADO avionic system

Navigation information is presented to the navigator on the Combined Radar Projected Map Display (CRPMD) and Television Tabular Displays (TV-TAB) and to the pilot on a Repeater Projected Map Display (RPMD). Flight director and weapon aiming symbology is presented to the pilot on the Head Up Display (HUD). Any other navigational information required may be extracted from the MC utilizing the TV-TAB's in the rear cockpit.

Basically the avionic system is composed of the following subsystems

- Navigation
- Terrain following/Autopilot
- Weapon delivery
- Displays and controls
- Communication
- Defensive aids.

Each subsystem contains several items of equipment composed of Line Replaceable Units (LRU).

The attention of this paper is limited to the navigation and terrain following subsystem.

Together with the other systems, such as communications, mapping radar and displays, the navigation subsystem with its precision navigation equipment and the Terrain-following subsystem-premitting low-level, high speed penetration sorties-are currently under flight test evaluation at MBB.

The avionic program started in September 1975 and to-date more than 80% of the total schedule has been completed.

NAVIGATION SUBSYSTEM

A functional flow diagram of the Navigation Subsystem shown in figure 3 may help one to appreciate the complexity of the system. The navigation information provided by IN, DOPPLER, SAHR, ADC and sensor data are fed into the main computer with Kalman filter. This Kalman filter as a mathematical model uses IN-data, DOPPLER-data and the available fixing data for statistic equations, thus the final navigation accuracy in MAIN mode will be considerably higher than the best accuracy provided by any single source. The main computer processes the incoming sensor signals, to make optimum use of system data and provide at any instant the best available steering and present-position information to be presented to the crew. The main computer also controls the subsystem moding and contains all information required to fly a route automatically.

The Inertial Navigator (IN) is the prime source of velocity, attitude, heading and present position data, the Doppler Radar (DO) providing velocity information, and the Air Data Computer (ADC) supplying pressure altitude data and true airspeed (TAS).

In the Navigation Subsystem, the aircraft present position is continuously calculated during flight. In order to improve the navigation accuracy this present position will be updated by accurately measured present position values, using various fixing methods.

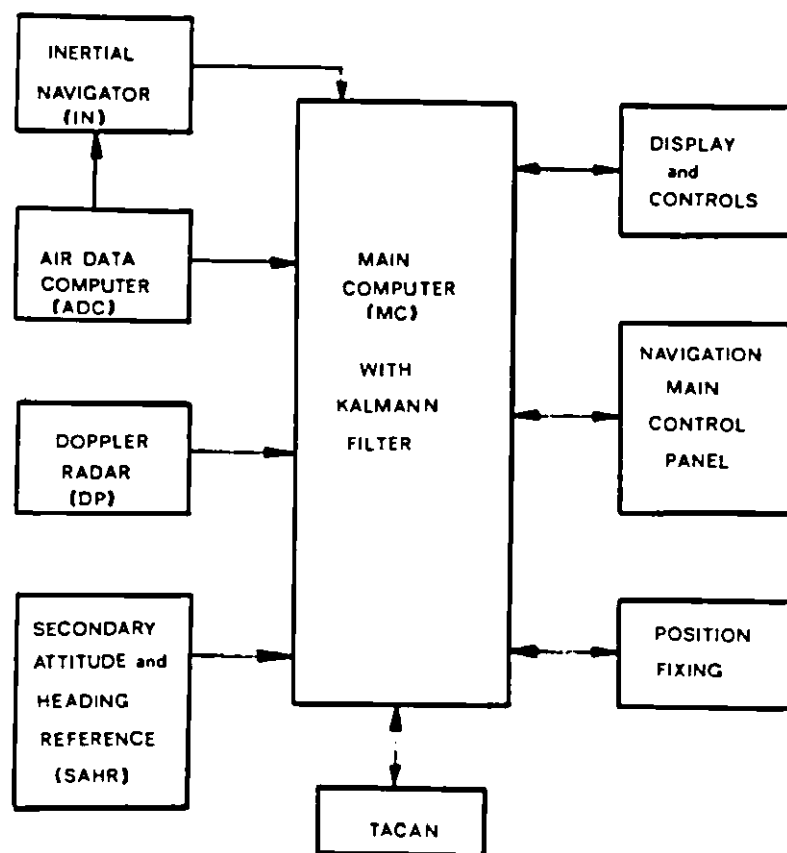


Figure 3 TORNADO navigation moding

	IN	DP	SR	ADC	MC
MAIN MODE	✗	✗	FAIL	✗	✗
INERTIAL NAVIGATOR (IN)/ MAIN COMPUTER (MC)	✗	FAIL	FAIL	✗	✗
DOPPLER (DP)/ SECONDARY ATTITUDE and HEADING REFERENCE (SR)	FAIL	✗	✗	✗	✗
AIR DATA COMPUTER (ADC)/ SECONDARY ATTITUDE and HEADING REFERENCE (SR)	FAIL	FAIL	✗	✗	✗
PURE IN	✗	FAIL	FAIL	FAIL	FAIL

Figure 4 Available navigation modes after equipment failure

Degraded operation is considered in the context of partial failures of system inputs which would not necessarily induce a mode change.

In case of primary equipment failure, the system automatically reverts to the next lower navigation mode with slightly degraded navigation performance. For example the system converts automatically to pure IN mode if the MC should fail, or to Doppler/Sahr mode when the IN fails and to the Air Data/Sahr mode when an IN and additionally a Doppler failure occurs. (Figure 4).

The navigator in the rear cockpit has use of two TV-tabular displays, he may feed into the main computer stores the coordinates of any desired waypoint, fixpoint or target, either before or during the flight; the aircraft will then continue to navigate automatically along the pre planned route although the crew retain the capability of updating the guidance data so as to maintain optimum navigation and weapon-aiming accuracy throughout the mission. Navigation steering and location information is displayed on both Head-up and Head-down instruments. On a combined radar and moving map display, (Figure 5), the aircraft's position and the terrain immediately ahead, is presented using a film or slides. The projected map is overlaid by the radar image, scale and orientation of this being automatically adjusted. It allows the navigator to interpret the radar image of the ground directly, without having knowledge of the radar picture beforehand.

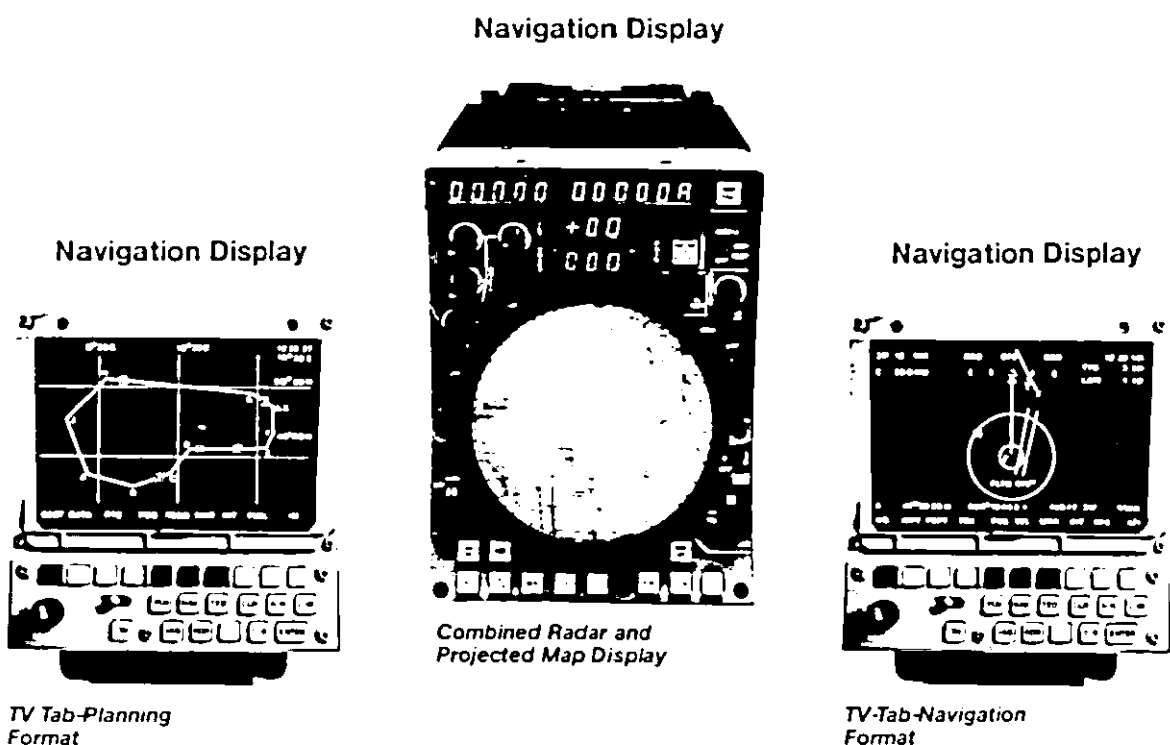


Figure 5 Displays rear cockpit

FLIGHT TEST METHOD

Navigation proving flights were carried out using a special route at a distance of approximately 100 NM around the home base. Main mode accuracy, pure IN performance and navigation performance with reversionary modes were quantified. During navigation trials the cockpit indications were all satisfactory and although most system switching was controlled from the rear seat, the pilot had no difficulty in remaining firmly in the loop.

It is a feature of this aircraft that crew co-operation is very important when flying this type of operation.

Two methods were used for navigation data evaluation.

NAVIGATION TESTS - TRACKING RADAR DATA EVALUATION

Apart from the airborne data recording system two RCA precision tracking radars MFP-36 were used for navigation accuracy measurement. It has been proven that the horizontal positioning accuracy of the tracking radar is better than 30 ft for ranges up to 70 NM when an airborne transponder is used.

The tracking radar measures range, elevation and azimuth angles in polar coordinates, which are recorded on magnetic tape. Together with digital data obtained from the tracking radar, an analogue plot is produced, presenting the aircraft position on a map (Figure 6). The route shown was flown in four different navigation modes, with autopilot engaged.

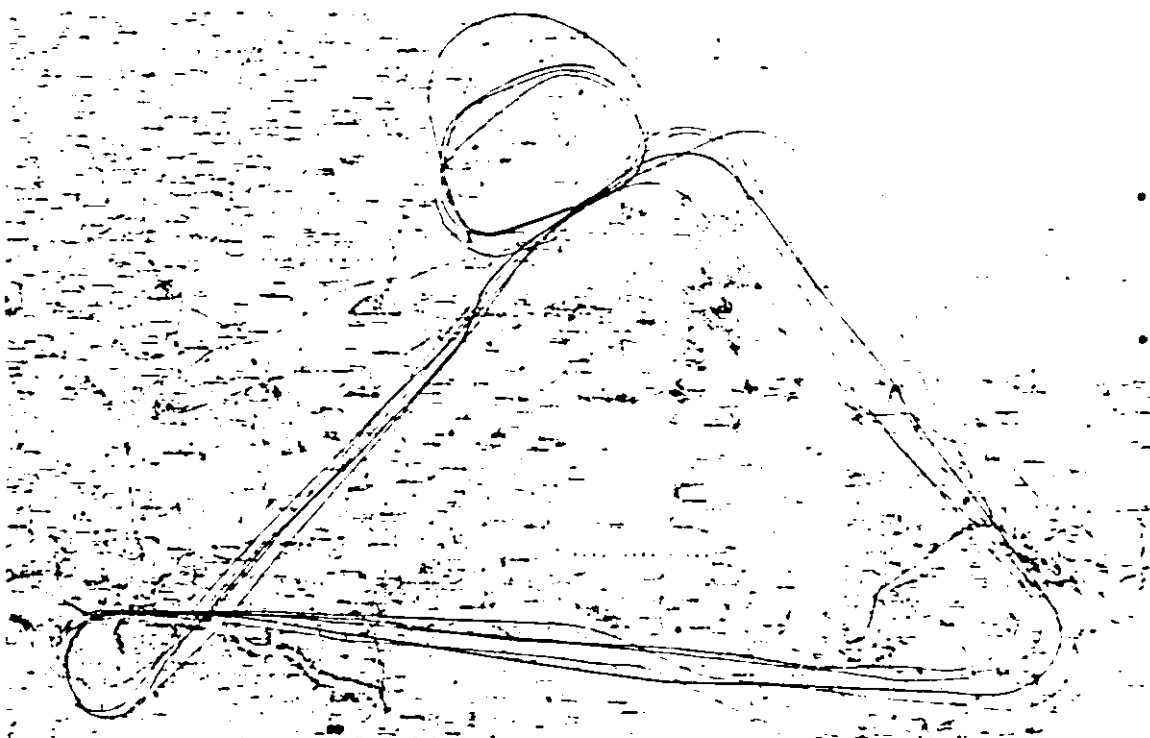


Figure 6 Route plotted by the tracking radar.

A computer programme was developed to relate the radar data to the same coordination system and to compare it to aircraft data recorded via FTI. To enable an accurate comparison between external tracking radar data and internal aircraft data, a precise time correlation has to be established. As part of the flight test instrumentations, a time code generator is installed onboard. The tracking radar has its own time code generator. By pressing the time synchronization button in the cockpit a 1000 Hz-tone is generated, recorded via FTI as well as being transmitted to the tracking radar. The time correlation accuracy between aircraft and tracking radar is at worst 10 msec., which limits the maximum position measurement error to less than 8 ft., depending on airspeed.

The advantage of the tracking radar used for precision measurement during navigation accuracy evaluation is its adaptability under all weatherconditions and all altitudes, without the need for special routes.

In order to continuously track the aircraft en route, the MPS 36 was sited on a hill north of the MBB flight test base of Manching.

The radar could be used in skin tracking mode without active equipment in the aircraft. However, to ease tracking, the aircraft was equiped with a transponder installed in the external camera pod mounted on the centerline station.

All modes of the navigation subsystem have been flight tested. Figure 7 shows a typical plot of navigational accuracy for a Schuler period. The evolution of the N-S, E-W and overall radial error is presented. The plots were obtained by using tracking radar and onboard data.

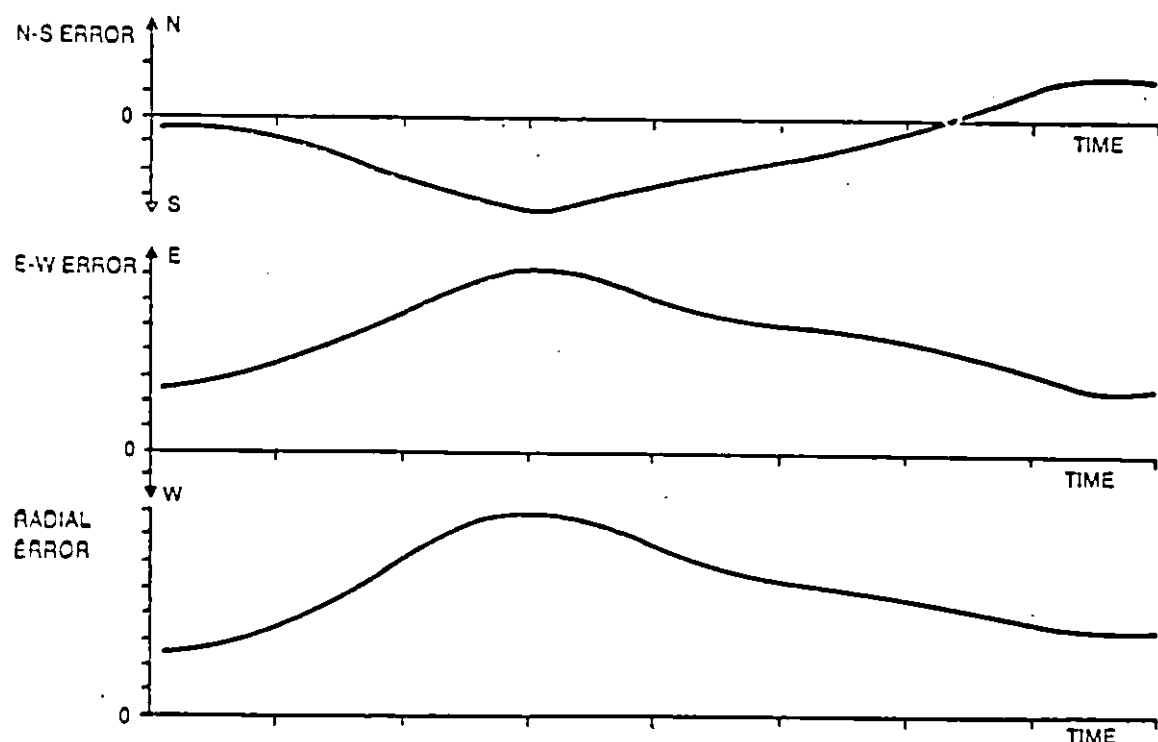


Figure 7 Navigation performance plot

NAVIGATION TESTS - PHOTO EVALUATION

As a back-up system for evaluation of navigation accuracy, a camera pod containing a downward and a forwardpointing camera was used. The pod is a converted external fuel tank mounted at the centerline station.

Flying a navigation route, pictures were taken over a fixpoint-area with well known coordinates and height MSL from at least two reference points. Figure 8 is a photographic picture from a fixpoint area with nine reference points, the area is approx. 3 by 3 miles. The number of frames taken over each fixpoint is about 20.



Figure 8 Fixpoint with nine reference points

The downward and forward pointing cameras are stereoscopic cameras. The stereo effect is generated by recording photographically two pictures at different times with an overlap of at least 60% on the two frames.

The developed films are evaluated by a stereo viewer which enables a precise identification of the reference points.

Via a special evaluation equipment (Weinberger, see figure 9) the X- and Y-coordinates are measured and automatically punched on a paper-tape, which is fed into the computer for data reduction.

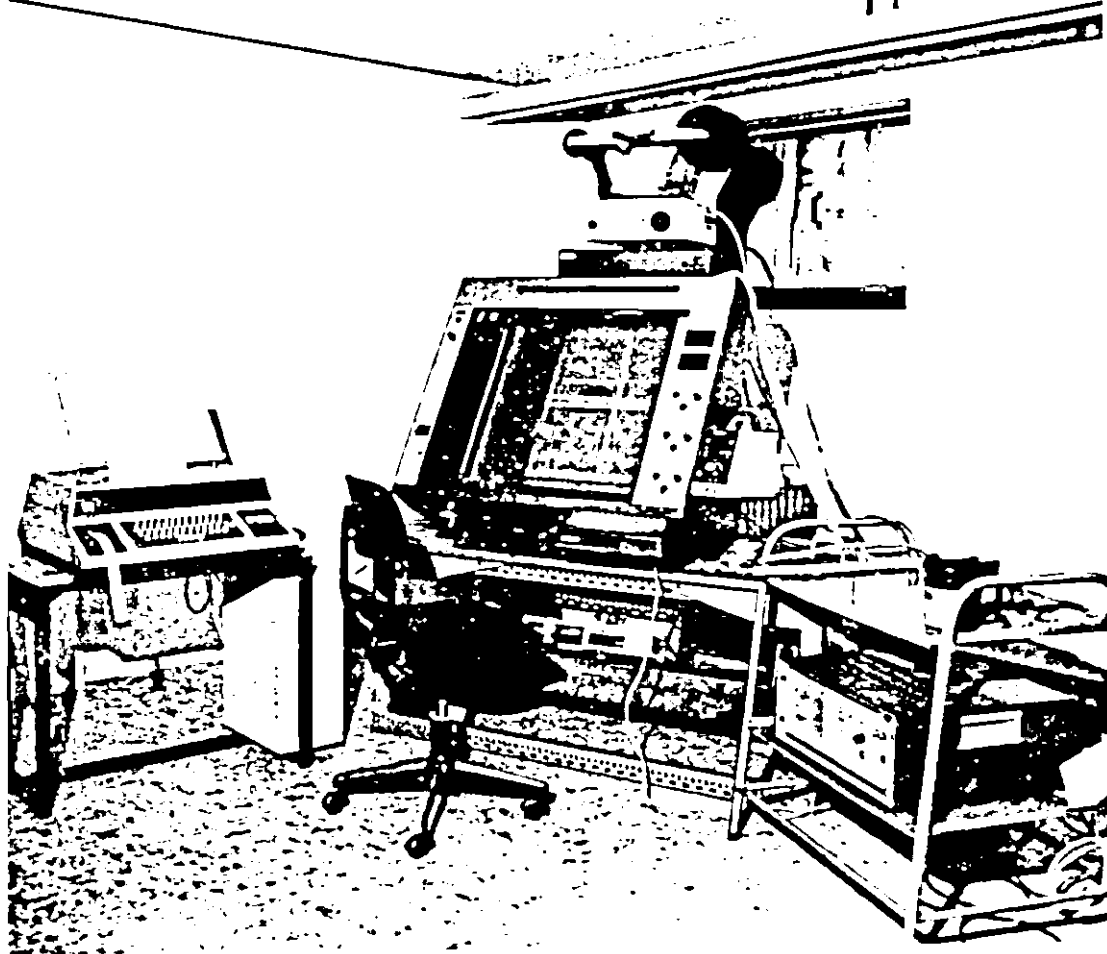
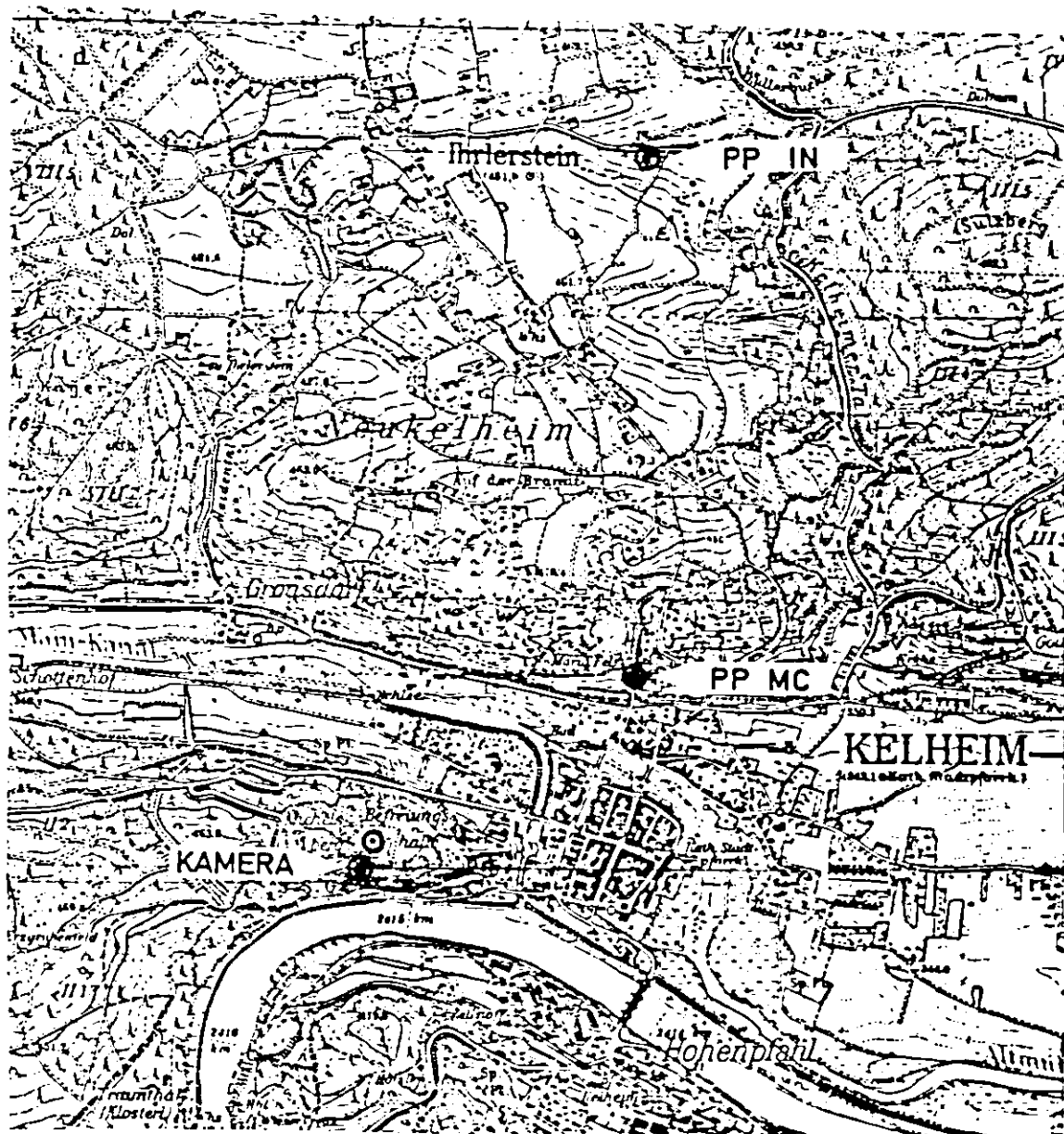


Figure 9 Weinberger evaluation equipment

The aircraft position and height is evaluated by a minimising calculation to satisfy the photo coordinates for each pair of reference points. Using this method a most precise present position determination is possible; and depending on an accurate harmonization of the cameras and height flown above ground, measurement errors of less than 10 ft for present position, 30 ft for height, have been obtained.

The shutter pulses of the cameras are recorded on the onboard flight test instrumentation (FTI) tape. To each shutter pulse, the time-correlated values of; - present position main computer (MC) and Inertial Navigator (IN), attitude and heading from IN and Secondary Attitude and Heading Reference (SAHR) and height from Airdata Computer (ADC) and baro IN, are recorded and compared to the camera data. A typical evaluation result is shown in figure 10. Due to limitations of the cameras and film format available, these evaluation may only be used when flying at test altitudes between 3000 ft and 7000 ft AGL.



PP IN = Present position IN
 PP MC = Present position MC
 KAMERA = Actual position aircraft

Figure 10 Test results

TERRAIN FOLLOWING (TF)/ AFDS SUBSYSTEM

The TORNADO TF/AFDS subsystem functional flow is presented in figure 11.

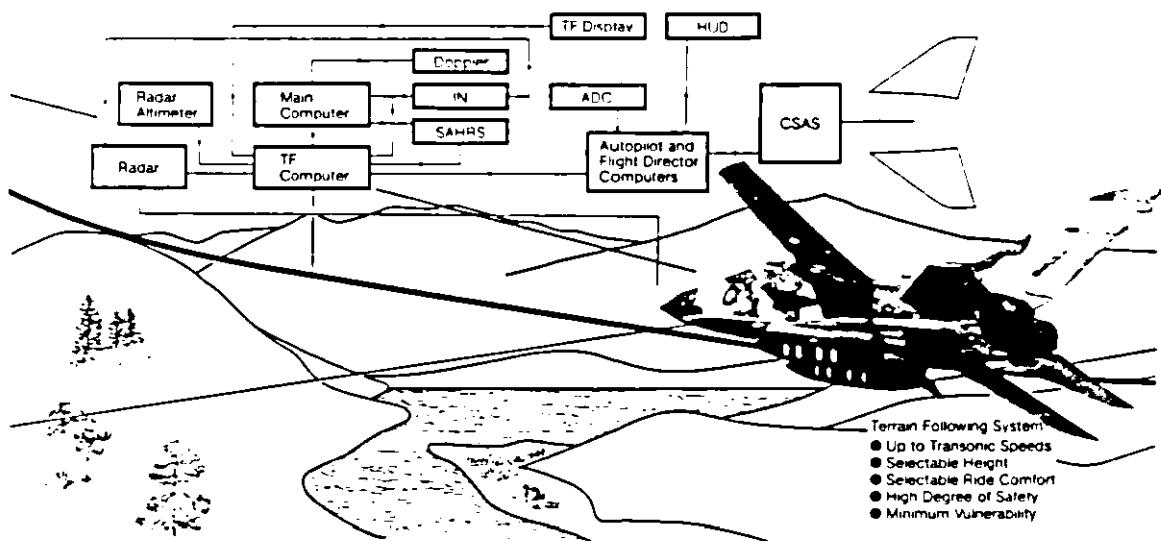


Figure 11 TF/AFDS functional flow

The TF subsystem was designed to ensure a safe flightpath over the terrain at high transonic mach number, at whatever clearance height, down to 200 ft, the pilot has selected; to be flown either manually or automatically under poor or zero ground visibility conditions for undetected penetration. The ride quality can be selected from "soft", with gentle manoeuvres (at the expense of less terrain following accuracy), to "hard", generating commands to keep the aircraft as close to the terrain as the aircraft performance and restriction allow for.

The TF radar (TFR) utilizes circular polarisation in addition to a high efficiency broadband random frequency agility mode to minimize weather and ECM problems.

The TFR scans the terrain ahead, in azimuth and elevation, along the aircraft track and measures range to the terrain as a function of elevation scan angle. Besides these signals, other inputs such as attitudes, groundspeed, height, from SAHR, IN and radar alitmeter are transmitted to the TF-computer and from there the TF-command is fed into the autopilot and flight director system which converts them either to flight control signals directly compatible to the flight control system, or displays the commands on the HUD for monitoring.

Substantial safety is built into the system, with continuous BITE testing being carried out. The autopilot and flight director system is a duplex system continually checking against each other, and with automatic recovery action being initiated should a fault be discovered.

The Head Up Display (HUD) is the primary display to the pilot when flying either manually according the flight director dot or for system performance monitoring. Except for the flight director, the radar altimeter digits and a symbol like a ".T." which indicates that TF mode is engaged, no additional information is displayed on the HUD during normal TF operation. In case of a TF data 'good removal' by the BITE or one of the safety monitors, a flashing break-away cross will appear, associated with a flight director fly-up command.

The E-scope is a display to the pilot for system performance monitoring during automatic terrain following flight. On the E-scope the zero "g" command line (shaped like a ski-toe depending on the inputs such as selected clearance height, ride mode, airspeed) and the actual TF-radar ground returns are displayed. Penetration of this zero command ski-toe locus will cause the TF-computer to generate a nose-up "g"-command. Ideally these discrete lines on the E-scope should merge together.

The ADI provides head-down flight director steering information according to the AFDS-modes selected. The instrument is situated next to the E-scope for verification of "g"-command generation when radar ground video penetrates the ski-toe.

Figure 12 presents the simplified terrain following control loop.

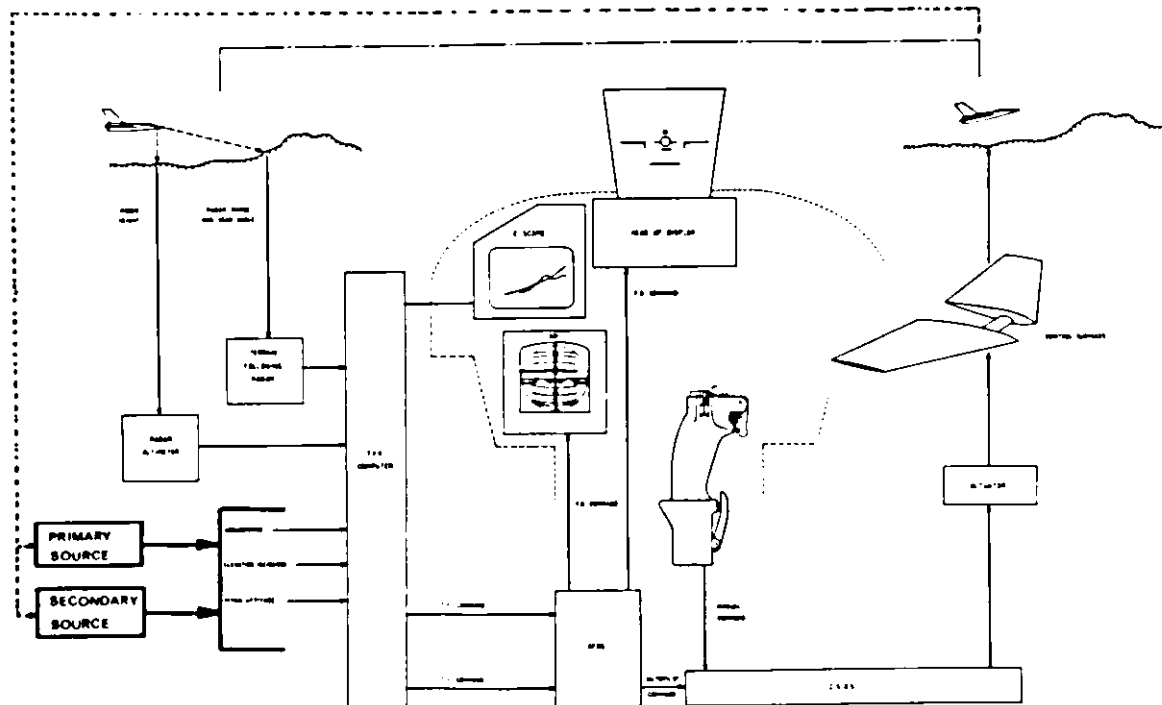


Figure 12 Simplified terrain following control loop

Figure 13 presents a terrain following flight profile and indicates that the selected clearance height has to be maintained over water, man-made obstacles or natural terrain.

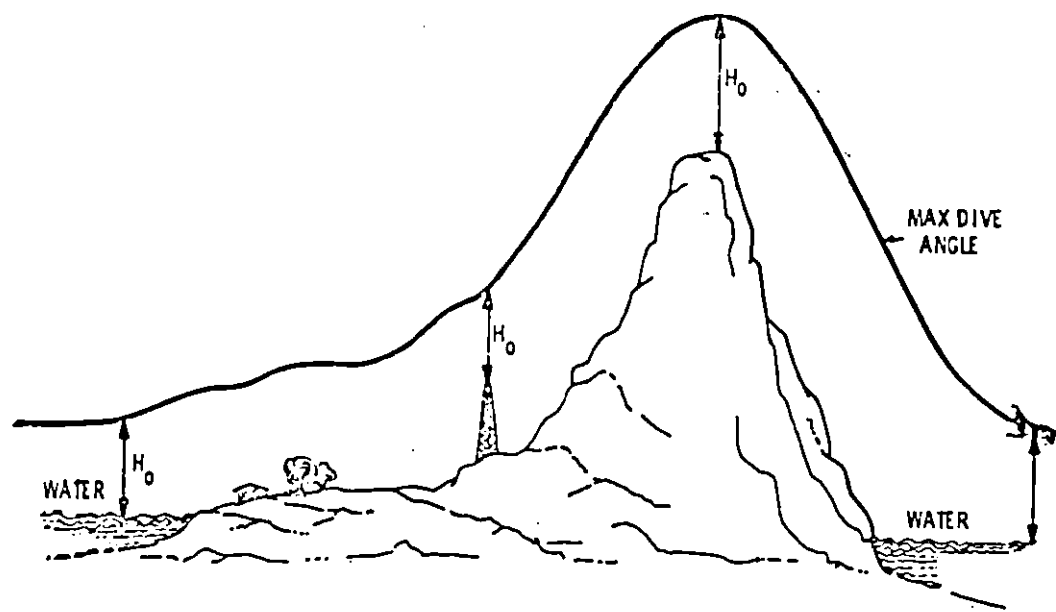


Figure 13 Terrain following flight profile

Actual flight test data of an automatic TF-flight, soft-ride, over moderate terrain in the Altmühl river valley are presented in figure 14.

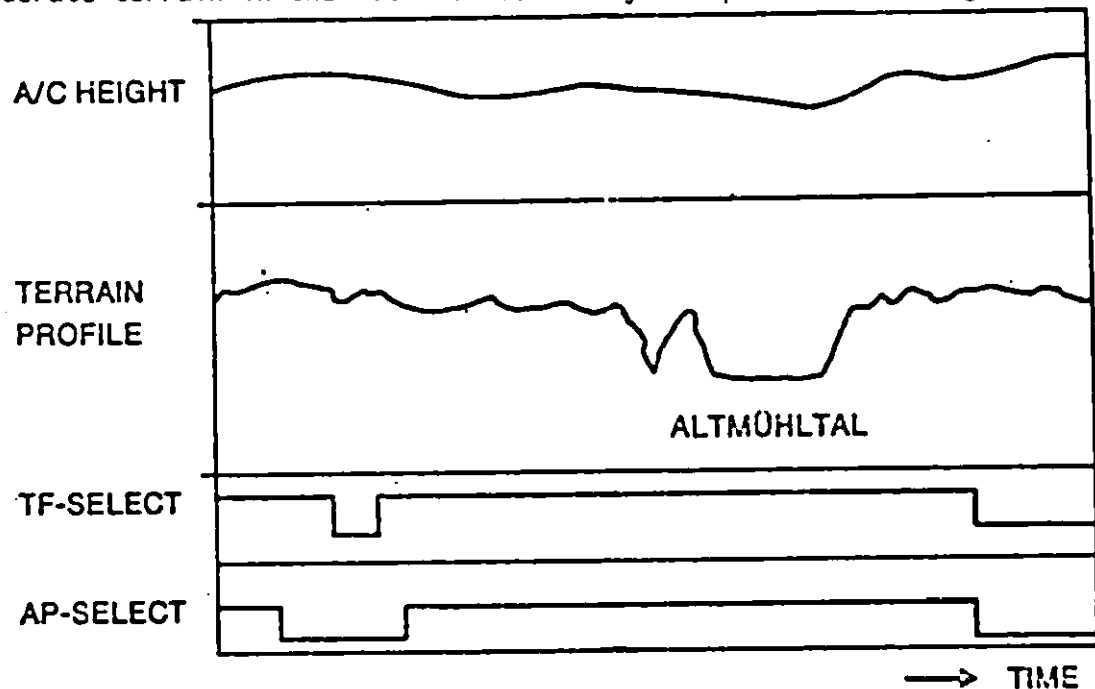


Figure 14 Automatic TF-flight data

FLIGHT TEST AND ANALYSIS METHODS

Flying was carried out over special routes which became progressively more demanding as confidence in the system grew. We started over flat terrain, with soft ride quality, maximum set clearance height and moved onto undulated rough terrain in manual and automatic mode. Except for cinetheodolites at the initial performance phase, for precise height determination, no ground based measuring device was used for evaluation of TF performance, since due to low level flight the tracking radar was not able to cover the flight path over long distances.

However, the camera pod with an oblique and downward pointing camera was used to identify the terrain and obtain data of actual height above ground, and present position. Data reduction is the same as used for navigation system evaluation. From the HUD-camerafilm, flight director and autopilot functioning was examined. The E-scope presentation was recorded via the E-scope camera, which provided some information about the functioning of the TF-system. The performance evaluation was carried out by comparing the characteristic aircraft parameters such as height above ground, aircraft attitude, barometric height, aircraft commands etc. measured in flight against the corresponding parameters obtained using a simulator working on the same terrain profile. The terrain profile fed into the simulator was reproduced by subtracting the radar altimeter height from the barometric height recorded and corrected via ADC and with an IN vertical term during the actual flight. Within the beam, the radar altimeter always measures the shortest distance to the ground, thus the radar altimeter height had to be corrected for the error when terrain slopes were overflowed (Figure 15).

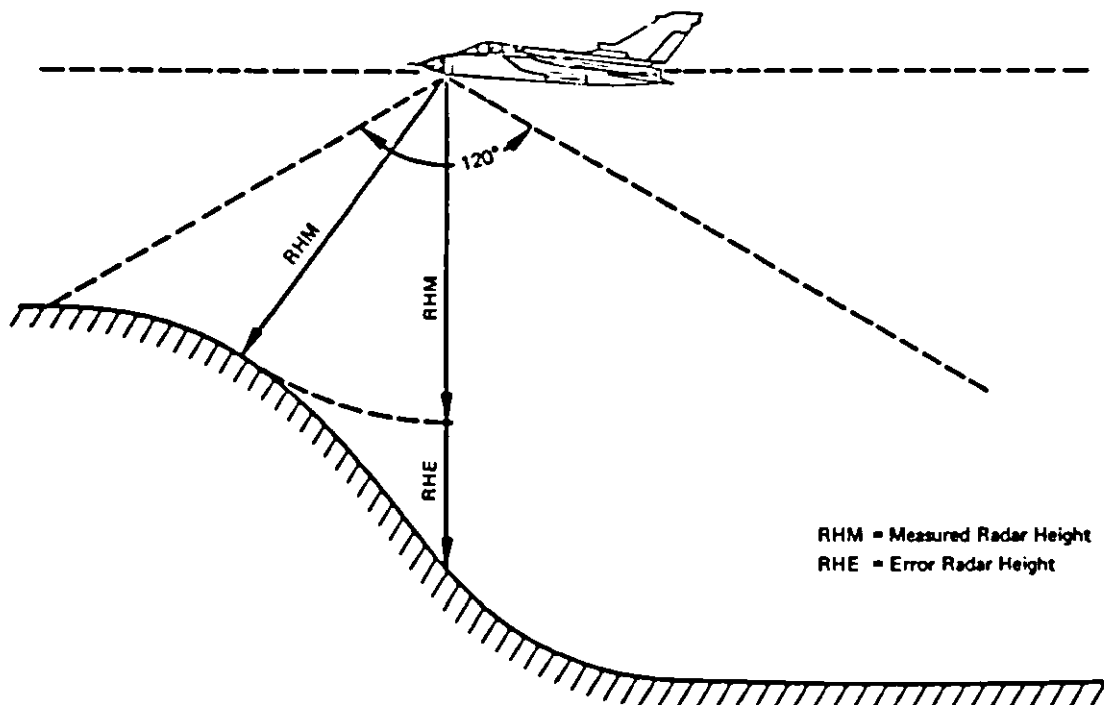


Figure 15 Radar altimeter measuring error

After these corrections have been applied the comparison between actual flight data and simulated error-free flight data was performed. As a result the actual flight path and the flight path provided by the simulator were plotted over the computed terrain profile. Within a specified tolerance band for sensor accuracy both, the actual and the simulated flight path overlap.

Inflight terrain following failure simulation with respect to terrain following radar failures were performed, which resulted in each case in an emergency pull-up as expected.

Radar altimeter failure simulations were carried out over all the kinds of terrain profile and no degradations in TF-performance were observed.

FLIGHT TEST INSTRUMENTATION

ON BOARD INSTRUMENTATION

In order to allow a comprehensive evaluation of the avionic system performance sophisticated instrumentation equipment has been developed (Figure 16).

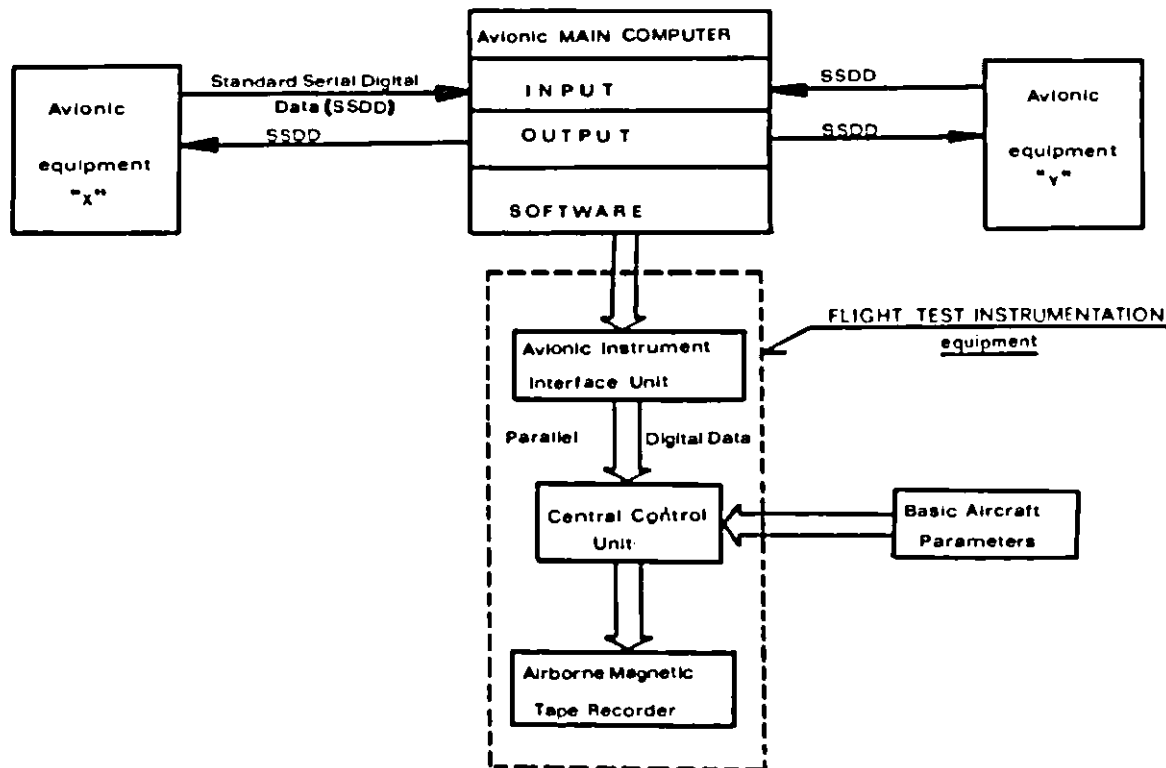


Figure 16 TORNADO main stream flight test instrumentation recording facility

The on board recording system is capable of recording analogue and discrete signals of general aircraft parameters, as well as, via an interface unit, recording the digital data word gathered from the avionic system. Most of the avionics equipment provide digital inputs to the MC. From this central digital unit, the data stream is fed via the Avionic Instrumentation Interface Unit (AIIU) to the central control unit where additional basic aircraft parameters are added.

The data is fed into the airborne magnetic tape recorder (AMTR) or transmitted via telemetry to the ground station for on-line data reduction (Figure 17). The sampling rate of analogue parameters is as high as 128 Hz, digital parameters can be sampled up to 2048 Hz. Up to 150 digital and a total of 500 parameters can be recorded simultaneously.

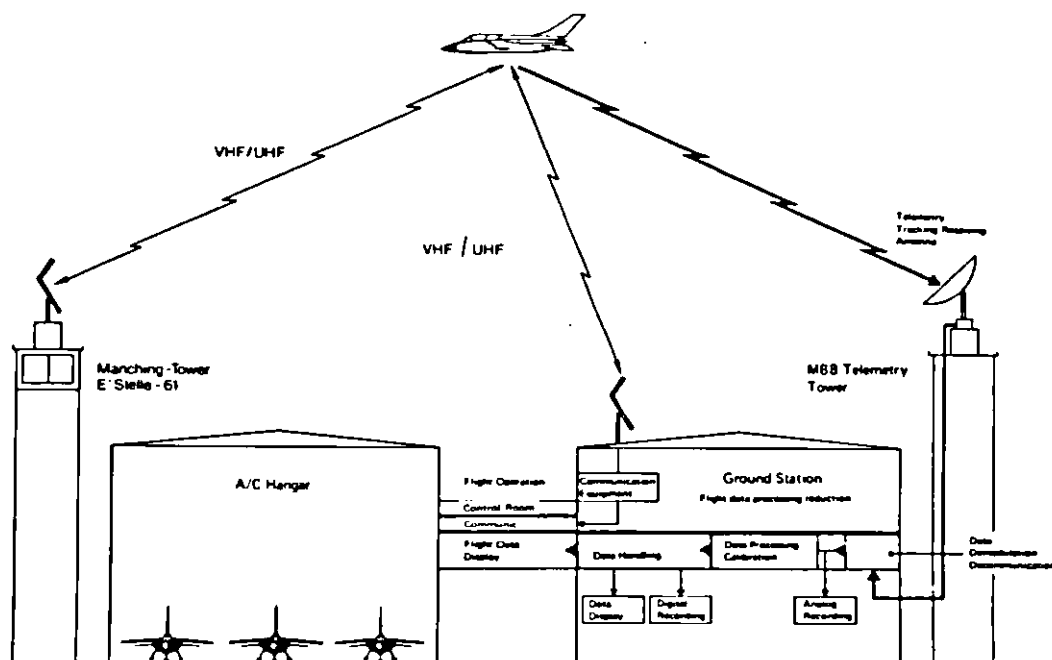


Figure 17 Control monitoring telemetry and communication

A camera pod mounted on the fuselage centerstation is provided with an oblique and down pointing camera to obtain photographic pictures for terrain identification and to gain data such as actual height and present position. A C-band transponder to identify the aircraft during radar tracking is contained within this camera pod.

GROUND BASED INSTRUMENTATION

The precision tracking radar and Asconia Kinetheodolites, furnished by the FRG government, are used as the most accurate data sources.

Characteristic points along special TF-routes are marked by flashing lights. For navigation fixing evaluation, special beacons and corner reflectors are used as artifical targets.

These have the benefit of producing consistent quality image returns ensuring no variation in signal return between any tests.

CONCLUSION

Up to now the avionic trials have been extremely successful. The tests have confirmed the systems predictions.

Of course, several problem areas were detected, however, solutions were found to either improve the system or solve the problem.

We have high confidence that the final TF-performance of the TORNADO will meet its specifications.

DESIGN, DEVELOPMENT AND FLIGHT TESTING OF A JET POWERED SAILPLANE

Bernard S. Smith
Caproni Vizzola Costruzioni Aeronautiche SpA
Vizzola Ticino, Italy

ABSTRACT

Sailplanes must be either towed to altitude or use a small onboard engine, which then makes them motorgliders (powered sailplanes). Common reciprocating engine-propellor combinations have inherent drag producing problems which a buried jet engine does not. To produce a jet powered sailplane capable of setting world records, solutions to problems are accomplished by Caproni through design, development and flight testing efforts.

INTRODUCTION

Sailplanes, traditionally called gliders, are certifiable heavier-than-air aircraft that are supported in flight by the dynamic reaction of the air against their lifting surfaces and whose free flight does not depend principally on engines. In order to enjoy free flight, the sailplane must have assistance to attain some initial altitude sufficient to allow time for an independent search for sustaining meteorological conditions. In early days, a bungee cord launch was used wherein several people on each end of a long 'rubber band' would run forward and outward while the middle of the cord was attached to a hook at the nose of the glider, which was restrained from moving by being held at its tail. When the bungee was fully extended, the glider pilot would signal for release of the tail hold-down and the resultant catapulting action would take them airborne. This was used successfully at the brow of ridges for a glide down to the bottom of the valley. When there was suitably directioned and sufficient wind, continued flight along the ridge in the rising air on the ridge's windward side was possible. The obvious altitude limitations of this type of launching device led to the use of automobiles to tow the glider aloft. Later, winches were developed and finally, tow behind an airplane, which is the method now widely used throughout the world as the most efficient launching style. It allows search, while on tow, for areas of lift, to preclude having to be launched with just the hope of finding rising air.

Although the Wright brothers had some measure of success in developing powered flight, that was preceded by very extensive flight evaluation in gliders. (1) But it would be improper to label their

Bernard S. Smith, Consultant for Caproni's Aircraft and Commercial Division

Wright Flyer as the first motorglider since a motorglider is a machine using the engine merely as the launching device as a substitute for the bungee, auto tow, winch, or airplane tow. However, the design and development of powerplant/sailplane combinations has been underway for many years (2) to provide that ultimate freedom in the search for lift. Even more freedom is realized because the motorglider can restart (hopefully) at the end of the soaring flight in order to climb away from an off-field landing, or to take off again after landing if such is desired. No expensive towplane retrieve or long trailer retrieve is needed. No extra crew members are necessary to fly the towplane or drive the car and trailer and glider disassembly is unnecessary. One solution to the powered sailplane concept is the Caproni A21J, from a company which began with a glider design in 1908 and more than forty years ago built one of the world's first jet thrust airplanes.

DESIGN CONSIDERATION

The A21 concept from the beginning (3) was for a production jet-powered sailplane. The jet wasn't entirely a new idea. Dr. Lippisch had considered and used reaction propulsion as early as 1928 in tests with model gliders (4). An all wood French CM8-13 glider, modified with a V-tail replacing its conventional tail and a small jet pod installed atop the fuselage behind the cockpit, flew successfully in 1950 as a forerunner to the Fouga trainer (5). A turbojet engine weighing 14 lbs. with 20 lbs. thrust installed on a Prue 215A sailplane in 1963 as an external mount similar to the Fouga could be used only as a sustaining aid while aloft (6). But the A21 design consideration was to give the highest possible performance either with or without its powerplant, with the capability of setting world records. (Although motorgliders had initially been given a Federation Aeronautique Internationale (FAI) record category in 1937 (7), powered sailplanes came into their own in 1971 when a specific motorglider category was established with procedures (8) to allow badge, contest and record flying.)

One of the major problems of a conventional Otto-cycle reciprocating-engined motorglider with a propellor is high drag. A number of solutions have been used. A conventional nose-mounted engine with feathering propellor (9) for drag reduction like the Sheibe SF-28A is quite common. Burying the engine in the fuselage with a shaft driving a folding propellor concentric with a tail boom (10) is another method, used on the C-10 in 1942. The 1949 Hummingbird design of Ted Nelson, Harry Perl and Don Mitchell led to production of several powered sailplanes which are still flying today as modern-looking ships, having pioneered the fully retractable engine-direct drive propellor combination (11). More recently (12) a buried engine with belt-driven retractable-propellor has been flown by Vern Oldershaw, who was a major helper on the Gossamer project. One unique retraction unit used a strut separating the propellor and its buried engine with both moving during retraction (13). All these methods have their problems,

but of course fuel consumption isn't one of them. Admitting to the higher fuel use and acquisition cost of a turbojet, the design proceeded. There were too many advantages to a jet to pass up no vibration in the 2Hz - 40Hz range, a structural problem with reciprocating engines; lack of complexity associated with reciprocating engines and retracting mechanisms; no CG shift as with retracting units; modern jet esthetics; and flush, closing air inlets for drag reduction.

Because of the very high performance of single-place sailplanes relative to that of two-place ships regarding existing world records, one major consideration was for a two-place ship. This could give additional engine space and weight allowance. The tadpole shaped fuselage depicted in Fig. 1 resulted from extensive wind tunnel and computer analysis providing lower drag than a tandem shape. The difference was because of fuselage lift. An attempt was made to measure this lift by installing

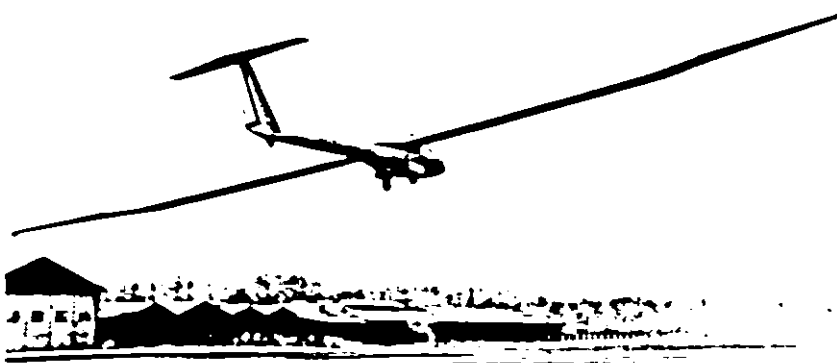


Fig. 1 A21J Landing at Factory

strain gauges on the wing to measure lift as a function of the bending moment. A cockpit readout was utilized by test pilot Zanetti, with a device which required commutation for each gauge. Results were inconclusive.

Since the design began with the turbojet installation concept, room for it was planned within the central core structure, a box shape which tied together the tail boom, wings and cockpit floor pan. The two-wheel design (See Fig. 1), abnormal for a glider, came about because that central core volume was necessary for the engine. This proved to be fortuitous for a number of reasons. Single-wheel sailplanes need people to run the wing for takeoff. The motorglider versions have drag inducing out-riggers ala U-2, or low wing designs with a dragging wingtip if there's no ground-handler, one of the reasons for having a motorglider in the first place. This means potentially control-losing turning forces either in takeoff as speed builds to aileron effectiveness or because of a possible asymmetric loss of wing lift when landing in a relatively low grass field if it reaches as high as the wing - one reason why most sailplanes have mid or high wings. The ability to easily taxi on any airport (See Fig. 2) in the wings level attitude (a rudder-pedal steerable tailwheel is incorporated on the powered version) is another dual wheel advantage. Braking energy is more quickly and safely utilized as well.



Fig. 2 A21J Taxiing at Palo Alto, CA

Selection of materials was important to the design. Because record-breaking high performance was the goal for a serial production ship incorporating a hot turbojet engine, the use of all metal stressed-skin structure for lightness, strength and high rigidity was indicated. For the wing, with an aspect ratio of 25.65, (See Fig. 3),

metal was selected for its modulus of elasticity compared to composites. The greater torsional stiffness of metal is important because of wing twisting forces which would result in higher drag with the twist experienced in a composite wing of these dimensions. Naturally, the airfoil section selected was of laminar type, the Wortman FX 67-K-170 for the rectangular section (See Fig. 4) and FX 60-126 in the tapered section. The 170 section has been extremely popular having been extensively used in the industry until very recently as some new tailored sections have been developed.

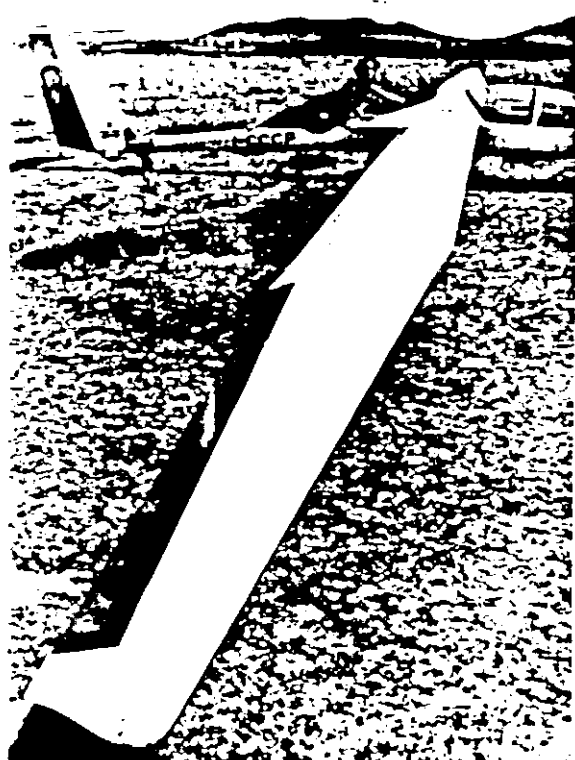


Fig. 3 A21S Shows Off its Aspect Ratio

FLAP/AIRBRAKE
As a result of flight-testing, two minor changes were made on the wing, one of which was simply a matter of observation. The outer wing dihedral was changed from 0° to $+1^\circ$ to provide more tip ground clearance. This required only a slight

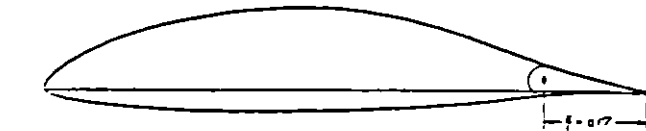


Fig. 4 Wortman
FX 67-K-170/17 wing
Section used on A21

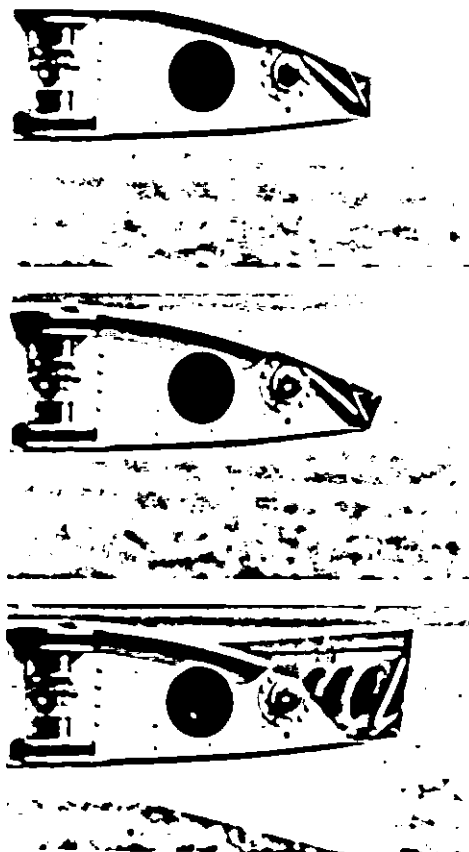


Fig. 5 -8°; +12° and
+87° Flaps/spoilers

most efficient flight over the complete speed range. At +12° flaps, which span 68% of the trailing edge, the upper surface aft hinged spoilers begin to open and can be fully modulated up to the maximum +87° flap setting (Fig. 5). Linkage from the cockpit is through a torsion tube with automatic engagement during wing assembly. Maximum attainable speed in vertical dive with full spoiler/flap deployed was determined by flight test to be 102kts. The testing was performed to assure that exact vertical was attained by noting speed reduction when going past the vertical and with markings on the canopy.

change in attach fittings in the airfoil transition section. Second, it was realized there would be considerable wake when the upper surface spoilers were deployed. One reason the T-tail design was selected was to preclude the wake from the in-board (center) wing section impinging on the horizontal stabilizer. However, it was readily apparent during flight testing that the tail was not high enough at slow speed so the upper surface spoiler was eliminated from the central wing section. The unique design of the flap/spoiler came about largely to satisfy the FAI requirements for restrictions against the use of both flaps and spoilers in Standard Class * category sailplanes concomitant with a means to limit vertical descent to 75% V_D .

Although the A-21 isn't a standard class ship, one was planned as a follow-on. (It was built but didn't go into serial production.) The flap/spoiler design works very well with a single handle allowing a continuous change of the wing camber within a range of -8° to +12° for

*Standard Class: Single-place, 15,000mm span with other cost reducing limitations, for world class competition.

The upper surface spoilers have the added advantage of balancing loads to reduce pilot operating forces which can be very high on speed limiting flap only operation. Prior to first flight, the flap/spoiler design was tested with a full scale 1m span wing section mounted above and ahead of a Fiat 1200 automobile. Running at 65 kts. with positive flaps, the front end of the Fiat was lightened enough to lose steering control effectiveness. Full flap deployment didn't completely stop the car, but was impressive enough to patent the design. A strain gauge was installed on the top of the tail boom at its midpoint in order to read tail loads. They were obtained in flight test at several speeds up to vertical to determine the wing moment coefficient with airbrakes open in order to calculate balance loads, required for certification, but not available from Wortman airfoil data. Ground tests with dummy loads provided calibration.

WING FILLET

Compared to conventional aircraft, because of the total overall effort in drag reduction on sailplanes, the effect of wing-body drag assumes more importance. Therefore, extensive flight testing of the wing fuselage fairing fillet was undertaken. Mirrors were mounted at both outer wing attach points (See Fig. 6) to enable in-flight viewing of wool tuft application in the affected area. A plastic forming material which could be easily altered was shaped, sometimes with a different contour on each side in order to better utilize the flight time. The original fairing caused resonance on the horizontal tail and even resulted in its stalling. After two months and ten hours of flight testing, the final shape was determined. It is much longer overall than the original fillet, with a lesser angle of incidence than the wing. This provides better alignment at negative flap settings. The concept was also tested on a Comanche 250 resulting in a reduction of 8.7 kts. in stall speed. On the A21, stall speed was reduced 5.4 kts. With the fillet, the sink rate is lower at high speeds but it is also good for positive flap settings.

MISCELLANEOUS

Flight testing for airspeed calibration used a vane anemometer. First installation was on the fuselage nose/canopy but was found to be too weak resulting in probe flutter. It was reengineered on the wing and the final result is a negative incidence pitot on the vertical stabilizer at the 77% span position measured up from the tail boom.

Fuel was to be carried in a 56 l tank mounted in the 4.8m span center wing box spar section which is directly above the engine location. Because it was known that considerable time would elapse prior to prototype engine availability, construction of the pure sailplane prototype proceeded, leading ultimately to certification of the A21 by RAI, FAA, LBA and SGAC. (Italian, U.S., German and French certifying authorities)



Fig. 6 Outer Wing Being Attached to Center Wing Section, Showing Flap/Airbrakes and Location For Mirror During Tufting tests.

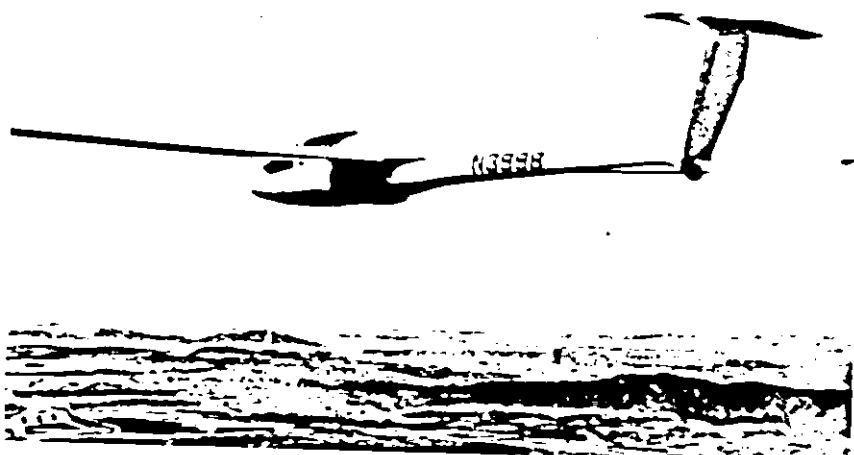


Fig. 7 A21J aloft over San Francisco Bay Area with engine exhaust bulge visible

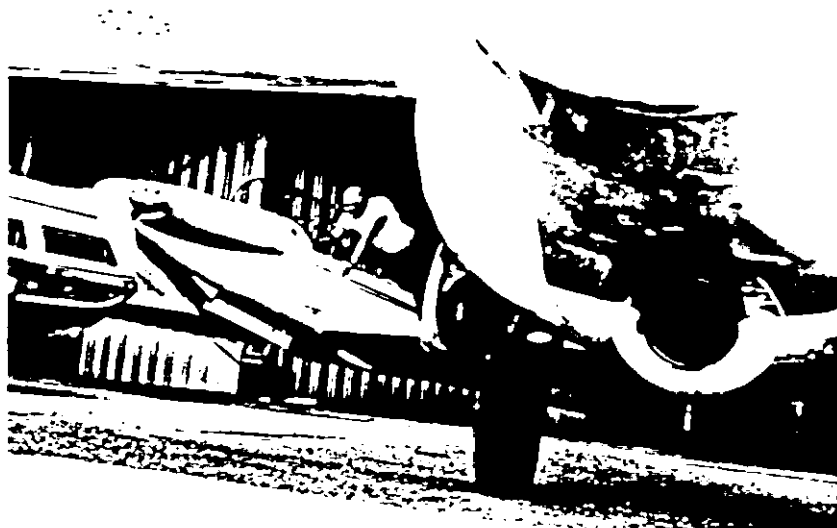


Fig. 8 A21J at Palo Alto with view of exhaust. RF5B motorglider in background

A21J ENGINE

The original central core engine location worked very well. Zanetti and I man-rated the small (0.3m diameter, 0.61m long, 30 kg wt.) engine with minimum operation in Italy and New York prior to demo at Dulles Transpo 72 which went without problem. I then flew over 100 hrs. in California (Fig. 7) on three different engines, building engine time and experience as Microturbo/Ames worked very closely with us. There were some problems. Fuel filter clogging was a major one only in that it took us a long time to determine that that was the reason for unexplained engine shutdown. It was no problem aloft except for tower operator excitement. They couldn't seem to understand that this aircraft sans engine at 1000' in the pattern really didn't have an emergency because flight time remaining at the very low sink rate was about 7.5 minutes. Or, if at 2000' altitude as far away as 25 kms. from the runway, a simple glide back to a landing was no problem. To protect our fuel we used triple filtering with final pour through a chamois. We changed ignitors, made many modifications to the electronic engine controller box, changed the fuel pump and finally determined that a 10 micron internal fuel filter had been used because the specified 50 micron one was unavailable (14). An intermediate size was obtained, installed and that problem ended.

As noted above, the electronics box was considerably modified as testing progressed. The single igniter was changed to two, which were relocated from the bottom of the chamber where the one became wet on engine shutdown due to fuel drainage, to positions about 30° up from the bottom. As certification proceeded on the engine, Microturbo made extensive changes which are not readily apparent. Take-off thrust of 100 kg is now more than 30% higher than our initial prototype engines. The prototype engine inlets were typical NACA flush shape, opening to a plenum section which contained the engine. Tests were made at all yaw and angle of attack combinations under full and idle power from sea level to 16000' with no evidence of engine surging/malfunction. Compressor stall was never induceable.

The central core engine location was ideal for CG positioning, but it did present problems (Fig. 8). Engine removal during the test program occurred quite frequently for various reasons, not the least of which was because it was easier than trying to work on components while installed. This meant developing a ramp to raise the fuselage so we could get under it with sufficient room to remove the engine. Additionally, FOD was visible on the compressor, even though the plenum chamber was helpful in foreign object removal prior to engine ingestion. But the chamber collected a lot because of the inlets' ground proximity. And airport managers viewed our exhaust plume's heat treatment of their asphaltic surfaces with dismay. We learned early to do all ground testing with the tail boom elevated to preclude any such ground erosion. Normally, to begin taxi, up to 80% breakaway thrust was required, and this left its mark. By making as few stops as possible which required such power, ground damage was kept minimal, but it was something to be aware of. Operation from grass and dirt

fields caused considerable visibility obscuration behind us. Fuel capacity in the center wing tank was limited and the engineering for it wasn't completed, so we used a temporary tank of similar capacity in the fairing over the wing behind the pilot's head plus a seat tank of 110 l capacity when necessary.

A21SJ ENGINE

All these negatives were overcome with the present engine installation. The tailboom was cut out and strengthened while the aft canopy contour was slightly reshaped so that the engine is still completely contained (Figs. 9-11). Before the change was made, though, a bifurcated exhaust duct had to be developed. I was concerned that the normal exhaust impinging on the tail would be unacceptable. Ground test with a fuselage and engine at Ames in New York confirmed this factor. Several differently shaped Y exhausts were manufactured to test various configurations. The present shape (Fig. 12) has been problem free. No fluidic gateing has occurred with testing, from idle to max thrust at all angles of yaw and attack. The closeable NACA inlet atop the aft canopy fairing is similarly problem free in flight test. Successful inflight engine start with the inlet closed has been accomplished, albeit unplanned! Previously, at the Toulouse, France factory, Microturbo had performed ground engine start and running with the air inlet closed to confirm calculations of available air. Engine inlet pressure reduction has been more than adequate to provide enough airflow into the engine plenum chamber, even, as noted, with the engine inlet closed.

There was some concern because the initial cockpit ventilation had been a small closeable NACA shape inlet atop the canopy with reverse flow to the forward canopy. The extensive flight testing in California had determined that it was so unsatisfactory that we had to use the small side canopy sliding window scoops which were noisy and drag inducing. New similarly shaped closeable ventilation inlets, still with reverse flow but much larger ducts, and larger diameter bends, have been installed below the wing and are very satisfactory. With the engine mounted, wing-fuselage fillet drag reduction is improved because of the longer fairing required for the split exhaust. Stall speed of the A21SJ is 2 kts lower, at a higher weight than the A21S. Stall performance is more symmetrical with the engine running, although it's good with the engine shut down.

OTHER CHANGES

The A21S is the second series of the original A21 model, incorporating other changes besides the ventilating inlets and engine location. The spar was strengthened to 5.3 G @ 625 kgs. (The third series, now underway is further strengthened to 5.3 G @ 808 kgs. - the original spar was 5.3 G @ 520 kgs.) The all-flying tail was altered to a fixed stabilizer with narrow chord elevator to provide more pilot feel. The sailplane accelerates extremely quickly and I had noticed a tendency for pilots to overcontrol the flying tailplane. A new trim



Fig. 9 A21SJ Engine compartment open (upper) and closed (lower).



Fig. 10 View looking forward from tail of A21SJ depicts wing fillets and engine exhausts

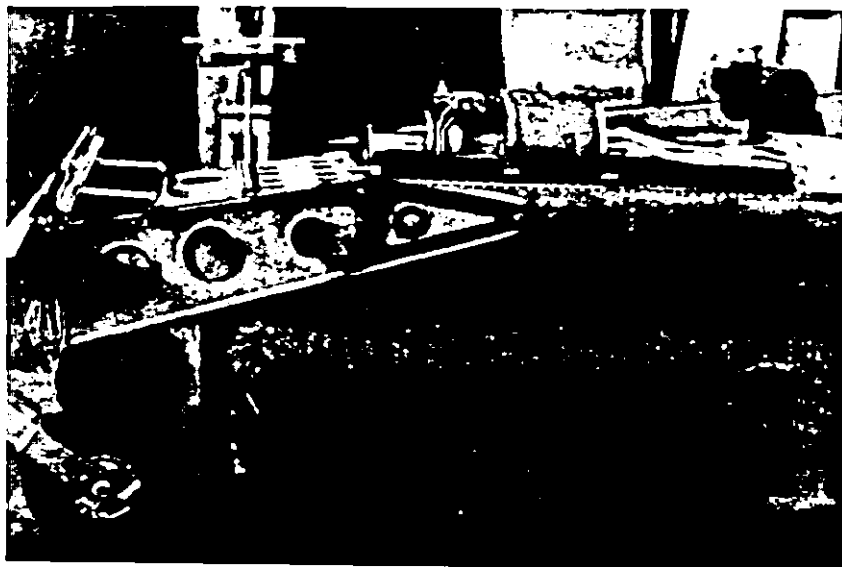


Fig. 11 A21SJ tail cone cut-out
with TRS-18 engine mounted.

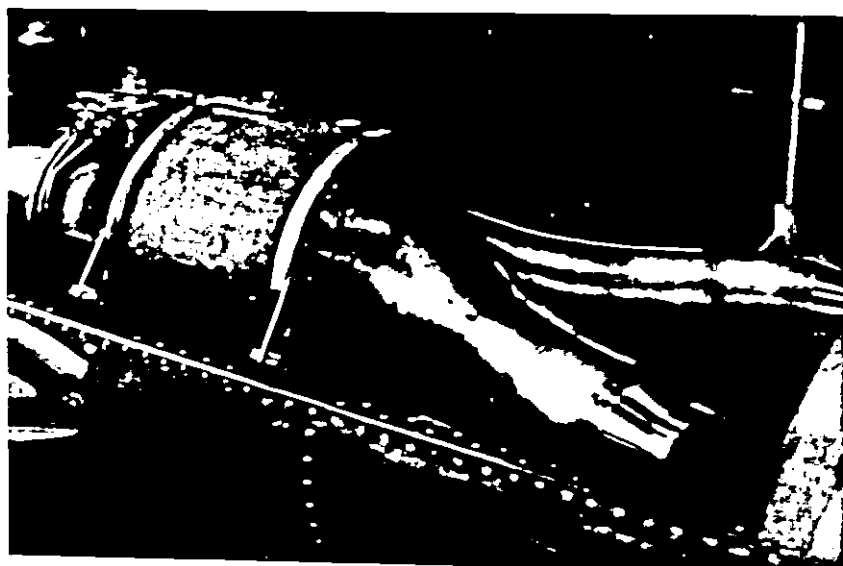


Fig. 12 TRS-18 engine with Y exhaust.

wheel was developed; flight testing had determined that the original ratchet lever could load up, and pop out at higher speeds. The new engine location frees the old space for an additional 60 l fuel capacity in the jet version. Because the engine is aft of the CG, single pilot flight with the engine installed is prohibited without batteries aboard in their fuselage location forward of the rudder pedals which have been modified to fold down for battery access.

The new engine compartment is stainless steel and titanium lined. Flight and ground testing was performed with temperature sensitive paint strips on engine inlet, compartment, case, tail boom and the tailplane. On the original engine location, the hottest spot was just forward of the tailwheel where the exhaust bounced up off the pavement. Now, the engine case over the turbine reaching 120°C after shutdown is the warmest location.

FLUTTER

After the first series was underway, Caproni developed a method for extruded metal flight control components during a development program for an extruded wing (15). These extrusions became quite important and are now used for all flight control surfaces except the rudder - including the 2.8m span aileron.

Throughout all the certification flight testing, including V_D hard-over stick demonstrations, 6-turn spins, my 150 + hours of flight in A21s and the A21J, a coast to coast race by a world champion soaring pilot, and many world record flights in Nevada at altitudes up to 22000', no wing or aileron flutter occurred, nor was there ever any evidence of it. We were certainly cognizant of the potential with such a design. The first report came from an A21 which had field-repaired aileron damage from a minor accident and repainted without close attention to factory specifications for weight of applied paint. This was followed by two other incidents on low maintenance, high time ships. It was determined that after about 300 hours, the decrease in flight control friction could allow flutter to occur.

It was not happening in most cases; however, a decision was made to perform an extensive flight, ground, analytical and wind tunnel analysis. Wing and tail vibration inputs were performed on a complete airframe elastically suspended at the main wing-fuselage fittings. The region explored was from 2 Hz - 27 Hz, utilizing an eccentric motor driven cam attached to the axle or the wing tip wheel and a vibrator on the end of the horizontal stabilizer. As a result, a bob weight is now used in the new extruded aileron, sized to provide considerable spanwise distribution and aileron balance is determined by measuring uninstalled trailing edge weight with tightly specified paint control. Flight results have been outstanding with tests up to 190 kts attempting to induce flutter with negative success. Flight above 33000' has been accomplished and single ship time in excess of 1000 hours has been accumulated with no flutter tendency.

REGULATORY ACTIONS

As noted previously, the airframe is certified by RAI, FAA, LBA and SGAC. The engine is certified by FAA and SGAC. A complete repeat of the airframe flight testing, totaling 20 hours, was required by SGAC in France who did not recognize the BCAR (British) standards used by RAI which were recognized in reciprocity by FAA and LBA. French government pilots performed a major portion of their flight test.

Certification of the engine installation is not completed; for the US it's a moot point because there is no FAA motorglider category, so experimental is the only certificate available. One US motor-glider did receive a type certificate in California in 1949. The Dragonfly (11), forerunner to the Hummingbird, was carried through under provision of the FAA's Glider Criteria Handbook. No one has been willing to take the financial risk since then because the Handbook does not have full regulatory standing, although it does continue to be used for pure gliders. It is quite out-moded, being over 40 years old. For long years many of us have been working with FAA on a rewrite to accomodate specific glider/motorglider rule-making without success in getting anything adopted although the present Joint Airworthiness Requirements (JARs) from Europe for these categories looks promising for U.S. acceptance.

CONCLUSION

The A21SJ program expended considerable talent of the highest caliber on design and development analysis to produce a world record class sailplane with the added attraction of having a jet engine. Flight testing, however, was absolutely essential to uncover and resolve the minor and major problems such as engine location, Y exhaust, flutter, ventilation, flap/airbrake position and drag reduction through fillet design alterations. One of the most enjoyable features of aiding in the flight testing was hearing tower operators caution aircraft following me on takeoff or landing to 'beware of my wake turbulence.' There's something about a jet!

ADDITIONAL FIGURES

Figures 13 - 15, following, denote specifications, dimensions and some flight test data. Figures 16 & 17 depict the cockpit and factory final acceptance line.

ACKNOWLEDGEMENTS

Dr. Livio Sonzio and Ing. Carlo Ferrarin are the designers of the Caproni A21 series of sailplanes and jet sailplanes described herein. Amleto Zanetti is the factory test pilot. Their assistance, along with Ing. Morganti, in preparing this paper, is gratefully acknowledged. They are rightfully proud of the marvelous achievement in bringing the A21SJ into being.

Fig. 13 Specifications and Dimensions (m)

	A21S	A21SJ
Empty Wt. Kg.	436	528
Useful Load Kg.	208	280
Max T.O. Wt. Kg.	644	808
Max Wing Loading Kg/m ²	39.8	49.9
Best Glide Ratio	43 @ 57 kts.	43 @ 65 kts.
Min Sink Speed m/sec	0.60 @ 43 kts.	0.68 @ 51 kts.
Stall Speed, flaps up kts.	38	38
Stall speed, flaps down kts.	34	34
Max Aero tow speed kts.	75	
Max Speed kts.	136	136
Wing span	20.38	
Chord at Root	0.90	at tip 0.32
Length	7.74	Height 1.79 (A21S) 1.84 (A21SJ)
Tailplane span	3.15	Chord 0.55
Aspect Ratio	25.65	Areas (m ²)
Ailerons	1.04	Flaps 2.07
Fin	0.71	Rudder 0.63
Tailplane	1.36	Elevator 0.34
		Wing (gross) 16.19
		Spoilers 0.91

Fig. 14 Climb Rate Measurements A21SJ Registration No. I JETT

Qnh 1011mb (800' elevation) 16 September 1977
 T 18°C - 20°C
 Delta Z 151.5m (1200' - 1700' ms1)
 Wt. Full fuel + Ferrarin & Zanetti 808 kgs.

CAS (km/h)	(kts)	Climb rate (m/sec - timed)		
208	112		2.39	
192	104		2.54	
176	95		2.89	
160	86	(1) 2.29	3.32	3.81 (2)
144	78		3.05	
128	69		2.89	

For comparison, rates are given for A21J at Palo Alto, N3998, at weight of 645 kgs in 1974 with lower thrust engine (1) and for A21SJ, verification uncompleted with new higher thrust (2).

Fig. 15 Takeoff Ground Run and 15m Obstacle Clearance Air Distance Measurements

Qnh 1013mb (1050' elevation, paved surface)
T 23°C 20 July 1977
Wt 808 kgs (1 - 4), 676.5 kgs (5 - 7)
RPM 96% (91.7 corrected for temp. and alt.)
CG 352mm (range: 212 - 408)

	Ground		Air		Total
	distance	time	distance	distance	time
1.	420 (m)	30 (sec)	210 (m)	630 (m)	- (sec)
2.	435	-	115	550	35
3.	420	31	160	580	41
4.	450	34	140	590	41
5.	300	24	150	450	32
6.	300	25	130	430	30
7.	300	24	130	430	30

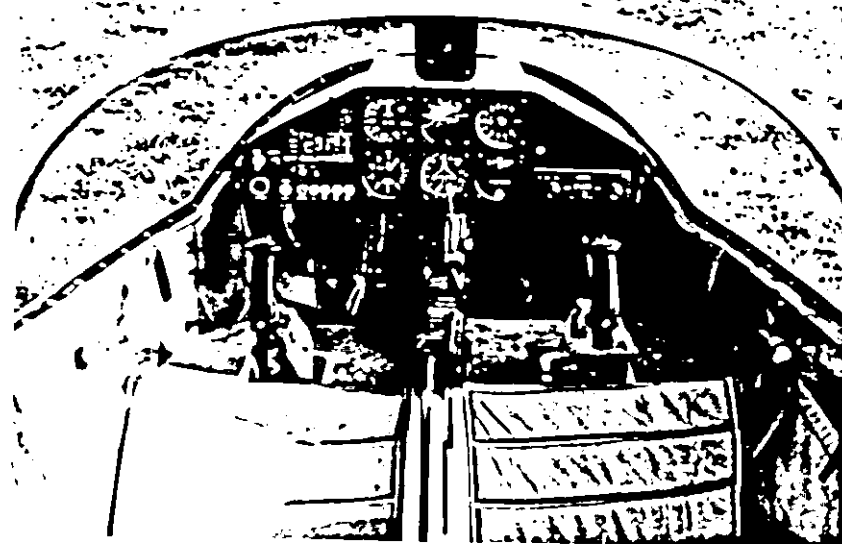


Fig. 16 A21SJ Cockpit

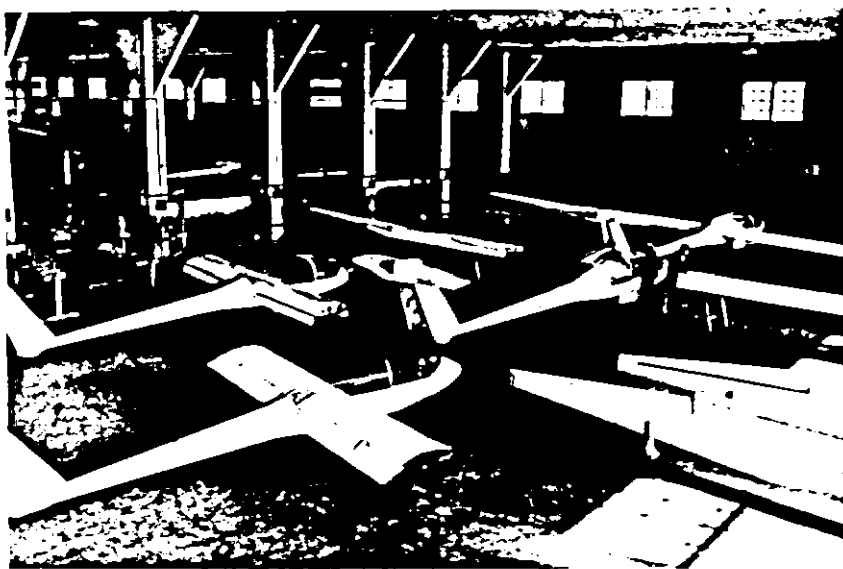


Fig. 17 Caproni Factory Final Assembly Line, A21s

REFERENCES

- (1) Wright, Wilbur, "Experiments and Observations in Soaring Flight," Oral presentation of a paper before the Western Society of Engineers, June 24, 1903.
- (2) Riedel, Peter, "Power Sailplanes," Soaring, Vol. 2, No. 2, Feb. 1938, p 2.
- (3) Klein, E., "Designing, Italian Style," Interview with L. Sonzio, Motorgliding, Vol. 3, No. 2, Feb. 1973, p 7.
- (4) Zrzywoblocki, Zbigniew, "Applying Jet Propulsion to Gliders," Oral presentation of a paper at the Motorless Flight Conference, Polytechnic Institute of Brooklyn, Aug. 1944.
- (5) Dawydoff, Alex, "Jet Propelled Sailplane," Soaring, Vol. 14, No. 3-4, Mar.-Apr. 1950, p 5.
- (6) Dreher, Max, "Auxiliary Turbo-Jet Engines For Sailplanes," Soaring, Vol. 27, No. 11, Nov. 1963, p 8.
- (7) Enyart, William, "N.A.A. Contest Board News," Soaring, Vol. 2, No. 1, Jan. 1938, p 3.
- (8) Smith, Bernald S., "CIVV Report," Soaring, Vol. 35, No. 4, Apr. 1971, p 33.
- (9) Uveges, George, Photograph, Motorgliding, Vol. 7, No. 1, Feb.-Mar. 1977, Front Cover.

- (10) Gorwin, Norman, "Propulsion for Self-Launching Sailplanes," Oral Presentation of a Paper at OSTIV Congress, Marfa, Texas, 1970.
- (11) Nelson, Ted, "Development of the Nelson Hummingbird Powered Sailplane," Soaring, Vol. 14, No. 5-6, May-June, 1950, p 3.
- (12) Monroe, Don, Photograph, Motorgliding, Vol. 6, No. 5, Oct.-Nov. 1976, Front Cover.
- (13) McGuinness, E.F., "The Powered HI 20," Soaring, Vol. 13, No. 5-6, May-June, 1949, p 5.
- (14) Smith, Bernald S., "The Caproni Caper," Motorgliding, Vol. 4, No. 4, Apr. 1974, p 4.
- (15) Morelli, Piero, "Extruded Light Alloy Aircraft Structures," Oral presentation of a paper at the First International Symposium on The Technology and Science of Motorless Flight, MIT, Oct. 1972.

SMALL SCALE FREE FLIGHT RESEARCH AT LOCKHEED-GEORGIA

Michael W. M. Jenkins*
Lockheed-Georgia Company
Marietta, Georgia

ABSTRACT

For several years a jet-powered Caproni A21J sailplane has been used, in conjunction with several remotely controlled research vehicles, for research into advanced technologies. The relatively contaminant free environment offered by this free flight research has been used to explore such areas as laminar flow control, spanwise blowing, parameter identification methods, fiber optics, airframe noise spectral elements, and command augmentation techniques. The manned Caproni A21J is fully instrumented, is capable of recording up to 32 channels of data and is operated at Mississippi State University. The 0.3 scaled, RCRV version of the Caproni is operated at Lockheed-Georgia in conjunction with other RCRV's. This vehicle which telemeters up to 24 channels of data, is flown by one operator. An overview of Lockheeds' program will be presented and some of the results will be discussed. Future plans will be outlined.

I. INTRODUCTION AND BACKGROUND

The concept of Small Scale Free Flight (S.S.F.F.) research at Lockheed-Georgia was initiated by Dr. J. J. Cornish III** in early 1976. He proposed that this in-flight research be conducted as a joint venture with Mississippi State University (MSU) and that the objective of the program should be the acquisition and demonstration of new technologies appropriate to transport aircraft. This was to be accomplished by the use of focused, clearly defined flight experiments covering a range of technology subjects.

*Michael W. M. Jenkins, Research and Development Engineer - Staff, Technical Director of Small Scale Free Flight Research at Lockheed-Georgia.

**Now Vice President - Engineering at Lockheed-Georgia Co.

At Lockheed we see this SSFF research capability as the third member of a TRIAD (See figure 1). Its purpose is to supplement and not replace both Wind Tunnel testing and ground-based flight simulation and so would be used to evaluate those technology aspects that could only be partially evaluated by the other two techniques. The need for in-flight research has always been recognized at Lockheed-Georgia, however, the key to this successful program has been the ability to identify the basic research requirements of each experiment and to adapt them for evaluation on a small, low-operating-cost flight research vehicle.

Another factor in searching for low cost flight research was the astronomical costs associated with any advanced aircraft program. (Figure 2). It is clear that development costs are becoming prohibitively high and wind tunnel test hours and costs, especially for military aircraft, excessive. Any method which provides meaningful data at a lower cost must be used. We believe that this is precisely what S.S.F.F. research at Lockheed-Georgia will do - get meaningful data at very low cost.

In May 1976 a Caproni A21 airframe and an Ames/Micro-turbo jet engine was purchased and sent to MSU at Starkville, Mississippi where installation work based on Lockheed designs was started. In June 1976 a Microturbo "Jaguar" gas generator was purchased and also delivered to MSU. Simultaneous with these events, the design and construction of an exact 0.3 aerodynamically and inertially scaled, remotely-controlled research vehicle (RCRV) version of the Caproni A21, was started at Lockheed-Georgia. Both the full and part scale versions were flying by the end of 1976.

II. FACILITY DESCRIPTION

The full scale Lockheed Caproni A21J (L-C A21J) in its current research configuration is shown in figure 3. Its basic structure is aluminum with fiber glass skinning in selected areas. The maximum weight is about 1900 lbs. and the vehicle has a span of 67 feet, wing area of 174 square feet and an aspect ratio of 25.8. The wing uses a Wortmann FX67-170 section out to the break station, and a Wortmann FX60-126 at the wing tip. The Ames/Microturbo TRS-18 engine is installed behind the side-by-side, two-place cockpit and delivers 200 lb. of static thrust at sea level. There are two 30 gallon underwing tanks fitted which gives a test duration in

excess of 1 hour. A detachable pod houses the gas generator which is capable of delivering 1 lb. of air per second at a pressure ratio of 3:1. The vehicle is fully instrumented and carries a Lockheed electronics tape recorder capable of recording up to 32 channels of data, multiplexed, on a stereo cassette tape system. The left hand seat is normally used for the sensor and instrumentation package.

All flying (figure 4) and flight operations are performed at the RASPET Flight Research Laboratory in Starkville, Mississippi. The normal operational mode is to tow the L-C A21J to altitude using a Stearman, the engine, when required, is then started, and, when the particular test is ended, the vehicle performs engine-off landings. All flying is performed by Gifford Bull of the MSU Aeronautical staff, and our excellent air-to-air photography is also an MSU function. To date we have had over 130 successful flights which have accumulated nearly 120 hours of flight test data.

The 0.3 scale version of the Caproni (figure 5) weighs close to 60 lb. and has a wing span of 20 feet. It is made of polystyrene foam, wood and fiberglass and has a payload of about 10 lbs. This was built at Lockheed and is test flown near Marietta, Georgia. A Royal Classic radio control unit working on 72.16 megahertz is used and 8 channels of control capability are available. Normally 5 are used for RCRV control and the remainder for specific experimental use. Driven by 3 Scozzi Ducted fans (using H.P. 40 model engines) speeds of up to 75 mph have been reached. Each engine gives about 4.0 lb. of static thrust at 18,000 RPM, resulting in a thrust-to-weight ratio of about 0.2 at a weight of 55 lb.

The standard launch technique is from the top of a moving vehicle (figure 6). After accelerating to lift-off speed, usually about 50 mph, the controller stationed at the side of the runway assumes command and flies the RCRV away from the launch platform. A self-releasing single-point mechanism ensures safe, positive detachment.

Fully instrumented, this RCRV telemeters up to 24 channels of data to a ground receiving station (figure 7). Operating at 173 megahertz frequency the digital data is recorded on a cassette in the portable receiving unit, and any two channels can be monitored real-time on dial readouts. Voice annotation of the data can also be used.

To date we have had 106 successful launches and have accumulated over 700 minutes of data.

III. FLIGHT RESEARCH

A summary of the technologies evaluated in-flight is shown in figure 8. Although in many instances scale research was performed in which both vehicles were used, this paper will address, primarily the full scale Lockheed-Caproni A21J programs. Further, it is not possible to cover four years work on one short paper, therefore only highlights of each test will be covered.

Spanwise Blowing

Flight testing on spanwise blowing was accomplished on the full scale and 0.3 scale vehicles (figure 9). Compressed air was ducted from the gas generator on the full scale vehicle to nozzles on the wing. A compressed air bottle was used on the RCRV. Spanwise blowing is a flow reattachment mechanism which is generated by ejecting a core of pressured air over a separated wing, (figure 10). A vortex forms, entrainment occurs and additional lift is generated depending on, among other things, the area of the wing influenced, diameter of jet, jet mass flow and jet penetration. In terms of recovered lift, ΔC_L , to jet momentum value, C_μ , ratios of as high as 8:1 have been acquired. This energy magnification had been pioneered at Lockheed-Georgia in many studies and wind tunnel tests and the demonstration in flight was considered necessary to prove the feasibility of this advanced concept.

Two-inch diameter ducts transferred air from the gas generator to a manifold on the wing, (figure 11). Provisions were made to explore (on each wing) three chordwise nozzle locations, 43, 54 and 65% x/c. One-half inch or 3/4 inch convergent nozzles could be fitted and all were located at the 45% wing semi-span location. The purpose of this experiment was to evaluate in flight the effectiveness of a flight worthy, practical spanwise blowing system for use both as a flow reattachment device and as a potential new control device.

Eighteen flights were made in 1977 and 15 more in 1978, for a total of 37.2 flight hours. Test altitudes, varied from 4000' to 11,000' and the test speeds ranged from 54 mph to 90 mph. Wing pressure surveys were made and were used to correlate the observed lift increments obtained. Extensive air-to-air photographic coverage

was obtained (figure 12) especially in the early stages of the program when knowledge of flow separation characteristics was needed, and was obtained by tufting the wing.

One measure of the efficiency of spanwise blowing is the ratio $\Delta C_L/C_\mu$. Figure 13 shows data obtained from the flights just described in terms of ΔC_L versus C_μ . At high C_μ values, $\Delta C_L/C_\mu = 5$ and at low C_μ values, the ratio approaches 8. Other data gathered confirmed the effectiveness of spanwise blowing both as a flow reattachment mechanism and as a primary control device. However, it is not possible to present all the data here due to space limitations.

Laminar Flow Control

Laminar flow control (LFC) on transport aircraft is of significant importance due primarily to its impact on drag and the corresponding reduction in fuel use. The objectives of this experiment were to expand our existing LFC data base and to provide improved LFC design criteria; to develop flow diagnostic instrumentation and the technical expertise required for successful flight testing of LFC aircraft; and finally to gather comparative wind tunnel data on the same glove. The latter dictated the need for a detachable glove design so that it could be tested in various tunnels in the U.S.

Initially the design concept was to have two gloves (figure 14) but preliminary calculations showed that one could easily be trimmed if it was mounted sufficiently inboard on the wing. One underwing tank was removed to accommodate the glove. The program was initiated in 1978 and is still in active status.

Early testing (figure 15) established the two dimensionality of the flow over the glove using wool tufts. The separation on the aft-end of the glove results from a designed continuity at this chordwise location (a flap exists here). The glove is 6 feet span and just under 4 feet chord. It is fitted with 50 pressure ports and is made of aluminum and fiberglass. The section profile was established by computer techniques to match the pressure distribution existing on an advanced transport airfoil at $M = 0.8$ at 40,000 feet. (figure 16). Six upper and six lower surface spanwise ducts form an integral part of the structure and provisions are made, in the suction system, to vary the chordwise and spanwise distribution of suction. During 1978 and

1979 a total of 18 flights were made and over 13 hours of flight test data were gathered. Test speeds ranged up to 110 mph and napthelene was used to establish transition regions.

Overall, the flight test program consists of three parts, which are: to establish transition locations, pressure distributions and boundary layer profiles on the unslotted glove, repeat this with the slotted glove without suction and finally a repeat again with slotted glove with suction. We are at present close to the end of part one.

For this test specialized instrumentation and sensors were designed, tested and developed. These were a bounday layer rake (figure 17), Preston tube arrays and boundary layer microphones (figure 18). The boundary layer rake consisting of 11, 0.02" O/D tubes was used to establish mean velocity profiles in the boundary layer (figure 19); the Preston tubes established transition location and characteristics, and the microphones established the spectral content of the total head in the boundary layer at fixed chordwise locations.

Transition characteristics established so far (figure 20) show that at about $\alpha = 4.5^\circ$ (about 78 mph) approximately 85% of the airfoil is in turbulent flow (natural transition occurs at 15% back from the leading edge). This flight condition will be used for slotted testing later in 1980.

Of interest is the turbulent wedge generated by a bug strike (figure 21) near the leading edge during napthelene testing. This classical pattern clearly indicates a fundamental problem associated with laminar flow on aircraft - i.e. loss of laminarity. As stated earlier, further testing is planned for 1980.

Airframe Acoustics

Airframe noise has been termed the "Ultimate Noise Barrier" of aircraft. Understanding the contributors to this noise will permit the design of quieter airframes and hence lower this noise barrier. Contributions include wings, flaps, landing gear, wheel wells, fuselage and so on, with the whole noise content being a very complex problem. No simple theoretical prediction model exists and so the present art depends upon test results. But large transport aircraft cannot, for safety reasons, be flown close to the ground, power-

off. Therefore, it was decided to use the L-C A21J Caproni and the 0.3 scale RCRV to generate data for use in a long-term airframe noise, evaluation study, (Figure 22).

During 1977 and 1979, a series of 24 flights were made and nearly 23 hours of power-off data gathered relating to the various contributors to the airframe noise. Phase I (1977) gathered data on wheels, wells and landing door noise spectra, and Phase II (1979) gathered data on the influence of flaps and flap gaps on the noise spectra.

The Caproni L-C A21J was flown power-off at fixed speeds at varying heights (40 to 300 feet) over a row of microphones situated on the extended center line of the runway (Figure 23). All flight test procedures were chosen to minimize the uncertainties associated with the randomness and transient nature of the far field noise measured with fixed microphones on the ground. To increase the statistical accuracy of the noise without increasing the error due to change of the aircraft (source) from the microphone, six B & K, $\frac{1}{2}$ " microphones were used on the ground at a spacing of 15 feet. Sanborn amplifiers and a Lockheed Electronic seven-channel recorder were used to record the data. The altitude and speed of the aircraft were monitored by photographic means.

The overall sound pressure level (OASPL - db) for the L-C A21J varies as the 5.8 power of velocity (Figure 24) and so does the OASPL of the 0.3 scale RCRV. Normalizing the data (100 ft. altitude, 100 mph) and comparing the results shows a scaling law proportional to the scale to the power of 3.8. This result is not yet fully understood and will require further evaluation.

General Radio real-time analyzers were used to obtain one-third octave band spectra of the peak value of the noise signatures. Typical noise spectra for the Phase I test series are shown in figure 25 where it is apparent that the wheels produce more noise than the wheel wells or doors. A common peak sound level occurs at 2000 hertz and this is attributed to wing vortex shedding and is a function of the airplane and not the landing gear configuration.

Phase II consisted of 16 flights in 1979 which accumulated 17.8 hours of flight test data on the effects of an extra flap and its gap on the noise spectra of the L-C A21J airframe. The same technique was used to

record these data as used in Phase I. The "extra-flap" is 13 feet 5 inches long and extends from each wing root outboard (figure 26); it has a chord of 7.25 inches, with a deflection capability of up to 20° - ground adjustable. Fourteen sub-miniature Knowles microphones were imbedded in the wing and flap at the 24.6% semi-span location. These were used to record fluctuating pressures intensity distribution for use in understanding the noise spectral content. The data were recorded on magnetic tape in the cockpit.

Similar tests were performed using the 0.3 scale RCRV in free flight (see figure 27) and a 0.2 scale wing section in our acoustic free jet facility at Marietta. In the latter case a 19 inch wing span model with a 7.8 inch chord was installed in the facility in a potential wind core of 27 inches and 6 microphones were used at a radius of 8 feet from the flap trailing edge to measure the far field noise. (Microphones were also imbedded in this model).

Analysis of this data is progressing now and there is evidence to show that the trailing-edge noise may not be the dominant source. Fluctuating pressures over the entire wing-flap surface could be the dominant source and these could be caused by the turbulent boundary layer. We hope to report on this at a later date.

Command Augmentation

In late 1977 and early 1978, 8 flights were made using a "command augmentation system" (figure 28). The objective of these tests was to demonstrate, in flight, the effectiveness of a unique lead-lag system aimed at enhancing the flying qualities of a transport aircraft. On future aircraft employing maximum use of CCV concepts the task of meeting handling qualities requirements is going to be very demanding on the control system. Therefore it is doubtful that the optimum flight control system will include mechanical inputs, rather it is most likely to be a Fly-By-Wire System. However, in the event of a complete loss of control due to, say, some electro-magnetic interference (i.e. a lightning strike), it is highly desirable that a back-up control system be available to prevent loss of the aircraft. Preliminary investigations at Lockheed in the use of unconventional augmentation techniques requiring no electrical power showed considerable promise. The whole philosophy of employing a command

augmentation system is to provide a phase lead in series with the pilot's commands to reduce or eliminate the requirement for the pilot to supply lead equalization. This reduction or elimination of the lead equalization appears to the pilot as a reduction in workload and so generates an improvement in flying qualities.

A side-stick controller was fitted over the instrumentation package (figure 29) in the left-hand seat of the test vehicle. This side-stick controller had a trigger switch for system engagement, is detented to the neutral position and exhibits a small increase in force with deflection. Electrical signals from the controller are used to drive, through amplifiers, an autopilot servo which connects to the elevator cross shaft in the cockpit floor.

The Fly-By-Wire system installed on the aircraft for command augmentation incorporated the capability of in-flight adjustment of the time constants, T_1 and T_2 , and the side arm controller to stabilator gain, K, of the transfer function given below.

$$\frac{K(T_1 S + 1)}{(T_2 S + 1)}$$

Prior to the first flight, servo output response to a step input via the side-stick controller, as shown in figure 30, was measured with a value of 1.2 for T_1 , 0.24 for T_2 , and 0.2 for K. All flights were made at approximately 5000 ft. and at an airspeed of approximately 90 mph.

Since the command augmentation system was designed to provide the appropriate phase lead to pilot commands for the 55% c.g. position, it was not expected to improve the pitch axis handling qualities at the 32% c.g. position. This expectation was verified during the first flight. The second, third and fourth flights were made with the c.g. at the 55% m.a.c. position, which is only 1% forward of the neutral point. The settings for T_1 , T_2 and K used in the first flight were used as the initial settings for the second flight. These settings produced a pilot rating of 6.0 to 7.0 for small (± 0.1 to $0.2g$) and moderate (± 0.4 to $0.5g$) inputs using the side-stick controller.

On the third and fourth flights, the lead-lag time constant ratio was held constant while the values of the time constant were varied. This has the effect of keeping the maximum lead phase angle constant and

varying the frequency at which the maximum phase occurs.

The ratio of lead to lag time constant selected was 5 which results in a maximum lead phase angle of approximately 40 degrees. The overall results are shown in figure 31 as Cooper Rating versus frequency in terms of $\frac{1}{\sqrt{T_1 T_2}}$. These data indicate that the best ratings were obtained when the maximum phase lead occurred at a frequency of 2.9 radians per second. The Cooper rating without command augmentation was 7.0; therefore the best compensation, in this case, resulted in an incremental Cooper Rating of about 3.5.

Parameter Identification Studies

Parameter Identification is a technique to extract stability and control derivatives from flight measured time histories by using a computer matching routine. In essence, estimates of time histories are compared, within a computer routine, with flight-measured quantities and continuous adjustments of the derivatives are made until a "best match" is reached. At this point the computer lists the derived derivatives as the best overall estimate of these quantities. Logic within the program determines the sequence of derivative changes and the "best" fit condition. This is a high speed technique which uses only 15-30 seconds of data but which requires accurate knowledge of vehicle c.g., weight and inertias.

The purpose of our study was first to develop the most cost effective method of obtaining parameter identification data and second, to crystallize specific testing techniques in terms of control inputs, type of maneuver and instrumentation sensitivities. A total flight time of 4.4 hours (3 flights) was obtained in 1977 on the first part and over 11 hours of data was gathered in 1978 on the second part of this flight test program, (8 flights). Similar testing was performed in 1978 on the 0.3 scale RCRV.

The test conditions covered speed ranges from 65 to 110 mph., c.g. was varied from 25% m.a.c. to 50% m.a.c., and flaps up and down were explored. Gross weights approaching 1800 lb. were used and the test altitude was close to 5000 feet. During this experiment data for over 700 separate flight conditions were obtained in the form of 18 separate channels of time history information per flight condition, recorded digitally on tape on board the airplane.

The Modified Maximum Likelihood Estimator (MMLE) Parameter I.D. program developed by NASA was used for data extraction, and typical final matching results are shown in figure 32 (longitudinal) and 33 (lateral-directional). Figure 34 illustrates some of the control input shapes evaluated, and Figures 35 and 36 show some typical correlation curves which resulted from the study.

Among the test variables explored were the following: minimum effective length of flight data to be analyzed, instrument sensitivity requirements, level of aircraft excitation, data repeatability, and the influence of c.g. location. In this paper only an overview of these results is possible.

Some stability derivatives are shown in figure 37 as a function of length of analyzed flight data. There appears to be a minimum acceptable data trace time for $C_{L\alpha}$ of about 4 seconds, and for $C_{M_{1t}}$ of about 6 seconds; but C_M and $C_{M_{1a}}$ appear to require about 15 seconds or more of time history data before settling to an unchanging value. In selecting a minimum acceptable data trace time for analysis, it is obviously important to include sufficient time after the cessation of control excursion, to permit damping derivative influences to be felt.

Instrumentation resolution requirements obviously depend upon the vehicle being tested. The Caproni flying at 5000 ft., and 100 knots with a 25% mac c.g. position has a short period of about 1.7 seconds, $\zeta = 0.57$ and a short period frequency w_{nsp} of about 4.5 radians/second. A typical high performance fighter may have w_{nsp} values of 7-9 radians/sec. In the latter case, the resolution, response and sensitivity requirements of the sensors (or instrumentation) will be entirely different than that used for the Caproni. It is imperative, therefore, to select instrumentation to match the anticipated requirements of the particular vehicle under test. A common failure is to select the most accurate and sensitive sensors without regard to overall and actual needs. This will inevitably drive costs up which may not be justified. For example, Figure 38 shows aileron resolution influences on the level of $C_{2\delta_a}$ extracted; resolution better than about 0.15 of a degree of aileron clearly cannot be justified.

An overview of the results is shown in figure 39 where best vehicle excitation levels, speed and c.g. location recommendations and derivative scatter are summarized for each derivative. An aft c.g. is recommended for all derivatives and generally high

vehicle velocity is desirable. Excitation levels vary significantly and so does derived derivative accuracy. A control doublet appears the best excitation driver.

The valuable experience gained on Parameter I.D. flight test techniques during this study is too large to catalogue in this current paper. However, one point cannot be over-emphasized and that is that the results of Parameter I.D. work are very sensitive to the weight, c.g. and inertia values of the vehicle. These must be accurately known if reliable and consistent derivative data is required.

Fly-By-Light (Fiber Optics)

The use of fiber-optic light pipes for signal transmission appears to offer excellent prospects of avoiding the Electro Magnetic Interference (EMI) problems of Fly-By-Wire (FBW) as well as providing additional cost and weight savings. All three services are involved with the evaluation of fiber-optic signalling system and as of 1978, no closed-loop servo system using fiber-optic links to transmit both command and feedback signals had been demonstrated in flight. The purpose of this experiment was therefore to get first-hand, practical experience with fiber-optic technology and to flight demonstrate a fiber-optic closed loop control system.

The electric side-stick controller and electro-mechanical auto-pilot servo used for the Command Augmentation experiment was used also for this test, and a schematic of the resulting fiber-optic system is shown in figure 40. Side-stick controller inputs to the system are triplex analog signals which are median selected and converted to digital signals for transmission over the three independent optic links which are 33 meters (108 ft.) long. The digital signals are then converted back to analog signals which are again median selected. The median signal is then summed with the servo position feedback signal and then transmitted to the servo amplifier which drives the existing Collins autopilot servo connected in parallel with the existing Caproni pitch axis control system. The servo output position feedback uses a single fiber-optic cable.

Hewlett-Packard HFBR-0001 fiber-optic transmitters were used in conjunction with Amphenol 801-Series connectors and Hewlett-Packard HFBR-0002 receivers. Two fiber-optic cables were evaluated. One was a Hewlett-Packard HFBR-0003 single fiber cable with a fiber optic core of 100 micrometers, and the other was a Galite 3000-LC-S

with a core diameter of 204 micrometers.

Bench tests showed cable and connector losses to be within the manufacturers specification with a total loss (cable plus two connectors) of 6.0 db. The integrated control system was subjected to a variety of tests to establish its frequency response and to determine the minimum data rate at which the system would function smoothly with no graininess. To perform this test, the side-stick controller was replaced with a Hewlett-Packard 3310A function generator. A Honeywell 906 C visicorder was used to record system response. Degradation of system response did not begin to occur until the bit rate was reduced to 1.0 KHz.

The system was first flight tested on September 10, 1979 with excellent results. The vehicle was flown to 6500 feet pressure altitude and the system smoothly engaged at 70 mph. Pitch maneuvers were performed at 80 to 100 mph through psuedo-sinusoidal control inputs. Slow, small amplitude inputs were used initially with the inputs gradually increasing in both amplitude and frequency. Finally fairly abrupt pitch inputs were evaluated. No graininess of control or erratic performance were detectable. The flight duration of approximately 40 minutes fulfilled the primary goal of this experiment in that a closed-loop, fiber-optic pitch axis control system was successfully demonstrated for what is thought to be the first time in aviation history.

Subsequent flights, for a total time of over 3.5 hours, confirmed the acceptability of the control system and illustrated the effectiveness of the fiber-optics feedback control system.

IV. FLIGHT RESEARCH FACILITY GOALS

The key elements of our very sophisticated free flight research facility are shown in figure 41. We have in operation now most of these elements, the remainder are due to be operable in a very short time. The manned L-C A21J Caproni vehicle and the unmanned 0.3 scale RCRV vehicle have been the subject of this paper, (with the latter only briefly touched upon). The manned L-C A21J has logged over 130 flights for nearly 120 hours of data gathering time. The 0.3 scale has accumulated 106 flights for over 700 minutes of data gathering time.

Telemetry has been extensively used during the unmanned

testing with reception occurring on a portable receiver unit. The data reduction system has been fully exercised (with Parameter I.D.), and the mathematical models of both vehicles have been established. Control console and computer center design is in hand and all data links are available. RCRV simulation equipment has been used in other studies and the tracking system will be based on, among other things, that used for our transport aircraft flight testing. We have been conducting flight research using this facility since 1976 and we expect to continue with increasing vigor in the future.

V. CONCLUSIONS

A very brief description of Lockheed Small Scale free flight research facility has been given and a brief overview of the experimental work performed since 1976 has been shown. The facility is proving to be very successful at gathering data at very low cost in clearly defined focused experiments. So far, in-flight experiments have been performed in the areas of spanwise blowing, acoustics, laminar flow control, parameter identification, command augmentation and fiber optics. Many more are planned.

In the interests of brevity, only passing reference has been made to the unmanned aspects of this program. However, this work is just as cost effective and important as that being performed on the full scale vehicle, and this too is anticipated to increase in the coming year.

VI. ACKNOWLEDGEMENTS

Many engineers and scientists at Lockheed-Georgia and MSU have been involved in this program, with the author, since 1976. Its success is therefore due primarily to their efforts and dedication. By now the number involved is too large to permit the identification of each by name in this acknowledgement. However, the contents of this paper rests solely on the shoulders of the author, and any errors and/or omissions are mine alone and cannot be ascribed to the fine team mentioned above.

VII. REFERENCES

1. Bauer, F., Garabedian, P., Korn, D., and Jamieson, A., "Supercritical Wing Sections II," Lecture Notes in Economics and Mathematical Systems, Vol. 108, Springer-Verlag, New York, 1975.

2. Keeble, T. S., "Development in Australia of a Thick Suction Wing," Third Anglo-American Conference, 1951.
3. "A Fortran Program for Determining Aircraft Stability and Control Derivatives from Flight Data," Maine and lliff, NASA TN D-7831, April, 1975.
4. G. N. Abramovich, The Turbulent Theory of Jets, The MIT press, Cambridge, Mass. 1963.
5. M. W. M. Jenkins and R. T. Meyer, Validation by Simulation Techniques of MIL-F-8785B as an RPV Flying Qualities Criteria Guide. AF Contract F33615-75-C-3012, March 11, 1975, Lockheed-Georgia Co.
6. Carlson, L. A., "Transonic Airfoil Flowfield Analysis Using Cartesian Coordinates," NASA CR-2577, August, 1975.
7. Bauer, F., Garabedian, P., and Korn, D., "Supercritical Wing Sections," Lecture Notes in Economics and Mathematical Systems, Vol. 66, Springer-Verlag, New York, 1972.
8. Cornish, J. J. III; "Method and Apparatus for Modifying Airfoil Fluid Flow," Patent 3,480,234, 25 November 1969.
9. Cornish, J. J. III, "High-Lift Applications of Spanwise Blowing," ICAS Paper No. 70-09, Presented at the Seventh Congress of the International Council of the Aeronautical Sciences, Rome, Italy, September 14-18, 1970.
10. Amcombe, A., and Williams, J., "Some Comments on High Lift Testing in Wind Tunnels with Particular Reference to Jet-Blowing Models," Agard Rpt. 63, August 1956.
11. Gaines and Hoffman, "Summary of Transformation Equations and Equations of Motion Used in Free-Flight and Wind-Tunnel Data Reduction and Analysis," NASA SP-3070, 1972.
12. Healy, G. J., "Measurement and Analysis of Aircraft Far-Field Aerodynamic Noise," NASA CR-2377.
13. McRuer, D. T. and Krendel, E. S., "Dynamic Response of Human Operators," WADC Technical Report 56-524, October, 1957.

14. McDonnell, J. D., "Pilot Rating Techniques for the Estimation and Evaluation of Handling Qualities," AFFDL-TR-68-76, December, 1968.
15. McRuer, D. T., et al, "A Systems Analysis View of Longitudinal Flying Qualities," WADD Technical Report 60-43, January, 1960.
16. Neal, T. P. and Smith, R. E., "An In-Flight Investigation to Develop Control System Design Criteria for Fighter Aircraft," AFFDL-TR-70-74, Volume 1, December, 1970.
17. Etkin, B., Dynamics of Atmospheric Flight, Wiley, 1972.

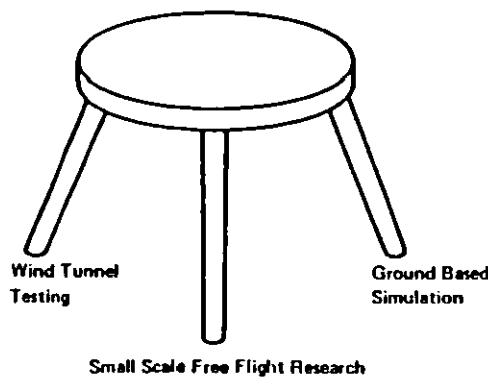


Figure 1. Technology Acquisition and Demonstration - A Triad

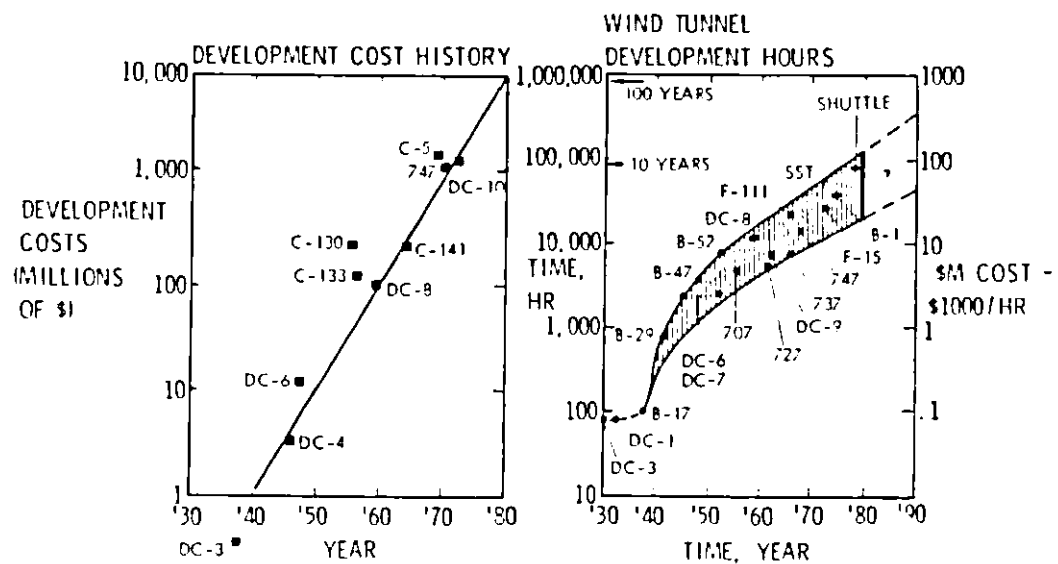


Figure 2. Need for Vehicle - Payoff

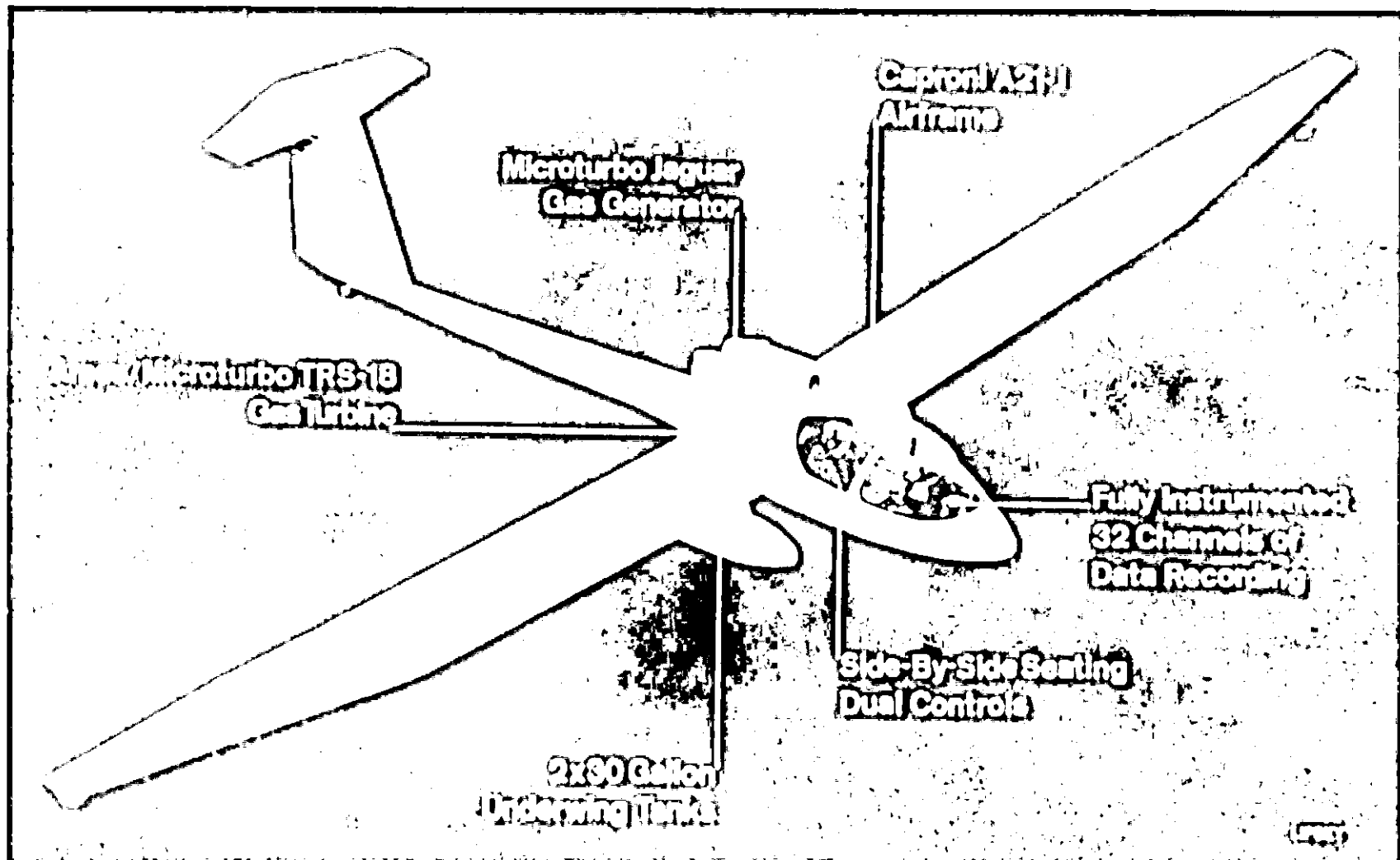


Figure 3. Lockheed-Caproni L-CA21 J Research Vehicle

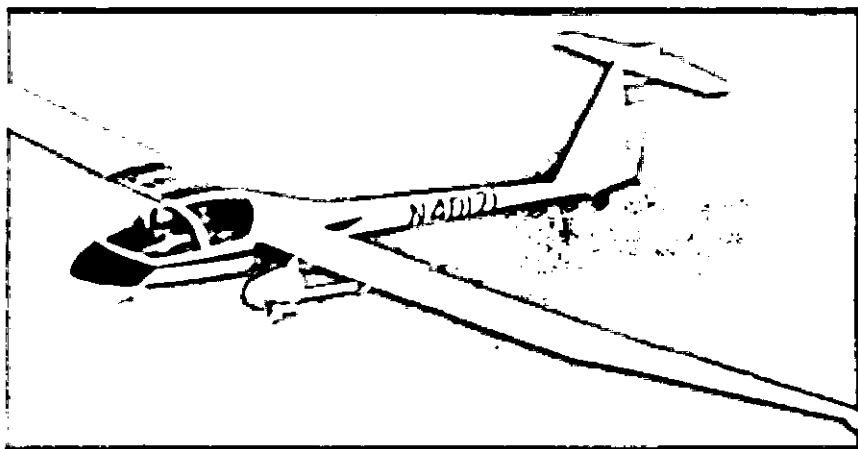


Figure 4. Research Vehicle in Flight



Figure 5. 0.3 Scale Caproni Research Vehicle

Figure 6. Early Launch Sequence of 0.3 Scale RCRV

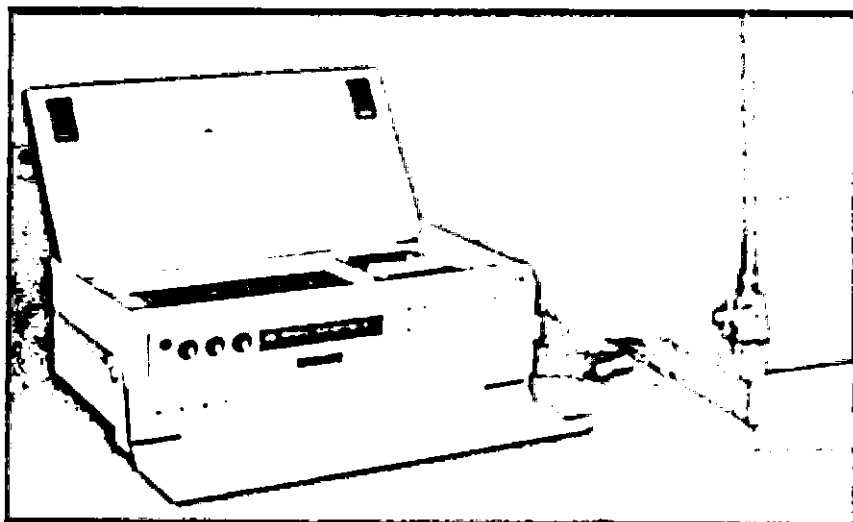


Figure 7. Portable Telemetry Receiving Station

- SPANWISE BLOWING
- LAMINAR FLOW CONTROL
- VORTEX DIFFUSERS
- AIRFRAME NOISE
- COMMAND AUGMENTATION
- PARAMETER IDENTIFICATION STUDIES

Figure 8. New Technologies for Free Flight Research

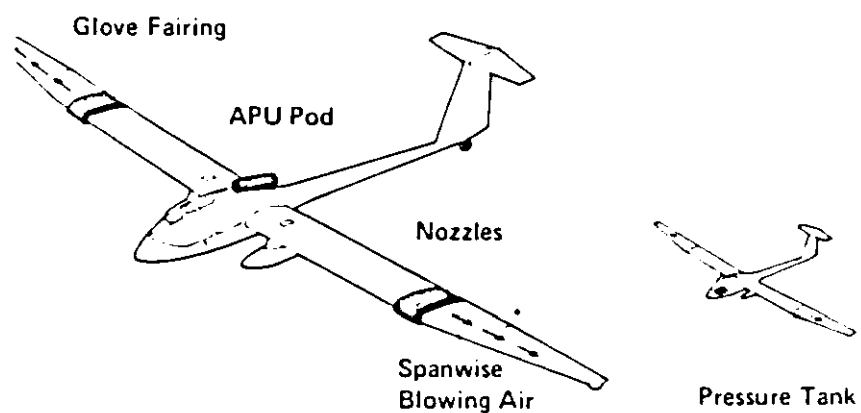


Figure 9. Spanwise Blowing - Flight Testing

STRAIGHT WING $\alpha = 20^\circ$

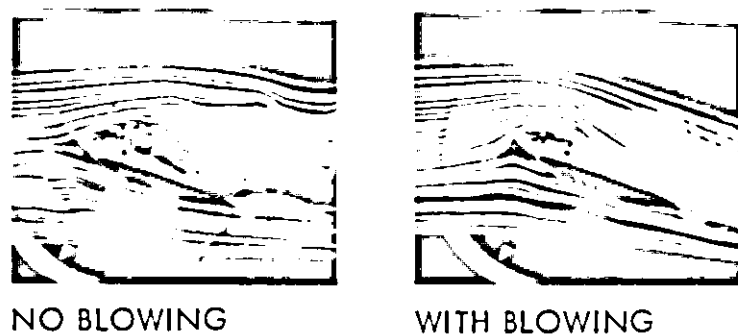


Figure 10. Spanwise Blowing - Smoke Tunnel Flow Visualization

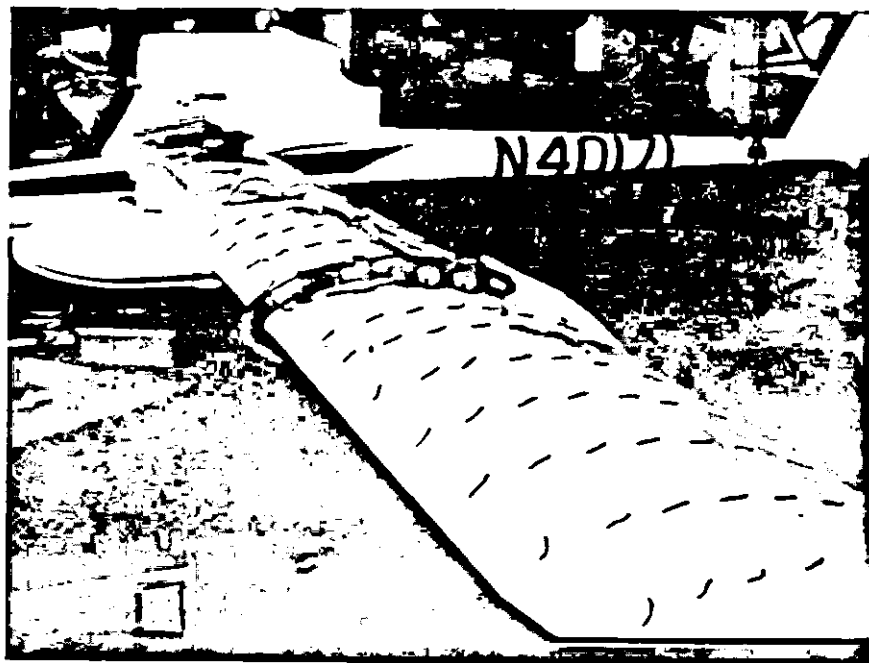


Figure 11. Spanwise Blowing Nozzle and Duct Arrangement

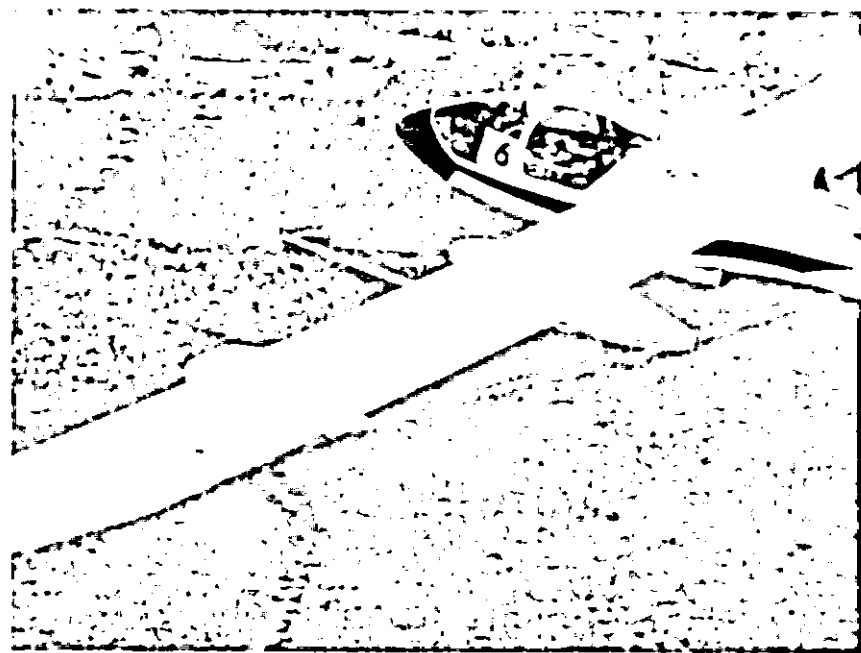


Figure 12. Spanwise Blowing in Flight

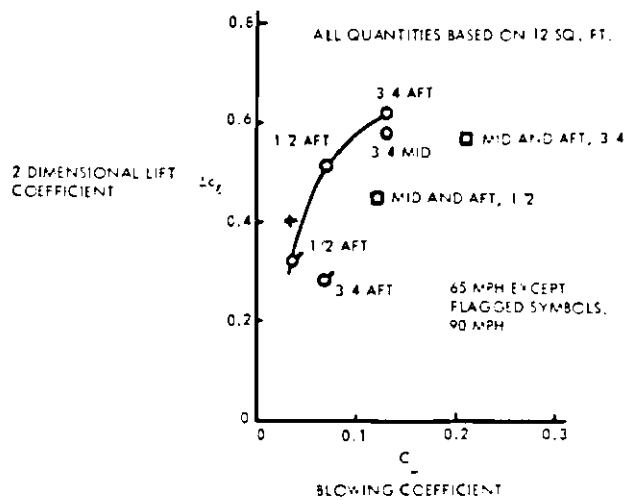


Figure 13. Effect of Blowing on Average Lift Increment

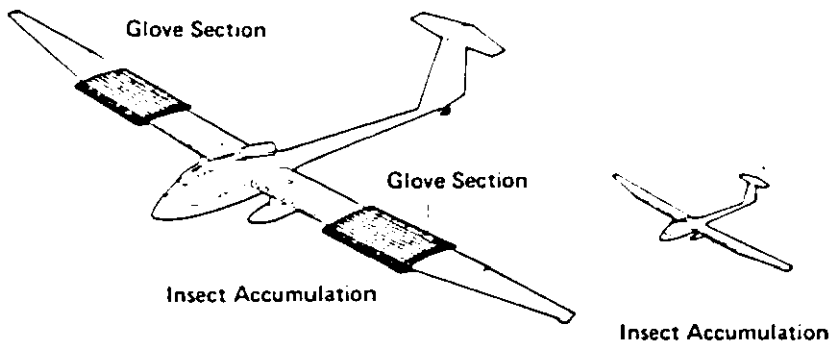


Figure 14. Laminar Flow Control Concept



Figure 15. Tufts Showing Two Dimensionality of LFC Glove

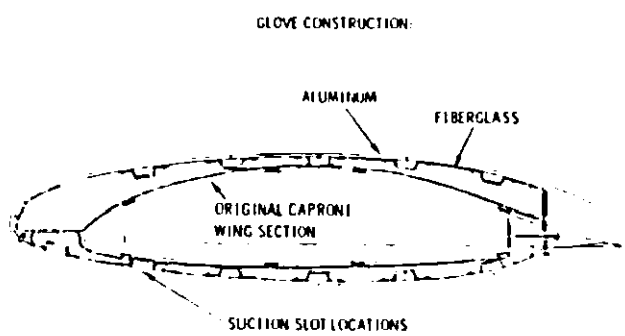


Figure 16. Cross Section of LFC Glove

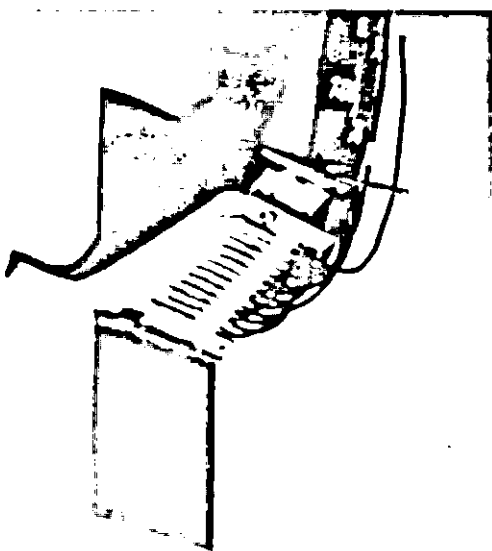


Figure 17. Boundary Layer Rake

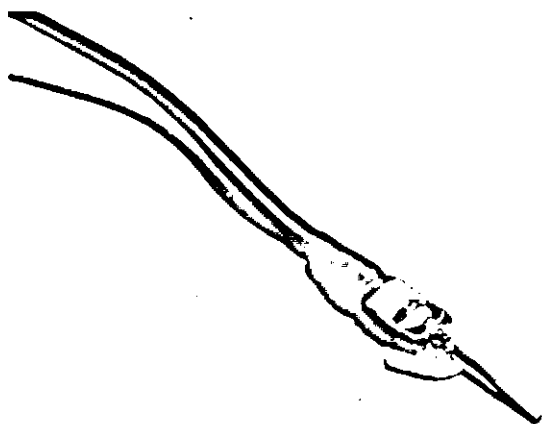


Figure 18. Boundary Layer Microphone

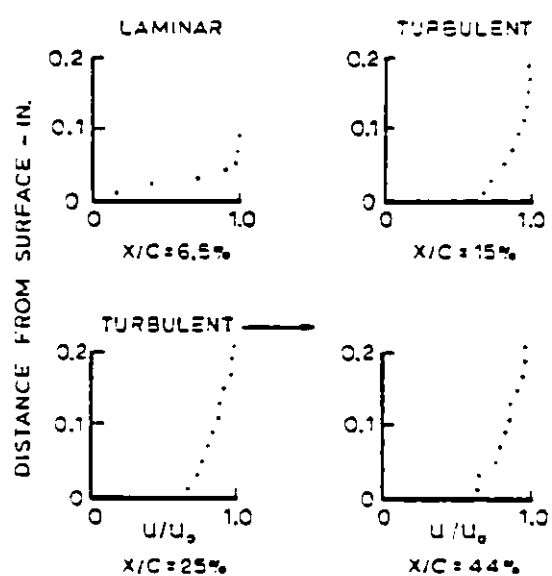


Figure 19. Typical Examples of the Mean Velocity Profiles Recorded by the Boundary Layer Rake
 $V = 60 \text{ mph}$

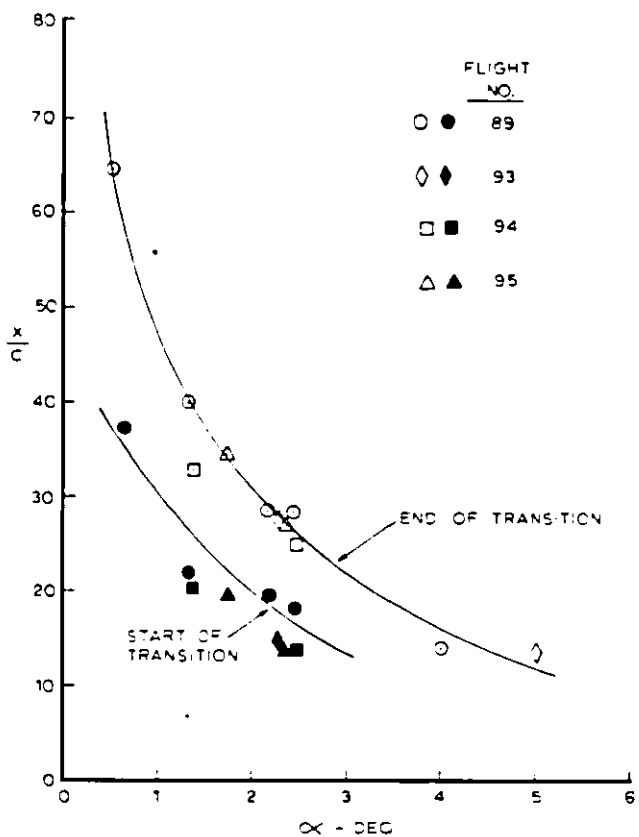


Figure 20. Beginning and end of Transition as Recorded by Preston Tubes

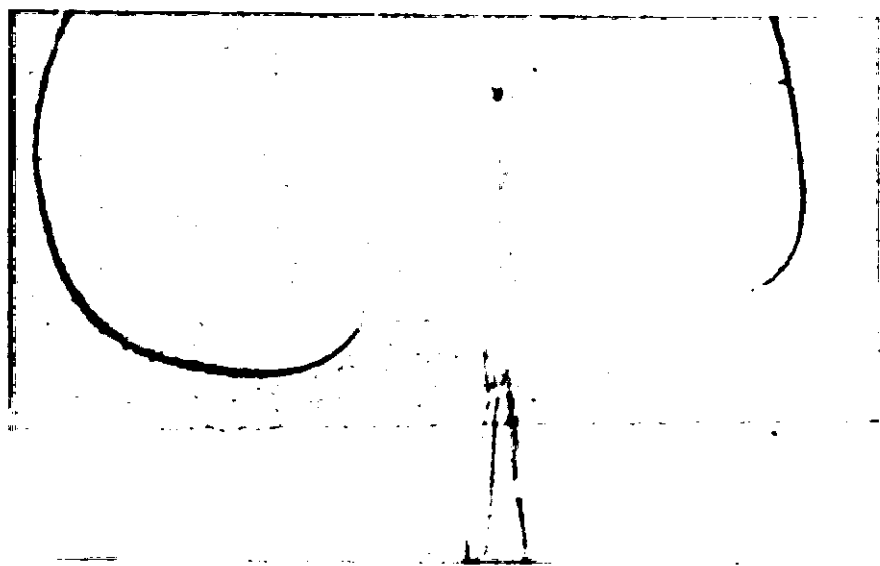


Figure 21. Turbulent Wedge Formed by Bug Strike in Flight

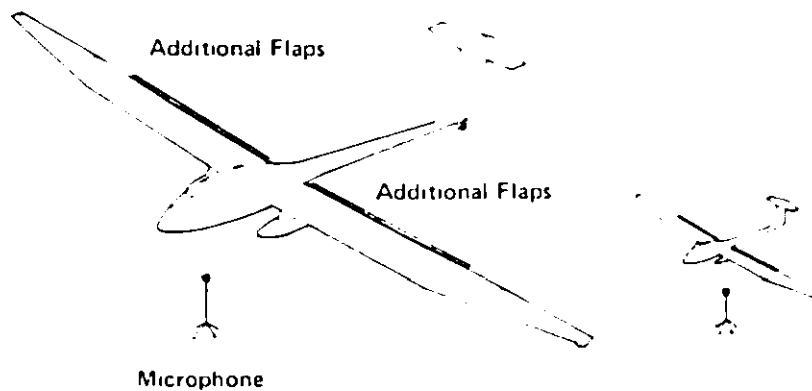


Figure 22. Airframe Noise Study

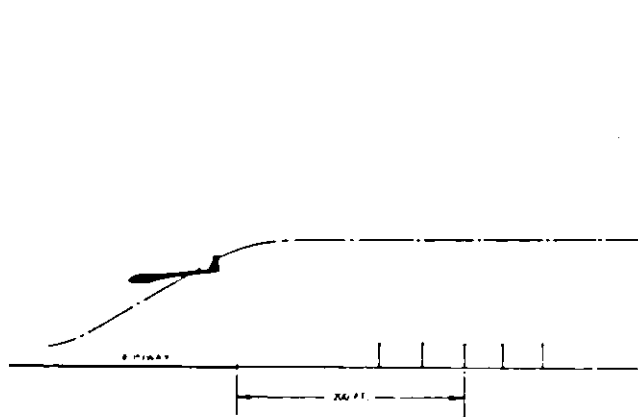


Figure 23. Acoustic Test Procedure

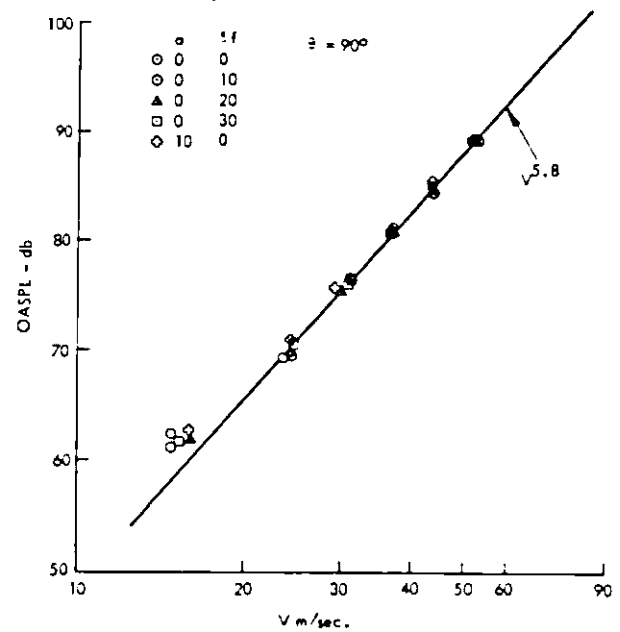


Figure 24. Variation of OASPL ~ db with Velocity

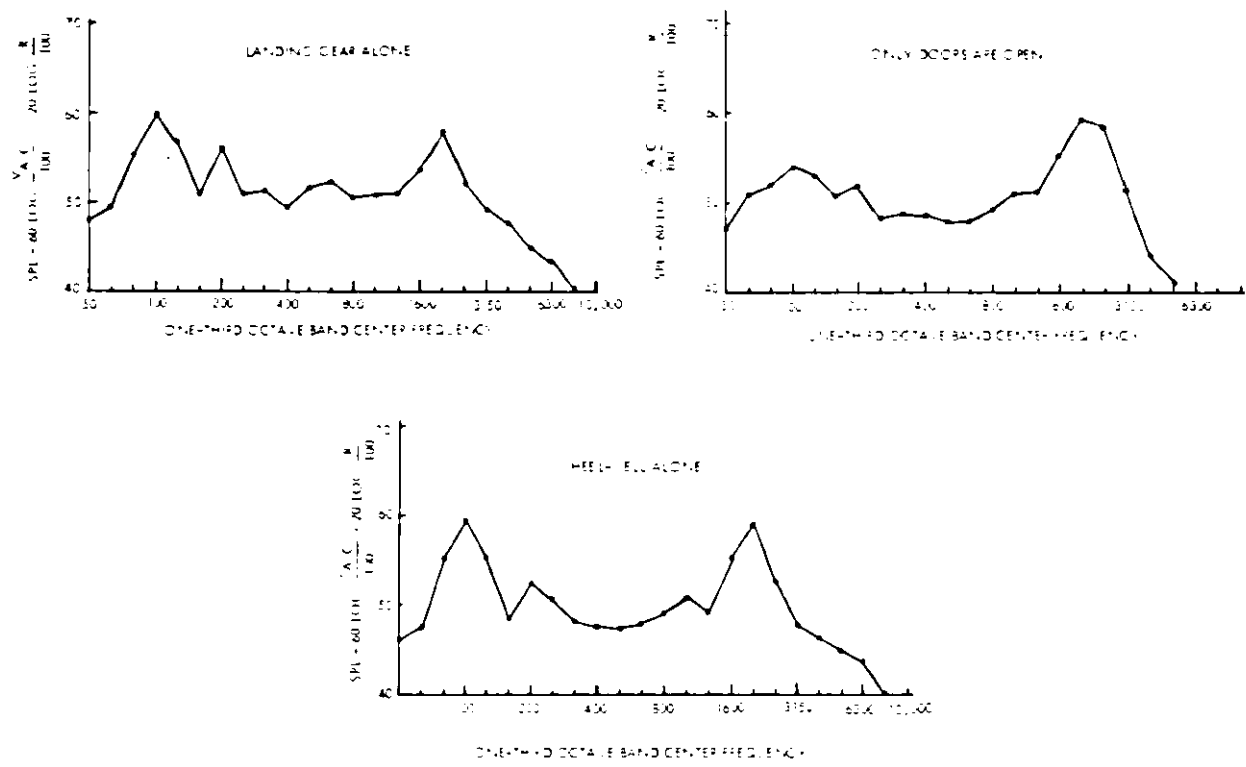


Figure 25. Noise Spectra Comparisons - Landing Gear, Wheel Well and Doors

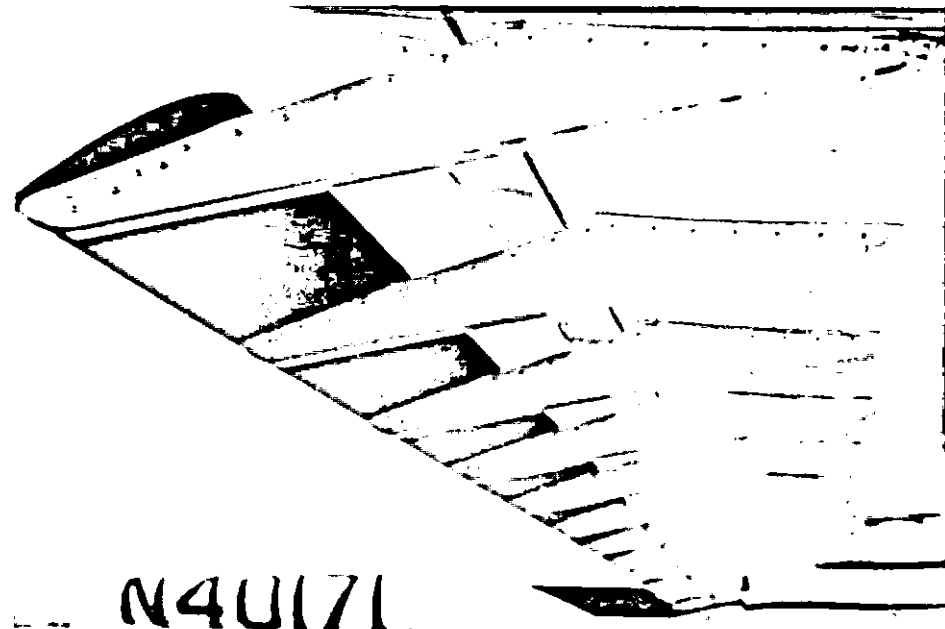


Figure 26. "Extra Flap" Configuration for Acoustic Testing



Figure 27. Acoustic Tests on 0.3 Scale RCRV - Typical Fly-by

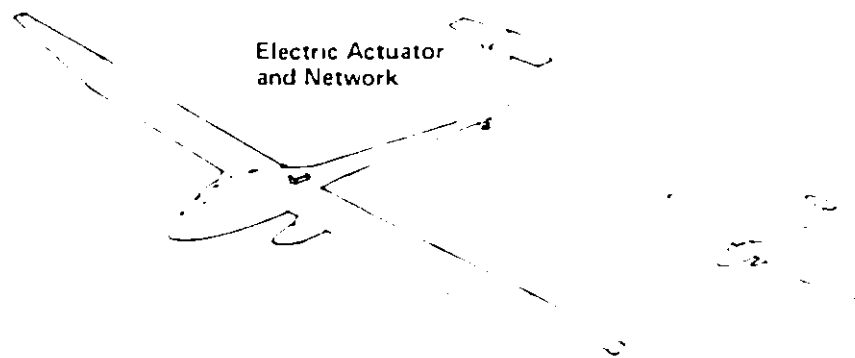


Figure 28. Command Augmentation Study

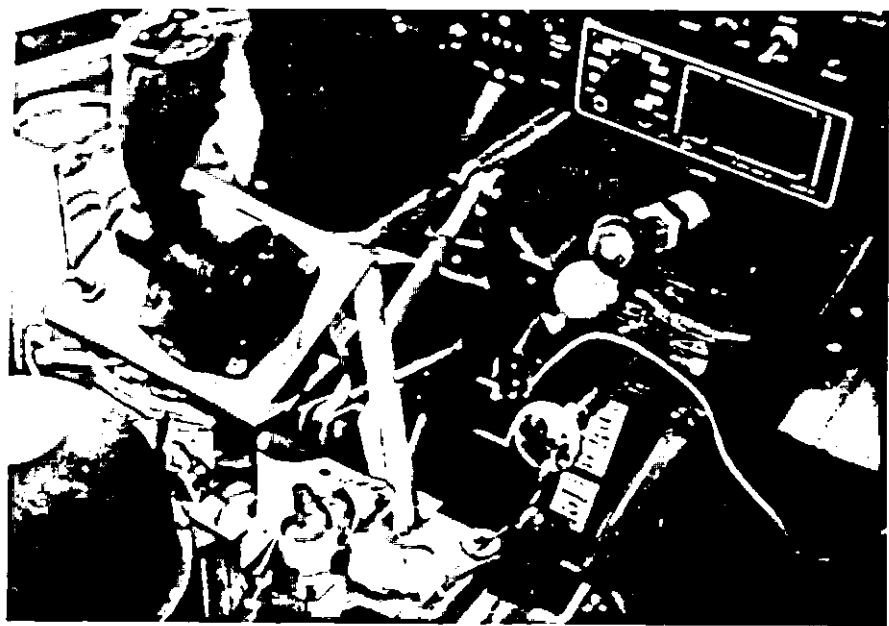


Figure 29. Side Stick Controller in Test Vehicle Cockpit

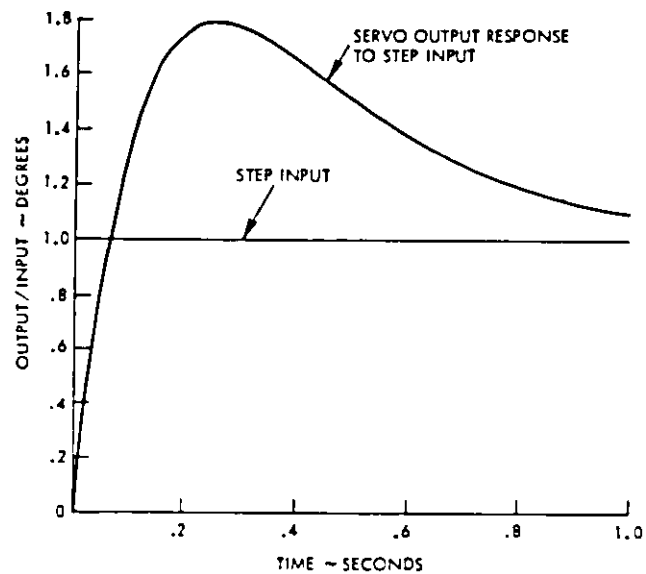


Figure 30. Output Response to Step Input - Side Arm Controller

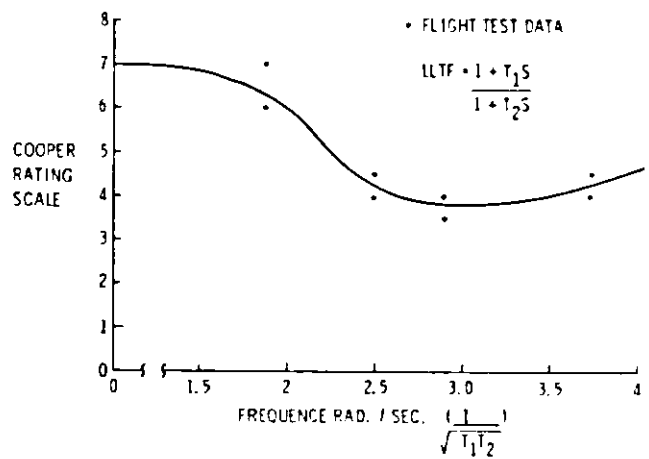


Figure 31. Command Augmentation Test Results

CAPRONI PARAMETER I.D FLIGHT 47

CASE G3

RUN CONDITIONS

G.W. = 1865 LB

C.G. = .47

ALT. = 5500 FT

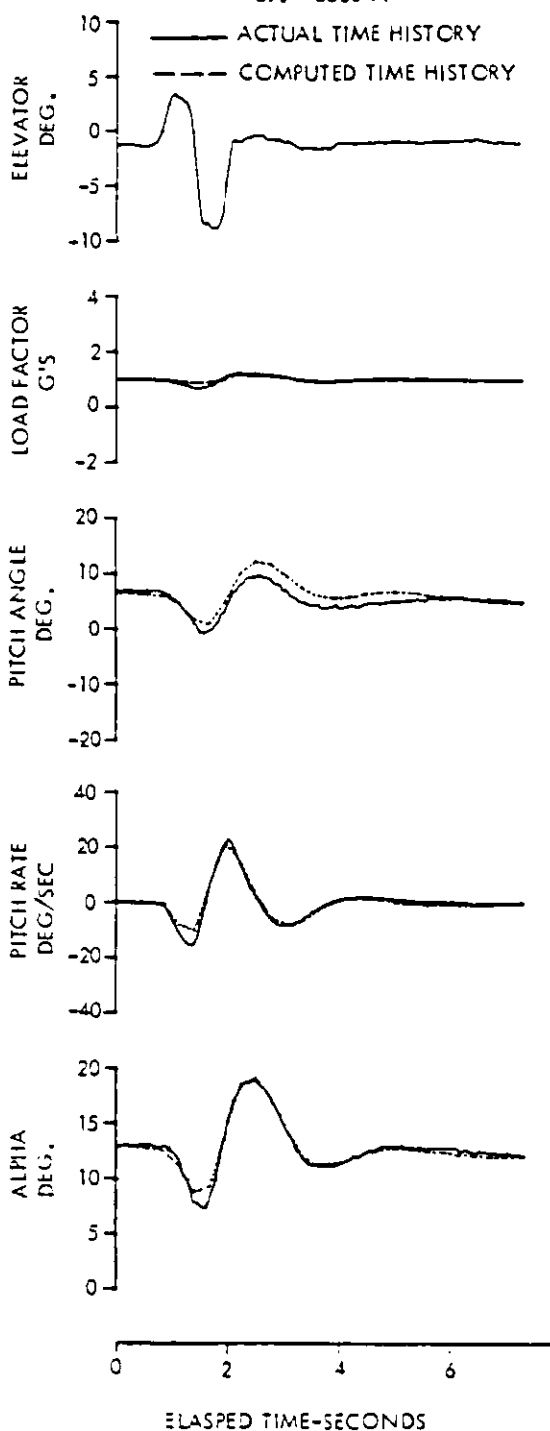


Figure 32. Longitudinal Parameter I.D. Matching

CAPRONI PARAMETER I.D FLIGHT 47

CASE G2

RUN CONDITIONS

G.W. = 1811 LB

C.G. = .32

ALT. = 7500 FT

LEGEND

TIME HISTORY

— ACTUAL

- - - COMPUTED

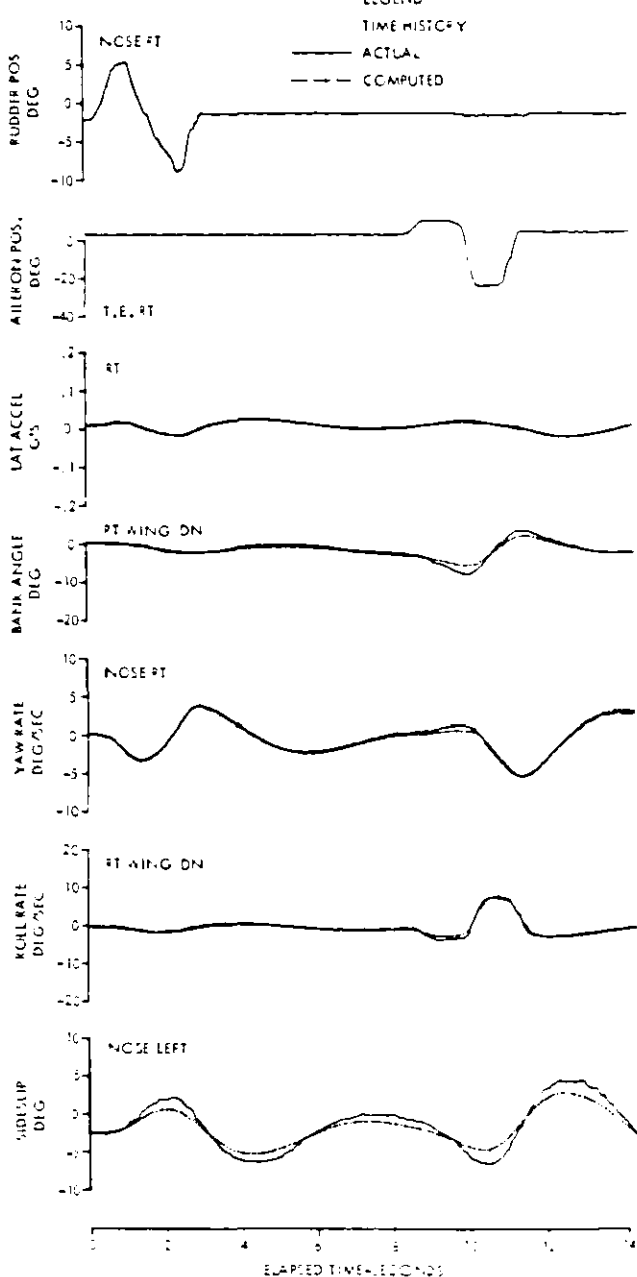


Figure 33. Lateral - Directional Parameter I.D. Matching

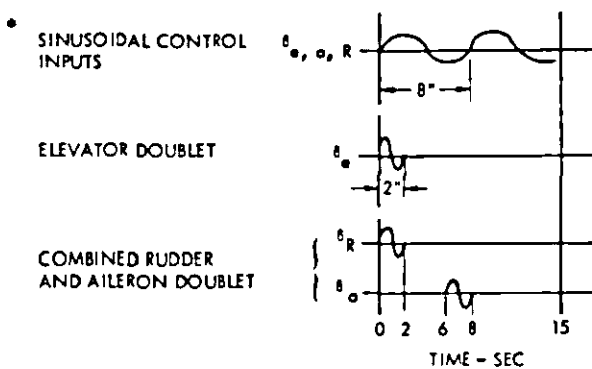


Figure 34. Sinusoidal, Doublet and Combined Doublet Control Input Shapes Evaluated

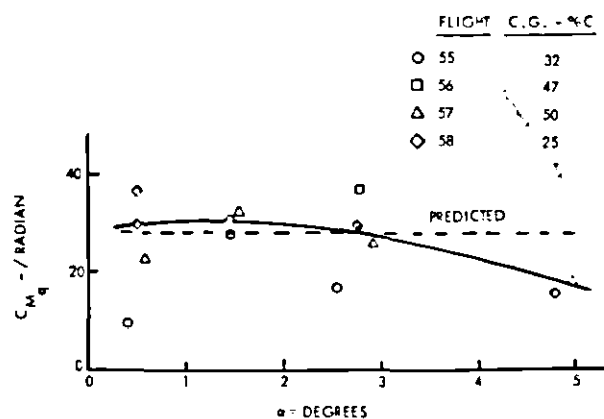


Figure 35. Correlation of C_{Mq} Predictions with Flight Test Data

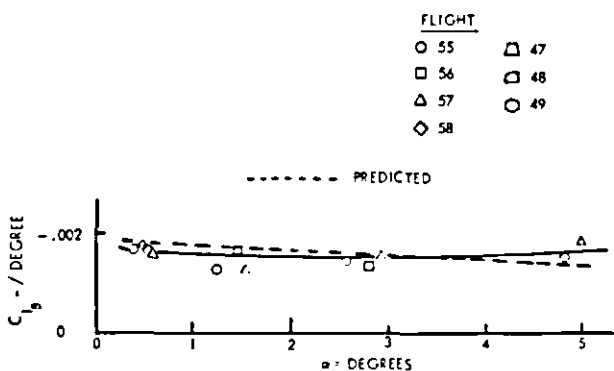


Figure 36. Correlation of $C_{l\beta}$ Predictions with Flight Test Data

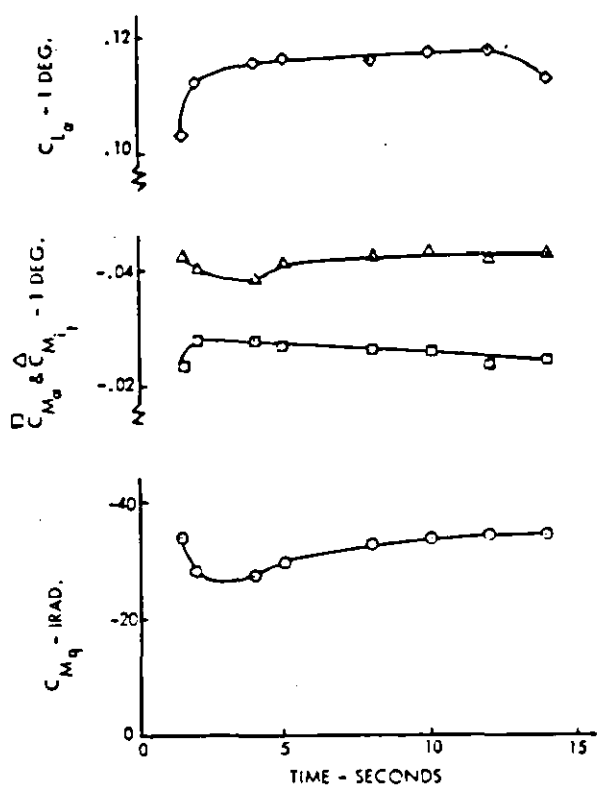


Figure 37. Influence of Analysis Time on Certain Derivatives

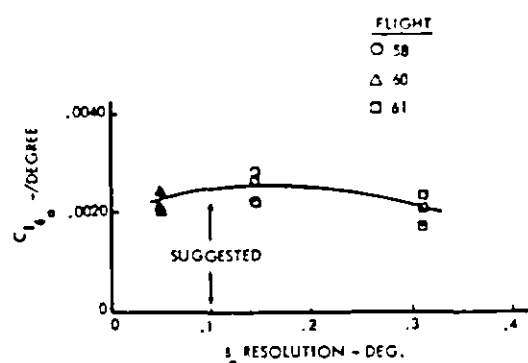


Figure 38. Influence of δ_α Resolution on $C_{l\beta\alpha}$

Derivative	Best Control Input	Best Excitation Level	Other Restrictions	Derivative Level		
				Predicted	Mean	Scatter
$C_{L\alpha}$	Elevator Doublet	$q(6-20^\circ/\text{sec})$.3129	.0494	$\pm 4\%$
$C_{L\dot{\alpha}}$	get from $C_{H\dot{\alpha}}$.0068		
$C_{H\alpha}$	Elevator Doublet	$q(6-20^\circ/\text{sec})$	aft C.G., high V	-.0160	-.0103	$\pm 1\%$
$C_{H\dot{\alpha}}$	Elevator Doublet	$q(6-20^\circ/\text{sec})$	aft C.G.	+.049	+.0155	$\pm 1.1\%$
C_{Hq}	Elevator Doublet	$q(6-20^\circ/\text{sec})$	aft C.G.	+.26.0	+.29.0	$\pm 25\%$
$C_{T\beta}$	Rudder Doublet	$\beta(\sim 10^\circ)$	aft C.G.	-.0050	-.0043	$\pm 2\%$
$C_{I\beta}$	Rudder Doublet	$\beta(\sim 10^\circ)$	aft C.G.	-.0020	-.0017	$\pm 1\%$
$C_{R\beta}$	Rudder Doublet	$\beta(3-12^\circ)$		-.0007	.0005	$\pm 15\%$
C_{I_p}	Aileron Doublet	$p(5-22^\circ/\text{sec})$		-.8258	-.8433	$\pm 1.2\%$
C_{R_p}	Rudder/Aileron Doublet	$p(5-22^\circ/\text{sec})$	high V	-.0592	-.0800	$\pm 18\%$
C_{I_t}	Rudder Doublet	$t(10^\circ/\text{sec})$	f(=1)	.1536	.1253	$\pm 6\%$
C_{R_t}	Rudder Doublet	$t(4-8^\circ/\text{sec})$		-.0139	-.0189	± 21
C_{Ig_a}	Aileron Doublet	$p(5-22^\circ/\text{sec})$	high V	.0026	.0019	$\pm 7\%$
C_{Rg_a}	Rudder Doublet	$t(4-8^\circ/\text{sec})$	aft C.G.	-.0006	-.0007	$\pm 3\%$
C_{yg_r}	Rudder Doublet	$t(4-12^\circ/\text{sec})$	aft C.G.	.0016	.0023	$\pm 6.7\%$
C_{Ig_t}	Rudder Doublet	$t(10^\circ/\text{sec})$	aft C.G.	-.00005	+.00004	----

Figure 39. Summary of Parameter I.D. Program

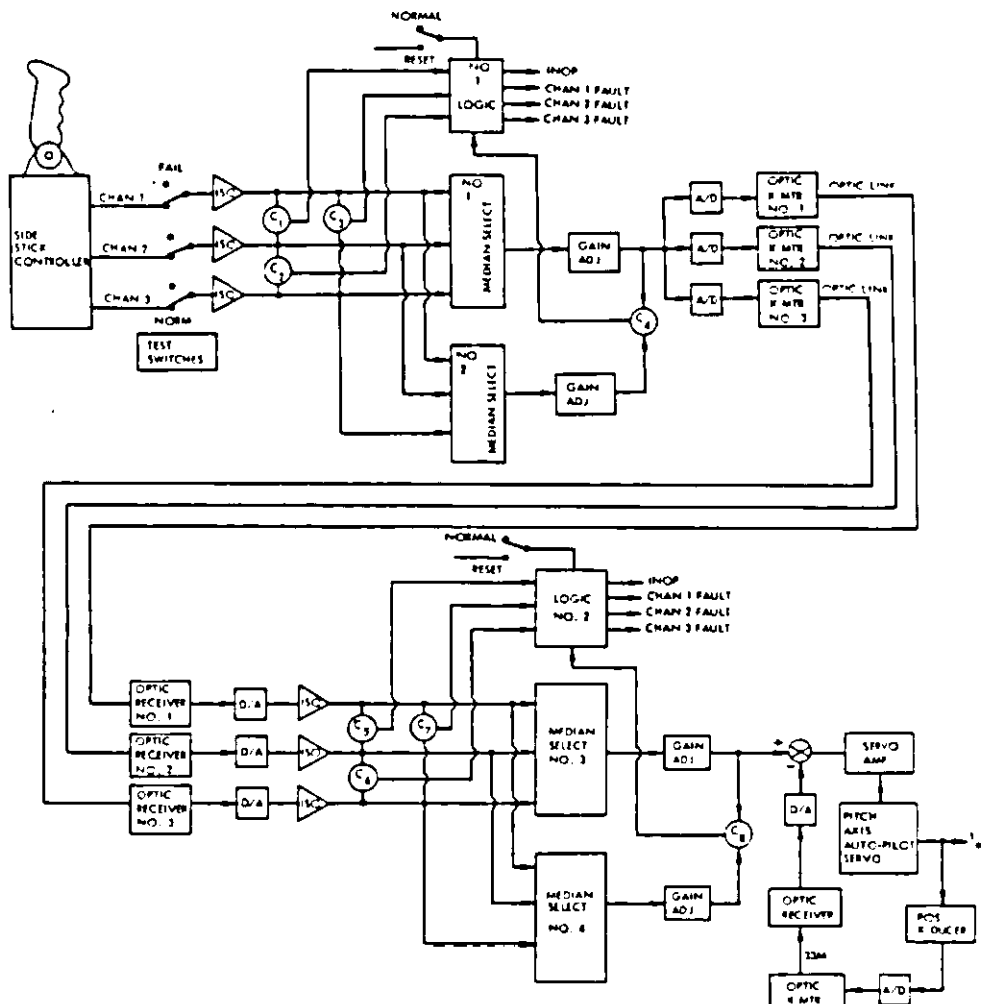
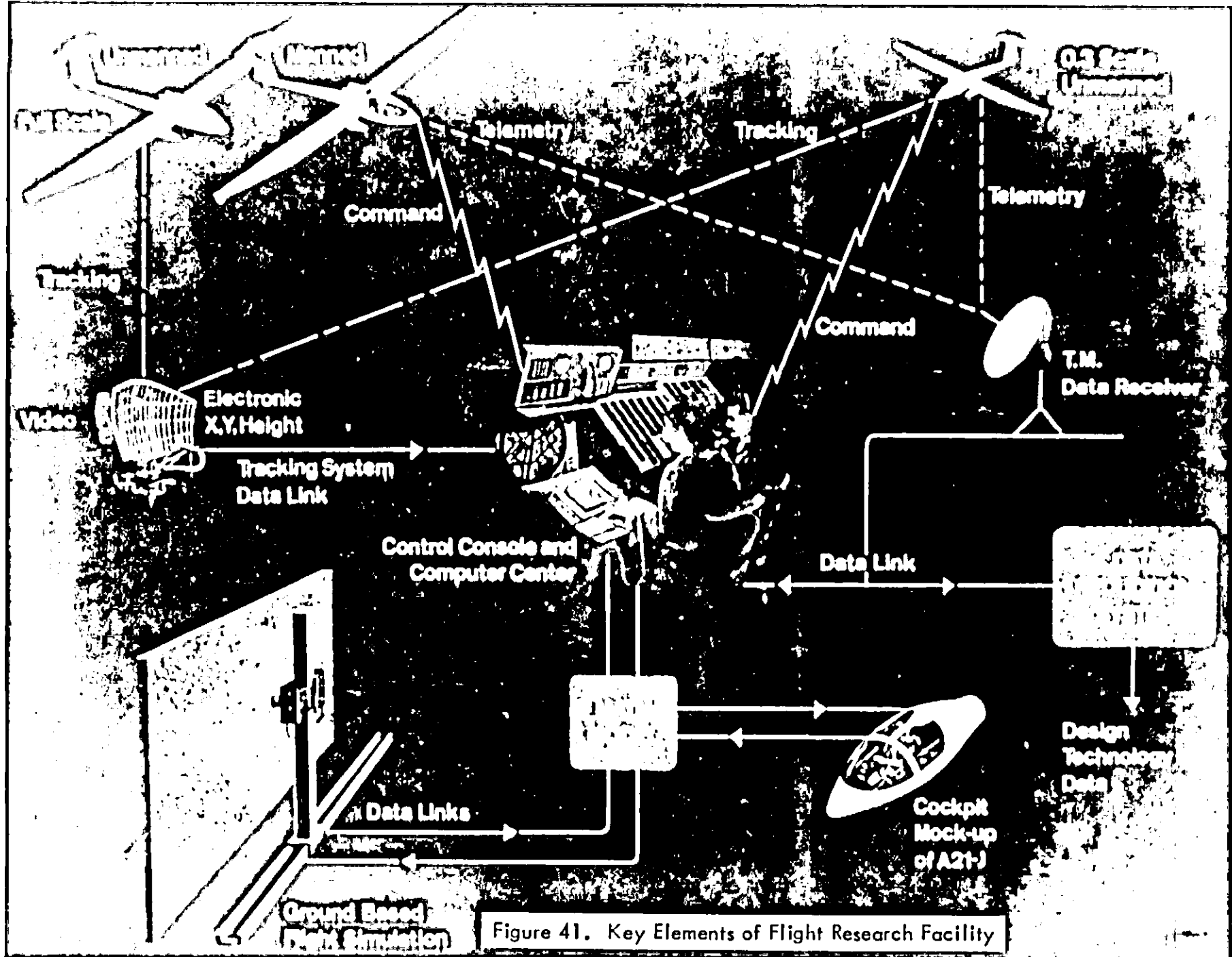


Figure 40. Electro-optic Pitch Axis Control System



PERFORMANCE FLIGHT TEST
EVALUATION OF THE BALL-BARTOE
JW-1 JETWING STOL RESEARCH
AIRCRAFT

Ralph D. Kimberlin*
The University of Tennessee Space Institute
Tullahoma, Tennessee

ABSTRACT

The Ball-Bartoe Jetwing is a single seat, jet, research aircraft powered by a JT15D-1 turbofan engine. It achieves supercirculation lift and STOL performance by ducting all engine air through the leading edge of the wing and ejecting it over the top surface of the wing through a slot nozzle. This nozzle extends along approximately 70% of the wing span. A Coanda flap is mounted at the trailing edge of the blown portion of the wing span. In addition to the main wing, a smaller wing panel is mounted above the slot nozzle. The air passage between the main wing and the smaller upper wing acts as an ejector to provide thrust augmentation. The mixing of the engine air with the ambient air in the ejector reduces jet noise levels and infrared signature.

This paper covers the initial portion of the Jetwing flight test program conducted by the University of Tennessee Space Institute for Naval Air Systems Command. Included are the flight test methods required to determine the performance of a powered lift aircraft, and the instrumentation approach necessary for inexpensive testing of a small aircraft.

INTRODUCTION

The need for a military aircraft that will operate from short, unimproved airfields, and the decks of smaller aircraft carriers, has increased as the number of overseas bases has decreased and the budget dollars shrink. Such an aircraft also needs to be fuel efficient, quiet, maneuverable, have a low infrared signature, and carry a large useful load.

The Ball-Bartoe "Jetwing" is a novel concept which offers the possibility of achieving these objectives. The "Jetwing" concept combines a thrust augmenting ejector with upper

*Associate Professor of Aviation Systems and Principal Investigator "Jetwing" Research Program.

surface blowing, and a Coanda flap in an attempt to achieve both thrust augmentation and powered lift. In this concept all engine air (fan bypass and core exhaust) is ducted to a slot nozzle on the upper surface of the wing. The nozzle is located at approximately 30 - 40% of the chord and extends along approximately 70% of the wing span. The fan by-pass air is ducted to the outboard portion of the wing while the core exhaust is ducted to the inboard portion of the wing as shown in Figure 1. Located above the nozzle is a separate, and much smaller wing surface which acts as the ejector. The Coanda flap is located along the portion of the wing span covered by the nozzle. A two dimensional sketch of the arrangement is shown in Figure 2.

In addition to providing supercirculation lift and potential thrust augmentation the concept offers several side benefits. They are: 1) Low infrared signature due to mixing of ambient air with the core exhaust in the ejector; 2) Low noise due to shielding, a slot nozzle, and ambient air mixing; and 3) Good lateral control at low airspeeds without a separate bleed air system for blowing the ailerons.

The "Jetwing" concept was conceived by Mr. O.E. "Pete" Bartoe while he was Vice President and General Manager of Ball Bros. Research. Mr. Bartoe was able to convince the management of Ball Corporation that his "Jetwing" ideas were worth spending corporate funds to develop. This led to the formation of a separate company, called Ball-Bartoe Aircraft Company (with Mr. Bartoe as its President), to develop the "Jetwing" concept into a research aircraft.

Development was started on the Jetwing airplane (Figure 3) in 1973 with Mr. Bartoe and one technician on a full time basis, plus a part time stress engineer. By December of 1976 the airplane was ready for test.

Testing started with the airplane in the 40' x 80' wind tunnel at NASA Ames Research Center. A large matrix of aircraft configurations were tested in the 40' x 80' tunnel, and data from these tests are available for comparison with flight test data. A sample of this data is shown in Figure 4. The tunnel data showed the airplane to be capable of achieving high lift coefficients, but to also be neutrally stable to unstable longitudinally at the center of gravity ranges where it was likely to be flown. As a result about 300 pounds of lead ballast was added to the nose prior to starting flight testing.

The first flight was conducted at Mojave, CA on July 11, 1977 by Mr. H. R. "Fish" Salmon. This flight confirmed the instability and an additional 100 pounds of lead ballast was added to the nose. Forty seven flights were flown at Mojave for a total of 34 hours. During this testing it was discovered

that the horizontal tail would stall whenever the flaps were lowered to angles in excess of 40° and when the air-speed was less than 50 knots indicated airspeed. As a result a safe flap angle of 35° was established. A certain amount of quantitative performance data were gathered during Mojave testing, but its usefulness is limited due to the lack of calibrations on instruments and airspeed system.

Upon completing testing at Mojave, the aircraft was ferried to Boulder, CO where some testing and demonstration flying continued. An additional 44 flights and 32 flight hours were accumulated during the ferry trip and test flying at Boulder.

In December of 1978, the Jetwing aircraft and its conceptual patents were donated to the University of Tennessee. During February 1980 the University of Tennessee received a \$99,232.00 contract from Naval Air Systems Command for a 105 hour flight test of the Jetwing aircraft. This paper describes the initial part of that testing.

DESCRIPTION OF THE TEST ARTICLE

The Jetwing research aircraft is a single engine, single seat, powered lift, jet aircraft with conventional landing gear. Figure 5 is a three view drawing of the aircraft showing configuration and dimensions. Table I lists other pertinent design features.

Two features of the design affect nearly all aspects of the flight test program. The first is the aircraft's small size, and the second is the location of the center of gravity when loaded with pilot and full fuel.

DESCRIPTION OF THE FLIGHT TEST PROGRAM

The purpose of the Jetwing Flight Test Program is to validate the 40' x 80' wind tunnel data by flight test, and to obtain performance, stability and control data sufficient to evaluate the Jetwing concept for future application to other flight vehicles. Included in the test program are:

1. Aircraft check out and pilot familiarization.
2. Airspeed calibration encompassing both high and low speed ranges.
3. Aircraft performance, including takeoff and landing performance.
4. Determination of aircraft lift capability, including lift variation with angle of attack.

5. Longitudinal stability to include neutral point determination, short period and long period dynamic stability characteristics, and flight path stability.
6. Maneuvering Stability
7. Determination of roll control power throughout the speed range and with several flap positions.
8. Lateral-directional stability to include both static and dynamic stability characteristics.
9. Critical evaluation of the landing approach characteristics, with particular emphasis on the STOL mode of operation.
10. A static determination of net thrust available using laser velocimeter measurements.

In this paper we will discuss the procedures and preliminary results of test program items (1) thru (3) except for takeoff and landing performance.

INSTRUMENTATION

The type and amount of flight test instrumentation was affected by three constraints. They are:

1. Cost
2. Size
3. Weight and Location

These are, of course, the same constraints that we face on any flight test program. However, with the Jetwing they took on new meaning.

First was the cost constraint. Although there are several flight test data collections systems available which will collect the data, make the instrument corrections, telemeter it to the ground, and display it on a console in real time, they also cost more than our entire budget! Needless to say, they were quickly passed by.

The other things about such systems is that they require a certain amount of space. Useable space on the Jetwing is at a premium. The space that is available is aft of the cockpit. If added there, they impact on the third constraint which is the empty weight center of gravity location. Since the center of gravity is already too far aft, addition of

instrumentation aft of the cockpit was kept to an absolute minimum.

The solution to this problem was to use calibrated flight instruments, and film the panel with a hand held 8mm movie camera. An alternative to this method is for the pilot to read the data by radio to a Flight Test Engineer in the chase aircraft or on the ground.

Figure 6 shows the instrument panel as configured for performance testing. The only piece of what might be described as sophisticated instrumentation is the SDI/Hoskins Fuel Management System. Our experience with this panel mounted system has confirmed the advertised 2% accuracy of fuel flow and fuel remaining.

In addition to the Fuel Management system a total pressure probe was installed in the hot and cold exhaust ducts and plumbed through a pressure switch to a single Δp gauge on the panel. The Δp gauge was referenced to static pressure by connection to the static ports of the airspeed boom.

The airspeed system consists of a wing mounted swivel boom containing both total and static sources. This boom is plumbed to a Kollsman F-1 sensitive airspeed indicator reading in knots. The static source is also plumbed to a sensitive altimeter and the Δp gauge. All other instrumentation is stock ship's instruments which have been calibrated.

TEST PROCEDURES

The initial performance testing consist of four seperate items:

1. Familiarization Flights
2. Airspeed Calibration
3. Thrust Calibration
4. V - γ Maps

FAMILIARIZATION FLIGHTS. The familiarization flights were used to obtain a qualitative evaluation and familiarization with the aircraft. In addition, the operating envelope was gradually expanded until an envelope of 50 to 200 KIAS had been explored. Items which received a preliminary evaluation during the familiarization flights included:

- a. Basic Static and Dynamic Stability (all axes)
- b. Low speed handling qualities, particularly in roll and pitch.
- c. Landing and takeoff techniques, CTOL, and STOL.
- d. Effects of configuration changes on trim.
- e. Power effects on airspeed calibration.

AIRSPED CALIBRATION. Since the aircraft it not equipped with an ejection seat, and safety is one of the prime concerns of the program, it was decided at an early date that the airspeed would be calibrated at altitude by the pace method. For this effort the Space Institute has available, and equipped for flight test work, a Cessna U3A (310) and a De Havilland DHC-3 Otter. The airspeed systems of both aircraft were calibrated over a speed course. The Otter is fitted with a wing mounted swivel boom, while the U3A has a trailing cone static with a Kiel probe for total pressure. Since neither of the aircraft was capable of the complete speed range of the Jetwing, two overlapping calibrations were required. The Otter was used to pace from 50 - 100 knots, while the U3A was used to pace from 90 to 170 knots. The Jetwing's airspeed system was calibrated in three seperate configurations.

- 1. Gear and flaps up from 70 to 160 knots in 5 knot increments.
- 2. Gear down and 15° flaps from 65 to 115 knots in 5 knot increments.
- 3. Gear down and 30° flaps from 65 to 95 knots in 5 knot increments.

Since power effects on the airspeed system were of some concern, power setting was recorded along with the airspeed. The ambient temperature probe correction factor was also determined during these tests.

THRUST CALIBRATION. The determination of gross thrust was of special concern. Although a limited calibration of gross thrust had been conducted in the 40' x 80' wind tunnel at NASA-Ames, this calibration had been done with the top wing removed. Since all of the flying in this program was to be conducted with the top wing installed, a calibration with the wing installed was required. Since it was not feasible to return the airplane to the 40' x 80' tunnel for another calibration a method had to be devised to accomplish the calibration locally. To accomplish this a bridle arrangement was fabricated which attached a dynamometer between the aircraft and an immovable object. We

were fortunate in that it was possible to attach the dynamometer and bridle to the aircraft through the thrust line. The test setup was on a slight incline so that the wheel friction was overcome and a slight preload placed on the bridle. This preload was later subtracted out of the thrust data. The test setup is shown in Figure 7.

Test data was taken for both increasing and decreasing values of thrust to evaluate hysteresis, and was corrected to standard conditions. In addition, calibrations were made with and without the upper wing installed. This was done so that comparison could be made between this method and the 40' x 80' wind tunnel calibration.

V - γ MAPS. Powered lift aircraft present an unusual problem for performance flight testing. This is because the thrust, drag and lift of a powered lift airplane are interrelated and cannot be easily separated. As a result, most analyses replace the drag coefficient (C_D) with the excess thrust coefficient (C_{Fex}). The excess thrust coefficient is defined by Williams, et al in Reference 2 as:

$$C_{Fex} = rC\mu - \frac{K C_L^2}{\pi A + 2C\mu} - C_{Do} - \Delta C_{DP}$$

where

$C\mu$ = the theoretical blowing coefficient.

r = a correction factor to account for boundary layer growth in the nozzle and scrubbing losses due to blowing the upper surface of the wing or flap.

K = a correction factor to account for the finite aspect ratio of the wing.

A = the geometric aspect ratio

C_{Do} = the drag at zero lift without flap deflection or blowing

ΔC_{DP} = additional lift dependent drag due to partial span flaps.

From this equation we can see that $C\mu$ appears in both the thrust term ($rC\mu$), and the drag terms ($K C_L^2 / \pi A + 2C\mu$) and ΔC_{DP} . As a result, a straightforward solution is difficult, if not impossible. It is possible, however, to determine the excess thrust coefficient (C_{Fex}) directly by flight test. If we are in a steady climb with no airspeed change, the excess thrust (F_{ex}) may be stated as:

$$F_{ex} = F_{AVAIL} - D = W \sin \gamma$$

where

F_{AVAIL} = thrust available

D = total drag

W = test weight

γ = flight path angle

If we assume small angles of γ we can say that $L \approx W$, and the equation may be rewritten in coefficient form as:

$$C_{Fex} = C_L \sin \gamma$$

Both C_L and $\sin \gamma$ may be determined by flight test, $\sin \gamma$ from sawtooth climb or level acceleration data, and C_L from airspeed and weight. A more convenient approach is to use a $V - \gamma$ map where flight path angle is plotted versus airspeed for a number of thrust settings from idle to maximum continuous. In this manner the performance can be mapped for a complete operating envelope. A method to normalize this data to standard conditions was developed by Parks and is given in Reference 3.

The $V - \gamma$ map was the approach adopted for performance measurement on the Jetwing. In addition, a decision was made to use the sawtooth climb method rather than the level acceleration technique to collect the data. Although sawtooth climbs require more flight test time, they are much easier to fly accurately with a neutrally stable to unstable airplane, and require less sophisticated data collection equipment.

TEST RESULTS

FAMILIARIZATION FLYING. A total of six familiarization flights were flown for a total of 2 hours and 55 minutes flying time. Flight durations were kept to 30 minutes or less in order to be back in the traffic pattern with at least one half of the fuel remaining. These flights confirmed earlier reports that the airplane was unstable longitudinally in nearly all configurations. The configuration which exhibits the most, positive longitudinal stability is gear down, flaps down 30°, and low power.

Landings were attempted using flap settings of 15° to 30°, and approach speeds from 65 to 90 knots indicated airspeed (KIAS). Power settings for these approaches varied between 76% N_1 and

68% N₁ with the higher settings corresponding to the lower airspeeds. The airplane was found to be quite difficult to land. The longitudinal instability, coupled with a conventional gear, and the unusual characteristics of a powered lift wing in ground effect go to make up some unconventional landing characteristics. For instance if the power is even 1 or 2% above idle, the main gear will not touch down. However, the longitudinal instability makes it quite easy to get the tail down. As a result, it is not unusual to find the airplane going down the runway with the tailwheel on the ground and the main gear two to six feet in the air. This is not a very comfortable position in which to find yourself since forward visibility is zero. The good thing about the landing characteristics is that the ground handling is excellent. In spite of the narrow main landing gear, there is no tendency to ground loop.

The familiarization flying confirmed the decision to use sawtooth climbs rather than level accelerations for collecting the performance data. The accelerations proved to be very difficult to fly due to the longitudinal instability, while the sawtooth climbs, although difficult, were easier than the accelerations.

AIRSPEED CALIBRATION. The airspeed calibration required 10 flights for a total of 6 hours and 40 minutes of flying time. Normally, the pace method of calibration would not require this much flying time, and there are several reasons why this was not the case. First, three flights had to be reflown due to leaks developing in the pitot-static system. In one case the plastic static line touched the hot skin in the wing root area and burned through. All pitot-static lines in this area were changed from plastic to stainless steel and the problem has not reappeared. Secondly, a large amount of flying time was consumed in obtaining stabilized formation on the pace airplane. This was primarily caused by the longitudinal instability of the Jetwing. This reason is related to the third reason which is the small fuel tank of the Jetwing. This makes the useable time at test altitude small with a lot of time spent climbing and descending.

The results of the airspeed calibration are shown in Figures 8, 9, and 10. The data scatter is somewhat larger than we would like. However, the majority of the scatter falls within 2% of the faired curve. We have not been able to relate any of this scatter directly to power effects. A comparison of data points with their respective power settings does not reveal any pattern which ties power setting to a data point location. We are still evaluating this aspect of the calibration. A majority of the data scatter is most likely due to the difficulty in obtaining good stabilized points with a longitudinally unstable airplane.

THRUST CALIBRATION. Figure 11 shows the results of the static thrust calibration with the upper wing removed. Plotted with that data are the results of the 40' x 80' wind tunnel calibration and the Pratt and Whitney of Canada test stand calibration of the JT15D-1 engine that is installed in the Jetwing. As can be seen from this plot the simple thrust calibration method used gives very good agreement with the wind tunnel calibration data. This increases our confidence in the data with the upper wing on obtained by this method. Figure 11 shows that there is a considerable thrust loss due to the ducting. Pratt and Whitney of Canada's original calculations on the ducting losses, conducted for Ball-Bartoe Aircraft, had estimated that it might be possible to achieve losses as low as 5 to 7%. The losses shown in Figure 11 are more on the order of 15 to 20%. Design iteration may be able to reduce these losses, and several areas for improving the ducts have been identified.

Figure 12 shows the results of the static thrust calibration with the upper wing installed. When compared with the data in Figure 11 we can see that the upper wing does not achieve thrust augmentation in the area of interest (high thrust settings). This was not unexpected since the 40' x 80' wind tunnel data had given indications of this. The wind tunnel data did show, however, that the upper wing provided beneficial aerodynamic effects at high angle of attack and low power settings.

V - γ PERFORMANCE MAPS. The flight testing to develop the V - γ maps is being conducted at the time this is being written and is not available for publication. We hope to publish this data at a later date.

CONCLUSIONS

Although the Jetwing flight test program has not progressed to the stage where significant conclusions may be reached about its performance, it is possible to say that such an aircraft can be flight tested without a large expenditure of funds providing unsophisticated techniques and instrumentation are used. In addition reasonable data may be obtained by these methods which will correlate well with other test methods as is demonstrated by the thrust calibration.

REFERENCES

1. "Jetwing from Colorado", Air International, Vol. 14, No. 2, (February 1978).
2. Williams, J., Butler, S. F. J., and Wood, M. N., "The Aerodynamics of Jet Flaps", Aeronautical Research Council R & M No. 3304, London, 1963.
3. Parks, Edwin K., "A Note on Performance Flight Testing of STOL Airplanes and the Application of Inertial Navigation Systems for Performance Testing", Office Memo, Performance and Flying Qualities Branch, AFFTC, Edwards AFB, CA, September 1975.

TABLE I. - JETWING TECHNICAL DESCRIPTION

Powerplant	Pratt & Whitney JT15D-1 Turbofan
Takeoff Thrust	2200 LB. S.T.
Maximum Continuous Thrust	2050 LB. S.T.
Maximum Continuous Thrust As Installed in Jetwing	1650 LB. S.T.
Fuel Capacity	106 GAL.
Maximum Gross Weight	3750 LBS.
Empty Weight	2500 LBS.
Ballast	400 LBS.
Center of Gravity Location With Ballast, Pilot & Full Fuel	37% M.A.C.
Wing Span	21.75 FT.
Wing Area	105 SQ. FT.
Mean Aerodynamic Chord	5.1 FT.
Aspect Ratio	4.5
Upper Wing Span	15.5 FT.
Length	28.6 FT.
Height	6.1 FT.
Landing Gear	Retractable, Conventional
Ejection Seat	None

FIGURE TITLES

- Figure 1.** Jetwing Ducting Arrangement (From Reference 1)
- Figure 2.** Two dimensional View of Jetwing Concept
- Figure 3.** Jetwing Research Airplane
- Figure 4.** Sample of NASA-Ames 40' x 80' Wind Tunnel Data on Jetwing Airplane.
- Figure 5.** General Arrangement Drawing of Jetwing Research Airplane
- Figure 6** Jetwing Instrument Panel Configured For Performance Testing
- Figure 7** Thrust Calibration Test Setup
 - Jetwing Airspeed Calibration
- Figure 8** Gear and Flaps Up
- Figure 9** Gear Down, Flaps 15°
- Figure 10** Gear Down, Flaps 30°
- Figure 11** Jetwing Thrust Calibration Upper Wing Removed Compared With Wind Tunnel Data and Engine Test Stand Data
- Figure 12** Jetwing Thrust Calibration With Upper Wing Installed

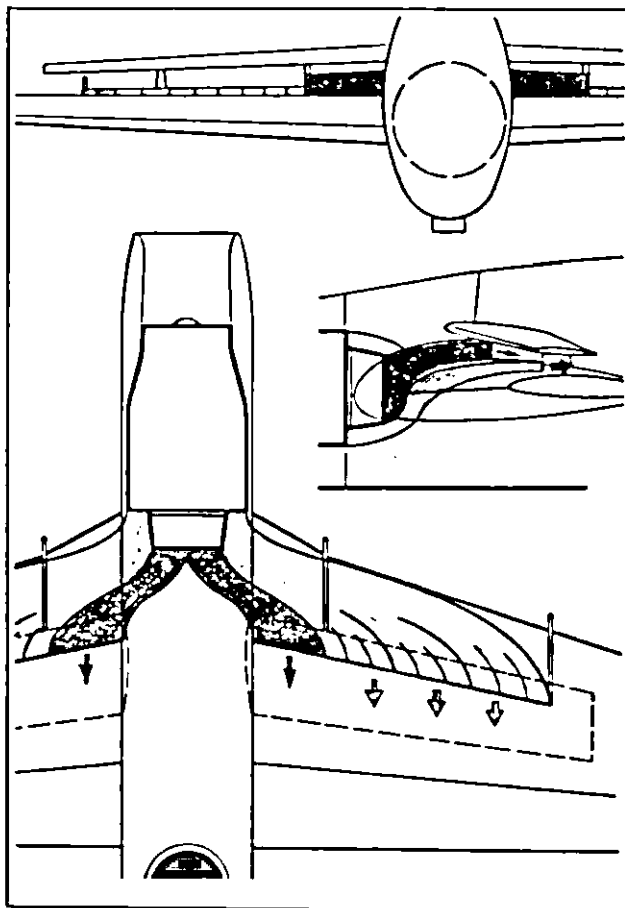


Figure 1. Jetwing Ducting Arrangement
(From Reference 1)

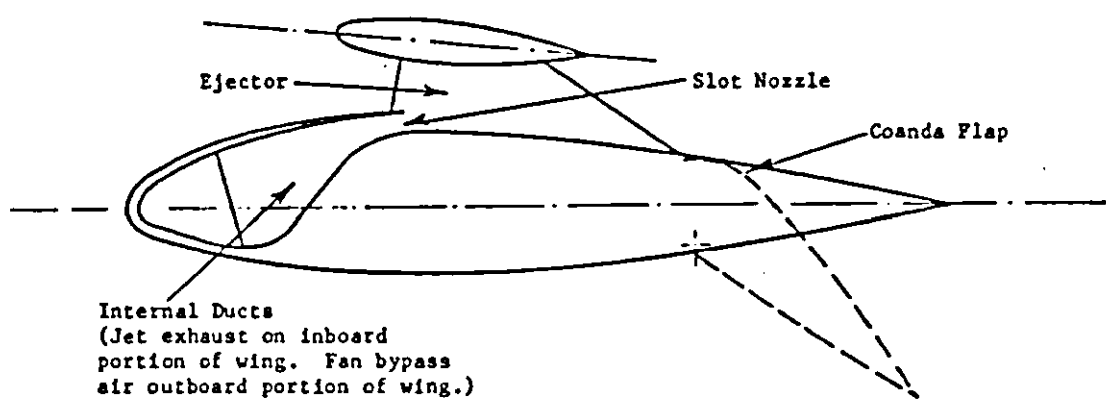


Figure 2. Two Dimensional View Of
Jetwing Concept

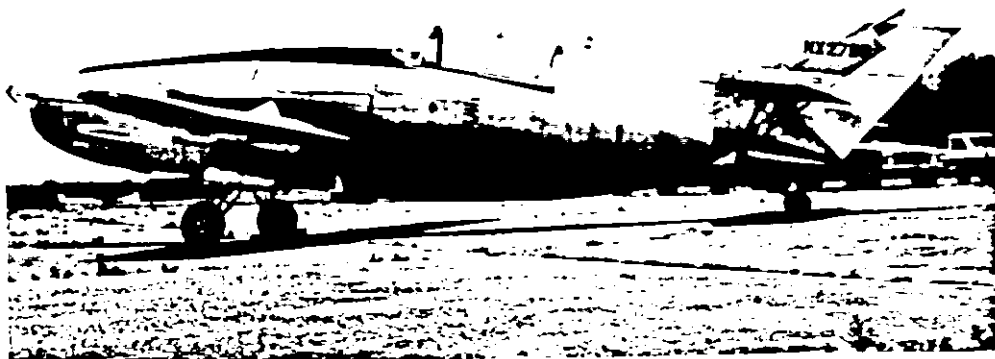


Figure 3. Jetwing Research Airplane

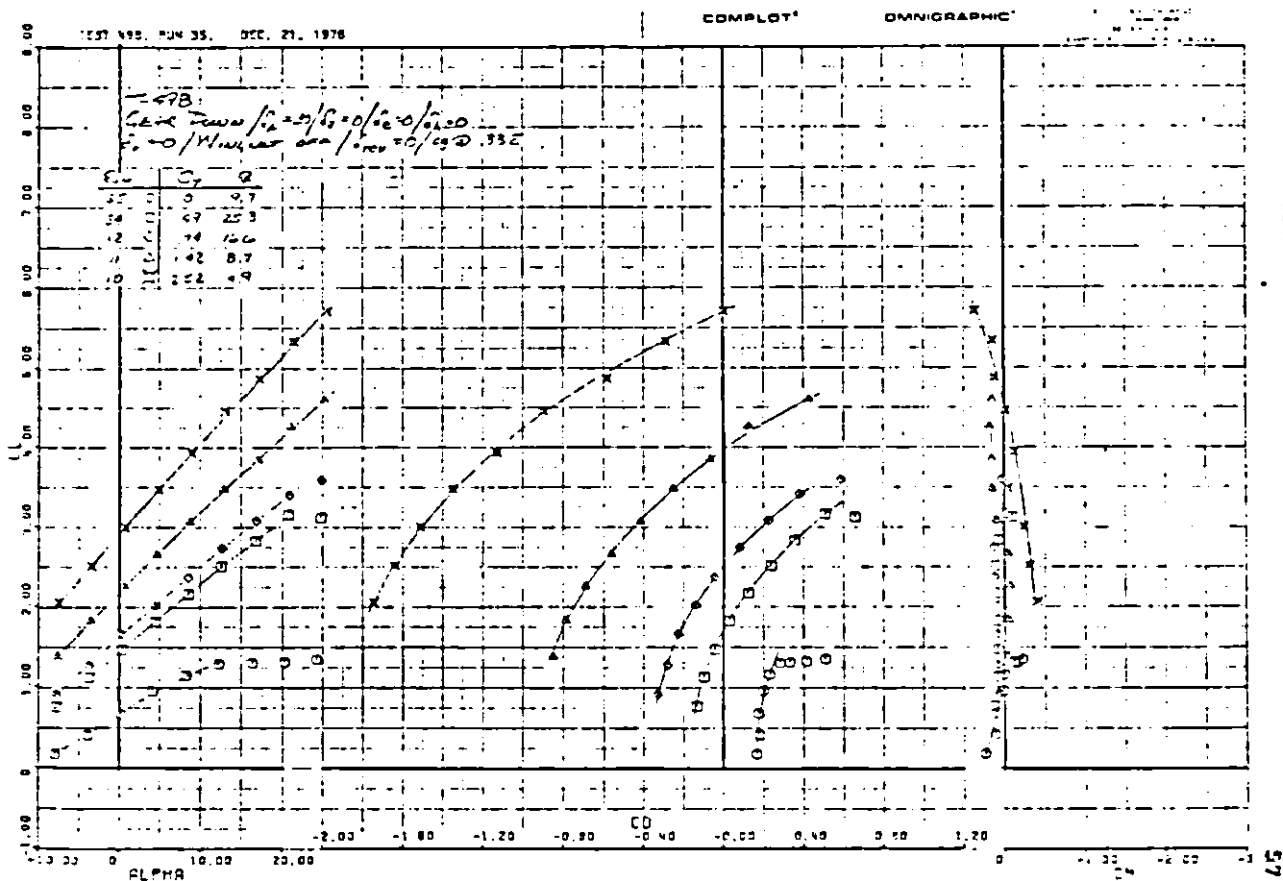


Figure 4. Sample of NASA-Ames 40' x 80' Wind Tunnel Data on Jetwing Airplane

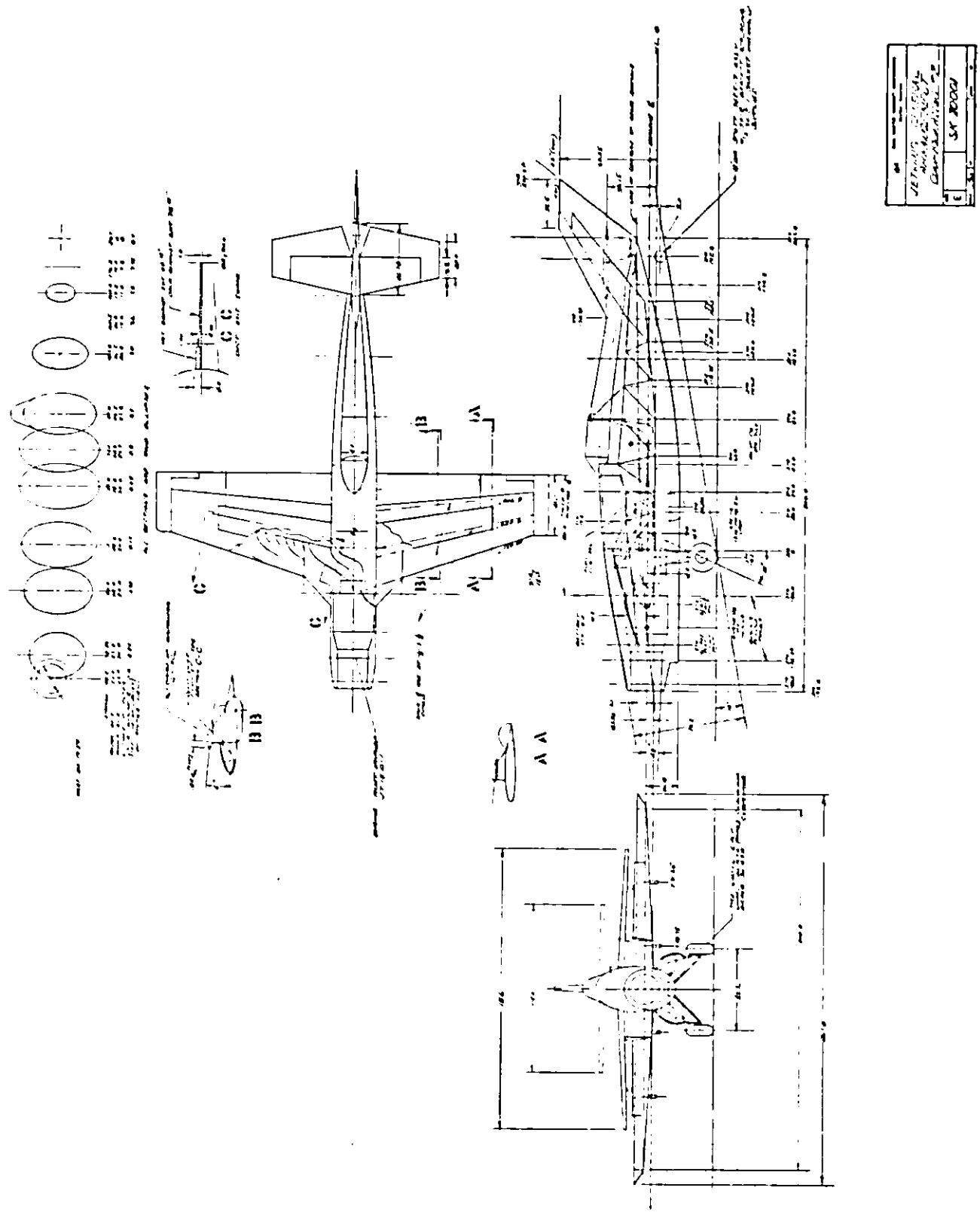


Figure 5. General Arrangement Drawing of Jetwing Research Airplane

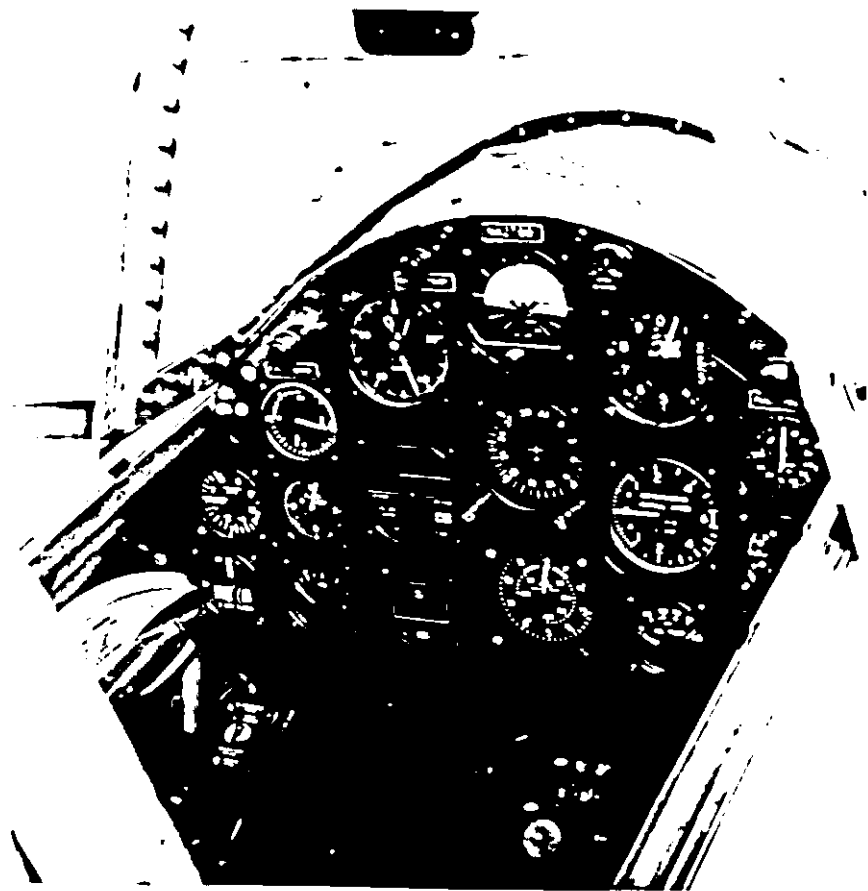


Figure 6. Jetwing Instrument Panel Configured For Performance Testing

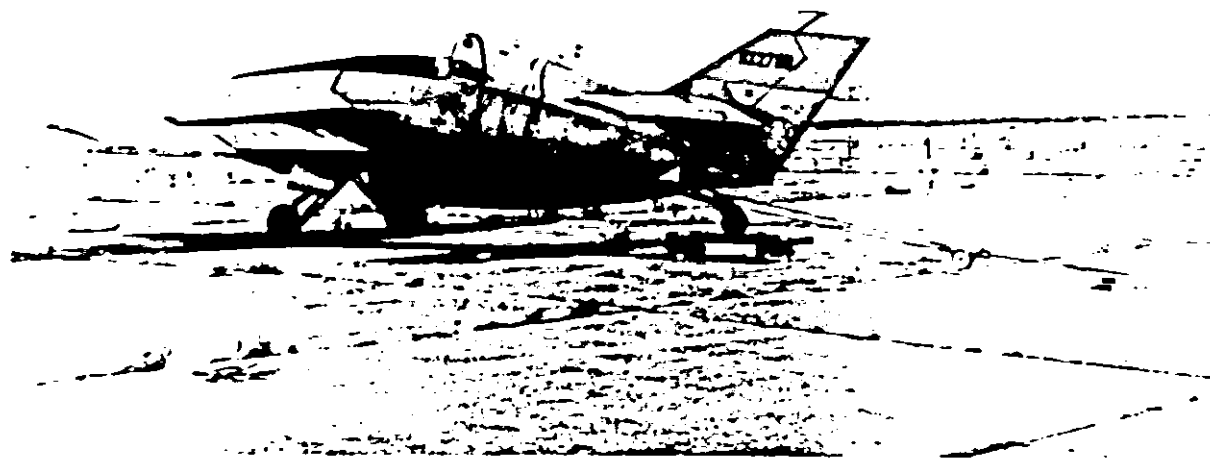
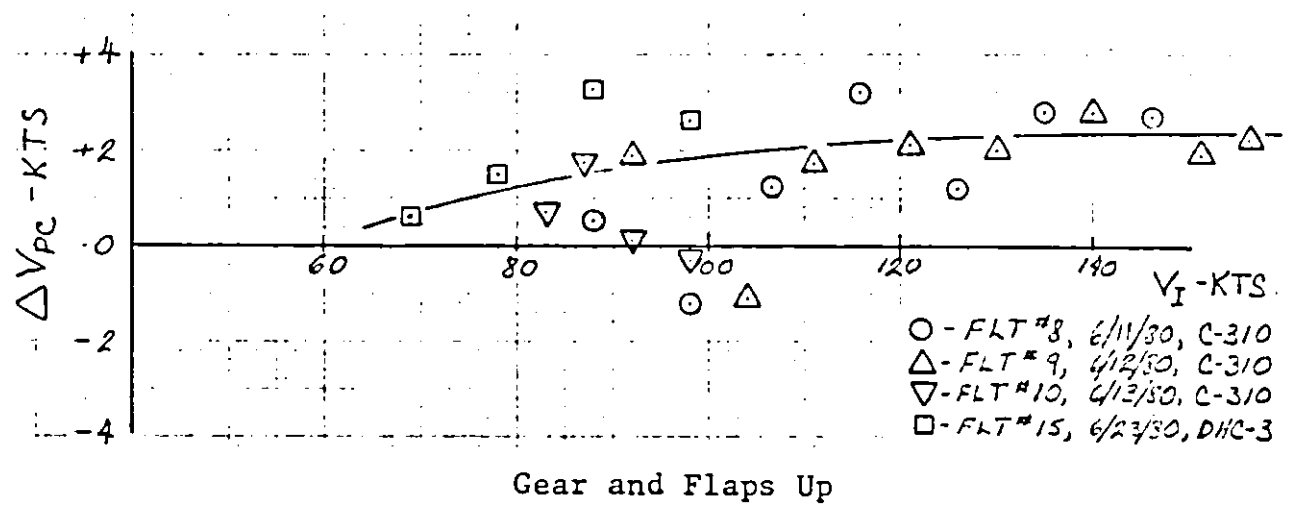
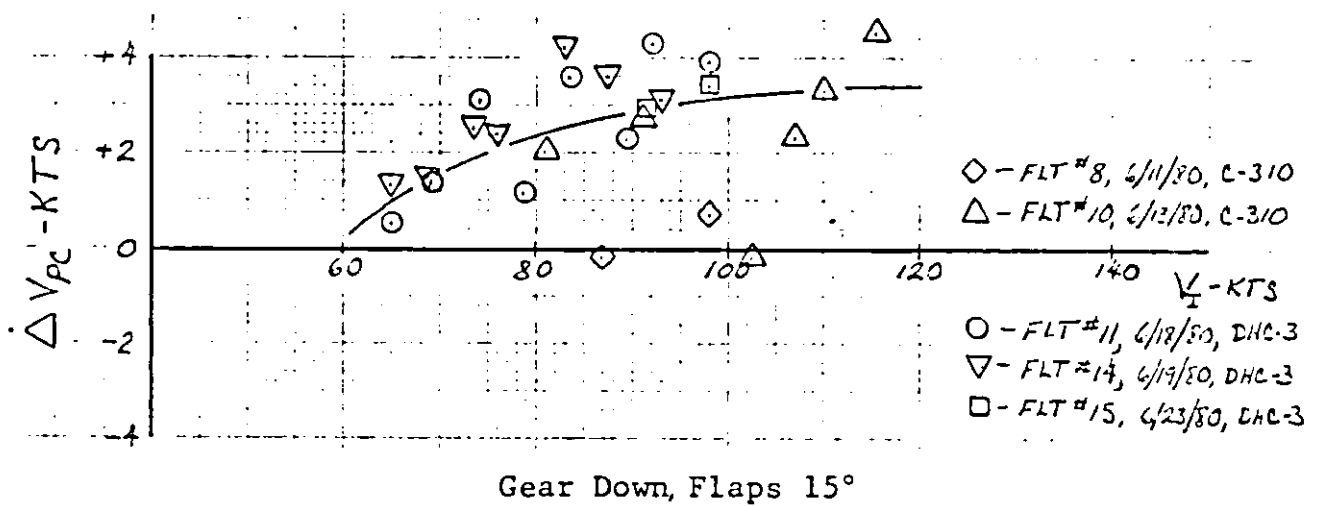


Figure 7. Thrust Calibration Test Setup

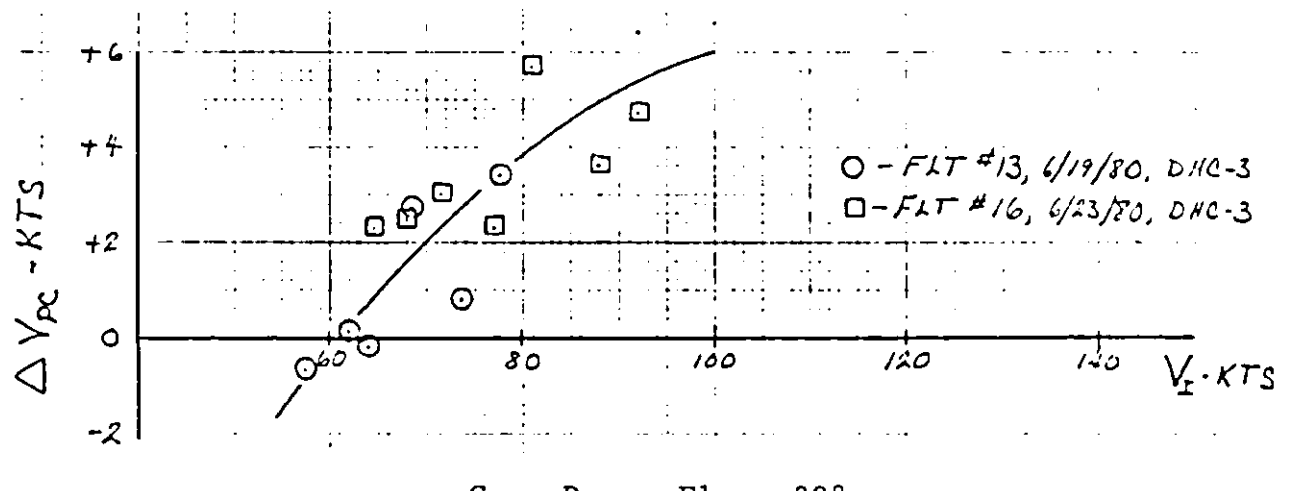
Figures 8, 9, 10. Jetwing Airspeed Calibration



Gear and Flaps Up



Gear Down, Flaps 15°



Gear Down, Flaps 30°

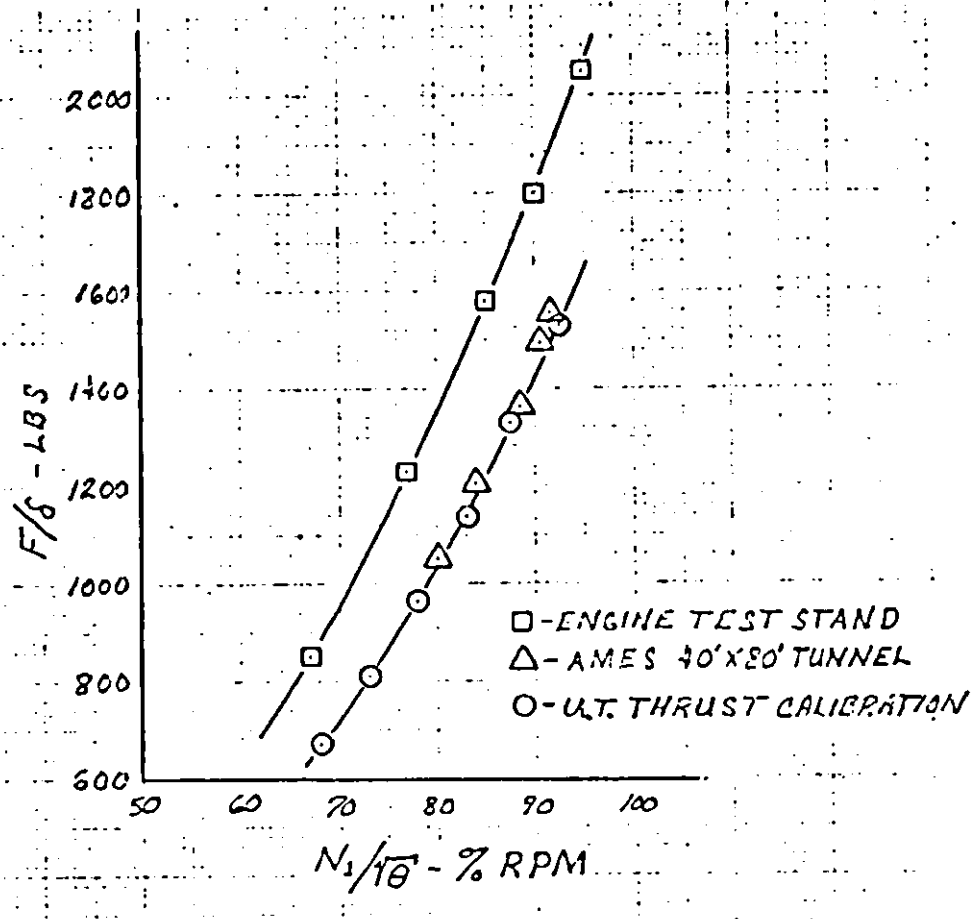


Figure 11. Jetwing Thrust Calibration Upper Wing
Removed Compared With Wind Tunnel And
Engine Test Stand Data.

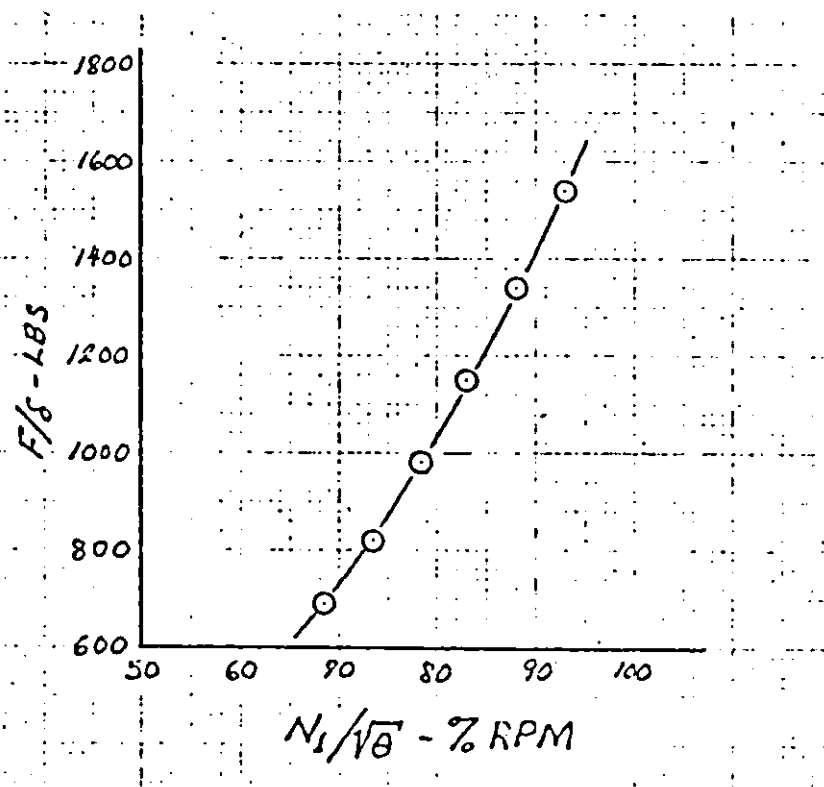


Figure 12. Jetwing Thrust Calibration
With Upper Wing Installed

ANALYSIS OF FLIGHT TEST MEASUREMENTS IN GROUND EFFECT

E. K. Parks*
University of Arizona
Tucson, Arizona

and

R. C. Wingrove†
Ames Research Center, NASA
Moffett Field, California

ABSTRACT

Three sources of errors, introduced into the air-data measurements of altitude and airspeed as a result of ground proximity, are evaluated. It is shown that the primary error results from ground constraint of the wing lifting pattern. Smaller errors result from constraint of the flow over the fuselage and of the engine exhaust. Equations are derived to provide corrections for the three error contributions. The equations are general and can be applied to airplanes of different geometries operating in different conditions. Applications illustrating different types of flight operations (takeoff and landing) are presented using CV-990 data. Applications illustrating the effect of different static orifice locations (fuselage and nose-boom) are presented with YC-15 data. Finally, an application to trajectory reconstruction is illustrated using DC-10 data.

INTRODUCTION

In analyzing test data obtained during aircraft operations near the ground, it is important to recognize the influence of the ground plane on the onboard measurements. Of particular importance is the effect of ground proximity on the air-data measurements of airspeed and altitude. This paper presents the development and application of a set of generalized equations for use in correcting air-data measurements for ground-effect errors.

The influence of ground proximity is familiar to pilots because of the "sag" in indicated airspeed and altitude observed during takeoffs and landings. Although the presence of these errors has long been recognized in flight operations, there has been no attempt to provide a systematic way of making corrections. During the recent flight test measurements of "ground effect" on the lift and drag of the Air Force YC-15 STOL airplane (Refs. 1, 2), it became apparent that some rational method was needed to correct the onboard airspeed and altitude measurements for

*Professor, Department of Aerospace and Mechanical Engineering.

†Research Engineer, Aircraft Guidance and Navigation Branch.

errors induced by ground constraint. Consequently, using wing-lifting line theory, an equation was derived with which the airspeed could be corrected for ground effect. A subsequent look at measurements made during takeoff and landing of other aircraft has indicated that although the major primary ground effect error in airspeed and altitude is induced by the wing lift, there are secondary effects caused by the ground-plane confinement of the jet-engine exhaust and of the flow about the fuselage. This report extends the work of Refs. 1 and 2 by providing a more general set of equations to account for the primary lift effects and, in addition, provides equations to account for the secondary engine and fuselage effects. The derived equations are general in nature and can be readily applied to airplanes of different geometries operating in different conditions.

The verification and use of the equations are illustrated by three recent applications at the Ames Research Center. The first is a set of tests that were conducted using the CV-990 to explain pilot-observed errors in the air-data instruments during takeoff and landing. The second is a flight test program that was conducted to measure the effects of ground proximity on the lift and drag characteristics of the YC-15. The third is a reconstruction of the time history from crash recorder data for the DC-10 Chicago accident (Ref. 3). Wherever possible, independent measurements of radar altitude are provided for verification of the analysis.

THEORETICAL DEVELOPMENT

General Considerations

The presence of a ground plane changes the magnitude of the air velocity over the static pressure orifice by an incremental amount ΔV . The related error in the barometric altitude can be determined by equating the momentum equation

$$\Delta p = -\rho V \Delta V$$

and the hydrostatic equation

$$\Delta p = -\rho g \Delta h ,$$

and solving for Δh ,

$$\Delta h = \frac{V^2}{g} \left(\frac{\Delta V}{V_\infty} \right) , \quad (1)$$

where p is the static pressure, ρ is the air density, h is pressure altitude, g is the gravitational constant, and V_∞ is the airspeed over static orifice when out of ground effect (OGE).

The error in dynamic pressure incurred by using the uncorrected airspeed becomes, to a first-order,

$$\frac{\Delta q}{q_\infty} = 2 \left(\frac{\Delta V}{V_\infty} \right) , \quad (2)$$

where $q_\infty = 1/2 \rho V_\infty^2$, the dynamic pressure. It follows that the error in the aerodynamic coefficients incurred by using the uncorrected dynamic pressure is

$$\frac{\Delta C_L}{C_{L_\infty}} \quad \text{or} \quad \frac{\Delta C_D}{C_{D_\infty}} = -2 \left(\frac{\Delta V}{V_\infty} \right). \quad (3)$$

Analytical Derivations

Three contributions to ground effect are developed. The first and major contribution results from ground constraint on the airplane's lift-dependent vortex pattern. The second effect comes from the ground constraint of the flow around the airplane fuselage. The third contribution, made by the airplane's engines, is thrust-dependent. The total incremental ground-effect error expressed in nondimensional form as the sum of the individual contributions is

$$\left(\frac{\Delta V}{V_\infty} \right) = \left(\frac{\Delta V}{V_\infty} \right)_L + \left(\frac{\Delta V}{V_\infty} \right)_F + \sum_{i=1}^{i=N} \left(\frac{\Delta V}{V_\infty} \right)_{E_i}, \quad (4)$$

where

$\left(\frac{\Delta V}{V_\infty} \right)_L$ = nondimensional velocity increment in ground effect (IGE)
induced by wing lift

$\left(\frac{\Delta V}{V_\infty} \right)_F$ = nondimensional velocity increment IGE due to fuselage constraint

$\left(\frac{\Delta V}{V_\infty} \right)_{E_i}$ = nondimensional velocity increment IGE due to jet-engine exhaust
constraint of the i th engine

N = number of engines

These ground effects are modeled mathematically by replacing the lifting wing, the fuselage, and the engines with an equivalent system of line vortices, sources, and sinks accompanied by their images mirrored in the ground. In using potential-flow methods, the following assumptions are made:

1. The flow is incompressible (the airspeed in operations near the ground usually is in the low subsonic range).
2. The pitot pressure is unaffected by the ground plane (i.e., the upstream potential is unchanged by ground proximity).
3. Image shape distortion due to ground constraint (mutual or paired interference) is negligible.

The equations representing the three contributions to the error, ΔV , as noted in Eq. (4) are derived in the following sections.

Wing lift effects. As previously stated, the major static pressure error induced by ground proximity results from constraint of flow around the lifting wing. Mathematically, the wing ground effect can be represented by replacing the lifting wing with an equivalent vortex pattern at a given height above the ground and a mirror image of the pattern at an equal distance below the ground (Refs. 4, 5).

For simplicity, the representation of ground effect will be made with a single "image" horseshoe vortex. Empirical constants necessitated by this simplification were adjusted to make the numerical results correspond to those obtained from a more rigorous solution employing many vortices.

Referring to Fig. 1, the velocity W_B induced at the static orifice by the image-bound vortex is, by application of the Biot-Savart law (Appendix A, Eq. (A3)),

$$W_B = \frac{\Gamma_0}{2\pi d_w} \frac{b'/2}{[d_w^2 + (b'/2)^2]^{1/2}} \quad (5)$$

where $d_w = [(2h + h_s + z_w)^2 + x_w^2]^{1/2}$ and $b' = \pi/4(b)$, for elliptical lift distribution (Ref. 4). In the single horseshoe vortex representation used here, b' is the length of the bound vortex (Appendix A) and b is the actual wingspan.

The component of W_B parallel to V_∞ represents the "lift" velocity error in normalized form,

$$\left(\frac{\Delta V}{V_\infty}\right)_L = -\frac{W_B}{V_\infty} \cos \chi = -\frac{\left(\frac{\Gamma_0}{V_\infty}\right)}{2\pi d_w^2} \frac{(2h + h_s + z_w)}{\left[1 + \left(\frac{2d_w}{b'}\right)^2\right]^{1/2}} .$$

For the case of a single horseshoe vortex and an elliptic spanwise lift distribution out-of-ground effect (OGE), from Ref. 2,

$$\frac{\Gamma_0}{V_\infty} = \frac{2C_L b}{\pi A} ,$$

where A is the wing aspect ratio.

Departures from the elliptic OGE spanwise lift distribution results from the application of flaps (Refs. 6-8) and from IGE changes of the spanwise downwash induced by the "image" trailing vortices.

In accounting for incremental IGE changes in spanwise circulation, it is shown in Appendix A (Eq. (A7)) that the ratio of the change at the root to that at the wing tip is

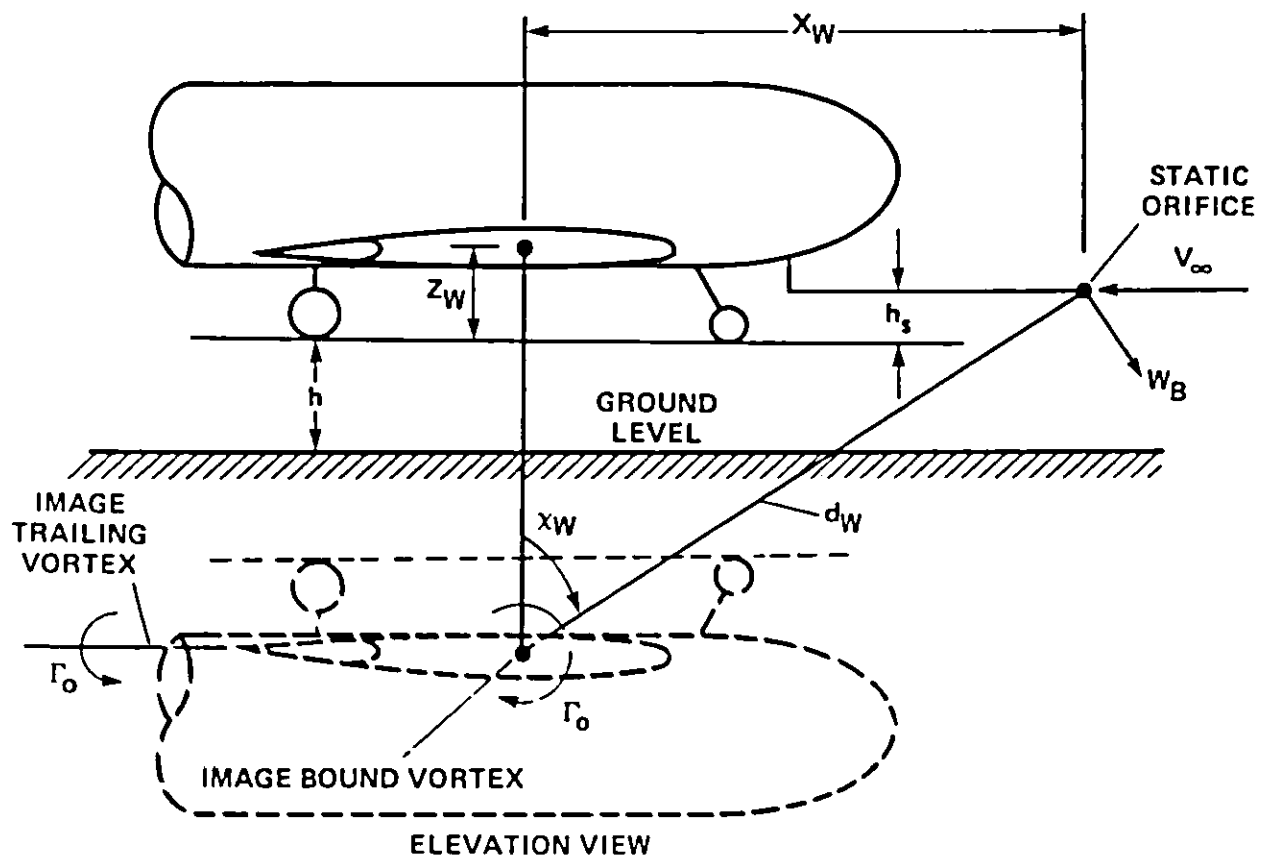
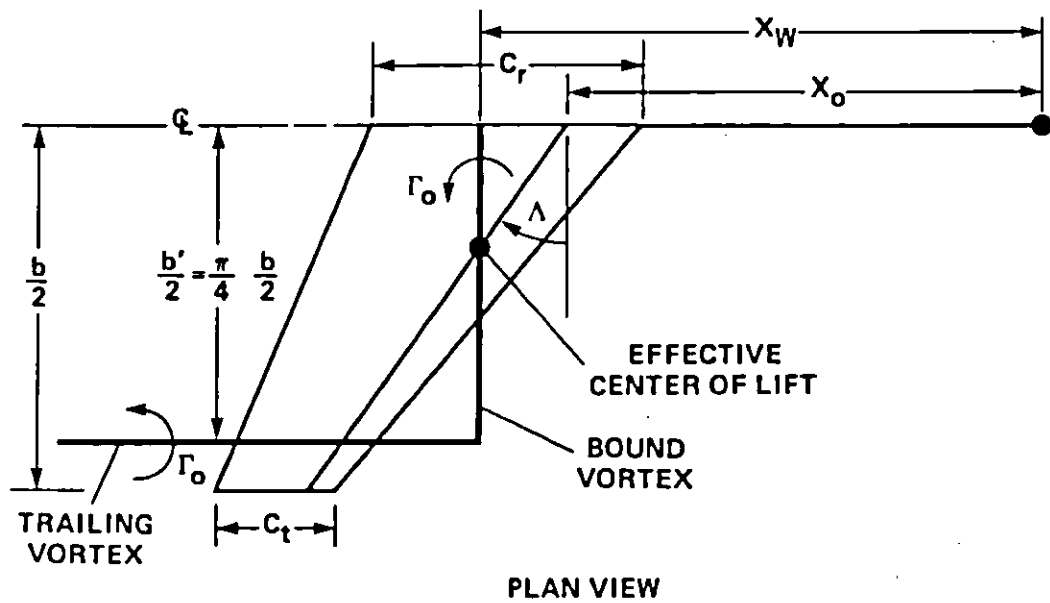


Figure 1.- Representation of "image" swept wing.

$$\frac{\Delta \Gamma_{\text{ROOT}}}{\Delta \Gamma_{\text{TIP}}} = \left(\frac{C_r}{C_t} \right) \frac{1 + \left[\frac{2(h + z_w)}{b} \right]^2}{\frac{1}{4} + \left[\frac{2(h + z_w)}{b} \right]^2}, \quad (6)$$

where C_r and C_t are the root and tip chord lengths. Consequently, it is assumed that

$$\frac{\Gamma_0}{V_\infty} = \frac{2C_L b}{\pi A} \frac{1 + \left[\frac{2(h + z_w)}{b} \right]^2}{k_1 + \left[\frac{2(h + z_w)}{b} \right]^2},$$

where k_1 is related to the spanwise location of the weighted average circulation.

Now assuming that $x_w = x_0 + k_2 b \tan \Lambda$, where x_0 is the distance from the root 1/4 chord forward to the static orifice, and Λ is the 1/4 chord sweepback angle, the value of d_w and hence $(\Delta V/V_\infty)_L$ is completely specified when suitable values of k_1 and k_2 are found.

Comparison of these simplified calculations of the lift effect with a more detailed analysis involving the superposition of a number of vortices permitted the determination of k_1 and k_2 ($k_1 = 0.8$ and $k_2 = 0.08$). Collecting terms results in Eq. (7), for the lift-effect error,

$$\left(\frac{\Delta V}{V_\infty} \right)_L = - \frac{C_L \left(\frac{2h + h_s + z_w}{b} \right) \left\{ 1 + \left[\frac{2(h + z_w)}{b} \right]^2 \right\}}{\pi^2 A \left(\frac{d_w}{b} \right)^2 \left[1 + 25.94 \left(\frac{d_w}{2b} \right)^2 \right]^{1/2} \left\{ 0.8 + \left[\frac{2(h + z_w)}{b} \right]^2 \right\}}. \quad (7)$$

Fuselage effects. In order to keep the fuselage ground-effect analysis simple and readily applicable to a general nose shape, with a forward fuselage or boom static source, fuselage ground image is represented by a single three-dimensional source of such strength as to produce a semi-infinite body of revolution of diameter equal to that of the fuselage (Fig. 2). The resulting equations are derived in Appendix B.

Applying the equations of Appendix B, the airspeed V at the static orifice becomes, in the notation of Fig. 2,

$$\frac{V}{V_\infty} = \left[1 + \left(\frac{D_F^2}{16 d_F^2} \right)^2 - 2 \frac{D_F^2}{16 d_F^2} \sin \chi_F \right]^{1/2},$$

which for $\left(\frac{D_F^2}{16 d_F^2} \right)^2 \ll 1$ is approximated by

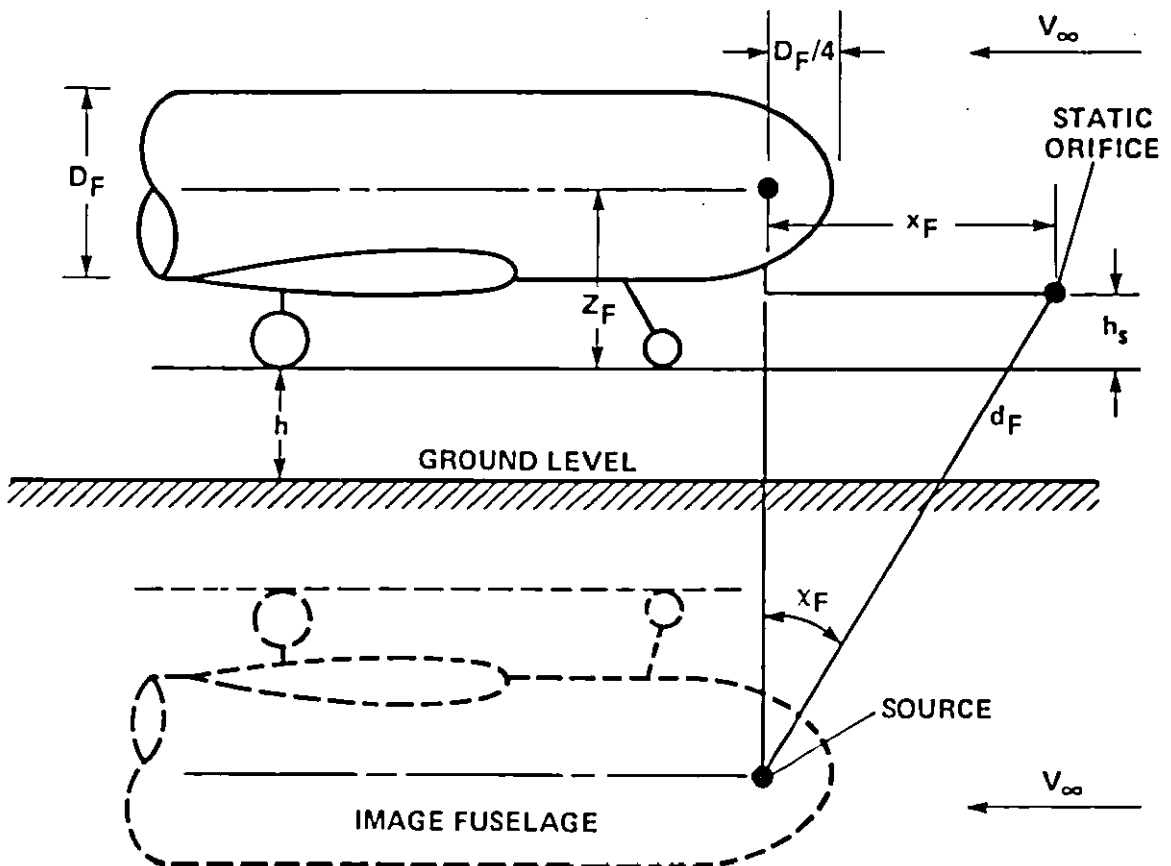


Figure 2.- Representation of "image" fuselage.

$$\frac{V}{V_\infty} = 1 + \frac{1}{2} \left[\left(\frac{D_F^2}{16 d_F^2} \right)^2 - \frac{2D_F^2}{16 d_F^2} \sin x_F \right].$$

The error due to ground effect is then given by

$$\left(\frac{\Delta V}{V_\infty} \right)_F = \frac{1}{2} \frac{D_F^2}{16 d_F^2} \left(\frac{D_F^2}{16 d_F^2} - 2 \sin x_F \right),$$

or, substituting for $\sin x_F$,

$$\left(\frac{\Delta V}{V_\infty} \right)_F = \frac{1}{2} \frac{D_F^2}{16 d_F^2} \left(\frac{D_F^2}{16 d_F^2} - \frac{2x_F}{d_F} \right). \quad (8)$$

Equation (8) is a first approximation for a general fuselage shape and a forward-mounted static source. A more exact representation of the fuselage in ground effect could be made by using a distribution of sources and sinks to accurately represent the fore and aft shape of the particular fuselage.

Because of the half-body representation, Eq. (8) should not be used to correct trailing-cone static pressure measurements for fuselage effects.

Engine effects. The ground effect of an engine on an upstream static pressure measurement is approximated by replacing the "image" engine with a three-dimensional sink of a strength chosen to satisfy the upstream flow conditions. The equations for the resulting velocity at the static orifice are derived in Appendix C.

Using Eq. (C4) of Appendix C, the perturbation velocity at the static source produced by the "image" engine is, with the dimensions of Fig. 3,

$$\left(\frac{\Delta V}{V_{\infty}}\right)_E = \frac{\left[\frac{-1 + (1 + C_j)^{1/2}}{2}\right] \pi r_j^2 x_E}{\pi [x_E^2 + y_E^2 + (2h + z_E + h_s)^2]^{3/2}}, \quad (9)$$

where

$$C_j = \frac{T}{(1/2)\rho V_{\infty}^2 A_j} = \text{engine thrust coefficient}$$

T = engine thrust

$$A_j = \pi r_j^2 = \text{area of jet exhaust}$$

r_j = radius of jet-exhaust stream-tube at the engine

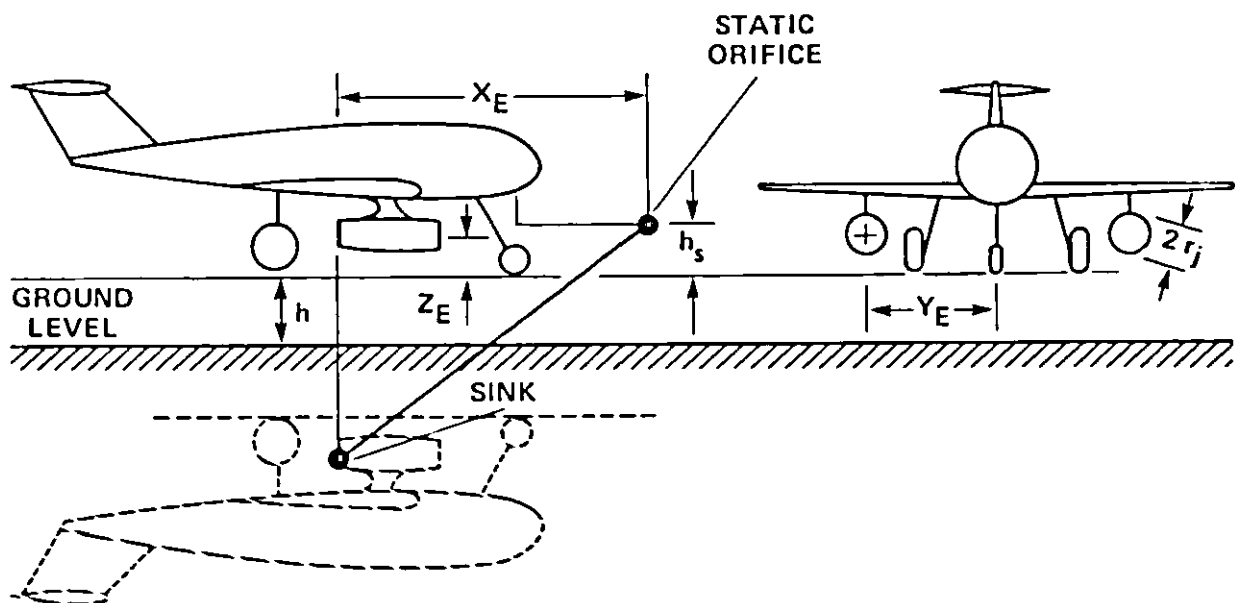


Figure 3.- Representation of "image" engine.

Equation (9) gives the perturbation velocity induced at the static orifice by the exhaust of the image engine. For a multi-engine airplane the contribution of each engine to ground effect must be considered separately unless the engines are paired symmetrically.

As mentioned in Appendix C, a more exact potential-flow representation of the jet-induced flow is made by using a line distribution of sinks to simulate the jet-exhaust flow (Refs. 9, 10). In the present paper the single-sink representation of the jet engine is used for simplicity. For ground-effect studies this is justified since the static orifice is more remote to the "image" engine than the locations considered in Refs. 9, 10.

APPLICATIONS

Ground Effects on Air-Data Measurements - CV-990 Takeoff and Landing

Figure 4 shows a time history of the altitude and airspeed during takeoff of the CV-990. These data show that prior to rotation the uncorrected altimeter reads too high. This error in altitude measurement is mainly due to the incremental velocity (at the orifice) induced by the engines and fuselage operating in ground effect. Upon rotation the wing contribution dominates and being of opposite sign causes the characteristic "sag" in the altitude and airspeed recordings. The specific contributions to the altitude and airspeed errors at lift-off, and at two subsequent heights, as computed by theory (Eqs. (7)-(9)) are shown in Table 1. These tabulated values show that the lift contributions to Δh and ΔV are of negative sign and that the fuselage and engine contributions are of positive sign. These data show that as the aircraft climbs out of ground effect the fuselage contribution tends toward zero more rapidly than the wing contribution. This is to be expected since the scaling factor in the former case is the fuselage diameter D_F , and in the latter case the wingspan, b (see Eq. (8)).

Figure 5 and Table 2 present the CV-990 landing data. A comparison of the wing effect during landing (Table 2) with that during takeoff (Table 1) shows a slightly smaller altitude error at touchdown than at lift-off. This difference is primarily due to the smaller value of gross weight during landing. Engine effects during landing are smaller than for takeoff due to the lower power settings.

The time histories of corrected barometric altitude in Figs. 4 and 5 are in reasonably good agreement with the radio altimeter measurements. This agreement, for both the takeoff and landing, is encouraging and indicates that the theory provides a practical way of correcting the measured static pressure for the effects of ground proximity.

Flight Tests in Ground Effect - YC-15

Airspeed and altitude measurements were made during a STOL landing of the YC-15 airplane using static pressures from both a fuselage orifice and from an orifice on a nose-boom. Time histories are shown in

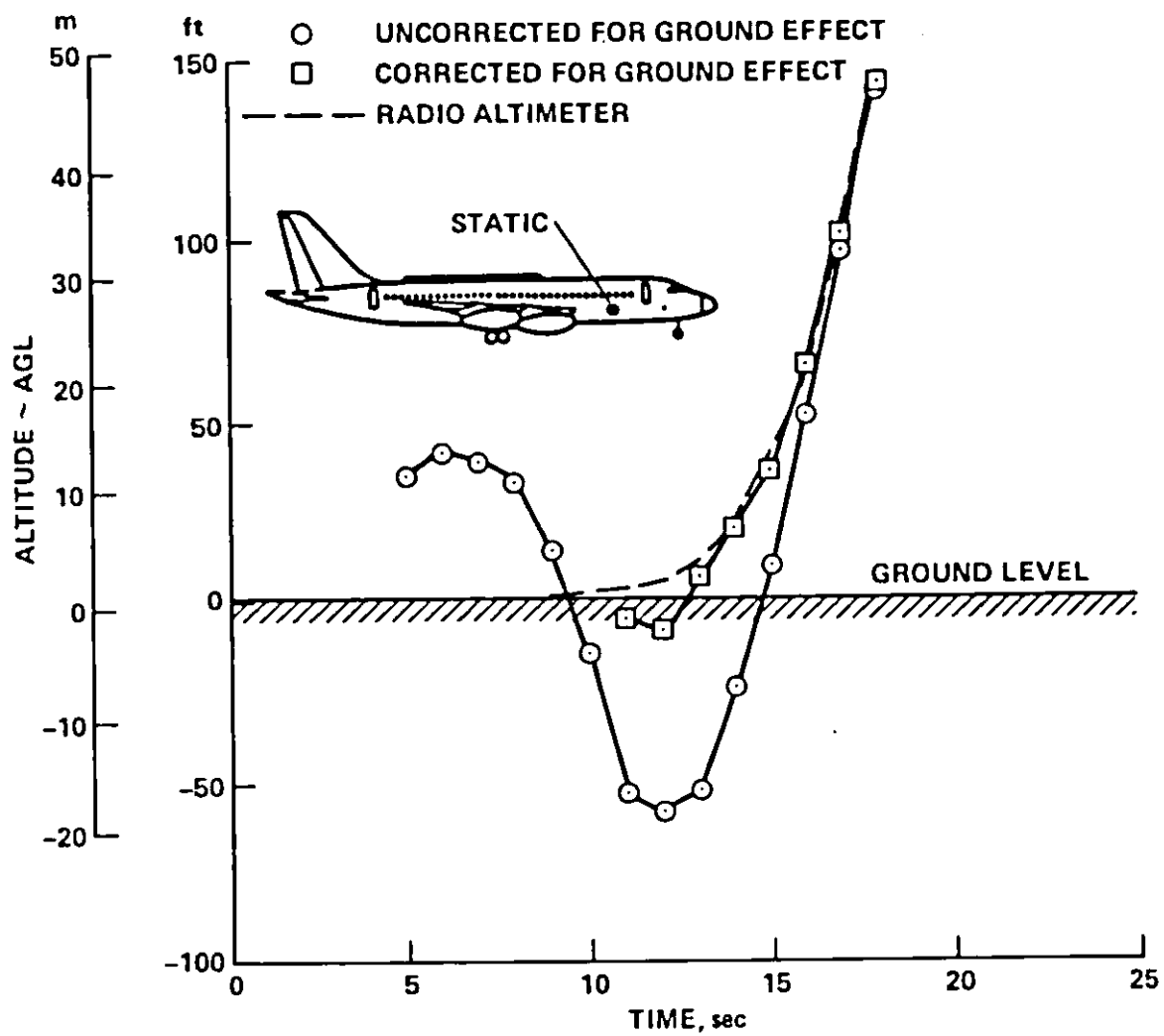
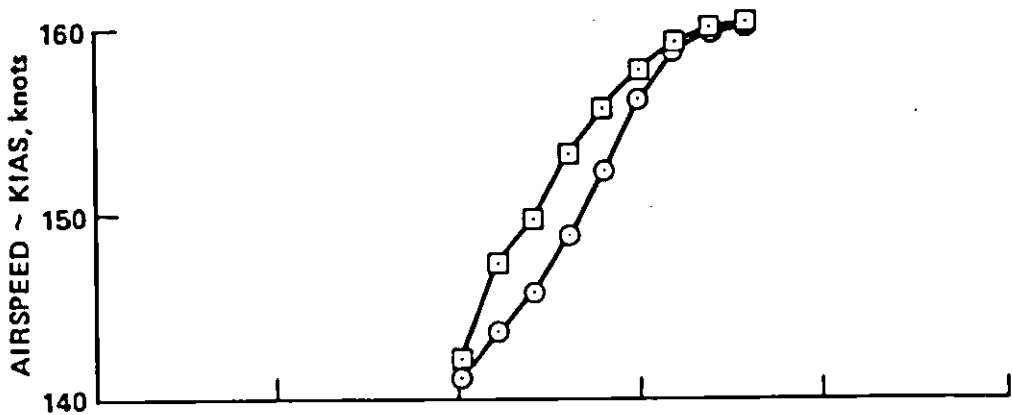


Figure 4.- CV-990 takeoff – altitude and airspeed time histories.

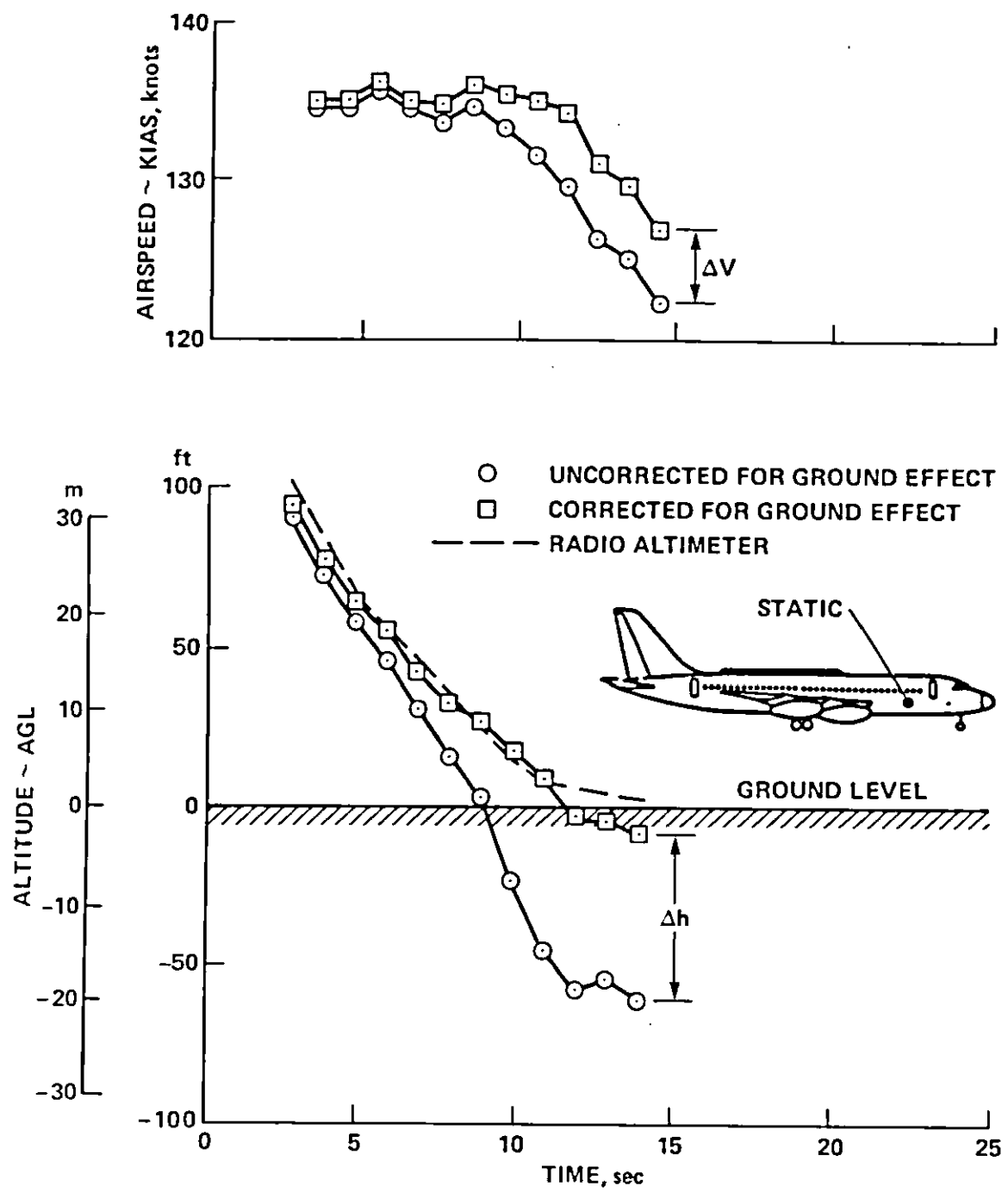


Figure 5.- CV-990 landing -- altitude and airspeed time histories.

TABLE 1.- LIFT, FUSELAGE, AND ENGINE CONTRIBUTIONS TO GROUND-EFFECT ERRORS IN ALTITUDE, AIRSPEED, AND DYNAMIC PRESSURE: CV-990 TAKEOFF

Wheel height (h), ft	Error contribution ^a								
	Lift		Fuselage		Engines		Total		
	Δh	ΔV	Δh	ΔV	Δh	ΔV	Δh	ΔV	$\Delta q/q^\infty$
2.6	-73.1	-5.7	+10.1	+0.8	+12.8	+1.0	-50.3	-3.9	-0.0536
18.9	-49.7	-3.7	+1.8	+0.1	+4.9	+0.4	-43.0	-3.2	-0.0420
66.9	-10.0	-0.7	+0.2	0	+0.9	+0.1	-8.9	-0.6	-0.0080

^ah in ft; V in knots.

TABLE 2.- LIFT, FUSELAGE, AND ENGINE CONTRIBUTIONS TO GROUND-EFFECT ERRORS IN ALTITUDE, AIRSPEED, AND DYNAMIC PRESSURE: CV-990 LANDING

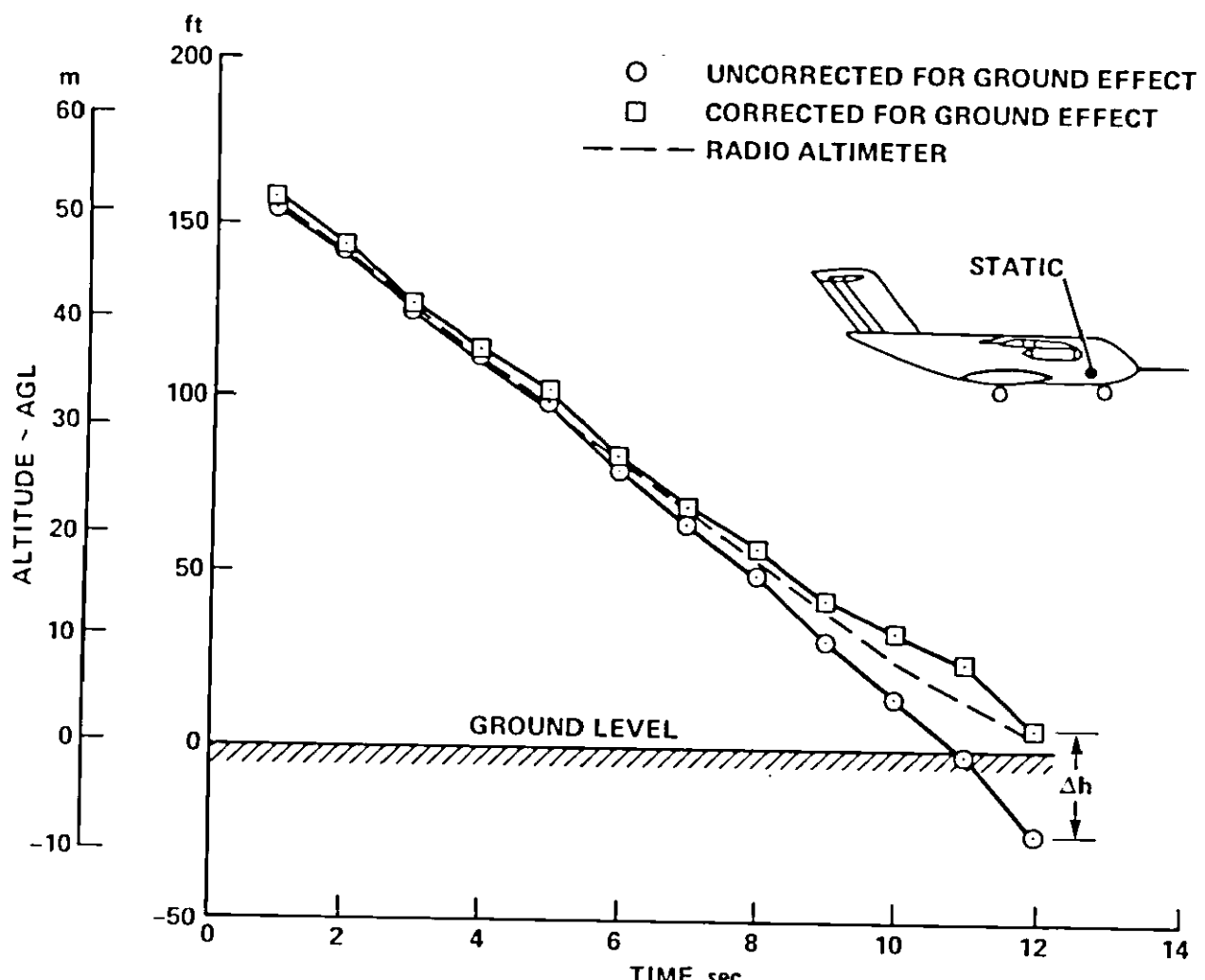
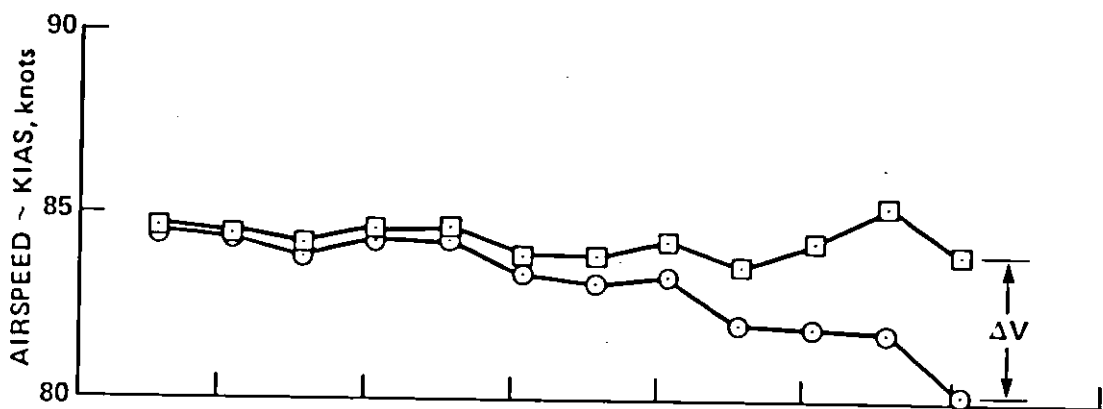
Wheel height (h), ft	Error contribution ^a								
	Lift		Fuselage		Engines		Total		
	Δh	ΔV	Δh	ΔV	Δh	ΔV	Δh	ΔV	$\Delta q/q^\infty$
66.5	-6.7	-0.6	+0.2	0	+0.3	0	-6.2	-0.5	-0.0076
25.1	-27.0	-2.3	+0.8	+0.1	+1.7	+0.1	-24.4	-2.1	-0.0310
4.8	-56.3	-5.1	+5.7	+0.5	+1.5	+0.1	-49.1	-4.4	-0.0706

^ah in ft; V in knots.

Figs. 6a and 6b. Tables 3 and 4 show the error contributions for the two orifice locations.

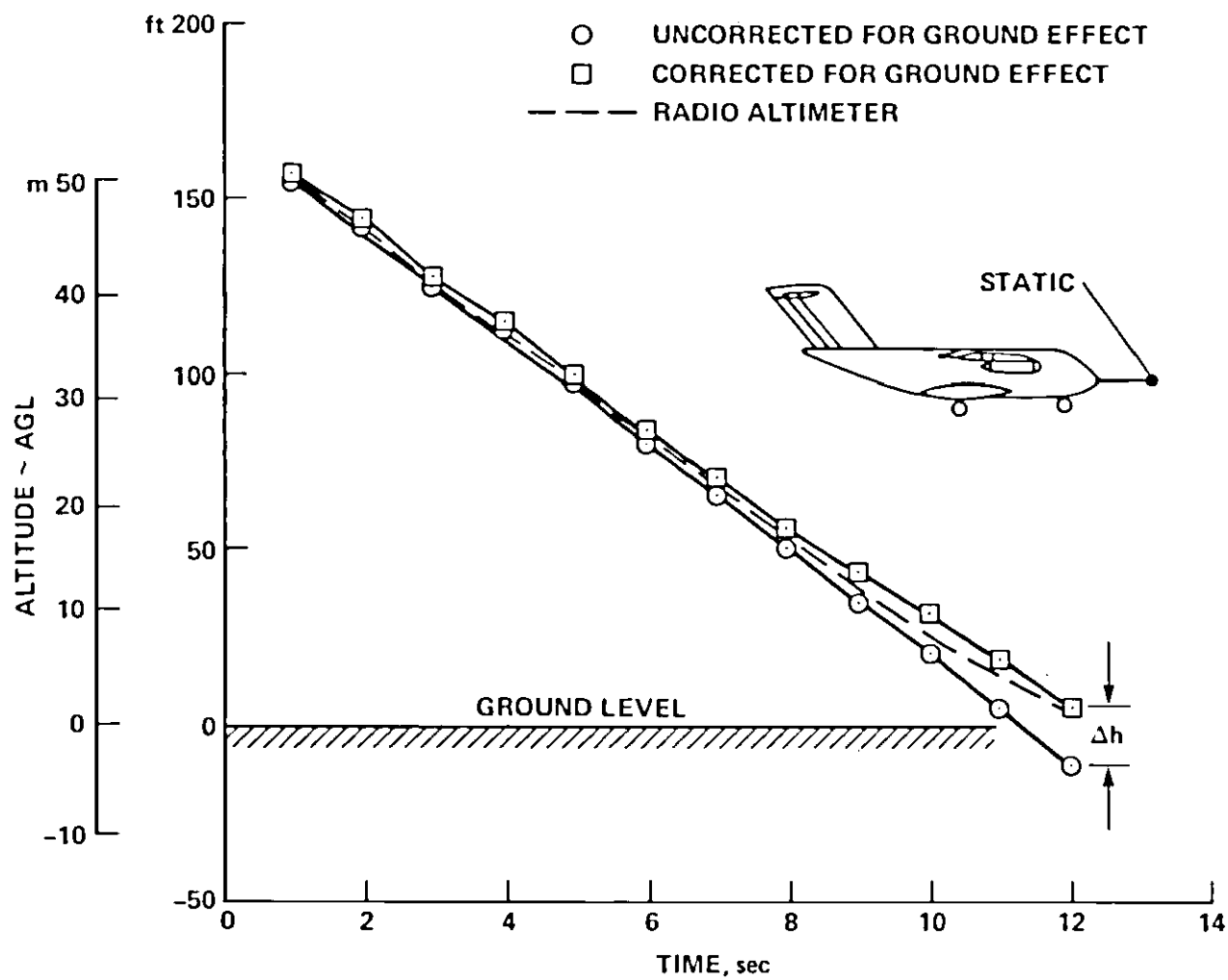
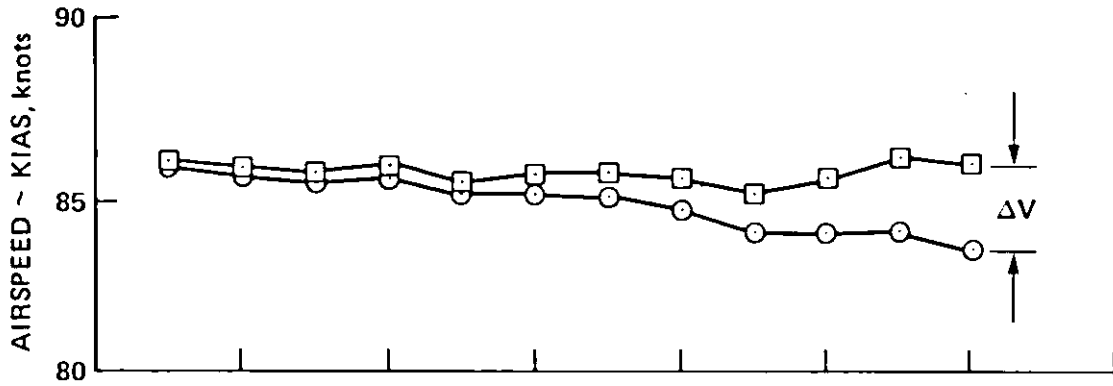
Comparing the two systems (fuselage vs boom), Fig. 6 and Tables 3 and 4, it is noted that boom-orifice measurements are less subject to ground-effect errors than those of the fuselage-orifice measurements. At a wheel height of 3.9 ft the altitude error, Δh , is -18.0 ft (Table 4) and -29.9 ft (Table 3) for the boom and fuselage systems, respectively. Also, note that the fuselage-error contribution shows a difference in sign between the boom and fuselage orifice locations. The distance X_F (see Fig. 2) has a positive value for the boom orifice and is negative in value for the fuselage orifice. Since the second term in the parentheses of Eq. (8) is dominant (i.e., $2X_F/d_F$) the fuselage-induced errors, Δh and ΔV , are negative for the boom orifice and positive for the fuselage orifice.

The lift increment produced by ground constraint ($\Delta C_L/C_{L^\infty}$) was measured at different wheel heights, using the method of Ref. 2; it is displayed in Fig. 7. Uncorrected as well as corrected airspeeds were used in the



(a) Fuselage static orifice

Figure 6.- YC-15 landing – altitude and airspeed time histories.



(b) Boom static orifice

Figure 6.- Concluded.

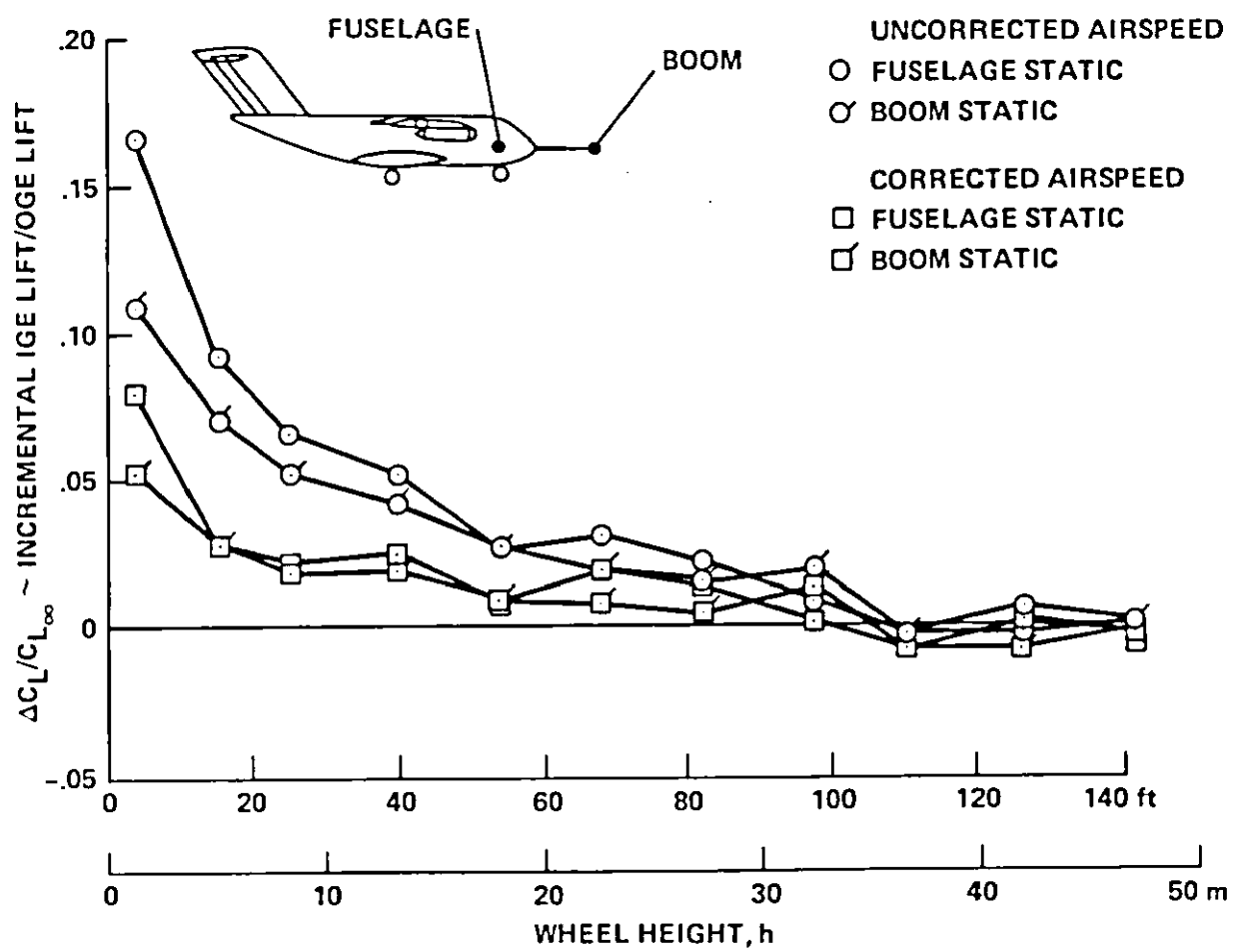


Figure 7.- Lift increment $\Delta C_L/C_{L\infty}$ in ground effect
versus wheel height: YC-15 landing.

TABLE 3.- LIFT, FUSELAGE, AND ENGINE CONTRIBUTIONS TO GROUND-EFFECT ERRORS IN ALTITUDE, AIRSPEED, AND DYNAMIC PRESSURE: YC-15 LANDING, FUSELAGE STATIC ORIFICE

Wheel height (h), ft	Error contribution ^a								
	Lift		Fuselage		Engines		Total		
	Δh	ΔV	Δh	ΔV	Δh	ΔV	Δh	ΔV	$\Delta q/q^\infty$
67.9	-5.9	-0.7	0	0	+0.2	0	-5.7	-0.7	-0.0166
24.9	-20.1	-2.5	+3.0	0	+1.7	0	-18.2	-2.3	-0.0548
3.9	-41.2	-5.2	+4.3	+0.5	+7.0	+0.9	-29.9	-3.8	-0.0940

^ah in ft; V in knots.

TABLE 4.- LIFT, FUSELAGE, AND ENGINE CONTRIBUTIONS TO GROUND-EFFECT ERRORS IN ALTITUDE, AIRSPEED, AND DYNAMIC PRESSURE: YC-15 LANDING, NOSE-BOOM STATIC ORIFICE

Wheel height (h), ft	Error contribution ^a								
	Lift		Fuselage		Engines		Total		
	Δh	ΔV	Δh	ΔV	Δh	ΔV	Δh	ΔV	$\Delta q/q^\infty$
67.9	-5.0	-0.6	-0.1	0	+0.3	0	-4.7	-0.6	-0.0150
24.9	-12.6	-1.6	-0.7	-0.1	+1.6	+0.2	-11.8	-1.5	-0.0382
3.9	-15.8	-2.0	-6.1	-0.8	+4.0	+0.5	-18.0	-2.3	-0.0590

^ah in ft; V in knots.

calculation of the lift coefficient. As pointed out by Eq. (3), errors in airspeed result in erroneous values of the lift coefficient. Referring to Ref. 7, the lift increment ($\Delta C_L/C_{L^\infty}$) due to ground effect, when calculated on the basis of the uncorrected fuselage airspeed, differs by a factor of 3 when compared with that based on corrected airspeed. This points out the serious errors that can result when airspeed data that have not been corrected for ground effect are used in the flight test measurements of the incremental changes in the aerodynamic coefficients induced by ground proximity.

Reconstruction of Time Histories for Accident Investigation - DC-10 Data

The data used in this illustration were recorded during the DC-10 takeoff accident in Chicago, May 25, 1979 (Ref. 3). In that situation, which is typical of many accidents, the problem is to reconstruct, from the barometric altitude record, the airplane's height above the runway and, from the recorded airspeed measurements, the aircraft's actual airspeed.

In this particular accident, one of the wing-mounted engines came off the aircraft at the time of rotation and lift-off. As discussed previously, each engine influences the airflow at the static pressure orifice. To account for the engine loss, the analysis was conducted in two steps.

First, the recorder altitude and airspeed measurements were corrected analytically for out-of-ground effect (OGE) position errors due to power effects; this was done by using Eq. (9), modified to reflect the influence of the "actual" engines on the velocity at the static orifice. Allowance was made for the loss of the wing engine at lift-off. Figure 8a shows the uncorrected recorder data and the data corrected for OGE position error.

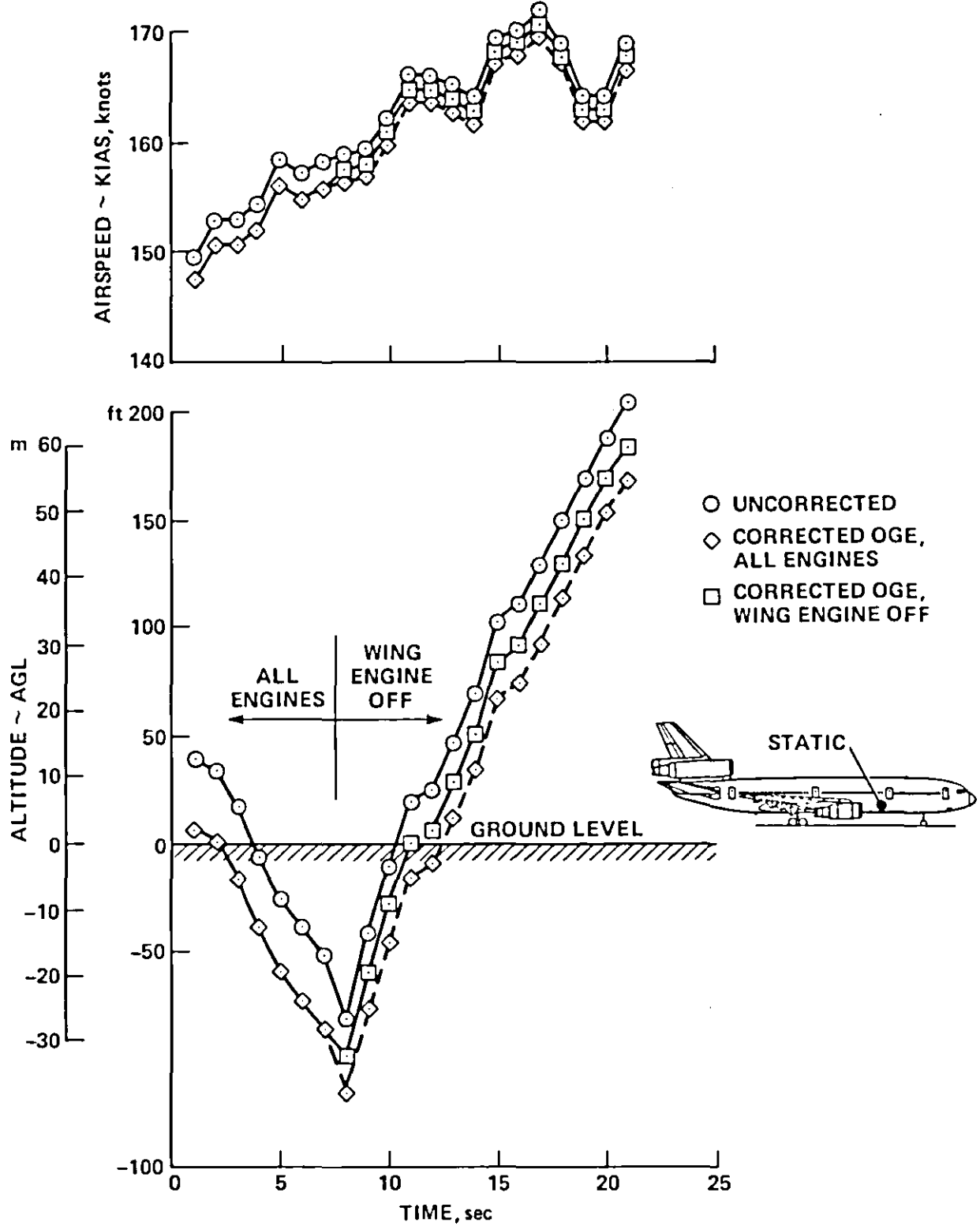
The next step involved solving simultaneously for two unknowns, the actual height, h , and the ground-effect correction Δh . The ground-effect corrections (Eqs. (7)-(9)) are dependent on the wheel height h , which was not accurately known initially; consequently, an iterative process was used for correcting altitude for ground-effect errors (in the absence of independent altitude measurements). Table 5 tabulates the ground-effect errors incurred during the ground roll, at lift-off, and at three subsequent wheel heights. The reconstructed altitude and corrected airspeed time histories are presented in Fig. 8b. In these data the altitude has been reconstructed for the time period prior to lift-off in order to provide some insight into the validity of the corrected altitude time history. During this time, when the aircraft was still on the runway, the results show that the reconstructed values are in good agreement with the actual value.

TABLE 5.- LIFT, FUSELAGE, AND ENGINE CONTRIBUTIONS TO GROUND-EFFECT ERRORS IN ALTITUDE, AIRSPEED, AND DYNAMIC PRESSURE

Time t, sec	Wheel height h, ft	Error contribution ^a									
		Lift		Fuselage		Engines		Total		Dyn. press., $\Delta q/q_\infty$	
		Δh	ΔV	Δh	ΔV	Δh	ΔV	Δh	ΔV		
1	0	-24.9	-1.8	11.5	0.9	25.5	1.9	12.1	0.9	0.0120	
7	0	-117.7	-8.2	11.3	0.8	23.3	1.6	-83.1	-5.8	-0.0736	
8	5	-121.9	-8.5	9.6	0.7	19.6 ^b	1.4 ^b	-92.8	-6.5	-0.0814	
10	24	-57.8	-3.9	3.8	0.3	4.3 ^b	0.3 ^b	-49.8	-3.4	-0.0418	
12	66	-15.6	-1.1	0.5	0	0.7 ^b	0 ^b	-14.4	-1.0	-0.0118	

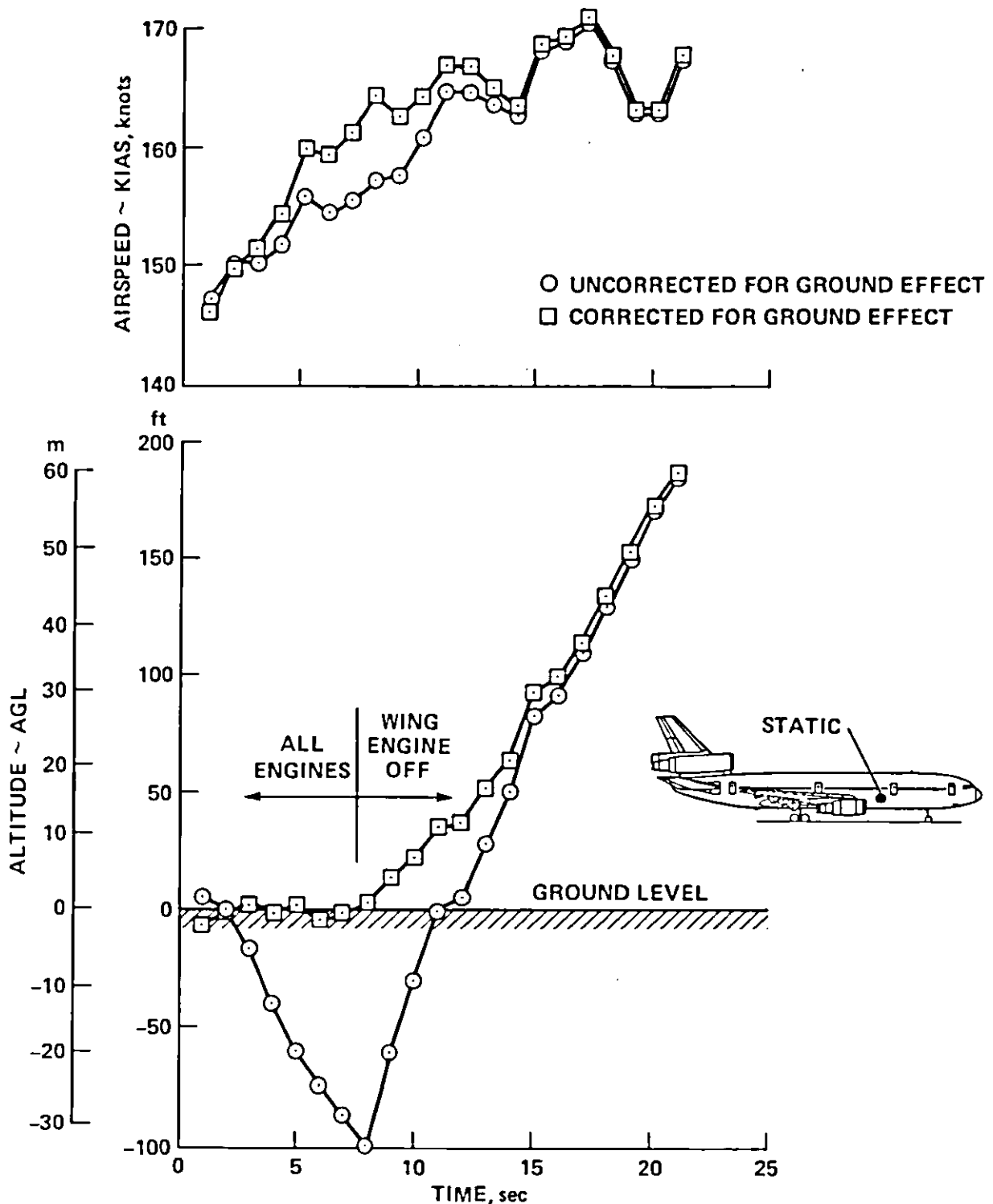
^a h in ft; V in knots.

^b Indicates one of wing engines is inoperative.



(a) Uncorrected recorder data and data corrected for OGE position error

Figure 8.- DC-10 takeoff – altitude and airspeed time histories.



(b) Data corrected for OGE errors and data corrected for IGE errors

Figure 8.- Concluded.

CONCLUDING REMARKS

Three sources of ground-effect error were identified and modeled. The primary error, termed the lift effect, results from the ground constraint of the wing lifting pattern. Smaller errors are induced by constraint of the flow over the fuselage and of the engine exhaust. Equations were derived for computing the three-error contributions; they are general and can be applied to airplanes of different geometries operating in different conditions.

The equations have been successfully applied to analyze measurements of airspeed and altitude for three applications where ground effect was significant. In addition to illustrating how the theory can be used to correct ground-effect errors, these applications also provide insight into the physical factors related to the incurrence of ground-effect errors. The results indicate that the corrected barometric altitude is in reasonably good agreement with independent measurements of the radio altimeter.

The flight test measurement of lift increments in ground effect, ($\Delta C_L/C_{L^\infty}$), were used to illustrate the distortion caused by the use of uncorrected airspeed. Finally, recorded data from a DC-10 takeoff accident were used to illustrate an application of the theory to the reconstruction of the altitude time-history.

APPENDIX A

The Biot-Savart Law

The velocity induced at a point P by a segment of vortex filament of strength Γ and vector length $d\ell$ is given by the equation

$$dw_B = \Gamma \frac{(d\ell \times \vec{r})}{4\pi r^3}, \quad (A1)$$

where \vec{r} is the vector distance between P and the vortex filament. This relationship is known as the Biot-Savart law (Refs. 4, 5, 11).

The magnitude of the induced velocity at P is

$$dw_B = \frac{\Gamma d\ell \sin \theta}{4\pi r^2} \quad (A2)$$

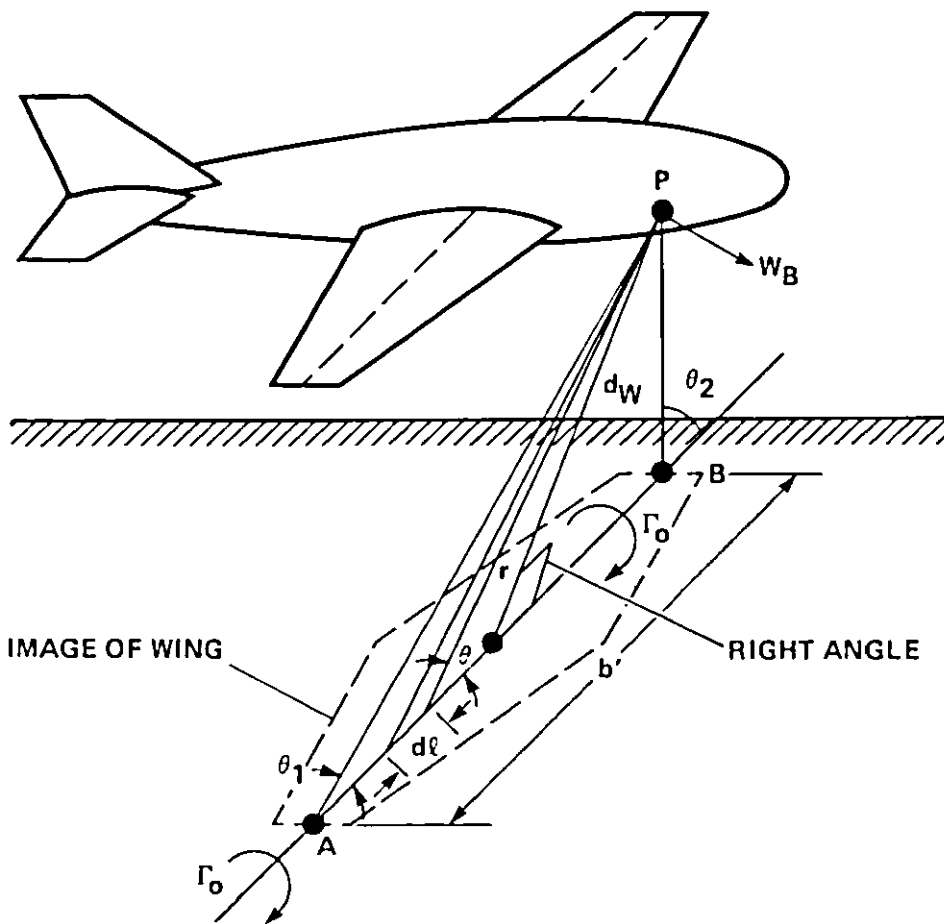


Figure 9.- Application of the Biot-Savart law to ground effect.

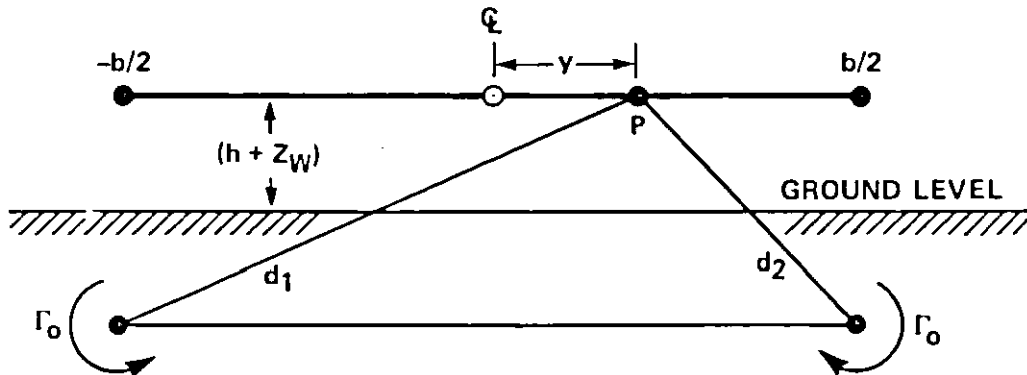
In Fig. 9, for the straight segment of vortex from A to B of constant strength Γ_0 , the induced velocity at P becomes, by integration,

$$W_B = \int_A^B \frac{\Gamma_0 \sin \theta \, dl}{4\pi r^2} = \frac{\Gamma_0}{4\pi d_w} (\cos \theta_1 - \cos \theta_2) \quad (A3)$$

$$W_B = \frac{\Gamma_0}{2\pi d_w} \frac{\frac{b'}{2}}{\left[d_w^2 + \left(\frac{b'}{2} \right)^2 \right]^{1/2}}$$

Spanwise Lift Distribution in Ground Effect

To account for the effect of ground constraint on the circulation in Eq. (A3), consider the reduction in downwash and the resulting change in sectional lift, ΔC_1 , induced by the image trailing vortices.



$$\Delta C_1 = a_o \Delta \alpha = \text{incremental change in sectional lift coefficient.}$$

where

a_o = sectional lift curve slope

$\Delta \alpha$ = change in angle of attack due to reduction of downwash

Applying the Biot-Savart law to point P at distance y from the centerline gives,

$$\Delta C_1 = \frac{a_o \Gamma_0}{4\pi V_\infty} \left\{ \frac{\left(\frac{b}{2} + y \right)}{\left(\frac{b}{2} + y \right)^2 + [2(h + z_w)]^2} + \frac{\left(\frac{b}{2} - y \right)}{\left(\frac{b}{2} - y \right)^2 + [2(h + z_w)]^2} \right\} \quad (A4)$$

The change in circulation is related to change in lift coefficient by

$$\frac{\Delta \Gamma}{V_\infty} = \frac{c}{2} \Delta C_1 .$$

Thus, the changes in circulation at the wing root ($y = 0$) and the wing tip ($y = b/2$) are,

$$\left(\frac{\Delta\Gamma}{V_\infty}\right)_{ROOT} = \frac{C_r}{2} \frac{a_0}{4\pi} \left(\frac{\Gamma_0}{V_\infty}\right) \frac{b}{\left(\frac{b}{2}\right)^2 + [2(h + z_w)]^2} \quad (A5)$$

and

$$\left(\frac{\Delta\Gamma}{V_\infty}\right)_{TIP} = \frac{C_t}{2} \frac{a_0}{4\pi} \left(\frac{\Gamma_0}{V_\infty}\right) \frac{b}{b^2 + [2(h + z_w)]^2}, \quad (A6)$$

where C_r and C_t are the root and tip chord lengths.

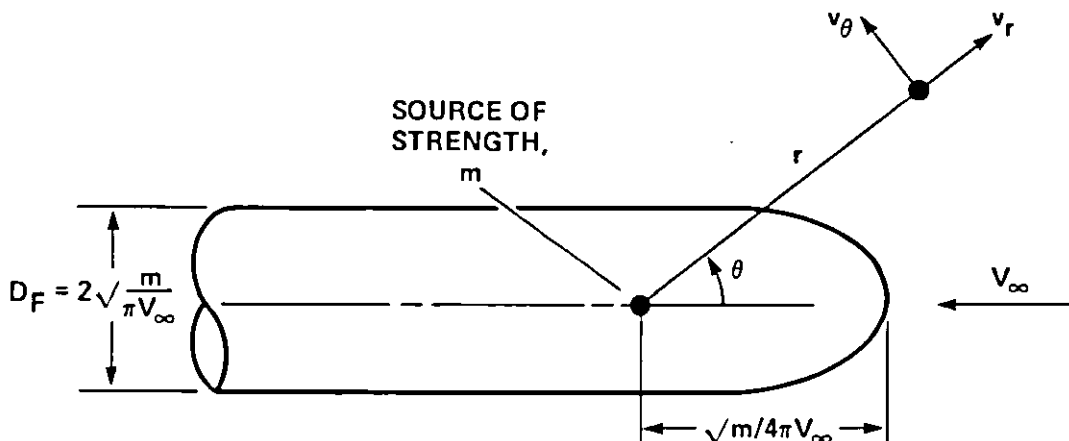
The ratio of the change in circulation at the root to that at the tip is,

$$\frac{\Delta\Gamma_{ROOT}}{\Delta\Gamma_{TIP}} = \left(\frac{C_r}{C_t}\right) \frac{1 + \left[\frac{2(h + z_w)}{b}\right]^2}{\frac{1}{4} + \left[\frac{2(h + z_w)}{b}\right]^2}. \quad (A7)$$

APPENDIX B

Flow Around a Semi-Infinite Body of Revolution

The stagnation streamline formed by placing a three-dimensional source of strength m into a uniform flow of velocity V_∞ represents, in potential-flow analysis, the flow over a semi-infinite body of revolution (Ref. 12, p. 322).



The velocity potential function in this case is,

$$\phi = \frac{m}{4\pi r} + V_\infty r \cos \theta$$

and

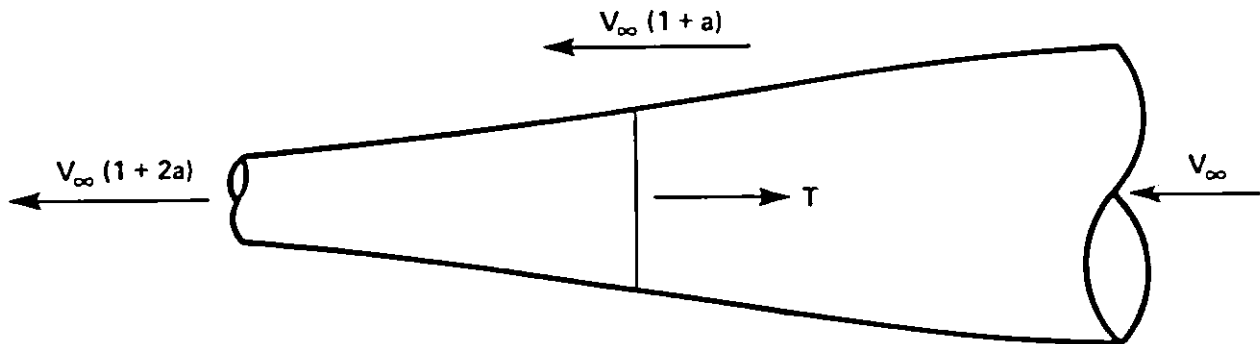
$$\left. \begin{aligned} v_r &= -\frac{\partial \phi}{\partial r} = \frac{m}{4\pi r^2} - V_\infty \cos \theta \\ v_\theta &= -\frac{\partial \phi}{r \partial \theta} = V_\infty \sin \theta . \end{aligned} \right\}$$

Radial and tangential velocity components

The diameter of the body of revolution far downstream is $D_F = 2(m/\pi V_\infty)^{1/2}$, and the forward stagnation point is a distance $(m/4\pi V_\infty)^{1/2}$, or $D_F/4$ upstream of the source.

APPENDIX C

Approximate Representation of Engine-Induced Flow



In the above sketch of the stream-tube of a thrusting propeller or other device, the velocity far upstream is V_∞ , and far downstream, where the flow has been energized by the propeller, the axial velocity is $V_\infty(1 + 2a)$ (Ref. 13). If the propeller is producing a thrust T , then, by the application of Newton's second law to the flow in the stream-tube,

$$T = C_j \frac{1}{2} \rho V_\infty^2 A_j = \rho A_j V_\infty (1 + a) 2a V_\infty ,$$

where C_j = the engine-thrust coefficient.

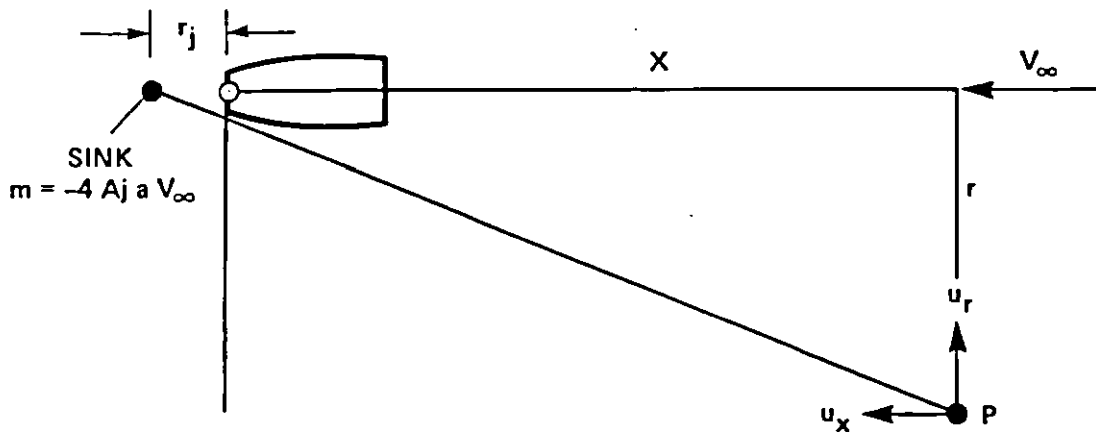
The above equation reduces to

$$4a^2 + 4a - C_j = 0$$

from which

$$a = \frac{-1 + (1 + C_j)^{1/2}}{2} \quad (C1)$$

A potential-flow representation of the flow upstream or downstream can be made satisfying conditions in the stream-tube. The upstream flow can be approximated by placing a sink of strength $4A_j a V_\infty$ at a distance r_j from the origin (Ref. 12).



The velocity potential function and velocity components are,

$$\begin{aligned}\phi &= V_\infty x - \frac{4A_j a V_\infty}{4\pi[(x + r_j)^2 + r^2]^{1/2}} ; \\ u_x &= \frac{\partial \phi}{\partial x} = V_\infty + \frac{A_j a V_\infty (x + r_j)}{\pi[(x + r_j)^2 + r^2]^{3/2}} ; \\ u_r &= \frac{\partial \phi}{\partial r} = \frac{A_j a V_\infty r}{\pi[(x + r_j)^2 + r^2]^{3/2}} ;\end{aligned}\tag{C2}$$

and

$$V = \sqrt{u_x^2 + u_r^2} \doteq V_\infty \left\{ 1 + \frac{A_j a (x + r_j)}{\pi[(x + r_j)^2 + r^2]^{3/2}} + \dots \right\} .$$

This expression for V results in the correct axial velocities far upstream ($x \rightarrow \infty$) and also at the origin where $V = V_\infty(1 + a)$.

Assuming $x \gg r_j$, the perturbation velocity at P is,

$$\left(\frac{\Delta V}{V_\infty}\right)_E = \frac{V}{V_\infty} - 1 = \frac{A_j a x}{\pi(x^2 + r^2)^{3/2}} \tag{C3}$$

Substituting for a and setting $A_j = \pi r_j^2$ where r_j is the radius of the jet-exhaust stream-tube at the engine,

$$\left(\frac{\Delta V}{V_\infty}\right)_E = \frac{(-1 + \sqrt{1 + C_j}) \pi r_j^2 x}{2\pi(x^2 + r^2)^{3/2}} . \tag{C4}$$

REFERENCES

1. Parks, E. K.; and Wingrove, R. C.: Flight-Test Measurements of Ground Effect - STOL Airplanes. Presented at the 8th Annual Symposium of the Society of Flight Test Engineers, Washington, D.C., Aug. 1977.
2. Parks, E. K.: Flight-Test Measurements of Ground Effect for Powered-Lift STOL Airplanes. NASA TM-73,256, 1977.
3. Aircraft Accident Report - American Airlines, Inc., DC-10-10. N 110 AA, NTSB Report No. AAR- 79-17, 1979.
4. McCormick, B. W.: Aerodynamics, Aeronautics, and Flight Mechanics. Chaps. 7 and 8, Wiley, New York, 1979.
5. Kuethe, A. M.; and Chow, C. Y.: Foundations of Aerodynamics: Basis of Aerodynamic Design. Chaps. 4 and 6, Wiley, New York, 1976.
6. Bollech, T. V.; and Hadaway, W. M.: The Low-Speed Lift and Pitching-Moment Characteristics of a Sweptback Wing of Aspect Ratio 8. NACA RM-L52K26, 1953.
7. Pearson, H. A.: Span Load Distribution for Tapered Wings with Partial-Span Flaps. NACA Rep. 585, 1937.
8. DeYoung, J: Theoretical Symmetric Span Loading Due to Flap Deflection for Wings of Arbitrary Plan Form at Subsonic Speeds. NACA 1071, 1952.
9. Ribner, H. S.: Field of Flow About a Jet and Effect of Jets on Stability of Jet-Propelled Airplanes. NACA ACR No. L6C13, 1946.
10. Squire, H. B.; and Trouncer, J.: Round Jets in a General Stream. R&M No. 1974, British ARC, 1944.
11. Bertin, J. J.; and Smith, M. L.: Aerodynamics for Engineers. Chap. 6, Prentice-Hall, New Jersey, 1979.
12. Karamcheti, K.: Principles of Ideal-Fluid Aerodynamics, Chap. 11, Wiley, New York, 1966.
13. Dwindell, J. H.: Principles of Aerodynamics. Chap. 13, McGraw-Hill, New York, 1949.

A Study of the Suitability of the
All Fiberglass XV-IIA Aircraft for Fuel
Efficient General Aviation Flight Research

George Bennett, Director
Raspet Flight Research Lab
Department of Aerospace Engineering
Mississippi State University
Mississippi State, Mississippi 39762

ABSTRACT

The impact of rapidly rising fuel prices upon future general aviation aircraft requirements is explored. The current configuration of the fiberglass XV-IIA aircraft is presented and it is shown that the aircraft can become a cost effective testbed for fuel efficient general aviation aircraft configurations. Several suitable research tasks for the aircraft are defined. A low cost method to produce master wing molds is proposed.

CURRENT GENERAL AVIATION AIRCRAFT DESIGN REQUIREMENTS

The rapid escalation of fuel prices from about \$.30/gal. to anticipated \$2.00/gal. in the immediate future has changed the design equation for general aviation (GA) aircraft. The cost of fuel now accounts for roughly 33% to 40% of the total operating cost of a GA aircraft, thus the aircraft fuel efficiency has become a very important parameter. The current general aviation aircraft fleet was designed before the large fuel cost increases, thus are not configured for the environment in which they must now operate. The GA situation is in danger of becoming analogous to the automobile market which the American manufacturers were configured for the large, low mpg models with disastrous results when the gasoline supply tightened and prices soared.

There has been some interest in fuel efficient aircraft configurations for some time, but the economics of aircraft manufacturing did not permit serious production. Figure 1 shows a configuration proposed by Raspet and Bryant of the Raspet Flight Research Laboratory (RFRL) in the middle 50's. This is an early low drag configuration which utilized an extended drive shaft to achieve a streamline body shape. In the early 1960's an all fiberglass turbine driven STOL aircraft, the XV-IIA, shown in Figures 2 and 3, was developed at the RFRL (Ref. 1, 2, 3). This configuration was the first powered aircraft to utilize fiberglass as the primary structure and to achieve low drag surface contours. The aircraft was flown for about 150 hours with no problems encountered with the extended shaft propeller drive system. Since the primary mission for the aircraft was to achieve high wing lift coefficients using suction boundary layer control to achieve high static thrusts using a shrouded propeller for short take-off distances, cruise fuel efficiency was not a major consideration.

The Lear Fan (Figure 4) is being developed using two currently available turbine engines in an extended shaft pusher configuration. This aircraft utilizes an advanced composite structure to achieve low drag and low structural weight (Ref. 4). This aircraft was chosen because it is well along in its development, but several other similar configurations are being proposed.

Two studies have been conducted by the MSU senior design class under the author's direction to investigate new directions in general aviation configurations. The Swift design, Figure 5, was a study to determine if 400 knot cruise speeds could be achieved for a small 4-place aircraft. It was found that if it was assumed that a 20% reduction of current values for engine sfc, structural weight, and aerodynamic parasitic drag were possible, that the goal was possible.

The Tumbleweed design, Figure 6, was a study conducted to explore the ultimate GA aircraft configuration. Variable sweep was proposed to be used to achieve pitch control at high lift coefficients. The aircraft has serious stability and control problems, but the rapid advances in avionics make such a concept feasible for the near future. The study assumed current state-of-the art structural weight, drag estimates, and non-supercharged reciprocating engine.

To show how these extended shaft pusher aircraft configurations can significantly improve general aviation aircraft fuel efficiency, a plot of passenger miles per pound fuel consumed is shown in Figure 7 for several aircraft. The current GA aircraft show a rapid decline in PM/lb with increasing cruise speed. The data for current aircraft was taken from Ref. 7. The fuel consumed included climb, cruise, and reserves for a typical GA mission.

The extended shaft configurations show a radical departure from the current aircraft. This characteristic signals a new era in aircraft design which is very similar to the large speed change brought on by the Learjet. It is most interesting that Bill Lear was instrumental in both of these GA aircraft developments, not the major airframe manufacturers. These new configurations appear to permit reductions in aircraft operating costs of about 20% which is significant. There are many problems to be worked out, but the state-of-the-art of powerplants, composite structures, and avionics have progressed to the point that such a radical configuration change as the extended shaft pusher can be seriously contemplated.

It should be pointed out in closing that the future of GA is far from bleak, even with current aircraft. The commercial airline rates are rapidly rising along with imposing a reduction in service. The RFRL has found that a Piper Twin Comanche serves as a very cost effective means of transportation. The University achieves significant travel account savings utilizing Piper Aztec aircraft.

CURRENT XV-11A CONFIGURATION

The XV-11A was developed as a testbed for STOL concepts in the early 1960's. It was an all fiberglass configuration to bring together the high lift and shrouded propeller technology under development at the RFRL into a high performance STOL light aircraft. The aircraft is shown in Figures 2 and 3 and details of its geometry are summarized in Table 1. The aircraft used an early version of the Allison light turbines, the T-63, with a prototype prop reduction gear box and an electric prop pitch control mechanism. A unique camber change flap was installed to improve the suction high lift characteristics. Figure 8 shows the details of the XV-11A construction. The auxiliary T-62 and the wing fuel tanks shown were never installed.

Since the aircraft was constructed early in the development of composite structures, only the fuselage floor is sandwich construction with the remainder of the aircraft conventional skin-stringer-rib construction of fiberglass. The fixed landing gear was suitable for the STOL task.

The wings were constructed in panels approximately 11 ft. long with conventional spars which attached to a carry-thru structure in the fuselage. This configuration allows easy removal of the wings and a wide range of wing planforms.

The aircraft was flown about 150 hours during the flight test program. The aircraft exhibited good handling qualities with the usual small problems of a low cost prototype. Full development of the aircraft was not achieved due to a shift of emphasis in Army R & D to helicopters. The aircraft has been inactive since 1970.

PROPOSED XV-11A CONFIGURATION

The author has been interested in utilizing the XV-11A as a research testbed for some time. Harned (Ref. 8) presented a paper which discussed ideas for fuel efficient aircraft configurations all of which were extended shaft pusher configurations. With this glimmer of interest from within the industry the author began to seriously look at the feasibility of modifying the XV-11A to become a testbed for the development of this new configuration for GA aircraft. The problem areas of the XV-11A considered were as follows:

1. Define a low drag configuration.
2. Determine preliminary performance characteristics.
3. Design a simple retractable landing gear system.
4. Determine the status of the power train.
5. Determine the integrity of the primary structure.

Figure 9 shows the proposed XV-11A for a fuel efficient research configuration. The propeller shroud has been removed and replaced with a conventional horizontal and vertical tail. It is proposed that the variable camber flaps be removed and a conventional single slotted flap used. The fuel will be placed in the wings using bladder tanks to eliminate the current fuselage fuel tank. The horizontal tail surface is attached at the bottom of the fuselage for installation simplicity, propeller protection, and to eliminate its wake from the propeller plane.

The performance characteristics of the modified XV-11A are most encouraging. The performance estimates were made using the following parameters.

Parameter	Conservative Estimate	Optimistic Estimate
C_{D_0} (drag coef.)	0.0162	0.0155
n_p (prop. eff.)	0.80	0.88
e^p (span eff.)	0.78	0.85

Figure 10 compares the estimated drag coefficient for the XV-11A with other aircraft. The small size of the XV-11A yields a very low equivalent flat plate area compared to other aircraft except the sailplanes. The sailplanes exhibit very low drags due to small fuselage areas and very smooth surface contours. The point might be made here that the sailplane manufacturing shifted to Europe when the European manufacturers adopted the fiberglass structure which increased the maximum L/D from 35 to about 50.

Figure 11 shows the aircraft maximum speed for two engine models which are dimensionally interchangeable. The aircraft is capable of about 300 knots with the high power engine. This speed yields a chord Reynolds number of 7.6×10^6 which is sufficient for airfoil developments. Preliminary range estimates show that the PM/lb performance, Figure 7, of the modified XV-11A is excellent in spite of the relatively high sfc and high value for the altitude power lapse rate of the Allison engine. This engine is configured for helicopters, thus, it is not optimum of high altitude cruise.

A simple retractable landing gear system has been devised for the XV-11A utilizing components from current aircraft. A Mooney nose gear was found to be useable. Figure 12 shows the main gear extended in a mockup. The main gear will be constructed using a Cessna spring steel gear and wheel/brake assembly. It was found that a rotation about a single axis could be used for this aircraft which is much simpler than other fuselage retraction systems. Additional structure will be required in the fuselage to maintain torsional stiffness around the main gear cutouts.

Since the T-63 was developed, Allison has upgraded the engine to 312 hp, and a 420 hp versions with the exterior dimensions remaining constant. The 250 B17C engine has a propeller gear box with a hydraulic prop pitch governor installed. For the extended shaft configuration the prop gear box is separated from the engine and installed in the aft fuselage. The engine installation is such that the prop shaft rotation is reversed which allows the utilization of conventional tractor propellers with a minor modification to the propeller shank.

The primary structure appears to be in excellent condition. The stringer/skin/rib construction allows easy inspection of joints and overall integrity. The large fuselage windows and doors in the fuselage must be divided into smaller segments for the high speed flight. Flutter speeds for the wing and fuselage are quite high - 600 knots.

RESEARCH TASKS FOR THE MODIFIED XV-11A

The author has reached the conclusion that the key impediment to the rapid adoption of composite structures is the high cost of constructing the master molds required for the initial prototype. In contrast to metal construction, the composite prototype aircraft requires high quality tooling. The staff of the Raspet Flight Research Laboratory are currently conducting an inhouse study to determine the feasibility of modifying the planer mill to be used to generate the master wing molds at a low cost. Figure 13 illustrates the concept. It is essential that the RFRL develop a low cost, rapid, method to generate the master wing molds to permit a wide range of experiments on the modified XV-11A and other aircraft. The short span of the XV-11A wing panel (11 ft.) will permit the rapid fabrication of experiments. The low power loading of the aircraft (6.67 lb/hp) permits a wide altitude-speed envelope.

The following fuel efficient GA aircraft experiments appear to be quite feasible and cost effective using the modified XV-11A.

1. Conduct a flight test program using the original wings sealed and modified to accomodate flaps and fuel. Define the aerodynamic drag parameters C_D , e , and propulsive efficiency, η , for the extended shaft pusher configuration. Explore the vibration and acoustic noise characteristics of the pusher propeller configuration. Define the effect of flap wake upon propeller vibration, noise, and efficiency. Define the control system/propeller interactions and handling qualities of the configuration.
2. Study the 2-D and 3-D characteristics of natural laminar flow airfoil sections. Explore the performance of the airfoils using the best possible full scale wing construction techniques. The first step would be to modify the shape of an existing XV-11A wing panel set. Then construct a complete wing using sandwich construction methods to achieve the best possible profile.
3. Study the 2-D and 3-D characteristics of slot and distributed suction laminar BLC systems. Verify concepts which can achieve significant laminar flow in an efficient manner. The aircraft performance change should be measurable. One wing panel could be built with a slot system and the other a distributed system. With this aircraft significant flight time could be acquired to define the operational problems with LFC, i.e., insect contamination, rain, etc.
4. Explore characteristics of this class of aircraft using significantly higher aspect ratios, i.e., greater than 10 and/or increased wing loadings. The fabrication techniques developed earlier would allow construction of these wings concurrently with airfoil development if interest warranted. Advanced structural materials would be used for spars and wing covers.
5. Demonstrate 2-D and 3-D characteristics of optimized multielement airfoil systems which have very low drag cruise characteristics

yet have high maximum lift coefficients with the flap extended. Verification of multi-element airfoil analysis programs and inflight measurements of turbulent b.l. including separated flows. A laser velocimeter can be mounted on the fuselage for these measurements.

A detailed study of the costs of various segments of the XV-11A development program are summarized as follows:

- | | |
|---|--------|
| 1. Initial XV-11A modification assuming a bailed C20 engine, and gloving current XV-11A wing to NLF profile | \$140k |
| 2. Master mold making machine assuming a bailed planer mill. | \$40k |
| 3. Prototype wings for XV-11A. Assume item 2 operational | |
| A. New wing (Natural Laminar Flow) | \$150k |
| B. New wing (Distributed Suction BLC) | \$200k |
| C. New wing (Slot Suction BLC) | \$250k |
| 4. Flight test costs. Assume 100-200 hrs/yr flight time also no major engine maintenance | \$36k |
| 5. Flight test support | \$35k |

These estimates do not include the cost of staff necessary to define and conduct the research program that the aircraft would support.

CONCLUSIONS

It has been shown that the extended shaft pusher GA aircraft configurations promise to yield greatly improved fuel efficiency. It has been proposed that the XV-11A aircraft can be modified to become a testbed for a wide range of flight test research to support the development of this new aircraft. The costs of building new wings and conducting flight test experiments are low using the XV-11A aircraft.

REFERENCES

1. Mertaugh, L. J., "XV-IIA Airplane Detail Specification", Aerophysics Department, Mississippi State University, May, 1967.
2. Roberts, S. C., et al, "XV-IIA Description and Preliminary Flight Test", Aerophysics Department 75, Mississippi State University, 1967.
3. Mertaugh, L. J., et al, "XV-IIA Flight Test Program", AASE Department 69-7, Mississippi State University, 1969.
4. Anon, "Lear Fan 2100, Description and Specifications", February, 1979.
5. Patrick, J., "The Swift Project", 1980 AIAA Bendix Design Competitions, May, 1980.
6. Pittman, J. L., et al, "Tumbleweed Project", 1975 AIAA Bendix Design Competition, May, 1975.
7. Anon, "1979 Planning and Purchasing Handbook", Business and Commercial Aviation, April, 1979.
8. Harned, M., "Industry Seeks Lighter Aircraft Weights", Aviation Week, May 21, 1979.

TABLE 1. XV-11A DESCRIPTION

Dimensions:

Span	26 ft. 2.5 in.
Length	23 ft. 3 in.
Height	8 ft. 6 in.

Weight and Loadings:

Maximum Takeoff Weight	2600 lb.
Maximum Wing Loading	24.5 lb./sq. ft.
Maximum Power Loading	10.4 lb./hp

Wing:

Aspect Ratio	6.5
Chord	4 ft. 10.2 in. on aircraft centerline, 3 ft. 2.8 in. at tip
Thickness/Chord Ratio	0.15
Dihedral	2 deg.
Incidence	1 deg. at root, -1 deg. at tip
Aileron Area	12.0 sq. ft.
Wing Area (Gross)	106 sq. ft.
M.G.C.	4 ft. 1.5 in.
Taper Ratio	.67
Sweep at 35-Percent Chord	0 deg.
Camber-Changing Span (Including Fuselage)	18 ft.
Aileron Span	3 ft. 6 in.
D Spar at 34.73-Percent Chord	
Wing Airfoil - Modified NACA 63615	

Tail Unit:

Duct	
Inside Diameter	5 ft. 6 in.
Chord	2 ft. 6 in.
Area	15.63 sq. ft.
Horizontal Tail Area	14.4 sq. ft.
Vertical Tail Area	7.3 sq. ft.
Incidence of Tail Unit	1.0 deg. (trailing edge up)

Power Plant:

A 250-horsepower T-63 gas turbine engine driving a two-blade propeller with electrically actuated pitch control. Engine is located in mid fuselage and drives the tail-mounted shrouded propeller through a 7-foot shaft and gearbox. Fuel tank, located under the rear seat position, has a 39-gallon capacity. Oil tank capacity is 7 quarts.

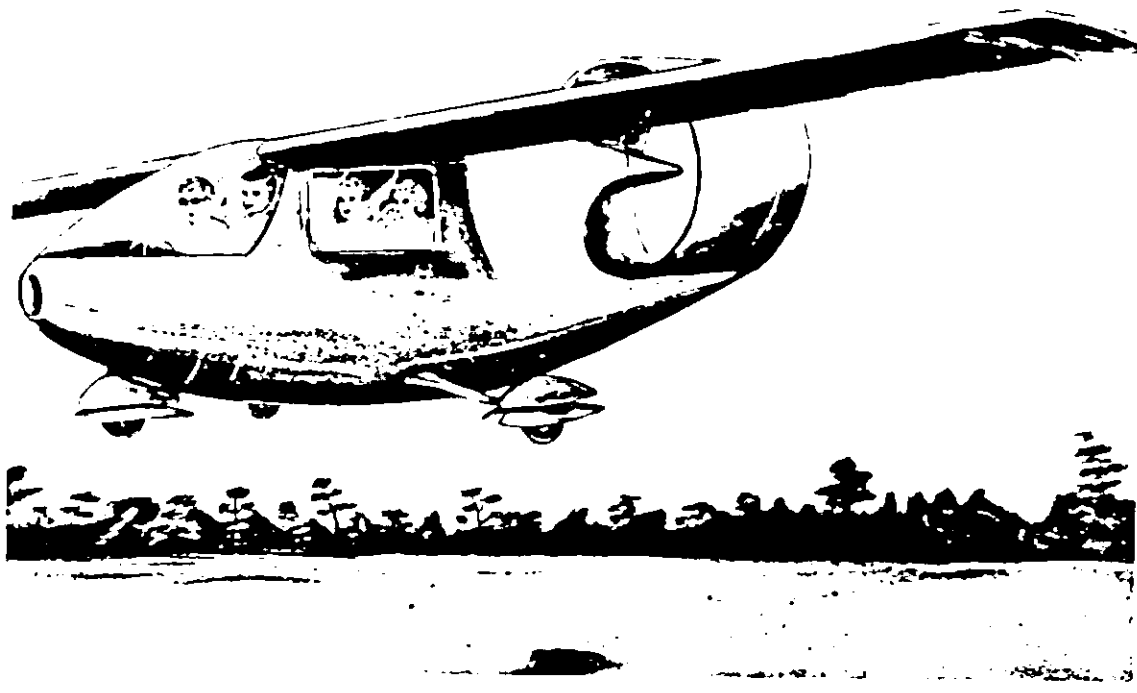


FIGURE 1: Fuel Efficient General Aviation Aircraft Proposed by Raspet and Bryant 1950's.

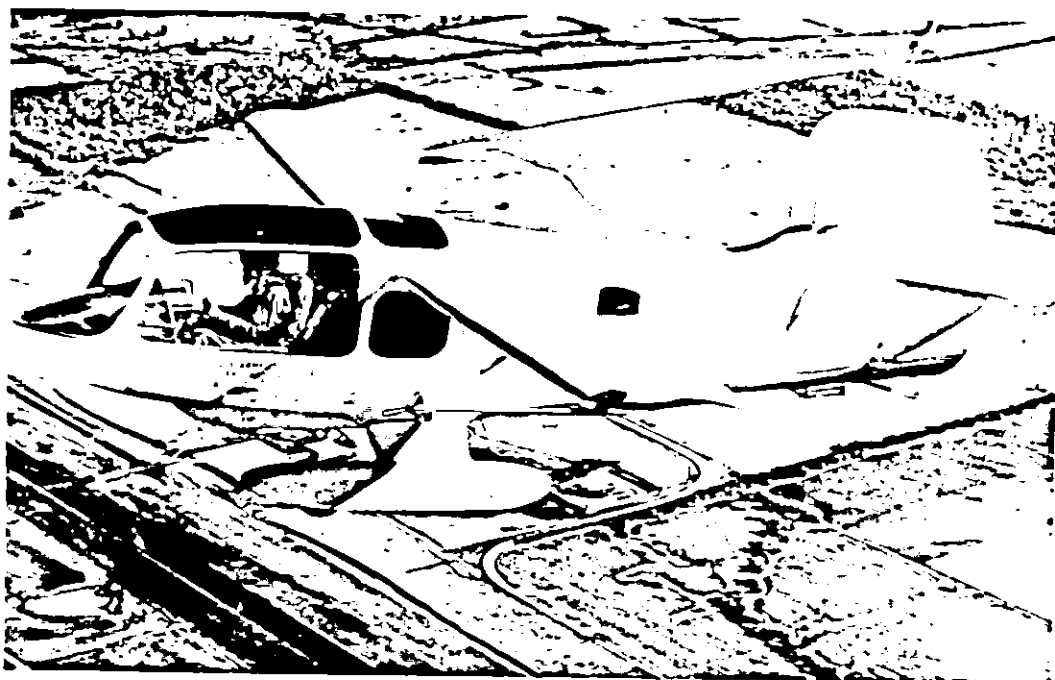


FIGURE 2: XV-11A STOL Research Aircraft

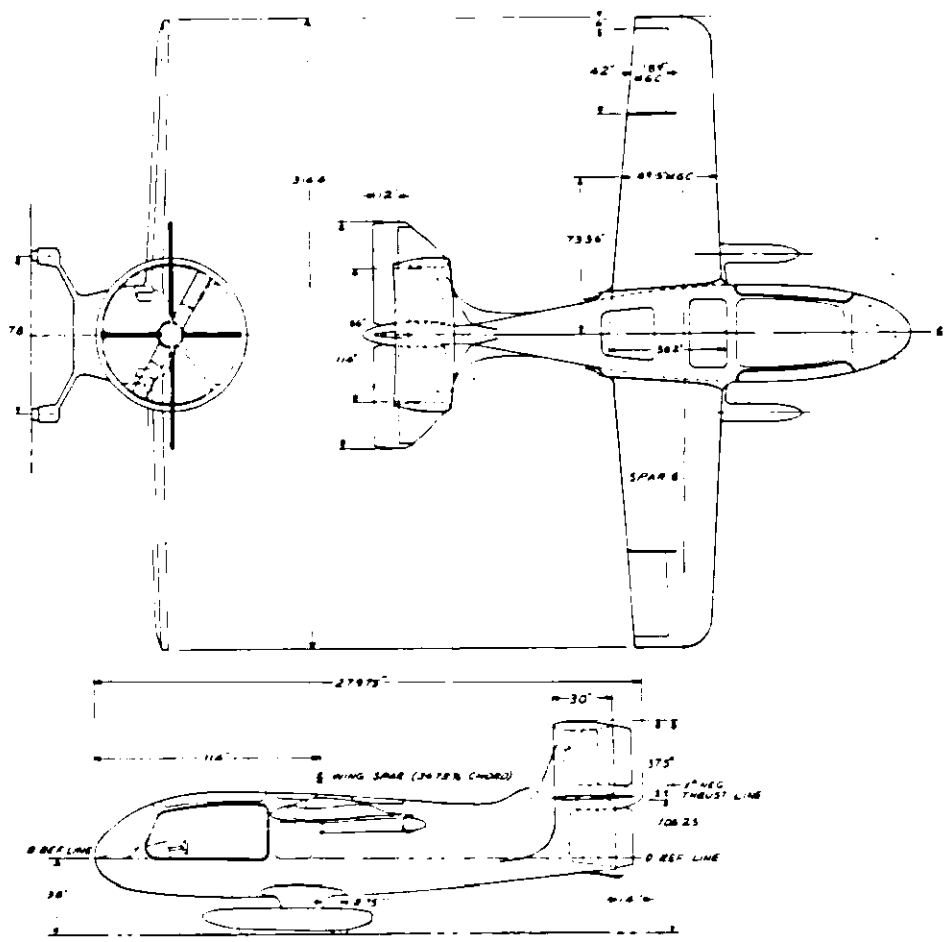


FIGURE 3: Three View of XV-11A

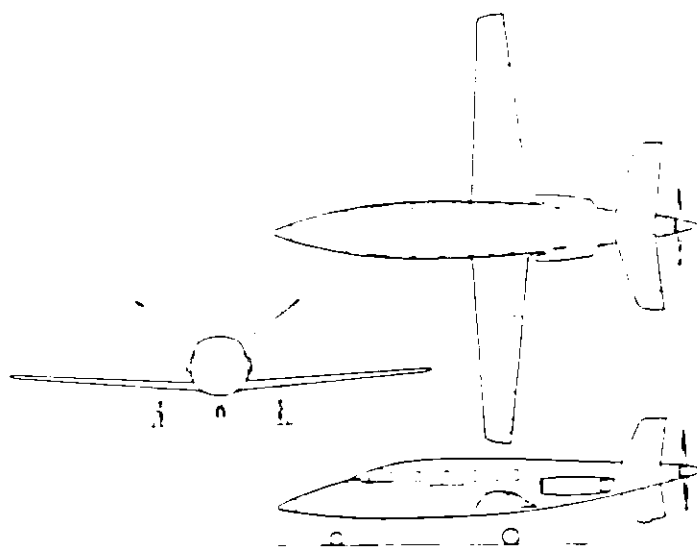


FIGURE 4: Lear Fan 2100

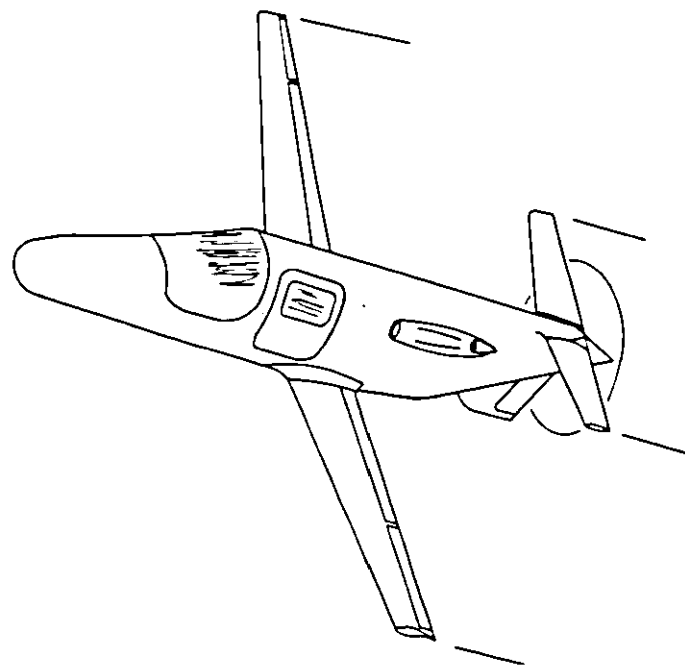


FIGURE 5: Swift High Performance 4-Place Aircraft

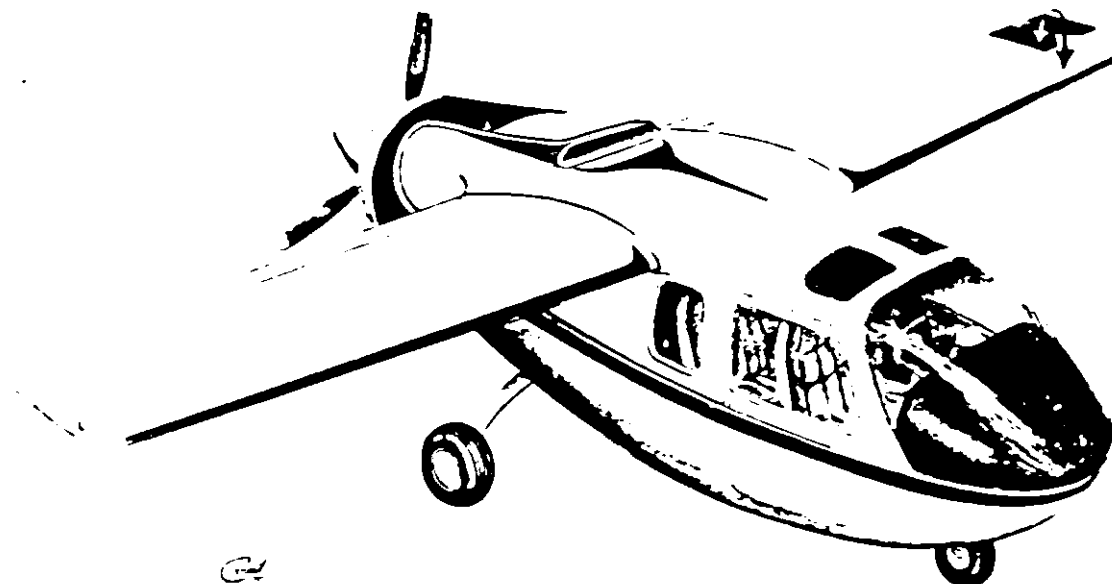


FIGURE 6: Tumbleweed High Performance 4-Place Aircraft

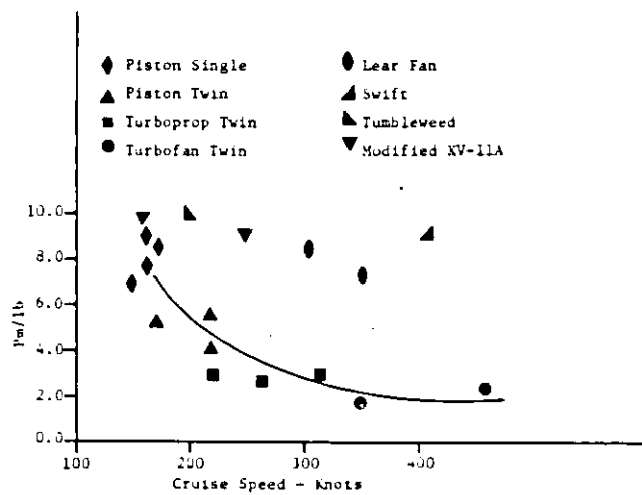


FIGURE 7: Passenger Nautical Mile Per Pound Fuel Versus Cruise Speed

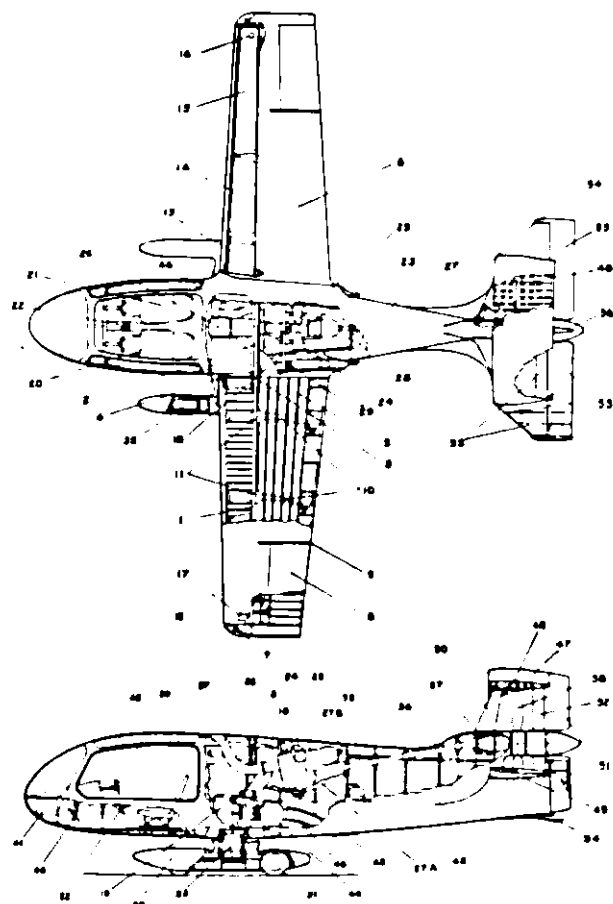


FIGURE 8: Details of XV-11A Layout

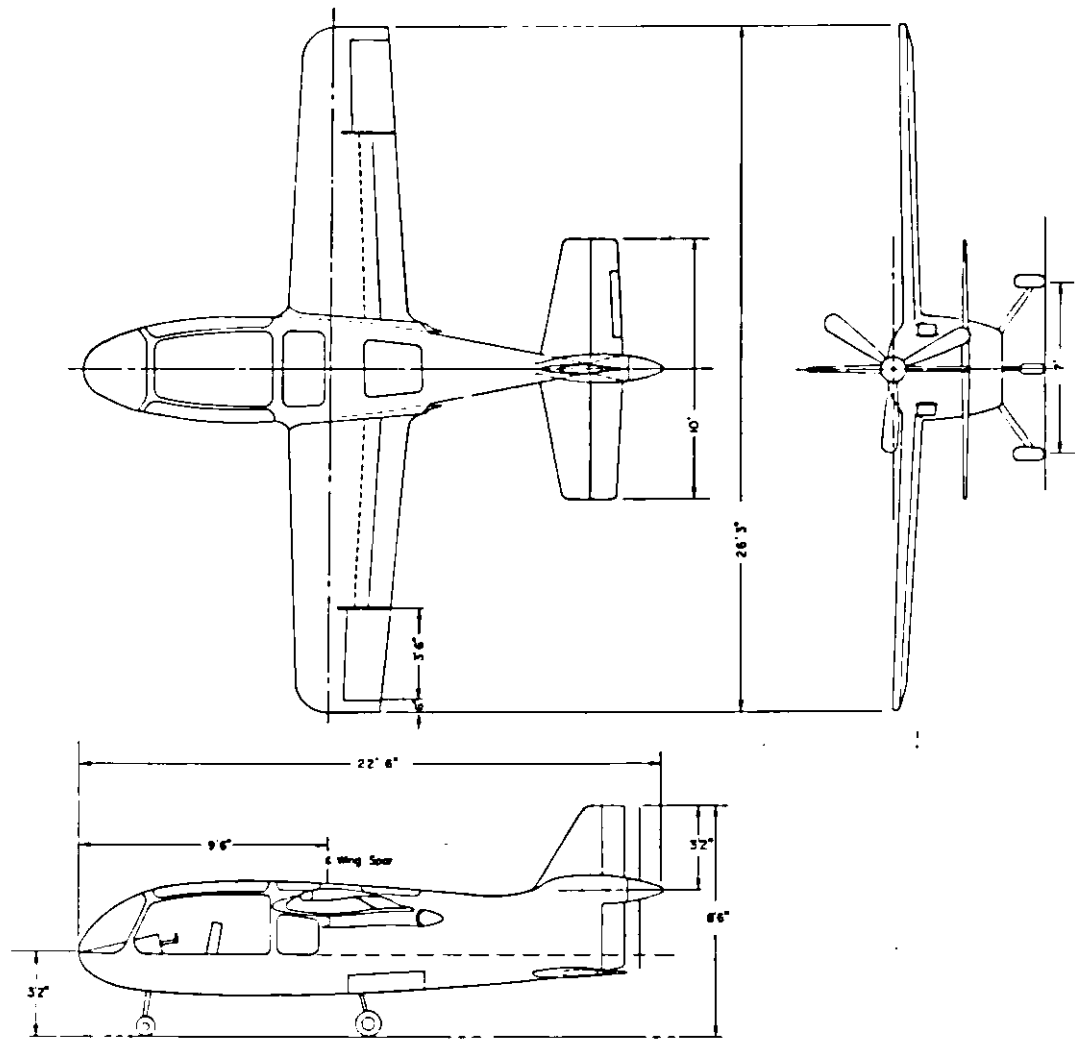


FIGURE 9: Modified XV-11A for Fuel Efficient Configuration Research

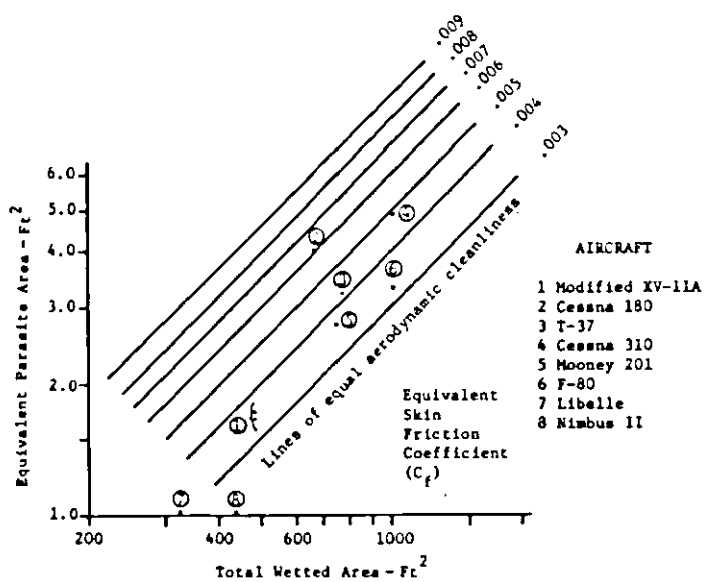


FIGURE 10: Comparison of Parasitic Drag for Several Aircraft

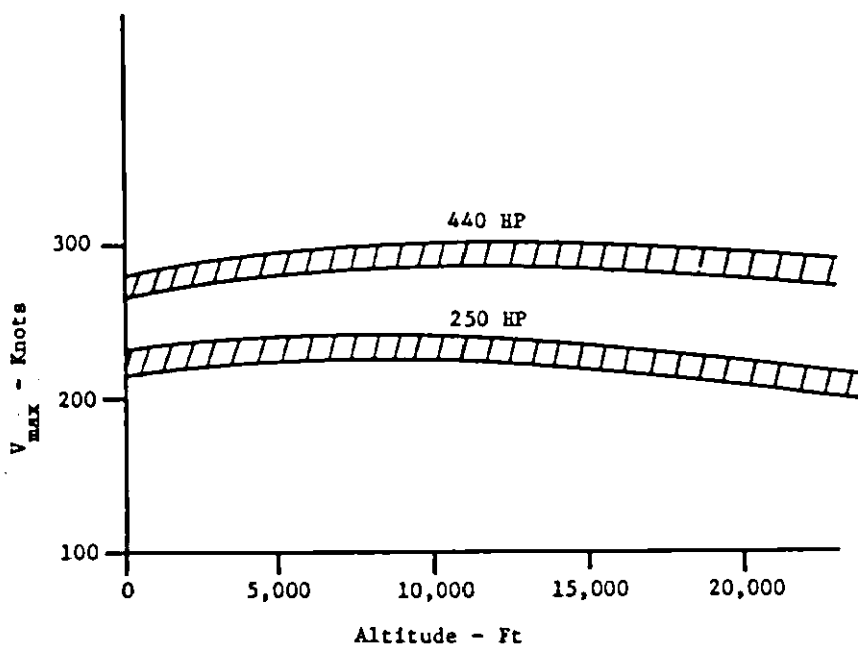


FIGURE 11: Modified XV-11A Estimated Maximum Speed

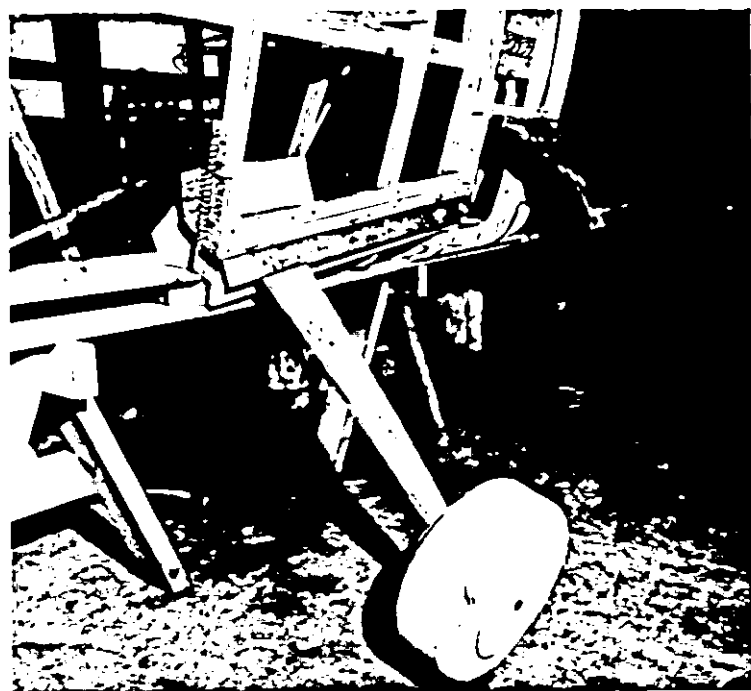


FIGURE 12: Mockup of Retractable Main Gear for XV-11A

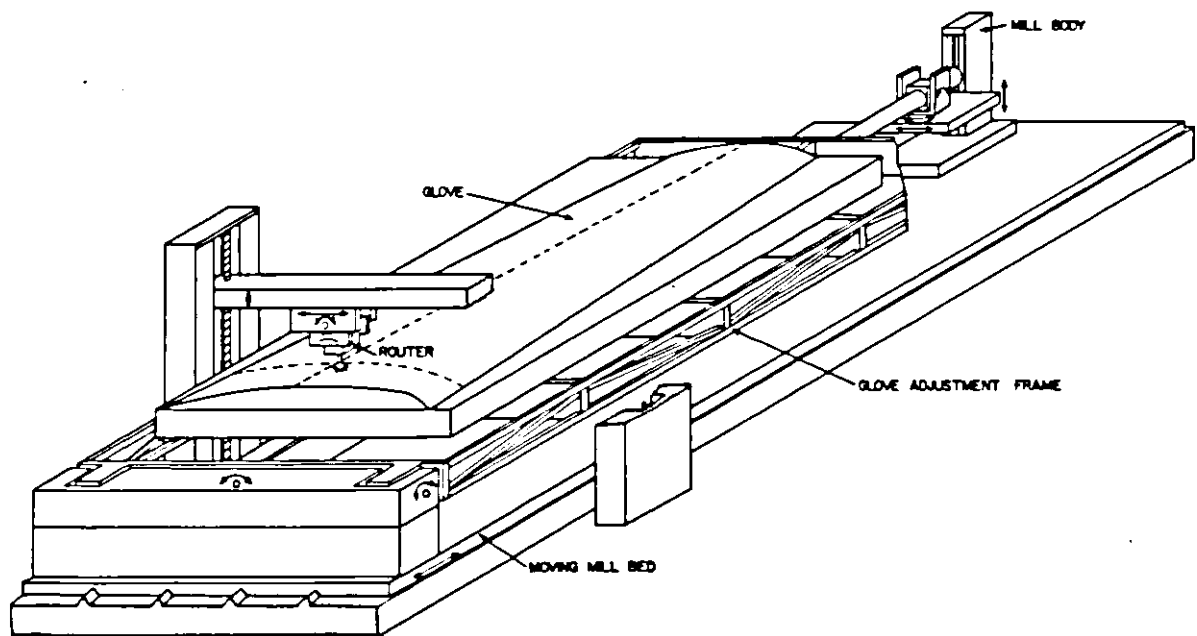


FIGURE 13: Proposed Planer Mill Setup to Produce Master Molds

A COMPREHENSIVE FLIGHT TEST FLYOVER NOISE PROGRAM

James W. Vogel
Engineering Flight Test
Lockheed California Company

ABSTRACT

Flyover noise testing is now an important part of the function of Flight Test organizations everywhere both because of the requirements of Federal Aviation Regulations (FAR), Part 36 - "Noise Standards: Aircraft Type and Airworthiness Certification", and of an increased public awareness of aircraft noise. Because of the large costs involved in flight testing it would be extremely advantageous to be able to predict flyover noise levels based on static tests.

This paper discusses some of the questions that must be answered in order that these predictions be made with acceptable accuracy. In addition, a test program is described which was conducted by the Lockheed-California Company and Rolls-Royce Limited in order to develop the required techniques and instrumentation and to acquire the data needed to answer the questions alluded to above. Some preliminary results of this program are also presented.

I. INTRODUCTION

It is almost a truism to say that noise makes news these days. Airports are awash in law suits, military bases get numerous complaints, and airframe and engine manufacturers are under great pressure to produce a quieter product. In the civil aviation field the law requires that certain categories of aircraft make no more than specified amounts of noise. For example, Federal Aviation Regulation (FAR) Part 36 sets the limits as shown in Figure 1 for subsonic transport category large airplanes and turbojet powered airplanes and in Figure 2 for propeller driven small airplanes (Reference 1).

In addition to the requirements of FAR Part 36, there are numerous airports with curfews, preferential runways, and, especially in Europe, individual airport noise requirements that may include monitoring.

James W. Vogel, Research Specialist Senior - Flight Analysis Department - Engineering Flight Test

Acknowledgement is hereby given to Rolls-Royce Limited for their conception and implementation of this program. Appreciation is also expressed for their support in the preparation of this paper.

All of the above is by way of saying that noise is an important part of flight testing today and promises to become even more important tomorrow. Thus Flight Test organizations everywhere are finding it necessary to conduct expensive and time consuming programs not only to certify the airplane initially and/or meet specific customer requirements but also to develop the data base and test techniques necessary to allow for product growth and to reduce future test time and costs.

The certification requirements are specific and all of us understand, for the most part, what is required. What is not so clearly evident, however, is the necessity to develop a data base from which future models of a particular aircraft may be certified, e.g., one of increased gross weight, one that is stretched, one that is shrunk, etc. Also, the requirement to support customer requests for expanded data relative to noise at different flap settings, climb-out procedures, etc. must be satisfied.

A further demand upon Flight Test is that of being able to certify an aircraft when the engine manufacturer makes changes in the engine. The Federal Aviation Administration (FAA), and the customer, hold the airframe manufacturer responsible for the noise (or at least most of it) but the airframe manufacturer must certify it and/or demonstrate compliance with customer guarantees. Thus, if an engine manufacturer increases an engine's thrust, or changes acoustic treatment, or makes any one of an infinite number of possible modifications, the airplane manufacturer must show compliance with FAR 36. This is not to say that this is unfair. This is just to say that the responsibility of showing compliance with FAR 36 rests with the airframe manufacturer.

It is clear then that there are many requirements for flyover noise testing today. Perhaps the easiest of these to understand is that dealing with the actual certification testing itself. FAR Part 36 delineates in great detail what is required in this case (Reference 2, for example). As previously mentioned, the testing required to develop a data base for future certification, customer requirements, and engine modifications is nowhere clearly defined, however. It is just such a flight test program involving the Lockheed L-1011 TriStar and the Rolls-Royce RB.211 engine that will be discussed in subsequent sections of this paper (Figure 3).

II. TEST PROGRAM

II.1 Background and objectives

As the Rolls-Royce RB.211 engine has progressed over the years, numerous changes have been made to different components of the engine. Many of these have had an effect on the certified noise levels of the L-1011 although these effects have not always been easy to assess. One of the reasons for this difficulty is the way in which the noise levels from the different engine components, e.g., fan bypass, core, primary jet, etc., combine to produce the total engine noise spectrum. Figure 4 illustrates the situation. If one of the lesser components is modified then the result will be that there is little or no effect on the

spectrum. If, however, one of the greater contributors is changed then the effect can be considerable. Part of the problem is to know the contribution of the individual components. What one generally measures is the total spectrum. Hence, it would be extremely advantageous to be able to sort out the contributions of the separate sources. These advantages accrue not only from being able to identify those sources that significantly influence the engine's noise spectrum, and those that are weak contributors, but also from being able to identify those sources where acoustic treatment or design can be applied most effectively. This knowledge and ability would be extremely useful in discussions with the FAA vis-a-vis the effect on noise certification of engine modifications and, also, in cost-effective engine design relative to noise.

In addition to the problem of the contribution of the several propulsive sources to the noise spectrum, there are airframe effects themselves to consider. Of considerable interest today is the aerodynamic noise (sometimes called "self-noise") of the airframe, i.e., the noise generated by the airflow over the surface of the wings, fuselage, flaps, landing gear, etc. (Reference 3, for example). This non-propulsive noise represents a so-called "floor" below which the noise cannot be reduced without an extensive redesign of the airframe. This can be seen by referring to Figure 4 which shows how the noise from individual components combines into the resultant noise spectrum. Even if the propulsive noise were reduced to less than the aerodynamic noise we would still have the problem of reducing the noise of the airframe/engine system, in this case dominated by aerodynamic noise. The state of the art is such that it could not be done, e.g., we don't know how to make the landing gear quiet. This hints at the importance of knowing the value of this floor in as much as there is little to be gained by setting noise requirements that are lower than this floor because they could not be attained even by the total elimination of the propulsive noise contributions and we certainly have not accomplished this yet!

Related to the self-noise problem is that of the impingement of the primary jet flow upon the flaps. Specifically, one wants to know if, in addition to the aerodynamic noise undoubtedly produced by the flaps, there is an additional noise source caused by the high velocity jet flow striking the flaps. If so then this is yet another area of the total noise signature that will be unaffected by acoustic treatment.

One further item requires mentioning and that is the effect of forward velocity on the noise (Reference 4). Engine manufacturers, out of necessity, acquire most of their data from static tests. These data are then input to the next design cycle and so on. It is important then that these static results carry over to the flight testing that will ultimately occur. If the effect of forward velocity produces noise signatures significantly different from those obtained statically then one could make erroneous decisions based upon such static tests. Thus one wants to know if there is a significant influence due to forward velocity on propulsive noise and, if so, how to predict it.

Based on the above problems and considerations it became clear that both Rolls-Royce and Lockheed had much to learn from a comprehensive flight test program investigating some of the aforementioned problems utilizing the L-1011 airframe and the RB.211 engine. Accordingly, such a program was devised and carried out. The details follow. It should be noted that in addition to the questions that the program was designed specifically to investigate, advantage was taken of the opportunity presented to study the effects of meteorological conditions and microphone placement on the data. Meteorological data were acquired by a tethered balloon complete with telemetry, an instrumented light airplane, and the test L-1011 itself. Temperature, relative humidity and wind speed and direction were also acquired at the conventional ten meters.

Microphone placement can effect the results primarily through the cancellation/reinforcement phenomenon due to the direct and reflected acoustic ray. To investigate this, microphones were mounted at ground level; at 1.2 meters (FAR 36 height) and at ten meters (Reference 4).

II.2 Tests Conducted

The test program itself was as shown in Figure 5. Note that Runs 1-14 and 17-25 were planned in order to determine the effects of aircraft speed on engine noise over the approach-power-to-takeoff-power range of the engine. Airframe noise was minimized by flying clean, i.e., flaps, slats, and gear up. Altitude over the center of the microphone array was also held constant (except for Runs 22 and 23) in order to minimize corrections to the data. Runs 22, 23 and 24 (conducted at a constant airspeed) serve as a check on the validity of the atmospheric absorption corrections applied to the data. Data measured at 300 and 600 feet can be corrected to 900 feet, for example, and compared with the results actually measured from the 900 foot flyover.

Runs 15 and 16 were designed to investigate the influence of flaps on the noise signature. Note that Run 16 was performed with all engines at flight idle and hence is a first measure of the contribution to the aerodynamic noise signature made by the flaps.

Runs 16, 26, and 27 had as their purpose the investigation of the self-noise generated by flaps and/or landing gear. Again, note that all engines were at flight idle.

Run 28 is a typical approach configuration.

It should also be pointed out that from Runs 24 and 25 an estimation of the installation effects can be made. The number two engine is tail-mounted with an S-duct on the L-1011 and the number one and number three engines are mounted in pods under the wings (Figure 3).

II.3 Test Procedures

Each condition was flown at least twice, i.e., until we had obtained two acceptable runs from the standpoint of the acoustical data, the aircraft speed and altitude, the engine power setting, and the meteorological conditions speed. Note that the restraint on speed was \pm 5 knots and on altitude \pm 50 feet. The weather conditions had to comply with the requirements of FAR 36, Amdnt 9, plus no temperature inversion. These are as shown in Figure 6.

The testing was accomplished at the Lockheed Flight Test Center in Palmdale, California. Figure 7 is an aerial view of the site. The passes were all made in one direction to simplify the procedure, as well as to aid in the integration of the light airplane (used for meteorological purposes) into the pattern. Two "marks" were given to the aircraft (via radio) from the ground:

- 1) One at the point of overhead of the microphone array in order to allow the crew to assess speed and altitude relative to the target values.
- 2) One at the end of each test run at which point engine power settings, aircraft ground track, etc. could be changed.

Speed and power were set by a geographic landmark, visible from the aircraft, and a mark was transmitted from the aircraft at this point. On the ground a stopwatch was started upon receipt of this mark. At the overhead mark the elapsed time between the marks was noted and this amount of time was allowed to transpire prior to transmitting the end-of-test mark. This insured that there would be sufficient data at constant speed and engine power, both before and after overhead, to perform the planned analysis.

Because the effect of airspeed, i.e., forward velocity, on flyover noise was under study so it was necessary that it remain constant for each individual pass. The effects of landing gear and flaps on noise were also under investigation and, thus neither device could be used to control speed. Hence, to avoid speed changes, it was necessary to allow the airplane to climb or descend once the speed and power were set. The only other way would have been to load the aircraft to the exact weight that would have allowed straight and level, unaccelerated flight. Since at least 56 passes were planned, all to be accomplished within stringent meteorological restraints, this was obviously impractical.

In order to determine where the starting point of the climb or descent should be (to bring the aircraft over the microphone array at the desired altitude) plots of rate of climb or descent versus aircraft gross weight were made. This was done for each desired airspeed for different flap settings, gear up or gear extended, and different engine power settings. One typical plot is shown in Figure 8. With the aid of these plots, plus one or two practice

flights, it was possible to select one starting point and vary the altitude over this point in such a way so as to arrive over the array at the proper height. One other device that aided in determining the height at which to begin the run was the use of a so-called "calibration run". For each new configuration tested a level flight pass was made, in that configuration, over the array. This run was conducted using the thrust required for level flight at the desired altitude and airspeed. This enabled the pilot to develop a good "feel" for just how the airplane really would fly at that particular weight. If the power settings called out in the flight card were greater than that required for level flight then the airplane would climb. If the power settings requested were less than that required for level flight then the airplane would descend.

II.4 Instrumentation and Set-Up

As mentioned, the test site is shown in Figure 7. A schematic of the instrumentation set-up is given in Figure 9. The test headquarters was in a specially equipped trailer shown in Figure 10. This housed most of the instrumentation and served as the base of operations for test coordination, communications, etc.

Note that the source location array (Figure 11) consisted of twenty-two microphones flush-mounted on a smooth asphalt surface. A close-up of this pad is shown in Figure 12. It was painted white to reduce the heat absorbed by the asphalt and thus to insure that the microphones that were lying on the surface were not exposed to too high a temperature and, also, to avoid large temperature gradients at the surface. The design of this asphalt surface was such that there were no parallel sides in order to prevent any standing waves between edges. The edges were made flush with the surrounding terrain to the extent possible. Note that the size of the pad was approximately 6500 square feet.

All microphone data were recorded on a thirty-two track tape recorder with signal conditioning (Figure 13) at the recorder in the trailer located about 230 feet from the microphone array. Thirty microphones were used with one track for voice annotation and one track for IRIG time code. Through this time code all data on the ground were synchronized with the airplane parameters. All microphones were calibrated using a pistonphone and both pink noise and white noise were recorded through each microphone system for response corrections.

The ten-meter microphones, i.e., those mounted ten meters above ground level, (Figure 14) were erected using telescoping masts with guy-wires for support. The 1.2 meter microphones were mounted on more conventional tripods.

The primary tracking instrument was a Rolls-Royce ground-based 70mm camera positioned on the expected ground track of the airplane, as shown in Figure 15. This system had a separate three-track tape recorder dedicated to it. IRIG time code and voice annotation were recorded on one track, the shutter pulses on another, and the

elevation and tilt angle of the camera (i.e., left or right of the expected ground track) on the third channel. This latter was accomplished by transforming voltages that were proportional to the two angles into two separate and distinct frequency bands. On playback, the merged signals could then be separated. From these inputs and scaling techniques involving the aircraft image the space position as a function of time could be obtained.

The back-up tracking system utilized an airborne camera on the test aircraft itself photographing surveyed ground targets.

The weather balloon (Figure 16) had its own paper tape recording system on which pressure, height, temperature, and relative humidity were recorded for later analysis. These parameters were telemetered to the recording station from the balloon as it ascended or descended and real-time read-out was available to determine that meteorological conditions above the surface were, or were not, acceptable for testing.

In addition to the balloon, a fully instrumented light aircraft was utilized to make spiraling descents through the test area immediately preceding the test airplane itself in order to obtain temperature and humidity data as a function of height above the surface for use in subsequent analysis. Real-time read-out of these parameters was again available for use in determining the suitability for testing. The data from the weather balloon and the light airplane were used in deciding whether to launch the test aircraft. The test airplane also carried instrumentation to determine temperature and relative humidity as a function of altitude.

Winds aloft were determined by pilot balloons (pibals). These were launched from the ground at the test site and tracked to obtain wind speed and direction as a function of altitude. Winds at ten meters were obtained from the ten meter weather tower.

Aircraft and engine parameters such as airspeed, altitude, total air temperature, engine pressure ratios, shaft speeds, fuel flow, and turbine gas temperatures were recorded onboard through the airplane data center for subsequent reduction and analysis, and correlation with the noise data.

III. RESULTS TO DATE AND CONCLUSIONS

The flight test program described in this paper has been completed. The principal areas associated with flyover noise that it was designed to examine were:

- 1) In-flight source location determination.
- 2) The effect of forward speed on the noise produced by coaxial jets over a power range from flight idle to takeoff.

- 3) The influence of airframe noise on the engine/airframe noise signature.
- 4) Engine/airframe installation effects.
- 5) Atmospheric effects on acoustic propagation.

The data obtained have been verified to be of high quality.

To date the data have been reduced only in terms of overall sound pressure level and for the test day atmospheric conditions, i.e., no corrections have been made for meteorological variations between test days. In addition, no corrections have been made as yet to normalize the data to a common altitude.

Although the data are still being analyzed, some preliminary conclusions can be drawn. One such conclusion is that in the rear arc engine noise dominates but in the forward arc the noise levels are airframe dominated. This can be seen in Figure 17 where the noise data for flight idle thrust are plotted for several different airspeeds. It can be seen that in the rear arc the data for the different airspeeds all come together, indicating that in this direction they are not a function of airspeed but, rather, of engine power which here is constant. However, in the forward arc they separate quite nicely as a function of airspeed. Figure 18 indicates that this is true for engine powers up to approximately 75% N₁, i.e., throughout the approach power range.

Another tentative finding from this program is that deploying either the flaps (to 33°) or the landing gear increases the overall noise level by approximately eight dB relative to the level associated with a clean airframe. Deploying both simultaneously adds about ten dB to the clean airframe overall noise level. These effects are shown in Figure 19.

There is also some evidence to indicate that there are less static-to-flight effects relative to the center engine than for the wing engines.

In addition, it appears likely that there is indeed a jet/flap interaction effect on noise. This appears to be true regardless of engine power setting and acts to increase the noise levels significantly, especially in the forward arc.

The investigation, primarily by Rolls-Royce personnel, is continuing into these latter two phenomena as well as all the other aspects of the program. It is anticipated that more definitive results will be available by the end of this year.

REFERENCES

1. Anon., Federal Aviation Regulations, Part 36, "Noise Standards: Aircraft Type and Airworthiness Certification", 1 December 1969.
2. Vogel, James W. "Flyover Noise: Measurement and Analysis", Society of Flight Test Engineers Eighth annual Symposium Proceedings, August 1977.
3. Fethney, P. and Jelly, A. H., "Airframe Self-Noise on the Lockheed L-1011 TriStar Aircraft", AIAA Paper 80-1061, 6th Aeroacoustics Conference, June 1980.
4. Szewczyk, V. M., "Coaxial Jet Noise In Flight", AIAA Paper 79-0636, 5th Aeroacoustics Conference, March 1979.

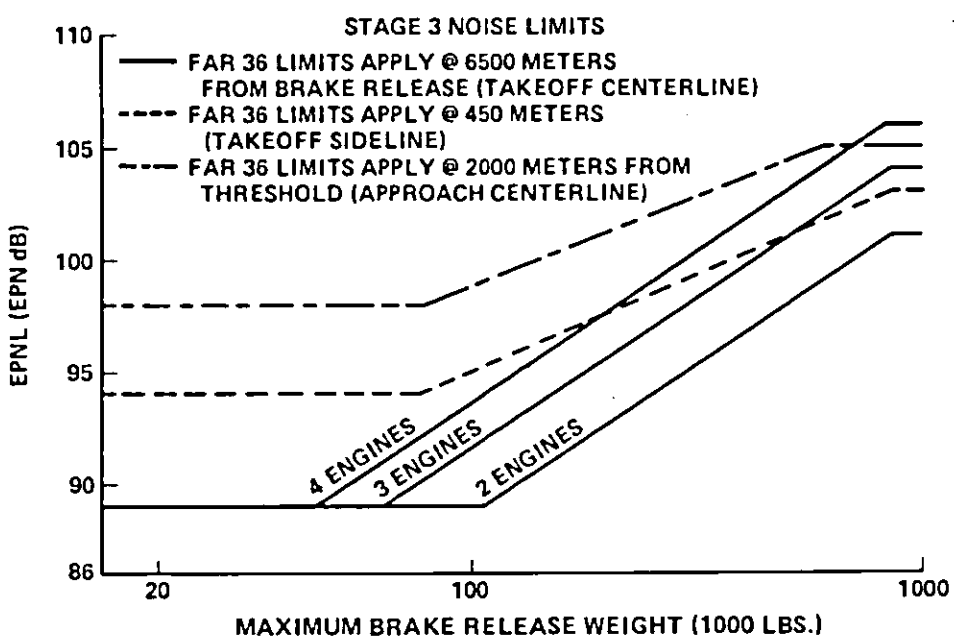


Figure 1. FAR 36 Noise Limits (Amdt. No. 36-8)

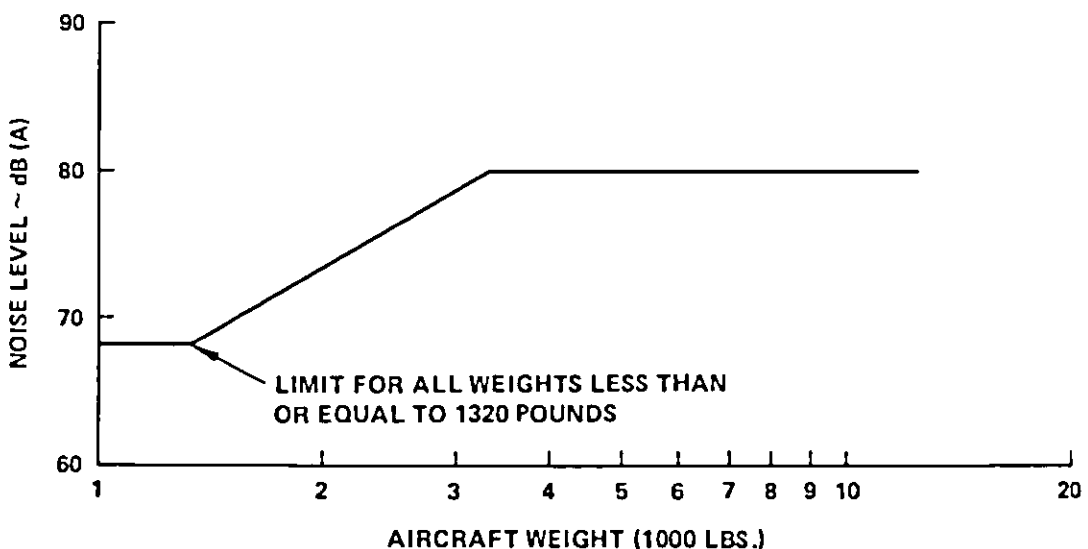


Figure 2. FAR 36 Noise Limits – Propeller Driven Small Airplanes

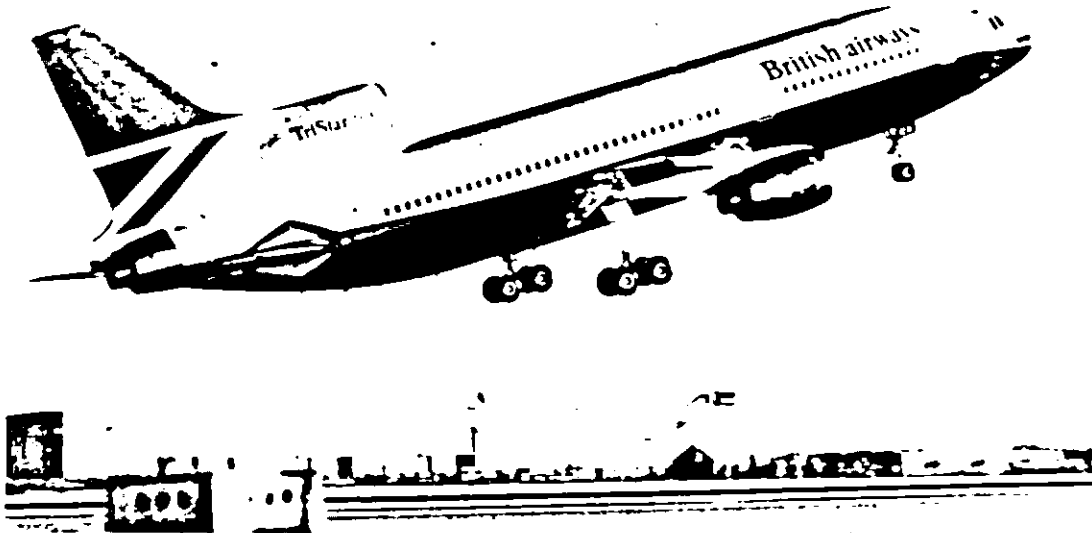
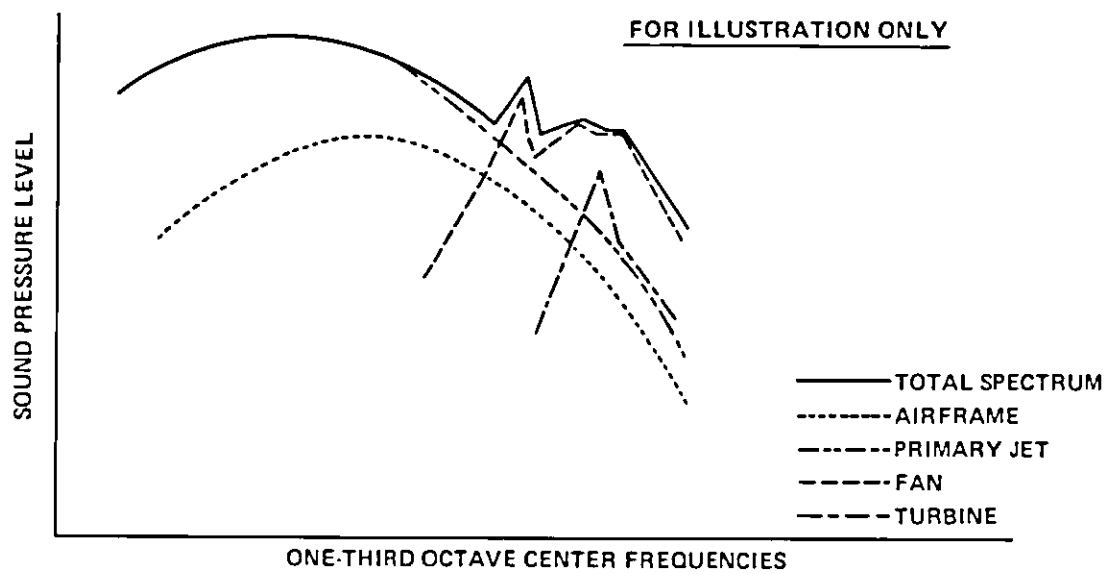


Figure 3. Lockheed L-1011 with Rolls-Royce RB.211 Engines



*Figure 4. Contribution of Individual Components
to Total Noise Spectrum (Logarithmic Addition)*

RUN NO.	AIRSPEED (KNOTS)	ALTITUDE (FEET)	FLAP (DEGREES)	GEAR	ENGINES NO 1 AND NO 3 (% FAN RPM)	ENGINE NO 2 (% FAN RPM)
1	210	600	UP	UP	100	FLIGHT IDLE
2					85	
3					75	
4					60	
5					FLIGHT IDLE	
6	170				100	
7					95	
8					90	
9					85	
10					75	
11					70	
12					65	
13					60	
14					FLIGHT IDLE	
15					70	
16	170				FLIGHT IDLE	
17			33		100	
18			33		85	
19			UP		75	
20					60	
21		600			FLIGHT IDLE	
22	170	900			85	
23	170	300			FLIGHT IDLE	
24	170	600			65	
25	240				FLIGHT IDLE	
26	170				60	
27	170				100	
28	150	600	33	DN	FLIGHT IDLE	
			33		70	FLIGHT IDLE

Figure 5. Test Program

- 1) No rain or other precipitation.
- 2) Ambient air temperature between 36°F and 95°F (2.2°C and 35°C), inclusively.
- 3) Relative humidity between 20% and 95%, inclusively.
- 4) Relative humidity and ambient temperature such that the sound attenuation in the one-third octave band centered at 8 KHz is not greater than $\frac{36.6 \text{ dB}}{1000 \text{ ft}} \left(\frac{12 \text{ dB}}{100 \text{ m}} \right)$
- 5) Wind not greater than 10 knots with the crosswind component 5 knots or less.
- 6) No temperature inversion.

Figure 6. Meteorological Restraints



Figure 7. Aerial View of Test Site

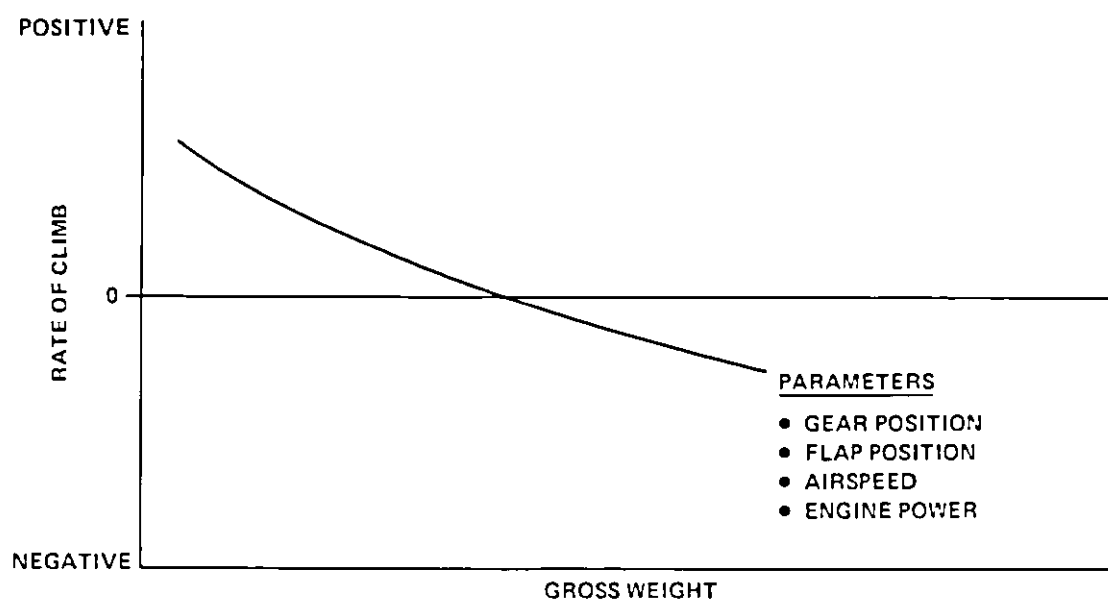


Figure 8. Aircraft Rate of Climb @ 600' AGL

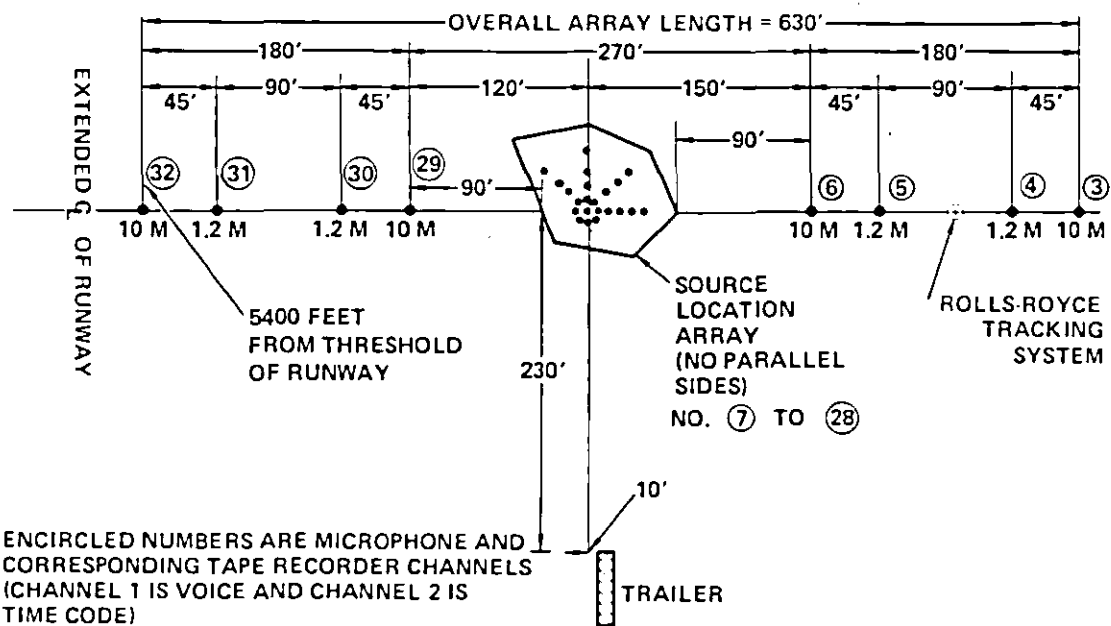


Figure 9. Instrumentation Schematic

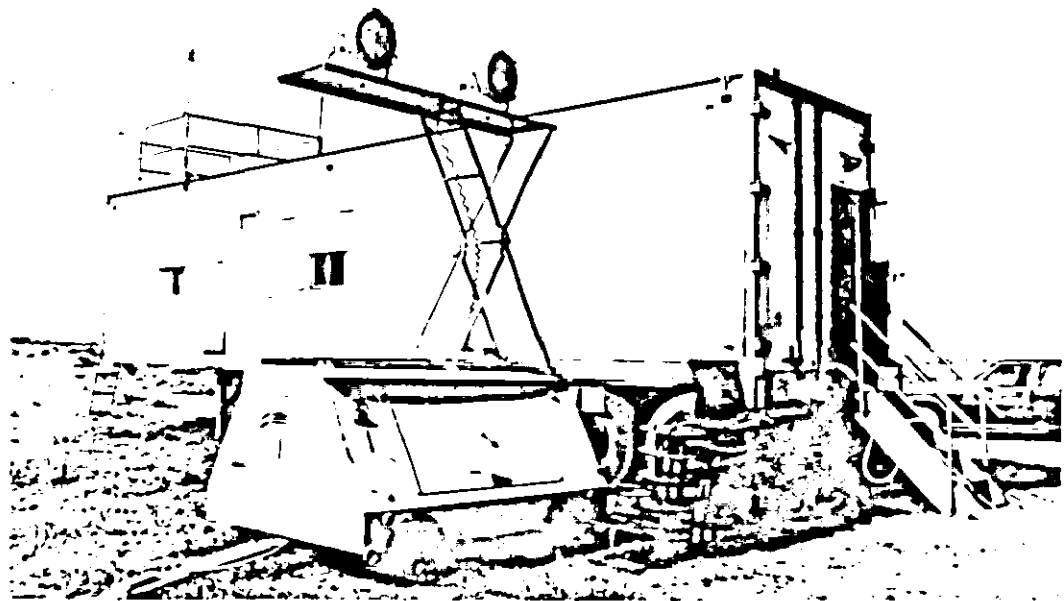


Figure 10. Test Headquarters



Figure 11. Source Location Array Pad

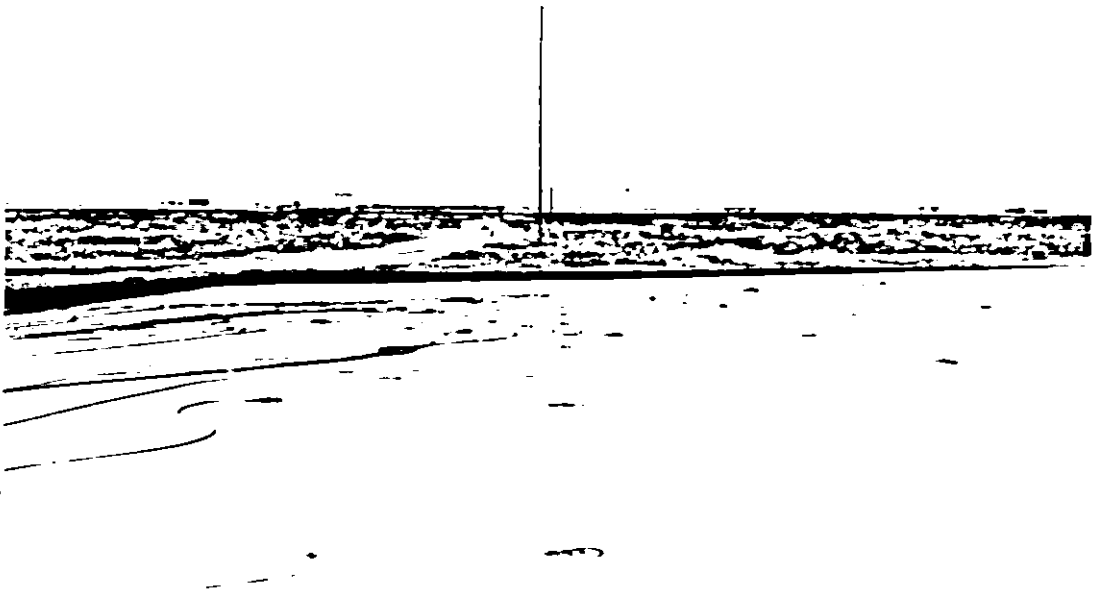


Figure 12. Close-Up of Source Location Array Pad

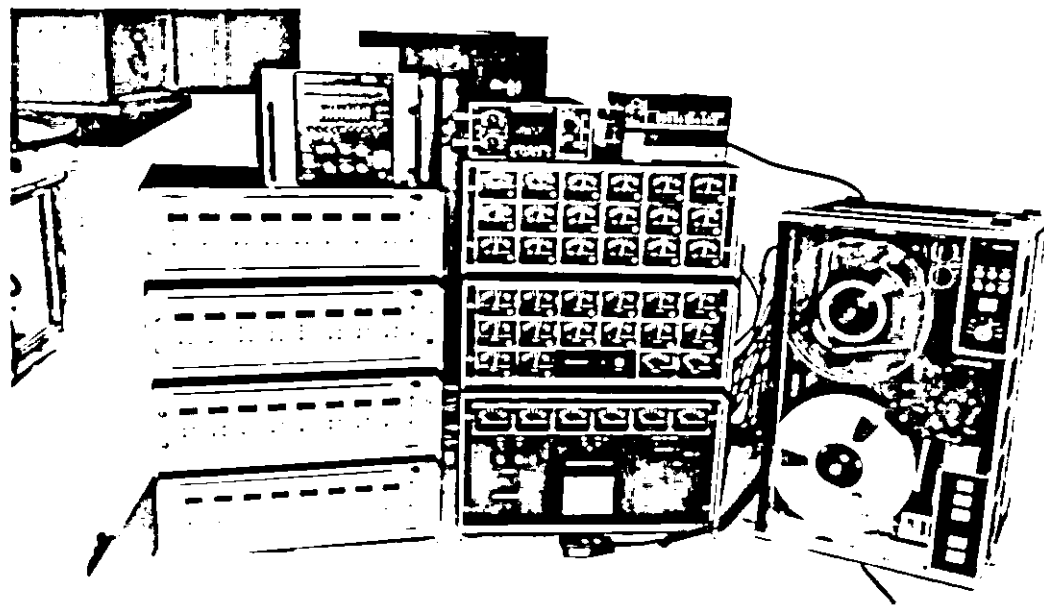


Figure 13. Tape Recorder and Signal Conditioning

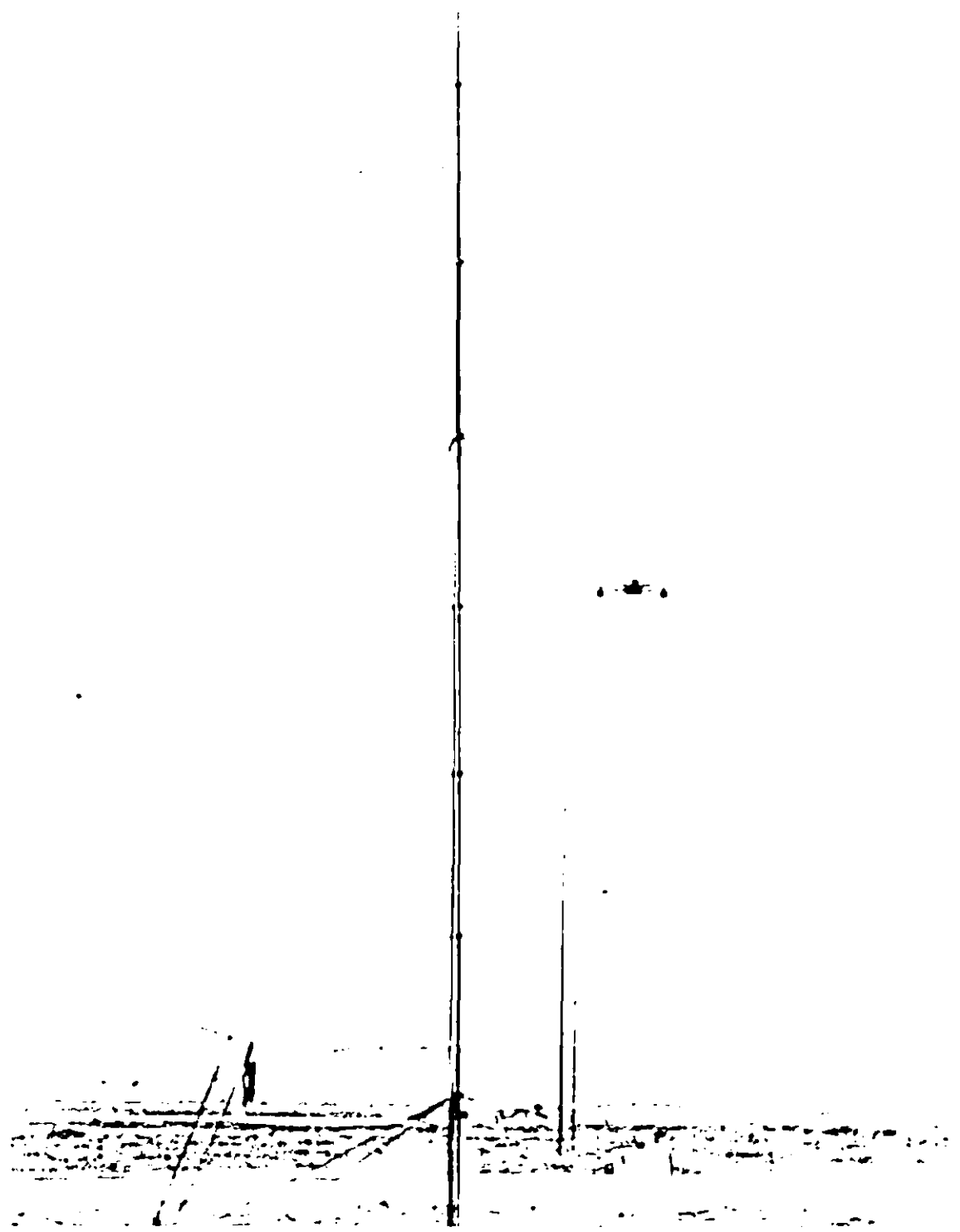


Figure 14. Ten-Meter Microphones

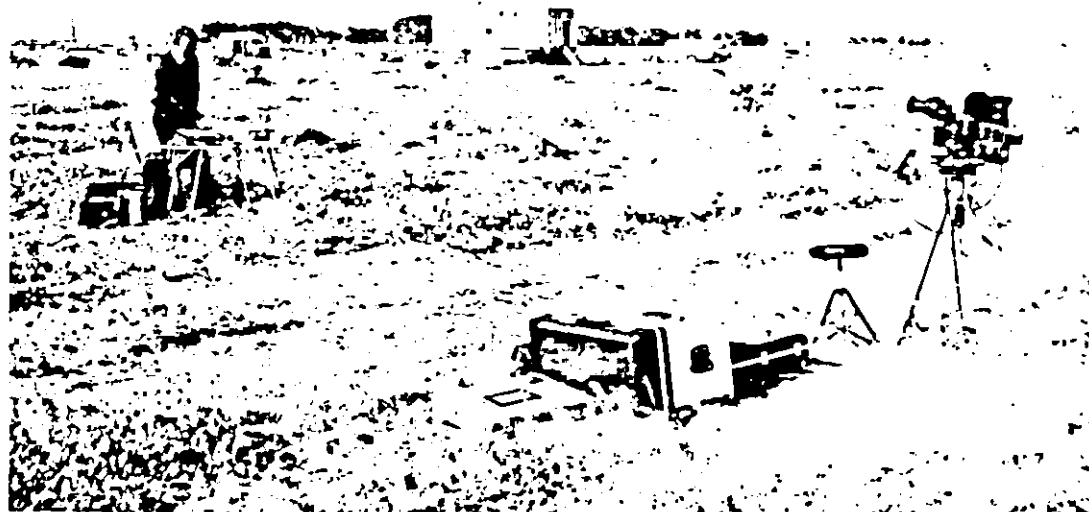


Figure 15. Primary Space Positioning System

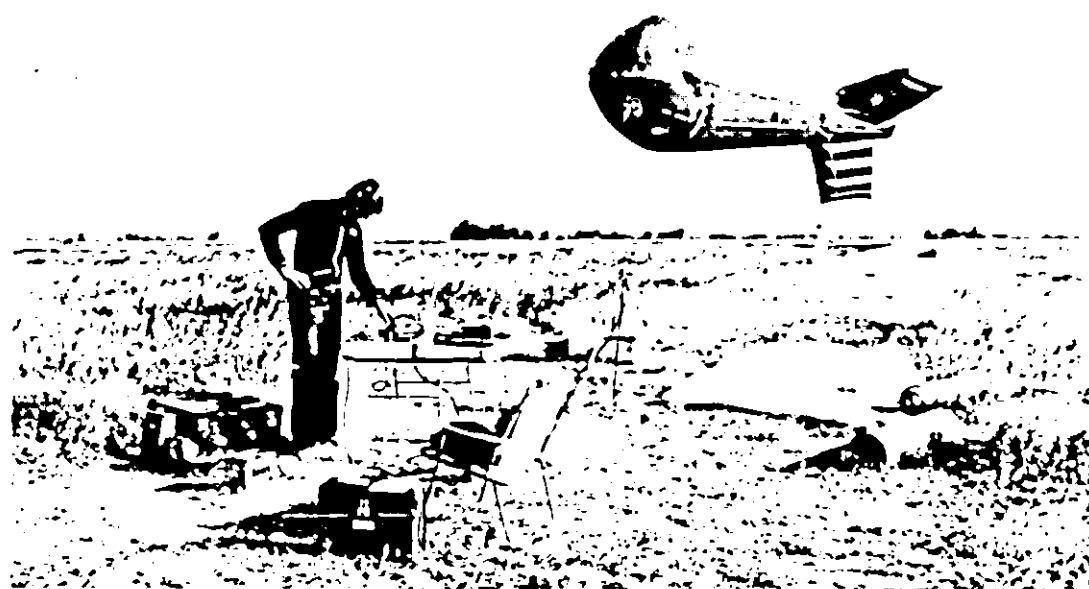


Figure 16. Meteorological Balloon

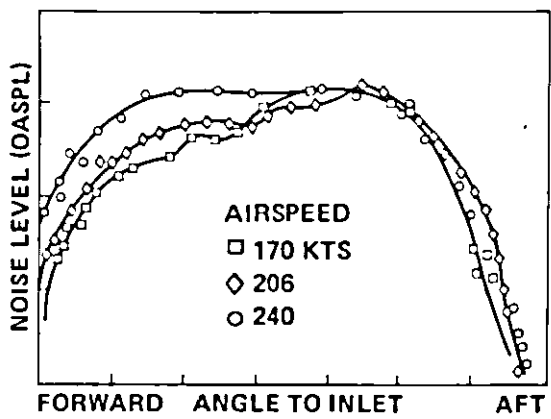


Figure 17. The Effect of Airframe Noise (All Engines @ FI)

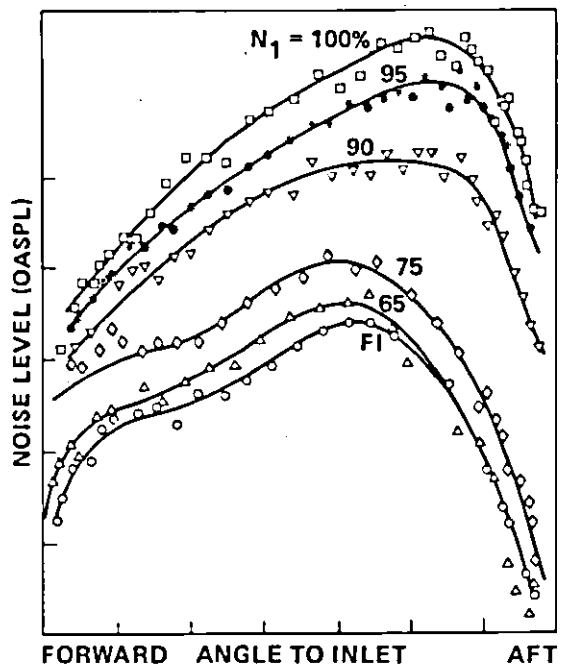


Figure 18. The Influence of Airframe Noise (@ 170 Knots)

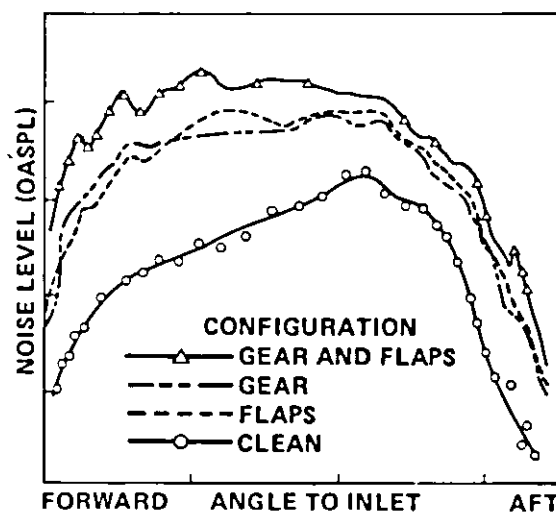


Figure 19. The Effects on Noise of Gear and Flaps (@ 170 Knots, All Engines @ FI)

SIZE REDUCTION FLIGHT TEST AIRBORNE DATA SYSTEMS

**J.W. Gierer
McDonnell Aircraft Company
St. Louis, Missouri**

ABSTRACT

During aircraft development, on board data systems are used to gather in-flight information. Generally there is not much unused space on a fighter aircraft and the electronic hardware of the data system displaces some of the normal aircraft equipment.

Electronics from the avionics suite is usually designed for easy removal and provides a more desirable location for the data system than that provided by removing other equipment such as fuel cells or ammunition drums. A data system that can fit into the removed avionics areas reduces installation and maintenance cost and facilitates the return of the test vehicle to the original configuration.

McDonnell Aircraft Company has recently used F-18 flight test experience to identify size reduction goals and establish guidelines for a data system that would fit into the "Removable Avionics" areas. Low power emerged as an important key to size reduction, since increasing the power density of the electronic boxes affects life and performance. An all-digital approach that includes multiplexers to handle often encountered transducers can also contribute to size reduction. High density electronic packaging plays a key role, too, and a packaging technique was developed based on the use of surface mounted electronic components and a multilayer substrate. In addition, a modular, building block arrangement is used to improve the efficiency of space utilization and tailor the data system to the measurand requirements of an aircraft.

It is estimated that a size reduction of 2.2 to 1 can be achieved by applying these concepts to the F-18 data systems. This would provide a data system small enough to fit into removable avionics areas on eight of the nine test aircraft. On the avionics test aircraft a 5 to 1 size reduction is needed in order to fit the data system into "Removable Avionics" areas.

INTRODUCTION

Over the years the airborne data system has evolved from note pads and photo panels into a sophisticated electronic system. The complexity can vary widely depending upon the nature of the aircraft test program. Data systems required to support development of a new fighter aircraft are complex electronic systems. Data is acquired via electrical interface to the avionics as well as from transducers installed especially for the flight test activity. Typically the information is formatted for on-board magnetic tape recording, with a portion being telemetered to the ground to support real time decisions. Selected information is also displayed to the pilot. Visual information in the form of film or video tapes is sometimes recorded on board the aircraft.

In recent years we have seen the return to smaller fighter and attack aircraft. Undesirable compromises are required, in some cases, to install the data system. The compromises include:

- 1) The use of difficult-to-access areas;
- 2) Lay up and re-configuration of the aircraft;
- 3) Structural modifications.

J.W. Gierer, Staff Engineer - Flight Test Engineering
Flight Test Data Systems

SIZE REDUCTION GOAL

The easy-access mounting areas available on the aircraft are usually occupied by the avionics suite. However, typically, some items of avionics can be removed for the flight test program. If the data system can be fitted into the "Removable Avionics" spaces, then installation and maintenance cost can be held to a minimum.

The F-18 flight test program was reviewed and equipment listed in Table 1 was classed as removable for eight of the nine aircraft. In the avionics aircraft only 43% of this space is available.

TABLE 1 - REMOVABLE AVIONICS

Part Number	Nomenclature
KY-58/T Sec	Secure Speech
KIT-1 A/T Sec	IFF Transponder Computer
CP-1269 AWG-25	Harm Weapon Control
JS-3053C AN/ALR-45	ECM Rec Set Analyzer
R-1764B/ALR-50	Radar Receiver
RT-1079	ICS Receiver/Transmitter

GP01 05525

In comparing the volume of the removable avionics to the average data system volume of the F-18 program, it was found that:

- 1) A size reduction of 2.2 to 1 would accommodate 8 of 9 aircraft;
- 2) A reduction factor of 5 to 1 would accommodate all aircraft.

AIRCRAFT SPACE USAGE

However, this assumes an aircraft installation factor of 2.5, whereas, on the F-18 the installation factor is 3.3 (See Figure 1). The present data system elements have a variety of shapes and sizes. Since the data system is not designed specifically to fit a particular area on the aircraft the efficiency of space usage can be expected to be less than the avionics removed from that area. In order to accomplish the improvement both the wiring and the installation access factors noted in Figure 1 need to be reduced.

Reducing the size of aircraft wiring or connectors does not appear feasible in the near future. The wire bundles must be rugged and the connectors sized for handling by maintenance personnel on the flight line. Reduction in the space used for wiring and connector access must come from other considerations. A review of the F-18 installation practices suggests a few possibilities:

- 1) Place the aircraft style connectors on the front surface of the package;
- 2) Use connectors efficiently and eliminate them when possible;
- 3) Multiplex groups of signals at the first opportunity.

The third item would involve the creation of signal multiplexers to handle the frequently encountered situations shown in Table 2.

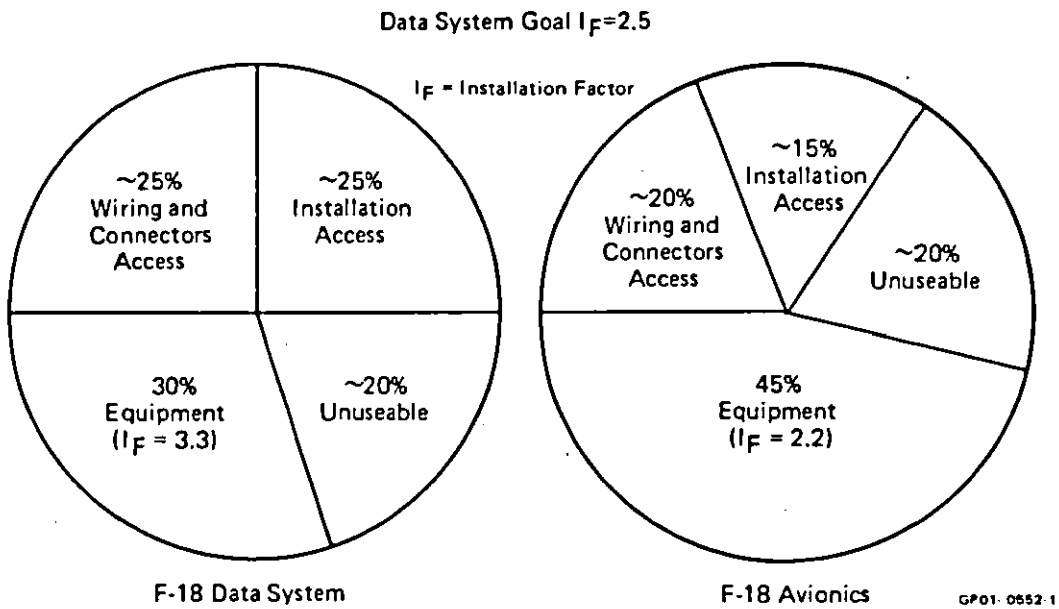


FIGURE 1 - TYPICAL AVIONICS BAY - SPACE UTILIZATION

TABLE 2 - MULTIPLEXER TYPES

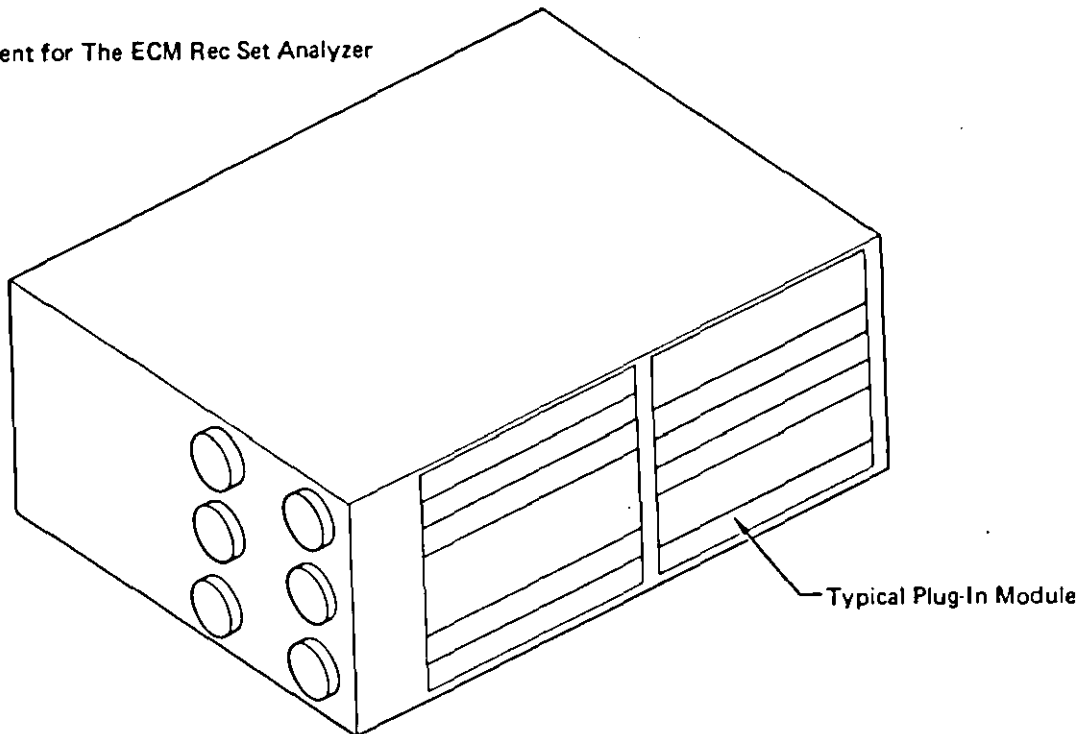
- 1. Vibration/Charge Amplifier
- 2. Bridge Transducer (Ratiometric)
- 3. Thermocouple
- 4. Voltage

GP01-0652-6

The variety of hardware shapes and sizes encountered during the F-18 program suggests that a standard form factor with a modular building block approach would allow better utilization of the space.

Such an arrangement is illustrated in Figure 2. An enclosure is constructed to take the place of the removed avionics, using the same aircraft mounting provisions. Small plug-in modules are assembled to the enclosure that contains mating high density connectors. The modules are interconnected using flex circuits or individual wires that are part of the assembly. The enclosure is connected to the aircraft wiring through the larger aircraft style connectors.

It is estimated that these wiring and installation concepts will allow the installation factor to attain the 2.5 goal.

**FIGURE 2 - MODULAR DATA SYSTEM****REDUCE HARDWARE VOLUME**

Another element considered was a reduction in the volume of the data system hardware. Again our F-18 experience was used to identify possibilities. The relative subsystem volumes are indicated in Figure 3.

Subsystem	F18 Average Percent of Total Equipment	Step 1 - Estimated	Step 2 - Estimated
		System Design Reduces Volume	Micro-Packaging Reduces Volume
Charge Amp and TC Ref	3%	0%	
Telemetry	4%	2%	2%
Excitation Power	4%	0%	
Conditioning	7%	7%	5%
Special	11%	11%	8%
TDMS	13%	13 + 15 + 1 = 29%	11%
Power and Dist	17%	8%	8%
FDMS	20%	0%	
Recorder	21%	12%	10%
Total	100%	70%	44%

FIGURE 3 - DATA SYSTEM VOLUME REDUCTION

GP01 0552 3

As a first step consideration was given to adopting system design concepts that would allow the design of smaller equipment. The use of low power circuitry surfaces as an important design goal. This would permit high density electronic packaging techniques while retaining power density levels compatible with reliable equipment performance. The use of high efficiency power supplies and low power circuits in each subsystem is expected to reduce power requirements to one fourth. This will allow a significant reduction in hardware size. The application of other system design concepts and high density electronic packaging techniques to each subsystem is outlined in the following paragraphs. An estimate of applying these concepts is noted in Figure 3.

Recorder

Local and remote control panels plus control relays are included in this subsystem. High bandwidth recording, currently operating in the laboratory and possibly in a few real world situations, may allow the size of the recorder to be reduced. Helical scan recording techniques are being applied to obtain a channel with 8 MHZ bandwidth and over one hour of record time. High density digital recording techniques are also being incorporated into linear machines and it is expected that this will reduce both tape quantity and machine size. Electronics contributes only a small portion of the recorder volume and electronic packaging is expected to contribute only a small additional reduction.

Frequency Division Multiplexing Subsystem (FDMS)

Higher signal frequencies have typically been recorded using FM multiplexing techniques. These systems require adjustments to set up the FM composite on the aircraft and corresponding set up in the ground station. A large inventory of FM hardware is also required to cover the various FM channels. In addition a valid error analysis of a many-parameter FM complex can be difficult. Progress in the development of linear and digital integrated circuits allows consideration of a digital sampling system to handle these parameters. The digital technique allows for time sharing of hardware and is expected to result in reducing hardware size. Figure 3 shows that the FDMS hardware can be reduced to zero and the digital subsystem (TDMS) increased to accommodate the high frequency parameters.

Power and Distribution

The 28 VDC transformer rectifier, circuit breaker panels, and power distribution boxes can be reduced in size since the overall power required by the other subsystems has been reduced. High density electronic packaging is not always compatible with power generation circuitry and no further size reduction is noted in Figure 3.

Time Division Multiplexing System (TDMS)

The transfer of parameters from the FDMS subsystem and the use of multiplexers to accommodate the charge amplifier, thermocouple, and bridge type signals initially adds to the volume of the digital subsystem as indicated in Figure 3. High density packaging can have a significant effect on a digital system. Standard and special large scale integrated (LSI) circuit chips are expected to contribute to reducing the size of digital equipment.

Special

Video equipment, film cameras, flutter exciter, and miscellaneous equipment are occasionally required on a flight test aircraft. Electronic packaging can reduce the size of the digital elements such as the flutter exciter. A slight reduction is forecast in Figure 3 for the overall volume of this equipment.

Conditioning

Signal conditioning is frequently needed to acquire data such as total air temperature, flight path acceleration, and fuel quantity. Electronic packaging is expected to contribute to reducing the size of this equipment.

Excitation Power

In the current F-18 data system the bridge-style transducers are excited from several high accuracy power sources. The ratiometric multiplexer listed in Table 2 would provide a stable excitation to the transducers. The same voltage is used as a reference within the multiplexer, so the absolute accuracy of the excitation is no longer critical. Thus, the stand-alone excitation power supplies can be eliminated, with only a minor size penalty in the digital subsystem.

Telemetry Subsystem

The telemetry equipment used on the F-18 provides about 40 watts of transmitter power. It is expected that the availability of large tracking antennas at the test sites will allow power to be reduced to as low as 5 watts for flight test activity, with a corresponding size reduction in the telemetry subsystem.

Charge Amplifier and Thermocouple Reference

These functions can be absorbed into the special purpose digital multiplexers. The devices currently are packaged separately and each has a connector and a separate power supply. In the multiplexer the connector and power supply are shared, resulting in a space savings.

MICRO PACKAGING

A high density electronic packaging scheme is an important factor in size reduction. The packaging approach, developed to support size reduction efforts, is illustrated in Figure 4.

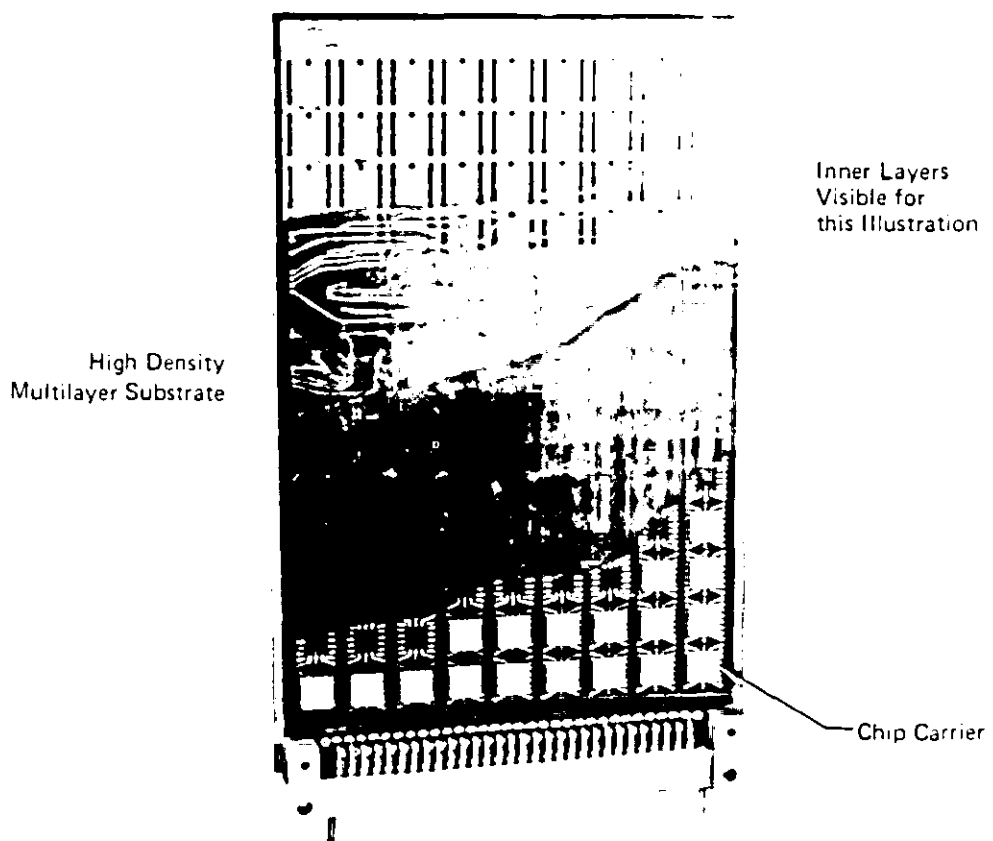


FIGURE 4 - MICRO PACKAGING

GPQ1.0552.4

Surface mounted electronic components are attached to a high density multilayer Kapton substrate. Surface mounting eliminates the through-the-board leads that can interfere with conductor routing in a multilayer structure. Kapton provides dimensional stability and high temperature performance superior to the standard epoxy glass printed circuit materials.

Integrated circuit chips, mounted in ceramic chip carriers, allow for handling and testing of the devices before they are attached to the substrate. Pre-testing is necessary in order to obtain a reasonable yield on a multi-chip assembly. Reflow solder techniques are used to attach the components to the substrate. The basic concept of using chip carriers mounted directly to a printed circuit board is not new to the industry (Reference 2, 3 and 4).

Low power integrated circuit technology, such as CMOS, Schottky, or I^2L can provide the key that allows high density equipment to achieve reliable performance.

CONCLUSION

In conclusion it can be seen that the concept of "Removable Avionics" is useful to establish a desirable size range for an airborne data system. Reduced costs for installation, maintenance, and return of the aircraft to the original configuration are expected.

A review of the F-18 data systems indicates that it is feasible to achieve a better than 2.2 to 1 size reduction, which allow the system to fit into the "Removable Avionics" spaces on 8 of the 9 development test F-18's.

The use of small functional building block modules will allow the data system to efficiently use the available space. The small modules will also allow the data system information capacity to be structured to fit the requirements. Mini data systems such as that used in the F-15 "MIDS" (Reference 1) can be set up from the same family of modules used for aircraft full scale development.

Continuing investigation of these techniques and others is needed to assure evolution of data systems optimized for use on board fighter aircraft.

REFERENCES

1. W.G. Densford and D.L. Jones, "MIDS - The Right Tool for Small Test Jobs", Society of Flight Test Engineers Symposium 1979.
2. Captain R.E. Settle, Jr., "A New Family of Microelectronic Packages for Avionics", Solid state Technology, June 1978, page 54.
3. J.E. Fennimore, "Using Leadless Components Technology on Printed Wiring Boards", Electronic Packaging and Production, December 1978, page 129.
4. F.L. Pinner, "Leadless Device Reflow Soldering is Reliable and Lowers Assembly Cost", Assembly Engineering, October 1977, page 50.

DATA SYSTEMS ORGANIZATION - A CHANGE FOR THE BETTER

by

**Robert D. Samuelson
Chief Flight Test Engineer - Data Systems
McDonnell Aircraft Company
McDonnell Douglas Corporation**

ABSTRACT

Flight Test Engineering Organizations have traditionally divided test data acquisition into two separate functions: instrumentation and data processing. In recent years, though, the interdependence of instrumentation and data groups has grown because test data requirements have become more complex. Recognition of this growing interdependence and concomitant overlapping of responsibilities have led McDonnell Aircraft Flight Test to consolidate these two functions into a single Data Systems organization with three branches:

- Operations Branch - Plans, directs, and controls data activities on a project by project basis.
- Processing and Support Branch - Maintains all airborne/ground systems and processes/distributes data.
- Design and Development Branch - Designs and develops hardware and software for future and advanced programs.

In addition to the immediate benefits of manpower savings and quicker turnaround, the Data Systems philosophy is being reflected in our advanced planning and design efforts and promises to be even more cost effective on future programs.

INTRODUCTION

Airborne instrumentation on a typical test aircraft has increased tenfold over the past 30 years, primarily because of increasing aircraft complexity. Even greater strides have been made with data processing.

But how has the management approach changed through the years to cope with increased data requirements? The most visible changes have been the corresponding increase in personnel and the emphasis on personnel qualifications. Organizational changes have tended to be more subtle.

Over the past decade McDonnell Aircraft Company (MCAIR) consolidated the traditional flight test instrumentation and data processing disciplines into a single data system organization.

The change can be considered from two aspects. First, as it was applied to the F-15 Program on a project basis, then on a departmental basis. The Data System organization is working well and we can see how it will benefit future programs.

BACKGROUND

The 'Data System' Concept

Until we began to think in terms of a flight test Data System, the standard approach was to instrument the aircraft with the best available equipment and, then, tailor the data processing as necessary. Instrumentation requirements were satisfied by combining vendor equipment with electronic signal conditioning and interface equipment developed in house. The data were processed using available capabilities either at MCAIR or at customer facilities. Naturally, data processing equipment was selected, and necessary adjustments made, to cope with the instrumentation in each aircraft. Years of operating in this mode established the following expectations for aircraft preparation and data processing:

- Aircraft Installation was very time consuming, particularly with respect to aircraft wiring.
- Aircraft Setup and Preflight required close coordination with the data group to ensure proper sensitivities, scale factors, and setup for data processing. Changes required close attention to the patch panel. Preflight checks took hours.
- Instrumentation Operations wiring and connector problems reduced reliability and performance. The system was susceptible to electromagnetic interference.
- Data Processing: Fast turnaround for limited quantities of 'high priority' data required for three or four days. Normal average for data turnaround was one to two weeks. Close coordination between the instrumentation engineer and data engineer was essential to establish the correct setup for processing. Two or three passes usually were required before all data were correct.

These expectations have been common for years, but the fixes to solve these operational problems were oriented traditionally to either instrumentation or data and involved agonizing appraisals to find the fault. Pressure by Flight Test Management for better solutions, ultimately led to simultaneous designs for an airborne system and a data processing network that were integrated. As described in Reference (a), a key element in this system was a common data base for setting instrumentation and data processing operations. The design concept was a 'system' that started with the sensor; included signal conditioning, encoding, recording, monitoring preprocessing, and processing; and ended with the display/plotting of data in final engineering format. At the same time, it was recognized that organizational changes also were needed to more effectively manage data system development and F-15 test support operations.

F-15 Project Data System Organization

The can-do atmosphere surrounding the F-15 Project at contract go-ahead was an ideal environment for a new organizational approach. It was well recognized that normal instrumentation/data processing test delays could not be tolerated in the schedule of this program. A Data System Project Supervisor, appointed within the Flight Test Organization, was given full responsibility for developing and operating the data system for the F-15 Program. The assigned instrumentation and data engineers still retained their traditional responsibilities, but with a stronger sense of cooperation and appreciation of each other's problems.

In this atmosphere, distinction between instrumentation-type problems, and data-type problems gradually disappeared. All problems became 'data system' problems to be solved without regard for normal instrumentation-data organizational boundaries.

This approach worked exceptionally well:

- New airborne and ground data systems were developed, procured, installed and operationally checked prior to first flight.
- Airborne instrumentation was rarely a cause for flight delay or flight abort.
- Average data processing turnaround time was reduced to one day from the seven to 14 days required during the F-4 Program.

- The MCAIR Category I Program goal of 10 flights per month per test aircraft was exceeded by 26 percent.
- All Category I Flight test Milestones were accomplished on schedule and within budget.

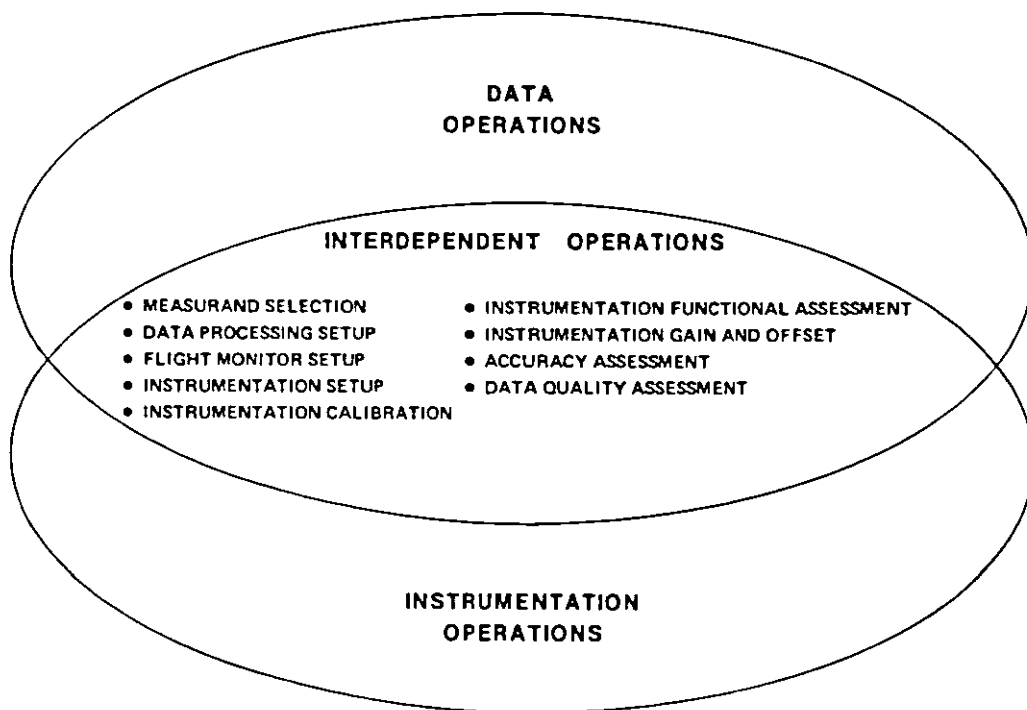
The Data System organization concept was accepted overwhelmingly by everyone closely involved with this program. Management assessment of F-15 results prompted a study for further reorganization on a functional department basis. The underlying objective of the reorganization was to improve effectiveness and reverse the long-term trend of increasing numbers of personnel required to support a test aircraft.

THE DATA SYSTEMS ENGINEERING DEPARTMENT

The Flight Test Management study revealed some key objectives to be considered in the reorganization:

- Strengthen project control over data and instrumentation operations.
- Combine data and instrumentation operations to broaden individual responsibilities and increase efficiency. (Figure 1 illustrates a number of the interdependent operations that existed before reorganization.)
- Manage data system development and test support activities separately to avoid priority conflicts between development and support. Get full-time personnel assigned to both activities.
- Combine data and instrumentation design activities to ensure optimum designs for future data systems.
- Combine supporting laboratories and supply operations where feasible.

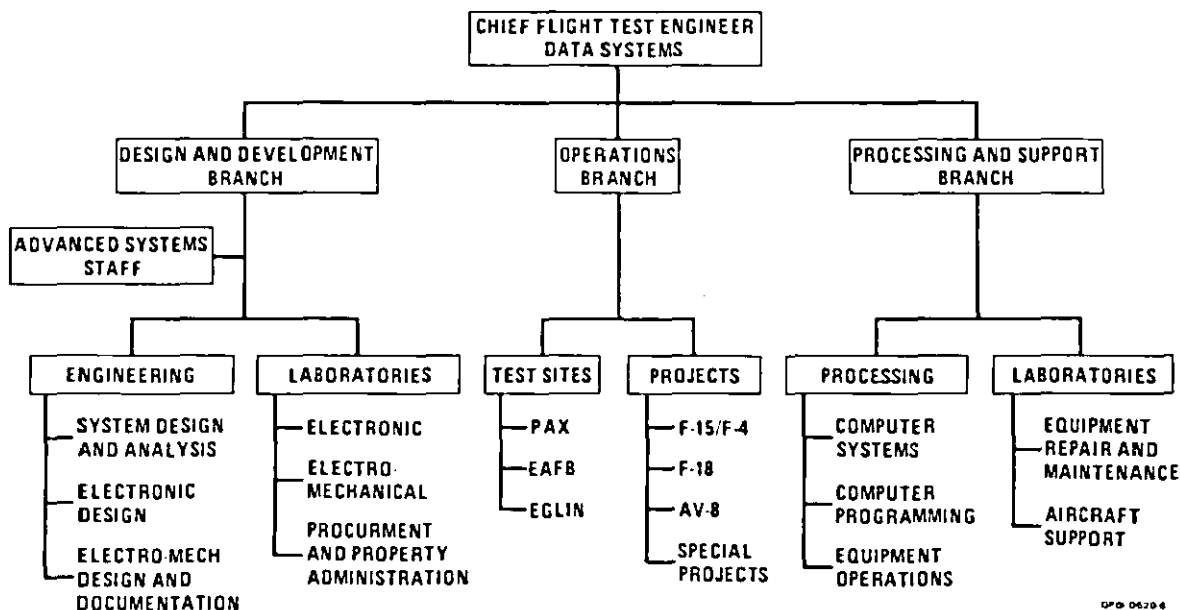
FIGURE 1
GROWING INTERDEPENDENCE BETWEEN
DATA AND INSTRUMENTATION GROUPS



OP-1-66206

The resulting Data Systems Engineering Department is shown in Figure 2. The three branches are results oriented:

FIGURE 2
FLIGHT TEST DATA SYSTEMS ENGINEERING
DEPARTMENT ORGANIZATION



Operations Branch - This branch is responsible for definition, implementation, and control of data systems for each project. During the planning and development phases of a program, Data System Engineers (DSE's) from this branch match the system to the project. Then, they designate specific responsibilities to the Design and Development Branch for design, development, fabrication, and procurement of major components and software. During flight test operations, DSE's are responsible for Data System operations and establish project support requirements for the Processing and Support Branch.

Design and Development Branch - Working to technical, budgetary, and schedule requirements from the project DSE, this branch is responsible for preparation, design, development, and procurement of all airborne and ground support equipment for Flight Test Data Systems. The Development Laboratory of this branch is used to fabricate, assemble, test, and evaluate equipment for support of individual projects. This branch also is responsible for refinement of data system methods and application of new concepts to existing or advanced data systems.

Processing and Support Branch - This branch is responsible for data processing, airborne data system preparation, and all facets of data system maintenance to support flight tests. The Data Processing Section has the necessary project support for computer program changes, computer operations, and equipment operations. The Laboratories Section provides aircraft technician support, and performs equipment maintenance and calibration.

Reorganization timing (after the F-15 development, before F-18 go-ahead) was ideal. We enjoyed the luxury of a transition period of nearly three years before the first flight of the F-18. In order to smooth the transition, cross-training classes indoctrinated all personnel in the complete spectrum of activities. In addition, operating procedures were redefined to cover the broader aspects of the data system discipline. Operations Branch personnel were affected the most by this change. Engineers who were formerly instrumentation specialists, learned the finer points of data computations, processing and analysis. Likewise, engineers with data analysis specialties learned instrumentation

principles. There was an excellent spirit of cooperation with much give and take between DSE's during the first two or three years of the new organization. There is still a tendency to assign the older engineers to jobs corresponding to their former strong suite. However, there is every indication that new graduates working as Data Systems Engineers tend to learn the over all data systems discipline very well.

Results to Date of Data System Engineering for the F-18 Program

It was recognized from the outset that to acquire tangible performance data to measure effectiveness would take several years. Comparisons with previous programs would require cumulative data on such factors as manpower expenditures and data turnaround times. Strong signals indicated very early, however, that we were right on track. The positive attitudes of personnel operating with lower budgets and yet meeting tough schedules were sufficient signs of progress to give Flight Test Management confidence in the new organization.

For the F-18 Program, a complete data assessment-preprocessing-transmission station was designed, fabricated, and installed at our Naval Air Test Center, Patuxent River, MD. It was checked out as part of the overall St. Louis data processing network (Figure 3). Data system manpower expenditures for all first flight preparations were less than on the previous program. Since much of the F-18 data system capabilities were replays of the F-15 data system, the F-18 data system preparations phase alone cannot be considered an accurate measure of productivity gains. We do, however, consider the level of manpower support for an average test aircraft to be a meaningful comparison, particularly with back-to-back programs such as the F-15 and F-18 which have comparable numbers of instrumented test aircraft.

**FIGURE 3
MCAIR FLIGHT TEST DATA PROCESSING NETWORK**

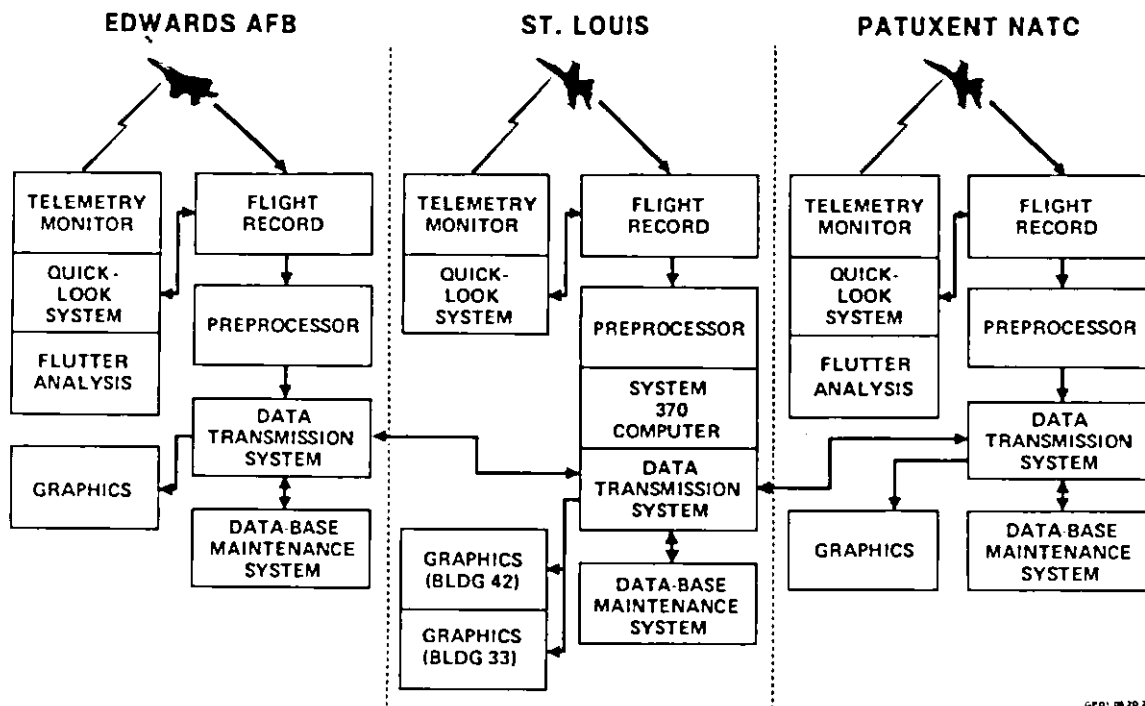
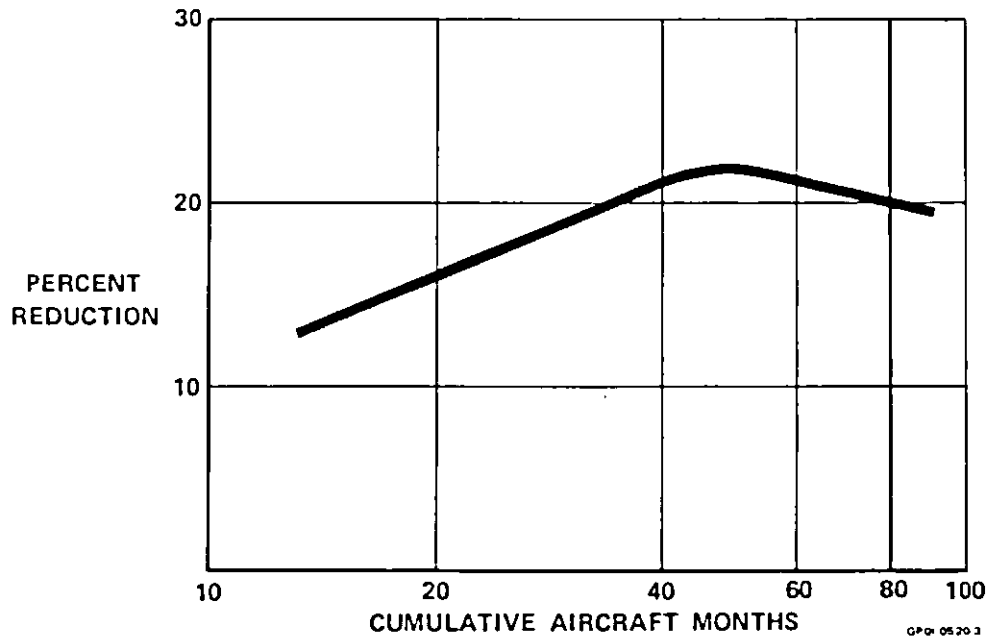


Figure 4 expresses the reduction of F-18 Data System Engineering personnel in terms of the F-15 baseline. The graph includes engineers and technicians. The cumulative 20 percent reduction, 18 months after the first flight, is as good as we expected to accomplish at this point in the program. Since F-18 staffing levels seem adequate, this nominal difference should hold throughout the program.

FIGURE 4
DATA SYSTEM MANPOWER REDUCTION
F-18 Program vs F-15 Program



The F-18 Program already is averaging essentially the same 24-hour turnaround as experienced at the mid-point of the F-15 Program. The biggest difference is that data are transmitted directly to the design team in St. Louis as part of the processing network. Much of the F-15 Program data transmittals in St. Louis were by company mail service, which adds several days to the process. Figure 5 shows F-18 data turnaround experience to date together with prior F-15 and F-4 Program results.

Developments for the Future

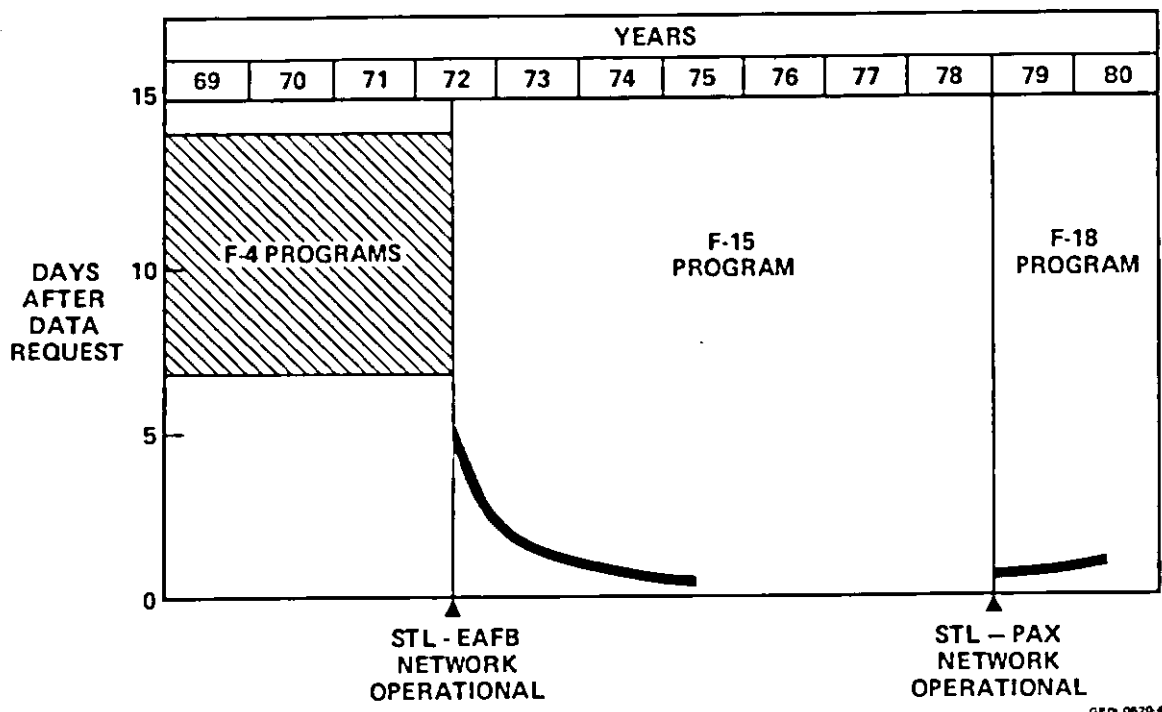
This is just the beginning. Our commitments for the future involve advanced designs of airborne equipment as well as data processing/analysis capabilities. We have an advanced data system design team reporting directly to the Design and Development Branch Chief in a staff capacity. Some of the key study areas currently being pursued promise more effective data systems in the future:

We propose to develop:

- An all-PCM airborne encoding system capable of handling the full range of dynamic data requirements.
- Micro-packaging techniques for further miniaturization of airborne systems. Reference (b).
- Fiber optics for airborne equipment.
- Interactive graphic display and analysis capabilities for enhanced assessment of flight test data.
- Earth satellite techniques for fast-response data processing networks.
- A hands-off preflight capability for the airborne equipment.

The 20-percent staffing level reduction seen during the F-18 Program came primarily as a result of department consolidation and organizational streamlining. The next 20-percent reduction in manpower support requirements will require the introduction of the more promising candidates for the data system improvement. Beyond that, who knows? But rest assured, we'll continue to probe and study how we can improve our flight test designs from one end of the data system to the other.

FIGURE 5
TRANSMISSION NETWORK SPEEDS FLIGHT TEST
DATA AVAILABILITY



CONCLUSIONS

Present and future flight test data acquisition problems can be addressed more effectively by a data systems organization which can view instrumentation and data processing in a total system perspective rather than as separate functions. Such reorganization at MCAIR has resulted in better project control of the flight test data acquisition process and increased productivity. A comparison of manpower support requirements for two similar programs shows that the Data System organization reduces expenditures 20 percent.

References:

- (a) DEVELOPMENT OF THE F-15 INTEGRATED DATA SYSTEM
Journal of Aircraft, Vol. 9, No. 9, September 1972
- (b) SIZE REDUCTION - FLIGHT TEST INSTRUMENTATION
1980 Symposium, Society of Flight Test Engineers

SIMULATOR DATA TEST INSTRUMENTATION FLIGHT TEST CHALLENGE OF THE EIGHTIES

William L. Curtice, III
U.S.A.F., Aeronautical Systems Division
Wright-Patterson Air Force Base, Ohio

ABSTRACT

This paper will address the development of a new test instrumentation system for flight simulators which is expected to significantly impact aircraft flight test data requirements during the next decade. Complex training systems are now in development for most current and some future aircraft, which will accurately simulate not only the airframe flight dynamics, basic cockpit flight instruments and controls, but will also provide complete integrated simulation of aircraft motion, the pilots' visual field of view, radar and electro-optical viewing systems, weapons release and guidance systems, and electronic warfare equipment. Conventional flight test data acquired for airframe performance evaluation and acceptance falls short of that needed to develop these integrated, high fidelity simulations. However, until recently, no practical means existed to measure a simulator's total performance, and compare it to flight test data. The recent development of the Simulator Data Test Instrumentation System (SDTIS) fills this need. The SDTIS is configured as a portable mini-system. It uses composite video techniques to concurrently record over 180 channels of digital or analog signal data in addition to TV camera acquired video information and voice audio. It also provides immediate, in-field automatic data reduction and analysis. Data acquired during simulator test may thus be directly compared to flight test data as a measure of simulation fidelity without dependence on large data processing systems. The SDTIS represents a significant advance in the state of the art for simulator instrumentation. Although not designed for use in an airborne environment, the techniques developed for the SDTIS appear suited to many airborne data collection tasks, and should warrant serious consideration by flight test instrumentation system designers.

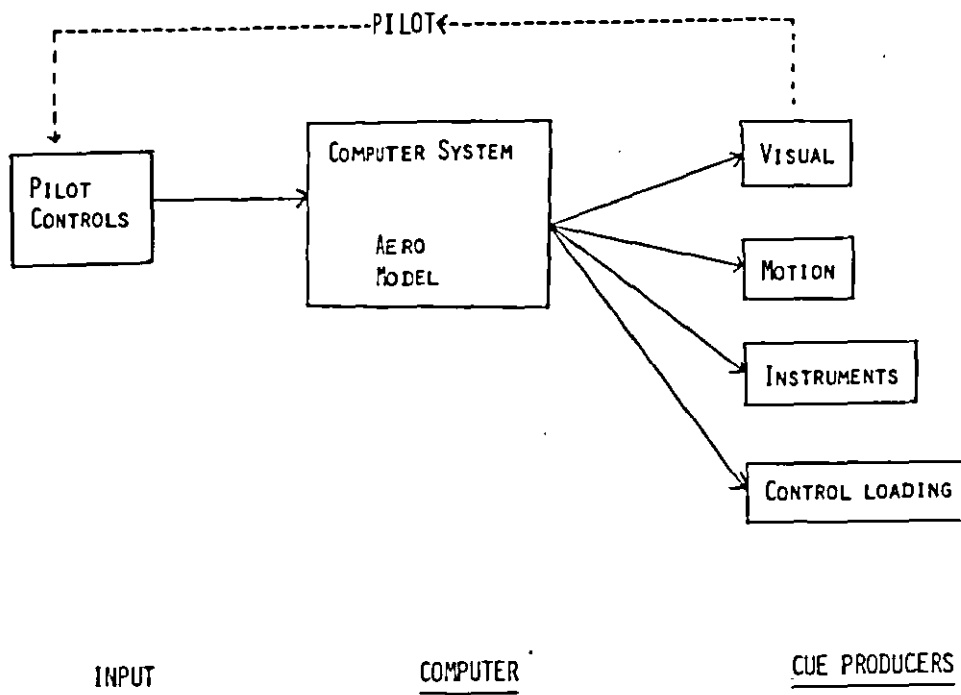
William L. Curtice is an electronics engineer within the Visual & Electro-Optical Branch, Flight Simulator Division, Directorate of Equipment Engineering. Mail: ASD/ENETV, Wright-Patterson Air Force Base, OH 45433. Phone (513) 255-4407.

INTRODUCTION

Background - Military and commercial use of flight simulators for crew training has expanded rapidly in recent years in response to the rising cost of energy and new aircraft. Simulator based training systems now enable commercial airlines to transition crews from one aircraft to another (i.e., DC-9 to DC-10) with as little as one hour of actual aircraft flight time. Current trends indicate that non-revenue (training) flights may be completely eliminated by some airlines in the near future as the effectiveness of both simulator hardware and related instructional systems is improved. Military flight simulation has traditionally been more demanding of technology than its commercial counterpart. When compared to airline flight operations, military flight tasks are more difficult, involve more diverse and complex systems, and demand development of vastly more complex simulators. Future military flight crew training programs will depend on use of a "family" of training equipment, ranging from table-top part task trainers to fully integrated weapons systems trainers (WST). The most complex of these simulate not only the airframe flight dynamics, basic flight instruments and controls, but also closely duplicate the control stick "feel", cockpit motion, vibration, buffet, and the pilot's complete external visual field of view. Visual displays provide a complete 360° out-the-window view of the sky, horizon, ground terrain, airbases, ground targets, ground threats, airborne surface to air missiles, and other aircraft. Radar and electronic viewing system sensor imagery (forward looking infrared television - FLIR) is also provided, in conjunction with simulations of imagery generated by precision guided munitions and other weapons release and guidance systems. Navigation systems and electronic warfare equipment functions are also simulated. Thus, the WST represents a fully integrated trainer.

As pressure to trade-off flying hours for simulator time has intensified, military simulator users in turn have demanded simulation fidelity far beyond that which would have been acceptable in years past. This leads to consideration of simulator "cue" fidelity and "cue" correlation, which are discussed in the paragraphs which follow. However, to appreciate the problem of cue fidelity, one must first understand basic flight simulator architecture.

Figure 1 illustrates a highly simplified simulator architecture. In a basic sense, the pilot makes "inputs" to the simulator through the various aircraft controls (stick, throttle, switches, etc.) These inputs are used to change variables in simulation equations which are solved by the central computer.



Simulator Architecture

Figure 1

For example, the stick and throttles are used as inputs for the simulator's aero model, a set of equations of motion which are repeatedly solved "in real time" at the system's iteration rate. Typical iteration rates for aero are 20 to 30 times per second. As the equations of motion are solved, basic flight parameters are produced (airspeed, rate of climb, pitch, roll, yaw, etc.) These parameters are then processed as required to drive simulator "cue producers"; i.e., the hardware systems which provide cues necessary for the pilot to fly the simulator (i.e., visual displays, motion platforms, instruments, etc.) When the pilot pulls back on the stick, he expects to see the horizon move downward, feel the motion system tilt the cockpit appropriately, see the instruments move, and feel the forces on the control stick change. These are cues. Thus, the flight simulator may be seen as a closed "man in the loop" system, wherein the simulator is expected to provide accurate cues in response to pilots' inputs. The architecture discussed above is, of course, highly simplified; the computer system, for example, is solving modules dealing not only with aerodynamics, but with navigation, electronic warfare, fire control, precision guided munitions, and more. However, the concept in each case is the same; the simulator pilot makes inputs through his controls, and expects to perceive appropriate "cues" in response.

Proper "correlation" of the simulator cues is essential for any simulation. Human physiology allows us to sense an event time difference as small as 100 milliseconds. For example, if a man operates a switch controlling a lamp, and the lamp does not illuminate within 100 ms after the man moves the switch, he will be aware of the time delay. Thus, it is important that the simulator produce accurate cues which are properly time correlated with the control movements and with the other cues produced. Visual or motion simulation systems which respond to control inputs 400 or 500 milliseconds after the panel instruments react will be of little value. Moreover, it is important that the cues not only start at the proper time, but also that their magnitude versus time be matched to the aircraft performance. Matching of simulator cue time histories with those perceived by pilots in the aircraft thus becomes a major simulator design task. Failure to do so inevitably results in unhappy simulator pilots who report that the simulator "doesn't fly like the airplane." Quite often they can't tell you why it doesn't fly right; they merely perceive a difference. In most cases, that difference can be quantitatively traced to poor cue fidelity, or poor cue correlation. Of course, simulation is a cheating game; it is not technically possible to perfectly duplicate many cues. Designers must therefore be both clever and innovative in "tailoring" the cues available within the state-of-the-art such that perception of cue errors is minimized.

Development of flight simulator cue fidelity is largely a "black art." Each contractor pursues the matter a little differently. Initial success is highly dependent on the quality of aerodynamic performance data available from aircraft flight test sources. More often than not, data available falls far short of that needed for development of a high fidelity simulation. Reasons are numerous. Quality data may be unavailable due to the fact that a simulator is being developed concurrently with the aircraft, forcing use of generic aero models, wind tunnel data, iron bird characteristics, etc. Quite often, the only aero data available is based on tests of previous aircraft configurations which differ considerably from that to be simulated. As a rule, the only aircraft test data recorded and preserved is that required for airframe acceptance or performance evaluation; data characterizing the full spectrum of systems and cues perceived by the pilot is not acquired or preserved. At best, data available allows simulator designers to develop a good aerodynamic model. However, one must recognize that the aero model represents only one link in the chain of signal processing which occurs between the pilot's control input and cues produced. Flight test data is normally not acquired which can be used to support the "end to end" test concept discussed above.

Past simulator acceptance tests have been based on performance of a "family" of tests. Wherever possible, peripheral systems (such as electronic warfare hardware) are tested independently. Limited tests of the computer's aero module (which look only at the aero model, and do not consider the extensive data processing of control inputs, cue drive outputs, linkage delays, etc. which occur before and after the aero model) are performed using spare computer digital to analog outputs and strip chart recorders. Handling qualities (including control stick response) are measured statically. No multiple axis, dynamic tests are performed quantitatively. These tests are left to test pilots who evaluate the simulator performance subjectively. Thus a pilot is the first evaluator of integrated simulator performance. Government test procedures have normally required a subjective simulator evaluation by teams of experienced pilots wherein the contractor was required to make hardware and software adjustments until the dynamic simulator performance matches the pilots' memory of aircraft performance. Unfortunately, pilots became "simulator acclimated" in just a few days. All too often, simulator performance acclaimed as adequate by one team was judged inadequate by the team that followed. This subjective procedure usually resulted in an endless iteration of tests. There was no method of tracking a performance fidelity baseline; neither the contractor nor the government knew where we were at, where we had been, or where we should go. Such handling qualities tests ultimately delayed simulator deliveries at great expense to both contractor and government.

Functional concepts for the Simulator Data Test Instrumentation System were developed by Air Force engineers based on their experiences in the subjective domain discussed above. The SDTIS embodied two basic concepts. They were:

1. That it should be possible to quantify simulator handling qualities and track handling qualities changes through use of "end to end" system measurements; i.e., a comparison of cue time histories versus control input time histories, and
2. That, if given identical control inputs, the simulator and aircraft would produce "comparable" cue time histories. The first concept is now well proven; the second is still on trial.

Functional SDTIS requirements included the ability to:

- a. Quantitatively measure and record the magnitude, phase, and time relationship of simulator cues produced in response to standard dynamic, multi-axis control inputs. The recording capability must include simultaneous, synchronous acquisition of analog and digital signal data, optically acquired data such as dial pointer positions and visual display positions, g-seat and g-suit forces, motion platform position and acceleration, stick position, and stick force.

b. Make measurements of cue time histories produced in response to multi-axis control inputs produced by a mechanized, automated, simulator stick (and rudder) mover. The control movers must be programmable to produce standard reference inputs (step, ramp, and sine) as well as to duplicate aircraft control movements made by test pilots flying missions from which simulator reference data was taken.

c. Automatically reduce data recorded into forms readily useable by simulator engineers. In field co-plots of time histories were required as a minimum. (Cross plots were subsequently added as a requirement.)

d. Automatically compare (through on-site, in-field plots) data recorded against that obtained from flight test and other data sources.

e. Self calibrate, automatically scale, and label all data recorded.

f. Be field portable such that the system could be easily transported (as airline luggage if necessary) to contractor facilities or Air Force field sites.

Development Status - Development of the SDTIS is now nearly complete. This work was performed over the last two years as an "in-house" development project within the Visual and Electro-Optical Branch at Wright-Patterson Air Force Base. Ninety per cent of the design, and 50 per cent of the fabrication was performed as an "additional duty" responsibility by Air Force simulator engineers, technicians, and cooperative engineering students who were also required to support simulator acquisition programs. The balance was performed as sub tasks by a local support contractor. All initial design objectives have been achieved; most have been expanded. Development cost to date is approximately \$300K for parts and contractor support.

System Description - The SDTIS system is shown in Figure 2, as represented by the block diagram of Figure 3. It consists of a family of sensors, video encoding and decoding electronics, a video recorder, a mini-computer, graphics terminal with hard copy unit, and a family of control movers. The functions of each subsystem will be discussed below.

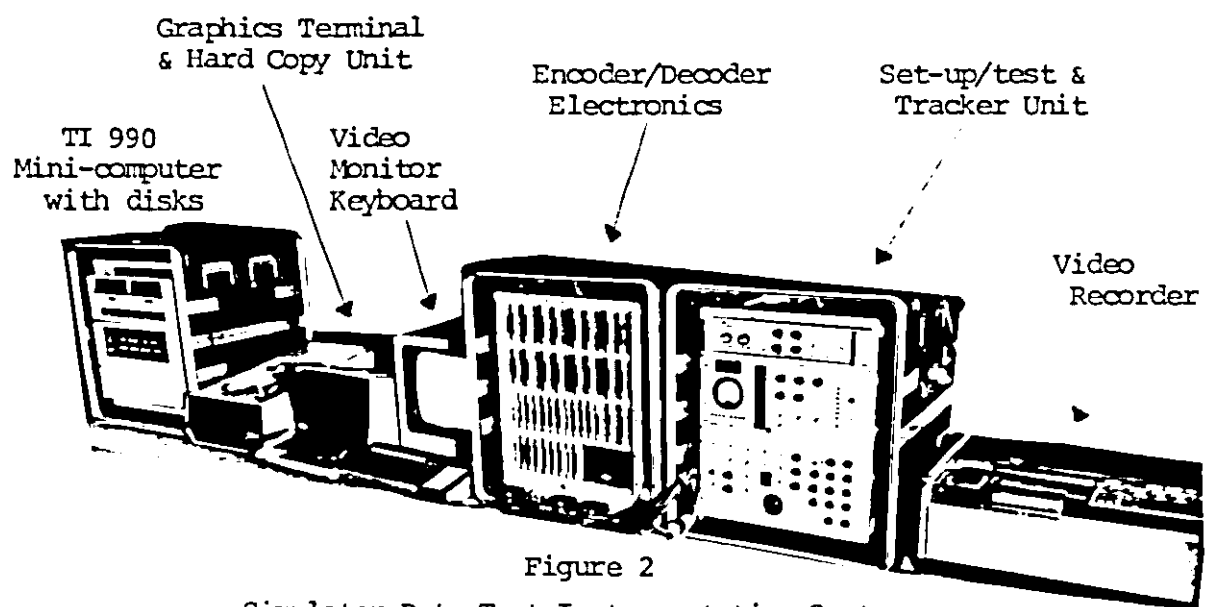


Figure 2
Simulator Data Test Instrumentation System

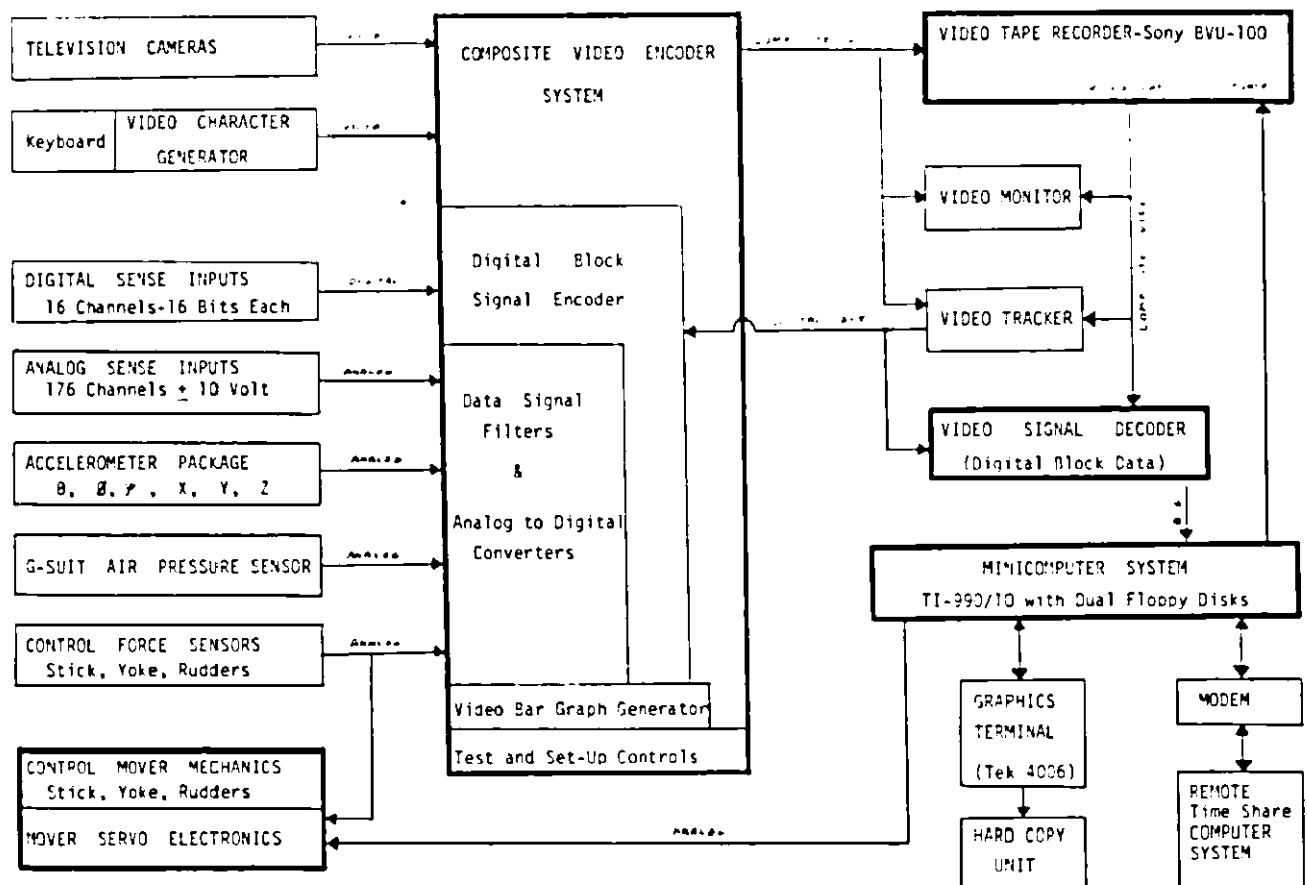


Figure 3
SDTIS Block Diagram

Sensors - Six basic sensors have been provided for simulator instrumentation. These are:

1. Analog signal inputs - The SDTIS system has the capacity to record 176 channels of analog signal data. The signal encoding, cabling, and filtering subsystems are physically and functionally organized into blocks of sixteen channels. Analog signals (from simulator electronics, back-planes, etc.) are acquired through the use of alligator clips, J-clips, push on connectors etc., and are connected to terminal blocks on J-boxes (or spider boxes). See Figure 4. Each J-box accommodates sixteen signals. Fifty foot lengths of multi-wire cable are then used to connect the J-boxes to the encoder electronics rack. Analog channel inputs are differential with input impedances which exceed one meg ohm (limited only by the cable capacitance). Portable, hand held, battery operated isolation electronics are used where signal loading is a problem and additional isolation is required. Simulator signals thus acquired include control force and position follow-up signals, command and follow-up signals for visual system servos, motion platform servos, panel instruments, and g-seat bellows.

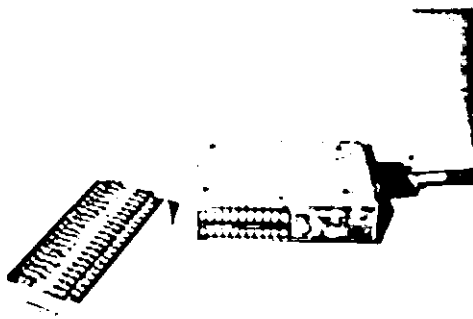


Figure 4

Analog and Digital Sense Boxes

2. Digital signal inputs - The SDTIS system, as currently configured has the capacity to record sixteen 16-bit digital channels. Signal input mechanics are configured much like the analog inputs discussed above, except that the J-boxes house active electronics which:

- a. provide additional isolation
- b. provide for digital word latching triggered by an external signal (master clock or signal valid), and
- c. accommodate digital inputs of varying thresholds, polarities, etc.

Each J-box handles one 16-bit input.

3. Motion Sensors - A motion sense package has been provided for motion platform acceleration measurements. The package consists of a three axis rate gyro, three linear accelerometers, and the associated electronics. (Rate gyros were chosen in lieu of angular accelerometers based on cost, availability and maintainability.) This package would normally be located at the pilot's seat; however, math exists and field operable software is under development that will permit comparison of measurements taken from anywhere on the motion platform with flight test measurements taken from anywhere on the airframe.

4. G-suit Air Pressure Sensor - A g-suit air pressure sensor has been provided to enable cue correlation between the g-suit, g-seat signal drives, and the motion platform.

5. External Position Follow-Up Sensors - Retractable string connected position sensors have been provided for measurement of control and servo movements in areas where internal simulator follow-up signals are unavailable or cannot be trusted.

6. Control Force Sensors - Force sensors have been acquired for stick, wheel/column and rudder control inputs.

7. TV Cameras - Three television cameras (one low light level intensified silicon vidicon, one Newvicon, and one silicon vidicon) have been provided for acquiring cues which are not available as electronic signals. Instrument panel dial pointer movements and visual display movements are of primary interest. Many simulator flight instruments are dc-servo replications of actual aircraft instruments - hence instrument response delays required to match aircraft instrument performance (cue correlation) are a simulator software function. Measurement of instrument command signals has been found inadequate for cue correlation work using the "end to end" test concept. A video tracker, capable of either edge or centroid tracking, has been provided to enable dial pointer/visual horizon position tracking. The tracker functions in conjunction with electronics which "mask" instrument or display geometry which may confuse the tracker. For example, a donut shaped mask is used to track dial pointers, so that the tracker is permitted to see only video from the arc transcribed by the dial pointer tip.

Data Encoder/Decoder - The encoder/decoder shown in Figure 5 is responsible for formatting all of the sensor signals discussed above into a composite video signal suitable for recording by a standard video recorder. The composite television picture format recorded is illustrated in Figure 6.

The first 15 per cent of each TV line is committed to hosting a 16-bit digital word. Thus, a "digital block" appears along the left edge of the TV picture which accommodates 240 words per TV field. All signal data is recorded in a digital format within the digital block. The remaining TV picture area (amounting to over 85 per cent of the active TV picture) is available for recording of TV camera video and for display of labeling information. Within the digital block, 176 words are assigned to analog signal data, 16 words to digital signal data and 48 words to data labeling information. Hardware signal filtering is available for selected analog input channels with various cut-off frequencies available from 30HZ to 240HZ.

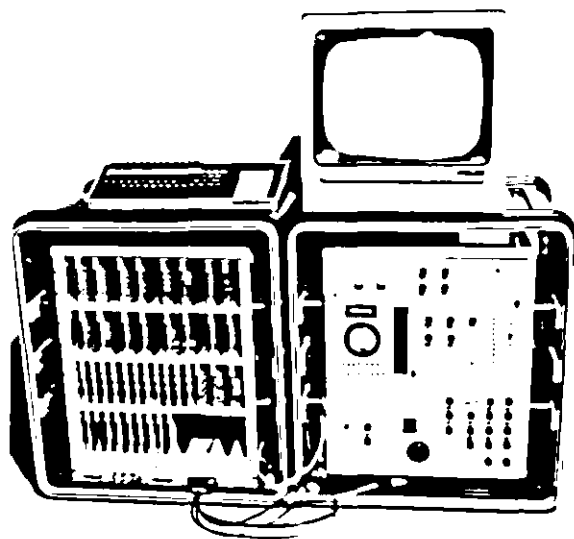


Figure 5

Encoder/Decoder Electronics
with Built-In Test/Set-Up Panel
and Video Tracker Controls.

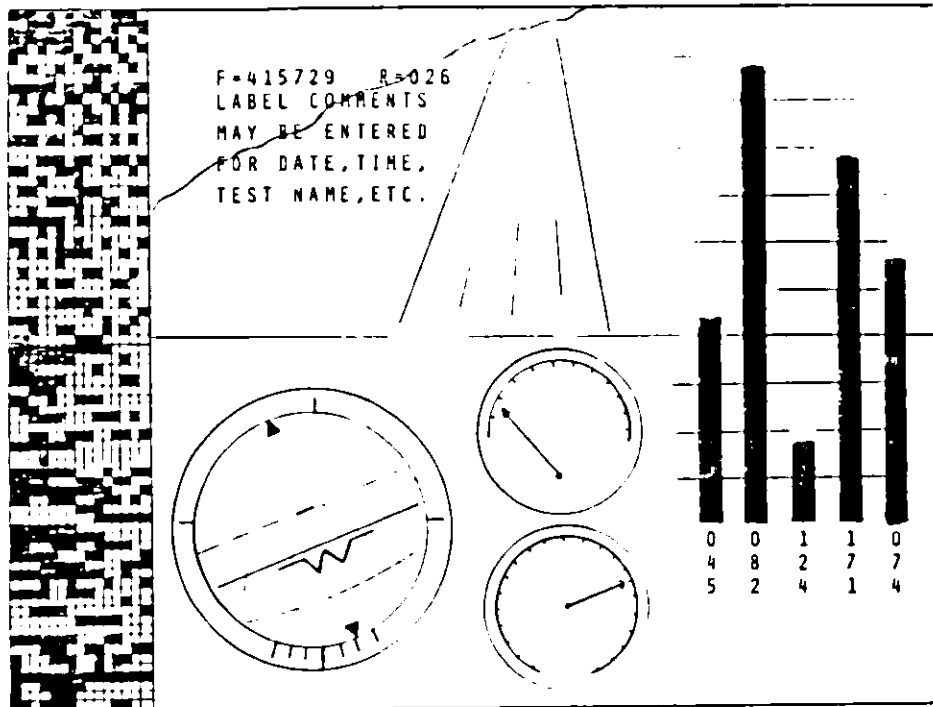


Figure 6
 SDTIS Video Format

A video bar graph system has been provided as a test and set-up tool. Up to ten vertical bar graphs may be added to the composite video picture. Any of the 176 analog channel signals may be assigned to any of the 10 bar graphs, with the bar height representing signal magnitude. Bar channel assignments are displayed at the base of each bar. The encoder electronics includes a video character generator for display of "labeling" information. Labeling is performed at two levels. First, each data run is identified with a label which appears continuously in the video picture, indicating run number, the ever changing TV field number, date, time, and miscellaneous comments. Second, each signal channel is labeled with a 64 character identification used to describe variable names, source, scaling, etc.. Channel labels do not continuously appear in the video picture as characters, although they are "scrolled" through the picture at the beginning of each data run. All label information is encoded in the digital block, thus making it available to the in-field computer for proper labeling of graphs and hard copy output data.

All labels, bar graph assignments and video image location assignments are controlled (entered) via a TV typewriter keyboard shown in Figure 7. Two channels of audio are concurrently recorded with the data discussed above. These are normally used to record simulator pilot intercom audio and test director comments.

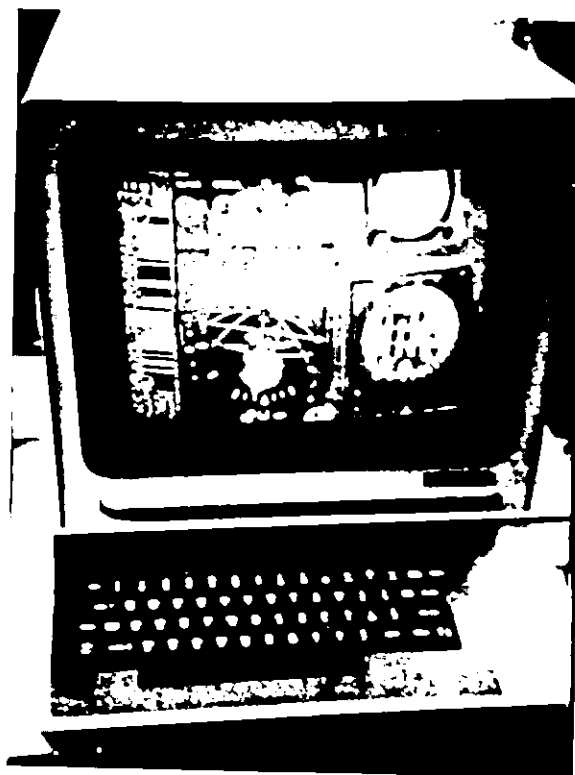


Figure 7
Television Monitor and
TV Character Generator Keyboard

Video Recorder - The SDTIS design concept is based on the use of a commercial, U-matic, 3/4 inch cassette, editing type, video tape recorder as the primary data recording device. (Figure 8 - Sony BVU-100) A video recorder was chosen because it:

1. was, in fact, a very wide bandwidth data recorder with information recording capacities which vastly exceeded those required for this effort, and
2. was available at very low cost, compared to available instrumentation recorders of comparable capacity, and
3. allowed integrated recording of audio and video data in addition to the digitally encoded multi-channel signal data, and
4. was easily interfaced to a digital computer allowing automation of data recording and reduction tasks.

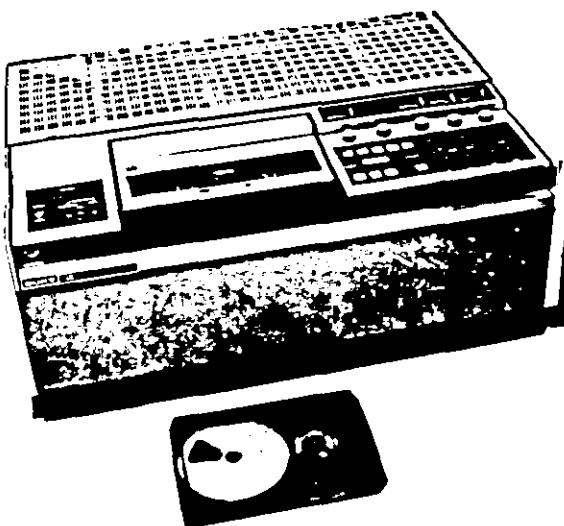


Figure 8
Sony BVU-100 U-Matic Video Recorder

The SDTIS design concept utilizes only 15 per cent of the active video field for recording the digital encoded signal data. This amounts to a 200 Killobit/second recording capability of one hour duration. If additional digital recording capability were required, the digital block could be expanded over the total active picture area to achieve a 1 megabit/second recording capability.

Recording Characteristics - The above paragraphs describe a very flexible data recording system. The inherent character of the TV signal format used provides a built-in 60HZ signal sample rate for all data recorded. In effect, each data channel is digitized, and recorded sequentially within the digital block. This means that each channel is sampled, sequentially in time 63 microseconds apart. The time shift of signal sampling normally provides no problem for typical simulator measurements - as all signals are sampled within 16.3 milliseconds - a recording time accuracy which exceeds all known requirements to date. However, software can be provided which will account for the line by line signal sample time offset in plotting. The sequential sampling does provide one advantage; signal sampling rates greater than the 60 HZ TV fixed rate are possible if the same signal is applied to two or more channels which are evenly spaced within the TV field. Thus, the system is capable of operating at a 120 or 240HZ samples rate, at the expense of the total number of channels available. To date, the 60HZ rate exceeds all simulator recording requirements.

Data Review - Once recorded, the video data may be reviewed by test personnel in much the same way you would review film with a film editor. Video recorder controls allow bi-directional tape playback at a variety of speeds running from field by field stop motion to twice real time. Test directors may listen to the audio and watch the movement of dials, indicators, and bar graphs representing selected signal data. As they slew through through the tape, they may also note the video field numbers appearing in the run data block. When a section of data of particular interest is located, the operator then need only note the field number appearing at the start of the data of interest.

Data Retrieval - The data retrieval system consists of a Texas Instrument TI-990/10 Minicomputer System, a Tektronix 4006 Graphics Terminal, and a Tektronix 4631 Hard Copy Unit. (See Figure 9.) The computer is a 16-bit minicomputer configured with 32K words of memory and dual floppy disk drives. Automated data retrieval is initiated using the graphics terminal keyboard to enter the beginning field number and the time duration for the data of interest. The computer will then take control of the video recorder, search for the data of interest, and transfer all digital block signal data from the video tape to the computer memory. Data is then sorted by channel and stored on a floppy disk. The operator will then be prompted to select the types of plots required. The graphics package will co-plot up to six channels of time history recordings, or will cross-plot ($X-Y_1 Y_2$) any three channels selected. See Figures 10 and 11 for examples of time-plot and cross-plot graphics. In each case, the plot packages will also label and scale the graphs using the run and channel labeling information entered prior to recording, and carried within the digital block. The hard copy unit will reproduce all graphics. It is significant to note that the plotting package and retrieve software process only sixty data points (samples across time) for each of the 192 channels recorded. The plotting resolution of the graphics hardware cannot practically handle more than 60 to 100 data points. Thus, if a data retrieve of one second is desired the computer will transfer and plot values for each channel from every TV field recorded during the one second period (60). However, if a two second retrieve period/plot is required, the computer would process and plot data for all channels from every other field. A ten second retrieve would result in data being taken from every tenth field, etc.. The system will retrieve and plot (on one sheet) data of any time interval from 1 second to 60 minutes using the sixty point sampling retrieve systems described above. Plotting of multiple 1 second graphs (most probably scotch taped end to end) is required in situations where every point recorded must be plotted. No simulator applications to date have required such plotting resolution.

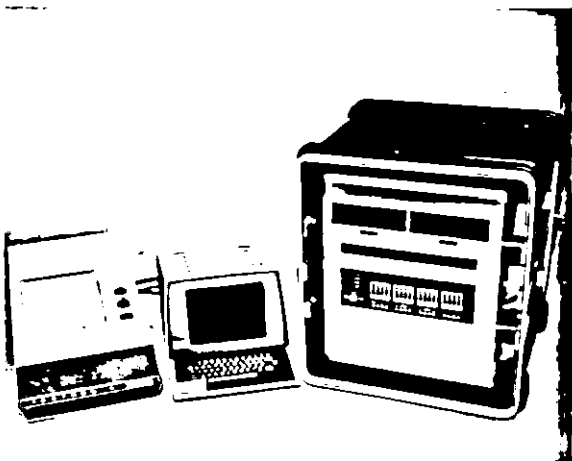


Figure 9

TI-990 Minicomputer
with Dual Floppy Disk

Tektronix 4006 Graphics
Terminal with 4631
Hard Copy Unit

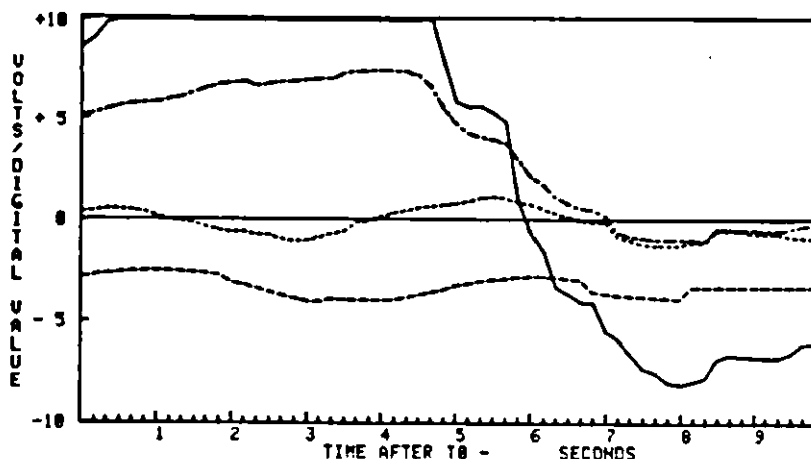


Figure 10
Time-Plot

RUN #:	5	GRAPH CHANNEL	LABEL INFORMATION	OFFSET/SCALE
START:	45888	19	819 STICK POS AILERON	0 1
STOP:	46685	28	820 PITCH RATE	0 1
RUN T-40.	5 SEP	21	821 ROLL RATE	0 1
1979. DEMO FOR		23	823 SIDESLIP ANGLE	0 1
MR. GIBINO AND				
COMPANY				

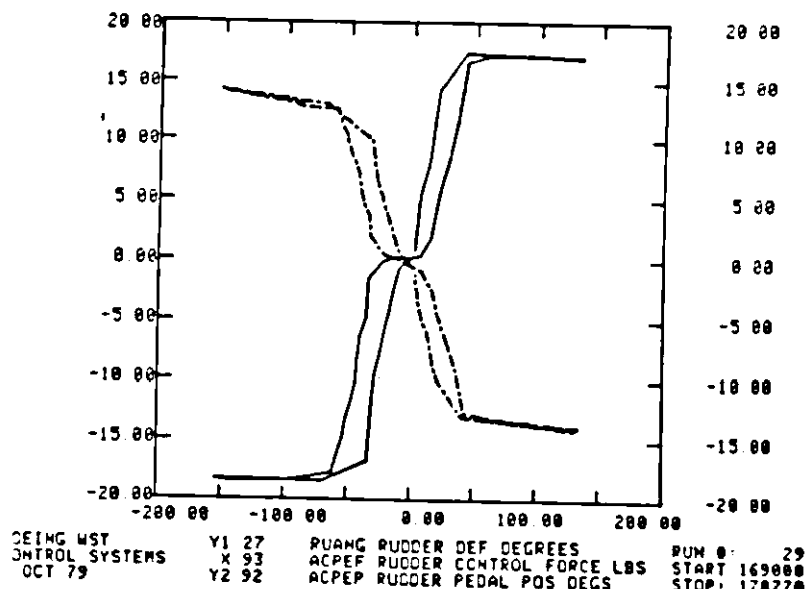


Figure 11
Cross-Plot

Data Analysis - A very limited amount of data analysis capability has been provided as part of the SDTIS software. Four programs will be available. They are:

1. Software Filtering - A three pole butterworth filter is available and can be used to process any 60 point time history retrieved from video tape.
2. Accelerometer Translation - An accelerometer package location translation program is in development which will allow pilot seat acceleration to be taken from anywhere on the motion platform.

3. Six Post Motion Platform Conversions - Many simulators today are designed with six post synergistic motion platforms. These systems provide six degrees of freedom movement, but the axis of platform motion is usually the synergistic product of the movement of six hydraulic drives. All simulator computer software is structured to drive these six hydraulic cylinders, with signals which are easily recorded. However, review of the six post drive values tells one very little - what is desired are the resulting values of platform pitch, roll, yaw, and heave (x, y, z). Transformations have been developed for this conversion. Thus, the six post drive/follow signals can be used to produce time histories of platform motion which can be directly compared to other simulator flight performance parameters or aircraft data.

4. X-Y Position to Angle Conversion-Routines for plotting video tracker X-Y position outputs as a function of dial pointer angle.

Extensive data analysis is possible if the SDTIS is linked to a larger computer system with a modem. This will permit use of techniques such as fast Fourier analysis which are generally beyond the capability of the SDTIS minicomputer. Software will be developed which will allow the SDTIS system to act as a data terminal to the General Electric Timeshare network. This arrangement should give simulator engineers the best of both worlds - independent data reduction to the maximum extent possible, coupled with the power of a large system when and where needed.

Control Movers - Previous sections of this paper have described the basic functions and design of the SDTIS - to sense cues, to record them, and to conveniently reproduce them as hard copy plots. However, the SDTIS (or any other instrumentation system) is incapable of fulfilling its intended "end to end" test roll without the ability to provide standard, controlled inputs for the simulator controls (stick and rudder). Comparison of cue time history data taken from run to run on the same simulator is not possible unless the control inputs (which caused the cues to be produced) were nearly identical. Even more significantly, comparison of simulator cue time histories with flight test data is not possible unless the simulator is flown under the same initial conditions, and with the same control inputs,

as the flight test airplane. Such controlled, standardized inputs are not possible using human operators (pilots). Thus, we see the need for a family of control movers that are capable of:

1. Three axis dynamic control inputs
2. Making standard control inputs which are likely to produce known results (ramp, sine, etc.)
3. Reproducing aircraft control inputs as recorded by flight test instrumentation, and
4. Operating in either a position or force mode (force versus time or position versus time).

Figure 12 shows the yoke and rudder movers with associated controls and electronics designed for this purpose. Test and system integration of the movers is now ongoing. When fully integrated, the control movers will be driven by pre-recorded control movement profiles which have been stored on floppy disks. Use of the movers will then complete our ability to perform a controlled "end to end" simulator system test. Figure 13 shows the yoke mover coupled to a control yoke. Note the force sensor located near the universal joint.

This completes the functional description of the SDTIS. As illustrated in the photographs above, all instrumentation hardware has been packaged such that it "could be" shipped as airline baggage by most carriers. However, the total system weight exceeds 2000 pounds. Air freight and truck are expected to be most often used.

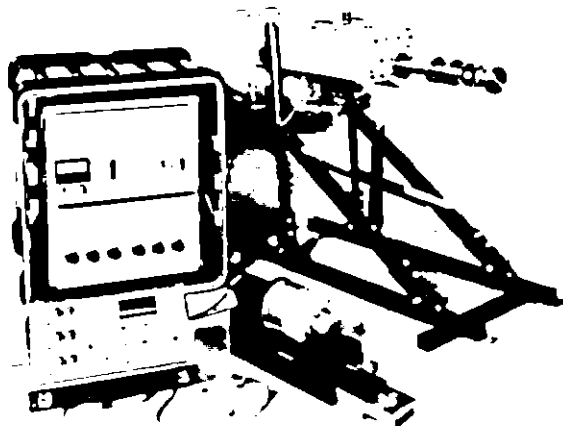


Figure 12
Control Mover Systems
(Yoke mover, Rudder
mover and associated
electronics)

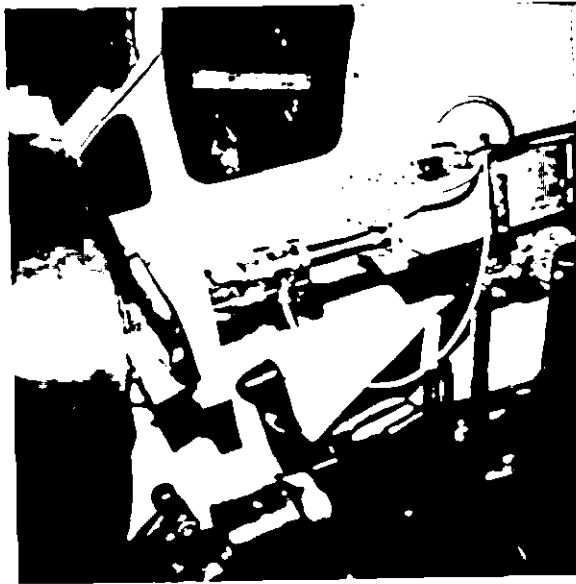


Figure 13

Yoke Mover Coupled
to T-40 Simulator Yoke

Future Systems - Data Bus Architecture - The current design concept of the SDTIS does little to consider the internal system architecture of the simulator. Of course, point to point signal tracing is possible - and was, in fact, a design objective. However, as simulator systems evolve, we expect to see the current analog interface systems replaced with architecture wherein both control inputs and cue producers (instruments and displays) are connected directly to a digital data bus. Thus, the signal tracing function will largely be replaced by a data bus monitoring function. Such is already the case with much electronic warfare (EW) simulation. The ability to eavesdrop on data bus communications is essential to system test and troubleshooting. An extension of the SDTIS to encompass data bus monitoring is now in design for the EW task. However, the basic "end to end" test concept of the SDTIS will remain unchanged. It is interesting to note too, that as aircraft systems architecture follow the data bus trend, high fidelity simulation may be even more difficult to produce. Aircraft controls and display technologists are now considering hierachal data bus structures, wherein data is processed (by asynchronous processors) and transferred from bus to processor to bus several times, may indeed be a challenge.

CONCLUSIONS

Simulator Procurement Impact - SDTIS availability is expected to significantly impact the Air Force procurement of flight simulators. Trainer handling qualities tests are expected to transition from a largely subjective activity, to a largely quantitative one, although subjective evaluation of handling qualities will probably never be eliminated completely. Use of SDTIS test procedures will be written into future procurement

specifications and the specifications themselves will be written in more quantitative terms than has been possible in the past. However, the degree of simulation fidelity achievable through use of SDTIS concepts is dependent on the degree to which the flight test instrumentation community can support simulator designers with high quality data.

Flight Test Impact - Use of SDTIS concepts in simulator procurement is expected to expand significantly during the 1980s. Thus there will be a demand for flight test data required to support the high fidelity integrated aircraft system simulation discussed at the beginning of this paper. This will likely impact the flight test instrumentation community in the form of requests for data from more sensors located in or near the cockpit, which are correlated with data obtained from other aircraft systems (engine, airframe, etc.). For example, accurate dynamic recording of stick and rudder position and force correlated to instrument readings, throttle setting and flight dynamics will be extremely valuable. Likewise, recordings of vibration, buffet, and g-forces experienced by the pilot and correlated to other flight dynamics will be critical to development of quality, dynamic motion simulation.. The nature of flight test data processing and massage may also be impacted. Complete time histories of control force or position may be needed in areas where only peak values were required before. This is illustrated by an example of pitch trim force. During level flight, when flaps are dropped, most aircraft will naturally assume either a pitch-up or pitch-down condition. The pilot must input some amount of control stick force to pull the nose back to straight and level. Aircraft specifications are usually concerned only with the peak stick force required to resume level flight. The only data which customarily shows up in the flight test report is that number - a single value. However, development of good simulation requires a knowledge of the complete stick force time history required to trim the aircraft. Thus, we can foresee a need for not only more data (from new sensors at additional locations) but also for expansions in reporting data that is currently recorded.

Application of SDTIS to Flight Test - The current SDTIS hardware was not designed to fly (although it could probably be tested and certified for airborne use assuming an aircraft had space to hold it). However, techniques developed for the SDTIS may provide solutions to some problems of concern within the flight test community. Of particular interest should be the use of digital encoded video recording techniques. One could expect an airborne instrumentation system based on such techniques to exhibit the following features:

1. Low Cost - Many test aircraft and almost all Air Force tactical aircraft are currently equipped with video recorders. The development and production of data signal encoding electronics required to exploit these recorders would be small compared to implementation of conventional flight test hardware.

2. Size and Weight - All electronics required to provide a 200 channel (either analog or digital) recording capability could be packaged into a $\frac{1}{2}$ ATR long case weighing less than 30 pounds. This assumes use of standard, commonly available components. Development and use of custom integrated circuits could reduce this size and weight considerably.

3. Recording Capability/Time - As currently configured, the SDTIS video system allows recording of 186 channels at a 60HZ sample rate, for a period of one hour, using standard cassette video tape. This recording capability is equivalent to a 200K-bit/second recording rate (and exhibits a bit error rate of 10^{-5}). As discussed previously however, expansion of the digital block concept could provide recording capabilities exceeding 1 mega-bit/second. Of course, the bit error rate may be improved as a trade off of picture area, number of channels, bit recording rate, etc.. Many cassette video recorders are limited in recording time to approximately 40 minutes. Yet, such a system (40 minutes, 1 mega-bit/second rate) may compare favorably to commonly used digital instrumentation system recorders.

4. Integrated Recording - Such a system would be capable of integrated video/data signal/audio recording (which is not possible using current IRIG/PCM standard equipment without adding time base generators, video recorders, or data links).

5. Independent, Stand-Alone Data Retrieval and Plotting - Current flight test instrumentation operations appear to be dependent on large computer complexes for data retrieval, reduction, and plotting. Such dependency often produces "priority" problems wherein low priority projects are delayed in order to permit expensive, saturated facilities to meet more urgent needs. Data retrieval, plotting, and even limited analyses are now performed by the SDTIS using hardware costing less than 50 thousand dollars. Pursuit of such a concept for flight test would permit each flight test engineer to have his "own" data reduction/plotting facility next to his desk. Moreover, the system could give him the ability to review aircraft data in ways not now possible.

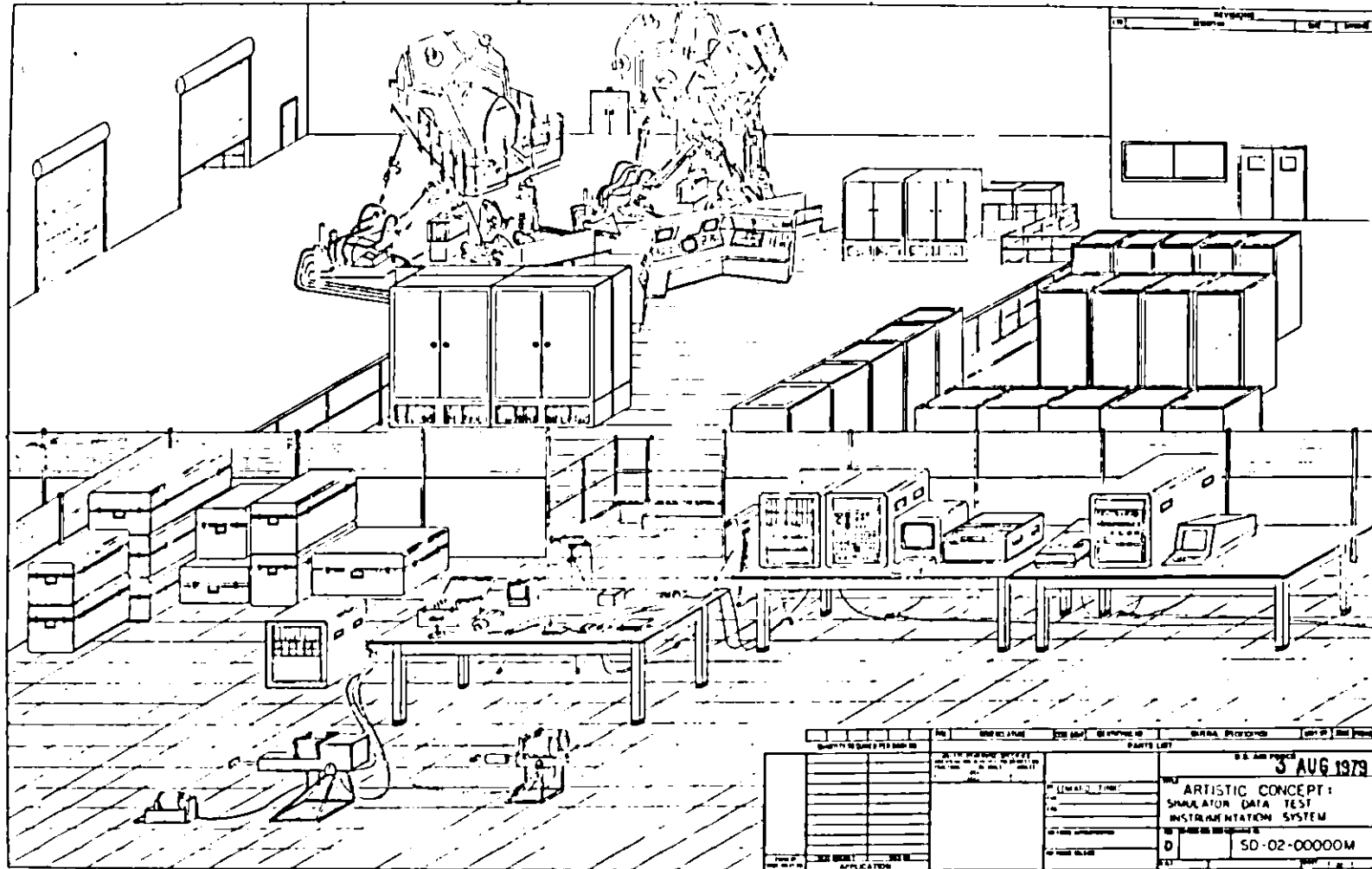
6. Inexpensive Media - The video tape cassette media is inexpensive, easily stored, and easily duplicated.

7. No Air-Ground Video Links - An on-board video recording capability with integrated signal data recording may reduce the need to use secure video data links to ground stations.

The SDTIS represents only one approach to exploiting a video technology that promises much capability at relatively low cost. Development of digital video sensors and recorders is now moving quickly due to the support of consumer and broadcast marketing interests. This work promises to yield future generations of advanced recording devices which may significantly surpass the capabilities of lesser developed recording technologies used conventionally for flight test instrumentation. The video techniques developed for the SDTIS should warrant serious consideration by designers of future flight test instrumentation systems.

SUMMARY

The Air Force has nearly completed development of a test instrumentation system for flight simulator fidelity evaluation. Use of this system in support of new flight simulator developments in the 1980s will result in new requirements for flight test data which surpass conventional practice. The simulator instrumentation system development itself proves several integrated video data recording concepts which are well worth consideration by flight test instrumentation designers.



SIMULATOR DATA TEST INSTRUMENTATION SYSTEM

THE BOEING FLIGHT TEST DATA SYSTEM 1980

Gerald J. Zanatta
The Boeing Commercial Airplane Company
Seattle, Washington

ABSTRACT

The 1980's bring a new and interesting challenge to Boeing Flight Test; two overlapping new airplane certification programs. In order to prevent the violent shifts in manpower experienced in the 1969/1970 time period, methods for increased productivity were required. The Flight Test Operating System was investigated and improvements began on its many parts. One part of that improvement effort is the redevelopment of the Flight Test Data System. This paper gives an overview of the Flight Test Data System as it will exist for the 767/757 test programs beginning in October of 1981.

INTRODUCTION

The 1980's present Boeing Flight Test with a new challenge. A challenge of two new airplane certification programs in an overlapping time span, the 767 and 757. At the same time product improvement programs for the 747, 737, and 727 airplanes will actively add to the Flight Test task. All of these programs are coming at a time when testing and data requirements have escalated due to general technical inflation in the aerospace industry. That inflation is generated by combinations of the following items:

- o The basic design of new airplanes has introduced new systems requiring new tests and new instrumentation.
- o The redundant nature of new airplane and system design has imposed requirements for repetitive testing to supply data for probability analysis.
- o Additional regulatory requirements have been imposed and existing regulation have become more stringent.
- o The use of simulation in design, performance checks, and crew training has added data and testing requirements in order to optimize the simulation data bases.

Gerald J. Zanatta, Supervisor, Flight Test Technology Group, Boeing Flight Test.

- o Tighter customer guarantees, resulting from higher direct operating costs, have caused more exacting performance analysis and consequently more instrumentation with greater accuracy.
- o Increased use of computerized data analysis systems throughout the engineering community has made the detailed analysis of larger volumes of flight test data a cost-effective and practical activity and hence increased demands for data.

To meet this challenge Boeing Flight Test began looking into ways of increasing productivity in the late 1970's. All aspects of Flight Test were investigated, a series of improvements identified, and redevelopment efforts started to optimize the Flight Test Operating System (FTOS). The FTOS consists of the people, machines, and procedures necessary to accomplish the Flight Test task. This paper will present an overview of one part of the FTOS - the Flight Test Data System.

FLIGHT TEST DATA SYSTEM

The Flight Test Data System exists to provide the various functions necessary to satisfy the Flight Test data functions. These functions include; calibration, conditioning, monitoring, recording, extraction, manipulation, analysis, and reporting of data obtained during an airplane test. These functions are graphically pictured in Figure 1. At Boeing Flight Test the systems required to accomplish these tasks have evolved from manual steps used by the industry in the past. Their nature and functions have not changed dramatically but the way the job is preformed has changed extensively. Today's systems all use computers to speed up and manage each system's operation. The computers vary from a large IBM 3033 main frame to small microprocessors used during data acquisition. The accumulation of systems being implemented to meet the 767/757 challenge are shown in Figure 2, and referred to collectively as the Flight Test Data System.

DATA ACQUISITION AND RECORDING SYSTEM

The current Data Acquisition and Recording System has been in operation since 1975 and the 747SP certification program. It is a system based on a Pulse Code Modulation (PCM) technology. The front end of the acquisition system interfaces with the transducer. It supplies an excitation voltage and electronic signal conditioning for outputting a signal to a Remote Multiplexer Demultiplexer Unit (RMDU). Currently there are 30 different signal conditioning networks used in conjunction with various types of transducers. The RMDU is programmable through a Programmable Read Only Memory (PROM) chip which provides the information to format transducer signals into a PCM bit stream. This bit stream is recorded on tape by a 14 track Honeywell tape recorder. The Boeing configuration uses a maximum of 6 RMDU's, each with a main frame format of either 128 or 250 words, sampled at a main frame speed of either 100 or 200 frames per second. Supercommutation (multiple main frame words to identify one parameter) allows parameter sampling rates up to a practical maximum of 800 samples per second.

Subcommutation (use of one main frame word for more than one parameter) provides a subcom table with a practical limit of forty levels or 2.5 sample per second data.

Part of the acquisition system is made up of various subsystems designed to reduce post test processing by manipulating data before recording. The following is a list of four such items.

- 1) Gross Weight and Center of Gravity Subsystem - This system provides a real time computed value of airplane gross weight, center of gravity, and moments of inertia. It also provides the means of changing center of gravity and gross weight with a water ballast control system. A microprocessor monitors fuel used, fuel manifold system status, tank quantities, and water ballast configuration to compute all required parameters. This output is recorded on tape, used by the onboard monitor and in post test processing.
- 2) Microwave Positioning System - An onboard minicomputer system which uses inputs from ground based transponders to calculate airplane position and altitude. This system provides real time space position answers both onboard and to a ground based system used in analyzing airplane noise data. It also provides computed values for recording on tape (requiring no post test calculations).
- 3) ARINC Capability - Provides interface to various ARINC data busses for extraction and conversion of data for the acquisition and monitoring systems.
- 4) Space Positioning Airborne Camera Equipment (SPACE) - An investigation is currently underway to determine the ability of an airborne TV videocom system to provide real time space position data for all types of testing. This system would digitize a video signal, feed a mini-computer and output space position parameters for use by the onboard monitoring and recording system.

AIRBORNE DATA ANALYSIS AND MONITOR SYSTEM

The Airborne Data Analysis and Monitor System (ADAMS) is an onboard real-time computer controlled system used for: instrumentation preflight activities, instrumentation monitoring, real-time test parameter monitoring, and onboard test analysis. The system uses a ROLM 1666 "Rugged NOVA" mini-computer with a 64K byte core as its central processor. The interface to the PCM acquisition system allows viewing of the data either before it is recorded or from a read head on the tape deck after it is recorded. Front end equipment consisting of PCM decommutators and programmable word identifiers (word ID), convert the PCM bit stream into a readable form for the central processor. The central processor is operator controlled through a keyboard allowing the channeling of data either directly to a Digital Analog Converter (DAC) or through the computer to the various output devices as shown in Figure 3.

The information necessary to set up the ADAMS input devices and central processor is available through a floppy disk produced from a central data base in the Flight Test Computing System, as explained later. The test engineer, through the floppy disk, specifies: the measurements required for the test, the various display device groupings necessary, and the application programs required for real time data analysis. The required measurement listing will provide a sequential display for the instrumentation preflight functions. The measurement grouping information will assign a single identifier for routing of those groups of measurements to individual output devices. The request for application programs will generate the input parameters, the algorithms needed and predefined output displays. Table 1 lists some of the current programs in use. The system can be operated as both a test engineer's analysis station and an instrumentation monitor station at the same time via separate terminals. Data output is via any of the devices noted in Figure 3. The CRT outputs alpha numeric data while the graphics system provides either time history or cross plot presentations. Any measurement signals can be routed through the DAC to the analog display devices. When combined with the playback capability of the Recording System the ADAMS can be used to do post test analysis. Figure 4 is a typical 2 station installation in a 747.

GROUND ANALYSIS STATION

The Ground Analysis Station (GAS) is a ground based duplication of ADAMS. It is a user oriented tool which provides a separate path "quick look" capability to troubleshoot test or data problems immediately after a test. The main differences between the GAS and ADAMS are in enhancements to the system display outputs, and capability to rapidly search the flight tape for test condition times. Figure 5 presents a block diagram of the system and indicates the modified components. The oscilloscope (visicorder) has the additional capability of printing coordination time on its output. The line printer is a 132 column machine with 600 lines per minute capability.

The system is capable of reading any measurement recorded on the flight tape. Any of the application programs available on the ADAMS are available for data manipulation. Output via any device, particularly the graphics station will be used for limited amounts of "final data". Figure 6 is a picture of the current layout in the Flight Test Center is Seattle.

TELEMETRY ANALYSIS STATION

The Telemetry Analysis Station (TAS) provides Boeing Flight Test the capability to handle "minimum crew" tests. Tests deemed "hazardous" are flown by a crew only large enough to operate the airplane and are monitored in real time through a telemetry link to the Flight Test Center in Seattle.

The GAS provides the central processor for this system. It is coupled with a antenna/receiver system at the front end and additional output devices, including a Fourier Analyzer on the output end. (Figure 7).

The signal transmitted from the airplane is received by an antenna/receiver at the Flight Test hangar, and sent via coax cable to the GAS facilities in the Flight Test Center. Two tracks of PCM data can be transmitted through the system simultaneously and routed by the engineer to any of the output devices in Figure 7. All gains and scaling are controlled by the engineer through the central processor. Additional analog output and tighter phase correlation is required during flutter tests, the biggest user of this system, so measurement selector hardware was added to route data directly from the Word ID to the double integrators or the analog output devices. A Hewlett-Packard Fourier Analysis System was added to the output side of GAS. This system will operate in near real time to produce modal parameters necessary to understand the dynamic behavior of the airplane. Figure 8 shows the system in use during a flutter test with 3 brush recorders monitoring acceleration and displacement data. Not pictured in the figure are the Fourier Analyzer and the central control console used by the test director during a test.

DATA PROCESSING GROUND STATION

The Data Processing Ground Station (DPGS), extracts data from the Flight Tape and passes that data to the Flight Test Computing System (FTCS) for processing. To accomplish this the DPGS uses a DEC PDP 11/70 computer to control an EMR Telemetry Front End for extraction and a disk/tape system for passing data to the FTCS. The Flight Tapes can be mounted on any of 4 tape recorders which are computer sequenced to allow data extraction to proceed while the other tapes are being searched for their next data time frame. The DPGS receives its extraction information from the FTCS data base electronically and then stores it in its own data base. During the extraction process the data may be passed through any of the following edit processes of an EMR data compressor.

1. Reject all data
2. Pass all data
3. Multiply by 1/n
4. Pass only when Bit change
5. Pass only when Bit match
6. Pass only when no Bit match
7. Pass when a specified delta difference
8. Pass when within certain limits
9. Pass when outside certain limits
10. Pass when equal to specified delta slope
11. Pass absolute min/max out of N samples
12. Cumulative Sum of N samples

The data can have calibration coefficient algorithms applied or be passed as counts to the FTCS via IBM compatible tape. Figure 9 is a block diagram of the system. Two such system using shared peripherals will be used during the 767/757 programs.

FLIGHT TEST COMPUTING SYSTEM

The Flight Test Computing System (FTCS) serves as the focal point for the flight test data base and provides the computing power for final test data processing. The functions necessary to accomplish this are:

1. Input to the data base
2. Maintenance of the data base
3. Output of data base information to other data systems
4. Handling of test data after its extraction from the flight tape
5. Support of interactive graphics for test data verification and analysis
6. Execution of various Flight Test scientific programs using test data and data base information
7. Batch output interface
8. Storage of selected test data for future use

The system which performs these functions is diagrammed in Figure 10. The system uses an IBM 3033 main frame computer as its central processor. IBM system software interfaces the mainframe and applications software which provide data base and test data processing functions. This software in turn interfaces with software designed to perform specific flight test tasks. It is split into three groups; Data Base Applications Software, Test Data Processing Software and Scientific Programs Software.

The data base applications software supports an interactive data base, transactions are carried out through IBM 3278 terminals (figure 11). These terminals are channel connected to the 3033 and allow direct data base interaction via keyboard entry. Each transaction uses screen menus to step the user through all necessary inputs for a particular data base application. Any part of the data base is available for interactive display however certain elements are password protected to prevent accidental modification.

Requests for test data processing are via a menu on the 3278 terminal. A request is set up in the data base for the DPGS to use for extracting test data from the flight tape. The DPGS sends output data to the 3033 storage system where it is accessed by an IBM 618 graphics station (Figure 12). This station provides interactive analysis of the test data. The data can be viewed before and/or after running through the scientific programs of the FTCS. It allows the engineer to verify, edit, or reformat test data before passing it to Flight Test customers. The equipment allows for display of the data graphically on the Tektronics scope and digitally on the 3277 alphanumeric terminal. Hardcopy output can be made at the station or sent to the batch output devices.

Scientific program software is an accumulation of standard flight test algorithms used to output calculated test data (i.e. thrust, airspeed). These software packages interface with the data base to obtain specific airplane information and input measurement information.

The FTCS also controls the electronic communication of processed data to the other Flight Test Data Subsystems and to various user systems. Data can be transferred to the main Boeing Engineering Computer System for storage in any of the staff or customer user accounts. Conventional output of data is handled through either on site plotting on Verstec plotters or a IBM 3800 Laser Printer capable of 20,000 lines per minute.

INSTRUMENTATION SUBSYSTEM

The Instrumentation Subsystem receives data base information from the FTCS and converts it into a form useable by the Airborne Data Analysis and Monitor System (ADAMS) and the Remote Multiplexer Demultiplexer Unit (RMDU). Data base information requested by the Flight Test engineer interactively via the 3278 terminals initiates a process which will electronically transmit format information to a Programmable Read Only Memory (PROM) programming machine to initialize an electronic chip which is the "brain" of the data acquisition system. Another interactive transaction in the FTCS will output that data necessary to produce a floppy disk for the ADAM System. This disk will carry the information to identify each measurement for display onboard, to apply calibration to each measurement and to group series of measurements into useful test packages.

The system is portable and can be taken to remote base sites to receive data from the FTCS in Seattle for update to the acquisition and ADAM systems.

CALIBRATION LABORATORY

The calibration laboratory provides a full range of metrology services for the Flight Test instrumentation systems. Precision electrical, mechanical and physical reference standards are maintained and periodically certified. In addition to performing periodic maintenance and calibration, the laboratory conducts evaluation, engineering acceptance and environmental testing of data acquisition and recording systems and components. Most sensing devices (transducers) and signal conditioning electronics are calibrated under closed-loop program control using mini or desk top computers. All calibration data is analyzed and formatted by a laboratory computer which transmits the calibration data and the resultant calibration coefficients to the Flight Test Computing System's data base. Check of proper data base entry is through the 3278 interactive terminals. Once entered into the data base calibration data is available for display to all users through the alphanumeric 3278 terminals or as plots on the 618 graphics stations.

ADAMS DEVELOPMENT LABORATORY

The ADAMS Development Laboratory provides the ADAMS operating system and application programs. This lab keeps the FTCS data base updated with the system software necessary to operate the Rolm 1666 computer and all peripheral equipment which make up the airborne monitor system. Another function is to produce application programs, from user

requirements, to operate on the ADAMS. These programs are of a changing nature due to airplane program requirements and require rapid updating as well as configuration control. A direct link to the FTCS data base provides for instantaneous updating. The quick access of the data base provides turnaround of the transportable media required by the ADAMS on a per test basis.

CONCLUSION

The Flight Test Data System will provide the Boeing Flight Test organization with the tool necessary to meet the certification schedules during the 767 and 757 time frame. The implementation of this group of systems into a coherent unit will increase the productivity of the Flight Test Engineer by bringing together in one data base all elements of the Flight Test task.

The interaction from engineer to computer and back to the engineer should eliminate or at least minimize all the manual processes needed to track test data requirements.

All parts of the Flight Test Data System are currently in various stages of design and implementation. The system will begin operation on January 1st, 1981 and be in full operation before the 767 first flight scheduled in early October of 1981.

- o Basic Airplane Parameters - Computes parameters that provide a base for most of the other test analysis programs. These include gross weight, airspeed, altitude and corrected lift coefficients.
- o Cruise Performance - This program calculates the drag coefficient parameters and specific range or fuel mileage of the airplane during a stabilized condition, making corrections for minor variations in airspeed and altitude.
- o Stall and Minimum Speed Performance - This program identifies the minimum flying speed of the airplane and calculates the stall entry rate, FAA lift coefficient, and the corrected lift coefficient values at the minimum speed.
- o Loads Performance - This program combines strain gage output to calculate shear, moment, and torsional load values while simultaneously checking a predefined list of measurements for out-of-limit conditions.
- o Takeoff Performance - This program calculates a number of parameters required for takeoff performance evaluation. These include thrust values for each engine, thrust-to-weight ratio, ground distance from brake release, and others.
- o Power Plant Parameters - This program calculates a collection of parameters related to engine operation and performance. These include many different pressures, pressure ratios, temperatures, temperature ratios, fuel flow, and rotor speeds.
- o Flight Control Parameters - This program calculates a collection of parameters used to evaluate the performance of the Flight Control System. These include a number of engine pressure ratios, thrust values, corrected airspeed, yawing moment coefficients, sideslip angle, and a corrected coefficient of lift.

TABLE I
ADAMS APPLICATION PROGRAMS

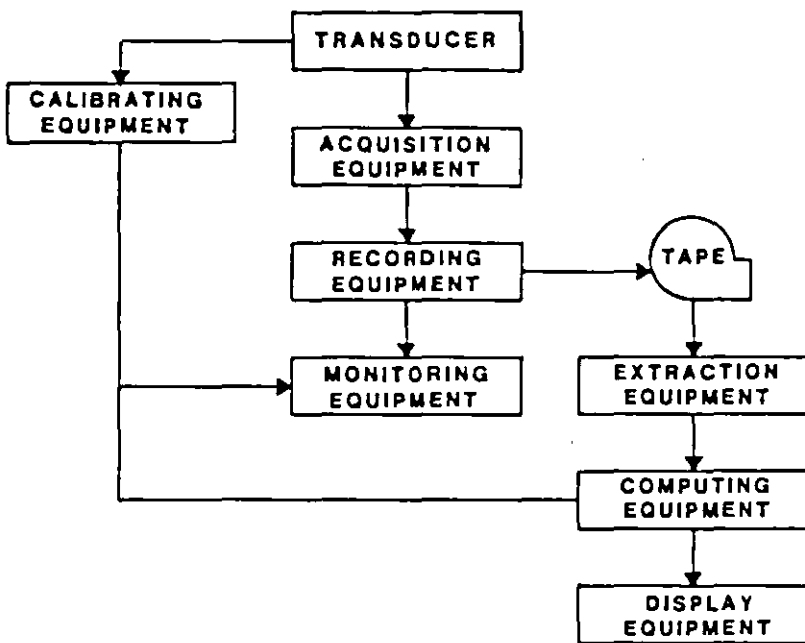


Figure 1
A Typical Flight Test Data System

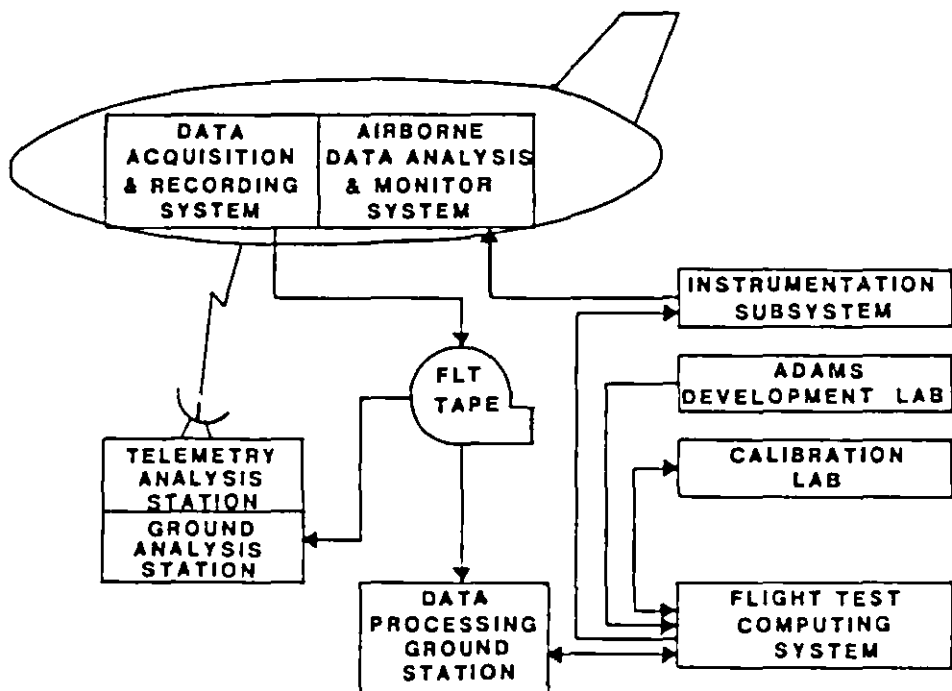


Figure 2
Boeing Flight Test Data System

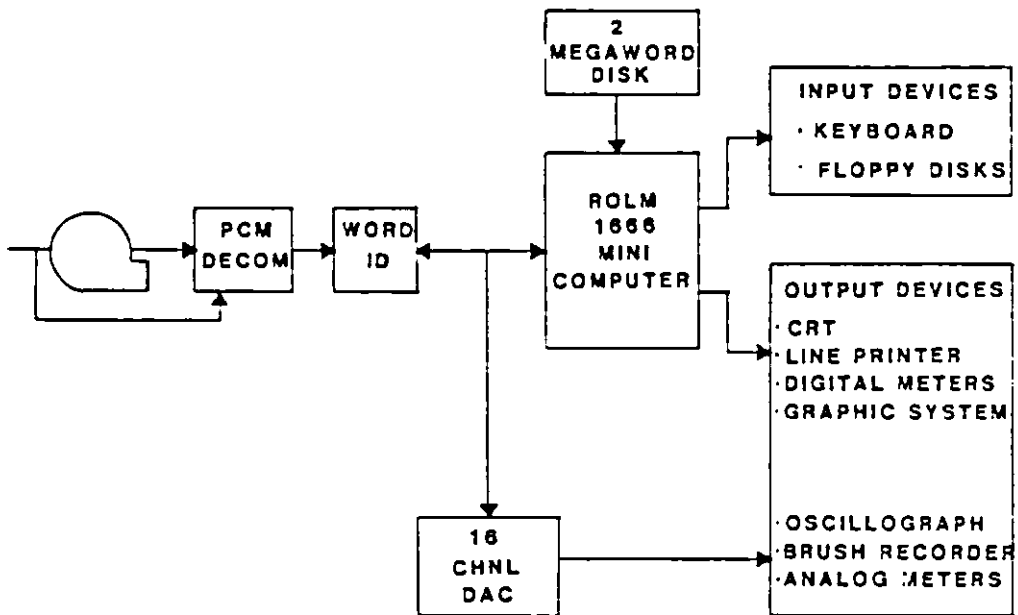


Figure 3
Airborne Data Analysis and Monitor System (ADAMS)



Figure 4
ADAM Analysis and Instrumentation Stations

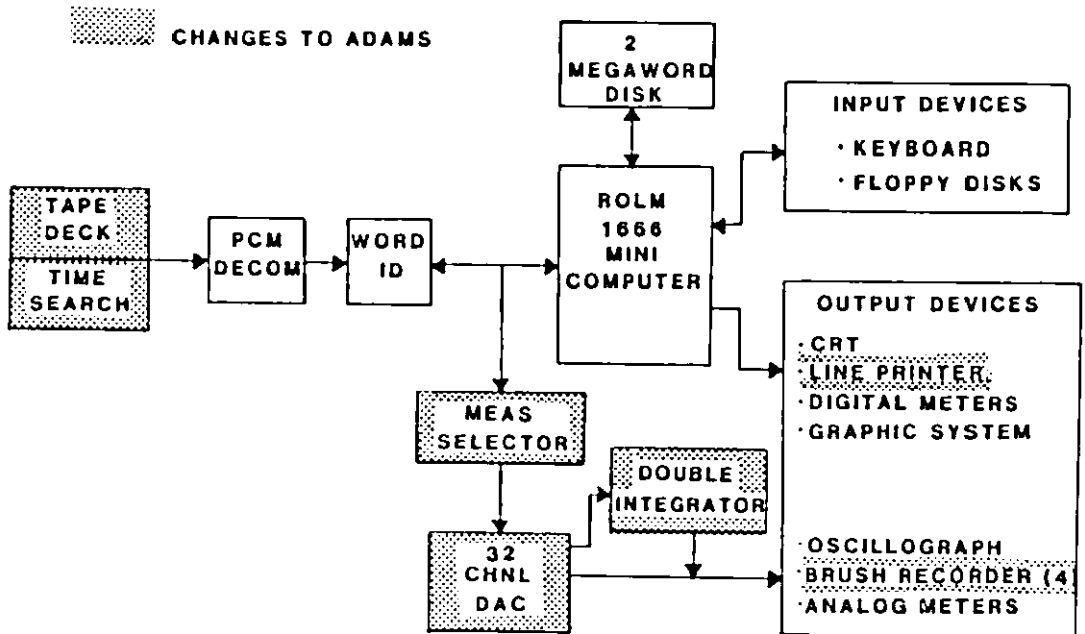


Figure 5
Ground Analysis Station (GAS)

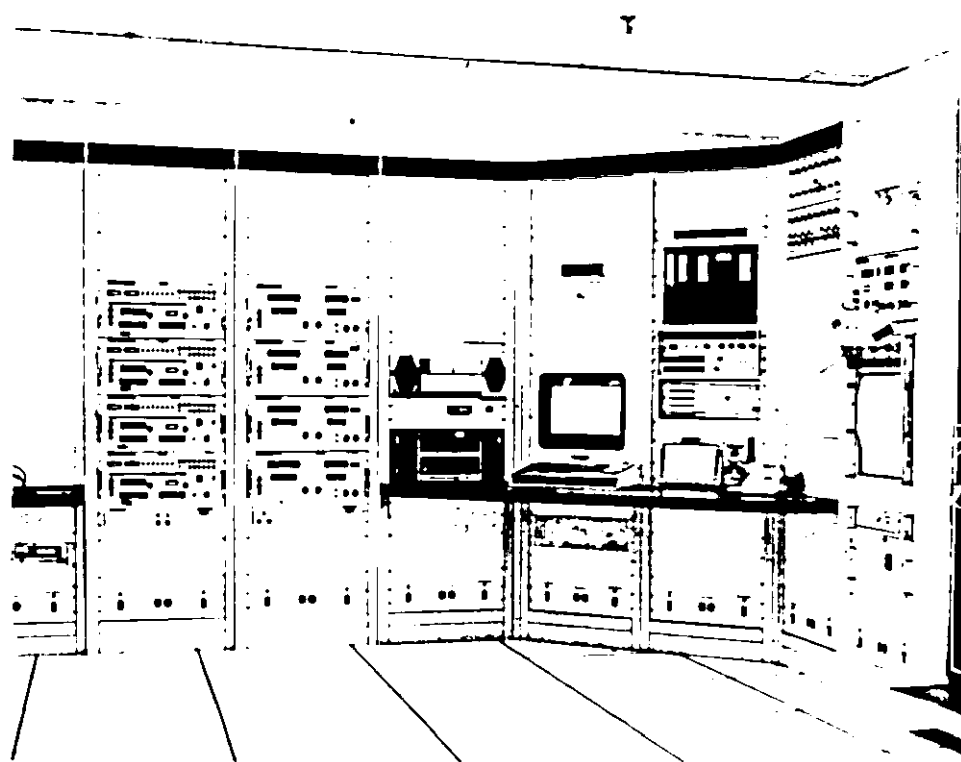


Figure 6
GAS Equipment in Flight Test Center

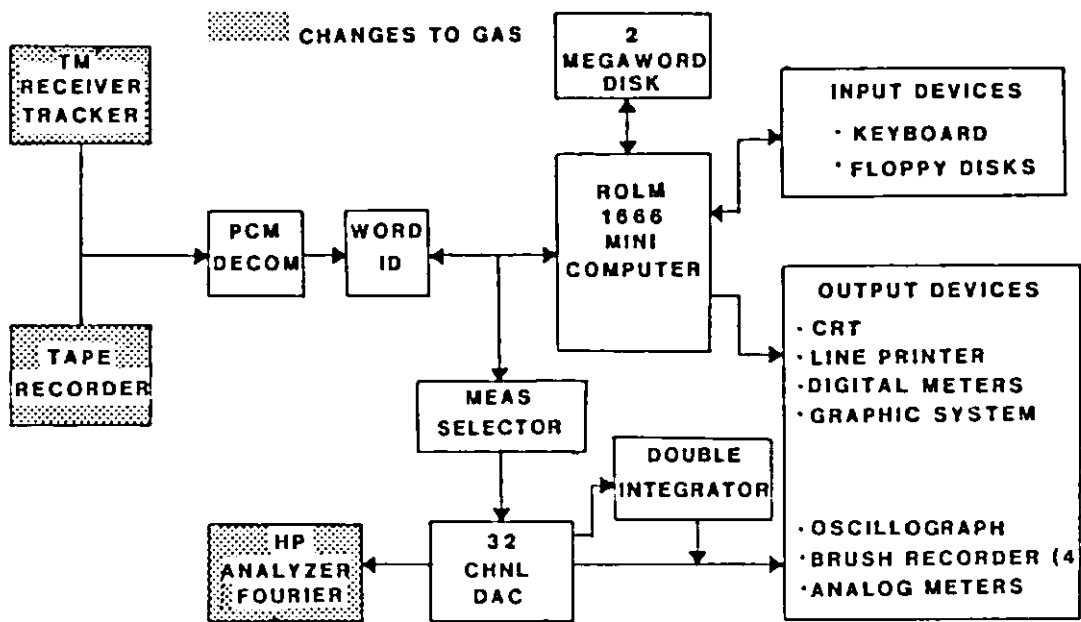


Figure 7
Telemetry Analysis Station (TAS)



Figure 8
TAS in Operation During a Flutter Flight

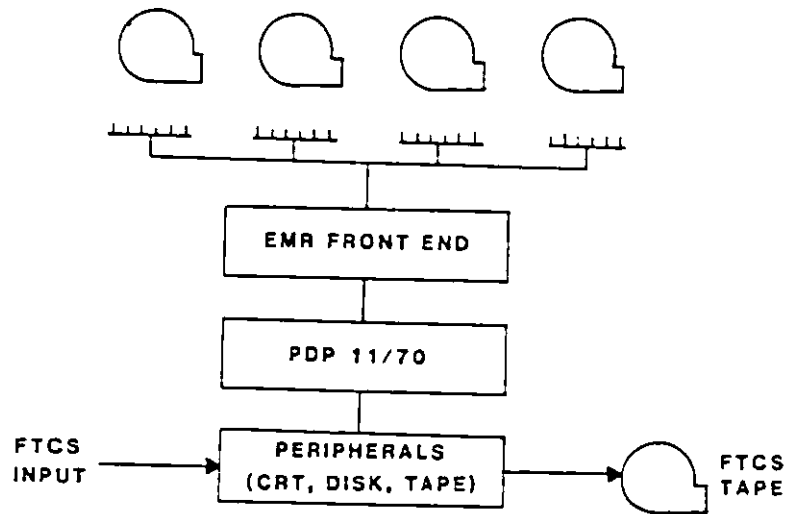


Figure 9
Data Processing Ground Station (DPGS)

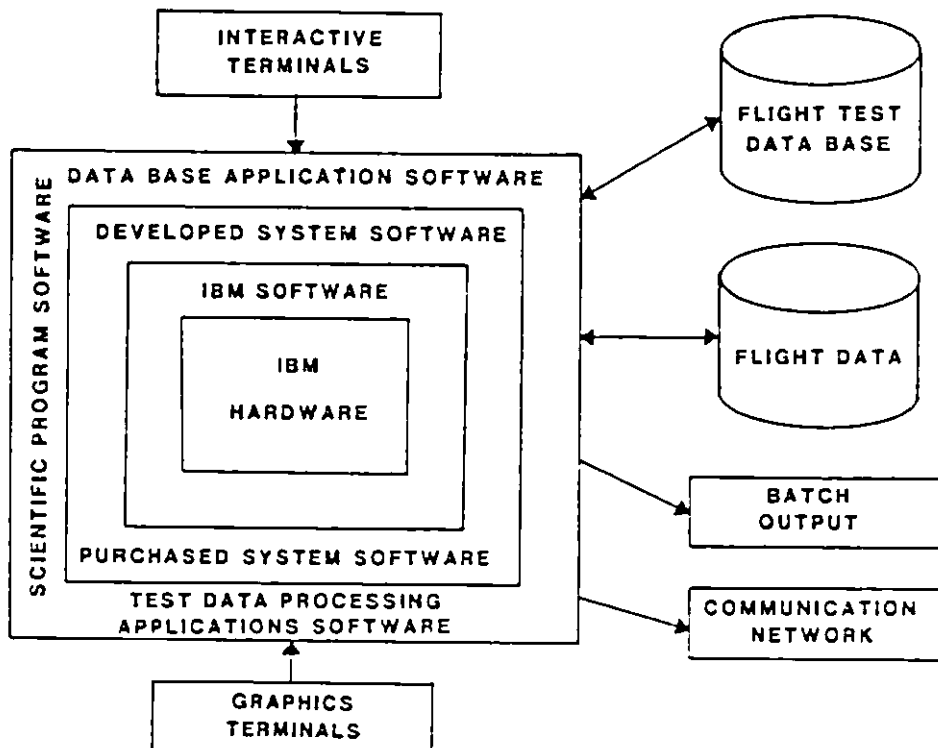


Figure 10
Flight Test Computing System (FTCS)

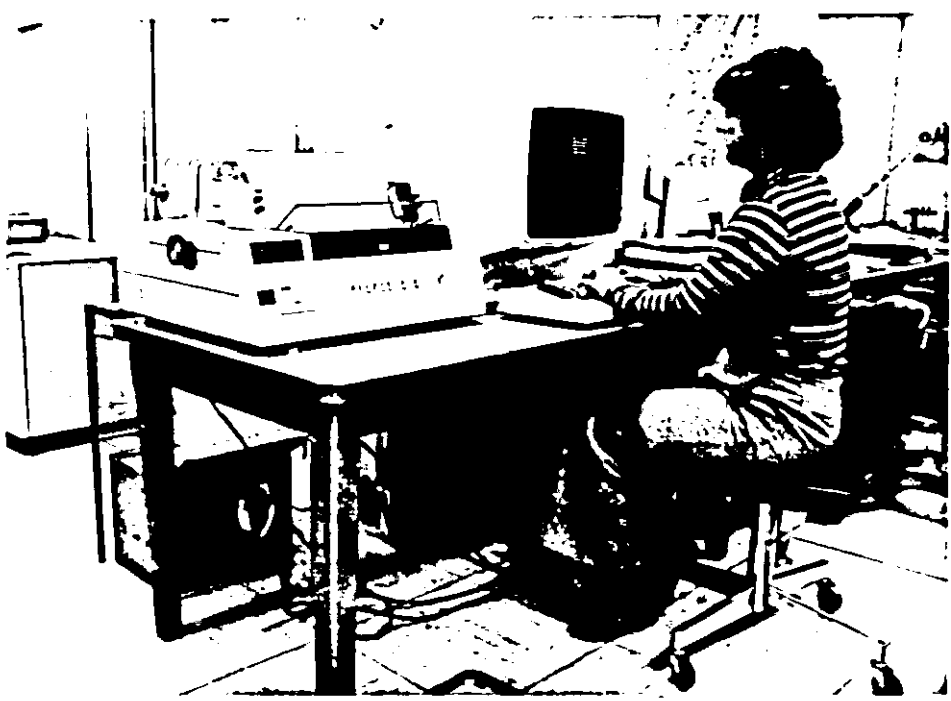


Figure 11
IBM 3278 Alpha-numeric Terminal and Printer



Figure 12
IBM 618 Graphic Station

INSTRUMENTATION REMOTE "MINI" GROUND STATION

Jack Nixon
Boeing Commercial Airplane Company
Seattle, Washington

With modern data and acquisition and monitor systems being capable of rapid changes to meet test conditions, the information necessary to make and monitor these changes must be readily available to the Instrumentation Engineer. With one centralized processing station, delays in the distribution of this information occur when airplanes are testing at an area remote from this central processing station, or when a large number of airplanes must use the same facility. At Boeing it is normal to have test airplanes located tens to thousands of miles from the central facility, and the 757/767 test phase will have both remote testing and large numbers of test airplanes.

What is being done to correct this problem is to "decentralize" this processing and place it directly in the hands of the Instrumentation Engineer. This is being done as part of a redeveloped Flight Test Computing System (FTCS) which will also allow the Instrumentation Engineer direct access to the Central Processing Computer via interactive Cathode Ray Terminals (CRT). Figure 1 shows the FTCS network.

Figure 2 shows the typical current flow of information from the Instrumentation and Operations Engineers back to the Instrumentation Engineer in order to prepare the Instrumentation system for an upcoming test.

The process begins with the Instrumentation Engineer filling out paper forms which describe the changes to be made to the Instrumentation Configuration, for example a transducer was replaced, new measurement added, etc. This form is then messenger delivered to the keypunch area where the information is transferred to cards and delivered to the large scale computer (IBM 3032). This deck, along with the Job Control Language (JCL) cards, is placed in the job cue for batch processing. The output of this process is a "Verification Report" which both verifies the changes made and reports any errors encountered in processing the changes. This report is printed at the large scale processor and messenger delivered back to the Instrumentation Engineer. When the Instrumentation Engineer is satisfied that all necessary configuration changes have been made correctly he inputs the "Instrumentation Ready" flag to the Request for Instrumentation Preflight (RIP) program via a CRT.

Jack Nixon, Senior Flight Test Engineer, Boeing Commercial Airplane Company, Instrumentation Projects Group.

When the R.I.P. is processed the Instrumentation Engineer receives a paper listing of the parameters to be preflighted, a punched mylar tape and, via the "Ground Station", a set of cartridge tapes. If changes have been made to the Instrumentation Configuration the mylar tape is then read through a programmable read only memory (PROM) programmer to produce the PROMS necessary to configure the Data Acquisition System for the changes. The cartridge tapes contain information necessary for the computerized onboard monitor system to acquire and convert the raw data to Engineering Units data using the same calibration coefficients as the large scale computer.

This information in its various forms (paper listings, PROMS and magnetic tape) is then taken to the airplane for preflight.

From this brief description it can be seen that the manual transportation of various items and having to route everything through a Centralized Processing area results in considerable delay if there is any amount of distance between sites and/or a large number of test airplanes to process through the single station.

The information flow that will result when the dedicated Instrumentation systems, which are called Instrumentation Sub-Systems (ISS for short), become active is shown in Figure 3.

The Instrumentation Engineer will be able to make the required configuration changes directly to the large scale computer via an interactive CRT and receive verification and/or error messages back in real time. This will eliminate the delay associated with the existing form fillout, messenger service, keypunching and the associated transcription type errors. Once the Instrumentation Engineer is satisfied that all changes to the Instrumentation Configuration have been made correctly, the "Instrumentation Ready Flag" is set as before.

What will happen now is considerably different than the previous information routing. All the information will be routed via a Remote Job Entry (RJE) data communications link to the Instrumentation Sub-System that has been designated as the system associated with the particular airplane of interest. If the system that the information is being routed to is "off-line" the information will be retained in the large scale computer and automatically routed to the ISS when it is brought back "on-line". This transfer will be made without intervention from either the ISS operator or the large scale operator. This is accomplished by assigning the RJE stream as "HOT". Each file that is transmitted will have header information which will supply such information as airplane number, test number and file type. A background program will automatically scan the headers on the data input via the RJE link and place the information in a file organized for an individual airplane.

Three types of files will be sent over the RJE link on a routine basis. These are PROM, Data Base and Listings. The Listing files will be routed directly to the Line Printer and the other two saved on disk.

With the previous "One station" concept, the Instrumentation Engineer had to either wait for the mylar tape to be punched by the large scale, delivered by messenger and manually run through the PROM programmer or manually make the required changes by reading the old information into the programmer and manually setting the required bit pattern changes. The new method will allow the Instrumentation Engineer to enter the Airplane Number, test number and PROM identification number into the ISS via a CRT terminal, and the PROMS will automatically be programmed from the information stored in the ISS. All manual programming and messenger service will be eliminated.

The data base information which is now placed on a 9 track tape by the large scale computer, delivered to the Ground Station, converted to cartridge tape and messenger delivered to the Instrumentation Engineer will be accomplished by the Instrumentation Engineer supplying the Airplane number and test number to the ISS and having Floppy disks programmed for the transfer of information to the Airborne Monitor system.

As an added advantage of the system, the ability of the System Technology Labs to transmit information from their computer, via the RJE link, to any or all of the ISS's allow for rapid dissemination of the Airborne Monitor system application and system programs which are also Floppy Disk based. This allows any changes or new programs to be quickly routed to the Airplanes that require the new information

With the RJE link information capable of being transmitted over telephone lines the Instrumentation Sub-Systems may be located anywhere a suitable modem can be installed. Presently six systems are being planned. One will be located at the Everett, Washington, 747/767 area, one at the Renton, Washington, 707/727/737/757 area, one at the Flight Test Facility at Boeing Field Seattle, Washington, and three systems assigned as "remote stations", capable of being moved to the areas where they are needed.

In summary, the Instrumentation Sub-Systems will be capable of being placed in the Instrumentation Engineers working area and give him direct control over the information he needs to assure data integrity. The replacement of messenger carried information with electronic communications will eliminate the delay between the request for information and the receival of the information. The interactive systems will eliminate transcription type errors and the immediate verification of the input data will eliminate the time lag now associated with batch operations.

SYSTEM DATA

CENTRAL PROCESSING UNIT: DEC PDP-11/34
128K words of memory
FP11A Floating Point Hardware
KG11A CRC/LRC Arithmetic Element

SOFTWARE: RSX11-M Operating System
Fortran IV +
BASIC Plus 2

DISKS: DEC RL11-AK Controller
two DEC RL01 5MB Disk Drives
AED 6200P Floppy Disk Controller
four AED Floppy Disk Drives

COMMUNICATIONS: DEC LA36 Decwriter for system communications
DEC DQ11-DA Synchronous DMA for RJE communications
DEC LP11-VA 300 LPM Line Printer
DEC DZ11-A RS232 8 Channel Comm. Interface
Interface for:
HP 2647A Terminal for user access
Data I/O System 19 Prom Programmer

DEC - Digital Equipment Corporation
AED - Advanced Electronic Design, Inc.
HP - Hewlett Packard

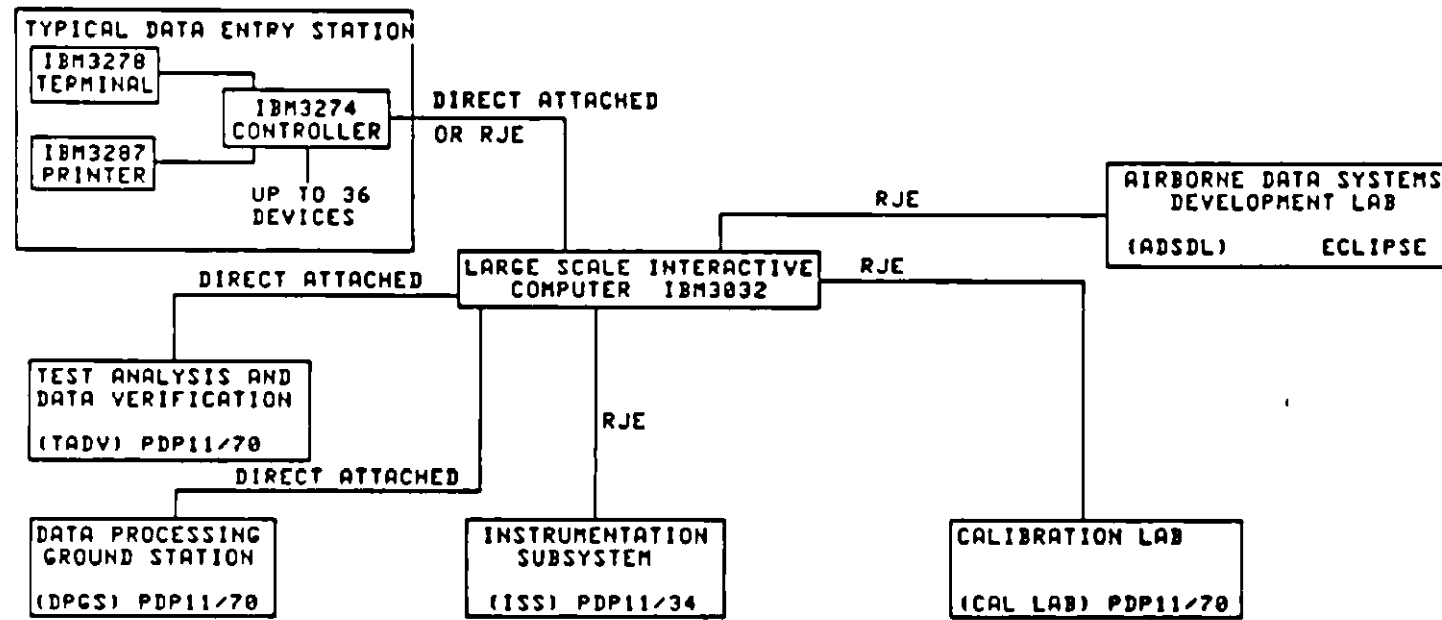


FIG. 1 FLIGHT TEST COMPUTING SYSTEM NETWORK

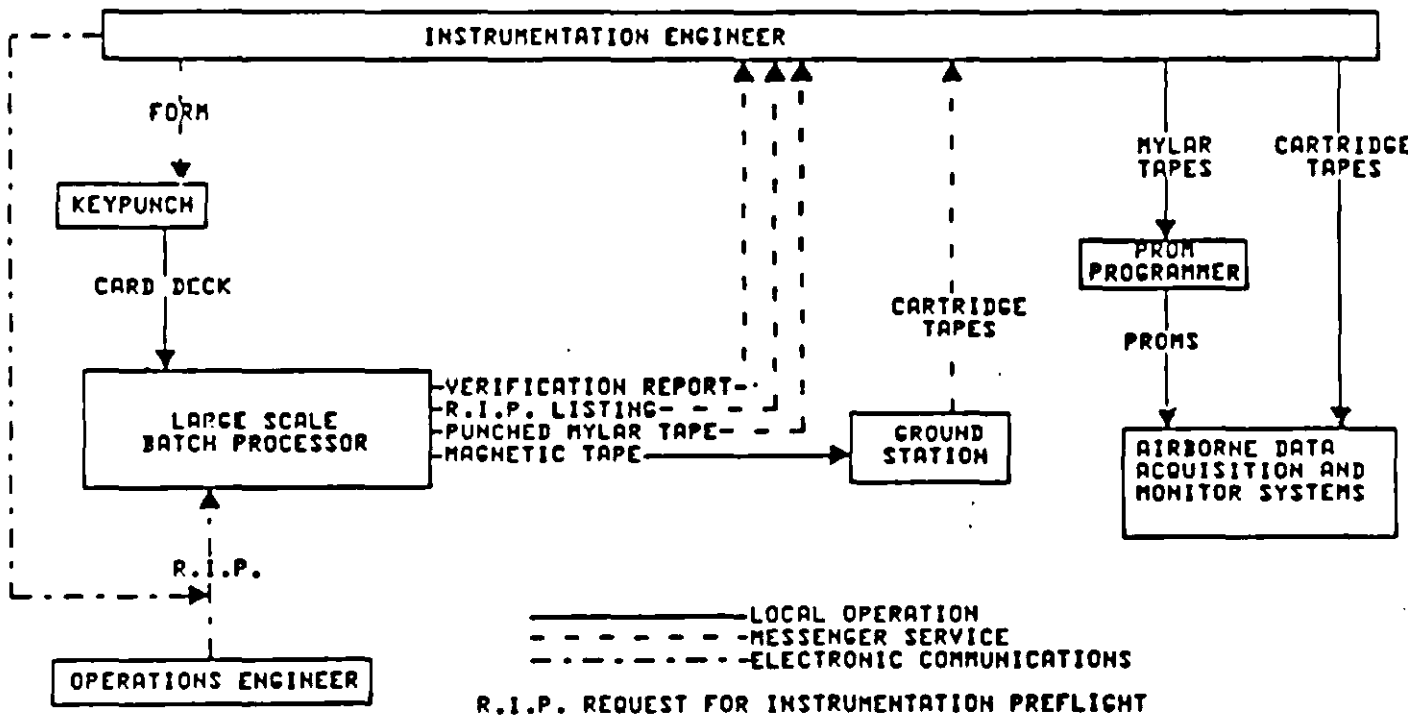


FIG. 2 PRESENT ROUTING OF R.I.P. INFORMATION

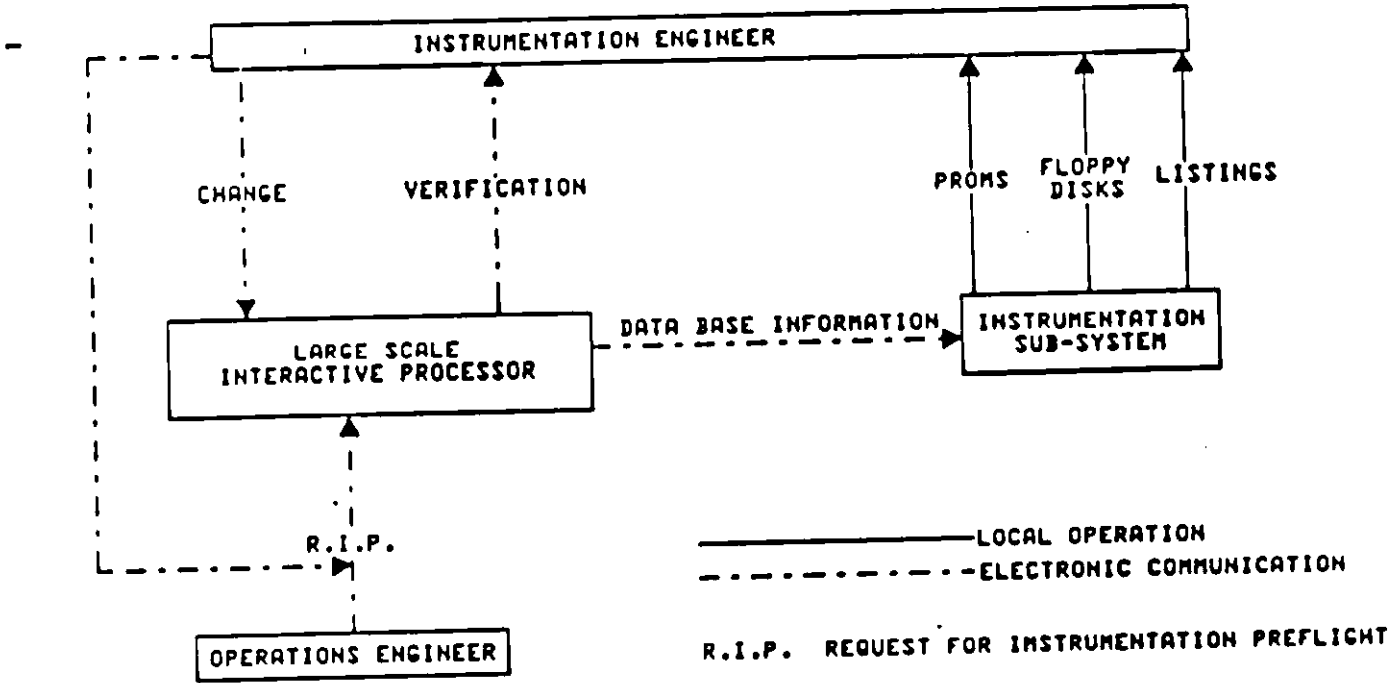


FIG. 3 ISS ROUTING OF R.I.P. INFORMATION

COLOR GRAPHICS BASED REAL-TIME
TELEMETRY PROCESSING
SYSTEM

Thomas M. Randall
Lockheed-Georgia Company
Marietta, Georgia

ABSTRACT

A phased development project was initiated at Lockheed-Georgia Company four years ago to establish a real-time telemetry processing facility capable of monitoring test data acquisition and performing interactive analysis of test results. The design of this system differs from its contemporaries in two important respects. All calibration, correction, and conversion of test data to engineering units, as well as computation of indirect measurements, are performed by integral computers in the air-borne PCM acquisition system, eliminating these tasks from the ground processing workload. Additionally, the principal man/machine interface in the telemetry processing system is a raster scan, color graphics display terminal instead of the monochrome stroke writing displays employed in other systems. To date, feasibility demonstration and prototype phases have been completed, with the prototype system utilized to support the Phase III flight test program on the stretch C-141B. For this phase, a unique display configuration was developed in conjunction with Ramtek Corporation to produce a scrolled time history format with the appearance of continuous motion. A series of computer analysis programs was also developed for the system to process test data stored on magnetic disc within two to three minutes of test run completion. Due largely to usage of the real-time system, the test program was completed ahead of schedule and under budget with better processing and analysis efficiency than had been expected. A production configuration phase is currently in progress to expand display capacity and increase computational resources through use of the VAX-11/780 digital computer.

Thomas M. Randall, Aircraft Development Engineer, Specialist for
Lockheed's Engineering Data Systems Department

INTRODUCTION

Four years ago, Lockheed-Georgia Company initiated a company-funded project to develop a telemetry processing facility capable of monitoring test data acquisition and performing interactive analysis of test results in near real-time. A coordinated, companion project had been previously initiated to develop an advanced airborne data acquisition system based upon computer control of data sampling and pulse code modulation (PCM) encoding of the data samples. In order to permit more accurate monitoring onboard the test aircraft and simplify the ground processing task, the functions of data calibration, correction, and conversion to engineering units, as well as calculation of indirect measurements, were allocated to the airborne acquisition system. The real-time processing system was to be developed around raster-scan, color graphics display equipment which would serve as the principal interface between operating personnel and the system's central digital computer. A phased approach was followed in the development of both systems.

The feasibility demonstration phase in the development of the Real-Time Telemetry System (RTTM) was completed in early 1977 and the resulting configuration was evaluated during the subsequent Phase II Flight Test Program on the C-141B. Several areas for potential improvement were noted during these tests and an appropriate set of design requirements was established to incorporate these improvements during the following prototype development phase. This phase was completed in mid-1979 in time for the system to be utilized as the primary data reduction facility for the C-141B, Phase III Flight Test Program. A third version is currently being developed to incorporate those features and capabilities that operating experience has shown to be desirable. The new version will be fully operational in late 1981 and will be utilized to support all subsequent flight test programs.

Since this "production" model is in an early stage of development, descriptions of the prototype are utilized to illustrate the composition, organization, capabilities, and features of the Real-Time Telemetry System. Specific changes that will be made in the current development phase to bring the system up to planned capabilities are then discussed to define the version that will exist in 1981.

DISCUSSION

System Composition

The composition of the system is illustrated in the simplified block diagram of Figure 1. Test data encoded in PCM format and IRIG-B time code information are input to the system through a telemetry link where they are converted to digital form by PCM ground station equipment and a time code translator. For postflight processing, data recorded onboard the test aircraft on magnetic tape are reproduced electronically and are then processed in the same manner as telemetered data. Digital data outputs from the PCM and time code equipment are input to the central computer through direct memory access (DMA) transfer, where they are processed in response to frame sync interrupts. The system software performs two types of processing. A selected group of key parameters is separated from the received frame of data, converted to display format, and presented on color-graphics CRT terminals as scrolled time-history plots

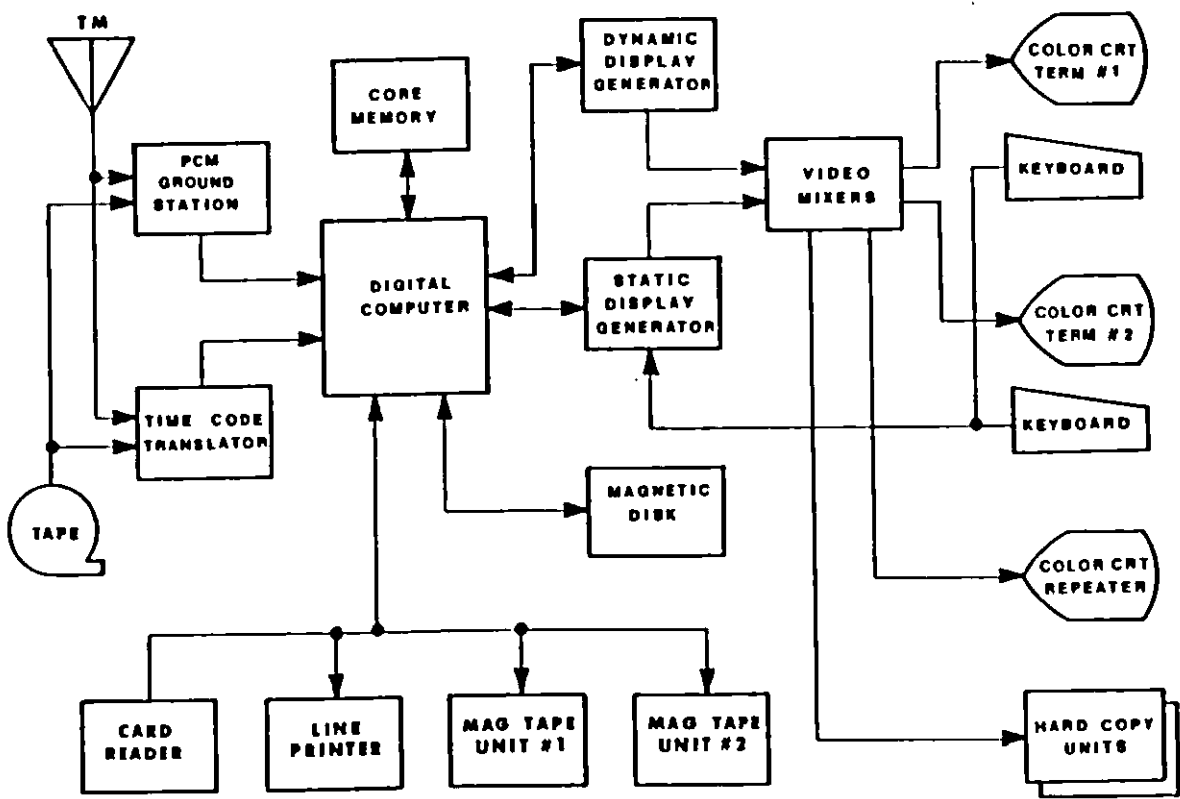


FIGURE 1: REAL-TIME TELEMETRY SYSTEM BLOCK DIAGRAM

for real-time viewing. Secondly, all received data are converted to fixed-point integer format, assembled into logical record blocks, and stored on the magnetic disk to form a rapid-access data base for subsequent analysis processing.

Analysis engineers monitor the scrolled time history displays to determine if test maneuvers are performed properly, desired test limits are reached, and valid measurements are being acquired. If discrepancies are noted, appropriate corrective directions are radioed to the aircraft and the test run is repeated. Once valid data are acquired from a test run, an analysis engineer selects appropriate processing software through terminal keyboard input, defines the time-code interval over which data are to be analyzed, and specifies the

processing options to be exercised by the analysis software. The computer then retrieves the specified interval of test data from the rapid-access data base and processes it to test result form, displaying the information in appropriate tabular and graphic forms on the color CRT terminals. Black and white hard copies of all pertinent display information needed to document test results are produced in response to operator initiation.

The component equipment with which the system is implemented can be categorized into three groups: the telemetry ground station, the digital computer, and the color graphics display subsystem. The telemetry ground station is comprised of a tracking antenna/receiver subsystem, magnetic tape recorder/reproducer, PCM decommutation subsystem, and time code translator. The antenna, manufactured by Scientific-Atlanta, is an 8-foot diameter parabolic dish with a beamwidth of six degrees. It is mounted on a pedestal that slews in both azimuth and elevation to provide hemispherical coverage. Installed on a 40-foot tower on the roof of a 6-story building, the antenna provides reliable telemetry reception over a range of 180 to 200 miles. Automatic tracking coupled with dual-diversity reception results in virtually drop-out free communications with a test aircraft throughout the full spectrum of test maneuvers. The PCM decommutation subsystem is comprised of EMR series 2700 modules that perform the signal conditioning, frame synchronization, digital-to-analog conversion, PCM simulation, and data distribution functions for pulse code modulation data conforming with IRIG standards. The time code translator is an Astrodata Model 6222 which processes standard IRIG time-of-day code and converts it to digital time information in hours, minutes, seconds, and milliseconds. Digital data from both the PCM decommutation subsystem and time code translator are input to the digital computer through a multiplexed I/O channel under direct memory access transfer. The magnetic tape unit is an Ampex Model FR 3030 wideband transport providing the capability for both recording/reproduction of telemetry transmissions and reproduction of tapes recorded onboard the test aircraft in telemetry format. This permits the system to be utilized in both an on-line, real-time mode and an off-line, interactive processing mode.

The digital computer is an EMR Model 6050 with 32K words of core memory, a 2.4 million word capacity magnetic disk, an 800 card per minute punched card reader, a 1000 line per minute line printer, and two multiple density seven-track magnetic tape units. The computer utilizes a 24-bit word structure, provides hardware floating-point processing, and operates with a memory cycle time of 2.0 microseconds. Four buffered input/output channels with direct memory access interface the computer with its peripheral equipment and the other major components of the Real-Time Telemetry System. Processor reaction to discrete events is provided by eight levels of vectored priority interrupt and 56 levels of vectored scanned interrupts.

The color graphics display system is comprised of two Ramtek HM-9300 display generators operating in tandem to drive two independent, 19-inch, high-resolution CRT monitors. Display information is divided into categories of static data and dynamic data depending upon whether the information is to be displayed in a fixed location on the screen or is to be scrolled across the screen in a dynamic manner. Data from both the static and dynamic generators are converted to synthetic video

signals which are combined in the video mixers to produce a single set of RGB video signals for each terminal. An additional monochrome video signal is produced for each terminal to drive a hard copy unit. A third color CRT monitor is connected by coaxial relays to either of the independent terminals to serve as a repeater scope. This CRT serves the test director who does not require independent data access but instead selects which terminal's data he wishes to view. Interactive inputs to the system are accommodated by alphanumeric keyboards at each of the independent terminals, which are interfaced to the computer through the static display generator.

Display System Operation

The most unique feature of Lockheed's Real-Time Telemetry System is the color graphics display equipment. While this system is comprised of standard Ramtek RM-9300 raster scan components, the particular configuration utilized is special and was devised jointly by Ramtek and Lockheed to provide the high-speed scrolling capability needed to implement a continuous-motion, time history display format. A simplified block diagram of the output section is shown in Figure 2 and will serve to show how the unique capabilities are derived. As with any modern raster-scan display, a graphics generation section utilizes a microprocessor to decode a series of instructions specifying the type, color, and screen location of the graphics to be generated and stores the series of picture elements (pixels) that comprise the graphics in a set of memory planes. Independently, a set of refresh readout circuits cyclically read the digital information from these memory planes and convert it to synthetic video to drive the CRT monitor. Data may be moved or scrolled across the display screen by either moving it to another set of storage locations within refresh memory or changing the starting memory address (origin) from which refresh readout is initiated. The former is called software scrolling and the latter is called hardware scrolling.

Software scrolling is useful when a small number of pixels are to be moved, but when an entire memory plane is to be scrolled, about 3 seconds is required to complete the process. Hardware scrolling, on the other hand, can be accomplished in hundreds of microseconds, but all information contained in all memory planes will be scrolled. This fact led to the use of the dual RM-9300 configuration. By separating information into static and dynamic categories according to whether it was to be displayed in a fixed position on the CRT screen or scrolled across the screen dynamically, the information could be routed to separate display generators and stored in separate sets of memory planes. Refresh readout from the two sets of memory planes is synchronized by a voltage-controlled oscillator tying the sync/timing circuits together and two sets of synthetic video representing red, green, blue, and hard copy are produced. The static and dynamic video signals are then combined in a set of video mixers to drive the CRT terminal and the hard copy unit. The dynamic data are scrolled vertically by altering the readout origin, erasing old data to be scrolled off the screen, and writing the new data to appear in appropriate locations in the refresh memory. This process is repeated at a rate of 10 times per second, which with the phosphor persistency, creates the effect of continuous motion.

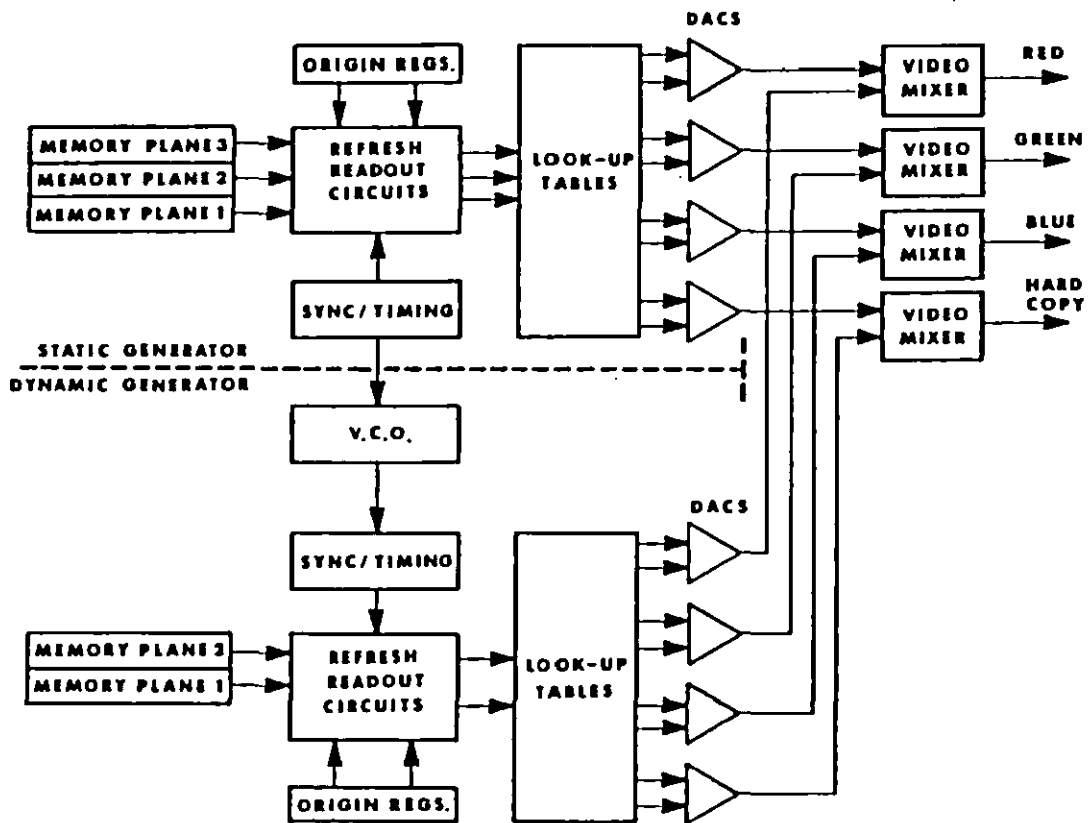


FIGURE 2: SIMPLIFIED BLOCK DIAGRAM OF COLOR GRAPHICS DISPLAY SYSTEM

The number of memory planes required for each display generator is a function of the number of colors desired. Three planes were chosen for the static generator, providing three bits of digital code for each pixel. This permits definition of seven colors plus black. For the dynamic generator, two planes were chosen to define three colors plus black. Each memory plane is organized as a matrix providing 512 lines of resolution vertically by 640 pixels horizontally. The actual color translation is fairly complex, involving two distinct look-up table translations which convert the 3-bit and 2-bit codes defining each pixel into four levels of intensity for each color: zero, one-third, two-thirds, and full. Digital to analog converters perform the final conversion from digital code to synthetic video.

System Software

The capabilities and limitations of the Real-Time Telemetry System are largely a function of its system software, which controls all aspects of acquisition processing and data base storage/retrieval. All pertinent characteristics of the data to be acquired and processed are defined by a project history file loaded into the computer from magnetic tape. This file together with a small deck of initialization cards define all information needed to set up the PCM ground station equipment, enable the system for data input, and display the set of selected channels in a graphical time-history format. Interactive access to this project history/initialization data for the operator is by means of the Initialization Data display format shown in Figure 3. This display is called by depressing the appropriate special function key on the alphanumeric keyboard, and presents, along with instructions for altering the data, all principal identification, selection, and process control information associated with the system. A capability is provided through this display format to alter title header data, change the measurement channels selected for display at the terminal, control the interval displayed in the scrolled time history by selecting the number of samples averaged

INITIALIZATION DATA

- INSTR. 1. POSITION CURSOR AT LINE TO BE CHANGED.
2. TYPE IN AND VERIFY NEW DATA.
3. DEPRESS ~~ENTR~~ KEY FOR CHANGE
4. REPEAT ABOVE STEPS FOR ADDITIONAL CHANGES.
5. DEPRESS SELECTED ~~ENTR~~ KEY WHEN CHANGES ARE COMPLETED.

A/C NAME =	C-141B	CHANNEL INITIALIZATION	
TAIL NO. =	7881	MEAS CODE =	HZCG
FLIGHT NO. =	129	SCALE FACTOR =	3
RUN NO. =	8A	+ MIN PLT VALUE =	0.50
FLIGHT DATE =	86JUL79	UNITS / DIV =	0.50
DATE REDUCED =	27MAY80	MEAS TITLE =	HZ CG
CHAN INIT DATA =	CCCC	UNITS LABEL =	G
DISP CHAN SEL =	X CCCC	DISP CONT =	14
TIME EXP FACTOR =	1	DISP CHANS	TIME EXPANSION
		CHAN MEAS CODE	FACTOR TIME(SEC)
		1 UCCK	1 16
		2 HZCG	2 32
		3 RUDD	4 64
		4 WPOS	10 160
		5 L915	20 320

FIGURE 3: SYSTEM INITIALIZATION DATA DISPLAY FORMAT

to produce each display point, and alter the sensitivity and offset with which each measurement is plotted. When all initialization parameters have been adjusted to the needs of the analysis engineer, he calls up the time history display through actuation of another special function key.

The scrolled time-history display format is shown in Figure 4. Its display area is divided such that 101 pixels horizontally by 320 lines vertically are allocated to each of five measurement channels. Grid lines are drawn and labeled with corresponding physical unit values for the measurement. Titles and unit labels are displayed above the grid structure of each measurement channel. A title header block containing all necessary identification information is displayed at the top of the format. Data points are displayed to scale within the grid structure, with time-code information in hours, minutes, and seconds shown to the left of the channel grids. Data and time code are scrolled from the top to bottom of the channel display area, with the oldest information disappearing from the screen when the bottom grid line is reached. The maximum and minimum measurement values contained within that portion of the time history currently appearing on the screen are tabulated in

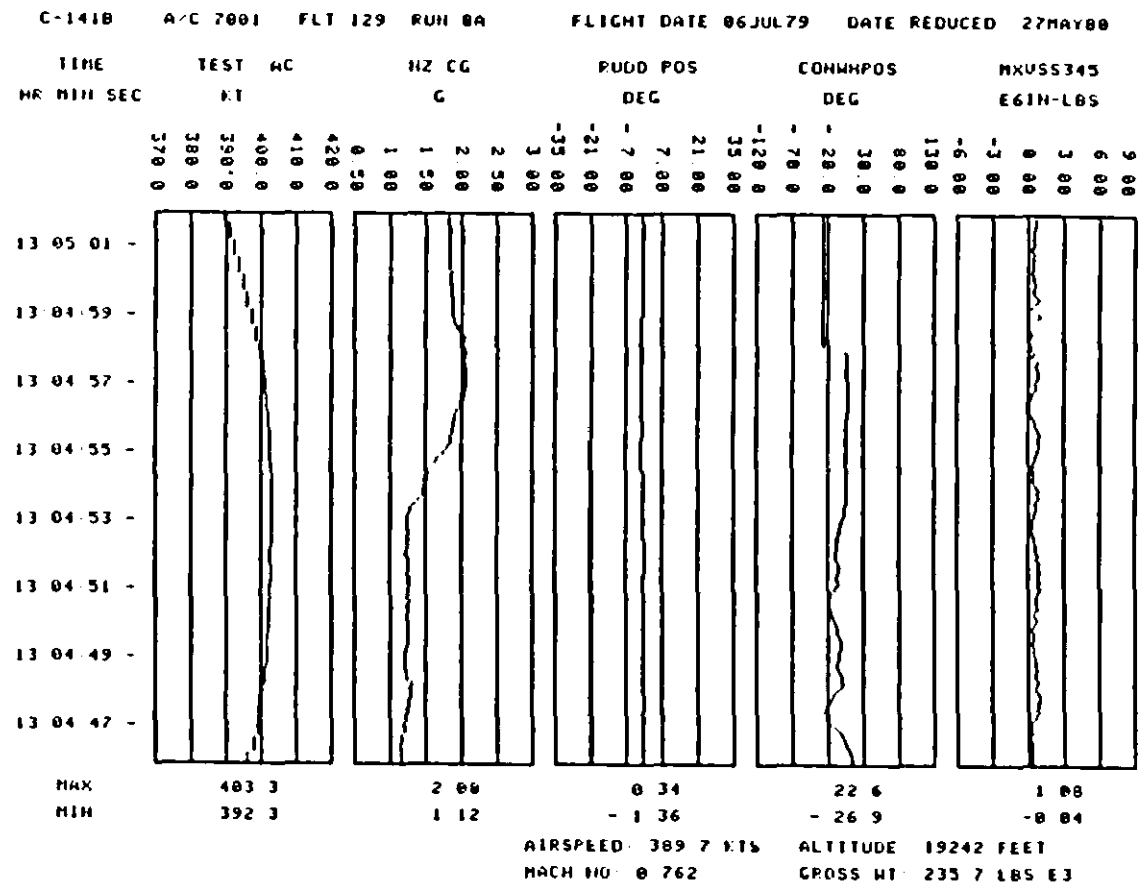


FIGURE 4: SCROLLED TIME HISTORY DISPLAY FORMAT

engineering units below the grid structure of each channel and are updated once per second. Thus limit values can be read directly without visual scaling. In addition, key test condition parameters of airspeed, altitude, Mach number, and gross weight are displayed in tabular form at the bottom right corner of the format and are also updated once per second. If a hard copy of the information appearing on the screen is desired at any point in time, depressing the copy function key initiates the copy sequence. Data update to both terminals is suspended to freeze information content and the copying process is automatically initiated. Approximately 12 seconds is required for the copy to be completed, after which, update scrolling is resumed automatically. Data being input to the system during the copy interval is stored in the data base, but is lost for real-time viewing.

As a general design philosophy, color is utilized in the scrolled time-history format and all other display formats for two major purposes. It is utilized to separate information categorically, and thereby reduce the apparent complexity of a display format so that operating personnel can find and interpret desired information more readily. Secondly, it is utilized to call the operator's attention to information of greatest importance and de-emphasize information of lesser significance in order to facilitate speed and accuracy of interpretation and usage.

Analysis Software

Whenever the system is operating in its data acquisition mode, all input test data are stored on magnetic disk to form a rapid-access data base for subsequent analysis processing. The data are stored such that when the capacity of 1.8 million words is reached, new data replaces the oldest stored data, resulting in a variable time interval of available data dependent upon sampling rate and number of channels. For a typical case where the PCM configuration was 128 mainframe channels sampled 20 times a second, storage capacity was the past 10.4 minutes of test data. This capacity may represent several test runs, however, since once a run is completed and all data of interest have been stored in the data base, the system is normally switched to the analysis mode for result processing while the aircraft sets up for the next run. When this mode switch is made, data flow to the disc is terminated, preserving the currently stored information until the mode is switched back to acquisition.

The analysis mode is entered by operator selection of a data analysis program through actuation of its associated special function key on the alphanumeric keyboard. Five such keys are allocated for the analysis software selection function and are given the undefined labels of PROG1, PROG2, PROG3, PROG4, and PROG5. Actual association of key with software is made within the system software itself, so that the repertoire of analysis programs can be easily altered according to the type of aircraft testing to be performed. An index display format is provided, as shown in Figure 5, to show the actual functions assigned to the special keys by the system software. This format is called for display by actuation of the key labeled INDEX.

INDEX OF FUNCTION KEYS

*	1010	TABLE OF KEYBOARD FUNCTIONS ASSIGNED BY SOFTWARE
*	1111	EDIT BUFFER REPEAT NON-REVERSED CHARACTERS
*	1112	HARD COPY - LOCAL TERMINAL ONLY
*	1113	MONITOR REAL TIME SCROLL HISTORY
11	1114	INITIALIZATION DATA DISPLAY
11	1115	LOADS ANALYSIS PROGRAM
11	1116	STALL PERFORMANCE / CHARACTERISTICS PROGRAM
11	1117	AIRSPED CALIBRATION SYSTEM PROGRAM
*	1118	LOADS MARGIN OF SAFETY ANALYSIS PROGRAM
*	1119	DIGITAL DATA RETRIEVAL AND RECORDING PROGRAM
1119	1120	CLEAR DISPLAY SCREEN (EXCEPT MHTR MODE)
1119	1121	STOP DISPLAY UPDATES (MHTR MODE)
1119	1122	CONTINUE PROCESS (DISPLAY UPDATES, NEXT SCREEN, ETC...)
1119	1123	HARD COPY - ALL ACTIVE DISPLAYS
1119	1124	CLEAR KEYBOARD ENTRY BUFFER
1119	1125	(NOT USED)
ENTER		PROCESS CURRENT KEYBOARD ENTRY (EDIT BUFFER)
SELECT		PRESET CURSOR POSITION (FUNCTION OF DISPLAY)
CORR		(NOT USED)
BLINK		BLINK CURSOR (IF ALREADY ON)
DISP		CURSOR DISPLACEMENT - HIGH/LOW SPEED
HOME		PRESET CURSOR POSITION (FUNCTION OF DISPLAY)
ON		CURSOR ON / STOP BLINK
OFF		TURN CURSOR OFF
		* -LOADS OR RESTARTS PROGRAM. ACTIVATES REQUESTING TERMINAL
		##-SYSTEM PARAMETER MODIFICATIONS, DEACTIVATES TERMINAL

FIGURE 5: INDEX OF FUNCTION KEYS DISPLAY FORMAT

When an analysis program is selected, the software is called up from storage on the magnetic disk and replaces the system software in main memory as an overlay. Execution then begins automatically with generation of appropriate interactive prompting messages on the CRT terminal. Since all analysis programs employ the same processing philosophy, they can be categorically described through use of a typical example. The example that will be used is a loads margin of safety program developed to support 80 and 100 percent loads demonstration testing of the C-141B. The initial prompting messages utilized for control of this analysis program are shown in Figure 6.

The first message displayed is a request to select whether 80 or 100 percent loads analysis is to be performed. An arrow points to the default choice and the analysis engineer is instructed on how to change the selection. If the default selection is correct, the continue (CONT) key is pressed in lieu of the selection entry sequence. Once the choice is made, a second message appears requesting specification of the desired

C-141B A/C 7081 FLT 129 RUN 8A FLIGHT DATE 06JUL79 DATE REDUCED 27MAY80

EXECUTING LOADS MARGIN OF SAFETY ANALYSIS PROGRAM

SELECT 80 OR 100 PERCENT LOADS ANALYSIS:

FORMAT: I,X ~~MMDD~~

-> A = 100 PERCENT ENVELOPE

B = 80 PERCENT ENVELOPE

ENTER SELECTED TIME CODE INTERVAL:

FORMAT: T,HHMMSS,HHMMSS ~~MMDD~~

ANALYSIS IN PROGRESS:

LOAD STATIONS TO GO - 19

FIGURE 6: LOADS MARGIN OF SAFETY ANALYSIS PROGRAM
QUEUE MESSAGES

analysis interval through entry of start and end time codes. When the time code interval is entered, a third message appears announcing that analysis is in progress and that there are 19 load stations to go. The specified interval of test data is retrieved from the data base and the measurements associated with the first load station are processed to determine maximum load encountered. When this has been accomplished, the load stations to go count is decremented to show progress and data for the next station are retrieved and processed. This procedure continues until data from all 19 stations have been processed. This typically requires approximately 2.5 minutes of processing time.

The final analysis results are then displayed in summary tabular form on both CRT terminals as shown in Figure 7. The maximum load encountered at each load station during the analysis interval is tabulated as a percentage of rated load together with an alphanumeric code identifying the station. The number displayed to the left of the station identification code is used for specification purposes when requesting substantiating data. In the lower-right corner of the format, the average value of principal test conditions for the analysis interval are tabulated together with the time-code interval over which analysis was performed.

C-141B A/C 7801 FLT 129 RUN 8A FLIGHT DATE 06JUL79 DATE REDUCED 27MAY80

LOADS MARGIN OF SAFETY ANALYSIS

PERCENT LOADS SUMMARY

<u>HING STATIONS</u>	<u>HORZ STAB STATIONS</u>	<u>FUSELAGE STATIONS</u>
1. MS135L - 82.5 X	9. HSS44L - 62.2 X	16. FS1048 - 58.3 X
2. MS135R - 85.2 X	10. HSS44R - 62.0 X	17. FS1048 - 58.3 X
3. MS214R - 85.8 X	11. HSS140R - 61.0 X	18. FS1398 - 62.1 X
4. MS293R - 92.2 X	12. HSS190R - 60.3 X	19. FS1688 - 67.2 X
5. MS396R - 93.9 X		
6. MS479R - 89.0 X	<u>VERT STAB STATIONS</u>	<u>TEST CONDITIONS</u>
7. MS688R - 79.1 X	13. USS343 - 23.2 X	HPC - 19183
8. MS778R - 88.2 X	14. USS412 - 22.8 X	UC - 398.0
	15. USS471 - 20.3 X	MACH - 0.037
		GW - 235.7

TIME 13:04:54 TO 13:05:02

FIGURE 7: LOADS MARGIN OF SAFETY TABULAR SUMMARY DISPLAY FORMAT

A system of color coding is employed in displaying percentage load to simplify interpretation. When the load value is under 70 percent of the demonstration limit, its value is displayed in white. Between 70 and 80 percent, the color is changed to green and between 80 and 90 percent, yellow is used. Above 90 percent, the load is displayed in red. At first glance, the analysis engineer can see the range of loads encountered, and which stations experienced the highest loads. A hard copy is normally made of the summary display and then substantiating data are requested for stations showing significant loads or loads that deviate from expected values. This data format is called by entering the characters I, X from the keyboard, where X is the number displayed to the left of the station code in the summary format.

Substantiation for the summary loads data is provided in the form of load envelope plots of the shear, bending, and torsion measurements at the load station in question, as shown in Figure 8. The data are cross plotted together with envelopes of constant rated load which show the combinations equivalent to 100 or 80 percent load. As the data points are plotted in rapid sequence, the buildup and decline in load can be noted together with

C-141B A/C 7001 FLT 129 RUN 8A FLIGHT DATE 06JUL79 DATE REDUCED 27MAY80

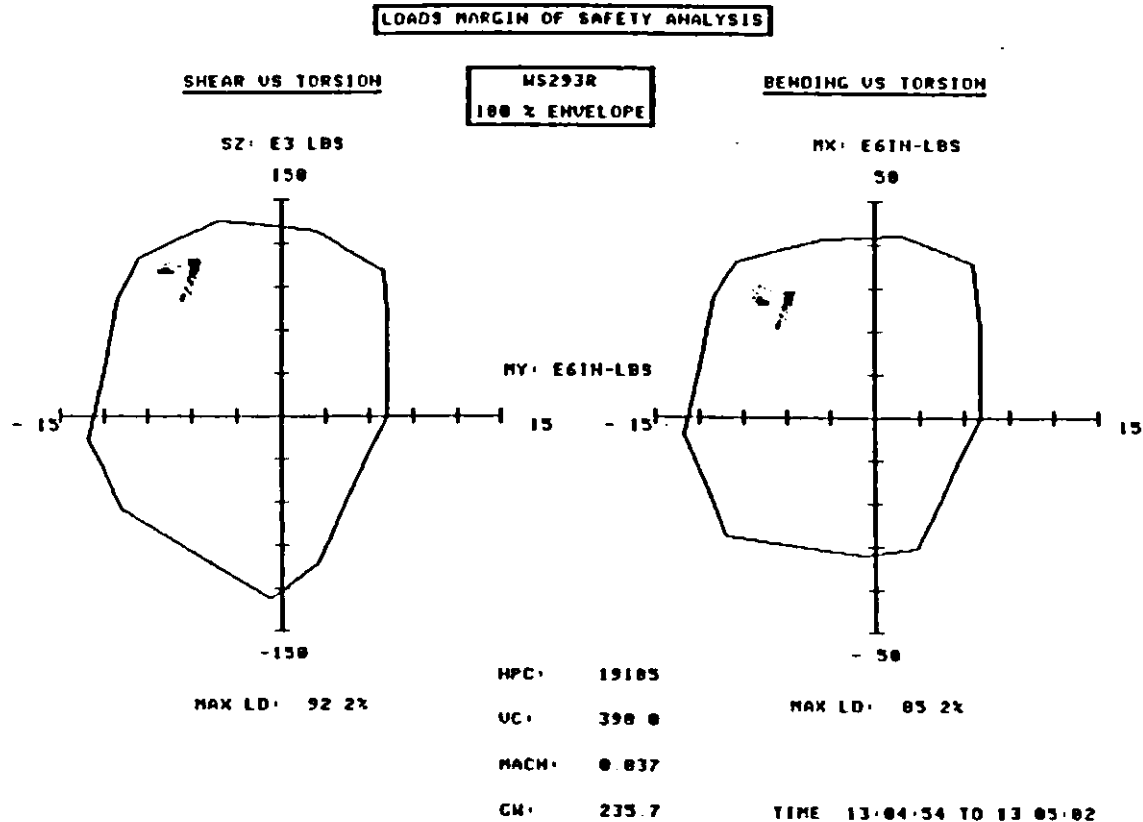


FIGURE 8: LOADS MARGIN OF SAFETY ENVELOPE PLOT DISPLAY FORMAT

the existence of any wild points that deviate from normal trends and which may bias the final result. Any such wild points may be eliminated by specifying a different analysis interval and re-running the program or by manually estimating the correct maximum load from the graphical presentation. As with the summary tabulation, average test conditions and the selected analysis interval are displayed at the bottom of the format. A hard copy of the presentation is generally made to document results and additional load station cross plots are called for display as needed for substantiation or documentation. When analysis activities are completed, actuation of the associated special function key causes the data acquisition software to be read into main memory from disk and the scrolled time-history display is brought up on both CRT's to complete transition back to the data acquisition mode.

Current Development Activities

The prototype system suffered from two principal limitations: inability to accommodate PCM data rates higher than 5120 samples per second and limited channel monitoring capacity resulting from availability of only

two independent terminals. Both of these limitations were imposed by the relatively modest computing capacity provided by the EMR-6050. Therefore, the primary objective of the current production configuration development phase was to replace the EMR-6050 with a modern, high-speed computer offering four times the capacity for real-time processing. After an evaluation of the currently available 32-bit super-minis, the Digital Equipment Corporation VAX-11/780 was selected and procured. Operating software is being rewritten to permit simultaneous acquisition and analysis processing of PCM data with frame lengths as high as 512 channels and sampling rates as high as 160 samples per second.

Display capacity will be expanded through incorporation of a new Remtek display system, the RM-9400. This color graphics display equipment provides unique capabilities which can be utilized to satisfy the principal faults of the RM-9300 for the real-time telemetry application. Resolution is increased to 1024 lines by 1280 pixels which will improve both the accuracy and quality of plotted data. Perhaps the greatest advantage, however, is that the increased resolution will accommodate twice the data rate in a scrolled time history display with the same level of dynamic movement on the CRT screen. Thus, the RM-9400 will accommodate real-time data rates as high as 80 samples per second with a rate of movement that is comfortable for human viewing while the RM-9300 will only support 40 samples per second. A special type of refresh memory plane is incorporated in the RM-9400, in addition to the standard type, which contains its own independent set of origin registers. Due to this feature, the scrolled time history format can be implemented with a single RM-9400 instead of the dual RM-9300 utilized in the prototype system. Two independent terminals can be driven from a single RM-9400 generator with 4 bits of conventional memory for static data, 2 bits of independently scrollable memory for dynamic data, and 1 bit of independently scrollable memory for hard copy allocated to each terminal. The use of a separate memory plane for hard copy data permits copies to be made without interruption to the scrolling operation on the CRT. Only input of dynamic data to the hard-copy plane need be suspended during the copying process.

A large number of changes will be incorporated into the operation software of the system to increase capacity and improve utility. Among these is the ability to accept narrow-band FM, wide-band FM, and digital data as well as PCM data in a non-real time, interactive processing mode. This mode will be used for detailed, post-flight analysis of test data recorded onboard the test aircraft or acquired and partially processed at off-site test facilities. A second change will involve greater allocation of magnetic disk capacity to the storage of the test data base. The exact allocation has not been set at this time, but disk storage has been increased by more than an order of magnitude with acquisition of the VAX-11/780, and an allocation on the order of two hours or more is likely. The third major area for software change is the introduction of new data display formats. Emphasis will be placed on greater use of dynamically updated tabular data to augment the scrolled time history display. The information actually being sought from many channels monitored as time histories has no relation to time rate of change of the parameter. In such cases, tabular presentation coupled with color change to indicate limit boundaries may prove the optimum method of presentation for acquisition monitoring.

CONCLUSIONS

While the real-time telemetry system and its component color-graphics display system described herein represents only a beginning, it does effectively demonstrate a philosophy of test data acquisition and analysis processing which shows great potential for improved efficiency and significant cost savings. This philosophy is to utilize modern computer and display technology in conjunction with the judgement and reasoning ability of the human operator to create an interactive processing chain capable of acquisition monitoring, interval selection editing, and analysis processing to final test results in a single, continuous operation. With the elimination of trial and error data acquisition and piecemeal analysis processing, attendant increases in efficiency and reductions in required test span produce dramatic cost savings. The key element in the interactive processing approach is the development of the custom system and analysis software. It is by far the most expensive single element in the system, representing six to eight man years of development effort. Its design is also critical, since the capabilities and features of the system are largely the result of software innovations. If this aspect is handled successfully, however, the cost savings over conventional methods will quickly amortize development costs and net savings can be achieved within the span of a single major test program.